INFORME FINAL DEL PROYECTO

MAGMATISMO, ACTIVIDAD HIDROTERMAL Y MINERALIZACIONES EN CINTURONES TRANSPRESIVOS: EL SO DE LA PENINSULA IBERICA

Salamanca, Diciembre 2007

En el marco de diversos proyectos del IGME (SICOAN 2000035, 2001058), parcialmente financiados por la Dirección General de Investigación en forma de proyectos del Plan General de Promoción del Conocimiento (DGI-FEDER BTE 2003-290) y dos Acciones Especiales y englobados en dos proyectos de la European Science Foundation (EUROPROBE y GEODE), se han realizado diversos estudios sobre la geología y geoquímica de las mineralizaciones situadas cerca del contacto transpresivo entre la Zona de Ossa Morena y la Zona Sudportuguesa con el fin de comprender la evolución metalogenética de las importantes mineralizaciones situadas cerca de esta sutura y la influencia que tiene el magmatismo y la tectónica en su génesis.
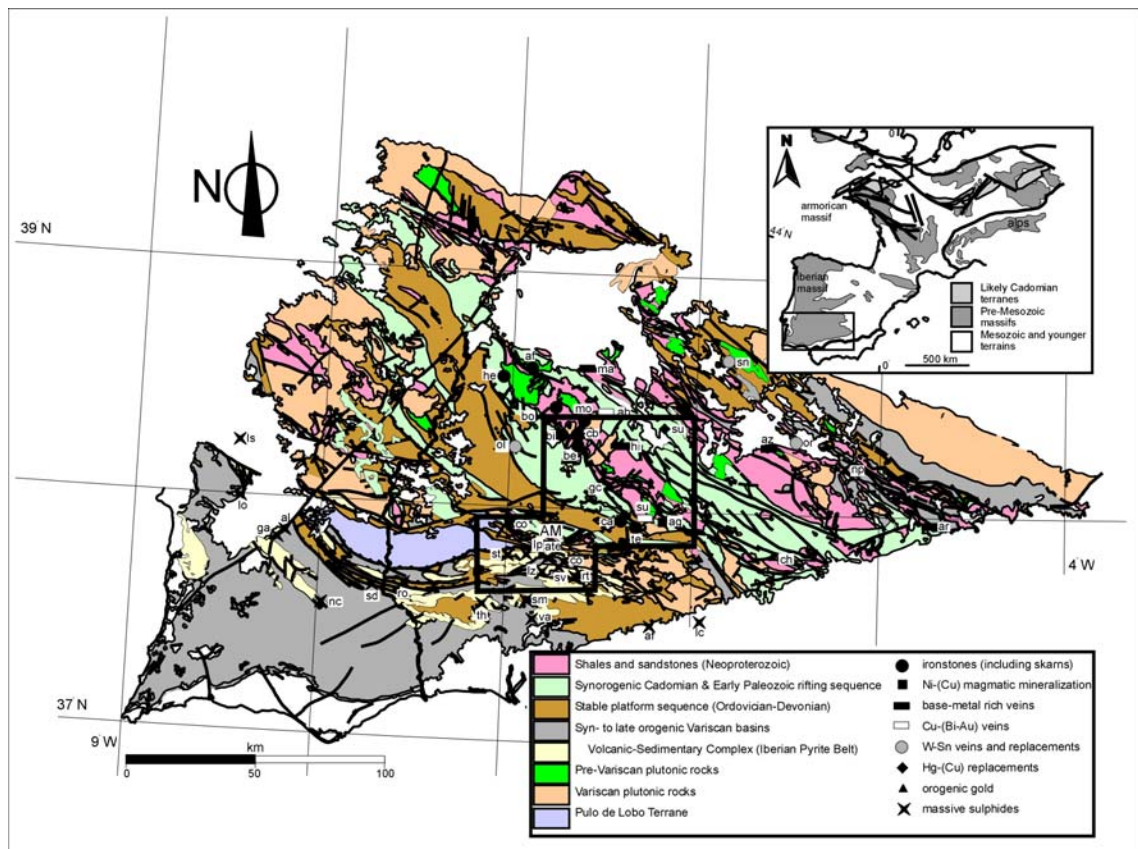

Figura 1. Localización de la zona de trabajo

Las conclusiones globales más importantes del proyecto son:

1. Establecimiento de las relaciones de la mineralización de Aguablanca con el complejo laminar profundo y propuesta de un nuevo tipo de mineralizaciones magmáticas de Ni-(Cu).

2. Modelo metalogenético para la Zona de Ossa Morena, proponiendo que las mineralizaciones de Ni-(Cu) e IOCG son la expresión del magmatismo profundo.

3. Propuesta de un esquema metalogenético para la FPI, en el que los sulfuros masivos de la zona meridional estarían formados por procesos exhalativos mientras que los depósitos de la zona septentrional se formarían por remplazamiento de rocas volcánicas.

El proyecto consta de dos partes diferenciadas, el estudio de la Zona de Ossa Morena y el de la Zona Sudportuguesa, como partes de un mismo proceso pero con una evolución metalogenética coetánea y ligada a la tectónica de desgarres Varisca pero totalmente diferentes.

En la Faja Pirítica los resultados fundamentales han sido:

• Realización de una cartografía de detalle y estudios geológicos, geoquímicos y estructurales en el depósito de Rio Tinto. A pesar de ser uno de los depósitos más emblemáticos y mayores del mundo, no había trabajos de detalle recientes en la mina y que encuadraran su geología en la del conjunto de la Faja Pirítica. Los resultados obtenidos (Mellado et al., 2006y González Clavijo et al., en preparación) muestran que su geología es muy similar a la de otras área de la FPI. Sin embargo, tiene una serie de características propias como son la aparente diacronía de los sulfuros masivos con los de otras zonas (Tournasiense vs Fammeniense) y la presencia de grandes cuerpos volcánicos félsicos bajo los sulfuros masivos.

• Estudio del encuadre geológico de los sulfuros masivos del sector septentrional de la FPI, en el sector entre Cueva de la Mora y San Telmo, con incorporación a un GIS de las cartografías anteriores y su reinterpretación a partir del análisis de facies volcánicas, estudio estructural y geoquímica. El estudio muestra que hay una serie de unidades volcánicas geoquímicamente diferenciables pero formadas por diversas facies de tipo domo e intrusivo. Los sulfuros masivos se encuentran sistemáticamente ligados a facies brechoides y/o ricas en pómez y vidrio laterales a los domos. No guardan una posición estratigráfica definida.

• Estudio global de los estilos de mineralización en la Faja Pirítica, mostrando que los sulfuros masivos en el sector meridional están encajados en pizarras y son de origen exhalativo mientras que los de la zona septentrional son remplazantes en la roca encajante, fundamentalmente rocas volcanoclásticas félsicas (Tornos, 2006).

• Estudio geoquímico (isótopos Sr, Nd, Os, O) mostrando que el origen de los metales y fluidos está más ligado a la evolución diagenética de la cuenca que a fluidos profundos ensueltos de magmas félsicos profundos (Tornos, 2006) y mostrando que la derivación de estas pizarras puede formar fluidos ricos en metales pero pobres en azufre capaces de ascender hasta el fondo marino, donde precipitarían por mezcla con azufre de origen biogénico (Tornos & Heinrich, enviado).

• Desarrollo de modelos sobre la formación de sulfuros masivos en fondos anóxicos por procesos de tipo "brine pool" a escala global (Solomon et al., 2004) o en la mineralización de Tharsis (Tornos et al., aceptado).

• Estudio de inclusiones vítreas en fenocristales de rocas volcánicas, mostrando que hay al menos dos tipos de magmas, uno de ellos con características similares a las de los leucogranitos ricos en Sn y que hipotéticamente podría ser la fuente última del Sn en la Faja Pirítica (Tornos et al., 2004).

• Desarrollo de modelos numéricos para explicar la evolución de los sulfuros masivos del sector meriodional de la Faja Pirítica para explicar la aparente coetaniedad de todas las mineralizaciones y la derivación de los fluidos. El modelo numérico desarrollado muestra de una manera clara que los sistemas hidrotermales convectivos generados expulsan los fluidos mas calientes y salinos (capaces de formar las mineralizaciones) en un evento corto (<1 Ma) y temprano dentro de la evolución de la cuenca mientras que los fluidos más tardíos son menos salinos y más fríos (Conde et al., 2005).

En la Zona de Ossa Morena, los resultados fundamentales del proyecto están orientados a interpretar las relaciones entre un cuerpo intrusivo máfico profundo y las mineralizaciones del área. Este cuerpo fue detectado por geofísica profunda (Simancas et al., 2003) y se encuentra situado bajo la casi completa totalidad de la Zona de Ossa Morena. Su intrusión parece haber condicionado toda la metalogenia de la zona. Los estudios fundamentales han consistido en:

• Cartografía de detalle de la mina de Cala (Carriedo et al., 2007), con especial énfasis en las relaciones entre el stock de Cala, los skarns, la mineralización y la estructura.

• Estudios isotópicos y geocronológicos por Re-Os de los yacimientos de de Aguablanca (Mathur et al., en preparación) y Cala (Stein et al., 2006). En el primero de los estudios los resultados han sido dispares y sugieren que la geoquímica del Re-Os en este sistema es muy complicada. Sin embargo, los resultados confirman una edad Varisca para la mineralización y que la mayor parte del Os es de origen crustal. En el yacimiento de Cala se ha obtenido una isócrona realmente buena – probablemente la mejor obtenida por Re-Os en el sistema pirita-magnetita – que muestra que la mineralización de magnetita es al menos 20 Ma más joven que el granito asociado. Las relaciones iniciales de Os indican también una derivación mayoritariamente crustal. Estos datos permiten reinterpretar la mineralización de Cala y sobre su base se están haciendo estudios mas detallados para confirmar el modelo.

• Síntesis general de la metalogenia de Ossa Morena (Tornos et al., 2004; Tornos et al., 2006) que actualizan los estudios de Locutura et al. (1990) y son una compilación de los yacimientos minerales de la zona y su interpretación genética.

• Estudio de la geoquímica isotópica del plomo en la Zona de Ossa Morena a escala global, mostrando que la zona se caracteriza por un contenido anómalo en plomo de origen mantélico que contrasta con el de los terrenos circundantes, de carácter mucho más crustal. Esta anomalía se interpreta como asociada a la intrusión del cuerpo plutónico profundo (Tornos y Chiaradia, 2004).

• Estudios sistemáticos y detallados en la mineralización de Aguablanca, con dataciones Ar-Ar, geoquímica Sr-Nd y estudio de detalle de la relación de la mineralización con las rocas encajantes y la estructura (Tornos et al., 2006). Este estudio confirma nuestros modelos anteriores realizados cuando el yacimiento se descubrió, pero con una mayor cantidad de información y a nivel de mas detalle.

• Estudio geológico y geoquímico de rocas que han demostrado pertenecer al complejo plutónico profundo y que afloran en el macizo de Aracena. Se han realizado dataciones Ar-Ar, litogeoquímica, geoquímica isotópica y estudios geológicos que muestran estas relaciones y que indican que este cuerpo interaccionó de una manera muy variable con las rocas encajantes. La comparación con Aguablanca abre importantes guías de exploración para el área y para el desarrollo de modelos para este estilo inusual de mineralización (Tornos et al., 2006).

• Modelo global para la metalogenia de la Zona de Ossa Morena, incluyendo las relaciones entre el cuerpo plutónico profundo, el magmatismo metalumínico y las mineralizaciones de Ni-Cu y de tipo IOCG. Se propone que la intrusión en la corteza media produjo un metamorfismo de alto grado-baja presión y deshidratación de las rocas encajantes acompañados de una asimilación de metasedimentos. Esto produjo por un lado la generación de un magma sulfurado inmiscible y por otro la generación de magmas poco fraccionados pero ricos en agua. Su intrusión a niveles epizonales produjo fluidos ricos en metales que dieron lugar a las mineralizaciones de tipo IOCG. En ambos casos, la presencia de pequeñas estructuras extensionales en un orógeno mayoritariamente compresivo favoreció la formación de los yacimientos. Se plantea que

este modelo puede ser extrapolable a otros cinturones del mundo donde las evidencias de sistemas similares no han sido observadas por la falta de erosión o por un mayor grado de deformación (Tornos y Casquet, 2005; Tornos et al., 2005).

Los objetivos no alcanzados en el proyecto son:
• Definición precisa de los modelos que necesitan un importante estudio geocronológico. Parte de la geocronología planteada para el proyecto no ha podido realizarse por saturación de trabajo en los pocos laboratorios existentes.
• El trabajo a realizar en la mina Sultana no se ha finalizado debido a que la mina estaba en proceso de desagüe y cuando éste ha finalizado se han observado aspectos que han obligado a cambiar muchas de las hipótesis establecidas.

El proyecto se ha revelado como demasiado ambicioso en lo que respecta al estudio geológico, estructural y geoquímica del sector septentrional de la Faja Pirítica. Las relaciones eran mucho más complicadas que las esperadas por lo que se ha decidido restringir la zona de trabajo.

Este informe final es complementario del realizado específicamente en el sector septentrional de la Faja Pirítica y que fue desglosado por tenerse que hacer un proyecto independiente que contemplara la contratación de personal. El informe relativo a ese proyecto (Apoyo cartográfico y estructural al estudio de los sulfuros masivos del sector septentrional de la Faja Pirítica Ibérica) se encuentra en el Área de Documentación del IGME.

Los trabajos realizados se agrupan en sintetizan en las siguientes publicaciones:

Zona de Ossa Morena
• Carriedo, J., and Tornos, F., 2006, Los yacimientos de óxidos de hierro y mineralizaciones de cobre-oro asociadas del SO Peninsular: un modelo vertical de evolución: Macla, v. 6, p. 135-136.
• Carriedo J, Tornos F, Velasco F, Stein H (2007) Complex structural and hydrothermal evolution of the Cala magnetite deposit, SW Iberia - an IOCG deposit? In: Andrew CJea (ed) Digging Deeper. Proceedings of the 9th Biennial SGA Meeting IAEG, Dublin, pp 975-978.
• Carriedo, J., Tornos, F., Velasco, F., and Terrón, A., 2006, Mineralizaciones de magnetita asociadas a skarns y bandas de cizalla: La mina de Cala (Huelva): Geogaceta, v. 40, p. 235-238.
• Cheilletz, A., Pelleter, E., Martin Izard, A., and Tornos, F., 2005, World Skarn Deposits - Skarns of Western Europe, in Hedenquist, J. W., Thompson, J. B., Goldfarb, R. J., and Richards, J. P., eds., Economic Geology 100th Anniversary Volume, Society Economic Geologists, p. appendix 1-10.
• Sanabria, R., Casquet, C., Tornos, F., and Galindo, C., 2005, Mineralizaciones ferríferas del coto minero San Guillermo (Jérez de los Caballeros, Badajoz, España): Geogaceta, v. 38, p. 223-227.
• Stein, H., Markey, R., Carriedo, J., and Tornos, F., 2006, Re-Os evidence for the origin of Fe-oxide-(Cu-Au) deposits in SW Iberia at the Frasnian-Famennian boundary: Geochimica Cosmochimica Acta - Goldschmidt Conference Abstracts 2006, v. 18, p. A612.
• Tornos, F., Boixereu, E., Florido, P., Gumiel, P., Locutura, J., Lopera, E., Urbano, R., Fernández Leyva, C., Bel-lan, A., Martínez, S., Ortiz, G., Pérez

Cerdán, F., Pérez Moras, F., Eguíluz, L., and Apalategui, O., 2006, Mapa Metalogenético de la provincia de Badajoz escala 1/200000: Madrid, IGME-Junta de Extremadura, 183 p. (no incluído).

- Tornos F, Carriedo J, Velasco F, Galindo C, Casquet C (2007) The relationship between large deep mafic sills, crustal contamination and the formation of Ni-(Cu) and IOCG deposits In: Andrew CJea (ed) Digging Deeper. Proceedings of the 9th Biennial SGA Meeting IAEG, Dublin, pp 975-978.
- Tornos, F., and Casquet, C., 2005, A new scenario for related IOCG and Ni-(Cu) mineralisation: the relationship with giant mid-crustal mafic intrusion, Variscan Iberian Massif: Terra Nova, v. 17, p. 286-290.
- Tornos, F., Casquet, C., and Relvas, J., 2005, Transpressional tectonics, lower crust decoupling and intrusion of deep mafic sills: A model for the unusual metallogenesis of SW Iberia: Ore Geology Reviews, v. 27, p. 133-163.
- Tornos, F., and Chiaradia, M., 2004, Plumbotectonic evolution of the Ossa Morena Zone (Iberian Peninsula): Tracing the influence of mantle-crust interaction in ore forming processes: Economic Geology, v. 99, p. 965-985.
- Tornos, F., Galindo, C., Casquet, C., Rodríguez Pevida, L., and Iriondo, A., 2006, La relación entre intrusiones laminares profundas y la mineralización de Aguablanca: las rocas intrusivas de Cortegana (Huelva): Macla, v. 6, p. 485-487.
- Tornos, F., Galindo, C., Casquet, C., Rodríguez Pevida, L., Martínez, C., Martínez, E., Velasco, F., and Iriondo, A., 2006, The Aguablanca Ni-(Cu) magmatic deposit (SW Spain). Geologic and geochemical controls and the relationship with deep magmatic layered complexes: Mineralium Deposita, v. 41, 737-768
- Tornos, F., Inverno, C., Casquet, C., Mateus, A., Ortiz, G., and Oliveira, V., 2004, The metallogenic evolution of the Ossa Morena Zone: Journal Iberian Geology, v. 30, p. 143-180.
- Tornos, F., Iriondo, A., Casquet, C., Galindo, C., 2004, Geocronología Ar-Ar de flogopitas del stock de Aguablanca (Badajoz). Implicaciones sobre la edad del plutón y de la mineralización de Ni-(Cu) asociada: Geotemas, v. 6-1, 189-192.

Zona Sudportuguesa

- Bellido, F., Díez Montes, A., and Ortiz, G., 2006, Estudio petrológico y geoquímico de las vulcanitas de los afloramientos de El Pimpollar, extremo nororiental de la Zona Surportuguesa: Geogaceta, v. 40, p. 127-130.
- Conde C, Tornos F, Doyle M (2007) Geology and lithogeochemistry of the unique Las Cruces VMS deposit, Iberian Pyrite Belt In: Andrew CJea (ed) Digging Deeper. Proceedings of the 9th Biennial SGA Meeting IAEG, Dublin, pp 1101-1104.
- Conde, C., Tornos, F., Matthai, S., and Geiger, S., 2006, Modelización del transporte de calor y fluido en los sulfuros masivos encajados en pizarras de la Faja Pirítica Ibérica, España: Macla, v. 6, p. 137-139.
- Díez Montes, A., Bellido, F., Cózar, P., and Monteserín, V., 2006, Caracterización geológica de los afloramientos de El Pimpollar, extremo nororiental de la Zona Surportuguesa: Geogaceta, v. 40, p. 123-126.
- Mellado, D., González Clavijo, E., Tornos, F., and Conde, C., 2006, Geología y estructura de la Mina de Río Tinto (Faja Pirítica Ibérica, España): Geogaceta, v. 40, p. 231-234.

- Sánchez España, J., Velasco, F., Boyce, A., and Tornos, F., 2006, Reply to the comments by Marignac and Cathelineau on the paper by Sánchez-España et al.: Source and evolution of ore-forming hydrothermal fluids in the northern Iberian Pyrite Belt massive sulphide deposits (SW Spain): evidence from fluid inclusions and stable isotopes (Mineralium Deposita 38: 519-537): Mineralium Deposita, v. 30, p. 749-754.
- Solomon, M., Tornos, F., Large, R. R., Badham, J. N. P., Both, R. A., and Zaw, K., 2004, Zn-Pb-Cu volcanic-hosted massive sulphide deposits: criteria for distinguishing brine pool- from black smoker-type sulphide deposition: Ore Geology Reviews, v. 25, p. 259-284.
- Tornos, F., 2006, Environment of formation and styles of volcanogenic massive sulfides: The Iberian Pyrite Belt: Ore Geology Reviews, v. 28, p. 259-307.
- Tornos F, Heinrich CA (2007) Shale basins, sulfur-deficient ore brines, and the formation of exhalative base metal deposits. Chemical Geology, in press.
- Tornos F, Heinrich CA (2007) The relationship between shale and giant massive sulphide deposits: More than a spatial coincidence? In: Andrew CJea (ed) Digging Deeper. Proceedings of the 9th Biennial SGA Meeting IAEG, Dublin, pp 1053-1056.
- Tornos F, Solomon M, Conde C, Spiro BF (2007) Formation of the Tharsis massive sulfide deposit, Iberian Pyrite Belt: geological, lithogeochemical and stable isotope evidence for deposition in a brine pool. Economic Geology in press. (no incluido)
- Velasco, F., and Tornos, F., 2006, Los sulfuros masivos (Cu-Zn-Au) de Lomero-Poyatos (Faja Pirítica Ibérica): Encuadre geológico, alteración hidrotermal y removilización: Macla, v. 6, p. 489-492.

4: Transpressional tectonics, lower crust decoupling and intrusion of deep mafic sills: A model for the unusual metallogenesis of SW Iberia

Fernando Tornos [a,*], César Casquet [b], Jorge M.R.S. Relvas [c]

[a] *Instituto Geológico y Minero de España, c/Azafranal 48, 37002 Salamanca, Spain*
[b] *Departamento de Petrología, Facultad de Ciencias Geológicas, Universidad Complutense de Madrid, 28040 Madrid, Spain*
[c] *CREMINER/Departamento de Geologia, Faculdade de Ciências da Universidade de Lisboa, Edifício C6, Piso 4, Campo Grande,
1749-016 Lisboa, Portugal*

Abstract

SW Iberia is interpreted as an accretionary magmatic belt resulting from the collision between the South Portuguese Zone and the autochthonous Iberian terrane in Variscan times (350 to 330 Ma). In the South Portuguese Zone, pull-apart basins were filled with a thick sequence of siliciclastic sediments and bimodal volcanic rocks that host the giant massive sulphides of the Iberian Pyrite Belt. Massive sulphides precipitated in highly efficient geochemical traps where metal-rich but sulphur-depleted fluids of dominant basinal derivation mixed with sulphide-rich modified seawater. Massive sulphides formed either in porous/reactive volcanic rocks by sub-seafloor replacement, or in dark shale by replacement of mud or by exhalation within confined basins with high biogenic activity. Crustal thinning and magma intrusion were responsible for thermal maturation and dehydration of sedimentary rocks, while magmatic fluids probably had a minor influence on the observed geochemical signatures.

The Ossa Morena Zone was a coeval calc-alkaline magmatic arc. It was the site for unusual mineralization, particularly magmatic Ni–(Cu) and hydrothermal Fe-oxide–Cu–Au ores (IOCG). Most magmatism and mineralization took place at local extensional zones along first-order strike-slip faults and thrusts. The source of magmas and IOCG and Ni–(Cu) deposits probably lay in a large mafic–ultramafic layered complex intruded along a detachment at the boundary between the upper and lower crust. Here, juvenile melts extensively interacted with low-grade metamorphic rocks, inducing widespread anatexis, magma contamination and further exsolution of hydrothermal fluids. Hypersaline fluids ($\delta^{18}O_{fluid} > 5.4$‰ to 12‰) were focused upward into thrusts and faults, leading to early magnetite mineralization associated with a high-temperature (>500 °C) albite–actinolite–salite alteration and subsequent copper–gold-bearing vein mineralization at somewhat lower temperatures. Assimilation of sediments by magmas led in turn to the formation of immiscible sulphide and silicate melts that accumulated in the footwall of the layered igneous complex. Further injection of both basic and sulphide-rich magmas into the upper crust led to the formation of Ni–(Cu)-rich breccia pipes.

---

* Corresponding author.
  E-mail address: f.tornos@igme.es (F. Tornos).

Younger (330 to 280 Ma?) peraluminous granitoids probably reflect the slow ascent of relatively dry and viscous magmas formed by contact anatexis. These granitoids have W–(Sn)- and Pb–Zn-related mineralization that also shows geochemical evidence of major mantle–crust interaction. Late epithermal Hg–(Cu–Sb) and Pb–Zn–(Ag) mineralization was driven by convective hydrothermal cells resulting from the high geothermal gradients that were set up in the zone by intrusion of the layered igneous complex. In all cases, most of the sulphur seems to have been derived from leaching of the host sedimentary rocks ($\delta^{34}S = 7‰$ to 20‰) with only limited mixing with sulphur of magmatic derivation.

The metallogenic characteristics of the two terranes are quite different. In the Ossa Morena Zone, juvenile magmatism played a major role as the source of metals, and controlled the styles of mineralization. In the South Portuguese Zone, magmas only acted as heat sources but seem to have had no major influence as sources of metals and fluids, which are dominated by crustal signatures. Most of the magmatic and tectonic features related to the Variscan subduction and collision seem to be masked by those resulting from transpressional deformation and deep mafic intrusion, which led to the development of a metallogenic belt with little resemblance to other accretionary magmatic arcs.

1. Introduction

Subduction-related orogens and accretionary plate margins are ore-forming environments of prime importance. Tectonic, magmatic and hydrothermal processes related to the subduction of an oceanic slab under an active margin and subsequent arc–continent or continent–continent collision are responsible for the formation of a wide variety of ore deposits, commonly related to the extrusion of large volumes of subaerial calc-alkaline andesite in the overriding plate. Such processes are well known in the Late Phanerozoic accretionary orogenic belts of the Pacific Ocean, Asia or eastern Europe (e.g., Mitchell, 1992; Camus and Dilles, 2001; Heinrich and Neubauer, 2002; Zengqian et al., 2003). Localized extensional zones were the preferred loci of ore deposits, including a wide spectrum of porphyry-related and epithermal systems, replacements (including skarns), veins and volcanogenic massive sulphides. However, not all collisional margins behave in the same way and less common ore-forming processes can prevail that depart from the well-known simple subduction/collision model.

Recent geological, geochronological and geophysical results in both the Ossa Morena (OMZ) and South Portuguese (SPZ) zones of SW Iberia show that the contrasting styles of mineralization found on both sides of the Variscan suture were broadly synchronous and formed in response to a unique tectonic evolution. In this paper, we examine the unusual features of this accretionary magmatic belt in which transpressional deformation and related magma emplacement controlled the tectonic, magmatic and hydrothermal evolution, masking other geological features typically related to subduction/collision and obduction.

2. The geological evolution of SW Iberia: tectonic framework

The Ossa Morena Zone is a continental Proterozoic terrane (Nd T_{DM} ages 1.4 to 2.0 Ga; Nägler, 1990) that was perhaps accreted to the autochthonous Iberian terrane during the Cadomian Orogeny at the Neoproterozoic to Cambrian transition (Abalos et al., 1991; Ochsner, 1993). During Variscan times, oblique collision of Gondwana with an exotic terrane, probably Laurentia (Silva et al., 1990; Quesada et al., 1991; Eguíluz et al., 2000; Matte, 2001), led to the amalgamation of the Iberian Variscan massif. The more currently accepted models propose that northdipping subduction of an intervening ocean was followed by ophiolite obduction and continental collision. Subduction and obduction were apparently proceeding in Early to Middle Devonian times, coming to an end in the Late Devonian to Late Visean (Silva et al., 1990; Oliveira and Quesada, 1998; Eguíluz et al., 2000). This old suture between the two continental terranes, the OMZ and SPZ, is now defined by the oceanic Pulo de Lobo terrane, the Acebuches-Beja ophiolite and the South Iberian

shear zone (Fig. 1). However, others claim that amalgamation of the Ossa Morena terrane to mainland Gondwana took place in Variscan times and that in consequence the Coimbra-Córdoba shear zone is the Variscan suture (e.g., Matte, 1986).

2.1. The Ossa Morena Zone

Pre-Variscan rocks of the Ossa Morena Zone consist of a thick sequence of dark shale with minor quartzarenite and amphibolite (Serie Negra, Neoproterozoic) that occurs in the cores of large anticlines. This is unconformably overlain by a thick calc-alkaline volcanic sequence and sedimentary rocks, formed in a Cadomian volcanic arc. Above them there are limestone, bimodal volcanic rocks and shale deposited in an extensional setting (Early to Middle Cambrian). Siliciclastic and calcareous rocks of Ordovician to Early Devonian age crop out in the core of major synclines (Fig. 1).

A key feature of the OMZ is the widespread evidence of left-lateral deformation during Variscan times, probably because of lateral escape promoted by orthogonal indentation of northern Iberia during collision (Silva et al., 1990). Transpressional strain within the OMZ was partitioned between NNE and SSW southward-verging fold-and-thrust zones, where orthogonal shortening predominated, and slightly younger strike-slip faults, which accommodated the lateral component of strain. Palaeogeographic reconstructions suggest that the minimum left-lateral displacement was in excess of 70 km, most of it concentrated along the Coimbra-Cordoba shear zone (Burg et al., 1981; Apalategui et al., 1990).

Upper crustal, subvolcanic I-type, high-K calc-alkaline plutons are widespread in the area and record crystallization ages between 352 ± 4 Ma (Early Tournaisian) and 332 ± 3 Ma (Visean) (Dallmeyer et al., 1995; Casquet et al., 1998; Montero et al., 2000). They are generally zoned and mainly made up of diorite, tonalite and granodiorite with minor gabbroic and noritic cumulates. This magmatism is well preserved in the Beja area, the Olivenza-Monesterio anticline and near the northern boundary of the OMZ (Figs. 1 and 2). A more restricted younger generation of peraluminous granites, ranging in composition from granodiorite to granite, is found as a few small granitic cupolas and dyke swarms, a feature which

contrasts with the widespread metaluminous magmatism of the area and the abundance of peraluminous granitoids in the Central Iberian Zone (Fig. 1). Variscan sedimentary rocks are scarce and located in minor pull-apart basins. They consist of continental to shallow marine siliciclastic sediments with minor limestone and volcanic rocks.

The recent IBERSEIS deep seismic reflection profile has shown that a 1- to 5-km-thick high velocity zone exists at about 10 to 15 km depth, where the large thrusts are rooted (Simancas et al., 2003). This zone is also characterized by high conductivities (Pous et al., 2004). From this evidence, along with complementary magnetic, gravity and geochemical information, Simancas et al. (2003) have suggested that the mid-crustal seismic reflector represents a large but discontinuous sheet of layered mafic–ultramafic rocks of Variscan age (IRB, IBERSEIS Reflective Body). A conservative estimate suggests dimensions of about $75 \times 70 \times 2.5$ to 5 km. A minimum volume of 15,000 to 30,000 km^3 can be inferred for such an intrusion, which thus becomes one of the largest layered mafic–ultramafic igneous complexes in the world, between the Bushveld (67,000 km^3) and Kunene (15,000 km^3) complexes (Pirajno, 2000). The Moho discontinuity, at about 30 km depth, is flat and no remnants of a subduction zone or orogenic roots have been preserved.

The geophysical and geological evidence also suggest that the IRB crops out, although tectonically disrupted, in the Aracena Massif, the southernmost part of the OMZ (Simancas et al., 2003). The Aracena Massif is a complex geological domain where gneiss, volcanic and carbonate rocks of Late Neoproterozoic to Cambrian age were intruded by several generations of igneous rocks (Fig. 1). The contacts with both the SPZ and the central OMZ are large faults (Crespo, 1991). Regional surveys and recent mapping by Rio Narcea Recursos (personal communication, 2003) in the Aracena massif show that significant amounts of Variscan mafic–ultramafic rocks intrude high-grade metamorphic rocks consisting of migmatite, pelitic and calc-silicate gneiss, marble and amphibolite. The mafic–ultramafic rocks, grouped as diorite in previous studies, include several 10- to 300-m-thick subhorizontal lenses made up of heterogeneous ultramafic cumulates, mostly peridotite and pyroxenite, norite and gabbronorite with disseminated to podiform
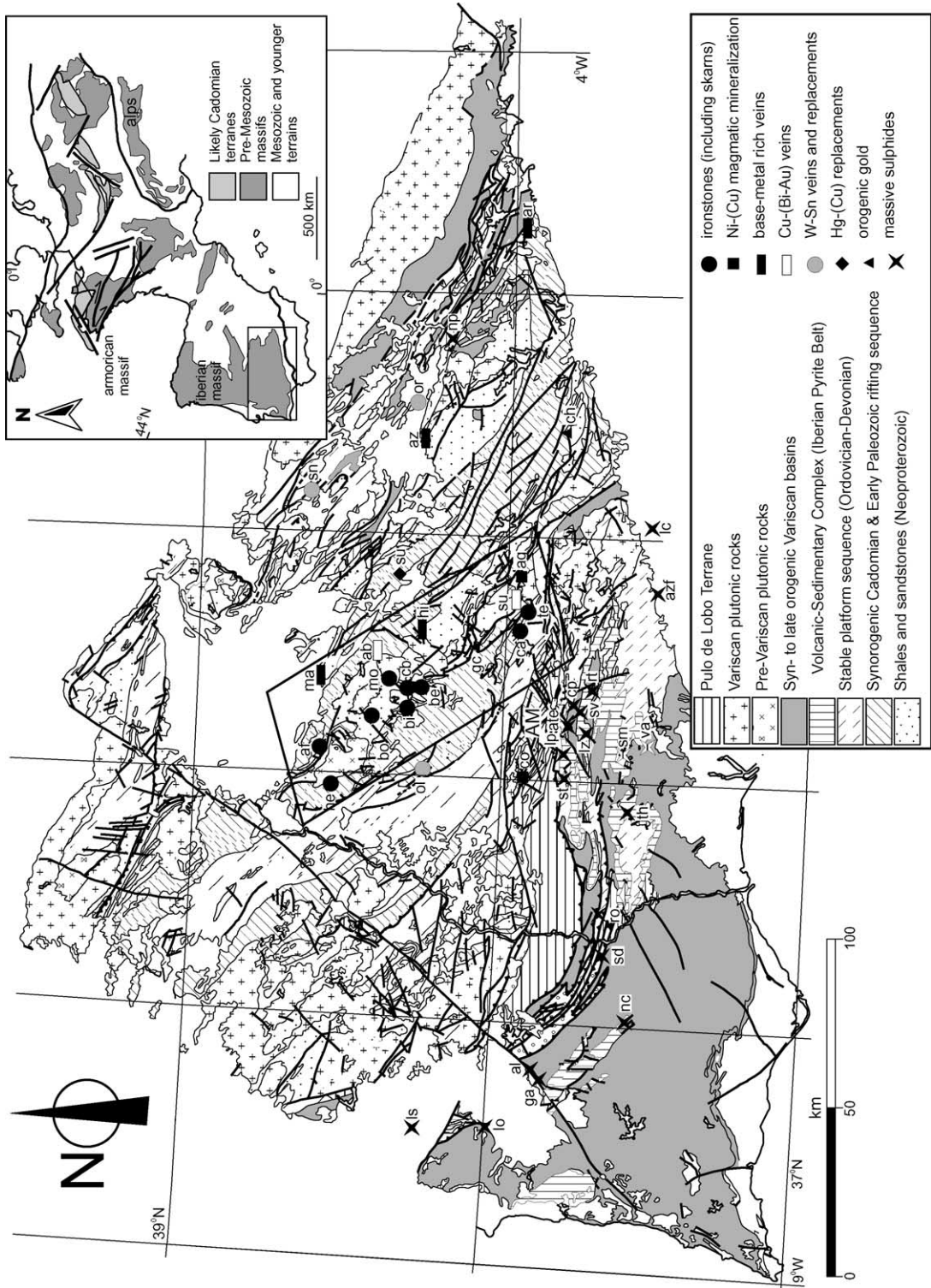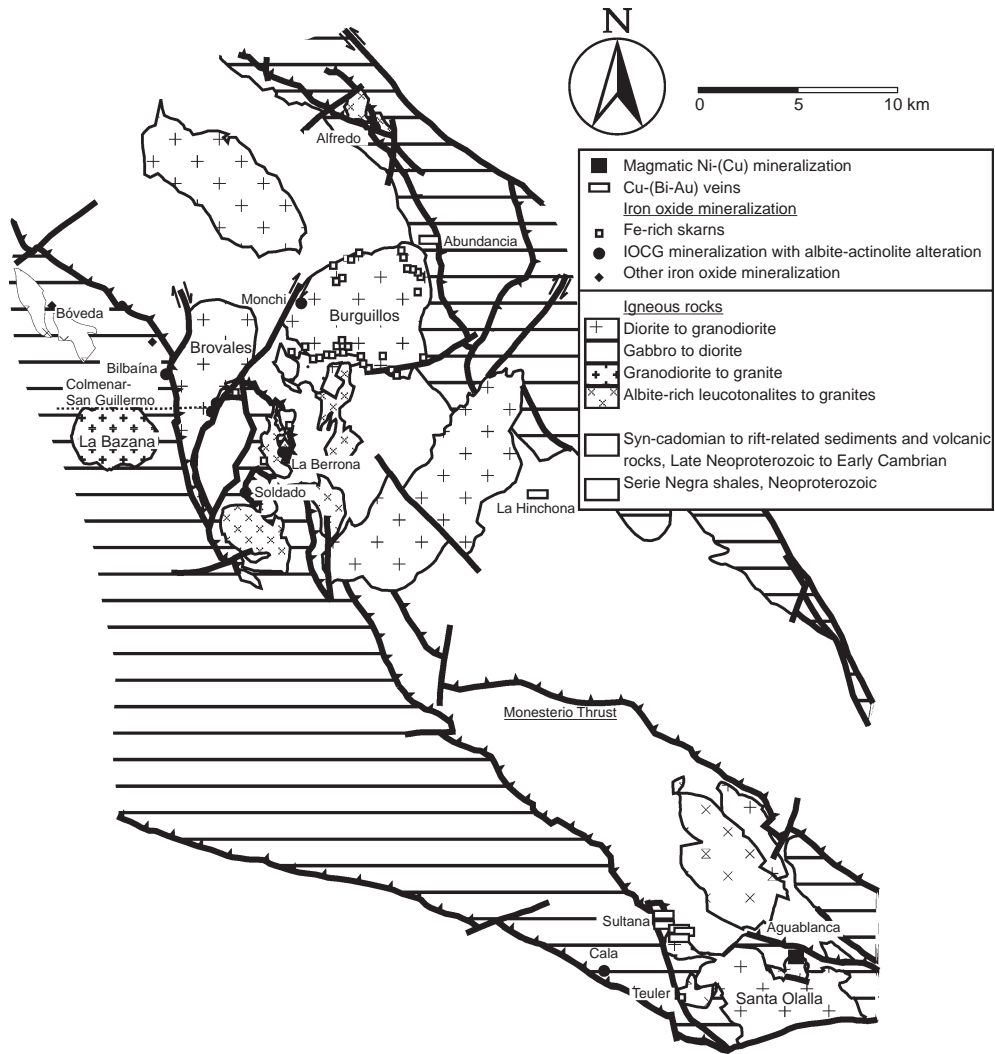
Fig. 2. Detailed geological map of the Olivenza-Monesterio structure of the Ossa Morena Zone showing the relationship between ironstones, Cu–(Au–Bi) veins, Ni–(Cu) magmatic mineralization and main structural and plutonic features of Variscan age. Modified from Tornos and Casquet (2005).

semi-massive sulphides, including pyrrhotite, pentlandite and chalcopyrite. These igneous rocks show widespread evidence of sediment–magma interaction including the presence of partially digested enclaves of the host anatexite, marble and pelitic and calc-silicate hornfels, in some places showing extensive

Fig. 1. Geological map of the southern Iberian Variscan Belt showing the location of the intrusions and ore deposits described in the text. Inset shows the location of SW Iberia in the Variscan Belt of Europe. Major ore deposits: ab: Abundancia; af: Alfredo; ag: Aguablanca; al: Aljustrel; ate: Aguas Teñidas Este; azf: Aznalcóllar-Los Frailes; az: Azuaga ore field; be: La Berrona; bi: Bilbaína; bo: Bóveda; ca: Cala; cb: Colmenar-Santa Bárbara; ch: Constantina-Huéznar; co: Cortegana; cp: Concepción-San Platón; ga: Gaviao; gc: Guijarro-Chocolatero; he: Herrerías; hi: La Hinchona; lc: Las Cruces; lo: Lousal; lp: Lomero Poyatos; ls: Lagoa Salgada; lz: La Zarza; ma: Santa Marta; mo: Monchi; nc: Neves Corvo; np: Nava Paredón; ol: Oliva; or: Oropesa; ro: Romanera; rt: Rio Tinto; sd: Sao Domingos; sm: Sotiel Migollas; sn: San Nicolás; st: San Telmo; su: Sultana; sv: Soloviejo; te: Teuler; th: Tharsis; va: Masa Valverde. AM: Aracena Massif. The box shows the location of the Olivenza-Monesterio structure, enlarged in Fig. 2.

development of skarn assemblages. The presence of abundant graphite and spinel in the igneous rocks is also indicative of the assimilation of large amounts of host rocks.

The Aracena Massif has been affected by high-temperature/low-pressure metamorphism, having tightly spaced isograds ranging from lower greenschist facies in the outer zone to widespread anatexis close to where the mafic–ultramafic rocks crop out (Crespo, 1991). The conditions (>920 to 1000 °C; 4 to 6 kb) deduced by Patiño Douce et al. (1997) and Díaz Azpiroz et al. (2004) are consistent with contact metamorphism produced by the intrusion of a large mafic pluton at intermediate crustal depths, leading to widespread anatexis of the host rocks. The estimated present depth to the IRB igneous complex, i.e., 15 km, is compatible with the metamorphic pressure estimate if account is taken of post-Variscan erosion equivalent to 1.5 kb ($\approx$ 5 km). ^{39}Ar/^{40}Ar ages of metamorphism range from 342.6 ± 0.6 to 328 ± 1.2 Ma (Dallmeyer et al., 1993; Castro et al., 1999; Fig. 3) and are coincident within error with those of the Variscan metaluminous magmatism.

2.2. The South Portuguese Zone

The South Portuguese Zone record the Early Devonian to Late Carboniferous geodynamic evolution associated with the accretion of this terrane to the Iberian Massif (e.g., Silva et al., 1990; Quesada et al., 1991).

The exposed stratigraphic column of the Iberian Pyrite Belt (IPB) begins with a thick unit (>2000 m; base unknown; Alonso, personal communication) composed of siliciclastic meta-sedimentary rocks deposited on a shallow marine platform (shale, quartz-wacke and quartzarenite; Phyllite–Quartzite Group; Fig. 1). In places, towards the top of the unit, these passive margin homogeneous characteristics gave way to sedimentary facies that testify collapse and fragmentation of the platform (sandstone bars, high-energy debris flows, limestone lenses; Moreno et al., 1996). This change marked the development of the basins where deposition of the Volcanic-Sedimentary (VS) complex took place during the following 20 to 30 million years (VS Complex of Fig. 1; Late Famennian to Middle Visean; Oliveira, 1990). Finally, the filling of the basin is represented by a synorogenic turbidite sequence up to 3000 m thick, derived par-

tially from the Ossa Morena Zone, which crops out in vast areas of the belt (Culm Group; late Visean to middle-late Pennsylvanian; Oliveira, 1990; Moreno, 1993).

The Variscan magmatism in the IPB consists of a bimodal, predominantly felsic suite that includes alkali to tholeiitic basalt, and low-Al–high-Nb calc-alkaline dacite to rhyolite. Andesite is scarce, mostly restricted to the northernmost part of the belt (Munhá, 1983). Felsic and mafic rocks evolved separately, and are not related by fractionation. The basic magmas could have been generated in the upper mantle as a result of decompression related to transcurrent tectonism (Munhá, 1983; Mitjavila et al., 1997; Solomon and Quesada, 2003). Petrogenetic modelling has shown that the felsic rocks could only have been generated by crustal melting at low pressures, which requires high heat flow and thus crustal thinning, magma underplating and/or significant emplacement of primary magmas within the crust (Munhá, 1983; Mitjavila et al., 1997; Rosa et al., 2004a,b).

The VS Complex is up to 1300 m thick, but seldom exceeds 600 m (Leistel et al., 1998b). It is characterized by rapidly changing lateral facies variations that conform with the strongly compartmentalized geometry of the basins (Oliveira, 1990). Volcanic facies include both intrusive and extrusive members of either coherent or volcaniclastic nature, but their relative proportions remain debatable. Some authors have emphasized the importance of sills as the main volcanic style within the IPB (Boulter, 1993; Soriano and Martí, 1999) while others maintain that sills are only predominant in restricted areas, the bulk of the volcanic edifice being dominated by felsic dome-crypto-dome-hyaloclastite complexes and thick pumice-rich and crystal-rich mass flows (Tornos et al., 2002; Rosa et al., 2004a,b; Tornos, 2005). Mafic lava flows and dykes are also common members of the volcanic architecture of the IPB. All these rocks occur intimately interbedded or interfingered with sequences of variable thickness of shale, sandstone and chemical precipitates such as massive sulphide, manganese oxide, and silica-rich rocks, chert and jasper.

Exposures of plutonic rocks are concentrated in the northeastern part of the belt, forming the Sierra Norte batholith; they are extremely rare in the remainder of the province. Their relationships with the adjacent volcano-sedimentary rocks are obscure due to the
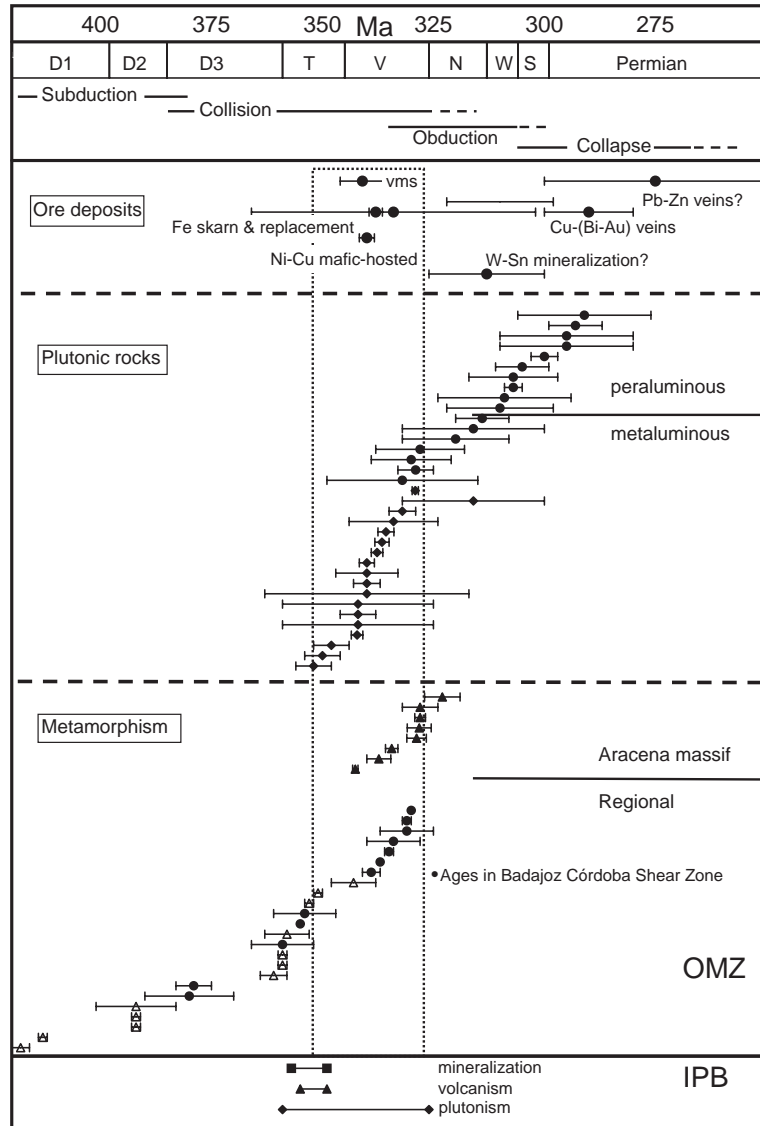
Fig. 3. Chronological relationships between Variscan magmatism, deformation and mineralization in the Ossa Morena Zone and Iberian Pyrite Belt. The data are mainly from compilations of Serrano Pinto et al. (1988), Schäfer (1990), Dallmeyer and Quesada (1992), Ochsner (1993), Ordoñez (1998), Castro et al. (1999), Montero et al. (2000), Casquet et al. (1998), Darbyshire et al. (1998), Tornos and Velasco (2002) and Table 1. The dotted box delimits the likely timing of intrusion of the deep mafic–ultramafic complex. The tectonic evolution is only an estimate and is based on the geological evolution of the Ossa Morena Zone.

complex tectonism. Some authors have postulated that the VS Complex and, at least part, of the Sierra Norte batholith are coeval and belong to the same magmatic suite, the granitoids representing the roots of the VS Complex (Schutz et al., 1987; Thieblemont et al., 1998). Other authors have argued that these relationships are equivocal, interpreting the intrusive rocks as

younger than the volcanism (e.g., Simancas, 1983). However, recent, very detailed and precise U–Pb ages are consistent with the first hypothesis (Barrie et al., 2002; Dunning et al., 2002).

The basement of the IPB is unexposed. Geophysical and radiogenic isotopic evidence suggests that it was limited at a depth of 10 to 15 km by a major mid-

Table 1
Representative Variscan ore deposits in SW Iberia

Deposit(s)	Age (Ma)	Morphology	Host rocks	Structural setting	Fluids and P/T	Radiogenic isotope	Comments
Ossa Morena Zone							
Aguablanca Cortegana, Beja Ni–(Cu–PGE)	337 ± 4	Subvertical breccia pipe with ultramafic fragments	Quartz-diorite, gabbro and gabbronorite	Intruded within a pull-apart structure near a major fault	$T = 1200$ to 1400 °C\n\nDepth $= 1$ to 3 km	$^7Sr/^{86}Sr = 0.7082$ to 0.71\n$\varepsilon Nd = -7.5$ to -6\nCP $= 0.51$ to 0.62\n$\delta^{34}S = 7.4‰$	Pervasive late hydrothermal alteration with widespread albite+actinolite+ scapolite
Monchi Fe–(U–REE)	338 ± 1.5\n\n$328 \pm 3$	Stratabound, lensoidal	Enclaves of limestone, dolostone, pelitic hornfels in tonalite, quartz-diorite	N–S trending shear zone	$T > 600$ °C\n\nDepth $= 1$ to 3 km\n$\delta^{18}O_{fluid} > 12‰$\nHypersaline brines	$^{87}Sr/^{86}Sr = 0.7109$ to 0.7121\n$\varepsilon Nd = -5.8$ to -4.8	B-rich deposit pre-dating magnesian and calcic skarns, associated with potassic alteration of host rocks
Colmenar-Sta Bárbara Cala, Herrerías Fe–(Cu)	334 ± 32	Stratabound	Tectonic contact between tonalite, calc-silicate rocks, schist and marble	N–S trending shear zone	$T > 500$ °C\n\nDepth $= 1$ to 3 km\n$\delta^{18}O_{fluid}$ 9‰ to 12‰	$^{87}Sr/^{86}Sr = 0.7093$ to 0.7104\n$\varepsilon Nd = -8.3$ to -4.7\nCP? 0.50\n$\delta^{34}S = 15.9‰$ to $19.2‰$	Pervasive albite–actinolite alteration pre-dating the skarns
Several skarns in roof pendants in Burguillos stock, Teuler Fe–(Cu)	350 to 330	Stratabound	Carbonatic rocks adjacent to intermediate plutons	Roof pendants and margins of plutons, locally along shear zones	$T = 400$ to 600 °C\n\nDepth $= 1$ to 3 km\n$\delta^{18}O = 10.11‰$ (early) $3‰$ to $8‰$ (late)	$^{87}Sr/^{86}Sr = 0.712$ to 0.7203\n$\varepsilon Nd = -8.0$ to -3.4\n$\delta^{34}S = 14.0‰$ to $14.7‰$	Potassic alteration on the adjacent granitoids
La Berrona, Alfredo Fe		Stratabound to irregular	Shale and carbonatic rocks adjacent to albititic granite	Regional shear zone?			Pervasive albite–actinolite alteration of igneous and sedimentary rocks
Sultana Cu–(Au–Bi)	313 ± 13	Low-dipping veins	Tonalite and host rocks, calc-silicate rocks and shale	Short extensional faults	$T = 290$ to $420°$\nDepth $= 3$ to 4 km\nImmiscibility fluid $> 30\%$ eq. wt. NaCl, CO_2-bearing (XCO_2 0.04)\n$\delta^{18}O_{fluid}$ 4.7‰ to 7.5‰	$^{87}Sr/^{86}Sr$ 0.7100\nCP $= 0.66$ to 0.69\n\n\n\n$\delta^{34}S = 11‰$ to $17‰$	Tourmaline, ankerite, albite and sericite in selvages
Burguillos, Au	330 ± 9	Quartz veins	Leucogranite	Tensional structures related to N–S shearing	Prof $= 3.5$ km\n$H_2O$–CO_2–NaCl–Kcl–$CaCl_2$–$FeCl_2$ moderate to high saline brines\n$\delta^{18}O_{fluid}$ 9.5‰ to 11.2‰		Pervasive albitization
San Nicolás, Oliva W–(Sn–Bi–Au)		Veins and disseminations in greisens above a granitic cupola	Shale overlying granite	Small pull-apart structure?	$T = 170$ to 320 °C\nDepth < 0.5 km\nImmiscibility fluid H_2O–CO_2–CH_4–NaCl (< 9 wt.% NaCl)	CP $= 0.56$	Pervasive greisenization of granitic cupola

Pb–Zn veins in Badajoz Córdoba Shear Zone (e.g. Azuaga)		Short and thick quartz-carbonate veins crosscutting shear zone	Gneiss, shale	Along tensional planes of the Badajoz-Córdoba Shear Zone	T_h < 200 °C	CP=0.53 to 0.63, 0.43 to 0.51 near granites	Potassification, sericitization, carbonatization, hydrothermal breccias. Epithermal environment
Nava Paredón Zn–(Cu–Pb)	341 ± 5	Stratabound	Contact between devitrified massive rhyolite and overlying polymictic mass flows	Pull-apart Carboniferous basin, adjacent to fault scarp		$^{87}Sr/^{86}Sr$=0.7080 to 0.7108 CP=0.43 to 0.52 $\delta^{34}S$=−0.2‰ to 6.5‰	Sub-seafloor replacement associated with pervasive sericitization and silicification
Usagre Hg–(Cu–Sb)		Stratabound to discordant	Limestone interbedded with shale	Controlled by strike-slip WNW–ESE regional faults	NaCl–H_2O 19 to 24 wt.% T_h=250 to 320 °C		Pervasive silicification of limestones. Dykes of microgabbro intruded along the same structures
Oropesa Sn–(Cu)		Vein-like, stratabound replacements	Shale, sandstone, limestone	Replacement of sediments in pull-apart basins		CP=0.69 to 0.71	Silicification of sediments
Guijarro-Chocolatero Constantina-Huéznar Au	413 ± 1 to 359 ± 1[a]	Veins and replacements	Volcanic and volcaniclastic rocks, sandstone	Major WNW–ESE shear bands and thrusts			Silicification
South Portuguese Zone							
Tharsis, Lousal	359	Stratiform orebodies	Grey shale	Third-order, pull-apart basins, adjacent to large strike-slip faults	NaCl–H_2O 3 to 12 wt.% T=60 to 350 °C	$^{7}Sr/^{86}Sr$=0.7073 to 0.7202 CP=0.60 to 78 $\delta^{34}S$=−33.2‰ to 20.7‰	Stratabound chloritization of underlying shales
Neves Corvo, Aznalcóllar-Los Frailes, Las Cruces, Sotiel-Migollas, Valverde	359	Stratiform to stratabound orebodies	Grey shale intercalated with felsic volcanic and volcaniclastic rocks			Neves Corvo has different CP values (0.65 to 0.82) and ε Nd=−11.3 to −0.4	Choloritization of underlying shales, cholorotization–sericitization of felsic volcanic rocks
Aguas Teñidas Este, La Zarza		Irregular to lensoidal	Volcaniclastic aprons or marginal facies of dacitic (crypto)-domes	Locally adjacent to synsedimentary faults			Cone-shaped chloritization–sericitization of felsic volcanic rocks. Silica-rich core
Aljustrel, Concepción, San Platón, Lagoa Salgada?		Sheet-like, stratabound to lensoidal	Pumice- or glass-rich mass flows adjacent to felsic domes				Stratabound to irregular sericitization with internal chloritization
Rio Tinto	345	Stratiform to lensoidal	Grey shale and dacitic sills				Large sericitic alteration with minor chloritization on mafic rocks, shale and near faults in felsic rocks

[a] Age of metamorphism (Dallmeyer et al., 1993). References in the text. CP is Crustal Proportion calculated following Carr et al. (1995) for the geological or assumed age of the mineralization.

crustal discontinuity (Simancas et al., 2003), and might consist of a continental Precambrian sequence with model ages younger than 1.2 Ga (Mitjavila et al., 1997). The IBERSEIS survey shows that the SPZ and the OMZ have major differences. The most important are that there is no evidence of the IRB body in the IPB and that the thrusts are clearly rooted on a basal detachment (Simancas et al., 2003).

The widespread massive sulphide deposition that occurred in the IPB during the Late Devonian to Early Carboniferous occurred in a geotectonic setting that is probably dissimilar from that of most other comparable ore-forming systems, both fossil and active, which are commonly associated with subduction-related arc and back-arc geodynamic settings (e.g., Barrie and Hannington, 1999). The IPB is interpreted as an ensialic, pull-apart basin type generated by left-lateral strike-slip faulting induced by oblique collision between the Iberian Massif and the South Portuguese terranes during Variscan times (Silva et al., 1990; Quesada et al., 1991). This elongated, first-order marine basin seems to have been segmented by regional-scale, east–west tectonic structures that define major second-order basins. Within these, local-scale faults, trending E–W to NE–SW, bounded smaller subbasins where most of the exhalative massive sulphide formation took place (Sáez et al., 1999; Tornos et al., 2002). These were characterized by a predominant half-graben geometry and contrasting relative subsidence (Oliveira, 1990; Moreno et al., 1996). Their tectonic boundaries may have had significant control on fluid flow paths, hydrothermal alteration and ore formation (Quesada, 1998; Solomon et al., 2004).

3. Ore deposits in the Ossa Morena Zone

The Ossa Morena Zone hosts a wide variety of ore deposits, with more than 650 mineral occurrences recorded. A feature that makes it different from the adjacent terranes is the presence of mineralization related to both the Cadomian and Variscan cycles as well as, to a lesser extent, the intermediate rifting stage of Early Palaeozoic age.

The Variscan metallogenesis is characterized by the presence of a rather unconventional suite of ore deposits including iron oxide-rich replacements and skarns, vein-like Cu–(Au–Bi), and Ni–(Cu–PGE)

magmatic ores as well as other more common styles such as orogenic gold, syn-metamorphic Cu, Fe and Zn–Pb veins, volcanogenic massive sulphides and granite-related base metal and W–Sn veins and replacements. Other mineralization styles include small epithermal vein-hosted Pb–Zn–(Ag) and replacive Hg–(Cu–Sb) deposits. In general, Variscan deposits within the OMZ can be provisionally grouped as: (a) deposits related to metaluminous plutonism; (b) those associated with peraluminous granodiorite to granite; (c) those related to metamorphic processes; (d) volcano-sedimentary deposits; and (e) epithermal deposits. Only the Variscan mineralization relevant to this work is described below. A more complete review of the metallogenesis of the OMZ can be found in Table 1 and in Tornos et al. (2004a).

3.1. Deposits associated with the metaluminous magmatism

Most of the mineralization spatially related to the metaluminous magmatism is found in the core of the Olivenza-Monesterio structure (Fig. 3). The Agua-blanca Ni–(Cu–PGE) orebody (Box 4-1; Martínez et al., 2005, this volume) occurs within one of the more mafic intrusives, the Aguablanca stock, which is a small intrusion with gabbronorite, gabbro and norite in the core and (quartz-)diorite at the margin. The deposit occurs in several lenses hosted by the more mafic rocks in which the ore occurs as: (a) an inner irregular zone in which the sulphides form large bleb-like masses or cement a breccia with fragments of the host igneous rocks, ultramafic cumulates (mainly pyroxenite) and sedimentary rocks; or (b) as a disseminated or pod-like mineralization in the host gabbro and norite, forming an aureole girdling the breccia.

Tornos et al. (2001) interpreted the formation of the orebody as a two-stage process, involving the early formation of a layered magmatic complex in the middle to upper crust. An immiscible sulphide melt, together with ultramafic cumulates, gravitationally settled to the bottom of the magma chamber. In a second event, tectonic disruption of the partially consolidated layered complex and injection of magmas high into the crust along a pull-apart structure, would have placed fragments of the cumulates in their present location, along with the molten sulphides and the residual gabbro-norite melt. Radiogenic isotope data

(Sr, Nd, Pb) are consistent with the interaction of a parental gabbroic magma with sedimentary rocks, very probably the Serie Negra. The abundance of hercynite and graphite, as well as the abundance of orthopyroxene in the cumulates, the presence of enclaves of metasedimentary rocks and the $\delta^{34}S$ values of the mineralization, all indicate extensive crust–mantle interaction in the source area (Casquet et al., 2001; Tornos and Chiaradia, 2004).

The age of this deposit is constrained by Ar–Ar dating of magmatic intercumular phlogopite (337 ± 4 Ma; Tornos et al., 2004b). Such an age is consistent with an earlier Rb–Sr errorchrone and U–Pb zircon dating of the cogenetic and adjacent Santa Olalla pluton (354 ± 17 Ma; Casquet et al., 2001; 332 ± 3 Ma, Montero et al., 2000) (Fig. 3).

The Aguablanca deposit is similar to magmatic Ni–(Cu) deposits elsewhere, sharing many common features including the relationship with mafic–ultramafic cumulates, the sulphide assemblage with pyrrhotite–chalcopyrite–pentlandite and the widespread mineralogical and geochemical evidence of crust–mantle interaction. What makes Aguablanca different from other deposits is the tectonic setting. Most of the other Ni–(Cu) magmatic deposits are located in Precambrian cratons affected by extensional events (e.g., Naldrett, 1999) and only a few are located in orogenic belts (Papunen, 2003; Shengao et al., 2003).

Probably coeval and also related to mafic–ultramafic rocks are other magmatic-hosted mineral occurrences in the Aracena Massif (Rio Narcea, personal communication, 2003) and the Beja Gabbroic Complex (Mateus et al., 2001) in which Fe–Ti–V oxide concentrations and Cu–(Ni) disseminations are hosted by Variscan olivine-bearing gabbro, troctolite and quartz-diorite with ages spanning that of the Aguablanca ore body (352 to 338 Ma; Dallmeyer et al., 1993).

Some magnetite ore bodies occur as stratiform lenses interbedded with Late Neoproterozoic to Cambrian volcanic rocks. They show sedimentary features and have been interpreted as low-temperature shallow replacive or exhalative deposits in third -order oxic basins (Tornos et al., 2004a). These deposits have been dated at ca. 500 Ma (Darbyshire et al., 1998), an age synchronous with that of the early Palaeozoic rift-related igneous activity (508 to 500 Ma; Galindo et al., 1990; Ochsner, 1993).

However, most Fe-oxide-rich deposits (see Box 4-2; Tornos et al., 2005, this volume) are made up of massive to banded magnetite replacing a wide variety of rocks, including limestone and dolostone, calc-silicate hornfels, metavolcanics, granitoids and, to a lesser extent, schist of Late Neoproterozoic to Early Cambrian age. These ore bodies occur as: (a) replacements within or near, N–S and WNW–ESE regional thrusts and strike-slip faults (Figs. 1 and 2); (b) replacements bordering epizonal albitized leucotonalite or strongly altered tonalite to granodiorite; and (c) skarns. The three styles can coexist in the same area. The total tonnage of these iron oxide deposits is about 150 to 200 Mt.

The ore occurs as stratabound to irregular bodies with minor breccias and veins that are enclosed in a halo of hydrothermal alteration. The alteration assemblage includes albite and tremolite–Fe–actinolite and smaller amounts of clinopyroxene (mainly salite), scapolite, biotite and adularia. The metasomatic column shows a zonation with an external aureole of albite and amphibole that is gradually replaced by amphibole and iron oxide and finally by massive iron oxide. However, this sequence is not everywhere present and massive iron oxide can locally replace the host rock. The assemblage includes significant proportions of REE- and U-bearing minerals, such as orthite, uraninite, allanite and monazite. Many of the deposits show an abundance of volatile-rich minerals such as vonsenite, scapolite, fluorite, axinite, tourmaline or apatite (Tornos et al., 2003; Tornos and Casquet, 2005). There is widespread evidence that the alteration was syntectonic and earlier, or synchronous with the intrusion of the adjacent igneous rocks. In the Monchi mine, intergrown mylonitic magnetite and vonsenite occur as enclaves in oriented tonalite, while in the Colmenar mine syntectonic tonalite is coeval with the albite–actinolite–magnetite assemblage. Magnetite dominates over hematite, which is only common at Las Herrerías (Fig. 1). The presence of albite paragenetic with (Fe-)actinolite and calcic pyroxene indicates that this alteration is different from that of conventional skarns, in which the stable plagioclase is Ca-rich and the assemblage includes variable amounts of grandite.

Adjacent to these metaluminous granitoids there are also classical iron calcic and magnesian skarns developed on limestone, dolostone and, only locally, calc-silicate and pelitic hornfels. They are commonly found in roof pendants, mostly in the Burguillos and

Santa Olalla plutons (Casquet and Velasco, 1978; Velasco and Amigó, 1981; Casquet and Tornos, 1991). Endoskarn is uncommon. The skarns do not show major deformation and, when spatially associated, they post-date the albite–actinolite–magnetite alteration. They have a prograde assemblage of grandite, salite–hedenbergite and idocrase replaced by later epidote, (Fe-)actinolite to hornblende and minor magnetite and ilvaite.

The sulphide assemblage is very variable between the different deposits but in almost every case postdated the albite–actinolite–magnetite assemblage and the prograde skarn. It includes pyrite, chalcopyrite, and pyrrhotite with smaller amounts of millerite, cobaltite and other Co–Ni–As–S minerals, bornite and bismuthinite. Copper contents are between 0.2% and 3%. Free gold has only been recorded in some of the deposits and tenors are usually low (<1 g/t, locally up to 7 g/t) but follow the same pattern as the sulphides. Commonly, the more deformed rocks have the higher sulphide and gold contents. Systematically, ironstones found away from shear zones are devoid of sulphides and gold.

Preliminary fluid inclusion and stable isotope data suggest that these orebodies and the related alteration assemblage formed due to the circulation of hot (>500 °C) saline (>25 eq. wt.% NaCl, enriched in $CaCl_2$ and $FeCl_2$) brines of deep origin ($\delta^{18}O$, 9‰ to 12‰). There are only a few radiometric data and so the timing of the mineralization is poorly constrained. Sm–Nd dating of the iron ore at the Colmenar ore body has yielded an age of 334 ± 32 Ma (Sm–Nd, Darbyshire et al., 1998), an age broadly synchronous with that of the host intrusion (340 ± 7 Ma, U–Pb Montero et al., 2000). At Monchi, allanite related to a skarn post-dating the magnetite ore has a concordia U–Pb age of 338 ± 1.5 Ma (Casquet et al., 1998). These ages are similar to that of the metaluminous magmatic suite of the OMZ (350 to 330 Ma) and confirm that both the albite–actinolite–magnetite alteration, the Ni–(Cu) mineralization and the metaluminous magmatism are broadly coeval.

As a whole, these Variscan ironstones share many features with the iron oxide-rich end-member of the IOCG style of mineralization (Hitzman, 2000). Equivalent deposits occur mostly in Archaean to Proterozoic belts such as the Cloncurry district (Mark et al., 2001) or the Fennoscandian Belt (Weihed and Eilu, 2003; Weihed et al., 2005—this volume); only the Andean Belt represents a major IOCG province developed in a Phanerozoic orogen (Marschik and Fontboté, 1996). Outstanding features of this style of ore deposits include the presence of a shallow epigenetic Fe-oxide-rich assemblage related to a high-temperature regional, structurally controlled, volatile-rich Na–Ca or potassic alteration, the presence of saline fluids with high $\delta^{18}O$ signatures and a hydrothermal assemblage rich in REE, Co and U-bearing minerals, as well as the relationship with magmatism of dominantly dioritic composition (Tornos et al., 2003; Tornos and Casquet, 2005).

Spatially unrelated to these deposits but hosted by the same igneous rocks, there are some high grade Cu–(Au–Bi) quartz–ankerite veins with chalcopyrite and pyrite and minor arsenopyrite and pyrrhotite. Some of the lodes have significant amounts of bismuthinite and maldonite, having high gold grades (Sultana Mine, average 15 g/t). The veins show a quartz–albite–tourmaline–sericite–ankerite alteration halo. Again, the stable isotope geochemistry is indicative of the presence of fluids equilibrated with deep sources ($\delta^{18}O$, 5.4‰ to 7.5‰), but formed in the 290 to 380 °C range, at lower temperatures than the iron oxide assemblage. The ore-forming process was probably related to the pulsatile unmixing of complex H_2O–CO_2–CH_4–NaCl–KCl–$CaCl_2$ brines with original salinities above 30 eq. wt.% NaCl (Tornos and Velasco, 2002). Such complex fluids have only been recorded in the Cu–(Au–Bi)-rich stage of IOCG mineralization (Skirrow and Walshe, 2002).

Sulphur isotopes in all these types of mineralization suggest mixing of sulphur derived from igneous and sedimentary sources. The Aguablanca Ni–(Cu) magmatic deposit has values of 7.1‰ to 7.8‰ (Casquet et al., 2001) while the skarns, replacements and veins have more variable and positive values, between 11‰ and 20‰ (Cuervo et al., 1996; Tornos and Velasco, 2002), and probably reflect a larger proportion of sulphur derived from sedimentary sources.

3.2. Deposits associated with the late peraluminous magmatism

As occurs in the other Iberian terranes, late orogenic granodiorite and granite have spatially related W–Sn and Zn–Pb veins. Intra- and peri-granitic tungsten-tin veins and greisens with significant propor-

tions of bismuthinite, fluorite and gold can be found in the apical zones of the intrusions. More eroded plutons only host some structurally controlled greisens with disseminated scheelite (e.g., La Bazana). Little is known about the geochemistry of these deposits. The fluid inclusion data of Gumiel (1988) suggest that the precipitation of wolframite and scheelite took place due to the immiscibility of H_2O–CO_2–CH_4–NaCl (<9 eq. wt.% NaCl) fluids at temperatures of 170 to 320 °C and shallow depth (<0.5 km). Leucogranite crosscutting the Burguillos pluton also hosts some gold occurrences. The gold occurs in sulphide-poor quartz veins within albitized leucogranite. The mineralization is related to the circulation of isotopically high ($\delta^{18}O$ 9.5‰ to 11.20‰) and chemically complex hypersaline H_2O–CO_2–NaCl–KCl–$CaCl_2$–$FeCl_2$ brines (Bachiller et al., 1997). This leucogranite has been dated at 328 ± 10 Ma (K–Ar sericite, Dupont et al., 1981) and 330 ± 9 Ma (Rb–Sr whole rock, Bachiller et al., 1997). The geological relationships suggest that the peraluminous granitoids post-date the metaluminous suite and were intruded along the same structures. In the Monchi area, late leucogranite developed a calcic skarn that crosscuts the earlier iron oxide ore, leading to a remobilization of the magnetite, growth of new sulphides and the precipitation of molybdenite and scheelite, minerals typical of a highly evolved igneous suite.

These rocks are geochemically and chronologically equivalent to those found in the Central Iberian Zone that are intruded along late extensional structures and have been dated between 330 and 281 Ma (Serrano Pinto et al., 1988).

4. Metallogenesis in the Iberian Pyrite Belt

Recent years have been witness to significant advances in the general understanding of the ore forming processes in the IPB (e.g., Leistel et al., 1998b; Relvas et al., 2001; Tornos, 2005), including the geology, structure and geochemistry of the host rocks (e.g., Munhá, 1983; Silva et al., 1990; Mitjavila et al., 1997; Quesada, 1998).

4.1. Environment of formation: volcanic versus shale-hosted massive sulphide deposits

The abundance and size of the IPB massive sulphide deposits stand out among VMS provinces worldwide (Large and Blundell, 2000), consisting of more than 2500 Mt of massive and stringer sulphides, distributed over about 88 deposits, of which 44 exceed 1 Mt, and 8 possess total tonnages in excess of 100 Mt (Fig. 4; Leistel et al., 1998b). The average IPB deposit (30.1 Mt at 0.85% Cu; 1.13% Zn; 0.53%
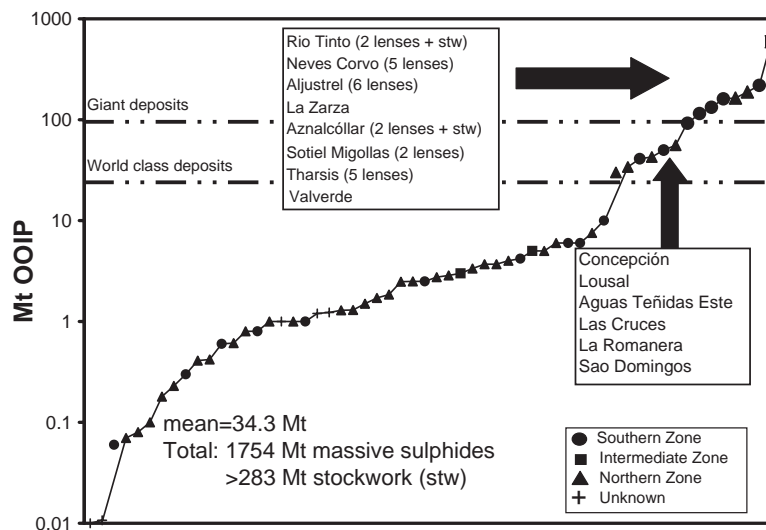

Fig. 4. Cumulative total tonnage diagram of massive sulphide deposits in the Iberian Pyrite Belt. Modified from Tornos (2005). OOIP: Original ore in place (estimated reserves+mined).

Pb; 38.5 g/t Ag; 0.8 g/t Au) is strongly pyritic with locally significant amounts of sphalerite, chalcopyrite and galena. Nevertheless, a few deposits have moderate to high base-metal contents (e.g., Neves Corvo, San Platón, Aguas Teñidas, Las Cruces). Most orebodies consist of clustered sets of two to six orebodies with a sheet-like to lensoid morphology. However, many were tectonically stacked or dismembered. Stratabound (e.g., Neves Corvo; Relvas et al., in press-a) to cone-shaped (Aljustrel; Barriga and Fyfe, 1988) ore-related hydrothermal alteration in felsic volcanic rocks is usually zoned, with a chlorite (sometimes associated with pyrophillite or donbasite) and/or quartz-rich core that is successively enveloped by sericite and paragonite-rich zones (Relvas et al., 1994, in press-a). These can extend for more than 1 km away from the axis of the mineralization (e.g., Barriga and Relvas, 1993; Sánchez España et al., 2000). When hosted by shale or basalt, the chlorite-bearing zone of the stockwork is particularly well developed (Tharsis; Tornos et al., 1998) and the sericitic zones are small or non-existent.

The northern and southern sectors of the belt exhibit considerable differences in the relative proportion of volcanic versus sedimentary rocks in the lithostratigraphic columns of the VS Complex (e.g., Oliveira, 1990; Oliveira and Quesada, 1998; Tornos, 2005). Thick successions of mudstone and sandstone, with or without intercalations of coherent volcanic rocks or volcaniclastic products, characterize the southern sector of the IPB. Conversely, shale is subordinate in the northern domains, where massive felsic domes and cryptodomes, their volcaniclastic aprons and pumice-rich mass flows dominate the VS sequence. In the southern sector, many massive sulphide orebodies are exclusively or predominantly hosted by shale (e.g., Tharsis, Lousal) or, at least, their immediate host rocks include shale units (e.g., Sotiel-Migollas, Neves Corvo, Valverde, Las Cruces, Aznalcóllar-Los Frailes).

The absence of oxidation of the ores, sedimentary dilution and remnants of chimneys or mound-derived breccias make unlikely a seafloor mound model for sulphide deposition in the IPB (Barriga and Fyfe, 1988; Tornos et al., 1998; Solomon et al., 2002; Tornos, 2005). Current models for the genesis of the massive sulphide deposits include sulphide precipitation in brine pools from vented brines on the seafloor (Tornos et al., 1998; Solomon et al., 2002, 2004) and near-seafloor replacement of mud strata below lithified caps of shale or chert (Almodóvar et al., 1998; Relvas, 2000). The mineralization styles recognized also include selective replacement of volcanic rocks by massive sulphides, particularly pumice mass flows, or massive rhyolite/rhyodacite in dome-cryptodome complexes beneath less permeable units or previously formed hydrothermal products. Most of the examples of this style of mineralization come from deposits in the northern sector of the IPB such as Aljustrel, La Zarza, Concepción-San Platón, some orebodies at Rio Tinto, Lomero Poyatos or San Miguel (Tornos, 2005). Relvas et al. (in press-a) have also described similar processes at Neves Corvo.

4.2. Six million years of highly productive hydrothermal activity

All the large, shale-hosted deposits of the southern sector dated so far cluster within a time span of 1 to 2 million years. Their hosting shale invariably yields Strunian ages (latest Famennian) (Pereira et al., 1996; Oliveira et al., 1997, 2004; Gonzalez et al., 2002). Limited palynological data on the host shale and U–Pb dating of dacitic intrusions affected by stockwork mineralization in the Rio Tinto area show that there the Strunian shale is barren and the mineralization is significantly younger, early Late Tournaisian in age (Barrie et al., 2002; Dunning et al., 2002; Rodríguez et al., 2002). Taking into account that some deposits might have formed a little before or after this, it is reasonable to assume that the ore-forming hydrothermal activity in the IPB spanned no more than 6 million years (Barrie et al., 2002; Oliveira et al., 2004).

4.3. Siliceous chemical rocks and low-temperature manganese mineralization

Silica (chert and jasper)-rich horizons and manganese-rich layers are very common in the IPB (Leistel et al., 1998a). They occur as regionally wide strata, often tens of metres thick, and host ca. 5 Mt of high-grade Mn-ores that were extracted from hundreds of small mines. Most of the Mn-rich rocks and the related jasper are hosted by a rather continuous unit of purple shale, which lies above the stratigraphic

level of the massive sulphide (Leistel et al., 1998a). However, discontinuous lenses of chert and jasper may occur in several other positions in the volcano-sedimentary complex. They have long been used as guides to VMS exploration due to the exceptional expression of these hydrothermal facies in the district and their frequent relationship with the orebodies.

The Soloviejo deposit (Huelva, Spain) was probably the most important of these deposits, with in excess of 175,000 t of manganese ores at 35% Mn. The primary manganese mineralization includes Mn-oxide, silicate and carbonate facies. Tectonic remobilization and supergene alteration account for significant Mn-enrichment. The Mn-bearing jasper was interpreted by Jorge (2000) as deposited on the sea-floor from poorly evolved seawater, being probably the result of low-temperature venting of sub-oxic hydrothermal fluids. The banded nature of the ores and their relationship with chert suggest that they should have formed in stratified but oxic basins.

Of particular importance are the silica-rich layers that cap the massive sulphides, either directly or separated from them by several m of shale. The best examples are found in Aljustrel and Tharsis (Barriga and Fyfe, 1988), Neves Corvo (Relvas, 2000), Rio Tinto and Aguas Teñidas Este (Tornos, 2005). The significance of these rocks is controversial. In Aljustrel, Neves Corvo and Tharsis, Barriga and Fyfe (1988) have interpreted them as being related to the regional-scale hydrothermal activity that pre-dated the massive sulphide-forming episode. Other authors, however, consider that these rocks are younger than the massive sulphides and resulted from direct precipitation during the waning hydrothermal activity or are due to the epigenetic, including syn-Variscan, formation of silica and iron oxides (e.g., Leistel et al., 1998a; Tornos, 2005).

5. Discussion

5.1. Geological and geochemical aspects of the metallogenic evolution of the OMZ

5.1.1. Metallogenesis related to a large mafic intrusion?

The geophysical data show that the IRB body can be traced below almost all the OMZ but does not

continue into the adjacent South Portuguese and Central Iberian Zones. Different geological and metallogenic data support the existence of a mid-crustal mafic–ultramafic layered intrusion and its link with the regional ore-forming processes. They include:

(a) The characteristic juvenile lead isotope signatures found in ores within the OMZ (Fig. 5). Lead isotope geochemistry of sulphides of the OMZ shows a remarkable regional $^{207}Pb/^{206}Pb$ depletion that is consistent with a significant input of mantle-derived lead. In the $^{207}Pb/^{206}Pb$ diagram, most of the samples plot below the average crustal and orogenic lead curves (Fig. 5). Only when the host rocks are Precambrian sediments with a long crustal history are there radiogenic signatures (Tornos and Chiaradia, 2004). These lead isotope signatures are interpreted as due to the mixing of lead derived from the host sediments with that scavenged from juvenile, deeply sourced rocks. Since the mantle is strongly depleted in lead relative to the crust, such an imprint can only be produced by the input of large amounts of juvenile lead high into the crust. The retarded lead isotope growth and the relatively low $^{207}Pb/^{204}Pb$ ratios are different from those of the adjacent South Portuguese and Central Iberian Zones, characterized by a long-lived crustal plumbo-tectonic evolution. Even the mineralization related to peraluminous granites, typically generated by crustal melting, shows evidence of significant mantle derivation.

(b) The Sr–Nd isotope geochemistry of the igneous rocks and mineralization that indicate extensive interaction between crustal rocks and deep magmas of mantle derivation at the district scale (Fig. 6; Casquet et al., 2001).

(c) The geophysical data showing the existence of a large subhorizontal conductive reflector at middle crustal depths (Simancas et al., 2003).

(d) The presence of a mafic–ultramafic cumulate complex in the Aracena massif, interpreted as a fragment of middle crust uplifted during late Variscan times.

(e) The existence of a magmatic-hosted Ni–(Cu) deposit (Aguablanca), probably derived from the magmatic–tectonic remobilization of an ear-
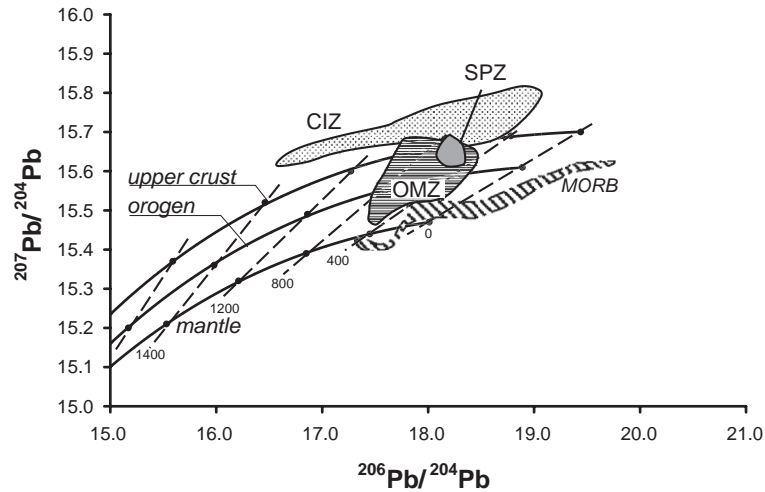
Fig. 5. Lead isotope data of the Variscan mineralization in the Ossa Morena Zone compared with those of the global reference curves (Zartman and Doe, 1981) and the regional data from the Iberian Pyrite Belt of Marcoux (1998), the Central Iberian Zone of Arribas (1993) and Garcia de Madinabeitia (2002) and the Ossa Morena Zone of Tornos and Chiaradia (2004).

lier sulphide immiscible melt deposited in a deep layered magmatic complex.

(f) The presence of iron oxide deposits sharing characteristics of the IOCG style of mineralization. In some places, this style of mineralization

has been interpreted as related to deep mafic intrusions (Oliver et al., 1991; MacCready et al., 1998; Oyárzun et al., 2003).

(g) The presence of a high-temperature shear zone-controlled hydrothermal alteration, that sug-
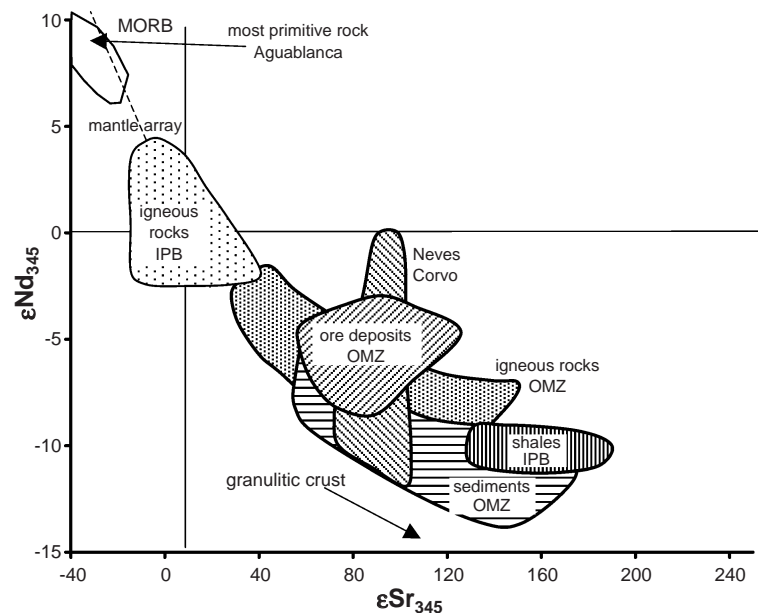

Fig. 6. εNd–εSr plot at 345 Ma of igneous and sedimentary rocks and of ore deposits in the Ossa Morena and South Portuguese Zones. Data from Mitjavila et al. (1997), Darbyshire et al. (1998), Mullane (1998), Casquet et al. (2001), Relvas et al. (2001), Tornos (2005) and unpublished data. The field of MORB is from Fauré (1986).

gests the existence of a deep crustal thermal anomaly.

(h) The existence of high geothermal gradients in the OMZ during late Variscan times, responsible for the formation of epithermal mineralization.

(i) The coincidence in ages of the contact metamorphism in the Aracena massif and the age of the metaluminous suite.

These data allow us to propose a new metallogenic model for the OMZ in which the regional mid-crustal intrusion of mafic rocks played a major role in the mineralization. The intrusion of a discontinuous laminar basaltic complex at the boundary between the upper and lower crust should modify the thermal balance of the area, leading to the formation of a superheated zone and promoting widespread high grade high-temperature/low-pressure metamorphism and anatexis (anorogenic metamorphism of Pirajno, 2000), crust–magma interaction and generation of large volumes of hydrothermal fluids (Tornos and Casquet, 2005). Such a process would produce an overlying gabbro-tonalite-dominated magmatism with a calc-alkaline geochemistry equivalent to that of continental magmatic arcs (Pitcher, 1993).

The location and the wedge-like shape of the intrusion are both consistent with the intrusion being controlled by the incomplete tearing of the lower crust along the major tectonic detachment located in the lower–upper crust boundary (Fig. 7). The intersection of such a sub-horizontal detachment, equivalent to that detected in the deep seismic profiles in both the OMZ and the SPZ (Simancas et al., 2003), with strike-slip sub-vertical faults generated during oblique collision can induce the subhorizontal decoupling of the lower crust with intrusion of mantle-derived magmas along the brittle–ductile transition.

Major Ni–Cu magmatic deposits in rifted intracratonic continental crust are interpreted as having formed in relation to mantle plumes (Norils'k, Naldrett, 1992; Voisey's Bay, Ryan, 2000). The same holds true for IOCG ores, which are also interpreted to be related to mantle plumes (Kiruna, Martinsson, 2003; Cloncurry district, Oliver et al., 1991, Andes, Oyárzun et al., 2003) or at least to the existence of large underlying mafic intrusions (Olympic Dam, Johnson and McCulloch, 1995; Cloncurry, MacCready et al., 1998). Mantle plumes have also been interpreted as having been responsible for the formation of epithermal deposits such as those of the Carlin trend (Oppliger et al., 1997). However, the interpretation of the deep seismic profile and the Ossa Morena geology suggests that mantle plumes are not necessarily the source of the deep mafic–ultramafic intrusion. The lack of evidence of lateral migration of a plume, the absence of a large igneous province with giant alkaline volcanism (LIP, Pirajno, 2000) and the short time span of the magmatism (about 20 to 30 million years) are all arguments that make a mantle plume origin unlikely.

Alternative models required for inducing melting of the upper mantle could have been derived by slab roll-back or by lithosphere delamination, with break-off and sinking of the subducted oceanic crust in the asthenosphere or detachment of a collisionally thickened lithospheric keel (e.g., Levin et al., 2000; Schofield and D'Lemos, 2000; Gutierrez Alonso et al., 2004). However, Castro et al. (1999) have shown that the magmatism in the Aracena Massif could well be related to the subduction of a ridge system.

5.1.2. The origin of the hydrothermal fluids

Hydrothermal fluids related to the iron oxide and Cu–(Au–Bi) mineralization are saline brines having high $\delta^{18}O$ values: those related to the iron oxide were saline, CO_2-poor brines whilst those related to the Cu–(Au–Bi) mineralization also had significant amounts of CO_2 and CH_4. The mineralogical and isotopic compositions show that the fluids were alkaline and hot (>500 °C) during the formation of the Fe-oxide ore, with intermediate redox conditions, and with magnetite stable instead of pyrrhotite and hematite and pyroxene and amphibole stable instead of garnet and epidote. The fluid inclusion and mineral assemblage of the Cu–(Au–Bi) veins indicate that ore forming fluids were more reduced, neutral to mildly acid and cooler (290 to 380 °C). The absence of sulphides in the iron oxide assemblage is interpreted as due to their high temperature of formation.

The radiogenic isotope data (Galindo et al., 1995; Darbyshire et al., 1998; Tornos and Velasco, 2002; Tornos and Chiaradia, 2004) indicate that fluids equilibrated with igneous and/or metamorphic rocks. Fluids equilibrated with mafic rocks or sediments at temperatures of 600 to 800 °C would have $\delta^{18}O$ compositions between 9.3‰ and 11.5‰ while those equilibrated
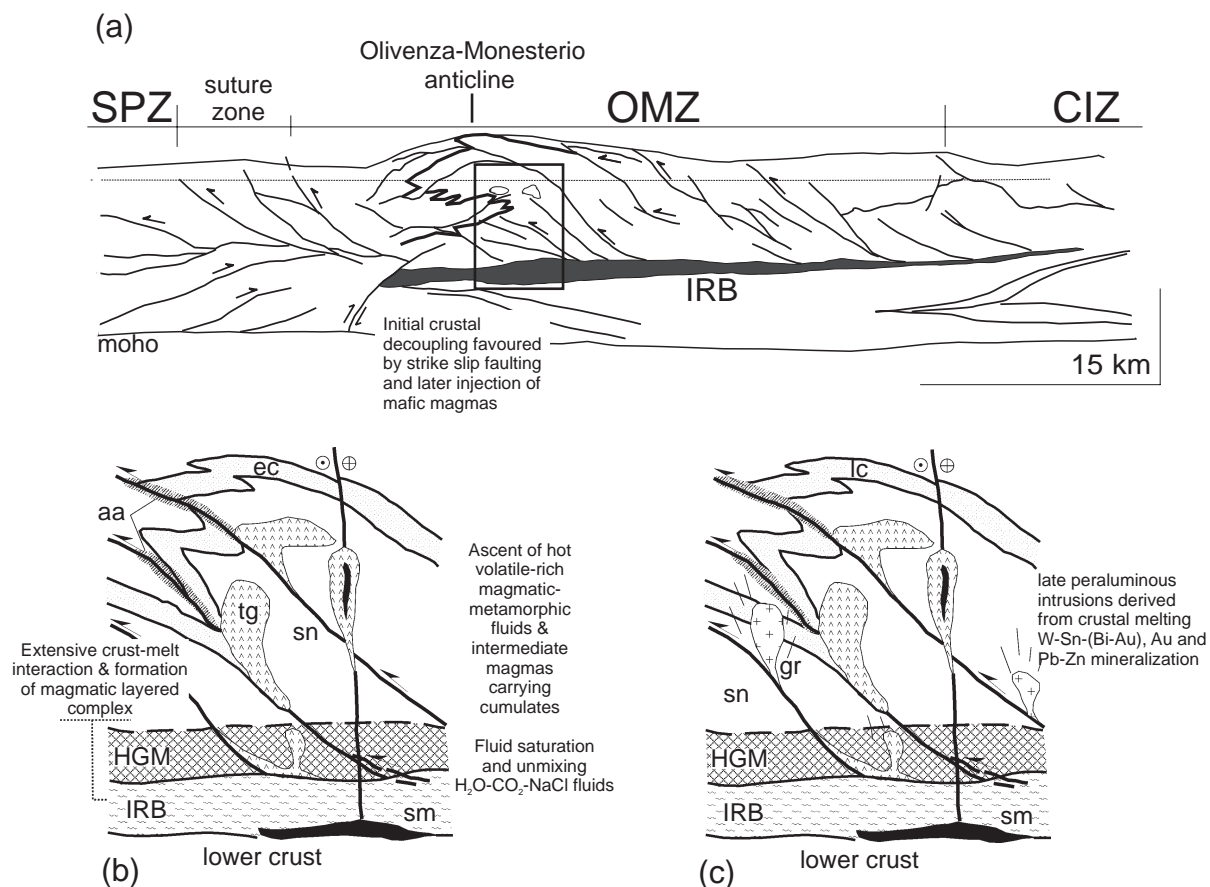
Fig. 7. Schematic sketch of the metallogenic evolution of the Ossa Morena Zone during Variscan times: modified from Tornos and Casquet (2005) and the interpretation of geophysical data of Simancas et al. (2003). (a) General sketch of the Ossa Morena Zone showing the relationship between the structure and the mafic–ultramafic layered complex. (b) Intrusion of the metaluminous magmatism and related iron oxide and Ni–(Cu) mineralization (350 to 330 Ma). sn: Serie Negra, grey shales and sandstones; ec: Early Cambrian siliclastic sediments and carbonatic rocks; aa: alkaline (Na–Ca) hydrothermal alteration; HGM. Zone of high-grade metamorphism and anatexis; LMC: layered magmatic complex; sm: sulphide-rich immiscible magma; tg: tonalite to gabbro-(norite). (c) Intrusion of peraluminous magmas and formation of related deposits (330 to 300? Ma). gr: peraluminous granodiorite and granite.

with a granitic source would be near 6.2‰ to 8.3‰ (e.g., Sheppard, 1986; Barrett and Friedrichsen, 1987). Thus, the high $\delta^{18}O$ values suggest that the fluids were of deep, magmatic or metamorphic, origin with minor interaction with surficial waters. An equivalent debate is found elsewhere for IOCG deposits where magmatic (Pollard, 2001) and sedimentary (Barton and Johnson, 1996) sources are proposed.

There are numerous examples to show that deep, layered intrusions can exsolve significant amounts of hydrothermal fluid. The presence of iron-rich pegmatite, pervasive alteration and hydrothermal breccias in the Bushveld Complex shows that fluid overpressures

can be significant in the upper part of the intrusion (Mathez, 1989; Boorman et al., 2003). In the Aracena Massif, intrusion of mafic magmas in pelitic rocks would tighten the isotherms and produce extensive metamorphic dehydration of shale and further anatexis. A combination of partial melting and assimilation of pelitic rocks with crystallization of anhydrous cumulates in the layered complex would dramatically increase the water pressure and promote fluid exsolution. High fluid pressures are shown by the abundance of intercumulus biotite/amphibole, the presence of pegmatite and of hydrothermal breccia. The presence of trondhjemitic and tonalitic anatectic melts (Castro et

al., 1999) is also consistent with high fluid contents. Fluids in equilibrium with mafic magmas tend to be CO_2- and iron-rich, as has been described in fluid inclusion studies (Kwak, 1986; Mathez, 1989), and can be inferred from the presence of magnetite-bearing pegmatite and of oxide-rich gabbro (Bushveld; Mathez, 1989). Fluid inclusion studies on gabbro show that there is an early generation of CO_2–CH_4-rich fluids followed by saline, up to 32 to 51 eq. wt.% NaCl, aqueous fluids, reflecting the early degassing of the more volatile species and the late exsolution of brines (Kelley and Früh-Green, 2001). Also, comparison with other areas where there is evidence of exsolution of fluids from basaltic magmas shows that the hydrothermal alteration is dominated by epidote, actinolite and magnetite (Galley, 2003), confirming that oxidized alkaline Ca–Fe-rich fluids dominated these systems. In this context, the oxide-rich gabbro reported in the Beja Massif (Mateus et al., 2001) could represent the late immiscible Fe-rich phase. This rock is enriched in P- and REE-bearing minerals, as occurs in the IOCG deposits, suggesting a common link between magmatic fluids and the IOCG deposits. The data of Boudreau and Kruger (1990) show that these fluids are enriched in volatiles such as fluorine and can carry significant amounts of alkaline and LREE elements. Sedimentary rocks are the most likely source of volatiles. Shale is one of the largest reservoirs of volatiles in the crust, having significant amounts of fluorine (average 740 ppm), boron (average 100 ppm) and phosphorus (average 700 ppm; Fauré, 1986).

A conservative estimate suggests that crystallization of a highly contaminated magma of the dimensions suggested above can liberate a vast amount of fluid, greater than 1200 km^3. Loss of 2% to 3% water due to the intrusion and contact metamorphic dehydration can account for sufficient fluid to form large ore deposits. This volume is in the range needed for forming large ore deposits, about 10^{12} to 10^{13} m^3 (e.g., Villas and Norton, 1977).

5.1.3. Hydrothermal fluids and other styles of mineralization

In a general scheme, the peraluminous intrusions are interpreted here as allochthonous magmas derived from anatexis induced by the layered intrusion. The high water content of these rocks probably inhibited the ascent of magma to epizonal levels, explaining why only a few small granites are found. Only water-depleted or volatile-rich magmas or those generated near major structures could rise high into the crust. Their high viscosity would imply a slower upward velocity than mafic melts and fluids, and thus a younger age of emplacement in the shallow crust.

However, these intrusions could equally well have been derived from fractional crystallization within the layered intrusion, as has been recorded at Bushveld. There, granites form a significant proportion of the layered complex, have high volatile (F, B) contents and can exsolve large amounts of fluids, causing Sn and W mineralization (Pollard et al., 1991). Perhaps equivalent to these rocks is the metaluminous pegmatitic leucogranite found in the Aracena Massif but none has been recorded in shallower environments.

Other hydrothermal mineral deposits include widespread low temperature, structurally controlled hydrothermal mineralization, including Pb–Zn–(Ag) and Hg–(Cu–Sb) veins and replacements. Most of the Pb–Zn–(Ag) veins are within the Coimbra-Córdoba Shear Zone, indicating that this structure channelized large amounts of fluids that scavenged metals from the adjacent rocks and precipitated them by boiling along tensional structures (Tornos et al., 2004a). Regional uprise of isotherms and generation of large convective cells should be a consequence of the magmatically induced regional high heat flow. Fluid flow should be channelized by regional WNW–ESE faults, leading to the formation of Hg–(Cu–Sb) mineralization. In fact, Hg-rich epithermal mineralization has been interpreted as related to abnormally high heat flow associated with deep mantle plumes, as has been described by Oppliger et al. (1997) in the Yellowstone area.

5.1.4. Structural controls on magma intrusion and fluid flow

Magmas and fluids derived from crust–magma interaction probably ascended along major structures to the upper crust. As explained above, Variscan WNW–ESE to NW–SE structures are widespread in the OMZ. Such structures have been detected by the IBERSEIS profile and seem to correspond to low-dipping (30° to 60°) discontinuities that have behaved episodically as thrusts or strike-slip faults (Simancas et al., 2003).

The geological relationships suggest that most of the hydrothermal flow was channelized along discrete

extensional zones. As shown in Fig. 2, the more sig-
nificant metaluminous magmatism and related miner-
alization are concentrated in two major zones, one of
about 900 km^2 located in the Brovales-Burguillos area
and another in the southern part of the terrane. In the
first area, plutonic and hydrothermal rocks are related
to a zone of rotation from WNW–ESE to N–S in the
trend of the tectonic structures (Fig. 2) that is resolved
by two strike-slip dextral shear zones on both sides of
the Brovales stock, giving it a drop-like morphology.
The second zone is adjacent to the large faults that
define the southern limit of the OMZ (Figs. 1 and 3)
but probably the situation is equivalent. The change in
trend can be interpreted as a major releasing bend zone,
probably reflecting a deep-seated tensional structure.
Other orebodies seem to be related to other localized
extensional zones. Both the Cala Fe-oxide deposit and
the Aguablanca Ni–(Cu) mineralization are hosted by
small pull-apart structures within the regional WNW–
ESE faults. The orientations of the breccias and frac-
tures and of the regional cleavage around the Agua-
blanca stock suggest that it intruded along a pull-apart
jog located between two major sinistral faults (Tornos
et al., 2002).

The presence of trans-crustal extensional zones
within a regional transpressional setting seems to be
critical for magma emplacement and hydrothermal
circulation. A drop in the geostatic pressure should
favour deep anhydrous melting and fluid exsolution as
well as quick ascent of the magmas to high crustal
levels. Under compression, the hydrothermal conduc-
tivity of faults can increase by several orders of
magnitude (Sanderson and Zhang, 1999). Thus, loca-
lized extensional zones such as pull-apart structures,
dilational jogs, deflection zones, releasing bends or
zones of fracture intersection are places for rapid and
high fluid flow. Sanderson and Zhang (1999) have
shown that in such a regime high permeabilities are
maintained even to considerable depths, promoting
high heat flow and the arrival to epizonal depths of
deep fluids with minor heat loss.

5.2. Geotectonic and geological factors leading to prolific VMS formation in the IPB

5.2.1. Heat, fluids and metals

Understanding the unusual, probably unique, geo-
tectonic setting of the IPB is the key to revealing how

numerous convergent processes led to highly favour-
able conditions for VMS generation in this region.
The transtensional opening of first order basins in an
active continental margin under an overall transcur-
rent tectonic regime (Tornos et al., 2002; Solomon and
Quesada, 2003) provided excellent conditions for
long-lasting high regional geothermal gradients,
magma generation and large fluid flow. Such a geo-
tectonic setting favoured the rise and shallow empla-
cement of super-heated, poorly fractionated felsic
magmas (Mitjavila et al., 1997). These conditions
should have also promoted fluid–rock interaction
and thus the generation of metal-rich solutions in
deep-seated hydrothermal aquifers, and contributed
to stabilize paths for fluid flow, focusing discharge
of the ore fluids (cf. Lydon, 1996). The role of syn-
volcanic tectonic processes in assisting and triggering
the circulation and upflow of the mineralizing fluids
was certainly crucial in the Iberian Pyrite Belt as
shale-dominated basins have low primary bulk perme-
ability (cf. Goodfellow et al., 1999).

Typical IPB deposits may result from different
extractions/leakages from similar crustal metal reser-
voirs. The available data on lead (μ, 9.6 to 10; Mar-
coux, 1998; Relvas et al., 2001), neodymium (most
εNd_i values between -11.3 and -5.5; Relvas et al.,
2001), strontium ($^{87}Sr/^{86}Sr_i$ between 0.7071 and
0.7221; Tornos and Spiro, 1999; Relvas et al., 2001;
Tornos, 2005) and osmium (γOs, 0.52 ± 0.17; Mathur
et al., 1999) isotopes suggest that, except perhaps for
the Neves Corvo deposit, there could have been a
common, large and mostly homogeneous reservoir
of metals for the whole province. Fluid inclusions in
the quartz from the IPB stockworks are mainly aqu-
eous and have salinities ranging between 3 and 12 eq.
wt.% NaCl (Almodóvar et al., 1998; Sánchez España
et al., 2003). These brines are interpreted as primary
ore fluids that could have led to the formation of
accumulations on the seafloor of immiscible saline
fluids (brine pools) responsible for massive sulphide
accumulation (Tornos et al., 1998; Solomon et al.,
2002).

Modified seawater has been interpreted as the main
fluid involved in most IPB systems (Barriga and
Kerrich, 1984; Munhá et al., 1986) but its exclusivity
is currently questioned by many authors. The gener-
ally high salinities of the IPB ore fluids and their
common heavy oxygen isotope signatures led several

authors to propose the involvement of magmatic fluids in all or, at least, in many IPB hydrothermal systems (e.g., Munhá et al., 1986; Halsall and Sawkins, 1989; Relvas et al., 2001; Sánchez España et al., 2003). According to Solomon and Quesada (2003), this fluid would have been intermittently swept (at depth and at high temperature) by the seawater-dominated convection cells, representing a minor component of the fluid budget but a major metal contributor for the overall system.

Alternative models consider mixtures of seawater with connate fluids (Sáez et al., 1996; Almodóvar et al., 1998), or even dominant connate waters equilibrated with the PQ Group (Tornos, 2005). The dry nature of the shallow-emplaced felsic magmatic systems in the belt (see Munhá, 1983; Thieblemont et al., 1998) mitigates against significant incorporation of aqueous fluid contributions in typical IPB hydrothermal systems. The metal ratios in typical IPB ores closely correlate with those of their underlying metasedimentary rocks, suggesting predominant metal leaching supply in the belt (Tornos and Spiro, 1999; Relvas, 2000). Volcanic rocks are nearly or completely absent from the footwall succession of some IPB deposits, (e.g., Tharsis, Tornos et al., 1998). Even when the deposits are hosted by volcanic rocks, the majority of the leached base metals in the massive sulphide ores must have been sourced by the Phyllite–Quartzite (PQ) Group (and an unknown proportion from older basement) and not from the VS Complex as, in general, this is less than 600 m thick. These circumstances, coupled with the overall large predominance of sedimentary over volcanic rocks in the footwall sequence, and the gigantic size of many deposits, led several authors to propose a volcanogenic/sedimentary-exhalative hybrid model for the IPB metallogenesis (Velasco et al., 1998; Sáez et al., 1999; Relvas et al., 2002).

Processes like low-grade metamorphic dewatering, and/or long time-resident, deeply circulated connate water or seawater through the PQ metasediments, seem more consistent with the chemically homogeneous signatures of the ores and radiogenic isotopes throughout the belt (Tornos and Spiro, 1999; Relvas, 2000; Relvas et al., 2001; Tornos, 2005). Fluids equilibrated with a mature siliciclastic sequence can explain the high salinities measured, heavy $\delta^{18}O$ isotopic ratios, and radiogenic signatures of the hydro-

thermal fluids, without requiring, in most cases, significant input of fluids of other derivation. Large trans-crustal faults and high heat flow could have fed energetically the processes of compaction-induced dewatering from a shale-dominated sequence, assisting in fluid migration and playing a critical role in homogenizing fluid–rock geochemical exchange, metal-extraction reactions, hydrothermal convection, and fault-controlled upflow of the resulting brines.

The case of the Neves Corvo deposit can arguably represent an exception to this general rule (Relvas, 2000; Relvas et al., 2001). The geochemistry of the Neves Corvo ores contrasts with that of typical IPB deposits, which generally possess high tonnages but low Cu grades. The copper content and the ratio of the Neves Corvo ores [100 Cu/(Cu+Zn)=47] significantly deviate from the IPB standards [15<(100 Cu/(Cu+Zn)<25]. In addition, the total tin content (>300,000 t), the tin grades attained by the stringer and massive cassiterite ores (up to 60% Sn), and the Cu–Sn metal association in the massive sulphide ores of Neves Corvo are truly unique among VMS deposits, not only in the IPB but also worldwide (Relvas et al., in press-a,b). The heavy $\delta^{18}O$ isotope ratios, the Nd and Pb isotope ratios, the subordinate occurrence of high-sulphidation ore mineral assemblages (bornite zone), and the Al-rich hydrothermal alteration pattern rich in donbasite are among the arguments invoked by Relvas (2000) for proposing a magmatic-hydrothermal model for formation of this deposit, involving direct magmatic contributions to its tin and copper contents.

Possibly, magmatic fluid and metal contributions in particular IPB deposits, if any, would have been related to deeper granitic bodies, independent from typical IPB felsic magmas (Relvas et al., 2001, in press-b). In fact, melt inclusion studies in dacitic subvolcanic sills show the presence of a population of quartz phenocrysts with melt inclusions that are different from those having compositions typical of the hosting volcanic rocks (Tornos et al., 2004c). These melt inclusions have compositions similar to those of the Sn-bearing granites and could reflect the existence of an independent suite of granites equivalent to those predicted by Relvas et al. (2001). However, Tornos (2005) finds no geological or geochemical arguments for invoking the presence of magmatic fluids in the IPB, including the Neves

Corvo system, leaving the igneous rocks only responsible for the high heat flow needed to provide fluid circulation.

5.2.2. Origin of sulphur, ore traps, and sulphide precipitation

Metal versus sulphur solubility constraints, the consideration of source geochemical characteristics, and the mineralogy and sulphur isotope composition of both the stockworks and the overlying massive sulphides, combine to indicate that the total content of metals in solution must have exceeded that of sulphur in the IPB ore fluids (Tornos, 2005). Fluid mixing of deep fluids having a low amount of sulphur with $\delta^{34}S$ values around 0‰ (-2.5‰ to 10.0‰) with surficial, H_2S-rich fluids having significantly lower $\delta^{34}S$ values, down to -33‰, is thus envisaged as the most suitable mechanism to provide the additional reduced sulphur needed to account for sulphide saturation and consequent massive sulphide precipitation. Two sources have been postulated for the reduced sulphur: (a) deep leaching of sediments and igneous rocks and/or abiogenic reduction of seawater sulphate at depth; and (b) biogenic reduction of seawater sulphate on or near the seafloor (Velasco et al., 1998).

In the massive sulphides formed by replacement, sulphide saturation would have been attained by mixing of ascending metal-bearing solutions with seawater circulating in suitable layers (hydrothermal aquifers). Reduced sulphur resulted from thermo-reduction of marine sulphate and/or leaching from the host succession (e.g., Barriga and Fyfe, 1988; Relvas et al., in press-a). In the less-permeable, shale-dominated systems, the ore fluids should mix with modified (reduced) seawater and precipitate the metals. For authors claiming a replacement origin for the shale-hosted deposits, the sulphides would be precipitated within the seawater-drenched uppermost part of the footwall sequence, whereas in the exhalative model they would vent on the seafloor, forming a brine pool and precipitating by reaction with H_2S generated by the biogenic activity in the chemocline (e.g., Tharsis; Tornos et al., in press). In these cases, the role of oxic/anoxic conditions at the bottom of the basin was critical not only in controlling sulphide preservation, but also in conditioning the existing biota.

5.2.3. Variscan tectono-metamorphism

The superimposed effects of a complex tectonism often obscure the relationships between orebodies and host lithologies in the IPB. The tectonic evolution of the belt led to compression-induced inversion of the early synsedimentary structures (Quesada, 1998), favouring the stacking or piling up of many massive sulphide bodies in a ramp and flat geometry, as has been quoted in Aznalcollar (Almodóvar et al., 1998), Tharsis (Tornos et al., 1998) and Neves Corvo (Relvas et al., in press-b). Tectonic dismembering into multiple lenses significantly biased the original aspect ratio of some deposits. This tectonic activity was accompanied by major ore remobilization and geochemical re-equilibration near the shear zones. Remobilization processes induced by post-ore deformation phenomena generated high Cu, Zn–Pb or Au grade oreshoots within some massive sulphides, enhancing their economic potential. This is the case in the Tharsis stockwork, where tectonic reconcentration of ductile minerals has produced Au–Cu–Bi–Te-rich zones (Tornos et al., 1998); an equivalent behaviour has been observed in the Rio Tinto stockwork, with Cu-enrichment controlled by Variscan structures (Gumiel et al., 2001). Syntectonic gold and base-metal enrichments have been described in many other massive sulphide deposits of the IPB, such as Aguas Teñidas Este, Lomero Poyatos or Concepción (Velasco et al., 2000).

The ore textures, sulphide paragenetic sequences and geochemistry of the Cu-rich massive and stockwork ores at Neves Corvo clearly indicate that long-lasting hydrothermal refining of the massive sulphides led to pronounced metal segregation at all scales, from the individual lenses to the overall deposit (Pinto, 1999; Relvas, 2000). The primary richness in chalcopyrite of this deposit strongly enhanced the consequences of tectonic remobilization, accounting for very significant copper enrichment in particular types of ore (up to 45% Cu). Noronha et al. (2000) and Relvas et al. (in press-a) have presented detailed descriptions of the mechanisms and fluids involved in the tectono-metamorphic copper enrichment of the Neves Corvo deposit.

5.2.4. Searching for analogues

Attempts to find modern or fossil analogues to the IPB deposits always face two major problems: the scale of the ore-forming processes involved, and the

Table 2
Synopsis of Variscan geological and metallogenic features of SW Iberia

| | Ossa Morena Zone | | South Portuguese Zone |
	Main OMZ	Aracena Massif	
Geotectonic setting	(Para-) autochthonous terrane accreted to the Iberian terrane during Cadomian orogeny. Overriding plate during Variscan collision	Same as Main OMZ, but probably representing mid-crustal rocks exhumed during late Variscan times. Includes pelitic and calc-silicate gneiss, marble, amphibolite and granulite	Allochthonous exotic terrane (Laurasia, Laurentia?) accreted to the Iberian terrane during the Variscan Orogeny through oblique continent–continent collision and subduction (?) of Rheic Ocean below the Ossa Morena Zone
Pre-Variscan stratigraphy	Proterozoic basement overlain by a Cadomian synorogenic sequence, rift-related carbonate, bimodal volcanic and siliciclastic rocks (early Palaeozoic) and siliciclastic-carbonate rocks deposited on stable platform (Ordovician to Devonian)	Proterozoic to Lower Cambrian rocks equivalent to those of the main OMZ	Thick (>2000 m) sequence of siliciclastic sediments deposited on a shallow platform (PQ Group, Upper Devonian) over an unknown basement
Structure	Thrust and overturned fold belt with major transcurrent component rooted in a basement shear zone. Major sinistral strike-slip component	S–SW-verging recumbent folds followed by subvertical folds	Fold and thrust belt
Metamorphism	Mostly greenschist facies with some restricted domes with up to amphibolitic conditions	Linear belt with tightly packed isograds. Low P/high T, with widespread anatexis in internal zones	Very low grade, reaching medium grade conditions near shear zones
Plutonism	Metaluminous suite (350 to 330 Ma) of gabbro-granodiorite followed by minor peraluminous granodiorite–granite (330 to 290 Ma) intruded in shallow environment	Complex magmatism dominated by (quartz)-diorite and ultramafic rocks intruded by younger granodiorite	Minor shallow quartz-diorites to granodiorites in the NE part of the belt
Sedimentary rocks	Minor pull-apart basins of Tournaisian-Visean filled with siliciclastic and carbonatic sediments deposited in a storm-dominated shelf with local subaerial facies	None recorded	Thick sequence including up to 1300 m of the Volcano-Sedimentary (VS) Complex, made up of volcanic rocks interbedded with shale and chemical sediments deposited in pull-apart basins and overlain by the Culm Group, with up to 3000 m of turbidites within a foreland basin
Volcanic rocks	Some WNW–ESE volcanic alignments of flows and (crypto)-domes of rhyolite to andesite of (K-rich) calc-alkaline geochemistry	None recorded	Abundant in the VS Complex as felsic volcanic rocks, including dome-cryptodome complexes, sills and thick mass flows, locally pumice-rich. More accessory basalt as sills and minor flows. Andesitic dome complexes restricted to the northern part of the belt

Table 2 (*continued*)

	Ossa Morena Zone		South Portuguese Zone
	Main OMZ	Aracena Massif	
Mineralization	Complex and variable including: (a) iron oxide, Cu–Au and magmatic Ni–(Cu) orebodies related to metaluminous plutonism; (b) W–(Sn) and base-metal veins and replacements associated with peraluminous plutonism; (c) minor volcanogenic massive sulphide and iron oxide mineralization; (d) synmetamorphic lode gold and Zn–Pb; (e) epithermal Hg–(Pb–Cu) and base-metal veins and replacements	Mostly disseminated to semi-massive sulphides in ultramafic rocks probably forming stratiform magmatic complexes	Dominated by large stratiform to stratabound volcanogenic massive sulphide orebodies in the VS Complex. Mn-oxide mineralization hosted by purple shale and jasper. Minor syntectonic to granite-related veins
Interpretation	Dominant magmatism and related mineralization due to crust-juvenile magma interaction at mid-crustal levels, with ascent of magmas and deep hydrothermal fluids to a shallow environment	Mid-crustal layered magmatic complex and host rocks	Mostly (sub)-exhalative massive sulphides related to focused discharge in zones of high heat flow. Fluids and metals mostly derived from accelerated compaction and dewatering of sedimentary sequence

geotectonic setting where they occurred. An exhaustive comparison with the major VMS districts worldwide is far beyond the scope of this article (Barrie and Hannington, 1999; Large and Blundell, 2000). The most frequently invoked parallels with the IPB mineralization are those of the massive sulphide deposits of the Bathurst camp (e.g., Lentz, 1999) and the Green's Creek deposit, Alaska (Taylor et al., 1999), in which footwall successions and ore characteristics have significant similarities with those of the Iberian deposits. However, at least in the case of Bathurst, the geotectonic setting envisaged for the host basin is different (back-arc environment) and the scale of the overall mineralization is beyond comparison.

Seeking modern analogues seems even more difficult as most hydrothermal fields investigated so far relate to mid-ocean ridge basaltic systems. Relvas et al. (2002) emphasized some similarities with the sulphide mineralization in the Pacmanus Basin, but, again, the back-arc complex tectonic setting of the field does not fit with that of the IPB metallogenesis. Some characteristics of the Bransfield Strait hydrothermal field, Antarctica are also reminders of important IPB features (Petersen et al., 2004). The geotectonic setting of the IPB, its geology and the

geometric configuration of the basin, the abundance of dark shale, the importance of biogenically derived sulphur and the involvement of large amounts of connate fluids derived from an underlying siliciclastic sequence make this belt perhaps unique as a highly favourable setting for the formation of giant massive sulphides.

6. Integrated model: metallogenesis in an unconventional tectonic setting

The Variscan Massif of Iberia is an orogenic belt where strike-slip deformation has had a major influence in its configuration. The exact nature and the polarity of the terrane amalgamation is poorly constrained due to the intense strike-slip deformation and the absence of any geophysical evidence of remnants of the subducted slab or of crustal thickening (Simancas et al., 2003). Despite global evidence in NW Iberia and the Appalachians that suggests the subduction of the Gondwana plate below the Laurentia plate (Martínez Catalán et al., 1997), most of the regional studies on SW Iberia postulate the opposite vergence, i.e., a north to eastward subduction of the oceanic

crust and further obduction of the exotic terrane above the autochthonous Iberian terrane. The main arguments for this model include the south to south–west vergence of the Variscan structures, the geological zonation in the presumed suture, the formation of a foreland basin in the SPZ and the presence of a calc-alkaline volcanism with orogenic signatures in the OMZ (Silva et al., 1990; Quesada et al., 1991; Oliveira and Quesada, 1998). In any case, the geophysical data, the absence of a well-defined orogenic magmatic arc and the presence of a regional metamorphism dissimilar to that of orogenic belts strongly indicate that the remnants of subduction and collision events, if any, have been masked by the strike-slip deformation. Transcurrent deformation on both sides of the suture induced the formation of magmatic-hydrothermal systems that overprinted equivalent ones that should be expected in conventional accretionary orogens.

The Variscan mineralization in the OMZ is polyphase and took place over a span of more than 50 million years (Table 2). Mineralization associated with the metaluminous magmatism occurred between 350 and 330 Ma, which related to the peraluminous magmatism, perhaps between 330 and 290 Ma. Other hydrothermal features seem to be within that same time span (Fig. 3). In the IPB, the situation is different and the bulk of the ore-forming events took place in a rather short time, probably between 360 and 350 Ma.

On both sides of the suture, mafic magmas induced crustal underplating, melting induced by decompression and felsic peraluminous magmas. What makes the OMZ and the SPZ different is the nature of the upper crust and the degree of crust–mantle interaction. Rocks of the SPZ are interpreted as having formed in an ensialic basin. The known upper crust is mainly formed by a thick mature siliciclastic sequence, the PQ Group, probably overlying an evolved continental basement. Thermally induced dewatering and diagenetic maturation and compaction of the PQ Group is probably the main source of fluids and metals (Tornos, 2005). Pull-apart structures favoured the intrusion of magmas, the rise of isotherms and convective circulation of the connate brines and seawater. Radiogenic isotope data show that both the felsic and mafic igneous rocks have initial εNd and $^{87}Sr/^{86}Sr$ ratios consistent with a major derivation from primitive sources. However, the few Nd, Sr and Os data of

hydrothermal rocks and the extensive Pb isotope database of the ores are consistent with derivation of hydrothermal fluids and metals from crustal sources and indicate only minor juvenile influence in the ore deposits of the SPZ. The IBERSEIS profile does not detect large mid-crustal layered intrusions (Simancas et al., 2003) and here the lower-upper crust boundary is clearly defined by the basal thrust detachment (Fig. 7). These features also agree with the composition of the massive sulphides, which are enriched in Cu, Zn and Pb. Massive sulphides with a significant mafic component are enriched in Cu–Zn and impoverished in Pb (e.g., Barrie and Hannington, 1999) in comparison with those derived from upper crustal sources, which are enriched in Cu–Zn–Pb.

In the OMZ, the situation is dramatically different. Sr and Nd isotope data show that magmatic rocks and ores have similar sources (Fig. 6). The stratigraphy is dominated by a thick sequence of metamorphic rocks of continental derivation. Hydrothermal systems seem to have been dominated by fluids, magmatic or metamorphic in origin, generated deep in the crust. The proportion of surficial fluids seems to be small and restricted to late orogenic convective cells. Dewatering of a sedimentary sequence also seems to be of minor importance, if any. The Pb, Nd and Sr isotope ratios suggest that the proportion of crustal component is high in both the igneous and hydrothermal rocks but a significant proportion of the lead was derived from a juvenile source.

The Variscan metallogenesis of the OMZ is interpreted as primarily controlled by the intrusion of a large layered mafic–ultramafic complex in the middle crust by incomplete decoupling of the lower crust and further magma intrusion. If this model holds true, then the layered complex would favour the formation of calc-alkaline rocks of intermediate composition, but inhibit the ascent of magmas generated at greater depths by underplating of mafic magmas at the base of the crust. The only peraluminous rocks to be formed should be related to the crustal melting associated with the deep magmatic complex. This can explain why the OMZ is impoverished in peraluminous granites when compared with the bulk of the Iberian Massif (Fig. 1).

In both terranes, localized extensional structures within the overall compressional setting played a major role in the ore-forming processes. Crustal exten-

sional heterogeneities such as transpressional dilational jogs, releasing zones, bending zones and pull-apart basins induced local stress relaxation, deep melting and quickly focused the ascent of magmas and hydrothermal fluids along well-defined pathways.

Despite both Ni–(Cu) and IOCG deposits being widely interpreted as having formed in equivalent tectonic settings and in relation to similar mafic igneous rocks, a genetic and spatial relationship has not previously been described. This could be due to the fact that most of them occur in highly deformed and metamorphosed Archaean and Proterozoic belts. The striking similarities between these ore belts and the OMZ suggest that this relatively young example has a metallogenic evolution similar to that of ancient continental margins, so perhaps associated IOCG and Ni–(Cu) mineralization in Precambrian belts formed by processes equivalent to those described above.

Acknowledgements

References

Abalos, B., Gil Ibarguchi, J.I., Eguíluz, L., 1991. Cadomian subduction/collision and Variscan transpression in the Badajoz Cordoba shear belt, southwest Spain. Tectonophysics 199, 51–72.

Almodóvar, G.R., Sáez, R., Pons, J.M., Maestre, A., Toscano, M., Pascual, E., 1998. Geology and genesis of the Aznalcollar massive sulphide deposits, Iberian Pyrite Belt Spain. Mineralium Deposita 33, 111–136.

Apalategui, O., Eguíluz, L., Quesada, C., 1990. Ossa Morena Zone: structure. In: Martínez, E., Dallmeyer, R.D. (Eds.), Pre-Mesozoic Geology of Iberia. Springer-Verlag, Berlin, pp. 280–291.

Arribas, A., 1993. Observations on the isotopic composition of ore Pb in the Iberian Peninsula. In: Fenoll, P., Torres, J., Gervilla, F. (Eds.), Current Research in Geology Applied to Ore Deposits. Universidad de Granada, pp. 29–32.

Bachiller, N., Casquet, C., Galindo, C., Quílez, E., 1997. Hydrothermal alterations in leucogranites from the Burguillos del Cerro intrusive complex, Badajoz, SW Spain—evidence for pulsatile mixing of igneous and meteoric fluids. In: Papunen, H. (Ed.), Mineral Deposits: Research and Exploration. Balkema, Rotterdam, pp. 605–608.

Barrett, T.J., Friedrichsen, H., 1987. Oxygen isotopic composition of basalts from young spreading axis in the eastern Pacific. Canadian Journal of Earth Sciences 24, 2105–2117.

Barrie, C.T., Hannington, M.D., 1999. Classification of volcanic-associated massive sulfide deposits based on host rock composition. In: Barrie, C.T., Hannington, M.D. (Eds.), Volcanic Associated Massive Sulfide Deposits: Processes and Examples in Modern and Ancient Settings, Reviews in Economic Geology, vol. 8, pp. 1–11.

Barrie, C.T., Amelin, Y., Pascual, E., 2002. U–Pb geochronology of VMS mineralization in the Iberian Pyrite Belt. Mineralium Deposita 37, 684–703.

Barriga, F.J.A.S., Fyfe, W.S., 1988. Giant pyritic base-metal deposits: the example of Feitais, Aljustrel, Portugal. Chemical Geology 69, 331–343.

Barriga, F.J.A.S., Kerrich, R., 1984. Extreme ^{18}O-enriched volcanics and ^{18}O-evolved marine water, Aljustrel, Iberian Pyrite Belt: transition from high to low Rayleigh number convective regimes. Geochimica et Cosmochimica Acta 48, 1021–1031.

Barriga, F.J.A.S, Relvas, J.M.R.S., 1993. Hydrothermal alteration as an exploration criterion in the IPB: facts, problems, and future. I Simpósio de Sulfuretos Polimetálicos da Faixa Piritosa Ibérica, October 3–6 1993, Évora, Portugal, Associação Portuguesa da Indústria Mineral, Abstract, vol. 1 (3), pp. 1–2.

Barton, M.D., Johnson, D.A., 1996. Evaporitic source model for igneous-related Fe oxide–(REE–Cu–Au–U) mineralization. Geology 24, 259–262.

Boorman, S.L., McGuire, J.B., Boudreau, A.E., Kruger, F.J., 2003. Fluid overpressure in layered intrusions: formation of a breccia pipe in the Eastern Bushveld Complex, Republic of South Africa. Mineralium Deposita 38, 356–369.

Boudreau, A.E., Kruger, F.J., 1990. Variation in the composition of apatite through the Merensky Cyclic Unit in the Western Bushveld complex. Economic Geology 85, 737–745.

Boulter, C.A., 1993. Comparison of Rio Tinto, Spain and Guaymas Basin, Gulf of California: an explanation of a supergiant massive sulfide deposit in an ancient sill-sediment complex. Geology 21, 801–804.

Burg, J.P., Iglesias, M., Laurent, P., Matte, P., Ribeiro, A., 1981. Variscan intracontinental deformation: the Coimbra-Córdoba Shear Zone (SW Iberian Peninsula). Tectonophysics 78, 15–42.

Camus, F., Dilles, J.H., 2001. A special issue devoted to porphyry copper deposits of northern Chile—preface. Economic Geology 96, 233–237.

Carr, G.R., Dean, J.A., Suppel, D.W., Heithersay, P.S., 1995. Precise lead isotope fingerprinting of hydrothermal activity associated with Ordovician to Carboniferous metallogenic events in the Lachlean fold belt of New South Wales. Economic Geology 90, 1467–1505.

Casquet, C., Tornos, F., 1991. Influence of depth and igneous geochemistry on ore development in skarns: the Hercynian Belt of the Iberian Peninsula. In: Augusthitis, E. (Ed.), Skarns, their Petrology and Metallogeny. Augusthitis, Athens, pp. 555–591.

Casquet, C., Velasco, F., 1978. Contribución a la geología de los skarns cálcicos en torno a Santa Olalla de Cala, Huelva-Badajoz. Estudios Geológicos 34, 399–405.

Casquet, C., Galindo, C., Darbyshire, D.P.F., Noble, S.R., Tornos, F., 1998. Fe–U–REE mineralization at Mina Monchi, Burguillos del Cerro, Spain: age and isotope (U–Pb, Rb–Sr and Sm–Nd) constraints on the evolution of the ores. Proceedings GAC-MAC-APGGQ Quebec 98 Conference, vol. 23,   p. A28.

Casquet, C., Galindo, C., Tornos, F., Velasco, F., 2001. The Aguablanca Cu–Ni ore deposit (Extremadura, Spain), a case of synorogenic orthomagmatic mineralization: isotope composition of magmas (Sr, Nd) and ore (S). Ore Geology Reviews 18, 237–250.

Castro, A., Fernández, C., El-Hmidi, H., El-Biad, M., Díaz, M., Rosa, J., Stuart, F., 1999. Age constraints to the relationships between magmatism, metamorphism and tectonism in the Aracena metamorphic belt, southern Spain. Contributions to Mineralogy and Petrology 88, 26–37.

Crespo, A., 1991. Evolución geotectónica del contacto entre la Zona de Ossa Morena y la Zona Surportuguesa en las Sierras de Aracena y Aroche, Macizo Iberico Meridional. Un contacto mayor en la Cadena Hercinica Europea. Unpublished PhD thesis, Universidad Granada, 327 pp.

Cuervo, S., Tornos, F., Spiro, B., Casquet, C., 1996. El origen de los fluidos hidrotermales en el skarn férrico de Colmenar-Santa Bárbara (Zona de Ossa Morena). Geogaceta 20, 1499–1500.

Dallmeyer, R.D., Quesada, C., 1992. Cadomian vs. Variscan evolution of the Ossa Morena Zone (SW Iberia): field and ^{40}Ar/^{39}Ar mineral age constraints. Tectonophysics 216, 339–364.

Dallmeyer, R.D., Fonseca, P.E, Quesada, C., Ribeiro, A., 1993. ^{40}Ar/^{39}Ar mineral age constraints for the tectonothermal evolution of a Variscan Suture in SW Iberia. Tectonophysics 222, 177–194.

Dallmeyer, R.D., García Casquero, J.L., Quesada, C., 1995. ^{40}Ar/^{39}Ar mineral age constraints on the emplacement of the Burguillos del Cerro Igneous Complex (Ossa Morena Zone, SW Spain). Boletin Geologico y Minero 106, 203–214.

Darbyshire, D.P.F., Tornos, F., Galindo, C., Casquet, C., 1998. Sm–Nd and Rb–Sr constraints on the age and origin of magnetite mineralization in the Jerez de los Caballeros iron district of Extremadura, SW Spain. Proceedings ICOG-9, Chinese Science Bulletin, vol. 43 supplement, p. 28.

Díaz Azpiroz, M., Castro, A., Fernández, C., López, S., Fernández Caliani, J.C., Moreno-Ventas, I., 2004. The contact between the Ossa Morena and the South Portuguese zones. Characteristics and significance of the Aracena metamorphic belt, in its central sector between Aroche and Aracena (Huelva). Journal of Iberian Geology 30, 23–52.

Dunning, G.R., Díez Montes, A., Matas, J., Martín Parra, L.M., Almarza, J., Donaire, M., 2002. Geocronología U/Pb del volcanismo ácido y granitoides de la Faja Pirítica Ibérica, Zona Surportuguesa. Geogaceta 32, 127–130.

Dupont, R., Linares, E., Pons, J., 1981. Premières datations radiométriques par le méthode potassium–argon des granitoides de la Sierra Morena Occidentale, Badajoz, Espagne: conséquences géologiques et metallogéniques. Boletin Geologico y Minero 92, 370–374.

Eguíluz, L., Gil Ibarguchi, J.I., Abalos, B., Apraiz, A., 2000. Superposed Hercynian and Cadomian orogenic cycles in the Ossa Morena Zone and related areas of the Iberian Massif. Geological Society of America Bulletin 112, 1398–1413.

Fauré, G., 1986. Principles of Isotope Geology, 2nd edition. Wiley & Sons, New York. 589 pp.

Galindo, C., Portugal Ferreira, M.R., Casquet, C., Priem, H.N.A., 1990. Dataciones Rb/Sr en el completo plutónico Táliga-Bancarrota (Badajoz). Geogaceta 8, 7–10.

Galindo, C., Darbyshire, D.P.F., Tornos, F., Casquet, C., Cuervo, S., 1995. Sm–Nd geochemistry and dating of magnetites: a case study from an Fe district in the SW of Spain. In: Pasava, J., Kribek, B., Zak, K. (Eds.), Mineral Deposits: From their Origin to Environmental Impacts. Balkema, Rotterdam, pp. 41–43.

Galley, A.G., 2003. Composite synvolcanic intrusions associated with Precambrian VMS-related hydrothermal systems. Mineralium Deposita 38, 443–473.

Garcia de Madinabeitia, S., 2002. Implementación y aplicación de los análisis isotópicos de Pb al estudio de mineralizaciones y la geocronología del área de Los Pedroches-Alcudia (Zona Centro Ibérica). Unpublished PhD thesis, Universidad del País Vasco, 207 pp.

Gonzalez, F., Moreno, C., Sáez, R., Clayton, J., 2002. Ore genesis age of the Tharsis Mining District, Iberian Pyrite Belt. A palynological approach. Journal of the Geological Society, London 159, 229–232.

Goodfellow, W.D., Zierenberg, R.A., ODP Leg 169 Shipboard Science Party, 1999. Genesis of massive sulfide deposits at sediment covered spreading centers. In: Barrie, C.T., Hannington, M.D. (Eds.), Volcanic Associated Massive Sulfide Deposits: Processes and Examples in Modern and Ancient Settings, Reviews in Economic Geology, vol. 8, pp. 297–324.

Gumiel, J.C., 1988. Estudio geológico y metalogénico de la mineralización de W–Sn–Bi–Mo asociada a la cúpula granítica de San Nicolás, Valle de la Serena (Badajoz). Unpublished Master Thesis, Universidad Complutense de Madrid, 221 pp.

Gumiel, P., Sanderson, D.J., Campos, R., Roberts, S., 2001. Fractal geometry of the Cerro Colorado stockwork, Rio Tinto Mine (Iberian Pyrite Belt). In: Tornos, F., Pascual, E., Sáez, R., Hidalgo, R. (Eds.), Unpublished abstracts, GEODE Workshop Massive Sulphide Deposits in the Iberian Pyrite Belt: New

Advances and Comparison with Equivalent Systems, Madrid, pp. 23–24.

Gutierrez Alonso, G., Fernández Suárez, J., Weil, A.B., 2004. Orocline triggered lithospheric delamination. Geological Society of America Special Paper no. 383, pp. 121–131.

Halsall, C.E., Sawkins, F.J., 1989. Magmatic-hydrothermal origin for fluids involved in the generation of massive sulphide deposits at Rio Tinto (Spain). In: Miles, D. (Ed.), Water–Rock Interaction. Balkema, Rotterdam, pp. 285–288.

Heinrich, C.A., Neubauer, F., 2002. Cu–Au–Pb–Zn–Ag metallogeny of the Alpine–Balkan–Carpathian–Dinaride geodynamic province. Mineralium Deposita 37, 533–540.

Hitzman, M.W., 2000. Iron oxide–Cu–Au deposits. What, where, when and why. In: Porter, T.M. (Ed.), Hydrothermal Iron Oxide Copper–Gold and Related Deposits: A Global Perspective. Australian Mineral Foundation, Adelaide, pp. 9–25.

Johnson, J.P., McCulloch, M.T., 1995. Sources of mineralising fluids for the Olympic Dam deposit, South Australia. Sm–Nd isotopic constraints. Chemical Geology 121, 177–199.

Jorge, R., 2000. Estudo mineralogico e metalogenetico do deposito manganesifero de Soloviejo, Huelva, Espanha, Unpublished Master Thesis, University Lisboa, 134 pp.

Kelley, D.S., Früh-Green, G.L., 2001. Volatile lines of descent in submarine plutonic environments: insights from stable isotope and fluid inclusion analyses. Geochimica et Cosmochimica Acta 65, 3325–3346.

Kwak, T.A.P., 1986. Fluid inclusions in skarns. Journal of Metamorphic Geology 4, 363–384.

Large, R.R., Blundell, D.J. (Eds.), 2000. Database on Global VMS Districts. CODES-GEODE. University of Tasmania, Australia. 179 pp.

Leistel, J.M., Marcoux, E., Deschamps, Y., 1998a. Chert in the Iberian Pyrite Belt. Mineralium Deposita 33, 59–81.

Leistel, J.M., Marcoux, E., Thieblemont, D., Quesada, C., Sánchez, A., Almodóvar, G.R., Pascual, E., Sáez, R., 1998b. The volcanic-hosted massive sulphide deposits of the Iberian Pyrite Belt. Review and preface to the special issue. Mineralium Deposita 33, 2–30.

Lentz, D.R., 1999. Petrology, geochemistry and oxygen isotope interpretation of felsic volcanic and related rocks hosting the Brunswick 6 and 12 massive sulfide deposits (Brunswick Belt), Bathurst Mining Camp, New Brunswick, Canada. Economic Geology 94, 57–86.

Levin, V., Park, J., Brandon, M.T., Menke, W., 2000. Thinning of the upper mantle during late Paleozoic Appalachian orogenesis. Geology 28, 239–242.

Lydon, J.W., 1996. Characteristics of volcanogenic massive sulphide deposits: interpretations in terms of hydrothermal convection systems and magmatic hydrothermal systems. Boletin Geologico y Minero 107, 15–64.

MacCready, T., Goleby, B.R., Goncharov, A., Drummond, B.J., Lister, G.S., 1998. A framework of overprinting orogens based on interpretation of the Mount Isa deep seismic transect. Economic Geology 93, 1422–1434.

Marcoux, E., 1998. Lead isotope systematics in the giant massive sulphide deposits in the Iberian Pyrite belt. Mineralium Deposita 33, 45–58.

Mark, G., Oliver, N.H.S., Foster, D.R.W. (Eds.), 2001. Mineralisation, Alteration and Magmatism in the Eastern Fold Belt, Mount Isa Block, Australia: Geological Review and Field Guide, Geological Society of Australia, Specialist Group in Economic Geology, vol. 5. 121 pp.

Marschik, R., Fontboté, L., 1996. Copper-(iron) mineralization and superposition of alteration events in the Punta del Cobre belt, Northern Chile in Andean copper deposits: new discoveries, mineralization, styles and metallogeny. In: Camus, F., Sillitoe, R.H., Peterson, R. (Eds.), Andean Copper Deposits: New Discoveries, Mineralization, Styles, and Metallogeny, Society of Economic Geologists Special Publication no. 5, pp. 171–190.

Martínez, C., Tornos, F., Casquet, C., Galindo, C., 2005. The Aguablanca Ni-(Cu-PGE) deposit, SW Spain. Box 4-1, Ore Geology Reviews 27, 164–165 (this volume).

Martínez Catalán, J.R., Arenas, R., Díaz García, F., Abati, J., 1997. Variscan accretionary complex of NW Iberia: terrane correlation and succession of tectonothermal events. Geology 25, 1103–1106.

Martinsson, O., 2003. Characterisation of iron mineralisations of Kiruna type in the Kiruna area, northern Sweden. In: Eliopoulos, D.G., et al., (Eds.), Mineral Exploration and Sustainable Development. Millpress, Rotterdam, pp. 1087–1090.

Mateus, A., Jesus, A.P., Oliveira, V., Gonçalves, M.A., Rosa, C., 2001. Vanadiferous iron–titanium ores in Gabbroic Series of the Beja Igneous Complex, Odivelas, Portugal. Remarks on their possible economic interest. Estudos Notas e Trabalhos do Instituto Geológico e Mineiro 43, 3–16.

Mathez, E.A., 1989. Vapor associated with mafic magma and controls on its composition. In: Whitney, J.A., Naldrett, A.J. (Eds.), Ore Deposition Associated with Magmas, Reviews in Economic Geology, vol. 4, pp. 21–44.

Mathur, R., Ruiz, J., Tornos, F., 1999. Age and sources of the ore at Tharsis and Rio Tinto, Iberian Pyrite belt, from Re–Os isotopes. Mineralium Deposita 34, 790–793.

Matte, P., 1986. Tectonics and plate tectonics model for the Variscan belt of Europe. Tectonophysics 126, 329–374.

Matte, P., 2001. The Variscan collage and orogeny (480–290 Ma) and the tectonic definition of the Armorican microplate: a review. Terra Nova 13, 122–128.

Mitchell, A.H.G., 1992. Andesitic arcs, epithermal gold and porphyry-type mineralization in the western Pacific and eastern Europe. Transactions-Institution of Mining and Metallurgy. Section B. Applied Earth Science 101, 125–138.

Mitjavila, J., Martí, J., Soriano, C., 1997. Magmatic evolution and tectonic setting of the Iberian Pyrite Belt volcanism. Journal of Petrology 38, 727–755.

Montero, P., Salman, K., Bea, F., Azor, A., Expósito, I., Lodeiro, F., Martínez Poyatos, D., Simancas, F., 2000. New data on the geochronology of the Ossa Morena Zone, Iberian Massif Variscan. Appalachian dynamics: the building of the Upper Paleozoic Basement. Abstracts 15th International Conference on Basement Tectonics, Galicia, vol. 2000, pp. 136–138.

Moreno, C., 1993. Postvolcanic Paleozoic of the Iberian Pyrite Belt: an example of basin morphologic control on sediment distribution in a turbidite basin. Journal of Sedimentary Petrology 63, 1118–1128.

Moreno, C., Sierra, S., Sáez, R., 1996. Evidence for catastrophism at the Famennian–Dinantian boundary in the Iberian Pyrite Belt. In: Strogen, P., Somerville, I.D., Jones, G.L. (Eds.), Recent Advances in Lower Carboniferous Geology, Geological Society, London, Special Publications no. 107, pp. 153–162.

Mullane, E., 1998. The geochemistry of the South Portuguese Zone, Spain and Portugal. Unpublished PhD thesis University Southampton, 234 pp.

Munhá, J., 1983. Hercynian magmatism in the Iberian Pyrite Belt. Memorias Servicio. Geologico Portugal 29, 39–81.

Munhá, J., Barriga, F.J.A.S., Kerrich, R., 1986. High ^{18}O ore forming fluids in volcanic hosted base metal massive sulfide deposits: geologic, ^{18}O/^{16}O, and D/H evidence from the Iberian Pyrite Belt, Crandon, Wisconsin and Blue Hill, Maine. Economic Geology 81, 530–552.

Nägler, T., 1990. Sm–Nd, Rb–Sr and common lead isotope geochemistry on fine-grained sediments of the Iberian Massif. Unpublished PhD thesis, Swiss Federal Institute of Technology, Zurich, 139 pp.

Naldrett, A.J., 1992. A model for the Ni–Cu–PGE ores of the Noril'sk region and the application to other areas of flood basalt. Economic Geology 87, 1945–1962.

Naldrett, A.J., 1999. World class Ni–Cu–PGE deposits: key factors in their genesis. Mineralium Deposita 34, 227–240.

Noronha, F., Cathelineau, M., Boiron, M.C., Ferreira, A., 2000. Neves Corvo, a metamorphosed VMS deposit: the textural and fluid inclusion evidence. Abstracts, Metallogeny 2000, vol. 1. Université Henri Poincaré-Nancy, pp. 121–122.

Ochsner, A., 1993. U–Pb geochronology of the Upper Proterozoic–Lower Paleozoic geodynamic evolution in the Ossa Morena Zone, SW Iberia: constraints on the timing of the Cadomian orogeny. Unpublished PhD thesis, Swiss Federal Institute of Technology Zurich, 249 pp.

Oliveira, J.T., 1990. South Portuguese Zone: introduction. Stratigraphy and synsedimentary tectonism. In: Martínez, E., Dallmeyer, R.D. (Eds.), Pre-Mesozoic Geology of Iberia. Springer-Verlag, Berlin, pp. 333–347.

Oliveira, J.T., Quesada, C., 1998. A comparison of stratigraphy, structure and paleogeography of the South Portuguese Zone and Southwest England, European Variscides. Annual Conference of the Ussher Society 9, 141–150.

Oliveira, J.T., Pacheco, N., Carvalho, P., Ferreira, A., 1997. The Neves Corvo Mine and the Paleozoic Geology of Southwest Portugal Geology and VMS deposits of the Iberian Pyrite Belt. Society of Economic Geologists Fieldbook Series 27, 21–71.

Oliveira, J.T., Pereira, Z., Carvalho, P., Pacheco, N., Korn, D., 2004. Stratigraphy of the tectonically imbricated lithological succession of the Neves Corvo mine area, Iberian Pyrite Belt, Portugal. Mineralium Deposita 39, 422–436.

Oliver, N.H.S., Holcombe, R.J., Hill, E.J., Pearson, P.J., 1991. Tectono-metamorphic evolution of the Mary Kathleen fold belt, northwest Queensland: a reflection of mantle plume processes? Australian Journal of Earth Sciences 38, 425–455.

Oppliger, G.L., Murphy, J.B., Brimhall, G.H., 1997. Is the ancestral Yellowstone hotspot responsible for the Tertiary Carlin mineralization in the Great Basin of Nevada? Geology 25, 627–630.

Ordoñez, B., 1998. Geochronological studies of the Pre-Mesozoic basement of the Iberian Massif: the Ossa Morena Zone and the allocthonous complexes within the Central Iberian Zone. Unpublished PhD thesis, Swiss Federal Institute of Technology Zurich, 235 pp.

Oyárzun, R., Oyarzún, J., Ménard, J.J., Lillo, J., 2003. The Cretaceous iron belt of northern Chile: role of oceanic plates, a superplume event, and a major shear zone. Mineralium Deposita 38, 640–646.

Papunen, H., 2003. Ni–Cu sulfide deposits in mafic–ultramafic orogenic intrusions—examples from the Svecofennian areas, Finland. In: Eliopoulos, D.G., et al., (Eds.), Mineral Exploration and Sustainable Development. Millpress, Rotterdam, pp. 551–554.

Patiño Douce, A.E., Castro, A., El-Biad, M., 1997. Thermal evolution and tectonic implications of spinel-cordierite granulites from the Aracena Metamorphic Belt, Southwest Spain. Proceedings GAC/MAC Annual Meeting Ottawa, vol. 22, p. A113.

Pereira, Z., Sáez, R., Pons, J.M., Oliveira, J.T., Moreno, C., 1996. Edad devónica, Struniense de las mineralizaciones de Aznalcóllar (Faja Pirítica Ibérica) en base a palinología. Geogaceta 20, 1609–1612.

Petersen, S., Herzig, P.M., Schwartz-Schampera, U., Hannington, M.D., Jonasson, I.J., 2004. Hydrothermal precipitates associated with bimodal volcanism in the Central Bransfield Strait, Antarctica. Mineralium Deposita 39, 358–379.

Pinto, A., 1999. Estudo da textura, mineralogia e química mineral dos minérios da massa de Corvo do Jazigo de Neves Corvo. Unpublished M.Sc. Thesis, University of Lisbon, 301 pp.

Pirajno, F., 2000. Ore Deposits and Mantle Plumes. Kluwer Academic Publishers, Dordrecht. 556 pp.

Pitcher, W.S., 1993. The Nature and Origin of Granites. Blackie Academic and Professional, London. 321 pp.

Pollard, P.J., 2001. Sodic(–calcic) alteration in Fe-oxide–Cu–Au districts: an origin via unmixing of magmatic H_2O–CO_2–NaCl–$CaCl_2$–KCl fluids. Mineralium Deposita 36, 93–100.

Pollard, P.J., Taylor, R.G., Taylor, R.P., Groves, I., 1991. Petrographic and geochemical evolution of pervasively altered Bushveld granites at the Zaaiplaats Tin Mine. Economic Geology 86, 1401–1433.

Pous, J., Muñoz, G., Heise, W., Melgarejo, J.C., Quesada, C., 2004. Electromagnetic imaging of Variscan crustal structures in SW Iberia: the role of interconnected graphite. Earth and Planetary Science Letters 217, 435–450.

Quesada, C., 1998. A reappraisal of the structure of the Spanish segment of the Iberian Pyrite Belt. Mineralium Deposita 33, 31–44.

Quesada, C., Bellido, F., Dallmeyer, R.D., Gil Ibarguchi, I., Oliveira, T.J., Perez Estaun, A., Ribeiro, A., 1991. Terranes within the Iberian Massif: correlations with West Africa sequences. In: Dallmeyer, D. (Ed.), The West African Orogens and Circum Atlantic Correlations. Springer-Verlag, Berlin. pp. 267–294.

Relvas, J.M.R.S., 2000. Geology and metallogeny at the Neves Corvo deposit, Portugal. Unpublished PhD thesis, University Lisbon, Lisbon, 319 pp.

Relvas, J.M.R.S., Barriga, F.J.A.S., Bernardino, F.B.C.P., Oliveira, V.M.S., Matos, J.X., 1994. Ore zone hydrothermal alteración in drill hole IGM-LS1, at Lago Salgada, Grohat;ndola, Portugal: a first report on pyrophylite in a central stockwork. Boletín Sociedad Española de Mineralogía 17, 157–158.

Relvas, J.M.R.S., Tassinari, C.C.G., Munhá, J., Barriga, F.J.A.S., 2001. Multiple sources for ore forming fluids in the Neves Corvo VHMS deposit of the Iberian Pyrite Belt, Portugal. Strontium, neodymium and lead isotope evidence. Mineralium Deposita 36, 416–427.

Relvas, J.M.R.S., Barriga, F., Pinto, A., Ferreira, A., Pacheco, N., Noiva, P., Barriga, G., Baptista, R., Carvalho, D., Oliveira, V., Munhá, J., Hutchinson, R.W., 2002. The Neves Corvo deposit, Iberian Pyrite Belt, Portugal: impacts and future 25 years after the discovery. In: Goldfarb, R., Nielsen, J. (Eds.), Integrated Methods for Discovery: Global Exploration in the 21st Century, SEG Special Publication, vol. 9, pp. 155–176.

Relvas, J.M.R.S., Barriga, F.J.A.S., Ferreira, A., Noiva, P.C., Pacheco, N., Barriga, G., in press-a. Hydrothermal alteration, replacement ore-forming mechanisms, chemical evolution and syn and post-ore deformation in the Corvo orebody, Portugal. Economic Geology.

Relvas, J.M.R.S., Barriga, F.J.A.S., Longstaffe, F., in press-b. Tin and base metal mineralization in the Neves Corvo volcanic-hosted massive sulfide deposit, Portugal: genetic implications from ore geochemistry and oxygen–hydrogen- and carbon-isotope data. Economic Geology.

Rodríguez, R.M., Díez, A., Leyva, F., Matas, J., Almarza, J., Donaire, M., 2002. Datación palinoestratigráfica del volcanismo en la sección de la Ribera del Jarama, Faja Pirítica Ibérica, Zona Surportuguesa. Geogaceta 32, 247–250.

Rosa, C.P.J., McPhie, J., Relvas, J.M.R.S., 2004a. Architecture of felsic volcanic succession hosting massive sulfide deposits in the Iberian Pyrite Belt, Portugal. In: McPhie, J., McGlodrick, P. (Eds.), Abstracts Volume 17th Australian Geological Convention, Hobart, p. 288.

Rosa, D.R.N., Inverno, C.M.J., Oliveira, V.M.J., Rosa, C.J.P., 2004b. Geochemistry of volcanic rocks, Albernoa area, Iberian Pyrite Belt. International Geological Review 46, 366–383.

Ryan, B., 2000. The Nain Churchill boundary and the Nain plutonic suite: a regional perspective on the geologic setting of the Voisey's Bay Ni–Cu–Co deposit. Economic Geology 95, 703–724.

Sáez, R., Almodóvar, G.R., Pascual, E., 1996. Geological constraints on massive sulphide genesis in the Iberian Pyrite Belt. Ore Geology Reviews 11, 429–451.

Sáez, R., Pascual, E., Toscano, M., Almodóvar, G.R., 1999. The Iberian type of volcano-sedimentary massive sulphide deposits. Mineralium Deposita 5, 549–570.

Sánchez España, F.J., Velasco, F., Boyce, A., Fallick, A.E., 2000. High $\delta^{18}O$ and low δD ratios of stringer systems of the northernmost IPP VHMS deposits: evidence for a magmatic input to the hydrothermal ore-forming fluids? Cuadernos do Laboratorio Xeolóxico de Laxe 25, 131–134.

Sánchez España, F.J., Velasco, F., Boyce, A.J., Fallick, A.E., 2003. Source and evolution of ore-forming hydrothermal fluids in the northern Iberian Pyrite Belt massive sulphide deposits, SW Spain. Evidence from fluid inclusions and stable isotopes. Mineralium Deposita 38, 519–537.

Sanderson, D.J., Zhang, X., 1999. Critical stress localization of flow associated with deformation of well-fractured rock masses, with implications for mineral deposits. In: McCaffrey, K.J.W., Lonergan, L., Wilkinson, J.J. (Eds.), Fractures, Fluid Flow and Mineralization, Geological Society, London, Special Publications no. 155, pp. 69–81.

Schäfer, H.J., 1990. Geochronological investigations in the Ossa Morena Zone, SW Spain. Unpublished PhD thesis, Swiss Federal Institute Technology Zurich, 153 pp.

Schofield, I., D'Lemos, R.S., 2000. Granite petrogenesis in the Gander Zone, NE Newfoundland: mixing of melts from multiple sources and the role of lithospheric delamination. Canadian Journal of Earth Sciences 37, 535–547.

Schutz, W., Ebneth, J., Meyer, K.D., 1987. Trondhjemites, tonalites and diorites in the South Portuguese Zone and their relations to the vulcanites and mineral deposits of the Iberian Pyrite Belt. Geologische Rundschau 76, 201–212.

Serrano Pinto, M., Casquet, C., Ibarrola, E., Corretgé, L.G., Portugal Ferreira, M., 1988. Sintese geocronologica dos granitoides do Macizo Hespérico. Geología de los Granitoides y Rocas Asociadas del Macizo Hespérico. Rueda publishers, Madrid, pp. 69–86.

Shengao, Y., Zhaochiong, Z., Denghong, W., Bailin, C., Lixin, H., Gang, Z., 2003. Kalatongke magmatic copper–nickel sulfide deposit. In: Mao, J., Gordfarb, R.J., Seltmann, R., Wang, D., Xiao, W., Hart, C. (Eds.), Tectonic Evolution and the Metallogeny of the Chinese Altay and Tianshan, IAGOD Guidebook Series, vol. 10, pp. 131–151.

Sheppard, S.M.F., 1986. Characterization and isotopic variations in natural waters. In: Valley, J.W., Taylor, H.P., O'Neil, J.R. (Eds.), Stable Isotopes in High Temperature Geological Processes, Reviews in Mineralogy, vol. 16, pp. 165–184.

Silva, J.B., Oliveira, J.T., Ribeiro, A., 1990. Structural outline of the South Portuguese Zone. In: Martínez, E., Dallmeyer, R.D. (Eds.), Pre-Mesozoic Geology of Iberia. Springer-Verlag, Berlin, pp. 348–362.

Simancas, J.F., 1983. Geología de la extremidad oriental de la Zona Sud Portuguesa. Unpublished PhD thesis, Universidad de Granada, 447 pp.

Simancas, J.F., Carbonell, R., Gonzalez Lodeiro, F., Perez Estaun, A., Juhlin, C., Ayarza, P., Kashubin, A., Azor, A., Martínez Poyatos, D., Almodóvar, G.R., Pascual, E., Sáez, R., Exposito, I., 2003. Crustal structure of the transpressional Variscan orogen of SW Iberia: SW Iberia deep seismic reflection profile (IBERSEIS). Tectonics 22, 1063–1078.

Skirrow, R.G., Walshe, J.L., 2002. Reduced and oxidized Au–Cu–Bi iron oxide deposits of the Tennant Creek Inlier, Australia: an integrated geological and chemical model. Economic Geology 97, 1167–1202.

Solomon, M., Quesada, C., 2003. Zn–Pb–Cu massive sulphide deposits: brine pool types occur in collisional orogens, black smoker types in backarc and/or arc basins. Geology 31, 1029–1032.

Solomon, M., Tornos, F., Gaspar, O.C., 2002. Explanation for many of the unusual features of the massive sulfide deposits of the Iberian Pyrite Belt. Geology 30, 87–90.

Solomon, M., Tornos, F., Large, R.R., Badham, J.N.P., Both, R.A., Zaw, Khin, 2004. Zn–Pb–Cu volcanic-hosted massive sulphide deposits: criteria for distinguishing brine pool-type from black smoker-type sulphide deposition. Ore Geology Reviews 25, 259–283.

Soriano, C., Martí, J., 1999. Facies analysis of volcano-sedimentary successions hosting massive sulfide deposits in the Iberian Pyrite Belt, Spain. Economic Geology 94, 867–882.

Taylor, C., Premo, W., Leventhal, J., Meier, A., Johnson, C., Newkirk, S., Hall, T., Lear, K., Harris, A., 1999. The Greens Creek deposit, southeastern Alaska: a VMS–SEDEX hybrid. In: Stanley, C.J., et al., (Eds.), Mineral Deposits: Processes to Processing. Balkema, Rotterdam, pp. 597–600.

Thieblemont, D., Pascual, E., Stein, G., 1998. Magmatism in the Iberian Pyrite Belt: petrological constraints on a metallogenic model. Mineralium Deposita 33, 98–110.

Tornos, F., 2005. Environment of formation and styles of volcanogenic massive sulfides: the Iberian Pyrite Belt. Ore Geology Reviews.

Tornos, F., Casquet, C., 2005. A new scenario for IOCG and Ni–(Cu) mineralisation: the relationship with giant midcrustal mafic sills, Variscan Iberian Massif. Terra Nova 17, 286–290.

Tornos, F., Chiaradia, M., 2004. Plumbotectonic evolution of the Ossa Morena Zone, Iberian Peninsula: tracing the influence of mantle–crust interaction in ore forming processes. Economic Geology 99, 965–985.

Tornos, F., Spiro, B.F., 1999. The genesis of shale-hosted massive sulphides in the Iberian Pyrite Belt. In: Stanley, C., et al., (Eds.), Mineral Deposits: Processes to Processing. Balkema, Rotterdam, pp. 605–608.

Tornos, F., Velasco, F., 2002. The Sultana orebody, Ossa Morena Zone, Spain. Insights into the evolution of Cu–(Au–Bi) mesothermal mineralization. Unpublished abstracts GEODE Study Centre, Grenoble, 25–28 Oct 2002, 2 pp.

Tornos, F., Gonzalez Clavijo, E., Spiro, B.F., 1998. The Filón Norte orebody (Tharsis, Iberian Pyrite Belt): a proximal low-temperature shale-hosted massive sulphide in a thin-skinned tectonic belt. Mineralium Deposita 33, 150–169.

Tornos, F., Casquet, C., Galindo, C., Velasco, F., Canales, A., 2001. A new style of Ni–Cu mineralization related to magmatic breccia pipes in a transpressional magmatic arc, Aguablanca, Spain. Mineralium Deposita 36, 700–706.

Tornos, F., Casquet, C., Relvas, J., Barriga, F., Sáez, R., 2002. The relationship between ore deposits and oblique tectonics: the SW Iberian Variscan Belt. In: Blundell, D., Neubauer, F., von Quadt, A. (Eds.), The Timing and Location of Major Ore Deposits in an Evolving Orogen, Geological Society, London, Special Publications no. 204, pp. 179–198.

Tornos, F., Casquet, C., Galindo, C., 2003. Hydrothermal iron oxide (–Cu–Au) mineralization in SW Iberia: evidence for a multiple origin. In: Eliopoulos, D.G., et al., (Eds.), Mineral

Exploration and Sustainable Development. Millpress, Rotterdam, pp. 395–398.

Tornos, F., Inverno, C., Casquet, C., Mateus, A., Ortiz, G., Oliveira, V., 2004a. The metallogenic evolution of the Ossa Morena Zone. Journal of Iberian Geology 30, 143–180.

Tornos, F., Iriondo, A., Casquet, C., Galindo, C., 2004b. Geocronología Ar–Ar de flogopitas del stock de Aguablanca (Badajoz). Implicaciones sobre la edad del plutón y de la mineralización de Ni–(Cu) asociada. Geotemas 6, 189–192.

Tornos, F., Simonov, V., Kovyazin, S., 2004c. Melt inclusions in quartz from subvolcanic sills of the Iberian Pyrite Belt: implications for magma evolution and hydrothermal alteration. Boletín Sociedad Española de Mineralogía 26, 93–106.

Tornos, F., Casquet, C., Rodriguez Pevida, L., Velasco, F., 2005. The Iron Oxide–(Cu–Au) Deposits of SW Iberia. Box 4-2, Ore Geology Reviews 27, 166–167 (this volume).

Tornos, F., Solomon, M., Conde, C., in press. The formation of the Tharsis massive sulfide deposit on the seafloor, Iberian Pyrite Belt: evidence for deposition in a brine pool from geology, host-rock compositions, and stable isotope data. Economic Geology.

Velasco, F., Amigó, J.M., 1981. Mineralogy and origin of the skarn from Cala, Huelva (Spain). Economic Geology 76, 719–727.

Velasco, F., Sánchez España, F.J., Boyce, A., Fallick, A.E., Sáez, R., Almodóvar, G.R., 1998. A new sulphur isotopic study of some Iberian Pyrite Belt deposits: evidence of a textural control on some sulphur isotope compositions. Mineralium Deposita 34, 1–18.

Velasco, F., Sánchez España, F.J., Yanguas, A., Tornos, F., 2000. The occurrence of gold in the sulfide deposits of the Iberian Pyrite Belt: evidence of precious metal remobilisation. In: Gemmell, J.B., Pongratz, J. (Eds.), Volcanic Environments and Massive Sulfide Deposits, Program and Abstracts, CODESUniversity of Hobart, Australia, pp. 221–223.

Villas, R.N., Norton, D., 1977. Irreversible mass transfer between circulating hydrothermal fluids and the Mayflower stock. Economic Geology 72, 1471–1504.

Weihed, P., Eilu, P., 2003. Gold, Fe oxide–Cu–Au and VMS metallogeny of the Fennoscandinavian shield. In: Eliopoulos, D.G., et al., (Eds.), Mineral Exploration and Sustainable Development. Millpress, Rotterdam, pp. 1123–1126.

Weihed, P., Arndt, N., Billström, K., Duchesne, J-C., Eilu, P., Martinsson, O., Papunen, H., Raimo Lahtinen, R., 2005. Precambrian geodynamics and ore formation: the Fennoscandian Shield. In: Blundell, D., Arndt, N., Cobbold, P., Heinrich, C. (Eds.), Geodynamics and Ore Deposit Evolution. Ore Geology Reviews 27, 273–322 (this volume).

Zartman, R.E., Doe, B.R., 1981. Plumbotectonics—the model. Tectonophysics 75, 135–162.

Zengqian, H., Hongwen, M., Zaw, K., Yuquan, Z., Mingjie, W., Zeng, W., Guitang, P., Renli, T., 2003. The Himalayan Yulong porphyry copper belt: product of large scale strike slip faulting in the Eastern Tibet. Economic Geology 98, 125–146.

Mineralizaciones de magnetita asociadas a skarns y bandas de cizalla: La mina de Cala (Huelva)

Magnetite deposits related with skarns and shear zones: The Cala mine (Huelva)

J. Carriedo [1], F. Tornos [1], F. Velasco [2] y A. Terrón [3]

[1] Instituto Geológico y Minero de España, Azafranal 48, 37001 Salamanca. j.carriedo@igme.es
[2] Departamento de Petrología y Mineralogía, Universidad del País Vasco, Apdo. 644, Bilbao
[3] Río Narcea Nickel S.A., Avda. de la Estación 22 bajo, 06300 Zafra (Badajoz)

ABSTRACT

The Cala iron deposit has been traditionally regarded as a classic iron skarn developed on Cambrian limestone adjacent to a Variscan monzogranitic stock. Ongoing studies show that the geologic setting is more complex and the mineralization is replacive on marble and calcsilicate and pelitic hornfels and controlled by syntectonic hydrothermal activity with a pull-apart structure. The skarn only forms a part of the hydrothermal alteration. Most of the magnetite is related to an biotite-quartz-ankerite-chlorite assemblage, while the pyrite-chalcopyrite ore seems to be slightly younger, replacing magnetite along extensional structures, sharing many features with the IOCG style of mineralization.

Key words: Ossa Morena Zone, Cala, replacement, IOCG, skarn.

Introducción

La mina de Cala se sitúa en el norte de la provincia de Huelva (hoja 1/50.000, 918), próxima al límite con la provincia de Badajoz. Esta mina es la última en actividad de la denominada provincia de hierros del SO, que ha sido trabajada intermitentemente desde 1901 hasta la actualidad; la máxima producción fue en 1975 con 610000 t de todo uno. Actualmente, es explotada por la empresa PRESUR, que extrae pequeñas cantidades de magnetita de alta calidad y áridos. Río Narcea Nickel SA está evaluando el depósito y definiendo zonas de alta ley en cobre y oro. No hay estimaciones fiables sobre el tonelaje total y reservas del depósito. El único estudio existente indica que en 1988 había cubicados 29 Mt con 39%Fe y 0.27%Cu.

El depósito se ubica en el flanco sur del antiforme Olivenza-Monesterio, flanco inverso compuesto por materiales del Cámbrico Inferior de naturaleza detrítica-carbonatada, y cerca del contacto con un pequeño (0.6 km^2) *stock* Varisco de naturaleza granodiorítica- monzogranítica. La mineralización de Cala ha sido considerada como un ejemplo típico de un skarn cálcico de hierro (Velasco, 1976; Casquet y Velasco, 1978; Casquet y Tornos,
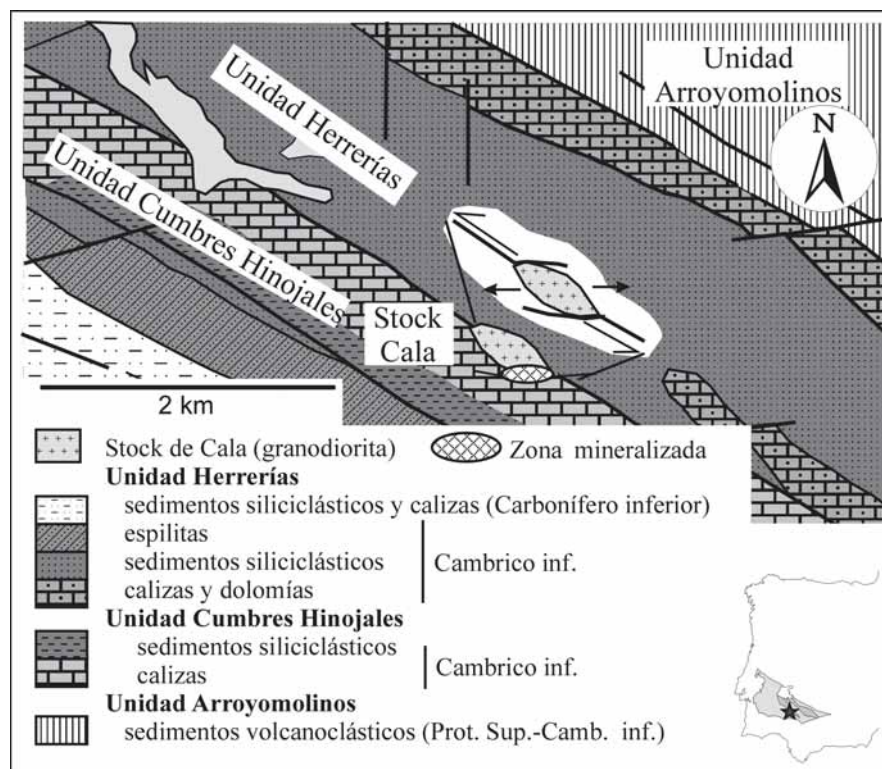

Fig. 1.- Contexto geológico esquemático de las inmediaciones de la mina de Cala, mostrando la relación de la mineralización e intrusión con una pequeña zona de *pull-apart* (modificado de Tornos *et al*., 2002).

Fig. 1.- Schematic geological setting of the Cala deposit, showing the relationship of the orebody and the intrusion with an small a pull apart structure (modified from Tornos et al., 2002).
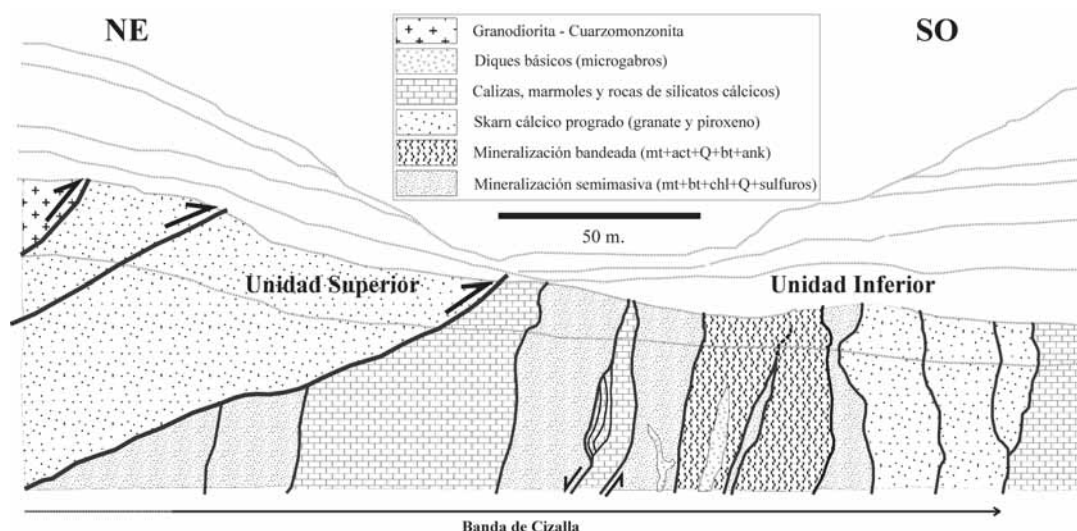
NE   SO

	Granodiorita - Cuarzomonzonita
	Diques básicos (microgabros)
	Calizas, marmoles y rocas de silicatos cálcicos
	Skarn cálcico progrado (granate y piroxeno)
	Mineralización bandeada (mt+act+Q+bt+ank)
	Mineralización semimasiva (mt+bt+chl+Q+sulfuros)

50 m.

Unidad Superior   Unidad Inferior

Banda de Cizalla

Fig. 2.- Corte esquemático mostrando la estructura general del yacimiento. Obsérvese que dentro de la banda de cizalla, los contacto litológicos están controlados por fallas.

Fig. 2.- Schematic section showing the general structure of the deposit. Notice that the lithologic contacts in the shear zone are controlled by faults.

1991). Sin embargo, un estudio de detalle sugiere que el skarn s.s. solo forma una parte de la mineralización y que la mayor parte de ésta tiene características similares a las de las partes someras de depósitos de tipo IOCG, con un importante control estructural (Tornos y Casquet, 2005).

Geología del depósito

En detalle, el depósito se encuentra en el contacto entre una pequeña estructura de tipo *pull apart* (Fig. 1) desarrollada en un contacto mayor de la Zona de Ossa Morena, una zona de cizalla senestra que pone en contacto la pizarra de la Unidad de Herrerías con la caliza, roca de silicatos cálcicos y pizarra de la Unidad de Cumbres-Hinojales (Tornos *et al.*, 2002). Esta estructura extensional ha favorecido el desarrollo de una importante actividad hidrotermal y la intrusión del Stock de Cala. La intrusión ha generado un intenso metamorfismo de contacto, dando lugar a corneana pelítica y calcosilicatada.

La zona mineralizada tiene una dirección NO-SE y una potencia de hasta 130 m. Cuenta con unos 1.100 m de longitud y pasa lateralmente a rocas aparentemente inalteradas y estériles; sólo localmente se ha observado la presencia de niveles estratoides de hematites y siderita de origen y significado desconocidos.

La morfología original de la mineralización está trastocada por cabalgamientos tardíos vergentes al SO, que han modificado casi completamente el contacto entre las rocas graníticas y el encajante (Fig. 2 y 3). Este hecho nos ha permitido establecer dos zonas diferentes: (1) La *Unidad Inferior*, que comprende una secuencia heterogénea de rocas cámbricas variablemente alteradas hidrotermalmente y deformadas. El skarn es poco abundante y presenta signos de deformación. La mineralización se presenta como tres lentejones discontinuos y subverticales de dirección N120-140ºE, siempre controlada por estructuras subparalelas a la cizalla. (2) La *Unidad Superior*, que engloba el Stock de Cala y un extenso skarn cálcico, fundamentalmente progrado. Ni el intrusivo ni el skarn muestran signos evidentes de deformación. Aquí, la mineralización de magnetita se haya preferentemente relacionada con la facies retrógrada del skarn.

La roca ígnea dominante es una granodiorita a monzogranito biotítico de grano medio a grueso, que parece ser un pequeño *offset* del cercano plutón de Santa Olalla, datado en 341±3 Ma (Romeo *et al.*, 2004) o 347±5 Ma (Spiering *et al.*, 2005). Su emplazamiento fue a presiones cercanas a 0.5 kb (Velasco y Amigó, 1981) y ha generado una importante aureola de metamorfismo de contacto super-
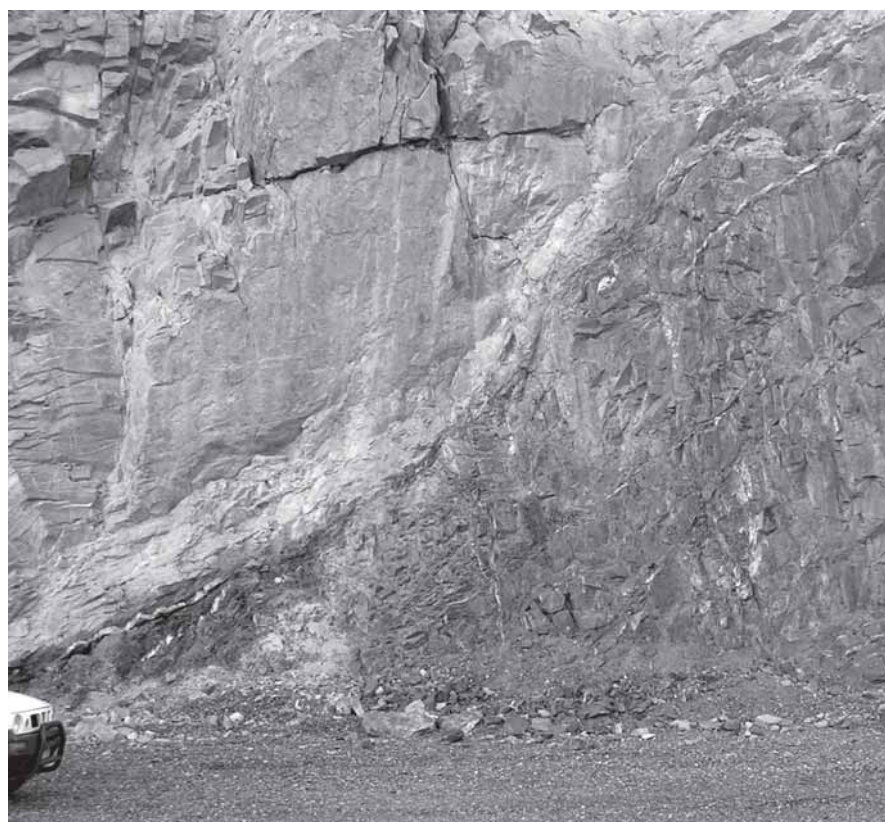

Fig. 3.- Cabalgamiento que pone en contacto el intrusivo granodiorítico (gris claro) con magnetita semimasiva asociada a la cizalla.

Fig. 3.- Thrusting of granodiorite on the shear-controlled semimassive magnetite.

puesto al regional de grado muy bajo. El granitoide muestra una intensa alteración potásica con desarrollo de biotita y feldespato K. Cerca del contacto es cortada por una alteración ácida de tipo greisen (cuarzo-moscovita) controlada por estructuras extensionales subhorizontales y que están rellenas por cuarzo, ankerita y clorita. Cuando el contacto es intrusivo se observa una zona cm a dm de endoskarn de clinoanfíbol, epidota y magnetita.

La Unidad Superior está poco deformada. Sin embargo, la Unidad Inferior engloba a una amplia banda de cizalla subvertical de unos 200 m de potencia, con abundantes estructuras SC y pliegues en vaina que indican un movimiento polifásico complejo. Ésta muestra una deformación de dúctil a frágil con predominio del desgarre senestro, pero también se reconocen estructuras indicativas de movimiento dextral y normal con hundimiento hacia el NE. Fuera de la zona mineralizada no se han encontrado evidencias de deformación, quedando la banda de cizalla restringida al contacto entre las dos unidades. Dentro de la zona de cizalla se reconocen rocas variablemente alteradas y siempre mineralizadas, pero poco skarn. Solo hay restos de un skarn granatítico residual, así como abundantes diques de microgabro.

En la mina hay grandes zonas de caliza remplazada por dolomía. Sin embargo, esta roca nunca es skarnificada.

La alteración hidrotermal y la mineralización de magnetita

La mineralización de magnetita aparece asociada al skarn (Unidad Superior) o controlada por estructuras (Unidad Inferior). En el primer caso, la caliza y corneana calcosilicatada están variablemente remplazadas por un skarn cálcico progrado clásico a favor de contactos litológicos, con desarrollo preferente de un skarn piroxénico (salita) sobre la roca de silicatos cálcicos y de granate (ad_{48-50}) sobre la caliza. No obstante, el tipo de skarn desarrollado no es función del encajante. La zona de granate es la dominante y es, a su vez, progradante sobre la piroxénica. Este skarn conserva el bandeado original del protolito.

El skarn retrógrado se concentra en la zona sudeste del depósito, pero es minoritario si se compara con el de sistemas similares. Está formado por clinoanfíbol y magnetita aunque son comunes los rellenos vacuolares en la granatita, formados por actinolita-Fe pargasita, epidota, calcita y cuarzo.

En la Unidad Inferior casi no hay skarn y la mineralización generalmente remplaza directamente a los protolitos inalterados. Aquí, la magnetita forma grandes lentejones discontinuos dentro de la banda de cizalla. Aunque la mineralización es generalmente masiva, localmente se reconocen estructuras bandeadas típicas de bandas de cizalla y relacionadas con una deformación polifásica. Las zonas más mineralizadas corresponden a zonas de intersección de fracturas o en pequeñas zonas extensionales. En esta unidad son muy comunes diques de microgabro.

La magnetita está intercrecida con proporciones muy variables de cuarzo, actinolita, ankerita y clorita; hay posible albita residual. Esta roca hidrotermal remplaza directamente a la corneana pelítica y de silicatos cálcicos. La caliza es remplazada por una mineralización bandeada y brechoide de magnetita y ankerita

La mineralización de Cu-(Au)

En relación con la magnetita, bien remplazando, bien en venillas cortantes, aparecen abundantes sulfuros, fundamentalmente pirita. En menor proporción existen calcopirita, pirrotita y, esporádicamente, oro nativo. La mineralización de cobre-oro también tiene un importante control estructural, y se deposita a favor de planos de deformación o de tensión dentro de las zonas con mayor deformación (Fig. 4). Algunas de
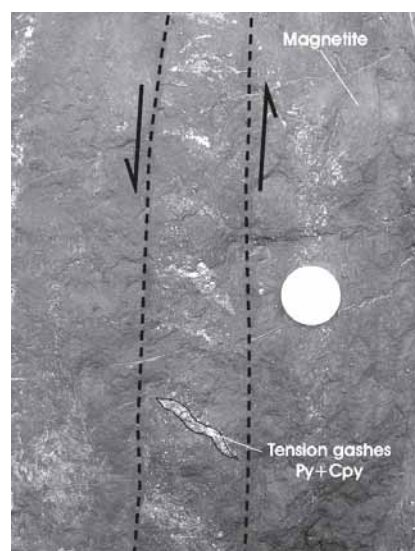

Fig. 4.- Grietas de tensión relacionadas con el movimiento de cizalla rellenas por sulfuros.

Fig. 4.- Tensión gashes shear zone related infilled by sulphides.

estas estructuras están a su vez deformadas sugiriendo que los sulfuros fueron sincrónicos con la deformación y sólo ligeramente posteriores a la precipitación de la magnetita. En general, las zonas enriquecidas en cobre son las más cercanas a la roca ígnea (Velasco y Amigó, 1981) y se encuentran en la Unidad Superior.

En el extremo occidental del depósito se localiza un filón de dirección N120-150ºE hasta un metro de potencia y relleno de cuarzo, ankerita, calcopirita e importantes contenidos en oro (Filón del Portugués) que parece ser similar a la mineralización de Cu-(Bi-Au) de la cercana Mina Sultana (Tornos y Velasco, 2002). Este filón y otros similares que se encuentran dispersos por el depósito y parecen ser posteriores a la mineralización anterior.

Aspectos geoquímicos

Los datos preliminares de isótopos de azufr e (d^{34}S, 14.3-16.5‰) sugieren que el azufre de los sulfuros proviene predominantemente de la secuencia sedimentaria y no tiene un origen magmático. Los isótopos de oxígeno indican que el skarn progrado se formó a partir de fluidos isotópicamente pesados (10-11.5‰), de posible origen magmático o metamórfico, mientras que la composición isotópica del anfíbol del skarn sugiere la presencia de fluidos meteóricos que se mezclaron con los anteriores. Sin embargo, la magnetita de la Unidad Inferior tiene composiciones inusualmente enriquecidas en ^{18}O (3.2 a 5.7‰), sugiriendo que precipitó de fluidos isotópicamente pesados (>10‰) y a altas temperaturas (>500ºC) y, por lo tanto, a partir de fluidos similares a los que dieron lugar al skarn progrado y no al retrógrado, confirmando su independencia del mismo.

Discusión y conclusiones

La mineralización de magnetita-(cobre-oro) de Cala muestra relaciones complejas con el Stock de Cala asociado. La mineralización de la Unidad Superior parece ser un típico skarn cálcico pero la de la Unidad Inferior muestra un importante control estructural, indicando que un simple proceso de skarn perimagmático no es el responsable de toda la mineralización. El aspecto relativamente indeformado de la roca ígnea aflorante, así como del skarn cálcico asociado, sugiere que se trata de un proceso posterior al desarrollo de la alteración hidrotermal y mineralización de la Unidad Inferior. Estos estarían bien relacionados con una intrusión más pro-

funda, bien ligados a la zona de cizalla regional que ha canalizado fluidos profundos hasta este ambiente somero. La presencia de diques de microgabro sugiere que la cizalla fue de importancia regional e implica condiciones localmente extensionales.

La magnetita probablemente precipitó en un ambiente caliente, alcalino y parcialmente oxidado en el que los sulfuros no eran estables. A menor temperatura, el ambiente oxidado facilitó el reemplazamiento de la magnetita por los sulfuros, permitiendo la desestabilización de los complejos tiosulfurados que los acompañan. En este marco, la formación de los filones tardíos de cuarzo-ankerita son probablemente independientes de la mineralización metasomática y representan un evento hidrotermal tardío en el que el Cu-Au precipitaron por inmiscibilidad de fluidos (Tornos y Velasco, 2002).

El modelo involucra la intrusión de plutones metalumínicos ricos en agua y derivados de la interacción en la corteza media de magmas juveniles con sedimentos en facies metamórficas de grado medio-bajo. Los fluidos magmáticos ricos en CO_2-CH_4 exsueltos durante la cristalización serían canalizados a lo largo de estructuras transcrustales hasta ambientes epizonales. Los fluidos mineralizantes aprovechan sistemáticamente planos de debilidad tales como fallas o zonas extensionales dentro de la banda de cizalla para su ascenso.

A escala regional, los depósitos de la Zona de Ossa Morena reúnen muchas de las características de los depósitos de tipo IOCG (e.g., Hitzman *et al.,* 1992; Williams *et al.,* 2003), con características comunes tales como relación con bandas de cizalla, alteración Na-K generalizada, fluidos implicados isotópicamente pesados y altas temperaturas (>500ºC) entre otros.

Si se compara con otros depósitos de Fe-(Cu-Au) cercanos, la mineralización de Cala se caracteriza por la poca proporción de albita hidrotermal y predominio de biotita-clorita-siderita, la ausencia de rocas ígneas albitizadas y los relativamente elevados contenidos en Cu-Au. En este contexto, la mineralización de Cala parece haberse formado en un ambiente relativamente somero donde la alteración hidrotermal está dominada por actinolita-cuarzo-ankerita y la deformación es de carácter dúctil-frágil. Sería, por lo tanto, más epizonal que otras del área, como Colmenar, La Berrona o Monchi (Tornos *et al.,* 2005).

Agradecimientos

Referencias

Casquet,C., Velasco,F. (1978). *Estudios. Geologicos*, 34, 399-405.

Casquet, C. y Tornos, F. (1991). En: *'Skarns, their petrology and metallogeny'* (Augusthitis, Ed.). Atenas 555-591

Romeo,I., Lunar,R., Capoe,R., Dunning,G.R., Piña, R. y Ortega,L. (2004). *Macla*, 2, 29-30.

Tornos, F., Casquet, C., Relvas, J., Barriga, F. y Saez, R. (2002). En: *The timing and location major or deposits in an evolving orogen.* (D. Blundell, F. Neubauer y A. von Quadt). *Geological Society London, Special Publications* 206, 179-198

Tornos, F., Casquet, C. y Relvas, J. (2005). *Ore Geology Reviews*, 27, 133-163.

Velasco, F. y Amigo, J.M. (1981). *Economic Geology*, 76, 719-727.

Velasco, F. (1976). *Serie Universitaria, Fundación Juan march*, 3, 34 pp.

Williams, P., Guoyi, D., Pollard, P., Broman, C., Martinsson, O., Wanhainen, C., Mark, G., Ryan y C.G., Mernagh, T. (2003). En: *Mineral Exploration and Sustainable Development, Millpress Rotterdam,* (D.G. Eliopoulos Eds.). 1127-1130.

Complex structural and hydrothermal evolution of the Cala magnetite deposit, SW Iberia – an ICOG deposit?

Jorge Carriedo & Fernando Tornos
Instituto Geológico y Minero de España, c/Azafranal 48, 37992 Salamanca (Spain).

Francisco Velasco
Dpto. Petrología y Mineralogía. Universidad País Vasco, Leioa, Bilbao (Spain)

Holly Stein
AIRIE Program, Department of Geosciences, Colorado State University Fort Collins, CO 80523-1482 (USA) and Geological Survey of Norway, Leiv Eirikssons vei 39, 7491 Trondheim, Norway

ABSTRACT: The Cala deposit is traditionally regarded as a classic calcic iron skarn, formed at the contact between Cambrian limestone and a Variscan monzogranitic stock. Ongoing studies show that the deposit is more complex and the mineralization consists of several stratabound, structurally controlled, lenses replacing calc-silicate and pelitic hornfels and marbles. Although skarn is part of the hydrothermal assemblage, most of the ore appears to be related to a quartz-ankerite-biotite-chlorite assemblage, sharing many features with shallow IOCG deposits. The mineralization formed in a multiply-reactivated pull-apart structure. Re-Os dating shows that most of the magnetite-sulphide ore predated by some 20 Ma the intrusion of the adjacent monzogranite.

KEYWORDS: Ossa Morena Zone, Cala, replacement, magnetite, IOCG, skarn.

1 INTRODUCTION

The Cala deposit is located in SW Iberia (Huelva province). It was one of the most important iron producers in Spain during the 20th century. Nowadays, the mine extracts a small tonnage of high quality magnetite but most of the production consists of granite and skarn for aggregate. Estimated reserves are more than 60Mt @ 39% Fe and 0.27% Cu but the deposit is open at depth. Currently, there is growing interest in the Cala deposit and systematic exploration is taking place.

Previously, this deposit was considered to be a classic calcic iron skarn directly associated with intrusion of an adjacent intermediate stock (Casquet & Velasco 1978, Velasco & Amigó 1981, Casquet & Tornos 1991). However, recent work suggests that the situation is more complex and the intrusion-related skarn is only a part of a larger IOCG-style mineralization.

2 GEOLOGIC SETTING

The Ossa Morena Zone (OMZ) is an accretionary terrane against the autochthonous Iberian Massif. Both are characterized by a complex geodynamic history (Eguíluz *et al* 2000). The presence of two orogenic cycles, Cadomian and Variscan, has superimposed several magmatic and tectonic events (Quesada 1990; Eguíluz *et al* 2000).

The Cala mine is located in the southernmost Olivenza-Monesterio belt (Fig. 1), a NW-SE trending kilometre-scale antiformal structure. Exposed in the core are Proterozoic schist, dark slate and quartzite (Serie Negra). Both limbs host a complex sequence of late Neoproterozoic-Cambrian synorogenic and rift-related rocks, including felsic and mafic volcanites, shale, sandstone, calc-silicate rocks and limestone. The region is host to widespread calc-alkaline Variscan magmatism. This includes several composite kilometre-size plutons made up of granodiorite, monzogranite and tonalite, with variably accompanying gabbro, diorite and granite.

Most iron deposits in the OMZ occur in the late Neoproterozoic-Cambrian sequence. Some deposits are interbedded with volcanic rocks and show exhalative features. Other deposits are clearly younger (presumably Variscan), replacing the same sequence. The exact relationship between both exhalative and replacements styles of mineralization is poorly understood.
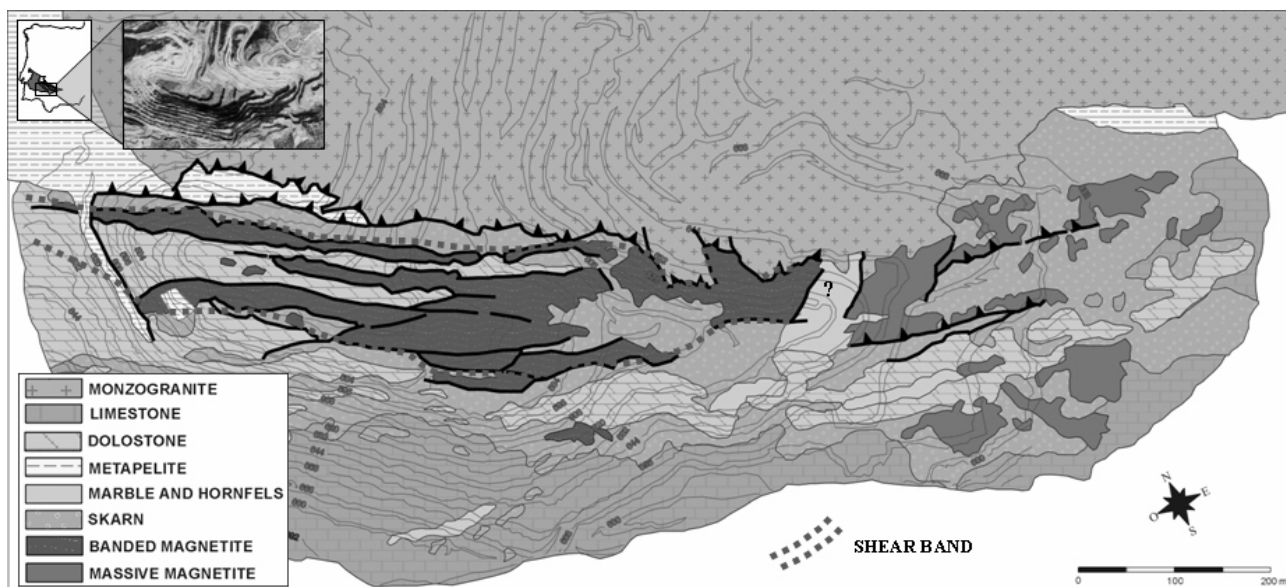
Figure 1: Geographic and geological map of the Cala Mine, showing main lithologies and structures.

In more detail, the Cala deposit is located in the southern limb of the Olivenza-Monesterio antiform, close to the major strike-slip faults that separate the OMZ from the South Portuguese Zone. The deposit itself is located within a major structural boundary and is directly adjacent to a small ellipsoidal monzogranitic stock. The stock was intruded at about 3km depth and produced an aureole of contact metamorphism (Velasco *et al* 1981). Recent U-Pb zircon dating yields an age of 352 ± 4 Ma for the Cala stock (Romeo *et al* 2006).
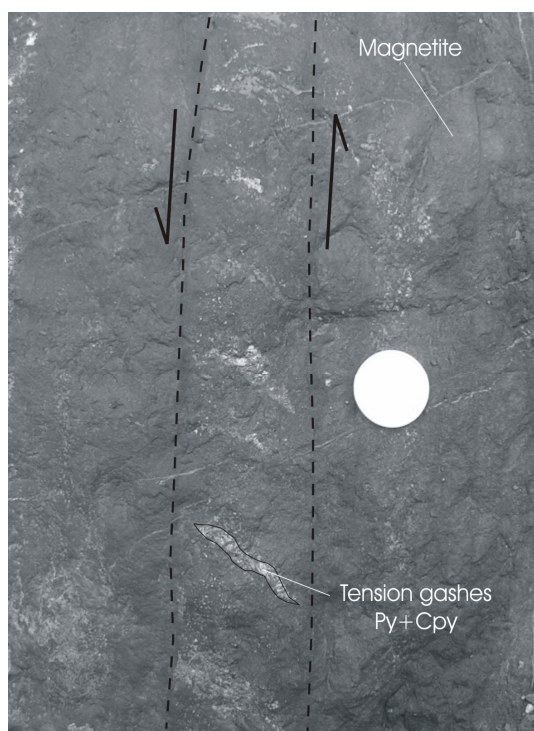

Figure 2: Tension gashes infilled by sulphides in the iron oxide mineralization

Detailed mapping has shown that both the orebody and the plutonic rocks were emplaced in a pull-apart structure formed during sinistral Variscan transpression. In detail, there are two major tectonic events:

Stage I – early sinistral brittle-ductile deformation was channeled along several 10 m-thick subvertical shear zones subparallel to the sedimentary layering; related to this event are abundant microgabbro dikes suggesting that these structures are deep regional ones.

Stage II – later N-S compression produced a system of low angle imbricated thrusts with a significant dextral component; these thrusts are mostly located along monzogranite contacts, obscuring the field relationship between igneous and metamorphic rocks.

3   HYDROTHERMAL ALTERATION

The area shows widespread hydrothermal alteration. Stage I has produced a pervasive alteration of limestone and calc-silicate and metapelitic rocks to a banded assemblage of quartz, ankerite, green biotite, phengite, ferroactinolite and chlorite along with massive magnetite. Locally, these rocks replace previous albitic and dolomitic alteration.

Most of the skarn postdates Stage I but predates Stage II; however, the presence of some skarnified boudins within the shear zone suggests that some skarn could be late Stage I. The more prominent skarn is mostly calcic, dominated by garnet, and occurs in the south-eastern part of the mine. Here, a prograde event

TIME	TECTONIC/MAGMATIC SETTING	HYDROTHERMAL ALTERATION & REPLACEMENT	AGE
↓	Sinistral shear band Localized extensional zones	Q-ser-ank-bt-act-mt-ab?-mt alteration	373.5 ± 3,2 Ma Stein *et al* 2006
	Dioritic intrusion ?	Calcic prograde skarn gr-px	
		Retrograde skarn ? mt-act (Q-ep-py-cc) alteration	
	Monzogranitic intrusion	Potassification bt-k-feldspar	352 ± 4 Ma Romeo *et al* 2006
	Thrusts SW vergence	Greisenization Q-chl-ank-ser	

Figure 3. Main tectonic, magmatic and hydrothermal processes associated with the geologic history at the Cala mine.

with banded to massive diopside-hedenbergite (Hd_{50} Di_{48} Jo_2) and grandite (Ad_{50} Gr_{39} $Sps-Al_{11}$) is exposed. Subsequent replacement by minor late andradite and actinolite, quartz, epidote, calcite, pyrite and magnetite is followed by vugh-filling quartz, epidote, calcite and magnetite. The retrograde component of the skarn is volumetrically small and includes massive ferroactinolite and magnetite.

Stage II thrusting produced only potassic alteration and greisenization in the monzogranite.

4 MINERALIZATION

Iron oxide ore at Cala is primarily magnetite with far subordinate to rare hematite. The earliest magnetite occurs as structurally-controlled massive replacement bodies related to Stage I (Fig. 2). The later magnetite associated with the retrograde skarn is always massive. While the early magnetite records evidence of deformation, the late skarn-associated magnetite is post-tectonic.

Cu-Au mineralization occurs within massive pyrite-chalcopyrite replacements, usually controlled by extensional, tension-gash structures (Fig. 2). The Cu-Au mineral assemblage includes some other sulphides such as pyrrhotite, nickelite, skutterudite, arsenopyrite, molybdenite and native gold. The proportion of sulphides is much more abundant in Stage I magnetite ores; however, Cu and Au grades are also high in the eastern part of the mine, where the retrograde skarn dominates.

5 GEOCHRONOLOGY

Because the field relationship between massive magnetite and the Cala stock could not be unequivocally determined in the field, a Re-Os study of Stage I mineralization was undertaken. Re-Os dating of magnetite and pyrite in the Stage I assemblage yields a well-constrained age of 373.5 ± 3.2 Ma (Stein *et al*. 2006). The initial $^{187}Os/^{188}Os$ ratio is 0.592 ± 0.043, indicating that metals are of crustal derivation. These data together with the recent U-Pb age for the Cala stock (352 ± 4 Ma, Romeo *et al* 2006) constrain previously ambiguous Stage I field relations destroyed by Stage II thrusting. Further field work affirms that the Cala stock is undeformed and hosts enclaves of banded magnetite. In addition, there is no associated endoskarn and, where visible, the Cala stock transects prograde skarn zonation suggesting that the monzogranite postdated even the prograde skarn.

Given the Re-Os and U-Pb geochronologic data, the tectonic-hydrothermal evolution of the Cala area is complex and spans at least 20 Ma (Fig. 3). Hypothetically, the skarn could be related to an unexposed intrusion located below the eastern part of the deposit, where the skarn dominates and where the Cu and Au grades are higher. In fact, in this eastern area we report some small outcrops of diorite-like intrusions affected by pervasive endoskarn that could correspond to shallow expressions of a deeper intrusion.

6 STABLE ISOTOPE GEOCHEMISTRY

Sulphur isotope data for pyrite ($\delta^{34}S$, 14.3-16.5‰) shows that most of the sulphur in the sulphides is of crustal derivation, probably derived from underlying shales and homogenized during hydrothermal transport.

Preliminary oxygen isotopic data show that fluids involved in both Stage I and skarn assemblages are of deep derivation. Calculated $\delta^{18}O$ values range from 9.9 to 11.1‰. If fluids forming the skarn and the Stage I magnetite were isotopically similar, then this magnetite precipitated at temperatures higher than those of the skarn, probably in the 500-600ºC range. $\delta^{18}O$ values of clinoamphibole and magnetite of the retrograde skarn record the influx of modified surficial fluids ($\delta^{18}O_{fl}$, 5.1-5.6‰; δD, -17 to -13‰). These results confirm different stable isotope histories for the two ore types.

Fluid inclusion data suggest that fluid circulation at the Cala deposit was complex and may have involved several events with CO_2-rich fluids and brines.

7 IOCG MINERALIZATION?

On the whole, the Cala deposit shares many features with epizonal IOCG deposits (Tornos and Casquet 2005). Stage I magnetite (Cu-Au) mineralization occurs as massive replacement of calcic-rich rocks. The mineral assemblage of Stage I is consistent with a K-Ca-Fe alteration event that overprinted an earlier (minor?) Na-rich alteration. Cala mineralization exhibits major structural control and hydrothermal fluids were most likely hot CO_2-bearing brines of deep origin. Compared to other iron oxide deposits of the OMZ, Cala has less pronounced Na alteration and no associated magmatic albitite, but exhibits higher Cu and Au grades. We suggest that Cala represents the shallow levels of a vertically extensive hydrothermal system. Other nearby Fe oxide deposits such as Monchi, Colmenar and La Berrona may represent deeper equivalents.

8 CONCLUSIONS

The iron oxide (Cu-Au) mineralization of the Cala mine shows a complex polyphase tectonic, magmatic and hydrothermal evolution, probably reflecting several tectonic and magmatic pulses. The Cala ore is concentrated in a small pull-apart structure. In the OMZ, small extensional structures in an overall transpressional orogen efficiently focussed fluids and magmatism in the crust (Tornos et al 2005). Although some of the ore is related to classic skarn processes, most of it seems to predate the skarn and magmatism. This earlier mineralization, associated with shear deformation, probably corresponds to the shallow portion of a hydrothermal system that shares many features with IOCG-style mineralization.

ACKNOWLEDGEMENTS

REFERENCES

Casquet, C., Tornos, F., 1991, Influence of depth and igneous geochemistry on ore development in skarns: *The Hercynian Belt of the Iberian Peninsula, in Skarns, their petrology and metallogeny,* Augusthitis ed., Athens, 555-591.

Casquet C, Velasco F (1978) Contribución a la geología de los skarns cálcicos en torno a Santa Olalla de Cala (Huelva-Badajoz). *Estudios Geologicos* 34: 399-405.

Eguiluz L, Gil Ibarguchi JI, Abalos B, Apraiz A (2000) Superposed Hercynian and Cadomian orogenic cycles in the Ossa-Morena zone and related areas of the Iberian Massif. *Geological Society of America Bulletin* 112(9): 1398-1413.

Quesada C (1990) *Ossa Morena Zone: introduction in pre-Mesozoic geology of Iberia,* Martinez E, Dallmeyer RD (eds), Springer Verlag, 249-251.

Romeo I, Lunar R, Capote R, Quesada C, Dunning GR, Piña R, Ortega L (2006) U–Pb age constraints on Variscan magmatism and Ni-Cu-PGE metallogeny in the Ossa Morena Zone (SW Iberia). *Journal of the Geological Society, London* 163: 837-846.

Stein HJ, Markey RJ, Carriedo J, Tornos F (2006) Re-Os evidence for the origin of Fe-oxide-(Cu-Au) deposits in SW Iberia at the Frasnian-Famennian boundary. *Geochimica Cosmochimica Acta* 70: A612. doi:10.1016/ j.gca.2006.06.1135

Tornos F, Casquet C (2005) A new scenario for related IOCG and Ni-(Cu) mineralization: the relationship with giant mid-crustal mafic intrusions, Variscan Iberian Massif. *Terra Nova* 17: 286-290.

Tornos F, Casquet C, Relvas J (2005) Transpressional tectonics, lower crust decoupling and intrusion of deep mafic sills: A model for the unusual metallogenesis of SW Iberia. *Ore Geology Reviews* 27: 133-163.

Velasco F, Amigo JM (1981) Mineralogy and origin of the skarn from Cala (Huelva, Spain). *Economic Geology* 76: 719-727.

The Aguablanca Ni-(Cu-PGE) deposit, SW Spain

Ossa Morena Zone: Lat. 37°57' N, Long. 6°11' W

C. Martínez [1], F. Tornos[2], C. Casquet [3], & C. Galindo[3]

[1] Rio Narcea Recursos SAU, Mina de Aguablanca, Monesterio, Badajoz, Spain
[2] Instituto Geológico y Minero de España, Azafranal 48, 37002 Salamanca, Spain
[3] Dpt. Petrología, Facultad de Geología, Universidad Complutense de Madrid, 28040 Madrid, Spain
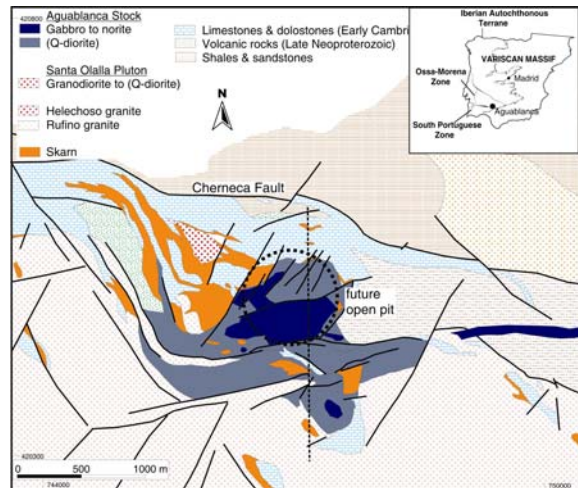
Geologic map of the Aguablanca orebody. Modified from Rio Narcea Recursos upub. mapping. The N-S dashed line is the projection of the section showed below.

Producing mining district: The only known economic deposit is Aguablanca, that started production in Octobre 2004. There are other minor prospects including several in the Cortegana-Aroche area.

Mining: Open pit and underground, scheduled between 2004 and 2013.

Metals: Ni, Cu, Pt, Pd, Co

Estimated annual production: 8000 t Ni, 5000 t Cu, 600 kg PGE (Pt+Pd).

Total resources: 17 Mt at 0.65 %Ni, 0.47 %Cu, 0.46 g/t PGE for a cut off of 0.2 %Ni. Geological reserves are 24 Mt.

Type: Magmatic hosted Ni-(Cu) deposit.

Morphology: Subvertical conical pipe with sulphide-supported breccias and massive sulphides hosted by gabbro and gabbronorite with disseminated and globular sulphides.

Age of mineralization: Intercumulus phlogopite has been dated at 337±4 Ma (Ar/Ar), an age consistent with that of other nearby equivalent intrusions (350-

330 Ma) (Tornos et al., 2004).

Ore minerals: Pentlandite, chalcopyrite, violarite, cobaltite, PGE-bearing minerals (Ortega et al., 2004).

Early magmatic mineralization: The breccia includes fragments of pyroxenite and minor peridotite, gabbro-gabbronorite and host rocks (marbles, skarn, hornfels) in a matrix of pyrrhotite, pentlandite and chalcopyrite with trace amounts of magnetite, cubanite, cobaltite, graphite and mackinawite. The disseminated and globular mineralization have the same assemblage but are impoverished in nickel.

Alteration: The primary magmatic assemblage is pervasively retrograded to amphiboles (actinolite, Mg-hornblende), biotite, epidote ss, talc, chlorite, calcite and illite. The alteration is accompanied by a major redistribution of the ore minerals, including the formation of coarse grained chalcopyrite, pentlandite, pyrite, pyrrhotite, and some mackinawite, bravoite, sulphosalts and Pd and Pt-Pd tellurides. The deposit underwent major supergene alteration with formation of violarite and marcasite.

Nature and age of the host rocks: Irregularly zoned plutons made up of calc-alkaline, K-rich quartz-diorite and gabbro. The orebody occurs in a small screen of more mafic rocks in the northern part. The pluton intruded limestone, felsic volcaniclastic rocks and hornfels of Upper Neoproterozoic-Early Cambrian age affected by high grade contact metamorphism.

Genetic model: Geochemistry shows that the mafic magmas at Aguablanca underwent major crustal contamination, probably with siliciclastic rocks within the crust of the Ossa Morena Zone, acquiring sulphur and developing an immiscible sulphide-rich magma (Casquet et al., 2001). Below the Ossa Morena Zone at about 10-15 km depth there is a large subhorizontal reflective body that has been interpreted as mafic sills (Simancas et al., 2003). The formation of localized transcrustal extensional structures within the regional transpressional setting probably induced partial crustal decoupling and

intrusion of juvenile magmas. Magma-crust interaction and partial crystallization took place in the deep magma chamber. Further reactivation of localized extensional structures allowed the injection to shallow crustal levels of molten sulphide melts, fragments of the partially consolidated mafic-ultramafic cumulates and residual melts of gabbroic-gabbronoritic composition (Tornos et al., 2001).

Selected photos of mineralization the Aguablanca deposit. Left: Breccia-like ore including fragments of pyroxenite supported by massive sulphides. The sulphides hosted mm-sized crystals of another pyroxene with equivalent composition. Size sample: 10 cm. Right: Gabbronorite with disseminated mineralization
.
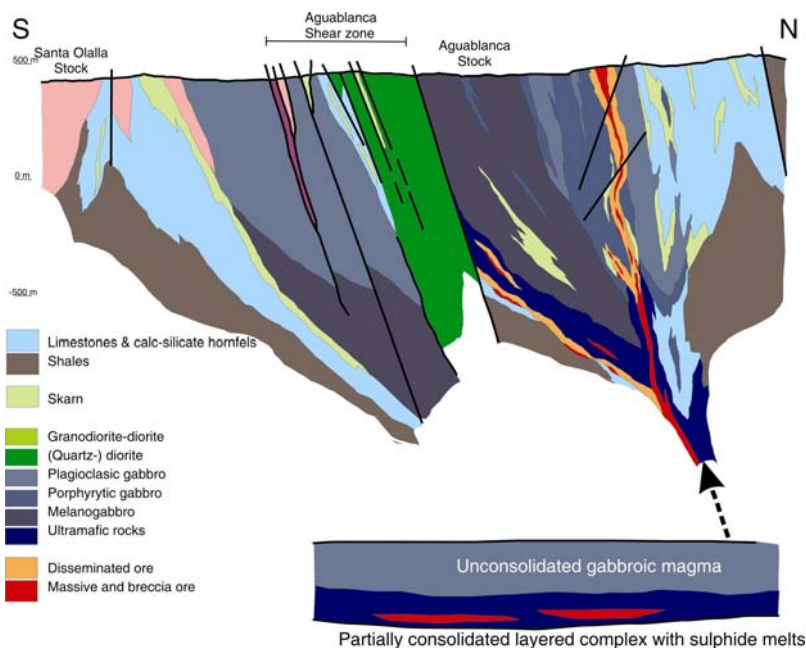
Interpretative N-S section of the Aguablanca deposit. The lower part of the figure represents a deep stratiform magmatic complex with immiscible sulphide melts perhaps equivalent to that mineralization found in the Aracena massif (Out of scale). Based on unpub.data of Rio Narcea Recursos and Tornos et al. (2001)

References:

Casquet, C., Galindo, C., Tornos, F., & Velasco,F., 2001. The Aguablanca Cu-Ni ore deposit (Extremadura, Spain), a case of synorogenic orthomagmatic mineralization: Isotope composition of magmas (Sr, Nd) and ore (S). *Ore Geology Reviews*, **18**, 237-250

Ortega,L., Lunar,R., Garcia Palomero,F., Moreno,T., Martin Estevez,J.R., Prichard,H.M., Fisher,P.C., 2004. The Aguablanca Ni-Cu-PGE deposit, Southwestern Iberia: Magmatic ore-forming processes and retrograde evolution. *Canadian Mineralogist*, **42**, 325-350

Simancas,J.F., Carbonell,R., Gonzalez Lodeiro,F., Perez Estaun,A., Juhlin., C., Ayarza,P., Kashubin, A.,Azor,A., Martinez Poyatos, D.,Almodóvar, G.R., Pascual, E., Saez, R., & Exposito, I., 2003. Crustal structure of the transpressional Variscan orogen of SW Iberia: SW Iberia deep seismic reflection profile (IBERSEIS). *Tectonics*, **22**, 1-16

Tornos, F., Casquet, C., Galindo, C., Velasco, F., & Canales, A., 2001: A new style of Ni-Cu mineralization related to magmatic breccia pipes in a transpressional magmatic arc, Aguablanca, Spain. *Mineralium Deposita*, **36-7**, 700-706

Las mineralizaciones ferríferas del coto minero San Guillermo (Jerez de los Caballeros, Badajoz, España)

Iron mineralizations of the San Guillermo mining district (Jerez de los Caballeros, Badajoz, Spain).

R. Sanabria [1], C. Casquet [1], F. Tornos [2] y C. Galindo [1]

[1] Departamento Petrología y Geoquímica, Universidad Complutense de Madrid. 28040, Madrid
[2] Instituto Geológico y Minero de España, Azafranal 48, 37001 Salamanca

ABSTRACT

Stratoid magnetite and skarn magnetite were mined at the San Guillermo mine district. Structural and textural evidence suggest that they formed by replacement of older rocks in Variscan orogeny times during a protracted process that begun with fluid flow and stratoid magnetite formation along thrusts. This was followed by the Brovales pluton emplacement probably controlled by an oblique shear zone. Exo and endoskarns with magnetite formed at this time, partly before and partly after complete crystallization of the pluton.

Key words: ore deposits, magnetite, skarn, Ossa Morena zone, Variscan

Introducción

Este trabajo se centra en las mineralizaciones de magnetita del coto minero San Guillermo (CMSG) (minas de San Guillermo, El Colmenar, Santa Bárbara y Santa Justa), en la localidad de Jerez de los Caballeros (Badajoz) (Fig. 1). Las minas estuvieron en explotación hasta el año 1978. El origen de las mineralizaciones de magnetita de este sector de la zona Ossa Morena, ha sido motivo de polémica. Por un lado la morfología estratoide de algunos depósitos y su ubicación, a menudo próxima a las rocas volcánicas del Cámbrico Inferior, condujeron a una intepretación volcanogénica (p.ej., Dupont, 1979). Por otro, la proximidad espacial de las mineralizaciones con los plutones varíscicos y su relación con formaciones de tipo skarn, propició un modelo alternativo epigenético (yacimientos hidrotermales) (p.ej., Casquet y Tornos, 1991). Los objetivos del trabajo son establecer las etapas mineralizadoras principales, determinar las posibles guías estructurales que controlaron la ubicación de las mineralizaciones y contribuir con nuevos datos a resolver el problema sobre el origen singenético *vs.* epigenético de las mineralizaciones de magnetita de esta zona.

Contexto geológico del coto San Guillermo

El CMSG se ubica en la faja metalogenética Olivenza-Monesterio, definida por Tornos *et al.* (2004) en la zona Ossa Morena, junto al contacto oriental del plutón varíscico de Brovales (340±4 Ma; Montero *et al.*, 2000) con el complejo metamórfico de Valuengo (Fernández Carrasco *et al.*, 1981) (Fig. 1). El Plutón de Brovales, de composición en buena parte tonalítica, se interdigita, en la zona estudiada, con el encajante metasedimentario en el que se aloja la mineralización y que constituye el flanco occidental del anticlinal de Valuengo (Fig. 1). Dicho flanco queda truncado a muy bajo ángulo por el contacto intrusivo y se verticaliza junto al mismo (Fig. 1). Este contacto se relaciona con una zona de cizalla sin-plutónica dextral de dirección aproximadamente N-S, que se continúa hasta el aledaño plutón de Burguillos del Cerro, al norte de la zona de estudio (Tornos *et al.*, 2002). Cortando a las tonalitas y al encajante hay diques de leucogranitos. Además, dentro del encajante se han reconocido, también, algunos cuerpos menores de gabros, envueltos por la estratificación y la foliación, ambas concordantes (Fig. 2) (Sanabria, 2001).

El encajante metasedimentario, en el que se localiza la mayor parte de la mineralización, está constituido por la formación detrítica de Las Mayorgas, esencialmente metarcosas, esquistos biotíticos, porfiroides y una capa de rocas metacarbonatadas (nivel «c») y por la formación Carbonatada de calizas y dolomías marmorizadas, carácterística del Cámbrico Inferior (Fernández Carrasco *et al.*, 1981) (Fig. 1).

Mineralizaciones de magnetita.

Hay dos tipos de magnetita. La mineralización principal del CMSG consiste en una concentración estratoide de magnetita (manto), de 2 a 30 m de poten-

O	Protolito: clinopiroxeno, *anfibol I* (hornblenda paragasítica) y plagioclasa
P	*Anfibol II* nematoblástico (hornblenda actinolítica)
M	*Magnetita* (mineralización principal)
E	*Anfibol III* (actinolita, fibroso-radiada). Reemplazamiento de todo lo anterior
I	Venas I y rellenos de cavídades: (*Anfibol IV* (ferro-actinolita) + cuarzo + calcita + epidota + albita + magnetita + pirita / calcopirita)
T	Venas II: Carbonatos, especularita, etc.

Tabla I.- Procesos ligados a la mineralización en la mina El Colmenar.

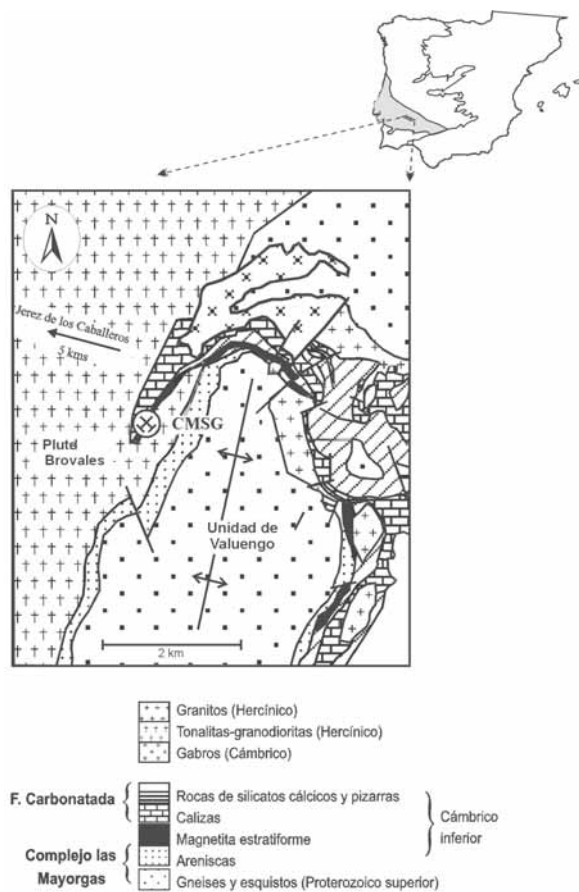*Table I.- Mineralization related processes at El Colmenar mine.*

Fig. 1.- Localización del coto minero San Guillermo.

Fig. 1.- Location of the San Guillermo mine district.

cia, que se sigue a lo largo de más de 5-6 km hacia el este, siguiendo el contorno del anticlinal de Valuengo. Fue objeto de explotación en diversas minas del propio coto y otras de menor entidad en el flanco oriental del pliegue (Bismarck, El Soldado, Las Galerías). El manto se adelgaza progresivamente hacia el sur, en el sector de mina San Guillermo, hasta desaparecer truncado a muy bajo ángulo por el contacto con la tonalita de Brovales (Fig. 1). En todo el área del anticlinal de Valuengo se ha reconocido, desde antiguo, la existencia de una capa guía discontinua, muy delgada, de rocas metacarbonatadas (mármoles y rocas de silicatos cálcicos) asociada a esta mineralización (nivel «c» de la formación detrítica de Las Mayorgas; Fernández Carrasco *et al.*, 1981), que se intercala entre esquistos y gneises biotíticos (Fig. 1). Este tipo de magnetita se ha considerado tradicionalmente vinculado con el vulcanismo ácido – básico, del Cámbrico Inferior (p. ej., Dupont, 1979).

Un segundo tipo de mineralización de magnetita es la asociada claramente con formaciones tipo skarn, tanto exoskarns sobre la Formación Carbonatada, como endoskarns, muy lo-

cales, sobre la propia tonalita de Brovales e intrusiones menores satélites. La descripción que sigue se refiere exclusivamente a la mina de El Colmenar (magnetita estratoide) y a la Santa Bárbara (magnetita de tipo skarn).

Mina El Colmenar

En ella se explotó el manto de magnetita estratoide que alcanza los 30 m de potencia (Fig. 2). La mineralización tiene un elevado buzamiento al oeste y limita a muro con la digitación de la tonalita foliada de Brovales, de la que queda separada por una faja filonítica. A techo hay esquistos y gneises migmatíticos. Además, dentro de la mineralización se encuentran restos del nivel guía carbonatado («c») (mármoles y rocas de silicatos cálcicos con granate, piroxeno y, en menor medida, anfíbol, escapolita y albita). Hacia el NE la mineralización se continua entre rocas de silicatos cálcicos, lo que sugiere su disposición ligeramente discordante con la estratificación. (Fig. 2).

Se pueden definir dos tipos de mineralización dentro de este cuerpo (Sanabria, 2001):

Tipo I

(*magnetita+ albita + anfibol*). Se trata de una roca granuda formada principalmente por plagioclasa (An_{10}) y magnetita y minoritariamente anfíbol (ANF-I, hornblenda pargasítica marrón, reemplazada por hornblenda actinolítica verde (ANF-II)) y clinopiroxeno hedembergítico. Accesoriamente hay esfena y, en menor proporción, circón idiomorfo. La mineralización es claramente posterior a la plagioclasa, al clinopiroxeno y a la hornblenda, pues se introduce a favor de los bordes de grano y avanza hacia el interior de los cristales, reemplazándolos. La presencia de circónes idiomorfos apunta hacia un protolito ígneo, probablemente una roca de grano fino formada por plagioclasa + clinopiroxeno ± hornblenda (leucogabro?). Afloramientos de esta roca se observan en diversos puntos. No obstante también se observan lentejones de mármoles y rocas de silicatos cálcicos dentro de la mineralización, parcialmente reemplazados.

Tipo II

(*mineralización bandeada de magnetita–anfíboles–sulfuros*). Está formada principalmente por niveles alternantes de magnetita + actinolita (agregados fibroso-radiados postectónicos; ANF-III) y de sulfuros (calcopirita + pirita) + hornblenda actinolítica (en crecimientos orientados paralelos al bandedado, sin-tectónicos; ANF-II). Se conservan relictos de piroxeno hedembergítico, de hornblenda (ANF-I) y de albita, igual que la mineralización Tipo-I. La magnetita (junto con los sulfuros) reemplaza al ANF-II y es, a su vez reemplazada por el ANF-III.

Dentro de la mineralización bandeada se observan estructuras tipo «boudinage» en litologías competentes que han sufrido estiramiento, en una etapa incipiente de la mineralización (Fig 4c; Tornos *et al.*, 2002). Además abundan filoncillos tardíos de albitita, que cortan a la mineralización principal y que muestran también fracturación, rotación, desmembramientos y reemplazamientos por magnetita y ANF-IV. Esta deformación tardía se corresponde con el desarrollo de fracturas extensionales rellenas con anfíboles de gran tamaño (actinolita-ferroactinolita; ANF-IV), calcita, cuarzo, epidota, albita, calcopirita / pirita, magnetita (+ esfena ± allanita). Estas venas llevan dirección aproximada E-O. Además esta mineralización, se encuentra también como relleno de cavidades de gran tamaño. Una segunda familia de venas muy tardía, presenta rellenos de carbonatos y especularita principalmente. En el Tabla I se resume el esquema de la evolución textural reconocida en la mineralización estratiforme.
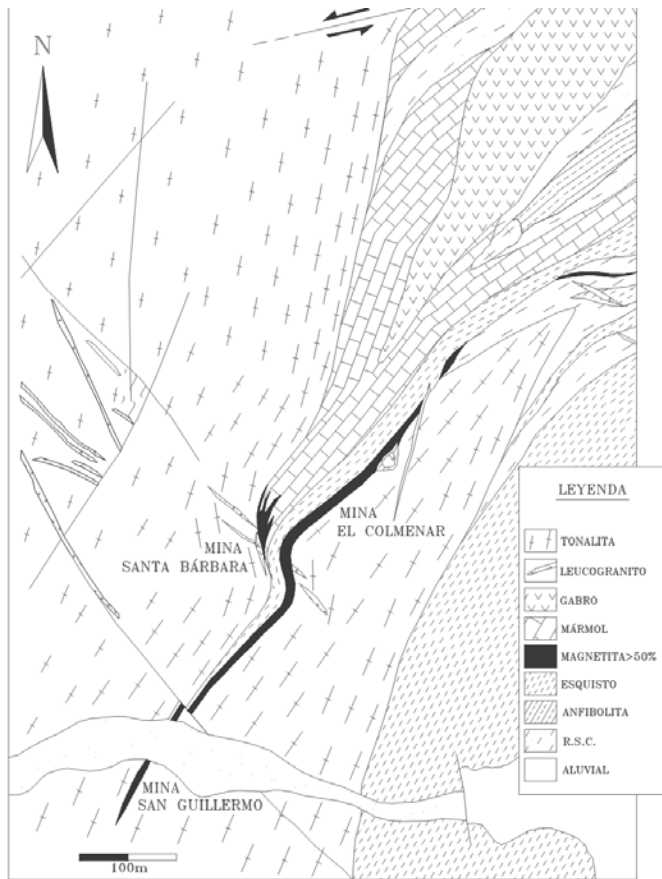
Fig. 2.- Mapa geológico de detalle del coto minero San Guillermo.

Fig. 2.- Detailed geological map of the San Guillermo mine district.

Mina Santa Bárbara

La mina Santa Bárbara se ubica junto a una inflexión del contacto con el plutón de Brovales (Fig. 3). La mineralización de magnetita es masiva y se asocia a dos skarns no deformados.

Skarn cálcico sobre mármoles

En este caso, la mineralización avanza a favor de las capas de mármol, dando lugar a una estructura flameada que coalesce en la zona de la mina (masa Santa Bárbara I) (Fig. 3). La zona de magnetita va precedida de una zona de actinolita, que la separa del mármol inalterado. Los frentes de reemplazamiento son netos y truncan a la estratificación. La actinolita se presenta en masas fibrosas arriñonadas, con una tendencia al crecimiento de las fibras perpendicular a los frentes metasomáticos. Este anfíbol es comparable al Anfíbol III de la mina El Colmenar. Las zonas son prácticamente monominerales, aunque hay algo de actinolita en la de magnetita y magnetita en la de actinolita. En este último caso se reconocen dos tipos de magnetita: una relicta (pre-actinolita), que forma alineaciones paralelas a la S_0 que se continúan en el mármol y otra posterior, relacionada con las formas arriñonadas de la actinolita. La zona de la actinolita reemplaza tanto al mármol como a la zona de magnetita masiva, por lo que parece ser más joven que ésta.

El skarn magnésico

En la mina Santa Bárbara, junto al contacto con la tonalita se encuentra un pequeño skarn magnésico caracterizado por la presencia de abundante flogopita y magnetita (masa Santa Bárbara II) (Fig. 3). El único contacto visible de esta masa es discordante con la S_0. El protolito parece haber sido en buena parte los gneises migmatíticos del complejo de Valuengo, ya que dentro de la mineralización se conservan circones relictos, textural y químicamente semejantes a los de dichos gneises (Sanabria, 2001). La tonalita de Valuengo no está afectada por este reemplazamiento. Junto a la flogopita y la magnetita hay clorita y grandes megacristales de pirita (piritoedros de hasta 10 cm). El conjunto a su vez está atravesado por venas tardías de cuarzo + carbonatos con hematites especular en masas de considerable tamaño. El proceso más interesante es la alteración potásica y magnésica en forma de una flogopitización masiva a la que se superpone en el tiempo una alteración retrógrada con diferentes tipos texturales de clorita. La secuencia de reemplazamientos observada en la masa Santa Bárbara II se resume en el Tabla II.

Discusión

Las mineralizaciones son, en los dos casos, de tipo epigenético. La mineralización estratoide, aunque ubicada dentro de la formación detrítica de Las Mayorgas, es oblicua, en detalle, a los límites entre unidades litológicas. Por otro lado, la magnetita reemplaza, a favor de bordes de grano y microfracturas, a un conjunto de minerales pre-existentes, que corresponden a una roca microgranuda de tipo leucogabro (Plag + Cpx ± Hb), roca de la que se encuentran restos dentro de la propia mineralización (junto a otras). Además, la precipitación de magnetita (y sulfuros) es parte de un proceso complejo de reemplazamientos en un contexto deformativo inicialmente dúctil y progre-

Tabla II.- Procesos ligados a la mineralización en la mina Santa Bárbara.

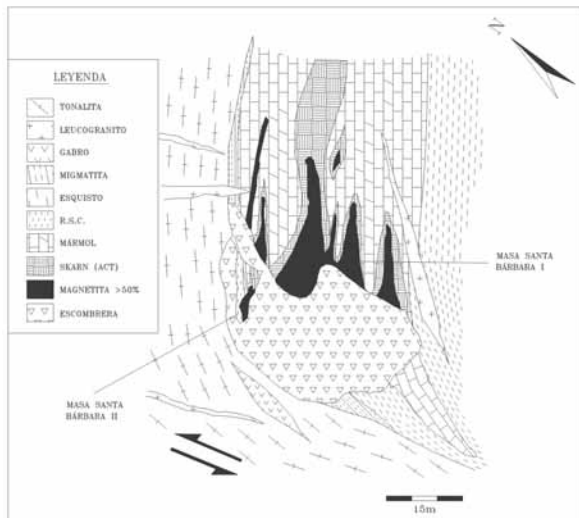*Table II.- Mineralization related processes at the Santa Bárbara mine.*

Fig. 3.- Mapa geológico de la mina Santa Bárbara.

Fig. 3.- Geological map of the Santa Bárbara mine.

sivamente más frágil, evidenciado por las sucesivas generaciones de anfíboles de tipo actinolítico que se han reconocido (ver Tabla I). Las evidencias de deformación dúctil se reconocen en las fábricas nematoblásticas del ANF-II y por estructuras de tipo «boudinage» dentro de la mineralización (Fig. 4c; Tornos *et al.*, 2002). Por otro lado, los filoncillos de albititas rotados, desmembrados y mineralizados que se encuentran en la mineralización bandeada y los rellenos de grietas de tensión con ANF-IV, así como el tapizado de cavidades sugieren condiciones progresivamente más frágiles hacia el final del proceso hidrotermal. Por otro lado, la mineralización estratoide se adelgaza progresivamente hacia el sur de la mina El Colmenar y queda truncada a bajo ángulo por el propio plutón de Brovales (Fig. 2), cuyo emplazamiento parece controlado por una zona de cizalla N-S (Tornos *et al.*, 2002). Además, la mineralización estratoide se continúa hacia el este, lejos del plutón (Fig. 1). Ambos hechos sugieren que la mineralización es anterior al emplazamiento definitivo del plutón y que está controlada por estructuras independientes al mismo. En este sentido, una datación Sm-Nd de concentrados de magnetita de las dos minas ha proporcionado una edad de 334±32 Ma (Darbyshire *et al.*, 1998), lo que confirma la edad varíscica de la mineralización y apunta hacia una proximidad temporal entre la mineralización y el magmatismo.

En cuanto a la estructura que constituye el metalotecto de la mineralización estratoide, resulta difícil de determinar, debido a su enmascaramiento por los reemplazamientos que tuvieron lugar en ella. Dado que la mineralización es

varíscica y anterior al emplazamiento definitivo del plutón de Brovales, pensamos que dicha estructura pudo ser un cabalgamiento también varíscico, frecuentes en el flanco meridional del anticlinal Olivenza – Monesterio (Azor *et al.*, 2004). Ello explicaría la ligera discordancia entre mineralización y contactos litológicos y el significado del problemático nivel carbonatado «c», reconocido solo en el complejo metamórfico de Valuengo, que podría ser el resultado de la repetición, por imbricación, de la formación Carbonatada.

El skarn de la mina Santa Bárbara se formó, probablemente, antes de la cristalización total del plutón de Brovales ya que, por un lado no hay endoskarn en la tonalita adyacente y por otro, el skarn no está deformado. Los controles fueron litológicos y estratigráficos. No obstante, en la digitación tonalítica a muro de la magnetita estratoide, hay también endoskarn sobre la propia tonalita (Sanabria, 2001).

Estas conclusiones están de acuerdo con el modelo recientemente propuesto por Tornos y Casquet (2005) para las mineralizaciones de Fe y de Ni-(Cu) de la región Olivenza – Monesterio. Los cabalgamientos varíscicos y otras estructuras asociadas habrían servido de vía de acceso para fluídos y magmas desde la corteza media, donde se habría emplazado, en el tránsito Devónico – Carbonifero, un complejo ígneo máfico-ultramáfico estratificado de grandes dimensiones (Simancas *et al.*, 2003). Los fluídos procedentes de la cristalización de este complejo fueron los responsables de las mineralizaciones de magnetita (+sulfuros). Los reemplazamientos se ubicaron en los propios cabalgamientos y precedieron a

las intrusiones, lo que explica las relaciones de temporalidad observadas y la frecuente relación espacial entre plutones y mineralizaciones.

Bibliografía

Casquet, C. y Tornos, F (1991). En: *Skarns, their genesis and metallogeny*. Ed. Theophrastus, 648 p.

Darbyshire, D.P.F., Tornos, F., Galindo, C. y Casquet, C. (1998). *Chinese Science Bulletin*, 43 supp. August.

Dupont, R. (1979). *Cadre Geologique et Metallogenese des Gisements de Fer du Sud de la Province de Badajoz (Sierra Morena Occidentale-Espagne)*. Tesis Doctoral, Inst. National Polytechnique de Lorraine, 395 p.

Fernández Carrasco, J., Coullaut, J.L. y Aguilar, M.J. (1982). *Mapa Geológico de España 1: 50.000, hoja nº 875 (Jerez de los Caballeros)*. IGME.

Montero, P., Salman, K., Bea, F., Azor, F., Expósito, I., Lodeiro, F., Martínez Poyatos, D. y Simancas, F. (2000). En: *Variscan Appalachian dynamics: The building of the Upper Paleozoic basement.* Basement Tectonics 15, La Coruña, Spain, Program y Abstracts, 136-138.

Sanabria, R. (2001). *Caracterización y evolución de las mineralizaciones ferríferas y de los skarns del Coto Minero San Guillermo, Jerez de los Caballeros (Badajoz).* Tesis de Licenciatura, Univ. Complutense Madrid, 97 p.

Simancas, F., Carbonell, R., Lodeiro, F., Pérez Estaún, A., Juhlin, C., Ayarza, P., Kashubin, A., Azor, A., Martínez Poyatos, D., Almodovar, J.R., Pascual, E., Sáez, R., y Espósito, I. (2003). *Tectonics*, 22, 1063.

Simon, A.C., Pettke, T., Candela, P.A., Piccoli, P.M. y Heinrich, A. (2004). *Geochemica et Cosmochemica Acta,* 68, 4905-4914.

Tornos, F. y Casquet, C. (2005). *Terra Nova* 17, 236-241.

Tornos, F., Casquet, C., Relvás, J., Barriga, F. y Sáez, R. (2002). En: *The timing and location of major ore deposits in an evolving orogen* (D. Blundell, F. Neubauer y A. von Quadt, Eds.). Geological Society of London Special Publication, 206, 179-198.

Evolution and dynamics of subduction zones from 4-D geodynamic models

D.R. STEGMAN[1], J. FREEMAN[2], W.P. SCHELLART[2], L.N. MORESI[1], D. MAY[1]

[1]Monash University, Australia (dave.stegman@sci.monash.edu.au)
[2]The Australian National University, Australia

Modeling the time-evolution of subduction in a 3-D geometry has a first order effect on nearly every aspect of understanding plate tectonics, in particular on the interpretation of geochemical signatures of the mantle Turner and Hawkesworth, 1998; Pearce et al., 2001.

We present models of free subduction (plates subducting due to their own negative buoyancy without the aid of imposed surface velocity boundary conditions or plate reconstructions) in which the subducting trench is allowed to migrate and evolve into curvatures which are fully consistent with the dynamics. A large emphasis has been put on communicating these results through the use of movies of the simulations.

We report the effect of the lateral width of subduction zones on the curvature of oceanic arcs (evolving towards either a concave or convex geometry) and trench migration rates (e.g. hinge rollback or hinge advance). We also observe a range of slab morphology in the upper mantle depending on the relative motion of the hinge during progressive subduction. For example, fast-retreating hinges result in a backward draping of a flat-lying slab atop the lower mantle.

However, hinges which are stable in a time-averaged sense (oscillating between phases of slow hinge retreat and slow hinge advance) result in the accumulation of slab material at the 660 km discontinuity alternating between forward- and backward-draping recumbent folds.

We quantify the energetics of these systems and provide a relation between the resultant plate kinematics (e.g. the speed of backwards trench migration vs. the forward velocity of the subducting plate) to plate driving forces (i.e. slab pull) and the resistive forces such as generation of the accompanying return flow. A significant component of this return flow is of a toroidal nature, which likely explains the preferred orientation of mantle fabric around slab edges as observed by shear wave splitting directions Russo and Silver, 1994 and geochemistry of volcanic rocks from arc and back-arc environments such as Tonga and Scotia.

References

Pearce, J.A., Leat, P.T., Barker, P.F., Millar, I.L., 2001. *Nature* **410**, 457–461.
Russo, R.M., Silver, P.G., 1994. *Science* **263**, 1105–1111.
Turner, S., Hawkesworth, C., 1998. *Geology* **26**, 1019–1022.

Re-Os evidence for the origin of Fe-oxide-(Cu-Au) deposits in SW Iberia at the Frasnian-Famennian boundary

H. STEIN[1,2], R. MARKEY[1], J. CARRIEDO[3], F. TORNOS[3]

[1]AIRIE Program, Department of Geosciences, Colorado State University, USA (hstein@warnercnr.colostate.edu)
[2]Geological Survey of Norway, 7491 Trondheim, Norway
[3]Instituto Geológica y Minero de España, Azafranal 48, 37002 Salamanca, Spain

To investigate the origin of economically important but poorly understood Fe-oxide-(Cu-Au) deposits, we collected three samples from the operating Cala mine (Spain) in the Ossa Morena Zone (OMZ) of SW Iberia. The OMZ is an accretionary magmatic arc that records the Variscan collision of the South Portuguese zone with the autochthonous Iberian terrane. Thick sequences of Neoproterozoic dark shale form the pre-Variscan basement in the OMZ. Cala Fe-oxide-(Cu-Au) ore is associated with a small pull-apart structure in a 200 m wide sinistral shear zone containing very low grade Early Cambrian carbonate and clastic rocks and a few small diorite porphyry dikes, all displaying a complex polyphase brittle-ductile deformation history. Juxtaposed to the immediate north is the granodiorite-monzogranite Cala stock, a presumed source for mineralizing fluids. The stock introduced a pyroxene-garnet skarn overprint on an earlier magnetite-rich mineralization. The Cala stock is presumed to be part of the nearby Santa Olalla pluton inprecisely dated at 350-330 Ma. Our dated samples are from the NW wall of the open pit where the early banded magnetite massively replaces hydrothermally altered limestone. The fine-grained magnetite ore is locally brecciated and pyrite ($\pm$ chalcopyrite and minor gold) penetrates and infills crackle zones.

Here we report the first magnetite-pyrite isochron for an Fe-oxide-(Cu-Au) deposit. Three pairs of magnetite-pyrite plus one magnetite replicate precisely define a 7-point 374 ± 3 Ma isochron with an unequivocally crustal initial $^{187}Os/^{188}Os$ of 0.592 ± 0.043 (MSWD = 1.4). Re and Os concentrations are in the low ppb to ppt and ppt range, respectively. We attribute the high precision of our result to sampling strategy and to strict analytical protocol, particularly for blank corrections. The Re-Os age for the deposition of Fe-oxide-(Cu-Au) at Cala places the onset of mineralization in the Early Variscan, $\sim$20 m.y. older than previous estimates. We suggest that prior to the widespread appearance of intrusions in the OMZ, dilational zones within deep transpressional shear zones served as channels for vapor-dominated upward transport of Fe and other ore components. The metals may have been liberated from Neoproterozoic basement shales as they were heated and dehydrated by underplating magma that later accessed higher crustal levels. As such, our initial Os ratio implies an $^{187}Os/^{188}Os$ for Neoproterozoic seawater that is less than 0.6.

A new scenario for related IOCG and Ni–(Cu) mineralization: the relationship with giant mid-crustal mafic sills, Variscan Iberian Massif

Fernando Tornos[1] and Cesar Casquet[2]

[1]Instituto Geologico y Minero de España, Salamanca; [2]Universidad Complutense de Madrid, Dpto. de Petrologia, Madrid, Spain

ABSTRACT

Both magmatic Ni–(Cu) and hydrothermal iron oxide–copper–gold mineralization coexist in ancient belts but their relationship remains poorly known. Geochronology and field geology evidence show that in SW Iberia both styles of mineralization were coeval with widespread metaluminous to peraluminous Variscan magmatism (350–330 Ma). We propose that mineralization was probably related to a hidden large layered mafic–ultramafic layered complex, recently inferred from geophysics, that was emplaced in a mid-crustal decollement zone. Contamination of a primitive mantle-derived magma with continental crust in the layered complex led to fractional crystallization accompanied by high-T–low-P metamorphism and the incorporation of volatiles into the melt. Hot hypersaline CO_2–CH_4-bearing brines were subsequently released and focused along major thrusts and strike-slip faults to produce the IOCG mineralization. Assimilation of continental crust also led to the formation of sulphide magmas that were tectonically injected high into the crust, leading to the formation of pipe-like breccia-hosted Ni–(Cu) ore bodies. All these processes took probably place as a consequence of oblique ridge– and/or continent–continent collision.

Terra Nova, 00, 1–6, 2005

Introduction

Iron oxide–copper–gold (IOCG) ore deposits have recently been recognized as constituting a new class of mineralization with high economic potential (Hitzman, 2000; Pollard, 2000). The deposits are dominated by magnetite or hematite, have variable amounts of Au and Cu and are usually enriched in U, LREE, Co, Ni, As, Mo, W and Te. Volatile-rich minerals are also common (e.g. Pollard, 2000). However, the geological setting and the source of the metals and fluids are still controversial, mainly because most of these ore bodies occur in highly deformed Proterozoic belts, such as the Fennoscandian shield (Weihed and Eilu, 2003) or the Cloncurry district (Australia) (Mark *et al.*, 2001). This style of mineralization show a direct relationship with large-scale faults and broad zones of sodium–calcium (albite–actinolite) or potassic (Kfeldspar or biotite) alteration. IOCG deposits span a range of depths and tectonic settings,

Correspondence: Dr Fernando Tornos, Oficina Proyectos Salamanca, Instituto Geologico y Minero de España, Azafranal 48, Salamanca 37001, Spain. Tel.: 00-34-923-265009; fax: 00-34-923-265066; e-mail: f.tornos@igme.es and ftornos.igme@telefonica.net

particularly extensional environments along subduction-related continental margins (Hitzman, 2000). In most cases the fluids involved were apparently part of large-scale deep-seated hydrothermal systems.

Here we report the case of the Ossa Morena Zone (SW Iberia), one of the domains of the Variscan European basement. Current geodynamic models suggest that the Ossa Morena Zone was an active continental margin during Variscan times, with a magmatic arc broadly similar to recent Andean or Pacific magmatic arcs (e.g. Quesada, 1991). The Ossa Morena Zone is unusual for the diversity of Variscan mineralization. It includes abundant IOCG (-REE-U) replacements as well as magmatic Ni–(Cu) mineralization, a diversity of periplutonic and intra-plutonic vein-type deposits [Cu-(Au–Bi), Zn–Pb, W–(Sn), Zn–Pb, and Au], Sn-rich replacements and epithermal Hg deposits (Tornos *et al.*, 2002). However, the district lacks the porphyry and epithermal deposits typical of subduction-related magmatic arcs (Mitchell, 1992). We will focus here on the first two types of mineralization.

This unusual metallogenesis was the consequence of Variscan oblique collision and the magmatic and hydrothermal activity resulting from the intrusion of a large layered igneous complex in the middle crust. This model provides new clues as to the genesis of the IOCG and Ni–(Cu) mineralization, and can help to better understand similar ore-forming systems in ancient metallogenic belts.

The Ossa Morena Zone: geological and geodynamic setting

The Ossa Morena Zone is a Proterozoic terrane that was accreted to the autochthonous Central Iberian Zone of the Iberian Massif (Fig. 1) during the Cadomian orogeny in late Neoproterozoic to early Cambrian times (Eguiluz *et al.*, 2000). The region was rejuvenated during the Variscan orogeny when the continental South Portuguese Zone, which is host to the world class volcanogenic deposits of the Iberian Pyrite Belt, was in turn accreted to the Ossa Morena Zone. Accretion involved subduction of intervening ocean-floor under the Ossa Morena Zone, ophiolite obduction, and oblique ridge and/or continental collision in Devonian to Lower Carboniferous times (e.g. Silva *et al.*, 1990; Quesada, 1991). Variscan deformation within the Ossa Morena Zone was partitioned between longitudinal southward verging fold-and-thrust zones and slightly younger strike-slip faults, the former involving a Cadomian basement and its unconformable Palaeozoic sedimentary cover. I-type
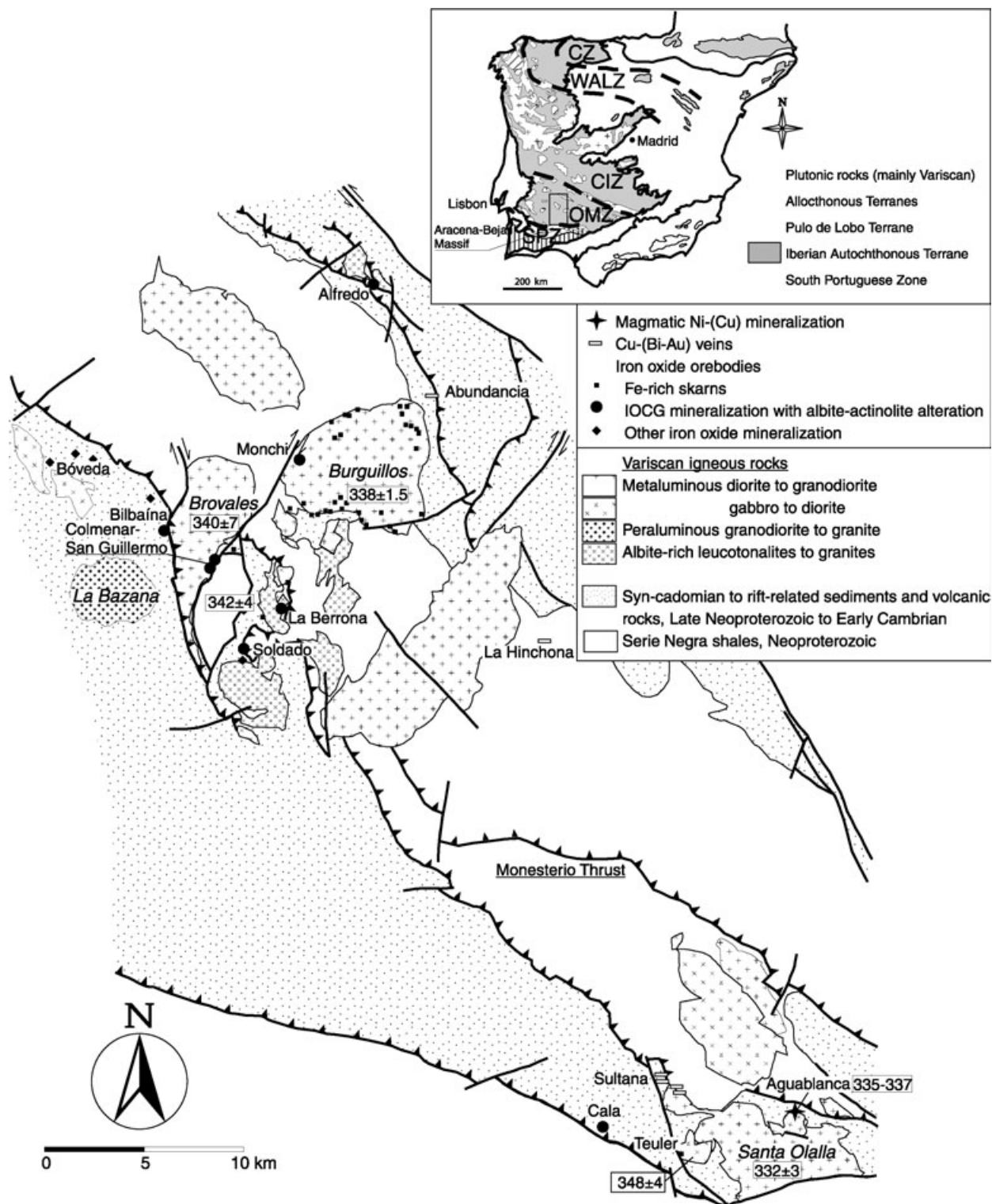
Fig. 1 Geological map of the Central Ossa Morena Zone, showing the relationship between different types of iron oxide-rich, Ni–(Cu) and Cu-Au ore bodies, magmatism and major Variscan structures. Ages are of Variscan plutonic rocks and related ore deposits. The inset shows the different zones of the Variscan Belt of Iberia: Cantabrian Zone (CZ), West Asturian Leonese Zone (WALZ), Central Iberian Zone (CIZ), Ossa Morena Zone (OMZ) and South Portuguese Zone. The box shows the area enlarged in the Fig. 2.

high-K calc-alkaline magmatism developed in the Ossa Morena Zone between 352 ± 4 Ma and 332 ± 3 Ma (Pin et al., 1999; Montero et al., 2000), consisting of composite plutons formed mainly by diorite and tonalite with local gabbronorite and gabbro, and only minor volcanic rocks. Peraluminous leucogranite dykes and small stocks are also common.

A seismic reflection survey across the Ossa Morena Zone (IBERSEIS) recently revealed a subhorizontal 1–5 km thick high velocity layer in the middle crust, about 15 km deep and 140 km long (Iberian Reflective Body; Simancas et al., 2003). This evidence, coupled with regional magnetic and gravity data and the inference that plutons had to be fed from a crustal magma chamber to account for their isotope geochemistry (Casquet et al., 2001), has led to the suggestion that the reflector is a large but discontinuous layered mafic complex underlying most of the Ossa Morena Zone (Simancas et al., 2003). The complex is probably Variscan, as major thrusts of this age merge at the depth of the intrusion (Fig. 2), suggesting emplacement along a main Variscan crustal decollement (Simancas et al., 2003).

Geophysical and geological evidence suggest that Variscan middle continental crust and dismembered parts of the layered complex crop out along the southern margin of the Ossa Morena Zone (Aracena–Beja domain) where a high-T–low-P metamorphic belt has been long recognized (Bard, 1969). Maximum pressures of 4–6 kb and peak temperatures of over 920 °C were determined by Díaz Azpiroz et al. (2004), and references therein. Anatexis is widespread in the core of the belt where discordant mafic–ultramafic intrusions with disseminated to semi-massive sulphides occur. Moreover, high-grade metamorphism has been recorded from some of these intrusions (Castro et al., 1999), suggesting that magmatism probably began close to the peak of metamorphism and continued further. Ar–Ar hornblende cooling ages for the Aracena metamorphism range between c. 328 and 342 Ma with the highest values found in the Beja domain (Dallmeyer et al., 1993; Castro et al., 1999). The discordant Beja gabbro has a U–Pb zircon age of c. 352 Ma (Pin et al., 1999), which is probably a minimum age for the peak of metamorphism.

Iron oxide(–Cu–Au) mineralization

Iron oxide mineralization is particularly abundant along the large Olivenza–Monesterio anticline in the central part of the Ossa Morena Zone (Fig. 1). The ore bodies occur as large massive stratabound lenses, always located within the fold-and-thrust belt that constitutes the southern limb of the anticline. The rocks involved are late Neoproterozoic–early Cambrian felsic volcanic rocks, siliciclastic sediments and reef carbonates that underwent low-grade regional metamorphism. A few ore bodies in the volcanic sequence probably formed from low temperature (sub)-exhalative hydrothermal fluids synchronous with the volcanism (Galindo et al., 1995); most iron oxide mineralization formed by replacement of the volcanic and carbonatic rocks along major thrust and strike-slip fault zones, usually close to epizonal (approximately 1.5 kbar equivalent to c. 5 km depth) Variscan intrusions (Fig. 1). Magnetite is allied to albite–actinolite–(salite–scapolite)-rich rocks that can be locally rich in allanite, uraninite, monazite and apatite. Where the host rock is marble, both magnesian and calcic Fe-skarns developed (Tornos et al., 2002, and references therein). Mineralization consists of massive or banded magnetite with subordinate sulphides (pyrite, chalcopyrite and trace amounts of millerite and cobaltite) and irregularly distributed gold; both sulphides and gold are always younger than the magnetite. Volatile-rich minerals such as vonsenite, fluorite, axinite, apatite
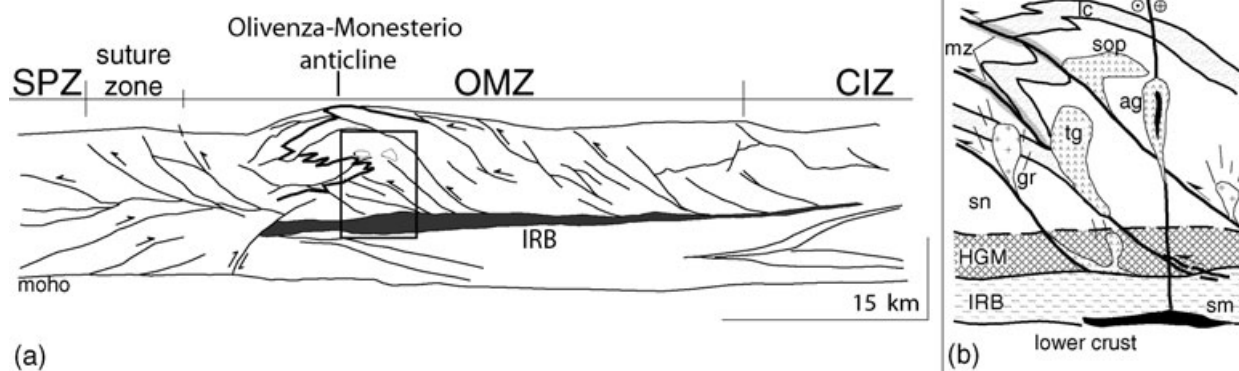
Fig. 2 (a) Schematic cross section of the Ossa Morena Zone (OMZ) and northern South Portuguese Zone (SPZ) as inferred from the IBERSEIS deep reflection seismic profile (Simancas et al., 2003). IRB, Iberian Reflective Body. Folded line represents Lower Cambrian sedimentary cover rocks. (b) Enlarged inset zone of cross-section showing an interpretation of relationships between Variscan mineralization, magmatism, metamorphism and tectonic structures. IRB is a layered mafic–ultramafic igneous complex; sm, sulphide-rich immiscible magma; HGM, zone of high-grade high-T–low-P metamorphism; sn, late Neoproterozoic-early Cambrian siliciclastic and volcanic rocks of the Cadomian basement; lc, Lower Cambrian sedimentary cover sequence; tg, tonalite-gabbro-(norite) plutons with Ni–(Cu)-rich massive sulphides and breccias; gr, peraluminous granite stocks and dyke swarms. sop. Santa Olalla Pluton; ag, Aguablanca pluton; mz, iron oxide-rich hydrothermal replacements with allied Na–Ca alteration. Only Variscan tectonic structures are shown.

and tourmaline are also common. Mineralization has been dated at 334 ± 32 Ma at Jerez (Sm–Nd, Darbyshire *et al.*, 1998) and 338 ± 1.5 Ma at Monchi (U–Pb, Casquet *et al.*, 1998). These ages are within error of those of Variscan plutonism referred to above but, in detail, most magnetite mineralization formed first, as evidenced by the presence of enclaves of magnetite within diorite. The range of Nd isotope compositions of the mineralization (εNd_{340} = −8.0 to −4.0; Galindo *et al.*, 1995; Darbyshire *et al.*, 1998) is comparable with that of local diorite and tonalite (εNd_{340} = −7.5 to −6; Casquet *et al.*, 2001). Fluid inclusion and stable isotope data show that the magnetite mineralization precipitated from hot (> 500 °C), hypersaline (> 25 wt% NaCl eq.) H_2O–$NaCl$–$FeCl_2$–$CaCl_2$ brines with heavy $\delta^{18}O$ values between +9 and +12‰ (Cuervo *et al.*, 1996). Local quartz-ankerite veins rich in chalcopyrite, bismuthinite and maldonite with albite–tourmaline–sericite alteration were probably synchronous with the sulphide-rich stage of the iron oxide ore bodies (Tornos and Velasco, 2002). These veins formed by pulsatile unmixing of H_2O–CO_2–CH_4–$NaCl$–KCl–$CaCl_2$ brines (30 wt% NaCl eq.) with heavy $\delta^{18}O$ values (+5 to +8‰).

Ni–(Cu) magmatic mineralization

The recently discovered economic Aguablanca magmatic Ni–(Cu) deposit is hosted by Variscan gabbronorite and norite, which form part of a small calc-alkaline pluton in the easternmost part of the Olivenza–Monesterio anticline (Fig. 1). The major ore body is hosted in a breccia pipe, with sulphides (mainly pyrrhotite with minor chalcopyrite and pentlandite) that are either massive or supporting fragments of the host rocks, pyroxenite, peridotite and metasedimentary rocks (Tornos *et al.*, 2001). Isotope (S, Sr, Nd and Pb) data are consistent with a model involving assimilation of Neoproterozoic upper crustal rocks, likely grey shale which forms most of the basement of the Ossa Morena Zone, by a mantle-derived magma and simultaneous fractional crystallization in an underlying magma chamber (Casquet *et al.*, 2001). These processes led to diversification of magma composition, formation of cumulates and generation of a sulphide immiscible melt. The deposit has an age of 335–337 Ma ($^{39}Ar/^{40}Ar$ age of phlogopite from breccia fragments; Tornos *et al.*, 2004), which is also interpreted as the crystallization age of the Aguablanca pluton. This age is embraced by those of nearby Variscan igneous rocks, which range between *c.* 332 and 348 Ma ($^{207}Pb/^{206}Pb$) single-zircon grain ages; Montero *et al.*, 2000).

A model for the Ossa Morena Zone deposits

Most ore bodies in the Olivenza–Monesterio anticline are found in the proximity of Variscan plutons and thrusts and strike-slip zones (Fig. 1) suggesting a genetic relationship. In fact, the mineralization was essentially coeval with the calc-alkaline metaluminous plutonism, between 352 Ma and 332 Ma. Variable mixing of juvenile magmas with continental crust has also been invoked to explain the isotope composition of the calc-alkaline igneous rocks (Casquet *et al.*, 2001). The available Nd isotope compositions of mineralization and igneous rocks are coincident, suggesting that fluids and magmas were in isotopic equilibrium. In turn, lead isotope compositions of ores from the Ossa Morena Zone systematically plot below the crustal and orogenic lead growth curves, indicating that significant amounts of juvenile lead mixed with crustal lead during the ore forming processes. Moreover, the $^{207}Pb/^{206}Pb$ ratios of ore bodies in the Ossa Morena Zone are significantly lower than those of the adjacent terranes and are significantly more juvenile than those of other Phanerozoic orogenic belts (Tornos and Chiaradia, 2004).

We propose here that the Iberian Reflective Body of Simancas *et al.* (2003) was the most probable source of magmas and fluids and that it largely controlled the Variscan metallogenic evolution of the Ossa Morena Zone, favouring the shallow intrusion of mafic-intermediate plutons in the Olivenza–Monesterio anticline area and developing a characteristic suite of mineralization. Emplacement of the mafic–ultramafic complex in the middle crust took

probably place in the Tournaisian–Visean as inferred from plutonic rock ages and the age of the related Aracena–Beja metamorphism. The process induced high-*T*–low-*P* metamorphism and partial melting of the shale. As quoted above, direct geological evidence of such processes can be seen in the Aracena–Beja domain. Present depth estimate to the igneous complex, i.e., 15 km, is compatible with metamorphic pressure estimate (4–6 kbar) if post-Variscan erosion equivalent to 1.5 kb (approximately 5 km) is accounted by.

Magmatic assimilation of siliciclastic sediments released sulphur and lithophile elements and induced water-enrichment in the evolving igneous body (Casquet *et al.*, 2001). The mafic–ultramafic rocks show evidence of high water activity at the time of crystallization, such as the presence of intercumulus phlogopite and amphibole, pegmatoids and high-*T* hydrothermal alteration. Thus, it is likely that hydrothermal fluids were exsolved from the contaminated magmas during the late stages of its crystallization. The fluid inclusion data suggest that fluids were CO_2–CH_4-bearing hypersaline brines similar to those found in IOCG deposits (Khin Zaw *et al.*, 1994) and that behaved immiscibility during upflow. A magmatic–metamorphic source for fluids is compatible with the high $\delta^{18}O$ values obtained for water in equilibrium with mineralization.

Assimilation of siliciclastic sediments resulted also in production of an immiscible sulphide melt that incorporated chalcophile elements from the magma. Batches of residual gabbroic to tonalite melts, along with minor molten sulphide magma and fragments of already crystallized ultramafic cumulates, were intruded episodically, giving rise to both the Aguablanca mineralization and the composite Variscan plutons. Minor peraluminous plutonism rose directly from anatexis of middle crust rocks.

Thrusts and strike-slip faults were the pathways to the upper crust. This model is consistent with the geophysical evidence showing that the south-verging thrusts that form the southern limb of the Olivenza–Monesterio anticline are rooted in the Iberian Reflective Body (Simancas *et al.*, 2003).

Apart from Aguablanca, few magmatic Ni–(Cu) deposits have been described from orogenic belts (Papunen, 2003). Most magmatic Ni–(Cu) deposits seem to be within giant mafic intrusions related to mantle plumes in rifted intracratonic settings, such as Noril'sk (Naldrett, 1992) or Voisey's Bay (Ryan, 2000). Many IOCG ore bodies have also been inferred to be related to mantle plumes (e.g. Kiruna, Martinsson, 2003; Cloncurry district, Oliver *et al.*, 1991). However, MacCready *et al.* (1998) have also invoked a hidden large mafic intrusion in the Cluncurry district, which as in the case of the Ossa Morena zone, is coincident with a regional compression decollement. A syn-orogenic mantle plume has also been invoked for Ossa Morena (Simancas *et al.*, 2003), although this possibility is difficult to prove.

We propose that the intrusion of the layered complex was directly related to the beginning of oblique collision at the Devonian–Carboniferous boundary (Fig. 2). The middle crust decollement became a zone of major crustal decoupling that favoured the injection of voluminous juvenile magmas and the consequent strong heating of the middle crust. One explanation for the proximity of hot mantle to the overriding continent is ridge-subduction, an idea first invoked by Castro *et al.* (1996). In this model, oblique collision of an oceanic ridge under the Ossa Morena margin evolved into a slab window from which juvenile magmas might have been released. However, the origin of the voluminous magmatism still remains conjectural.

Conclusions

The intrusion of a large mafic–ultramafic layered complex into the Ossa Morena crust (SW Iberia) during oblique collision is probably the reason of the unusual metallogeny of the area, which lacks the conventional suite of ore deposits commonly found in subduction-related magmatic arc environments. Interaction of mantle-derived melts with upper crustal metasedimentary rocks led to extensive contamination and complementary immiscibility of a sulphide melt, as well as fluid saturation and consequent exsolution of iron- and volatile-rich saline brines. Silicate and sulphide magmas and hydrothermal fluids were focused into major thrusts and strike-slip faults and formed IOCG and magmatic Ni–(Cu) deposits at epizonal depths. This is the first time that coexisting IOCG and nickel sulphide deposits have been recognized in a Phanerozoic magmatic belt, showing that orogenic environments can be the loci of magmatic sulphide mineralization and that they may have a genetic link with IOCG mineralization.

References

Bard, J.P., 1969. *Le metamorphisme regional progressif de Sierra de Aracena en Andalousie occidentale* (*Espagne*). These d'Etat, Université de Montpellier, Montpellier, 397 pp.

Casquet, C., Galindo, C., Darbyshire, D.P.F., Noble, S.R. and Tornos, F., 1998. Fe-U-REE mineralisation at Mina Monchi, Burguillos del Cerro, Spain: age and isotope (U-Pb, Rb-Sr and Sm-Nd) constraints on the evolution of the ores. *Proc. GAC-MAC-APGGQ Quebec 98 Conf.*, **23**, A28.

Casquet, C., Galindo, C., Tornos, F. and Velasco, F., 2001. The Aguablanca Cu-Ni ore deposit, Extremadura, Spain), a case of synorogenic orthomagmatic mineralisation: isotope composition of magmas, (Sr, Nd) and ore, (S). *Ore Geol. Rev.*, **18**, 237–250.

Castro, A., Fernández, C., De la Rosa, J.D., Moreno-Ventas, I., El-Hmidi, H., El-Biad, M., Bergamín, J.F. and Sanchez, N., 1996. Triple-junction migration during Paleozoic Plate convergence: the Aracena metamorphic belt, Hercynian Massif, Spain. *Geol. Rundsch.*, **85**, 108–185.

Castro, A., Fernández, C., El-Hmidi, H., El-Biad, M., Diaz, M., Rosa, J. and Stuart, F., 1999. Age constraints to the relationships between magmatism, metamorphism and tectonism in the Aracena metamorphic belt, southern Spain. *Contrib. Mineral. Petrol.*, **88**, 26–37.

Cuervo, S., Tornos, F., Spiro, B. and Casquet, C., 1996. El origen de los fluidos hidrotermales en el skarn férrico de Comenar – Santa Bárbara (Zona de Ossa Morena). *Geogaceta*, **20**, 1499–1500.

Díaz Azpiroz, M., Castro, A., Fernández, C., López, S., Fernández, J.C. and Moreno-Ventas, I., 2004. The contact between the Ossa Morena and South Portuguese Zones. Characteristics and significance of the Aracena metamorphic belt, in its central sector between Aroche and Aracena. *J. Iberian Geol.*, **30**, 23–52.

Dallmeyer, R.D., Fonseca, P.E, Quesada, C. and Ribeiro, A., 1993. ^{39}Ar/^{40}Ar mineral age constraints for the tectono-thermal evolution of a Variscan Suture in SW Iberia. *Tectonophysics*, **222**, 177–194.

Darbyshire, D.P.F., Tornos, F., Galindo, C. and Casquet, C., 1998. Sm-Nd and Rb-Sr constraints on the age and origin of magnetite mineralisation in the Jerez de los Caballeros iron district of Extremadura, SW Spain. *Chinese Sci. Bull.*, **43**, 28.

Eguiluz, L., Gil Ibarguchi, J.I., Abalos, B. and Apraiz, A., 2000, Superposed hercynian and cadomian orogenic cycles in the Ossa Morena Zone and related areas of the Iberian Massif. *Geol. Soc. Am. Bull.*, **112**, 1398–1413.

Galindo, C., Darbyshire, D.P.F., Tornos, F., Casquet, C. and Cuervo, S., 1995. Sm-Nd geochemistry and dating of magnetites: a case study from an Fe district in the SW of Spain. In: *Mineral Deposits: from their Origin to Environmental Impacts* (J. Pasava, B. Kribek and K. Zak, eds), pp. 41–43. Balkema, Rotterdam.

Hitzman, M.W., 2000. Iron oxide–Cu–Au deposits. What, where, when and why. In: *Hydrothermal Iron Oxide–Copper–Gold and related deposits: A Global Perspective* (T.M. Porter, ed.), pp. 9–25. Australian Mineral Foundation, Adelaide.

Khin Zaw, Huston, D.L., Large, R.R., Mernagh, T. and Hoffmann, C.F., 1994. Microthermometry and geochemistry of fluid inclusions from the Tennant Creek gold-copper deposits: implications for ore deposition and exploration. *Mineral. Deposita*, **29**, 288–300.

MacCready, T., Goleby, B.R., Goncharov, A., Drummond, B.J. and Lister, G.S., 1998. A framework of overprinting orogens based on intepretation of the Mount Isa deep seismic transect. *Econ. Geol.*, **93**, 1422–1434.

Mark, G., Oliver, N.H.S. and Foster, D.R.W., eds, 2001. *Mineralisation, Alteration and Magmatism in the Eastern Fold Belt, Mount Isa Block, Australia. Geological Review and Field Guide*, Vol. 5. Geological Society Australia, Specialist Group Economic Geol, Townsville, 121 pp.

Martinsson, O., 2003. Characterisation of iron mineralisations of Kiruna type in the Kiruna area, northern Sweden. In: *Mineral Exploration and Sustainable Development* (D.G. Eliopoulos, *et al.* eds), pp. 1087–1090. Millpress, Rotterdam.

Mitchell, A.H.G., 1992. Andesitic arcs, epithermal gold and porphyry-type mineralisation in the western Pacific and eastern Europe. *Trans. Inst. Min. Metall.*, **101**, b125–b138.

Montero, P., Salman, K., Bea, F., Azor, A., Exposito, I., Lodeiro, F., Martinez Poyatos, D. and Simancas, F., 2000. New data on the geochronology of the Ossa Morena Zone, Iberian Massif Variscan. In: *Proceedings of the Appalachian dynamics: The building of the Upper Paleozoic basement*. Galicia.

Naldrett, A.J., 1992. A model for the Ni-Cu-PGE ores of the Noril'sk region and the application to other areas of flood basalt. *Econ. Geol.*, **87**, 1945–1962.

Oliver, N.H.S., Holcombe, R.J., Hill, E.J., Pearson, P.J., 1991. Tectono-metamorphic evolution of the Mary Kathleen fold belt, northwest Queensland: a reflection of mantle plume processes? *Austr. J. Earth Sci.*, **38**, 425–455.

Papunen, H., 2003. Ni-Cu sulphide deposits in mafic–ultramafic orogenic intrusions - Examples from the Svecofennian areas, Finland. In: *Mineral Exploration and Sustainable Development* (D.G. Eliopoulos *et al.* eds), pp. 551–554. Millpress, Rotterdam.

Pin, C., Paquete, J. and Fonseca, P.E., 1999. 350 Ma (U-Pb zircon) igneous emplacement age and Sr-Nd isotopic study of the Beja Gabbroic Complex (S. Portugal). *J. Conf. Abs.*, **4-3**, 1019.

Pollard, P.J., 2000. Evidence for magmatic fluid and metal source for Fe-oxide Cu-Au mineralisation. In: *Hydrothermal Iron Oxide Copper-Gold and related deposits: A Global Perspective* (T.M. Porter, ed.), pp. 27–41. Australian Mineral Foundation, Adelaide.

Quesada, C., 1991. Geological constraints on the Paleozoic tectonic evolution of tectonostratigraphic terranes in the Iberian Massif. *Tectonophysics*, **185**, 225–245.

Ryan, B., 2000. The Nain Churchill boundary and the Nain plutonic suite: a regional perspective on the geologic setting of the Voisey's Bay Ni-Cu-Co deposit. *Econ. Geol.*, **95**, 703–724.

Silva, J.B., Oliveira, J.T. and Ribeiro, A., 1990. Structural outline of the South Portuguese Zone. In: *Pre Mesozoic Geology of Iberia* (E. Martinez and R.D. Dallmeyer, eds), pp. 348–362. Springer Verlag, Berlin.

Simancas, J.F., Carbonell, R., Gonzalez Lodeiro, F., Perez Estaun, A., Juhlin, C., Ayarza, P., Kashubin, A., Azor, A., Martinez Poyatos, D., Almodovar, G.R., Pascual, E., Saez, R. and Exposito, I., 2003. Crustal structure of the transpressional Variscan orogen of SW Iberia: SW Iberia deep seismic reflection profile (IBERSEIS). *Tectonics*, **22**, 1063.

Tornos, F. and Chiaradia, M., 2004, Plumbotectonic evolution of the Ossa Morena Zone, Iberian Peninsula, Tracing the influence of mantle-crust interaction in ore forming processes. *Econ. Geol.*, **99**, 965–985.

Tornos, F. and Velasco, F., 2002. The Sultana orebody (Ossa Morena Zone, Spain): Insights into the evolution of Cu-(Au-Bi) mesothermal mineralisation. In: *Abstracts GEODE Study Centre, 25–28 October 2002.* pp. 16–17. Grenoble.

Tornos, F., Casquet, C., Galindo, C., Velasco, F. and Canales, A., 2001. A new style of Ni-Cumineralisation related to magmatic breccia pipes in a transpressional magmatic arc, Aguablanca, Spain. *Mineral. Deposita*, **36**, 700–706.

Tornos, F., Casquet, C., Relvas, J., Barriga, F. and Saez, R., 2002. The relationship between ore deposits and oblique tectonics: the SW Iberian Variscan Belt. In: *The Timing and Location of Major Ore Deposits in an Evolving Orogen* (D. Blundell, F. Neubauer and A. von Quadt, eds), *Spec. Publ. Geol. Soc. Lond.*, **206**, 179–198.

Tornos, F., Iriondo, A., Casquet, C. and Galindo, C., 2004. Geocronología Ar-Ar de flogopitas del stock de Aguablanca, Badajoz). Implicaciones sobre la edad del plutón y de la mineralización de Ni-(Cu) asociada. *Geotemas*, **6**, 189–192.

Weihed, P. and Eilu, P., 2003, Gold, Fe oxide-Cu-Au and VMS metallogeny of the Fennoscandinavian shield. In: *Mineral Exploration and Sustainable Development* (D.G. Eliopoulos *et al.* eds), pp. 1123–1126. Millpress, Rotterdam.

Plumbotectonic Evolution of the Ossa Morena Zone, Iberian Peninsula: Tracing the Influence of Mantle-Crust Interaction in Ore-Forming Processes

FERNANDO TORNOS[†]

Instituto Geológico y Minero de España, Azafranal 48, 37002 Salamanca, Spain

AND MASSIMO CHIARADIA[*]

Department of Mineralogy, University of Geneva, Rue des Maraichers 13 CH-1211, Geneva 4, Switzerland

Abstract

The Ossa Morena zone in the Variscan belt of the Iberian Peninsula is characterized by a complex geotectonic evolution. It hosts a Neoproterozoic-Paleozoic sequence that records the existence of two orogenic events (Cadomian and Variscan) separated by rift and stable platform stages (Middle Cambrian to Late Devonian). Volcanogenic and sediment-hosted massive sulfides, skarns, magmatic Ni-(Cu) deposits, synmetamorphic and intragranitic and perigranitic veins, and replacement bodies are related to different magmatic-hydrothermal systems ranging in age from 650 Ma to about 250 Ma. The lead isotope signatures from 26 different mineral deposits show variable ratios of $^{206}Pb/^{204}Pb$ (17.49–18.44), $^{207}Pb/^{204}Pb$ (15.47–15.67) and $^{208}Pb/^{204}Pb$ (37.37–38.78) that have low average μ values (9.7) but high ω values (38.3). As a whole, the lead isotope data define an irregular cluster that plots around the Stacey and Kramers (1975) growth curve but clearly marks the existence of two main ore-forming events during Cadomian and Variscan times.

The most radiogenic samples are from some minor Zn-Pb stratiform (sedimentary exhalative) mineralization. They are interpreted as having a dominantly crustal derivation (μ >10.1) in which most of the lead was leached from a pre-Cadomian continental basement with a long crustal history. This basement has strong geochemical affinities with the oldest rocks of the Iberian terrane. However, most of the ore samples investigated plot below the Stacey and Kramers (1975) reference curve, indicating polyphase but variable mixing of lead from upper crustal and mantle lead reservoirs at the terrane scale. Clear mixing lines between the two end-member reservoirs are evident only in the oldest volcanic rock- and sedimentary rock-hosted massive sulfide deposits related to the Cadomian (late Neoproterozoic-Early Cambrian) magmatic arc; in the other deposit types lead isotopes have more restricted values. The crustal lead is interpreted as having been derived from ancient crust (2.1–2.5 Ga) and the derived shales (Montemolín Formation) that predated the Cadomian orogeny. The mantle-derived lead may have been derived from three different sources: Neoproterozoic tholeiitic orthoamphibolite, syn-Cadomian calc-alkaline andesite, or calc-alkaline metaluminous plutonic rocks intruded during the Variscan orogeny. The first two sources probably controlled the lead isotope signatures of the Cadomian massive sulfide deposits and the Variscan synmetamorphic veins.

The input of primitive lead is especially significant during Variscan times (350–300 Ma) and is interpreted as having been related to the existence of a large primitive reservoir that controlled the Variscan magmatic, metallogenic, and hydrothermal evolution of the Ossa Morena zone. This primitive lead is recognized in most of the magmatic-hydrothermal deposits, including the typically crust-derived W- and Pb-bearing perigranitic hydrothermal systems. Likewise, associated plutonic rocks have more primitive lead isotope signatures than their counterparts in other Iberian terranes. The lead isotope evolution of the region is consistent with recent geophysical data that suggest that a deep, large mafic sill was intruded below the Ossa Morena zone during Variscan times. This sill was a likely key factor in the different Pb isotope evolution of the Ossa Morena zone compared with the nearby Iberian terranes and the entire Western Mediterranean province, which are characterized by lengthy crustal histories with very little input of primitive lead. The extensive mantle-crust interaction probably explains the wide variety and the unusual metallogenic features of the Ossa Morena zone.

Introduction

THE OSSA MORENA zone is a major tectonostratigraphic unit situated in the southwestern margin of the Variscan belt of Europe. It is one of the most complex terranes in the belt and contains sedimentary rocks belonging to a complex polyphase accretionary system ranging in age from late Riphean to late Carboniferous. The geotectonic evolution of the Ossa Morena zone also involves the intrusion of large volumes of igneous rocks belonging to three magmatic events: the Cadomian orogenic cycle, the Variscan orogenic cycle, and an intermediate extensional phase of early Paleozoic age (e.g.,

Sanchez Carretero et al., 1990; Quesada et al., 1991; Ochsner, 1993; Eguíluz et al., 2000). This geologic evolution has produced an abundance of diverse ore deposits and mineral showings, including iron-oxide skarns and replacements, magmatic Ni-(Cu) deposits, and Cu-(Au-Bi) veins, making the Ossa Morena zone differ metallogenically from adjacent terranes that host abundant volcanogenic massive sulfides (South Portuguese zone) or gold-bearing mesothermal systems and shallower W-Sn and Cu-Pb-Zn veins (Central Iberian zone). Most of the ore deposits of the Ossa Morena zone are related to both the Cadomian and Variscan orogenies (Locutura et al., 1990; Tornos et al., 2004). This relative chronology has been traced by the preliminary lead isotope data presented by Tornos et al. (1998) and Marcoux et al. (2002b).

[†]Corresponding author: e-mail, f.tornos@igme.es
[*]Present address: Centre for Geochemical Mass Spectrometry, School of Earth Sciences, University of Leeds, Leeds LS2 9JT, United Kingdom.

Systematic lead isotope investigations have been carried out in most terranes of the Variscan belt of Iberia, including the West Asturian Leonese zone (Tornos and Arias, 1993; Tornos et al., 1996; Arias et al., 1997), the Central Iberian zone (Lillo, 1992; Arribas, 1993; García de Madinabeitia, 2002), the South Portuguese zone (Marcoux and Saez, 1994; Marcoux, 1998), and the Pyrenees and adjacent areas (Velasco et al., 1994; Cardellach et al., 1996; Canals and Cardellach, 1997). Other studies have dealt with the lead isotope geochemistry of the Alpine deposits in the Betic Ranges (Arribas and Tosdal, 1994) and the Mississippi Valley-type deposits in the post-Variscan zones (Velasco et al., 1996). However, little is known about the lead isotope geochemistry of the Ossa Morena zone.

Recent geophysical data have shown that below the Ossa Morena zone, at depths of 10 to 15 km, lies a heterogeneous reflective layer about 2 to 3 km thick. This layer is currently interpreted as a mafic sill intruded during Variscan times at the boundary between the lower and upper crust above a mantle plume (IBERSEIS: Simancas et al., 2003). If true, such a large intrusion should exert a major control on the Variscan plutonism and the related ore-forming processes.

Previous lead isotope studies on the Ossa Morena zone, on the basis of a limited number of samples (Tornos et al., 1998; Marcoux et al., 2002b) have shown that some mineralization derived its lead from a deep, primitive reservoir. Here, we have carried out a larger lead isotope survey in order to determine whether the peculiar metallogenesis of the Ossa Morena zone is related to this anomalous input of mantle-derived metals and to assess the relationship between plumbotectonics of the Ossa Morena zone and the adjacent terranes. The data presented here illustrate how the juxtaposition of many different deposit types in a small area can reflect a complex history of mantle-crust interactions.

Geologic Setting

The Ossa Morena zone is located between the Central Iberian zone and the South Portuguese zone of the Variscan belt of Iberia (Fig. 1). It consists of (1) heterogenous, dismembered pre-Cadomian sequences that contain high-grade metamorphic rocks and a thick siliciclastic sequence deposited in a passive margin, (2) a synorogenic Cadomian unit that contains backarc to intraarc sequences of late Neoproterozoic-Early Cambrian age, (3) a volcanosedimentary unit formed during an intracontinental rift phase of early Paleozoic age, (4) a passive margin sequence (Ordovician-Early Devonian), and (5) syn-Variscan sedimentary rocks that were deposited in restricted basins (Table 1) (Quesada et al., 1987, 1991; Eguíluz et al., 2000). The Ossa Morena zone itself is thought to have been accreted onto the Iberian autochthonous terrane during the Cadomian orogeny (late Neoproterozoic-early Paleozoic); it became the locus of another magmatic belt in Variscan times (late Paleozoic) during its collision with the exotic South Portuguese zone. This superposition resulted in a complex architecture that is not fully understood. Figure 2 and Tables 1 and 2 provide a simplified structural and stratigraphic framework of the Ossa Morena zone on the basis of Quesada et al. (1987, 1991), Sánchez Carretero et al. (1990), Galindo et al. (1990), Quesada and Munhá

(1990), Abalos and Eguíluz (1992) and Eguíluz et al. (1995, 2000).

The southern boundary of the Ossa Morena zone is a major suture (the South Iberian shear zone) with the South Portuguese zone. In the northern part the Badajoz-Córdoba shear zone probably represents an imbricated Cadomian suture (Burg et al., 1981) that in Variscan time had major sinistral displacement. The Obejo-Valsequillo domain, located between the Ossa Morena zone and the Central Iberian zone (Fig. 1), is characterized by the presence of a Neoproterozoic sequence with affinities to the Ossa Morena zone but with an overlying detrital Paleozoic sedimentary cover more typical of the Central Iberian zone (Apalategui et al., 1985).

Mineralization in the Ossa Morena Zone

There are more than seven hundred mineral occurrences in the Ossa Morena zone. Only the Cala iron mine is currently (2004) operating, but the area has been a major producer of iron from the San Guillermo-Colmenar, Alfredo, and Monchi mines, and of lead from the Azuaga vein field. The Ossa Morena zone also includes widespread W-Sn, Hg, Au, Mn, and Cu mineralization. Recent discoveries include the Puebla de la Reina and Nava-Paredón volcanogenic massive sulfide deposits, the Fuenteheridos sedimentary-exhalative deposit, the Oropesa replacement Sn deposit and the Aguablanca Ni-Cu magmatic mineralization. Only those mineral occurrences and deposits included in the lead isotope study are briefly described here (Table 3). A more general overview can be found in Locutura et al. (1990) and in Tornos et al. (2004) and references therein.

Mineralization in the Cadomian volcanic sequence (types 3, 4, 5, and 6)

In the Cadomian volcanic rocks there are several massive sulfide orebodies (type 3 in Table 3) that are thought to be related to calc-alkaline submarine magmatism in an arc environment. The major deposits are Maria Luisa and nearby showings (including Santa Ana) and Puebla de la Reina (15 in Fig. 1). The Puebla de la Reina orebody is located in the northern part of the Ossa Morena zone and is hosted by a succession of alternating andesitic and dacitic volcanic rocks with minor shales and limestones. The mineralization occurs as a stacked replacive strata-bound lens with an underlying diffuse stockwork (Conde et al., 2001).

In the southernmost part of the Ossa Morena zone an equivalent volcanic sequence hosts abundant strata-bound deposits in an intensely deformed and metamorphosed setting (Aracena belt; Fig. 1). The Maria Luisa mine, which was worked for Cu-Zn, consists of several ca. 100-m-long massive sulfide lenses interbedded with orthoamphibolite and metarhyolite as well as minor schist, volcaniclastic rock, and carbonate rock. Underlying the massive sulfides are small Cu-rich stockworks in chloritized volcanic rocks. The mineralization was subsequently replaced by a skarn assemblage that modified most of the original features (Vazquez, 1972). The nearby Fuenteheridos deposit is the most important of several carbonate rock- and volcanic rock-hosted Zn-Pb barite strata-bound deposits grouped in the Portel-Aracena belt of Schermerhorn (1981) (type 4 in Table 3; Tornos et al., 2004). Some barite-bearing lenses with abundant galena and
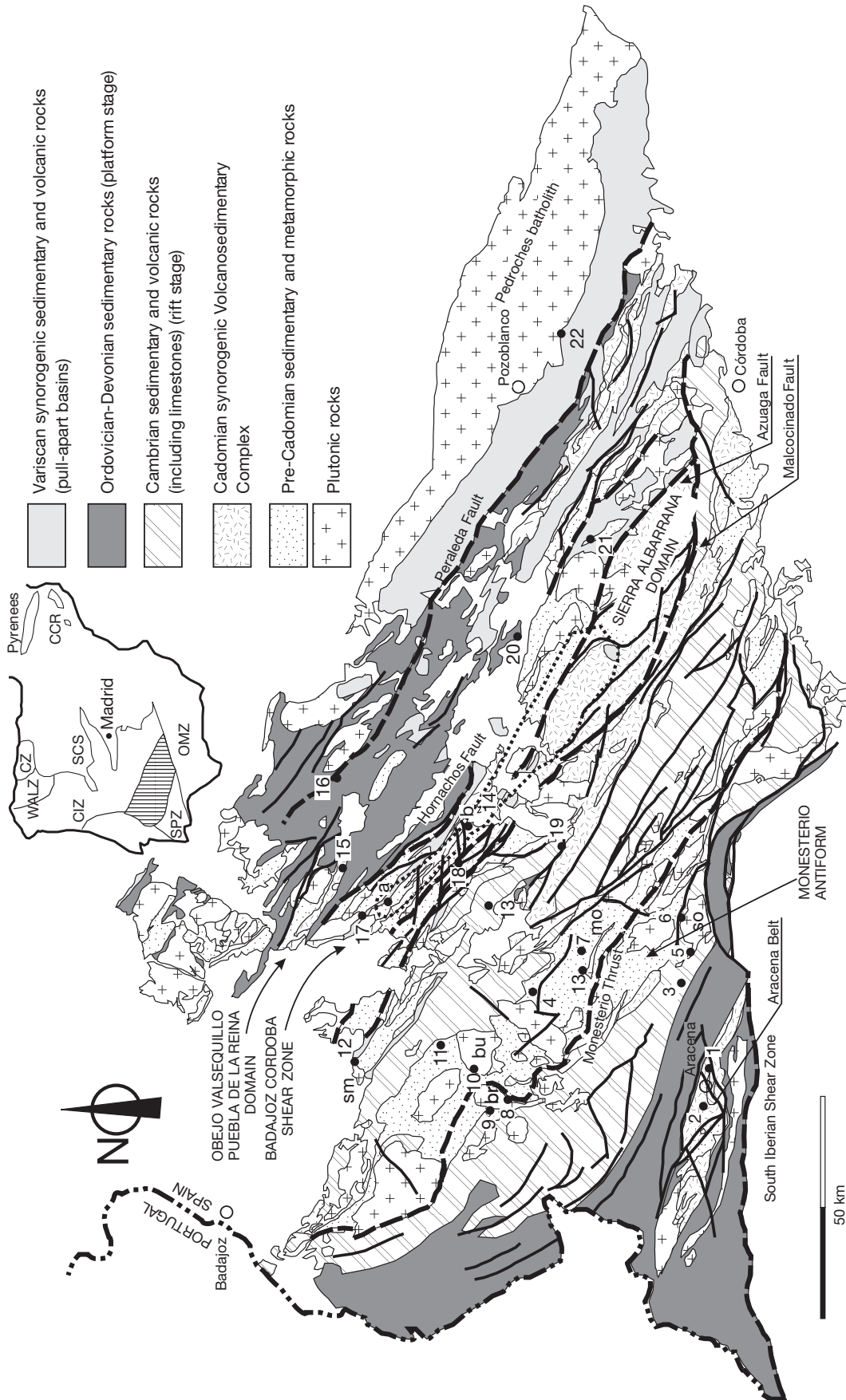
FIG. 1. Geologic map of the Ossa Morena zone with the location of deposits, showings, and localities described in the text and listed in Table 3. Modified from Locutura et al. (1990) and Tornos et al. (2004). 1. Aracena belt, including Fuenteheridos (type 4). 2. María Luisa (type 3). 3. Cala (type 11). 4. La Hinchona (type 10). 5. Sultana (type 13). 6. Aguablanca (type 12). 7. Pb-Zn veins Monesterio structure (Aguilar, Aguila and Nogalito) (type 10). 8. Colmenar (type 11). 9. Bilbaína (type 11). 10. Monchi (type 7). 11. Abundancia (type 13). 12. Santa Marta (type 20). 13. Usagre (type 19) and Las Minas (type 5). 14. Pb-Zn veins in the Badajoz-Córdoba shear zone (Azuaga vein field, limited by dotted line) a. Afortunada b. Arroyo Conejo (type 20). 15. Puebla de la Reina (type 3). 16. San Nicolás (type 15). 17. Matachel (type 14). 18. Retín (type 6). 19. Llerena (type 5). 20. Oropesa (type 18). 21. Nava Paredón (type 9). 22. Espiel (type 16). Thick discontinuous lines are the major faults that limit geologic domains. Inset maps show the zones in the Variscan belt of Iberia. br = Brovales metaluminous Variscan pluton, bu = Burguillos metaluminous Variscan pluton, CCR = Catalonian Coastal Ranges, CIZ = Central Iberian zone, CZ = Cantabrian zone, mo = Monesterio anatectic Cadomian granodiorite and dome, OMZ = Ossa Morena zone, SCS = Spanish Central system, sm = Santa Marta peraluminous Variscan stock, so = Santa Olalla metaluminous Variscan pluton, SPZ = South Portuguese zone, WALZ = West Asturian Leonese zone.

TABLE 1. Major Tectonostratigraphic Units of the Ossa Morena Zone

Orogenic cycle	Tectonostratigraphic Unit	Lithology	Setting	Age	Comments
Syn-Variscan		Turbiditic sediments, sandstones, and shales with limestones, coal seams, and conglomerates; minor alkaline basalt and rhyolite	Restricted foreland, pull-apart and intermontane basins with strike-slip faulting	Devonian to Permian	
Pre-Variscan		Shales and sandstones; local volcanic rocks	Shallow stable passive platform	Ordovician to Early Devonian	Northeast and southwest zones of the Ossa Morena Zone
		Limestones and siliciclastic sediments below bimodal (sub)alkaline to tholeiitic volcanic rocks interbedded with shales and sandstones	Rift-related continental to oceanic basin	Early to Middle Cambrian	
Syn-Cadomian	Aznaga Formation	Turbiditic sediments	Foreland basin	Late Riphean to Early Cambrian	
	Malcocinado Formation	Debris flows, graywackes, conglomerates, limestones, and shales with abundant calc-alkaline volcanic rocks	Magmatic island arc	Late Riphean to Early Cambrian	
	Serie Negra	*Tentudia Formation:* turbiditic shales and graywackes with calc-alkaline volcaniclastic intercalations in the uppermost part	Back-arc to intra-arc	Middle to Late Riphean; the uppermost Tentudía Formation has zircons younger than 564 ± 30 Ma suggesting that it belongs to the Cadomian synorogenic sequence	Core of antiformal structures; up to 3,000 m thick
		Montemolín Formation: biotitic schists with accessory graywackes, black quartzites, volcaniclastic rocks, marbles, and abyssal tholeiitic orthoamphibolites	Passive margin setting with mature continental source		
Pre-Cadomian	Aznaga Gneiss Group	Highly deformed and metamorphosed massive felsic volcanic rocks; minor biotitic paragneisses, marbles, black quartzites, orthoamphibolites (continental tholeiites), and eclogites	Early rifting	Middle Riphean	Crops out in the deepest Badajoz Córdoba shear zone
	Sierra Albarrana Group	Sandstones and shales deposited in a shallow marine shelf platform	Passive margin setting	Proterozoic? Ordovician?	Debated origin; exotic Proterozoic terrane or Ordovician sediments with Central Iberian zone affinities

Based on Quesada et al. (1987, 1991), Eguiluz et al. (2000), Bandrés et al. (2002) and references therein
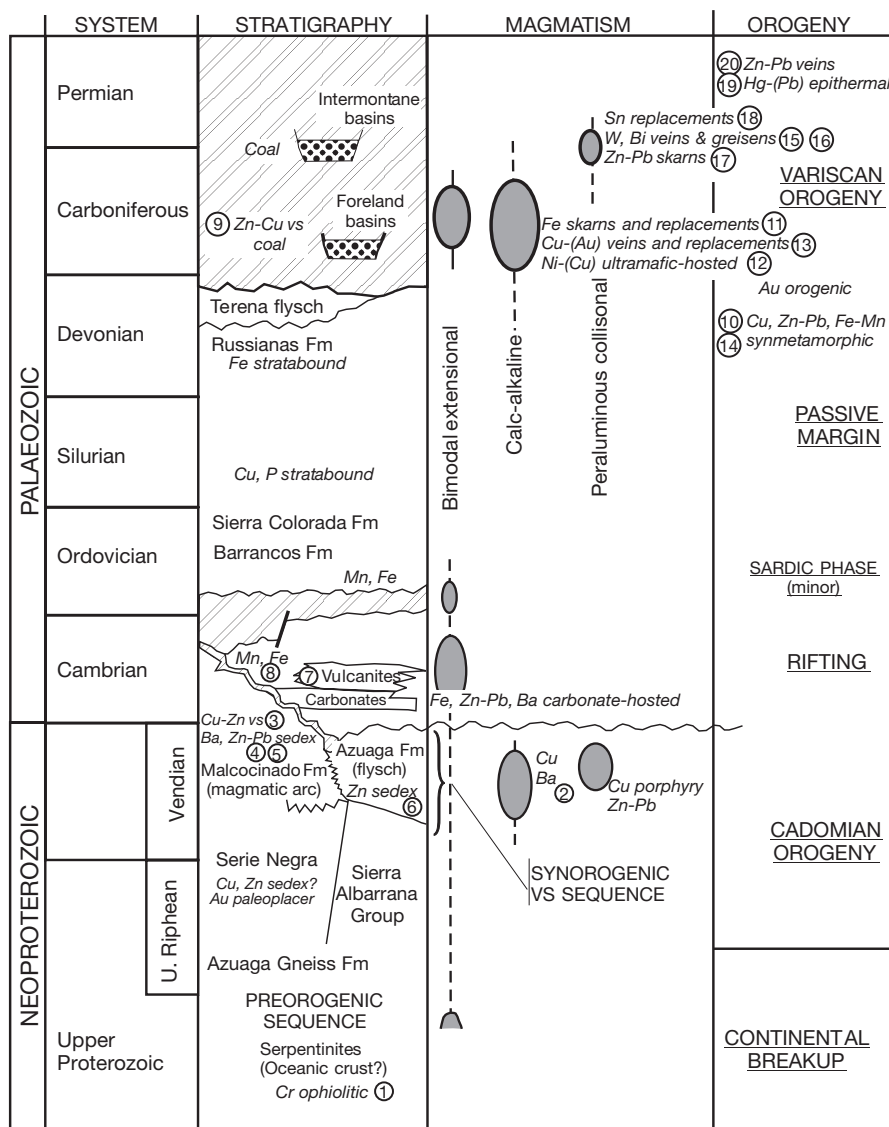
FIG. 2. Summary of the tectonometamorphic and metallogenic evolution of the Ossa Morena zone. Modified and adapted from Quesada (1992) with data of Tornos et al. (2004). Circled numbers refer to the types of deposits described in Tables 3 and 4. Other types of mineralization in the area are also noted. Irregular horizontal lines represent unconformities and diagonal stripes indicate the absence of sedimentary rocks (except in basins).

cinnabar in limestones in the central Ossa Morena zone (Las Minas, 13 in Fig. 1; type 5 in Table 3) are probably stratigraphically equivalent to the Fuenteheridos deposit (Tornos and Locutura, 1989). Sulfur isotopes of the volcanogenic massive sulfides range between 13.0 and 19.5 per mil, indicating that the sulfur was probably leached from a sedimentary sequence.

In the Azuaga Formation, a few stratiform shale-hosted Zn-Pb ore showings are associated with silica- and manganese-rich exhalites and basaltic flows. These occurrences are meter-thick lenses of sphalerite and galena in highly sericitized and chloritized rocks (Retín, 18 in Fig. 1; type 6 in Table 3) and have been interpreted as sedimentary-exhalative deposits (Locutura et al., 1990). Their host rocks belong to the Sierra Albarrana domain and lie unconformably above

epicontinental sedimentary rocks of uncertain age and origin. The existence of late Neoproterozoic and early Paleozoic intrusive rocks in this sequence suggests that they are pre-Cadomian (Quesada et al., 1991; Table 1), but other models propose that they are Paleozoic in age (Apalategui et al., 1990; Azor et al., 1993).

Base metal-bearing veins near the Monesterio granodiorite (type 10)

Abundant small quartz- and carbonate-bearing veins with pyrite, chalcopyrite, sphalerite, and galena occur in the core of the Monesterio antiform, adjacent to the anatectic Cadomian granodiorites, granites, and migmatites, where they are always enclosed by Neoproterozoic dark shales and quartzites (Serie Negra, Table 1). Most of the veins hosted by the

TABLE 2. Main Tectonic, Magmatic, and Metamorphic Events in the Ossa Morena Zone

Orogenic cycle	Deformation	Metamorphism	Interpretation	Age	Magmatism[1]
Variscan	Sinistral displacement along west-northwest–east-southeast structures; abundant north-verging thrusts and folds	Badajoz Córdoba shear zone: high-grade; in other areas below greenschist facies	Northward collision of the South Portuguese zone with the Iberian terrane	390–280 Ma	(4) Late orogenic peraluminous epizonal granodiorites to leucogranites intruded along extensional zones (330–290 Ma)
				Metamorphism 368–331 Ma	(3) Large felsic intrusions, including monzogranites and two-mica granites
					(2) Large, locally zoned, calc-alkaline plutons; ultramafic rocks to granodiorites with dominant tonalites to granodiorites (350–330 Ma)
					(1) Epizonal intrusions and volcanic rocks within pull-apart basins
Early Variscan	Graben formation		Rifting	510–450 Ma	Anorogenic (sub)alkaline to peralkaline igneous rocks, from gabbro to syenite and amphibole-bearing granites (510–500 and 475–470 Ma)
Cadomian	Recumbent folds and thrusts with northeast-southwest and north-south trends	Medium to high grade low-pressure metamorphism with local anatexis	Continent collision, basin inversion and overthrusting	620–480 Ma	(3) Late Cadomian K-rich biotitic granodiorites and granites (530–516 Ma)
					(2) Calc-alkaline intermediate to felsic epizonal intrusions (522–514 Ma)
				Metamorphism 562–524 Ma	(1) Anatectic granodiorites to granites (552–495 Ma)
	East-west-trending isoclinal folds and thrusts	Low-grade intermediate pressure regional metamorphism	Cadomian subduction and deposition of the Tentudía Formation		

Based on Quesada et al. (1987, 1991) and Eguíluz et al. (2000)
[1] Numbers refer to various magmatic units

Montemolín Formation, northeast of the Monesterio granodiorite, are Pb-Zn-rich (Nogalito, El Aguilar, El Aguila; 7 in Fig. 1), whereas veins located in the eastern and southwestern zones and hosted by the Tentudía Formation are rich in chalcopyrite and pyrite (La Hinchona; 4, Fig. 1). Many of these veins have a boudin-like morphology, are subparallel to the regional cleavage, and exhibit only subtle hydrothermal alteration in the selvages. These features led Locutura et al. (1990) to propose that the veins were synmetamorphic, generated during the granodiorite intrusion and regional metamorphism in the Cadomian times. The differing mineralogy of the veins was attributed to the different source rocks.

The Variscan volcanic rock-hosted massive sulfides (type 9 and 14)

The Nava-Paredón orebody (21 in Fig. 1) is the largest of several small massive sulfide prospects located in the Variscan pull-apart basins of the northern Ossa Morena zone (Gabaldón et al., 1985). The mineralization occurs as several strata-bound to irregular lenses up to 3 m thick, located near the contact between rhyolite and overlying heterolithic volcaniclastic rocks of Visean age (Baeza et al., 1981; Tornos et al., 2004). The massive sulfides are pyrite poor but sphalerite, chalcopyrite, and galena rich. They overlie pervasively silicified and sericitized massive rhyolites that host disseminated pyrite with locally high Cu and Au contents. The mineralization is interpreted as synchronous with volcanism and as a replacement deposit along the permeable contact between partially devitrified rhyolite and overlying fault-scarp related mass flows. Sulfur and strontium isotopes suggest that the precipitation of the sulfides took place by mixing of two fluids, one equilibrated with the underlying rhyolite and another corresponding with modified seawater.

Chloritized and silicified volcaniclastic rocks of the Carboniferous volcanic sequence also host other Zn-Cu-Pb disseminations and veins of unknown origin (Matachel; 17 in Fig. 1; type 14 in Table 3). They could correspond with root zones of massive sulfides or be related to their late hydrothermal remobilization.

Mineralization associated with Variscan mafic to intermediate intrusions (types 11, 12, and 13)

Historically, most of the mining in the Ossa Morena zone has been that of iron ores located at the contact between Variscan gabbroic to granodioritic intrusions (350–330 Ma) and the volcaniclastic rocks and limestones of late Neoproterozoic-Early Cambrian age. Three styles of mineralization of type 11 occur (Table 3; Tornos et al., 2003): (1) early replacive ores with semimassive magnetite and accessory pyrite and chalcopyrite associated with actinolite-hornblende, albite, clinopyroxene, calcite and quartz, usually located along major shear bands (Colmenar mine; 8 in Fig. 1); (2) massive magnetite- and vonsenite-rich replacements in tonalite and in calc-silicate and pelitic hornfels, which are also enriched in U, rare earth elements (REE), and Co (Monchi mine; 10 in Fig. 1) (Arribas, 1962; Casquet et al., 1998); (3) calcic skarn with a prograde anhydrous assemblage of andraditic garnet and hedenbergite replaced by actinolite, epidote, magnetite and sulfides, that postdate the former magnetite replacements (e.g., several deposits around the Burguillos and Brovales

intrusives: Cala; 3 in Fig. 1) (Velasco and Amigó, 1981; Casquet and Tornos, 1991; Cuervo et al., 1996). The total tonnage of the different iron orebodies was more than 150 Mt, containing 25 to 45 percent Fe (Vázquez, 1989). The magnetite ± albite ± actinolite replacements that predate the skarns have many similarities to iron oxide-copper-gold deposits (Tornos et al., 2003).

Several copper-bearing quartz-ankerite veins (e.g., mina Abundancia; 11 in Fig. 1), sometimes hosting significant gold and bismuth and averaging 3.2 percent Cu and 15 g/t Au (mina Sultana; 5 in Fig. 1; type 13 in Table 3), are spatially associated with the same plutonic rocks. Geochemical and fluid inclusion data show that metals, sulfur, and fluids had the same sources as the iron-oxide mineralization and that the ores precipitated by fluid immiscibility of CO_2-rich hypersaline liquids (up to 50 wt % NaCl equiv; Tornos and Velasco, 2002).

The Aguablanca deposit (6 in Fig. 1) is apparently unique in the Ossa Morena zone and probably in the Variscan belt of Europe (type 12 in Table 3). It consists of a subvertical pipe-like orebody hosted by heterogeneous diorite, gabbro, and norite of the small Aguablanca stock. The mineralization, dominated by pyrrhotite, chalcopyrite, and pentlandite, occurs as sulfide-supported breccias with fragments of ultramafic (mainly pyroxenitic) and sedimentary rocks, as large bleb-like massive sulfides, and as irregular disseminations in the host gabbro and norite. The intrusive rocks are pervasively replaced by a complex hydrothermal assemblage with actinolite, biotite, sericite, talc, pyrite, magnetite, and late sulfides—mainly chalcopyrite and pyrite.

Ortega et al. (2001) interpreted the mineralization as an overturned pre-Variscan layered complex. However, Tornos et al. (2001) proposed that it is a chimney-like discordant orebody resulting from the injection of magmatic sulfides and derived from a disrupted Variscan-age stratiform complex formed at depth. Isotopic data indicate a major contamination of juvenile magmas by sedimentary rocks, very likely shales of the underlying Serie Negra (Casquet et al., 2001), accompanied by the incorporation of large amounts of reduced sulfur from the host rocks.

Variscan granite-related mineralization (types 15, 16, and 18)

W-(Sn-Bi-Au) vein and stockwork mineralization in strongly greisenized and tourmalinized slates (type 15 in Table 3) is found in the apical zones of sporadic small Variscan peraluminous epizonal leucogranite stocks. In most of the occurrences, an early quartz-wolframite-(cassiterite) assemblage is replaced by later sulfides and scheelite with minor carbonates and fluorite (e.g., Ovtrach and Tamain, 1977; Gumiel et al., 1987; Gumiel, 1988). The best example is the San Nicolás mine (16 in Fig. 1). Minor quartz-ankerite veins with native bismuth occur near the presumed source intrusions in the Pedroches area (22 in Fig. 1; type 16 in Table 3).

The poorly known tin-rich Oropesa deposit (20 in Fig. 1) is hosted by pervasively silicified and chloritized conglomerate, sandstone, and shale with minor carbonate of Late Carboniferous age. These sedimentary rocks occur in a Variscan pull-apart basin that has been intruded by felsic sills. The mineralization consists of cassiterite, arsenopyrite, pyrite, and

TABLE 3. Major Styles of Mineralization within the Ossa Morena Zone

Timing, type number, and mineralization	Host rock	Geologic setting	Examples	Economic data	Comments
Pre-Cadomian					
1 Podiform Cr in ophiolite	Serpentinites (Pre-Vendian?)	Olistoliths within the Malcocinado Formation	Calzadilla	<0.03 Mt, 25.1% Cr	Some scarce prospects
Cadomian (Upper Vendian-Lower Cambrian)					
2 Porphyry Cu	Disseminations and veins in hydrothermally altered tonalites	Andean-type continental margin with calc-alkaline volcanism; Malcocinado Formation and coeval synorogenic sequences	Ahillones / El Mosquil	Prospect / Prospect	Currently subeconomic
3 Zn-Cu-(Pb) massive sulfides	Mafic and felsic massive and volcaniclastic rocks	Andean-type continental margin with calc-alkaline volcanism; Malcocinado Formation and coeval synorogenic sequences	Maria Luisa and Ana (2) / Puebla de la Reina (15)	1.5 Mt, 0.8% Cu, 3.0% Zn, 0.5% Pb, 0.55 Mt, 1.6% Cu,11% Zn, 1.2% Pb, 32 g/t Ag	Pb-rich and Ba-poor in limestones, Zn-, Fe-, and Ba-rich in volcanosedimentary rocks; subeconomic
4 Strata-bound Zn-Pb-(Ba)	Contact between limestones and bimodal volcanic rocks	Andean-type continental margin with calc-alkaline volcanism; Malcocinado Formation and coeval synorogenic sequences	Aracena (1) / Fuenteheridos (1)	2–3% Zn, 0.4% Pb, 50 g/t Ag ≈4.0 Mt, 2.0% Zn, 0.2% Pb, 80 g/t Ag	
5 Strata-bound Ba-Pb-(Cu)	Felsic volcaniclastic rocks, shales, limestones, cherts	Andean-type continental margin with calc-alkaline volcanism; Malcocinado Formation and coeval synorogenic sequences	Llerena (19) / Las Minas (13)	0.7 Mt 50% barite	Abundant lenses; major barite deposits of Spain
6 Strata-bound Zn-(Pb)	Lenses in shales	Turbiditic sequence in the Azuaga Fmornation above the Sierra Albarrana Group	Retín (18)	Prospect	No obvious relationship with igneous rocks
Post-Cadomian (Lower Cambrian-Devonian)					
7 Volcano-sedimentary Fe-(Cu)		Rift-related volcanism bimodal (alkaline to tholeiitic); facies change to limestones and shales in semigraben structures	La Bilbaína (9) / La Bóveda	7.85 Mt, 52.5% Fe; 0.11% Cu 43.9% Fe	Numerous prospects; subeconomic
8 Volcano-sedimentary Mn	Volcanic rocks, limestones and shales (Early-Middle Cambrian)		Zahínos	Small mines	Lateral? to Fe-(Cu) mineralization; subeconomic
Variscan (Upper Devonian-Permian)					
9 Zn-Cu-Pb massive sulfides	Felsic domes and related volcaniclastic rocks (Late Tournaisian-Early Visean)	Pull-apart basins with bimodal volcanism in island arc(?) margin; deltaic and lagoon sediments	Nava-Paredón (21)	0.3 Mt, 2% Cu, 4.7% Pb, 11% Zn, 183 g/t Ag	Other minor prospects; subeconomic; roughly equivalent to the Pyrite belt and related to volcano-sedimentary Fe oxides
10 Cu, Zn-Pb veins	Schists, graywackes (Serie Negra)	Near Monesterio Cadomian anatectic granodiorite and high-grade metamorphic structure	La Hinchona (4) / El Aguilar (7) / El Aguila (7) / El Nogalito (7)	Small mines and prospects	Abundant but very small veins with Cu in southern part and Pb-Zn in northern part

TABLE 3. (*Cont.*)

Timing, type number, and mineralization	Host rock	Geologic setting	Examples	Economic data	Comments
11 Fe-(Cu) calcic skarns and replacements	Marbles and calc-silicate hornfelses (Late Vendian-Early Cambrian) in contact with Variscan tonalites to granites	Magmatic arc with calc-alkaline I-type granitoids	Colmenar (8), Cala (3), Monchi (10), La Berrona	31 Mt, 35.3% Fe; 50 Mt, 40% Fe, 0.4% Cu; 66% Fe; 23.6 Mt, 24.8% Fe	Abundant prospects and some mines; locally economic; some deposits similar to IOCG deposits
12 Mafic-hosted Ni-Cu	Diorites to ultramafic rocks of Santa Olalla pluton	I-type zoned syntectonic calc-alkaline intrusion	Aguablanca (6)	31 Mt, 0.62% Ni, 0.46% Cu	Deposit under evaluation
13 Cu-(Bi-Au) veins	Veins hosted by Serie Negra, Malcocinado Formation or Variscan igneous rocks	With or in the thermal aureole of calc-alkaline tonalites to granodiorites	Cu: Abundancia (11), Cu-Au: Sultana (5)	<1 Mt, 3.15% Cu, 15 g/t Au	Uncommon; subeconomic
14 Cu-Zn-(Pb) veins	Epiclastic sediments and shales (Late Carboniferous)	Stockworks or late remobilization of type 9	Matachel (17)	Prospect	
15 W-(Sn) veins and greisens	Siliciclastic metasediments with contact metamorphism	Adjacent to minor late Variscan peraluminous epizonal intrusions of leucogranite	San Nicolás (16), Oliva	0.36 Mt, 3% WO_3, 0.25% Bi	Old mines; subeconomic
16 Bi-(Co-Ni) veins	Schists with contact metamorphism	Adjacent to minor late Variscan peraluminous epizonal intrusions of leucogranite	Espiel (22)	No data	Old mines; subeconomic
17 Zn-(Pb-Sn) calcic and magnesian skarns	Marbles (Late Vendian-Early Cambrian) in contact with Variscan leucogranites	Adjacent to minor late Variscan peraluminous epizonal intrusions of leucogranite	Cerro Muriano		
18 Sn replacement deposits	Replacement of Carboniferous detrital sediments or veins in nearby Ordovician quartzites	Pull-apart basins with synchronous felsic and mafic hypoabyssal intrusions	Oropesa (20)	18 Mt, 0.25% SnO_2	Subeconomic
19 Epithermal Hg-(Pb)	Replacement and veins in Lower Cambrian limestones	Spatially related with major late Variscan west-northwest-east-southeast faults and mafic dikes	Usagre (13)	0.11 Mt, 5–7% Hg, 2% Cu	Ancient mine and other prospects
Late to post-Variscan					
20 Pb-Zn-(barite-fluorite) veins	0°–45° and 80°–100° trending veins in Azuaga Group	Related to late (late to post-Variscan) left lateral movement on Badajoz Cordoba shear zone; minor granodiorites	A° Conejo (14), Azuaga ore field (14), Santa Marta (20), Afortunada (14)	Small mines (<1 Mt each)	Numerous old mines, past leading Pb producer; currently subeconomic

Modified from Locutura et al. (1990) and Tornos et al. (2004) where specific references to the deposits can be found (see text); numbers after mines refer to Figure 1

chalcopyrite in stockworks or as replacive bodies (Locutura et al., 1990). Nearby, abundant subvertical quartz-cassiterite veins are hosted by Ordovician quartzite. The mineralization is interpreted to be distal replacements and veins associated with late Variscan subvolcanic peraluminous granitoids similar to those of the Renison Bell deposit in Tasmania (e.g., Patterson et al., 1981).

Late Variscan to post-Variscan Zn-Pb veins (type 20)

The easternmost Ossa Morena zone was the world's leading producer of lead at the end of the nineteenth century. Hundreds of small mines in quartz-carbonate-ankerite veins with sphalerite and Ag-rich galena occur along the Badajoz-Córdoba shear zone and near the adjacent Azuaga fault (14 in Fig. 1). The veins are short (<200 m in length), subvertical and oblique to the strike of the shear zone, with north-south and northeast-southwest trends, and they are almost always hosted by the most brittle rocks (gneisses, amphibolites, and ultramylonites) or the shales of the Azuaga Formation. The veins are particularly abundant and sulfide rich near the late Variscan Santa Marta granodiorite (12 in Fig. 1) (Tornos et al., 2004). The hydrothermal fluids were low-temperature (ca. 200°C), boiling, low-salinity, aqueous fluids (Chacón et al., 1981).

Lead Isotopes

The evolution of lead in the Earth's crust has been modeled on the basis of the U/Th/Pb ratios in the different bulk reservoirs (Doe and Zartman, 1979; Zartman and Haines, 1988) and stages of global isotopic homogenization (Stacey and Kramers, 1975; Cumming and Richards, 1975). However, these global models have limited application at the district scale. Recent studies have tried to develop growth curves for specific terranes with a homogeneous lead isotope evolution (e.g., Andrew et al., 1984, Ludwig et al., 1989; Sinclair et al., 1993; Carr et al., 1995). These models try to incorporate regional homogenization processes such as fine-grained sedimentation, igneous melting, hydrothermal leaching, or supergene alteration at different ages.

Only limited lead isotope data are available for the rocks of the Ossa Morena zone. Nägler (1990) presented some lead isotope analyses of Cambrian shales of the Ossa Morena zone and of the late Neoproterozoic shales of the Central Iberian zone, which are equivalent to those of the syn-Cadomian Tentudía Formation of the Ossa Morena zone (Quesada et al., 1987). These data define a trend close to the Stacey and Kramers (1975) evolutionary curve, in which μ ($^{238}U/^{204}Pb$) values are near 9.75 (curve P in Fig. 3). The high ε_{Nd} values (>–4) and the bulk geochemistry of the shales (Ugidos et al., 1997) are consistent with a significant input of mantle-derived rocks during the late Neoproterozoic and early Paleozoic (i.e., during the Cadomian orogeny). Geochemical signatures indicate that the shales were mostly derived from the erosion of the Cadomian magmatic arc (Bandrés et al., 2002). A second group of shales, of Tremadoc to Visean age, have higher μ values (9.9–10.4) and lower ε_{Nd} values (between –13 and –7), suggesting that they were derived from the erosion of older supracrustal rocks, very likely the old basement in the Central Iberian zone. Locally, these signatures have been partially disturbed and homogenized during the Variscan metamorphism (Nägler et al., 1993). Since these shale curves should represent the average lead signatures of sedimentary rocks (Nägler, 1990), lead isotope data that plot below them must indicate the input of primitive lead from a source external to the basin.

The $^{207}Pb/^{206}Pb$ model age (Stacey and Kramers, 1975) of most of the studied deposits (Table 4) broadly corresponds with the true geologic age, where it is known. Although the model ages cannot accurately define the timing of the ore-forming events, these data help to distinguish Cadomian and Variscan ore-forming events.

Analytical methods

Lead isotope analyses were performed on sulfides and other ore minerals from a wide range of representative deposits and prospects of the Ossa Morena zone (Table 4). Ore minerals were dissolved in sealed Teflon beakers at 180°C with a 3:1 mixture of 7M HCl and 14M HNO$_3$. Lead was purified through chromatography with AG1-X8 and AG-MP1 resins in hydrobromic medium or by electrodeposition (galena). Fractions of the purified lead were loaded onto rhenium filaments using the silica-gel technique. The lead isotope ratios were measured on a Finnigan MAT 262 mass spectrometer at the Department of Mineralogy of Geneva (Switzerland). Lead isotope ratios were corrected for fractionation by a +0.08 percent amu correction factor on the basis of more than 150 analyses of the NBS981 international standard. The analytical uncertainties (2σ) were 0.05 percent for $^{206}Pb/^{204}Pb$, 0.08 percent for $^{207}Pb/^{204}Pb$, and 0.10 percent for $^{208}Pb/^{204}Pb$. Procedural blanks were always <120 pg Pb. The μ ($^{238}U/^{204}Pb$) and ω ($^{232}Th/^{204}Pb$) values were calculated with reference to the Stacey and Kramers (1975) curve. Because most ore samples have high Pb/(U + Th) ratios no correction for in situ radiogenic decay was required.

Three samples of Variscan metaluminous granitoids (Burguillos and Brovales stocks) and one of the Neoproterozoic orthoamphibolite belonging to the Montemolín Formation were analyzed (Table 4) following the methodology described by Chiaradia and Fontboté (2003). These authors showed that the analysis of massive felsic rocks after acid attack yields lead isotope ratios similar to those of the common lead and need not to be corrected for in situ radiogenic lead.

Results

The ore lead isotope results, including the data of Marcoux et al. (2002b), show rather variable $^{206}Pb/^{204}Pb$ (17.49–18.44), $^{207}Pb/^{204}Pb$ (15.47–15.67), and $^{208}Pb/^{204}Pb$ (37.37–38.78) ratios (Table 4; Figs. 3 and 4). As a whole, the lead isotope data do not define any clear trend and have a spread that is larger than in any other zone of the Iberian Peninsula (Arribas, 1993; Tornos and Arias, 1993; Arribas and Tosdal, 1994; Velasco et al., 1994; Cardellach et al., 1996; Tornos et al., 1996; Velasco et al., 1996; Arias et al., 1997; Canals and Cardellach, 1997; Marcoux, 1998) and possibly larger than in any single terrane in the European Variscan belt.

On the $^{207}Pb/^{204}Pb$ versus $^{206}Pb/^{204}Pb$ diagram (Fig. 4), the ore samples plot both above and below the average crust model curve of Stacey and Kramers (1975) and between the mantle and upper crustal growth curves of Zartman and Doe (1981). In the $^{206}Pb/^{204}Pb$-$^{208}Pb/^{204}Pb$ diagram most samples
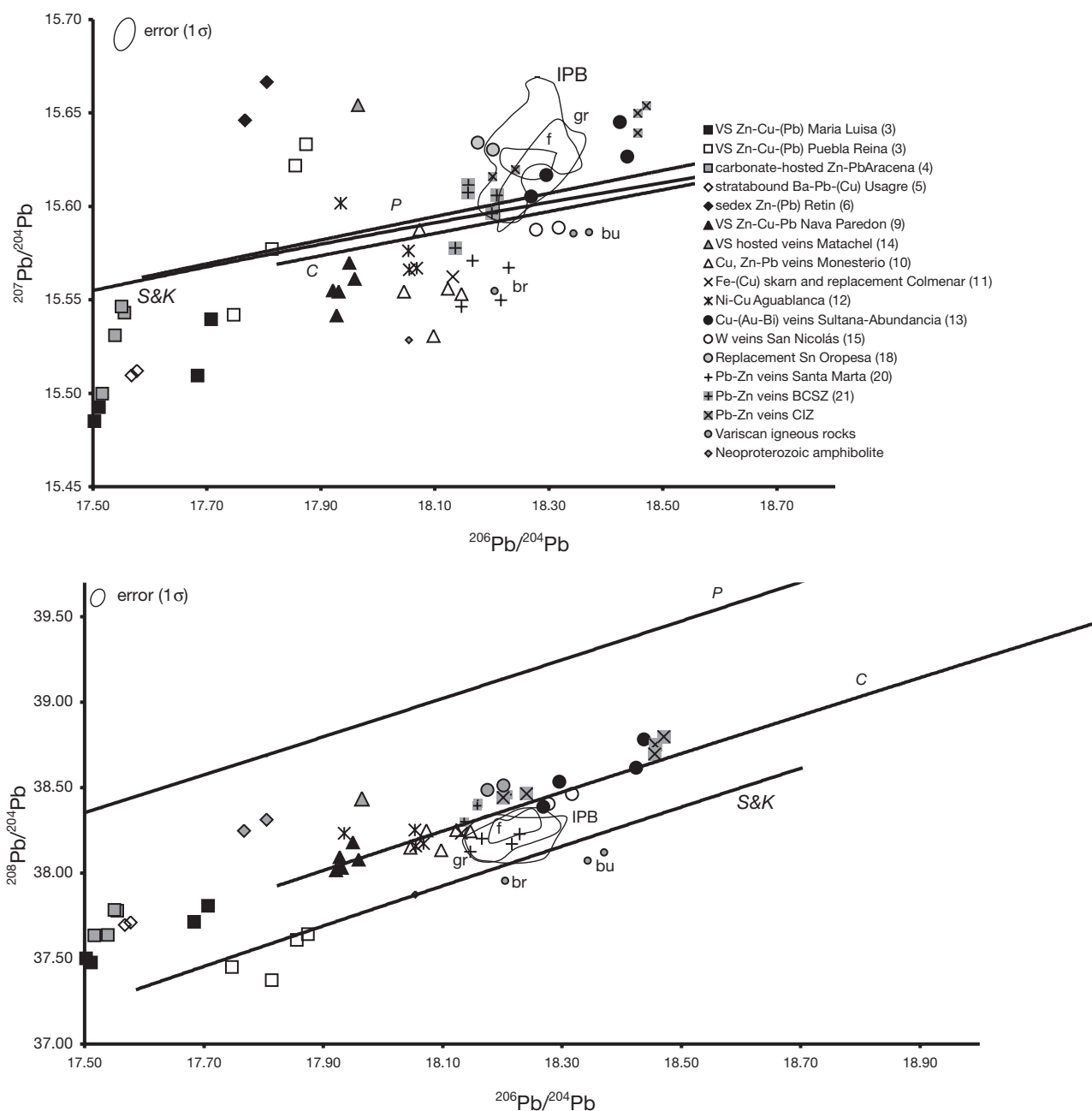
Fig. 3. Lead isotope compositions of mineralization in the Ossa Morena zone. For comparison, the crustal growth curve of Stacey and Kramers (1975) is shown (S&K). The fields of other lead isotope data of the Iberian Peninsula are as follows: br = Brovales pluton, bu = Burguillos pluton, F = Pb-Zn veins of the Pedroches batholith (Arribas, 1993), gr = feldspars of granites of the Variscan belt of Iberia (Michard Vitrac et al., 1981; Arribas, 1993), IPB = massive sulfide deposits of the Iberian pyrite belt (Marcoux, 1998). Curve P is the evolution curve of the sample AL-1 of Nägler (1990) from a late Neoproterozoic shale of the Central Iberian zone, equivalent to the uppermost Serie Negra of the Ossa Morena zone. Curve C is the evolution curve of the sample ZAF-5 of Nägler (1990), a Cambrian shale of the Ossa Morena zone. Numbers in the legend refer to the types of mineralization described in the Table 3. The overall analytical precision exceeds ±0.009 (^{206}Pb/^{204}Pb), ±0.012 (^{207}Pb/^{204}Pb), and ±0.039 (^{208}Pb/^{204}Pb).

plot above the upper crust, mantle, and orogen average values, indicating a major contribution of Th-derived lead.

The combination of geology and timing of the ore deposits (Table 3) with lead isotope data allow us to divide the mineralization into seven groups: (1) stratiform deposits in the Azuaga Formation, (2) volcanosedimentary and sedimentary exhalative mineralization hosted by syn-Cadomian volcanosedimentary rocks in both the northern and southern Ossa Morena zone, (3) synmetamorphic veins near the Monesterio anatectic granodiorite, (4) Variscan massive sulfides,

TABLE 4. Lead Isotope Composition of Sulfides, Oxides, and Plutonic Rocks

Sample	Locality	Type[1]	Mineral	$^{206}Pb/^{204}Pb$	$^{207}Pb/^{204}Pb$	$^{208}Pb/^{204}Pb$	Geologic age (Ma)	Model age (Ma)	μ	ω
SANA–1	Santa Ana (MªLuisa)	3	Sp	17.707	15.539	37.808	522–514	571	9.6	38.2
SANA–11	Santa Ana (MªLuisa)	3	Sp	17.684	15.509	37.714		529	9.5	372
ML–1	Maria Luisa	3	Py–sp	17.511	15.492	37.477		629	9.5	369
	Maria Luisa [2]	3	Ms	17.491	15.470	37.406		601	9.4	36.2
	Maria Luisa [2]	3	Ms	17.503	15.485	37.499		621	9.4	36.9
209–9	Puebla Reina	3	Sp	17.874	15.633	37.641		626	10.0	37.8
209–10	Puebla Reina	3	Sp	17.856	15.622	37.608		619	9.9	37.6
PR–2	Puebla Reina	3	Gn	17.747	15.542	37.449		547	9.6	35.9
	Puebla Reina [2]	3	Gs	17.814	15.577	37.372		564	9.7	35.6
	Puebla Reina [2]	3	Gs	17.819	15.587	37.404		580	9.8	35.9
AR–7	Aracena	4	Gn	17.555	15.543	37.778		694	9.7	39.5
AR–8	Aracena	4	Gn	17.517	15.500	37.634		640	9.5	38.0
AR–8a	Aracena	4	Gn	17.551	15.546	37.785		702	9.7	39.6
	Fuenteheridos [2]	4	Ds	17.539	15.531	37.637		683	9.6	38.5
LM–1	Las Minas	5	Gn	17.568	15.510	37.698	Early Cambrian	620	9.5	38.1
LM–2	Las Minas	5	Gn	17.577	15.512	37.712		617	9.5	38.2
219–5	Retín	6	Sp	17.767	15.646	38.249	See text	728	10.1	42.7
219–6	Retín	6	Sp	17.805	15.666	38.312		736	10.2	43.2
PAR–1	Nava-Paredón	9	Gn	17.950	15.570	38.181	340 ± 5	448	9.7	38.9
N–13A	Nava-Paredón	9	Py	17.931	15.554	38.031		431	9.6	37.9
N–18	Nava-Paredón	9	Cpy	17.959	15.561	38.079		423	9.6	38.1
NP–1	Nava-Paredón	9	Gn	17.927	15.542	38.095		409	9.5	38.0
	Nava-Paredón [2]	9	Ms	17.921	15.555	38.018		440	9.6	37.9
HI–1	La Hinchona	10	Cp	18.073	15.588	38.251	Variscan	392	9.7	38.7
HI–2	La Hinchona	10	Cp	18.046	15.554	38.148		343	9.6	37.6
68–72–1	El Aguila (Monesterio)	10	Gn	18.147	15.553	38.245		263	9.5	37.4
68–49–1	El Nogalito (Monesterio)	10	Gn	18.123	15.556	38.253		288	9.6	37.6
68–51–1	El Aguilar (Monesterio)	10	Gn	18.097	15.531	38.134		255	9.5	36.7
S–300	Colmenar	11	Mt	18.132	15.562	38.234	332 ± 3	294	9.6	37.6
AG–5	Aguablanca	12	Po	17.935	15.602	38.232	Variscan	522	9.8	40.1
AG–18	Aguablanca	12	Po	18.054	15.576	38.252		382	9.7	38.6
	Aguablanca [2]	12	Ms	18.055	15.566	38.159		361	9.6	37.9
	Aguablanca [2]	12	Ms	18.068	15.567	38.174		353	9.6	379
AB–2	Abundancia	13	Cp	18.269	15.605	38.387	Variscan	279	9.7	38.3
AB–6	Abundancia	13	Cp	18.425	15.645	38.615		244	9.9	39.1
SU–10	Sultana	13	Cp	18.296	15.617	38.534	313 ± 13	283	9.8	39.1
SU–21	Sultana	13	Gn	18.438	15.627	38.782		197	9.8	39.5
248–4	Matachel	14	Gn	17.965	15.654	38.434	Variscan	599	10.0	42.2
SN–3	San Nicolás	15	Wolfr	18.317	15.589	38.463	300–280	209	9.7	38.0
SN–4	San Nicolás	15	Wolfr	18.278	15.587	38.404		234	9.7	37.9
ESP–1	Espiel	16	Py	18.398	15.632	38.460		237	9.8	38.2
OR–1	Oropesa	18	Apy	18.202	15.630	38.513	300–280	379	9.9	40.0
OR–2	Oropesa	18	Cp–py	18.176	15.634	38.485		406	9.9	40.2
SM–1	Santa Marta	20	Gn	18.216	15.550	38.172	300–280	204	9.5	36.4
SM–1a	Santa Marta	20	Gn	18.229	15.567	38.229		230	9.6	36.9
SM–2	Santa Marta	20	Gn	18.166	15.571	38.203		286	9.6	37.4
SM–2b	Santa Marta	20	Gn	18.146	15.546	38.125		249	9.5	36.6
213–2	Afortunada	20	Gn	18.159	15.611	38.407		373	9.8	39.4
213–10	Afortunada	20	Gn	18.158	15.607	38.395		366	9.8	39.2
213–10a	Afortunada	20	Gn	18.136	15.578	38.300		324	9.6	38.3
215–4	Arroyo Conejo	20	Gn	18.200	15.596	38.430		312	9.7	38.8
215–4a	Arroyo Conejo	20	Gn	18.209	15.606	38.459		326	9.8	39.2
CEN–1	Centenillo	[3]	Gn	18.201	15.616	38.443	≈220	352	9.8	39.3
CEN–2	Centenillo	[3]	Gn	18.241	15.620	38.465		330	9.8	39.2
AS–1041	Asturiana	[3]	Gn	18.456	15.639	38.752	145 ± 18	208	9.8	39.5
AS–1042	Asturiana	[3]	Gn	18.471	15.654	38.798		228	9.9	39.9
HIE–1	Hiendelaencina	[3]	Gn	18.456	15.650	38.698	Early Alpine	231	9.9	39.4
PC–1	Orthoamphibolite Montemolin Formation		WR	18.054	15.529	37.874	Late Neoproterozoic			
BP–130	Burguillos granodiorite		WR	18.371	15.586	38.120	338 ± 2			
BP–130R	Burguillos granodiorite		WR	18.343	15.585	38.072				
BRO–130	Brovales tonalite		WR	18.205	15.555	37.956	340 ± 7			

Model ages, μ and ω values calculated from Stacey and Kramers (1975)
Geological ages are from Tornos et al. (2004)
Analytical precision exceeds 0.05% ($^{206}Pb/^{204}Pb$), 0.08% ($^{206}Pb/^{204}Pb$) and 0.10% ($^{206}Pb/^{204}Pb$).
Apy = arsenopyrite, Cp = chalcopyrite, Ds = disseminated sulfides, Gn = galena, Gs = gossan, Ms = massive sulfides, Py = pyrite, Sp = sphalerite, Wolfr = wolframite, WR = whole rock; μ = $^{238}U/^{204}Pb$, ω = $^{232}Th/^{204}Pb$
[1] As listed in Table 3
[2] Data from Marcoux et al. (2002)
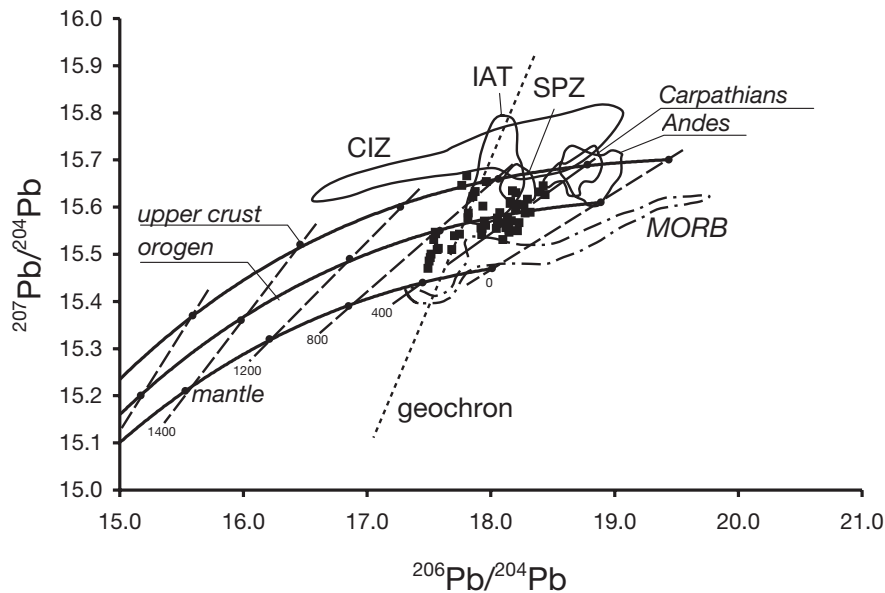[3] Samples belonging to the Central Iberian zone, outside the map in Figure 1

FIG. 4. $^{206}Pb/^{204}Pb$ vs. $^{207}Pb/^{204}Pb$ diagram showing the lead isotope composition of the studied ore deposits compared with those of adjacent terranes. For reference, the global curves of upper crust, orogene, and mantle of the plumbotectonic model of Zartman and Doe (1981) are also plotted. The field Central Iberian zone represents the estimated lead isotope composition of sedimentary rocks derived from the ancient crust of the Central Iberian zone in the 600 to 300 Ma interval, as calculated from data of Nägler (1990). The field of MORB is from Zindler and Hart (1986), and the lead isotopic composition of sulfides from the Carpathian zone and the Andes are from Chiaradia and Fontboté (2002) and Marcoux et al. (2002). The geochron is the isochron representing lead having t = 0; all modern single-stage leads in the Earth and in the meteorites lie on it. Dashed lines are isochrons in 400 Ma intervals. IAT = Iberian autochthonous terrane, including the Central Iberian (CIZ), West Asturian Leonese, and Cantabrian zones (Fig. 1), SPZ = South Portuguese zone.

(5) iron oxide, copper-gold, and Ni-(Cu) mineralization related to Variscan metaluminous magmatism, (6) mineralization related to Variscan peraluminous magmatism, and (7) post-Variscan Pb-Zn veins spatially associated with the Badajoz-Córdoba shear zone. These groups are described below.

Stratiform deposits in the Azuaga Formation (type 6): These deposits (18 in Fig. 1) are characterized by high U/Pb ratios (μ = 10.1–10.2) and model ages between 736 and 728 Ma. The results are consistent with the leaching of metals during the upper Neoproterozoic from an older basement isotopically equivalent to that of the Central Iberian zone, with μ values between 9.9 and 10.4 (Nägler, 1990). The lead isotope data support the hypothesis of Quesada et al. (1991) that the siliciclastic sequence underlying the mineralization, and belonging to the Sierra Albarrana domain, is of Neoproterozoic age and has geochemical affinities with the Central Iberian zone.

Volcanosedimentary and sedex mineralization hosted by syn-Cadomian volcanosedimentary rocks in the northern and southern Ossa Morena zone (types 3 and 4): These deposits have lead isotope compositions that in the $^{206}Pb/^{204}Pb$ versus $^{207}Pb/^{204}Pb$ diagram (Fig. 3) define a linear array with a positive slope that cannot be interpreted as a secondary isochron or as the result of analytical error. As a whole, the data indicate that the metals were derived from a heterogeneous mixture of crustal and mantle reservoirs.

Both the carbonate- and volcanic-hosted massive sulfides of the Aracena massif (Aracena, 1 in Fig. 1; María Luisa and Santa Ana, 2 in Fig. 1) are characterized by rather homogeneous signatures and low μ values (9.4–9.7) (Fig. 3). The broadly synchronous carbonate-related mineralization in the central Ossa Morena zone (Las Minas, 13 in Fig. 1) has similar primitive signatures (μ = 9.5–9.7). The fact that these isotope data plot below the Stacey and Kramers (1975) curve in the $^{206}Pb/^{207}Pb$ diagram indicates that lead could have been derived from the incomplete mixing of lead from orogenic and enriched-mantle reservoirs with no significant input from an unmodified upper crust.

The volcanogenic massive sulfides in the northern Ossa Morena zone (Puebla de la Reina, 15 in Fig. 1) have more variable lead isotope signatures. The highest U/Pb ratios (μ = 10) indicate that the radiogenic lead was derived from a continental crust, probably from the same source as the sedimentary-exhalative mineralization in the Albarrana domain. The less radiogenic samples have compositions equivalent to those from the southern and central Ossa Morena zone.

The $^{207}Pb/^{206}Pb$ model ages of these massive sulfides range between 702 and 529 Ma (late Neoproterozoic-Early Cambrian). These ages are maximum geologic ages owing to the significant proportion of mantle lead. In fact, the youngest model ages are broadly equivalent to those of the Cadomian igneous rocks (573–524 Ma). If these ages are true geologic ages, then the volcanic rocks of the Aracena region can be correlated with the Cadomian synorogenic volcanic complex and are not Silurian in age, as proposed by Crespo (1991).

Veins adjacent to the Monesterio anatectic granodiorite (type 10): These deposits are characterized by relatively non-radiogenic signatures ($^{206}Pb/^{204}Pb$ = 18.146–18.197; $^{207}Pb/^{204}Pb$ = 15.531–15.588) and broadly Variscan (392–255 Ma) model

ages. The lead isotope results plot below the regional shale curves and the Stacey and Kramers (1975) growth curve (μ = 9.5–9.7) and suggest that a significant fraction of the lead was derived from a primitive source. The dominant regional metamorphism and the granitoids of the Monesterio dome have been dated as Cadomian (Ordoñez, 1998; Salman et al., 1999), and the veins were also considered to be Cadomian (Locutura et al., 1990). However, their $^{207}Pb/^{206}Pb$ model ages are more consistent with a Variscan age.

Variscan massive sulfides (type 9): The Nava-Paredón deposit (21 in Fig. 1) has lead isotope ratios that define a rather tight cluster below the orogen growth curve. The compositions are significantly more homogeneous than those of the Cadomian massive sulfides, and the $^{206}Pb/^{207}Pb$ ratios are identical within analytical error (Fig. 3). The rather primitive signatures are responsible for model ages (450–410 Ma) that are retarded as compared with geologic ages (340 ± 5 Ma; Table 4).

The sample of the Matachel vein (17 in Fig. 1) shows a significantly more crustal signature (μ = 10.1) than does the Nava Paredón mineralization. This lead was most likely derived from the adjacent pre-Cadomian shales and gneisses, and it received only a minor contribution of the primitive lead that characterizes the massive sulfides. The lead isotope ratios indicate that these veins probably represent a Variscan mineralization with no genetic relationship to the massive sulfides hosted by the same sequence.

Iron oxide, copper-gold, and Ni-(Cu) mineralization related to the metaluminous Variscan magmatism (types 11 and 12): These deposits include diverse mineralization spatially related to the Variscan gabbros to granodiorites. Lead isotope compositions of three of four samples from the mafic rock-hosted Aguablanca magmatic Ni-Cu deposit (6 in Fig. 1) are very similar, suggesting a high degree of magmatic homogenization. Sample AG-5 is more radiogenic, a feature that may be due to the strong superimposed hydrothermal alteration (Tornos et al., 2001). The low U/Pb ratios of pyrrhotite (Marcoux et al., 2002b) indicate that the variation cannot be due to an uncorrected radiogenic lead addition. The lead isotope data plot slightly below the growth curves of the host Neoproterozoic and Cambrian rocks (μ = 9.6–9.7), indicating a significant degree of mixing between a primitive lead and a more radiogenic lead. The model ages of the Aguablanca orebody (383–352 Ma) are consistent with a Variscan age and agree with the age of the adjacent plutons (332 ± 3 Ma U/Pb age of Salman et al., 1999) and a 359 ± 18 Ma Rb/Sr reference line (Casquet et al., 2001).

The lead isotope composition of sulfides of the nearby Cu-bearing veins (5 and 11 in Fig. 1) plot above the Stacey and Kramers (1975) curve. This location is consistent with the derivation of most of the lead from upper crustal sources (μ = 9.7–9.8), very likely the Serie Negra, with a minor contribution from the associated igneous rocks belonging to the Burguillos and Santa Olalla intrusions (Fig. 1).

Except for one sample from the Colmenar mine (S-300), which yields geologically consistent results, the other magnetite lead isotope data yield future model ages. This feature is probably due to the existence of minute inclusions of U- and Th-bearing minerals in the magnetite. Recent REE and Sm/Nd studies have shown that magnetite from skarns in southwestern Spain includes abundant inclusions of allanite, monazite and other U- and Th-bearing minerals (Darbyshire et al., 1998). The magnetite sample S-300 has a rather primitive signature intermediate between that of the sedimentary rocks and the adjacent plutonic rocks, again suggesting the mixing of lead from the sedimentary rocks and the adjacent metaluminous Variscan rocks (Fig. 3).

Mineralization related to Variscan peraluminous magmatism (types 15 and 18): This mineralization, represented by the W-(Bi) veins of the San Nicolás mine (16 in Fig. 1) and the replacive Sn ores of the Oropesa deposit (20 in Fig. 1), shows very different but internally homogeneous results. At Oropesa, the sulfides have radiogenic lead signatures (μ = 9.9) indicating an upper crustal derivation without significant juvenile contamination. The lead isotope compositions are similar to those of the Zn-Pb mineralization and of feldspars of the granitoids of the Iberian zone and are markedly different from other deposit types of the Ossa Morena zone (Fig. 3).

In contrast, the wolframite of the San Nicolás perigranitic vein system has an unexpectedly primitive signature, plotting below the Stacey and Kramers (1975) growth curve (μ = 9.7). These veins are hosted by late Paleozoic sedimentary rocks of the northern Ossa Morena zone, which have Central Iberian affinities and should have strong crustal signatures (Nägler, 1990). They are spatially and genetically related to peraluminous epizonal granites similar to those hosting W-(Sn) veins all along the Variscan belt of Europe and are regionally characterized by dominantly crustal sources. This unusual situation can only be interpreted as being related to the existence of a deep nonradiogenic lead reservoir that has controlled the geochemistry of the late orogenic epizonal felsic magmatism of the area.

Post-Variscan Pb-Zn veins spatially associated with the Badajoz-Córdoba shear zone (type 20): These veins can be divided into two different groups. Most of them show no obvious relationships with Variscan granitoids (Afortunada, A°Conejo, 14 in Fig. 1) and are characterized by $^{206}Pb/^{204}Pb$ values between 18.136 to 18.209 and corresponding $^{207}Pb/^{204}Pb$ values of 15.578 to 15.611, with μ = 9.6 to 9.8. A second group of samples belong to veins hosted by gneiss within the Badajoz-Córdoba shear zone but adjacent to a Variscan granodiorite (Santa Marta; 12 in Fig. 1). These samples have equivalent $^{206}Pb/^{204}Pb$ signatures but lower $^{207}Pb/^{204}Pb$ ones, and μ = 9.5 to 9.6 (Table 4), reflecting a larger contribution of mantle-derived lead. An independent group of samples corresponds with other Pb-Zn-(Ag) veins outside the Ossa Morena zone (not shown in the Figure 1), which include El Centenillo (northern Los Pedroches batholith), Asturiana, and Hiendelaencina (Spanish Central system, inset in Fig. 1). All of them have high μ values (9.8–9.9).

An outstanding problem in the metallogenic evolution of the Iberian Peninsula is the age and origin of the widespread Pb-Zn(-barite-fluorite)-veins that occur all along the Ossa Morena zone, the Central Iberian zone, and the Pyrenees. These veins are usually related to Variscan granitoids (granodiorites to monzogranites), occurring both inside and peripheral to them. Some authors have suggested a late Variscan age related to the waning stages of perimagmatic hydrothermal systems (Concha et al., 1992; Lillo et al., 1992). Such an

hypothesis is plausible for some vein fields characterized by a zonal peribatholithic arrangement with intraplutonic copper veins and zonally arranged Pb-Zn and Sb lodes, as in some areas of the Los Pedroches batholith (Ovtrach and Tamain, 1977). However, studies on other veins suggest that most of them do not have any genetic link with the related granitoids. Crosscutting relationships with Mesozoic sedimentary rocks, radiometric dating, and stable isotope data support a genesis related to regional, low-temperature convective hydrothermal cells that were mostly recharged by meteoric or basinal waters (Tornos et al., 1991; Johnson et al., 1996). The veins can be interpreted as having formed during a large span of time ranging from the Permian to the Tertiary (e.g., Halliday and Mitchell, 1984; Canals and Cardellach, 1992; Galindo et al., 1994; Fanlo et al., 1998).

The veins within the Central Iberian zone and the Catalonian Coastal Ranges (inset in Fig. 1) are interpreted as Late Jurassic to Cretaceous in age (Canals and Cardellach, 1992; Galindo et al., 1994). Their lead isotope model ages are broadly consistent with this interpretation (Table 4). However, the lead isotope signatures of the veins associated with the Los Pedroches batholith plot in the field of the feldspars of the spatially associated granitoids, indicating that they must have an age close to that of the hosting granites. A Permo-Triassic age is consistent with the oldest K-Ar data presented by Halliday and Mitchell (1984) and with the crosscutting relationships of the veins with the Permo-Triassic sedimentary rocks unconformably lying upon the granitoids (Font and Thibieroz, 1981).

The lead isotope ratios of the Pb-Zn veins in the Badajoz-Córdoba shear zone suggest that they are late Variscan and are older than the Jurassic-Cretaceous veins. The formation of these veins is interpreted to be related to the waning stages of movement of the Badajoz-Córdoba shear zone. The last major tectonic activity along this shear zone, in the Late Carboniferous, was strike-slip displacement in a brittle environment. Such conditions are consistent with the formation of the mineralized veins in tensional gashes resulting from left-lateral movement (Tornos et al., 2002, 2004).

Discussion: Implications for the Geology and Metallogeny of the Ossa Morena Zone

Origin of lead in the massive sulfides

The lead isotopes of the volcanogenic and sediment-hosted massive sulfides of Cadomian age define a mixing array plotting between crustal and mantle lead curves; the best fit is for an age of 630 Ma (Figs. 3 and 4). Mixing lines are typical of volcanogenic massive sulfides, as has been described in the Hokuroko district (Fehn et al., 1983), the Caledonian massive sulfides (Bjorlykke et al., 1993), the Lachlan belt (Carr et al., 1995), and the Abitibi belt (Thorpe, 1999). They are interpreted as reflecting the synvolcanic reaction of hydrothermal fluids with the host and underlying rocks. Usually, single deposits have homogeneous lead isotope signatures, reflecting homogenization of lead sources in large hydrothermal cells (e.g., Fehn et al., 1983; Carr et al., 1995; Thorpe, 1999), but in some cases a major isotopic variation exists at the deposit scale (Bjorlykke et al., 1993). This behavior traditionally has been interpreted as related to the degree of isotopic homogenization within the hydrothermal cell, the mixing lines reflecting mixtures of lead derived from basement and host volcanic rocks (Fehn et al., 1983), the underlying volcanic rocks and the nearby sedimentary rocks (e.g., JADE hydrothermal field, Halbach et al., 1997), or modified mantle and synorogenic sedimentary rocks (Carr et al., 1995).

The volcanic and volcaniclastic rocks hosting the Cadomian massive sulfides in the Ossa Morena zone are mainly of andesitic composition and were likely the source of nonradiogenic lead. The lowest U/Pb values are consistent with the derivation of such lead from a slightly contaminated mantle. This is consistent with recent geochemical data of Pin et al. (2002), which suggest that the parental magma of the syn-Cadomian andesites was derived from a mantle reservoir and that it did not interact with the old crustal basement during its ascent.

The most significant volcanogenic massive sulfides of the Ossa Morena zone (Puebla de la Reina and Maria Luisa) show variable lead isotope values possibly indicating that the hydrothermal cells were small (e.g., Fouquet and Marcoux, 1995). The deposits within the Aracena massif have a noticeable degree of isotopic homogenization, which may indicate that the hydrothermal cells were long-lived and theoretically large enough to form a large deposit (e.g., Loveless, 1975; Carr et al., 1995).

The different lead isotope composition of deposits in the northern and southern zones of the Ossa Morena zone can be attributed to their different environments of formation. Current models propose that the Cadomian magmatism and deformation are related to southward subduction under Gondwana of the Cadomian ocean (Sánchez Carretero et al., 1990; Quesada et al., 1991; Eguíluz et al., 2000). Isotopic signatures dominated by crustal lead in deposits in the northern part of the belt (e.g., Puebla de la Reina) are consistent with the development of a volcanic arc on a continental crust (Eguíluz et al., 2000). The more primitive signatures found in the central and southern Ossa Morena zone indicate that these massive sulfides could have formed in a back-arc basin, now represented by the Aracena massif and by the volcanic rocks within the central-southern Ossa Morena zone.

The unique candidate for the source of the more radiogenic lead is a pre-Cadomian mature crustal sequence. Carbonate-hosted Zn-Pb mineralization (Aracena, 2 in Fig. 1) with primitive signatures similar to those of the volcanogenic Cu-Zn-Pb deposits seems to contradict the generally accepted models of formation for this deposit type, in which lead is derived from the crust (e.g., Large, 1992). A similar situation has been described by Bjorlykke et al. (1993). The lead isotopic features of the Nava Paredón orebody (21 in Fig. 1) are also markedly different. Although the lead isotope ratios are homogeneous at the deposit scale, they have rather primitive signatures that cannot be explained by simple derivation from the underlying mature siliciclastic rocks and strongly suggest the existence of a deep primitive lead source.

The Variscan massive sulfides are broadly coeval with those of the Iberian pyrite belt. Mineralization in both cases has formed in Late Devonian-early Visean pull-apart basins related to the oblique Variscan collision (Tornos et al., 2002). Within the Ossa Morena zone, the basins are shallow marine,

the volcanism of minor regional importance, and the massive sulfides scarce (Gabaldón et al., 1985). They probably formed in a Variscan continental magmatic arc located on the overriding plate. The giant massive sulfide deposits of the Iberian pyrite belt precipitated in a large, locally deep, forearc trench basin hosting major volcanic activity. In both cases, mafic magmatism was present and broadly synchronous with the massive sulfides (Gabaldón et al., 1985; Leistel et al., 1998). However, the lead isotope signatures of sulfides of the Iberian pyrite belt have crustal U/Pb ratios (μ. 9.8) and model ages consistent with geologic ages, indicating that the metals were extracted from a homogeneous crustal reservoir with a negligible contribution of juvenile lead (Marcoux, 1998).

Origin of lead in the synmetamorphic veins

The veins hosted by the Serie Negra (10 in Fig. 1) have more primitive lead ratios than would be expected for simple derivation of the lead from the host shales (μ >9.7). There is no evidence of Cadomian or Variscan mafic magmatism in the area, and it seems unlikely that the fluids equilibrated with distal lead sources. The small size of the deposits, the lack of major hydrothermal alteration, and the alignment of most of the veins parallel to the regional cleavage suggest that the fluids were locally derived and were probably metamorphic in origin. A likely source for the primitive lead is the tholeiitic orthoamphibolite in the Montemolín Formation, an interpretation that is consistent with the lead isotope analysis of a sample of amphibolite (Table 4 and Fig. 3).

Origin of lead in mineralization related to the Variscan igneous rocks

Magnetite-bearing skarns and replacements (Cala, Colmenar, Monchi: 3, 8, and 10 in Fig. 1), Ni-(Cu) magmatic mineralization (Aguablanca, 6 in Fig. 1) and intraplutonic to periplutonic Cu-(Bi-Au) veins (Sultana, Abundancia, 5 and 11 in Fig. 1) are all related to metaluminous calc-alkaline plutonic rocks of Variscan age (350–330 Ma).

In the $^{207}Pb/^{206}Pb$ diagram (Fig. 3), lead isotopes of the magmatic Ni-(Cu) and the iron-oxide replacive mineralization plot below the orogene curve, suggesting contributions from both mantle-derived and crustal lead. As discussed above, the most likely source of the radiogenic lead are the dark shales of the Serie Negra, which crop out in the core of the Olivenza-Monesterio structure and form the host rocks of the intrusions (Fig. 1). Whereas in the hydrothermal systems lead sources can be mixed by fluid-rock interaction, in the magmatic Ni-(Cu) deposits sedimentary rocks must be assimilated by the magmatic rocks. Geologic evidence of such a process includes the abundance of xenoliths in the Aguablanca breccia pipe and the presence of spinel and graphite in the gabbros and norites (Tornos et al., 2001). However, the extent of crustal contamination required is difficult to estimate because the upper crust is on average about 770 times richer in lead (23.1 ppm) than the mantle (0.03 ppm) (Zartman and Haines, 1988). Assimilation of only 9 weight percent of the radiogenic pre-Cadomian shales of the Serie Negra (average, 20 ppm Pb) by the mafic magma would result in a lead isotope composition of the magma almost totally (90%) controlled by the contaminant. Nd, Sr, and S isotope studies of these rocks suggest 1:1 mixing between the

mafic magmas and the pelitic rocks (Casquet et al., 2001).

The Cu-(Bi-Au) vein deposits have more radiogenic signatures, reflecting a larger contribution of lead from the shales. Whereas the Ni-(Cu) breccia pipe and the iron-oxide replacement deposits occur in areas dominated by magmatic rocks, the copper-bearing veins are hosted by or adjacent to large outcrops of Neoproterozoic shale (Fig. 1).

The Sn-W mineralization in younger (330–290 Ma) peraluminous granitoids (Oropesa deposit, 20 in Fig. 1) has radiogenic lead isotope signatures typical of the Central Iberian zone (Michard Vitrac et al., 1981; Arribas, 1993). The San Nicolas tungsten deposit has more primitive signatures reflecting a significant and unexpected mantle input in crust-related W-Sn-bearing granites. This signature suggests that peraluminous Variscan intrusions are not simply derived from melting of the upper crust but that other processes such as magma mixing must have occurred during their evolution. Deposits located in areas adjacent to the Pedroches batholith (i.e., the limit with the Central Iberian zone) have more typical radiogenic lead isotope signatures.

Origin of lead in late Variscan to post-Variscan Pb-Zn veins

The Pb-Zn veins within the Badajoz-Córdoba shear zone have lead isotope signatures significantly different from the signatures of similar veins of the Iberian Variscan belt. Data from the Linares-La Carolina area (Arribas, 1993), the Catalonian Coastal Ranges (Canals and Cardellach, 1997), and from Table 4 show that these veins always have μ values above 9.8. The feldspars of the Variscan granitoids of the Iberian autochthonous terrane also have high μ values that, in the case of the Los Pedroches batholith, overlap those of the associated veins. In contrast, the lead from the veins in the Ossa Morena zone is systematically less radiogenic, indicating significant lead contribution from a primitive source. This is particularly evident in the veins adjacent to the Santa Marta stock, a peraluminous epizonal Variscan intrusion (Fig. 1), which are characterized by μ values of 9.5 to 9.6. Such an hypothesis is consistent with the lead isotope data of the wolframite veins (San Nicolás) related to equivalent granitoids. The lead isotope ratios of the veins are significantly different from those of the adjacent sedex mineralization hosted by the Azuaga Formation (type 6 in Table 3) and therefore cannot be interpreted as simple hydrothermal remobilization of earlier stratiform ores.

Lead isotope evolution of the Ossa Morena zone in the framework of the Southern Variscan belt

The existence of a Variscan Southern Europe lead isotope province with an evolutionary trend characterized by high μ and ω values has been described by several authors (Michard Vitrac et al., 1981; Brevart et al., 1982; Köppel, 1983; Köppel and Schroll, 1988; Ludwig et al., 1989; Caron et al., 1993; Sinclair et al., 1993; Tornos and Arias, 1993; Arribas and Tosdal, 1994). Many of them have interpreted this feature as a result of prolonged crustal reworking with polyphase extraction from a reservoir with constant U-Pb ratios. The high Th/Pb values could indicate that the thorogenic lead was scavenged from the lower crust. However, the coincident high μ and ω ratios are interpreted to indicate U/Th decoupling during weathering and erosion (Köppel, 1983).

In contrast, the lead isotope data of the Ossa Morena zone are interpreted to reflect a polyphase metallogenic evolution with mixing of lead derived from at least two distinct reservoirs during the Cadomian and Variscan orogenic cycles (Fig. 5). The less radiogenic reservoir has μ values close to 9.3 and ω values of 36 whereas the more radiogenic reservoir had μ values of 10.1 and ω values of 42. The first is interpreted to be a Pb-enriched mantle, and the second a long-lived upper crust reservoir.

Samples with $^{207}Pb/^{206}Pb$ isotope ratios above the Stacey and Kramers (1975) evolution curve, the orogen global growth curve (Doe and Zartman, 1979) and the evolutionary curves of the regional shales are thought to derive from a dominantly upper crustal reservoir with only negligible mantle-derived lead. Four types of mineralization with this signature are all associated with pre-Cadomian sedimentary rocks or can be related to rocks of Central Iberian affinity. They include the Zn-Pb sedex mineralization in the Proterozoic Sierra Albarrana terrane, most of the Pb-Zn veins in the Badajoz-Córdoba shear zone, excluding those adjacent to the Santa Marta stock, the Cu-(Bi-Au) veins, and the Sn replacements near the Central Iberian zone (Oropesa).

The veins near the Monesterio dome, the iron-rich hydrothermal replacements, the massive sulfides of Nava Paredón, the Ni-(Cu) Aguablanca mineralization, and the periplutonic veins of Santa Marta and San Nicolás plot below the curves of the Serie Negra shales. These relative positions strongly indicate the existence of a deep juvenile lead reservoir. Intriguingly, most of the analyzed samples plot below the Ni-Cu magmatic ores that intuitively should have the most primitive lead.

The most outstanding feature of the Ossa Morena zone from the plumbotectonic point of view is the dramatically different lead isotopes signatures when compared with adjacent Central Iberian and South Portuguese zones (Fig. 4). The mineral deposits of the Ossa Morena zone have systematically lower $^{207}Pb/^{204}Pb$ values for equivalent $^{206}Pb/^{204}Pb$ values, a mantle signature that is not found in any Iberian terrane nor perhaps in southwest Europe. On average, the lead isotope ratios are also significantly depleted in $^{207}Pb/^{204}Pb$ compared with Phanerozoic magmatic arcs such as the Andes (Chiaradia and Fontboté, 2002) or the Carpathians (Marcoux et al., 2002a) (Fig. 4) suggesting that a conventional Phanerozoic magmatic arc cannot account for such a large input of primitive lead.
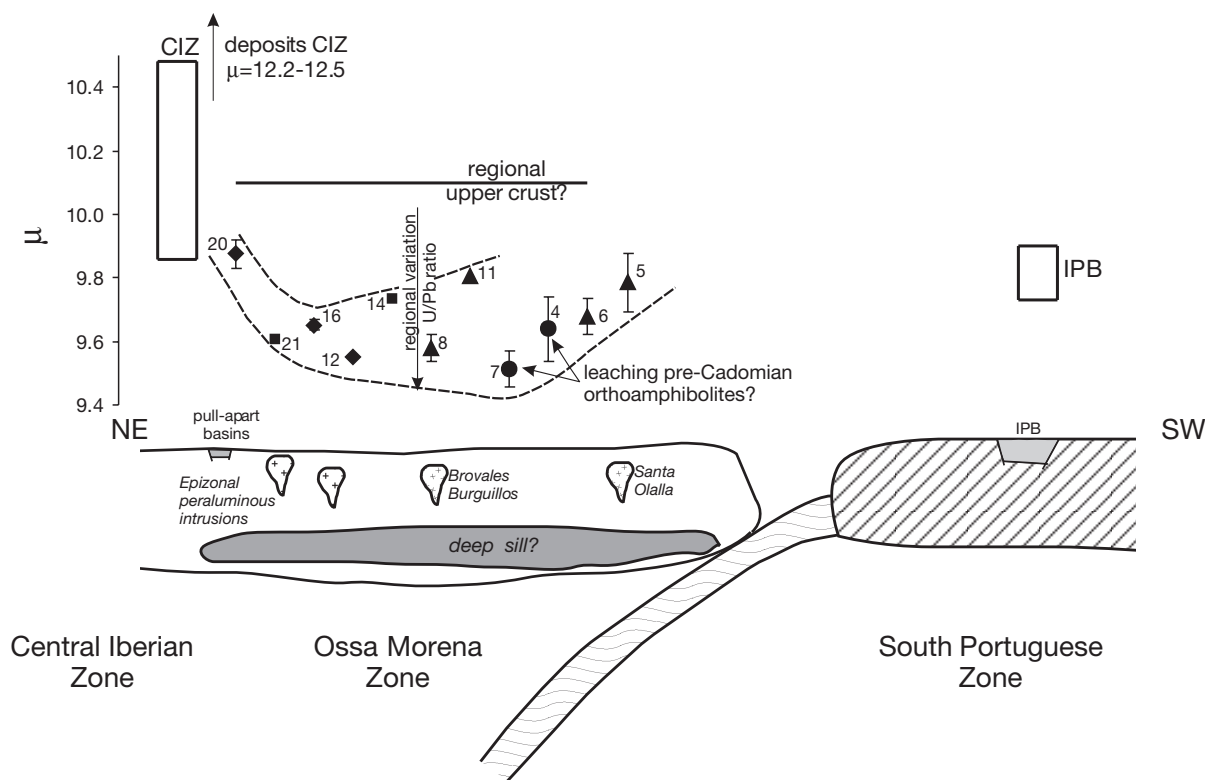

FIG. 5. Regional variations of the μ value of the Variscan ore deposits of the Ossa Morena zone along a theoretical northeast-southwest profile, showing the significant depletion in the U/Pb ratio compared with the deposits of the Central Iberian and South Portuguese (represented by the Iberian pyrite belt, IPB) zones (Arribas, 1993; Tornos and Arias, 1993; Tornos et al., 1996; Arias et al., 1997; Marcoux, 1998). Except in the samples from the mines near the Monesterio granodiorite (4 and 7) in which primitive lead could be leached from nearby orthoamphibolites, all other lead isotope signatures can be interpreted as having been influenced by the input of primitive Variscan lead derived from the deep basaltic sill. The numbers represent the mines in the Table 3 and Figure 1. (▲): Deposits associated with synorogenic metaluminous basic to intermediate plutonic rocks; (◆): Deposits associated with late peraluminous granitoids; (●): Deposits hosted by sedimentary rocks near the Monesterio anatectic core; (■): other styles of mineralization.

The Central Iberian and South Portuguese zones are characterized by high U/Pb ratios, indicating a long crustal history. A significant but only local primitive lead input occurred during the Cadomian orogeny (Ugidos et al., 1997), but it had only a limited influence on the overall metallogenic signatures of the Central Iberian zone. The composition of the basement of the South Portuguese zone is unknown, but the Pb and Nd isotope data suggest that there was no late Neoproterozoic to post-Neoproterozoic primitive mantle contribution to the crust (Mitjavila et al., 1997; Marcoux, 1998; Rosa et al., 1999),

However, in central and southern Europe, Ludwig et al. (1989) and Kober and Lippolt (1985) documented significant post-Archean mantle-crust mixing and transfer of mantle lead. In Sardinia and northern Iberia, Caron et al. (1993) and Tornos and Arias (1993) have also shown that during the Early Cambrian the dominant crustal lead was mixed with a less radiogenic lead, probably of mantle origin. Kober and Lippolt (1985) proposed a model in which a restricted mantle lead contamination of granites in southwestern Germany occurred at about 500 Ma, coincident with the Cadomian orogeny, near the Neoproterozoic-Cambrian boundary.

Crustal signatures in the Ossa Morena zone

The most radiogenic lead signatures of the Ossa Morena zone are found in the sedimentary-exhalative mineralization hosted by the schists of the Azuaga Formation. These signatures are fully consistent with those of the Central Iberian zone and reflect the derivation from a long-lived upper crust reservoir (Arribas, 1993; Tornos and Arias, 1993). Nd and Pb model ages indicate that this reservoir was as old as 2.5 to 2.1 Ga (Nägler, 1990; Schäfer et al., 1992; Casquet et al., 2001). However, crustal signatures are also found in other deposits of the Ossa Morena zone. Except the Oropesa deposit, all other deposits with radiogenic lead are characterized by a relationship with the lowermost Serie Negra (Montemolín Formation) or the underlying Azuaga Gneiss. These sequences predate the synorogenic Cadomian rocks and the proposed input of mantle-derived lead. Thus, the most radiogenic lead of the Ossa Morena zone seems to be derived from a pre-Cadomian crustal basement and the lowermost Serie Negra.

Origin of the primitive lead

The lead isotope composition of the different styles of mineralization in the Ossa Morena zone suggests that the primitive lead has a multiple origin. Three different sources can be envisaged: the metabasic rocks of the Montemolín Formation, the andesites of the Cadomian synorogenic complex as well as their plutonic equivalents and derived sedimentary rocks, and the widespread Variscan metaluminous plutons.

It is unlikely that the amphibolites of the Montemolín Formation can be the source of lead for mineralization other than the veins adjacent to the Monesterio dome, were these amphibolites are particularly abundant. The lead from the syn-Cadomian massive sulfides is most reasonably interpreted as derived from the mixing of very different proportions of upper crustal lead and lead derived from the Cadomian volcanosedimentary complex, which was derived from deep mafic magmas in an arc setting. Conversely, the limited

volume of the syn-Cadomian volcanosedimentary rocks as well as their isotopic signatures make them an unlikely source of primitive lead for the younger Variscan mineralization. The geologic relationships indicate that the primitive lead of the Variscan mineralization is mainly derived from the coeval magmatic rocks, via assimilation, fluid phase separation, or hydrothermal leaching. Evaluation of the results of lead isotope studies alone cannot discriminate between these processes.

In some of the deposits, such as the replacive iron-oxide mineralization or the Ni-(Cu) magmatic sulfides, the logical source of lead is the associated mafic to intermediate igneous rocks. However, the analyzed plutonic rocks are less radiogenic than their equivalent in the Central Iberian zone (Table 4 and Fig. 3). Similarly, the perigranitic tungsten and base metal veins of San Nicolás and Santa Marta have lead isotope signatures that can only be explained by the contribution of primitive lead in the cogenetic peraluminous granitoids. In Nava-Paredón, the lead isotope signatures also suggest the equilibration of fluids with an unexposed deep source of primitive lead.

The IBERSEIS deep seismic profile in southwest Iberia has detected a discontinuous reflective body in an upper-lower crust decollement (Simancas et al., 2003). This body, interpreted as a mafic sill 175 km long and 2 to 3 km thick, appears to lie beneath almost all of the Ossa Morena zone, as can be inferred from regional magnetic patterns. If the geophysical model of Simancas et al. (2003) is correct, the existence of a large midcrustal stratiform intrusion of mantle derivation below almost all the Ossa Morena zone should exert a major control on the Variscan plutonism and the related ore-forming processes.

The areal extent of lead isotope depletion is consistent with a deep reservoir of primitive lead underlying most of the Ossa Morena zone. The high Pb_{crust}/Pb_{mantle} ratio (10^3) implies that only the input of large amounts of primitive lead from such a source could have produced the observed ^{207}Pb depletion.

Conclusions

The Ossa Morena zone has a plumbotectonic evolution controlled by the systematic input of mantle-derived lead and that differs from adjacent terranes and from the whole of the Southern Variscan belt of Europe. The lead isotope ratios of the investigated ore samples are interpreted to trace the link between ore-forming processes and large-scale mantle-crust interaction, and the Ossa Morena zone has behaved as an open system with mixed crustal and mantle parentage. Most of the lead can be attributed to two long-lived reservoirs, an old pre-Cadomian crustal basement with μ values as high as 10.1 and a mantle reservoir with μ as low as 9.3, introduced during the Cadomian and Variscan orogenies. Samples with the largest crustal signatures are usually associated with the pre-Cadomian lithologies and their reworked materials. The primitive lead was first introduced into the crust via the intrusion of andesites within the Cadomian magmatic arc. However, the primitive signatures found in most of the Variscan deposits can probably be traced back to a large midcrustal sill of mantle-derived basalt. The deep mafic rocks are here interpreted as possibly being responsible for forming the magmatic Ni-(Cu) and replacive iron-oxide mineralization as

well as for contributing primitive lead to the volcanic-hosted and the perigranitic mineralization, including base metal and tungsten-bearing veins. Thus, the major metallogenic difference between the Ossa Morena zone and the adjacent terranes seems to be related to the existence of a deep mafic intrusion that conditioned the Variscan metallogenesis of the Ossa Morena zone. The regional extent of the lead isotope anomaly and the marked ^{207}Pb depletion indicate that very large amounts of primitive lead were introduced into the crust by magmatic and hydrothermal systems. Finally, the data support the hypothesis that the Ossa Morena and South Portuguese zones belong to two different terranes with distinct isotopic compositions, that they were accreted during the Variscan orogeny (Silva et al., 1990), and that the rocks of the Ossa Morena zone did not contribute to the formation of the magmatic rocks and massive sulfides of the Iberian pyrite belt.

Acknowledgments

February 28, 2003; February 9, 2004

REFERENCES

Abalos, B., and Eguíluz, L., 1992, Evolución geodinámica de la zona de cizalla dúctil de Badajoz-Córdoba durante el Proterozoico Superior-Cámbrico Inferior, *in* Gutierrez Marco, J.C., Saavedra, J., and Rábano, I., eds., Paleozoico Inferior de Ibero-América: Universidad de Extremadura, p. 577–592.

Andrew, A., Godwin, C.I., and Sinclair, A.J., 1984, Mixing line isochrons: A new interpretation of galena lead isotope data from southern British Columbia: ECONOMIC GEOLOGY, v. 79, p. 919–933.

Apalategui, O., Borrero, D., and Higueras, P., 1985, División en grupos de rocas en Ossa Morena Oriental: Temas Geológicos Mineros, v. 5, p. 73–80.

Apalategui, O., Eguíluz, L., and Quesada, C., 1990, Ossa Morena zone: Structure, *in* Martinez, E., and Dallmeyer, R.D., eds., Pre-Mesozoic geology of Iberia: London, Springer Verlag, p. 280–291.

Arias, D., Corretgé, L.G., Súarez, O., Villa, L., Cuesta, A., and Gallastegui, G., 1997, Lead and sulfur isotope compositions of the Ibias gold vein system (NW Spain): Genetic implications: ECONOMIC GEOLOGY, v. 91, p. 1292–1297.

Arribas, A., 1962, Mineralogía y metalogenia de los yacimientos españoles de uranio: Burguillos del Cerro (Badajoz): Estudios Geológicos, v. 28, p. 173–192.

——1993, Observations on the isotopic composition of ore Pb in the Iberian Peninsula, *in* Fenoll, P., Torres, J., and Gervilla, F., eds., Current Research in Geology Applied to Ore Deposits: Society for Geology Applied to Mineral Deposits, Proceedings, p. 29–32.

Arribas, A., and Tosdal, R.M., 1994, Isotopic composition of Pb in ore deposits of the Betic Cordillera, Spain: Origin and relationship to other European deposits: ECONOMIC GEOLOGY, v. 89, p. 1053–1073.

Azor, A., González Lodeiro, F., and Simancas, J.F., 1993, Cadomian subduction/collision and Variscan transpression in the Badajoz Cordoba shear belt,

southwest Spain: A discussion on the age of the main tectonometamorphic events: Tectonophysics, v. 217, p. 343–346.

Baeza, L., Ruiz, C., Ruiz, M., and Sánchez, A., 1981, Mineralización exhalativo sedimentaria de sulfuros polimetálicos en la Sierra Morena Cordobesa (España): Boletín Geológico Minero, v. 92, p. 203–216.

Bandrés, A., Eguíluz, L., Gil Ibarguchi, J.I., and Palacios, T., 2002, Geodynamic evolution of a Cadomian arc region: The northern Ossa Morena zone, Iberian massif: Tectonophysics, v. 352, p. 105–120.

Bjorlykke, A., Vokes, F.M., Birkeland, A., and Thorpe, R.I., 1993, Lead isotope systematics of strata-bound sulfide deposits in the Caledonides of Norway: ECONOMIC GEOLOGY, v. 88, p. 397–417.

Brevart, O., Dupré, B., and Allegre, C.J., 1982, Metallogenic provinces and the remobilization process studied by lead isotopes: Lead-zinc ore deposits from the Southern massif central, France: ECONOMIC GEOLOGY, v. 77, p. 564–575.

Burg, J.P., Iglesias, M., Laurent, P., Matte, P., and Ribeiro, A., 1981, Variscan intracontinental deformation: The Coimbra-Córdoba shear zone (SW Iberian Peninsula): Tectonophysics, v. 78, p. 161–177.

Canals, A., and Cardellach, E., 1992, Strontium and sulphur isotope geochemistry of low-temperature Ba-F veins of the Catalonian Coastal Ranges (NE Spain): A fluid mixing model and age constraints: Chemical Geology (Isotope Geology Section), v. 104, p. 269–280.

——1997, Ore lead and sulphur isotope pattern from the low temperature veins of the Catalonian Coastal Ranges (NE Spain): Mineralium Deposita, v. 323, p. 243–249.

Cardellach, E., Canals, A., and Pujals, I., 1996, La composición isotópica del azufre y del plomo en las mineralizaciones de Zn-Pb del Valle de Arán (Pirineo Central) y su significado metalogenético: Estudios Geológicos, v. 52, p. 189–195.

Caron, C., Lancelot, J., and Orgeval, J.J., 1993, Heterogeneites isotopiques du plomb dans les amas sulfures a encaissant carbonaté Cambrien inferieur de l'Iglesiente (SO Sardaigne): Effects de melange entre sources crustales differenciees: Compte Rendu Academie Sciences Paris, v. 317-II, p. 1073–1080.

Carr, G.R., Dean, J.A., Suppel, D.W., and Heithersay, P.S., 1995, Precise lead isotope fingerprinting of hydrothermal activity associated with Ordovician to Carboniferous metallogenic events in the Lachlean fold belt of New South Wales: ECONOMIC GEOLOGY, v. 90, p. 1467–1505.

Casquet, C., and Tornos, F., 1991, Influence of depth and igneous geochemistry on ore development in skarns: The Hercynian belt of the Iberian Peninsula, *in* Augusthitis, A., ed., Skarns, their petrology and metallogeny: Athens, Augusthitis, p. 555–591.

Casquet, C., Galindo, C., Darbyshire, D.P.F., Noble, S.R., and Tornos, F., 1998, Fe-U-REE mineralization at mina Monchi, Burguillos del Cerro, Spain: Age and isotope (U-Pb, Rb-Sr and Sm-Nd) constraints on the evolution of the ores, GAC-MAC-APGGQ, Quebec'98 Conference, Proceedings, p. 23.

Casquet, C., Galindo, C., Tornos, F., and Velasco, F., 2001, The Aguablanca Cu-Ni ore deposit (Extremadura, Spain), a case of synorogenic orthomagmatic mineralization: Isotope composition of magmas (Sr, Nd) and ore (S): Ore Geology Reviews, v. 18, p. 237–250.

Chacón, J., Herrero, J.M., and Velasco, F., 1981, Las mineralizaciones de Zn-Pb de Llera (Badajoz): Proceedings I Congreso Español Geología, v. 2., p. 447–455.

Chiaradia, M., and Fontboté, L., 2002, Lead isotope systematics of Late Cretaceous-Tertiary Andean arc magmas and associated ores between 8° N and 40° S: Evidence for latitudinal mantle heterogeneity beneath the Andes: Terra Nova, v. 14, p. 337–342.

——2003, Separate lead isotope analyses of leachate and residue rock fractions: Implications for metal source tracing: Mineralium Deposita, v. 38-2, p. 189–195.

Concha, A., Oyarzun, R., Lunar, R., Sierra, J., Doblas, M., and Lillo, J., 1992, The Hiendelaencina epithermal silver-base metal district, central Spain: Tectonic and mineralizing processes: Mineralium Deposita, v. 27-2, p. 83–89.

Conde, C., Tornos, F., and Baeza, L., 2001, Los sulfuros masivos cadomienses de Puebla de la Reina (Badajoz): Boletín Sociedad Española Mineralogía, v. 24A, p. 153–154.

Crespo, A., 1991, Evolución geotectónica del contacto entre la zona de Ossa Morena y la zona Surportuguesa en las sierras de Aracena y Aroche (Macizo Ibérico Meridional): Un contacto mayor en la cadena hercínica europea: Ph.D. dissertation, Servicio Reprografía, Facultad Ciencias, Universidad Granada, 327 p.

Cuervo, S., Tornos, F., Spiro, B., and Casquet, C., 1996, El origen de los fluidos hidrotermales en el skarn férrico de Colmenar-Santa Bárbara (zona de Ossa Morena): Geogaceta, v. 20, p. 1499–1500.

Cumming, G.L., and Richards, J.R., 1975, Ore lead isotope ratios in a continuous changing earth: Earth Planetary Science Letters, v. 28, p. 155–171.

Darbyshire, D.P.F., Tornos, F., Galindo, C., and Casquet, C., 1998, Sm-Nd and Rb-Sr constraints on the age and origin of magnetite mineralization in the Jerez de los Caballeros iron district of Extremadura, SW Spain: Chinese Science Bulletin, v. 43 sup., p. 28.

Doe, B.R., and Zartman, R.E., 1979, Plumbotectonics, the phanerozoic, *in* Barnes, H.L., ed., Geochemistry of hydrothermal ore deposits—second edition: New York, Wiley, p. 22–70.

Eguíluz, L., Apraiz, A., Abalos, B., and Martínez Torres, L.M., 1995, Evolution de la zona d'Ossa Morena (Espagne) au cours du Proterozoique superior: Correlations avec l'orogene cadomien nord armorican: Geologie de la France, v. 3, p. 35–47.

Eguíluz, L., Gil Ibarguchi, J.I., Abalos, B., and Apraiz, A., 2000, Superposed Hercynian and Cadomian orogenic cycles in the Ossa Morena zone and related areas of the Iberian massif: Geological Society America Bulletin, v. 112, p. 1398–1413.

Fanlo, I., Touray, J.C., Subías, I., and Fernández Nieto, C., 1998, Geochemical patterns of a sheared fluorite vein, Parzan, Spanish central Pyrenees: Mineralium Deposita, v. 33, p. 620–632.

Fehn, U., Doe, B.R., and Delevaux, M.H., 1983, The distribution of lead isotopes and the origin of Kuroko ore deposits in the Hokuroko district, Japan, *in* Ohmoto, H., and Skinner, B.J., eds., The Kuroko and related volcanogenic massive sulfide deposits: ECONOMIC GEOLOGY MONOGRAPH 5, p. 488–506.

Font, X., Thibieroz, J., 1981, Los filones plumbíferos de Linares, Jaen, son continuos hasta el paleocaliche de la base del Trias: Acta Geológica Hispánica, v. 16, p. 211–213.

Fouquet, Y., and Marcoux, E., 1995, Lead isotope systematics in Pacific hydrothermal sulphide deposits: Journal of Geophysical Research, v. 100 (B4), p. 6025–6040.

Gabaldón, V., Garrote, A., and Quesada, C., 1985, El Carbonífero Inferior del Norte de la zona de Ossa Morena (SW de España), Congreso Geología Carbonífero, 10°, Instituto Geológico y Minero de España, Proceedings, p. 173–185.

Galindo, C., Portugal Ferreira, M.R., Casquet, C., and Priem, H.N.A., 1990, Dataciones Rb/Sr en el completo plutónico Táliga Barcarrota (Badajoz): Geogaceta, v. 8, p. 7–10.

Galindo, C., Tornos, F., Darbyshire, D.P.F., and Casquet, C., 1994, The age and origin of the barite-fluorite (Pb-Zn) veins of the Sierra del Guadarrama (Spanish central system): A radiogenic (Nd, Sr) and stable isotope study: Chemical.Geology, v. 112, p. 351–364.

Garcia de Madinabeitia, S., 2002, Implementación y aplicación de los análisis isotópicos de Pb al estudio de mineralizaciones y la geocronología del área de Los Pedroches-Alcudia (zona centro Ibérica): Unpublished Ph.D. dissertation, Bilbao, Spain, Universidad del País Vasco, 207 p.

Gumiel, J.C., 1988, Estudio geológico y metalogénico de la mineralización de W-Sn-Bi-Mo asociada a la cúpula granítica de San Nicolás (Valle de la Serena, Badajoz): Unpublished M.Sc.thesis, Universidad Complutense Madrid, Madrid, Spain, 221 p.

Gumiel, P., Lunar, R., Sierra, J., and López , J.A., 1987, Contribución al conocimiento de las mineralizaciones de W, Bi del distrito de Oliva de la Frontera (Badajoz): Revista Materiales y Procesos Geológicos, v. 1, p. 229–248.

Halbach, P., Hansmann, W., Köppel, V., and Pracejus, B., 1997, Whole-rock and sulfide lead-isotope data from the hydrothermal JADE field in the Okinawa back-arc trough: Mineralium Deposita, v. 32, p. 70–78.

Halliday, A.N., and Mitchell, J.G., 1984, K-Ar ages of clay-size concentrates from the mineralisation of the Pedroches batholith and evidence for Mesozoic hydrothermal activity associated with the break up of Pangea: Earth Planetary Science Letters, v. 68, p. 229–239.

Johnson, C.A., Cardellach, E., Tritlla, J., and Hanan, B.B., 1996, Cierco Pb-Zn-Ag vein deposits: Isotopic and fluid inclusion evidence for formation during the Mesozoic extension in the Pyrenees of Spain: ECONOMIC GEOLOGY, v. 91, p. 497–506.

Kober, B., and Lippolt, H.J., 1985, Pre-Hercynian mantle lead transfer to basement rocks as indicated by lead isotopes of the Schwarzwald crystalline, SW Germany. I. The lead isotope distribution and its correlation: Contributions Mineralogy and Petrology, v. 90, p. 162–171.

Köppel, V., 1983, Summary of lead isotope data from ore deposits of the eastern and southern Alps: Some metallogenic and geotectonic implications, *in* Schneider, H.J., ed., Mineral deposits of the Alps and of the Alpine epoch in Europe: London, Springer Verlag, p. 162–168.

Köppel, V., and Schroll, E., 1988, Pb-isotope evidence for the origin of lead in strata-bound Pb-Zn deposits in Triassic carbonates of the Eastern and Southern Alps: Mineralium Deposita, v. 23, p. 96–103.

Large, R.R., 1992, Australian volcanic-hosted massive sulfide deposits: Features, styles and genetic models: ECONOMIC GEOLOGY, v. 873, p. 471–510.

Leistel, J.M., Marcoux, E., Thieblemont, D., Quesada, C., Sanchez, A., Almodovar, G.R., Pascual, E., and Sáez, R, 1996, The volcanic-hosted massive sulphide deposits of the Iberian pyrite belt. Review and preface to the special issue: Mineralium Deposita, v. 33, p. 2–30.

Lillo, J., 1992, Vein-type base-metal ores in Linares-La Carolina (Spain): Ore-lead isotopic constraints: European Journal of Mineralogy, v. 4, p. 337–343.

Lillo, J., Oyarzun, R., Lunar, R., Doblas, M., González, A., and Mayor, N., 1992, Geological and metallogenic aspects of late Variscan Ba-(F)-(base-metal) vein deposits of the Spanish central system: Transactions of the Institution Mining Metallurgy, v. 101, p. b24–b31.

Locutura, J., Tornos, F., Florido, P., and Baeza, L., 1990, Ossa Morena zone: Metallogeny, *in* Martinez, E., and Dallmeyer, R.D., eds., Pre-Mesozoic geology of Iberia: London, Springer Verlag, p. 321–332.

Loveless, A.J., 1975, Lead isotopes—A guide to major mineral deposits: Geoexploration, v. 13, p. 13–27.

Ludwig, K.R., Vollmer, R., Tuti, B., Simmons, K.R., and Perna, G., 1989, Isotopic constraints on the genesis of base-metal ores in southern and central Sardinia: European Journal of Mineralogy, v. 1, p. 657–666.

Marcoux, E., 1998, Lead isotope systematics in the giant massive sulphide deposits in the Iberian pyrite belt: Mineralium Deposita, v. 33, p. 45–58.

Marcoux, E., and Sáez, R., 1994, Geoquímica isotópica del plomo de las mineralizaciones hidrotermales tardihercínicas de la faja pirítica Ibérica: Boletín Sociedad Española Mineralogía, v. 171, p. 202–203.

Marcoux. E., Grancea, L., Lupulesco, M., and Milesi, J.P., 2002a, Lead isotope signatures of epithermal and porphyry type ore deposits from the Romanian Carpathian Mountains: Mineralium Deposita, v. 37, p. 173–184.

Marcoux, E., Pascual, E., and Onezime, J., 2002b, Hydrothermalisme ante-Hercynien en Sud-Iberie: Apport de la geochimie isotopique du plomb: Compte Rendu Geoscience, v. 334, p. 259–265.

Michard Vitrac, A., Albarede, F., Allegre, C.J., 1981, Lead isotopic composition of Hercynian granitic K-feldspars constrains continental genesis: Nature, v. 291, p. 460–464.

Mitjavila, J., Martí, J., and Soriano, C., 1997, Magmatic evolution and tectonic setting of the Iberian pyrite belt volcanism: Journal of Petrology, v. 38, p. 727–755.

Nägler, T., 1990, Sm-Nd, Rb-Sr and common lead isotope geochemistry on fine-grained sediments of the Iberian massif: Unpublished Ph.D. dissertation, Swiss Federal Institute of Technology, Zurich, 139 p.

Nägler, T., Schäfer, H.J., and Gebauer, D., 1993, A new approach for the determination of the age of partial or complete homogenization of Pb isotopes: Example: Anchimetamorphic detrital sediments of the central Iberian zone, Spain: Chemical Geology (Isotope Geology Section), v. 107, p. 191–199.

Ochsner, A., 1993, U-Pb geochronology of the upper Proterozoic-lower Paleozoic geodynamic evolution in the Ossa Morena zone (SW Iberia): Constraints on the timing of the Cadomian orogeny: Unpublished Ph.D. dissertation, Swiss Federal Institute of Technology, Zurich, 249 p.

Ordoñez, B., 1998, Geochronological studies of the Pre-Mesozoic basement of the Iberian massif: The Ossa Morena zone and the allochthonous complexes within the central Iberian zone: Unpublished Ph.D. dissertation, Swiss Federal Institute of Technology, Zurich, 235 p.

Ortega, L., Lunar, R., García Palomero, F., Moreno, T., and Prichard, H.M., 2001, Removilización de minerales del grupo del platino en el yacimiento de Ni-Cu-EGP de Aguablanca (Badajoz): Boletín Sociedad Española Mineralogía, v. 24-A, p. 175–176.

Ovtrach, A., and Tamain, G., 1977, Tectonique, migration des centres chaudes et mineralisations dans le sud de la meseta iberique (Espagne), *in* Les roches plutoniques dans leurs rapports avec les gites mineraux: Paris, Masson et cie., p. 191–211.

Patterson, D.J., Ohmoto, H., and Solomon, M., 1981, Geological setting and genesis of cassiterite-sulfide mineralization at Renison Bell, western Tasmania: ECONOMIC GEOLOGY, v. 76, p. 393–438.

Pin, C., Liñan, E., Pascual, E., Donaire, T., Valenzuela, A., 2002, Late Neoproterozoic crustal growth in the European Variscides: Nd isotope and geochemical evidence from the Sierra de Córdoba andesites (Ossa Morena shear zone, Southern Spain): Tectonophysics, v. 352, p. 133–151.

Quesada, C., 1992, Evolución tectónica del Macizo Ibérico (una historia de crecimiento por acrecencia sucesiva de terrenos durante el Proterozoico superior y Paleozoico, *in* Gutierrez Marco, J.C., Saavedra, J., and Rábano, I., eds., Paleozoico Inferior de Ibero-América: Mérida, Spain, Junta de Extremadura, p. 173–192.

Quesada, C., and Munhá, J., 1990, Ossa Morena zone: Metamorphism, *in* Martinez, E., and Dallmeyer, R.D., ed., Pre-Mesozoic geology of Iberia: London, Springer Verlag, p. 314–320.

Quesada, C., Florido, P., Gumiel, P., Osborne, J., Larrea, F., Baeza, L., Ortega, C., Tornos, F., and Sigüenza, J., 1987, Mapa geológico minero de Extremadura: Mérida, Spain, Junta de Extremadura, 131 p.

Quesada, C., Bellido, F., Dallmeyer, R.D., Gil Ibarguchi, I., Oliveira, T.J., Pérez Estaun, A., and Ribeiro, A., 1991, Terranes within the Iberian massif: Correlations with West Africa sequences, *in* Dallmeyer, R.D., ed., The West African orogens and circum-Atlantic correlations: London, Springer Verlag, p. 267–294.

Rosa, J., Castro, A., and Jenner, G., 1999, Age and relationships between the deep continental crust of South Portuguese and Ossa Morena zones in the Aracena metamorphic belt revealed by zircon inherited cores: Reunion Geologia Oeste Peninsular, 15th, Badajoz, Spain, University of Badajoz, September 26–October 3, Extended Abstracts, p. 81–88 (Journal Conference Abstracts, 4–3, p. 5).

Salman, K., Montero, P., and Bea, F., 1999, Rb-Sr and single-zircon grain [207]Pb/[206]Pb chronology of Monesterio granodiorite and related migmatites (Ossa Morena zone, SW Iberian massif): Journal of Conference Abstracts, v. 4, p. 669.

Sánchez Carretero, R., Eguíluz, L., Pascual, E., and Carracedo, M., 1990, Ossa Morena zone: Igneous rocks, *in* Martinez, E., and Dallmeyer, R.D., eds., Pre-Mesozoic Geology of Iberia: London, Springer Verlag, p. 292–313.

Schäfer, H.J, Ochsner, A., and Gebauer, D., 1992, The Pre-Mesozoic evolution of the SW Iberian massif (Spain) based on geochronological data, *in* Rábano, I., and Gutierrez Marco, J.C., eds., Reunión de Ossa Morena: 8th, Mérida, Spain, Junta de Extremadura, May 8–12, Abstracts, p. 13.

Schermerhorn, L.J.G., 1981, Framework and evolution of Hercynian mineralization in the Iberian Meseta: Leiden Geologische Mededelingen, v. 52, p. 23–56.

Silva, J.B., Oliveira, J.T., and Ribeiro, A., 1990, Structural outline of the South Portuguese zone, *in* Martinez, E., and Dallmeyer, R.D., eds., Pre-Mesozoic Geology of Iberia: London, Springer Verlag, p. 348–362.

Simancas, J.F., Carbonell, R., Gonzalez Lodeiro, F., Perez Estaun, A., Juhlin, C., Ayarza, P., Kashubin, A., Azor, A., Martinez Poyatos, D., Almodovar, G.R., Padcual, E., Saez, R., Exposito, I., 2003, Custral structure of the transpressional Variscan orogen of SW Iberia: SW Iberia deep seismic reflection profile (IBERSEIS): Tectonics, v. 22, (in press).

Sinclair, A.J., Macquar, J.C., and Rouvier, H., 1993, Reevaluation of lead isotopic data, southern massif Central, France: Mineralium Deposita, v. 28, p. 122–128.

Stacey, J.S., and Kramers, J.D., 1975, Aproximation of terrestrial lead isotope evolution by a two stage model: Earth and Planetary Science Letters, v. 26, p. 207–221.

Thorpe, R.I., 1999, The Pb isotope linear array for volcanogenic massive sulfide deposits of the Abitibi and Wawa subprovinces, Canada Shield, *in* Hannington, M.D., and Barrie, C.T., eds., The giant Kidd Creek volcanogenic massive sulfide deposit, western Abitibi subprovince, Canada: ECONOMIC GEOLOGY MONOGRAPH, v. 10, p. 555–576.

Tornos, F., and Arias, D., 1993, Sulphur and lead isotope geochemistry of the Rubiales Zn-Pb ore deposit (NW Spain): European Journal Mineralogy, v. 5, p. 763–773.

Tornos, F., and Locutura, J., 1989, Mineralizaciones epitermales de Hg en Ossa Morena (Usagre, Badajoz): Boletín Sociedad Española Mineralogía, v. 12, p. 363–374.

Tornos, F., and Velasco, F., 2002, The Sultana orebody (Ossa Morena zone, Spain): Insights into the evolution of Cu-(Au-Bi) mesothermal mineralization: GEODE Study Centre, Grenoble, France, October 25–28, Abstracts, p. 25–28.

Tornos, F., Casquet, C., Locutura, J., and Collado, R., 1991, Fluid inclusion and geochemical evidence for fluid mixing in the genesis of Ba-F (Pb-Zn) lodes of the Spanish central system: Mineralogical Magazine, v. 55, p. 225–234.

Tornos, F., Ribera, F., Arias, D., Loredo, J., and Galindo, C., 1996, The carbonate-hosted Zn-Pb deposits of NW Spain: Stratabound and discordant deposits related to the Variscan deformation, *in* Sangster, D.F., ed., Carbonate hosted lead zinc deposits: Society of Economic Geologists Special Publication 4, p. 195–203.

Tornos, F., Chiaradia, M., and Fontboté, L., 1998, La geoquímica isotópica del plomo en las mineralizaciones de la zona de Ossa Morena (ZOM): Implicaciones metalogenéticas y geotectónicas: Boletín Sociedad Española Mineralogia, v. 21A, p. 206–207.

Tornos, F., Casquet, C., Galindo, C., Velasco, F., and Canales, A., 2001, A new style of Ni-Cu mineralization related to magmatic breccia pipes in a transpressional magmatic arc, Aguablanca, Spain: Mineralium Deposita, v. 36, p. 700–706.

Tornos, F., Casquet, C., Relvas, J., Barriga, F., and Sáez, R., 2002, Transpressional tectonics and ore deposit formation: The southwestern margin of the Iberian Variscan belt, *in* Blundell, D., Neubauer, F., and von Quadt, A., eds., The timing and location of major ore deposits in an evolving orogen: Geological Society London Special Publication 206, p. 179–198.

Tornos, F., Casquet, C., and Galindo, C., 2003, Hydrothermal iron oxide (-Cu-Au) mineralization in SW Iberia: Evidence for a multiple origin, *in* Eliopoulos, D.G. et al., eds., Mineral exploration and sustainable development: Rotterdam, Millpress, p. 395–398.

Tornos, F., Inverno, C., Casquet, C., Mateus, A., Ortiz, G., and Oliveira, V., 2004, Metallogenic evolution of the Ossa Morena zone: Journal of Iberian Geology, v. 30, p. 143–180.

Ugidos, J.M., Armenteros, I., Barba, P., Valladares, I., and Colmenero, J.R., 1997, Geochemistry and petrology of recycled orogen-derived sediments: A case study from upper Precambrian siliclastic rocks of the central Iberian zone, Iberian massif, Spain: Precambrian Research, v. 84, p. 163–180.

Vázquez, F., 1972, Génesis de la mina Maria Luisa, La Nava (Huelva). Una mineralización zonada: Boletín Geológico Minero, v. 834, p. 377–386.

——1989, Mineral deposits of Spain, *in* Mineral deposits of Europe: The Institution of Mining and Metallurgy, v. 4/5, p. 105–196.

Velasco, F., and Amigó, J.M., 1981, Mineralogy and origin of the skarn from Cala (Huelva, Spain): ECONOMIC GEOLOGY, v. 76, p. 719–727.

Velasco, F., Herrero, J.M., Gil, P.P., Avarez, L., and Yusta, I., 1994, Mississippi Valley-type, Sedex and iron deposits in Lower Cretaceous rocks of the Basque Cantabrian basin, northern Spain, *in* Fontboté, L., Boni, M., eds., Sediment hosted Zn-Pb ores: Special Publication Society.Geology applied Mineral Deposits, London, Springer Verlag, v. 10, p. 246–270.

Velasco, F., Pesquera, A., and Herrero, J.M., 1996, Lead isotope study of Zn-Pb ore deposits associated with the Basque-Cantabrian basin and Paleozoic basement, northern Spain: Mineralium Deposita, v. 31, p. 84–92.

Zartman, R.E., and Doe, B.R., 1981, Plumbotectonics—The model: Tectonophysics, v. 75, p. 135–162.

Zartman, R.E., and Haines, S.M., 1988, The plumbotectonic model for Pb isotopic systematics among major terrestrial reservoirs—A case for bi-directional transport: Geochimica et Cosmochimica Acta, v. 52, p. 1327–1339.

Zindler, A., and Hart, S., 1986, Chemical geodynamics: Annual Review of Earth Planetary Sciences, v. 14, p. 493–571.
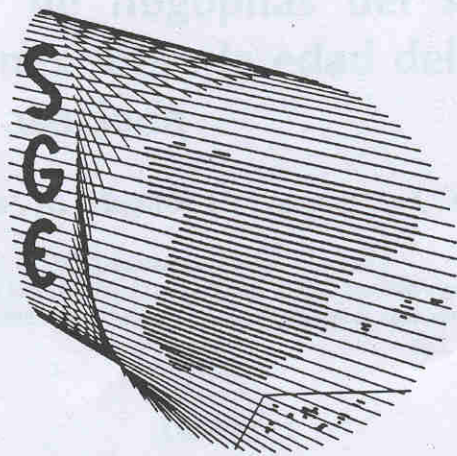
VI CONGRESO GEOLÓGICO DE ESPAÑA

Editores

Carlos Luis Liesa Carrera

Andrés Pocovi Juan

Carlos Sancho Marcén

Ferrán Colombo Piñol

Ángel González Rodríguez

Ana Rosa Soria de Miguel

Instituto Geológico
y Minero de España

Geocronología Ar-Ar de flogopitas del *stock* de Aguablanca (Badajoz). Implicaciones sobre la edad del plutón y de la mineralización de Ni-(Cu) asociada

F. Tornos[1], A. Iriondo[2], C. Casquet[3], y C. Galindo[3]

1 Instituto Geológico y Minero de España, Azafranal 48, 37002 Salamanca. f.tornos@igme.es
2 U.S. Geological Survey, Argon Thermochronology Lab., Denver, CO 802250046, EEUU. iriondo@usgs.gov
3 Dpto. Petrología, Universidad Complutense de Madrid, 28040 Madrid. casquet@geo.ucm.es, cgalindo@geo.ucm.es

ABSTRACT

Ar-Ar dating of intercumulus phlogopite for both a websterite fragment within the mineralized breccia pipe of the Ni-(Cu) Aguablanca magmatic deposit, and the host gabbronorite has yielded ages of 335±2 to 338±3 Ma, i.e., Visean (Mississippian). These values are within error and suggest that the mineralization and the host rock are Variscan in age. Moreover this age is compatible with a previous model which interprets the sulfide mineralization as intrusive (vertical pipe) into the Aguablanca gabbronorites.

Keywords: *Ar-Ar dating, nickel, copper, magmatic-hosted mineralization.*

INTRODUCCIÓN

La mineralización de Ni-(Cu) de Aguablanca se encuentra asociada a las facies más básicas del *stock* del mismo nombre, situado en el extremo SE de la antiforma Olivenza – Monesterio (Zona Ossa Morena) (Fig. 1). La edad de la intrusión y el significado del stock ha sido objeto de diversos estudios, fundamentalmente orientados a la interpretación genética de la mineralización. El yacimiento de Aguablanca es, por el momento, único a escala peninsular y su génesis es controvertida. Actualmente hay dos modelos geológicos muy diferentes. El primero propone que el depósito corresponde a un yacimiento magmático estratiforme, que ha sido plegado y verticalizado durante la orogenia varíscica (Lunar *et al.*, 1997; Ortega *et al.*, 2002). El segundo modelo propone que la intrusión de Aguablanca es de edad Varíscica y que la mineralización se encuentra en una chimenea (*pipe*) magmática (Casquet *et al.*, 2001; Tornos *et al.*, 2001). La adopción de un modelo u otro es fundamental para establecer modelos de exploración, orientando la búsqueda a los plutones pre-Varíscicos o Varíscicos de la zona.

En este marco, una datación precisa del *stock* de Aguablanca y la mineralización es un argumento de primera importancia para apoyar uno u otro modelo.

GEOLOGÍA

El *stock* de Aguablanca es una pequeña intrusión zonada localizada junto al plutón de Santa Olalla del que se ha considerado tradicionalmente parte (Casquet, 1980). El plutón de Santa Olalla presenta un zonado inverso continuo, con granitos y monzogranitos en la parte central y facies algo más básicas, granodioritas, tonalitas y cuarzodioritas, en la zona externa. El *stock* de Aguablanca está formado por rocas máficas, fundamentalmente cuarzodioritas y dioritas, aunque en su zona NE y cerca del contacto con el encajante, hay un área rica en gabros, gabronoritas y noritas que es donde se localiza la mineralización (Fig. 2). Las rocas encajantes son esquistos, rocas volcanoclásticas félsicas, mármoles y rocas de silicatos cálcicos afectados por un metamorfismo de contacto de alto grado. Los mármoles y rocas de silicatos cálcicos están afectados por complejos procesos de skarnificación (Casquet, 1980). El *stock* probablemente intruyó a favor de una zona de *pull apart* dentro de un importante desgarre sinestral.

En detalle, la mineralización tiene la estructura de una chimenea subvertical, de sección elipsoidal que se adelgaza en profundidad. Está constituida por sulfuros masivos y brechas en las que los sulfuros soportan fragmentos de rocas ultramáficas y ultrabásicas (orto- y clinopiroxenita, websterita, en menor proporción peridotita y cantidades subordinadas de gabro-gabronorita-norita, y rocas encajantes). Esta chimenea está rodeada por gabronorita y norita con mineralización diseminada. En ambos casos la mineralización está formada por pirrotita, con cantidades algo más accesorias de calcopirita y pentlandita, y trazas de magnetita, cubanita, mackinawita, grafito y cobaltita. Las rocas mineralizadas muestran una alteración hidrotermal de desarrollo muy irregular y a la que se asocia la formación de Mg-hornblenda-actinolita, biotita, epidota *ss*, talco, clorita, calcita e illita. La mineralización está también removilizada localmente, con
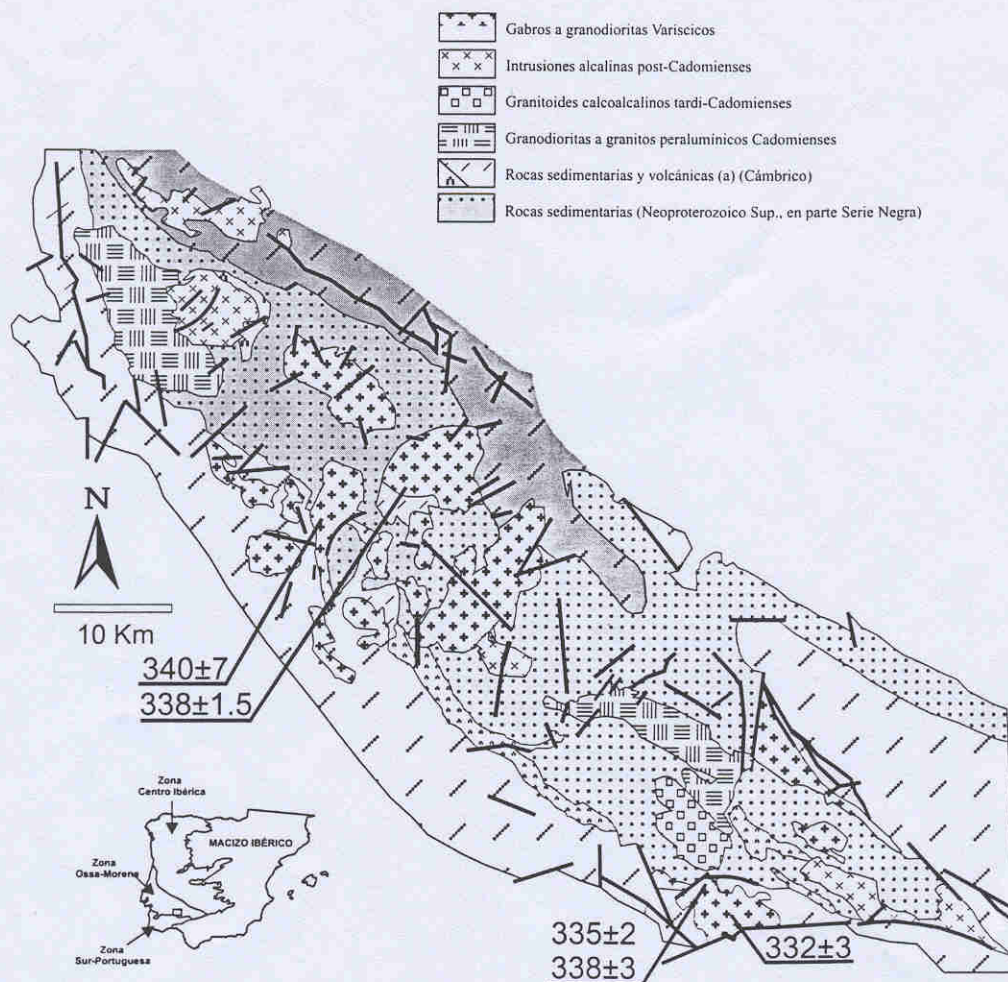
FIGURA 1. *Mapa geológico del sector central de la Zona de Ossa Morena mostrando dataciones de plutones metalumínicos Varíscicos y de la mineralización de Aguablanca.*

neoformación de granos gruesos de los mismos minerales, así como de pirita, violarita, marcasita y minerales del grupo del platino (Ortega *et al.*, 2002).

DATACIÓN AR-AR

La datación $^{40}Ar/^{39}Ar$ se ha realizado en los laboratorios del USGS, a partir de concentrados de flogopita de dos rocas máficas de grano medio a grueso, que no muestran procesos secundarios superpuestos. Una de las muestras (AG-38), tomada en la galería de exploración, corresponde a un fragmento de gabronorita de la brecha mineralizada.; la otra (AG-68) es un gabro de la zona externa y procede del sondeo S-6758 (679,3 m). Ambas rocas contienen flogopita (X_{flog} 0,49-0,70) y clinoanfíbol (edenita) intercumulares (Fig. 3), que forman agregados de entre 0,2 y 1 mm intersticiales entre plagioclasa, también intercumular, y el piroxeno. Las edades *plateau* y las isocronas Ar-Ar coinciden en ambas muestras. Los resultados son: 335±2 Ma (AG-38) y 338±3 Ma (AG-68), que corresponden al Viseense (Missisipiense). La similitud de ambos resultados dentro de los límites de error (335-337 Ma), y la coincidencia entre edades *plateau* e isocrona de cada muestra, indica que los dos concentrados analizados son semejantes e isotópicamente homogéneos. Ello es compatible con una interpretación de las edades en términos de edades de cristalización magmática en un contexto de enfriamiento rápido (Edad de cierre (Ar) » Edad cristalización), como el que hay que esperar en el caso de plutones epizonales. La ausencia de alteración hidrotermal apreciable y el valor relativamente alto de la temperatura de cierre para la difusión del Ar de la flogopita (en torno a 400-450°C) refuerzan esta interpretación. De acuerdo con el modelo de Tornos *et al.* (2001), la brecha intruiría a unos 1000-1400°C siendo los fragmentos de acumulado transportados desde la cámara magmática en una matriz todavía fundida de sulfuros. Las edades obtenidas serían las de enfriamiento *in situ* de la brecha y por lo tanto las del stock de Aguablanca y de la mineralización.

DISCUSIÓN

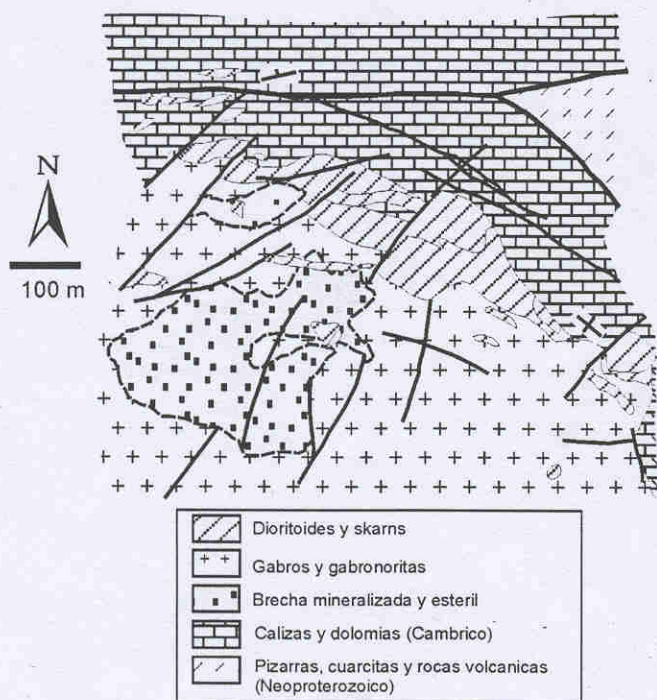Uno de los problemas básicos para la datación del stock y la mineralización de Aguablanca es la existencia de

FIGURA 2. *Esquema geológico del plutón de Aguablanca. Modificado de Tornos et al. (2001).*
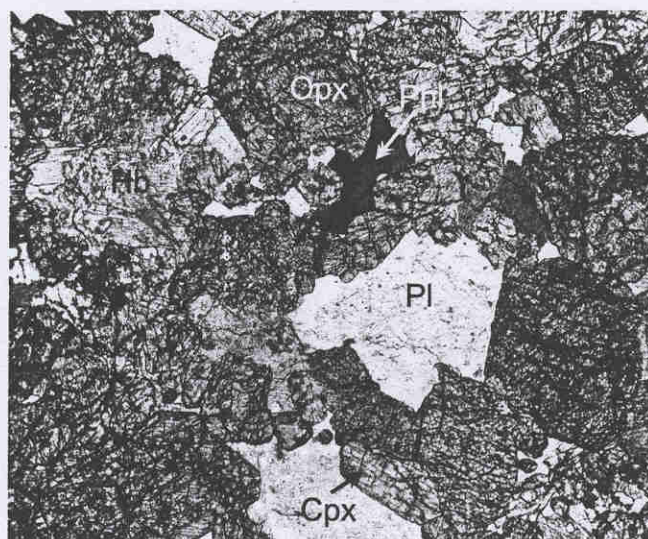

FIGURA 3. *Flogopita y edenita intercumulares entre ortopiropiroxeno y plagioclasa de norita encajante de la mineralización. La escala gráfica es 0,25 mm.*

importantes procesos de mezcla de magma básico y corteza continental en una cámara magmática probablemente ubicada en la corteza superior (Casquet *et al.*, 2001). Estos procesos son fundamentales para la génesis de la mineralización ya que la adición de sílice y azufre al magma promueve la inmiscibilidad del magma sulfurado. En el caso de Aguablanca hay múltiples evidencias de asimilación cortical. Los resultados isotópicos de Sm-Nd, Rb-Sr, Pb-Pb, Re-Os (datos inéditos) y del azufre, son todos ellos interpretables en términos de mezcla de un magma juvenil de composición basáltica y una corteza continental probablemente siliciclástica (Casquet *et al.*, 2001, Tornos *et al.*, 2001). Los elevados valores de oro, la presencia de grafito, de microenclaves peralumínicos con espinela, corindón y sillimanita y de fragmentos parcialmente asimilados de roca de caja en la brecha, son también consistentes con este modelo.

La asimilación ha motivado que las composiciones isotópicas Sm-Nd y Rb-Sr den líneas de mezcla y no isocronas y que, por lo tanto, las edades de regresión obtenidas sean valores máximos. Este es probablemente el caso de la edad Rb-Sr del plutón de Santa Olalla (359 ± 18 Ma; MSWD = 17,1) (Casquet *et al.*, 2001). Este valor es algo más alto que el obtenido a partir de circones (332 ± 3 Ma; edad ^{207}Pb/^{206}Pb; Montero *et al.*, 2000) (Fig. 1). Por otro lado, las relaciones ^{207}Pb/^{206}Pb de la pirrotita de Aguablanca también indican edades modelo aproximadamente Varíscicas (382-353 Ma; Tornos y Chiaradia, 2004).

Las edades Ar-Ar obtenidas son consistentes con los resultados de Rb-Sr y de Pb, y con las edades de otros plutones similares de la Zona de Ossa Morena. Así, el cercano plutón de Brovales tiene una edad ^{207}Pb/^{206}Pb (circón) de 340 ± 7 Ma (Montero *et al.*, 2000) y la mineralización de allanita de la Mina Monchi, junto al plutón de Burguillos, 338 ± 1,5 Ma (U-Pb; Casquet *et al.*, 1998). Este último valor coincide con la edad Ar-Ar obtenida a partir de anfíboles de rocas ígneas de Burguillos del Cerro (entre 342 y 329 Ma; Dallmeyer *et al.*, 1995). Todo ello sugiere que, en su conjunto, el plutonismo varíscico tuvo lugar entre los 350 y 330 Ma (Carbonifero Inferior / Missisipiense).

CONCLUSIONES

La datación Ar-Ar de flogopitas magmáticas intercumulares del stock y brecha mineralizada de Aguablanca indican que la intrusión del gabro y de la mineralización son de edad Viseense (335 - 337 Ma) y por lo tanto varíscicos. Esta edad es consistente con las de otros plutones geoquímicamente equivalentes de la zona.

AGRADECIMIENTOS

REFERENCIAS

Casquet, C. (1980): *Fenómenos de endomorfismo, metamorfismo y metasomatismo en los mármoles de la*

Rivera de Cala (Sierra Morena). Tesis Doctoral, Univ. Complutense de Madrid, 295 p.

Casquet, C., Galindo, C., Darbyshire, D.P.F., Noble, S.R. y Tornos, F. (1998): Fe U REE mineralization at Mina Monchi, Burguillos del Cerro, Spain: age and isotope (U Pb, Rb Sr and Sm Nd) constraints on the evolution of the ores. En: *Proceedings GAC MAC APGGQ Quebec 98 Conference*, 23: A28.

Casquet, C., Galindo, C., Tornos, F. y Velasco, F. (2001): The Aguablanca Cu Ni ore deposit (Extremadura, Spain), a case of synorogenic orthomagmatic mineralization: Isotope composition of magmas (Sr, Nd) and ore (S). *Ore Geology Reviews*, 18: 237 250.

Dallmeyer, R.D., Garcia Casquero, J.L. y Quesada, C. (1995): 40Ar/39Ar mineral age constraints on the emplacement of the Burguillos del Cerro Igneous Complex (Ossa Morena Zone, SW Spain). *Boletín Geológico Minero*, 106: 203-214.

Lunar, R., Garcia Palomero, F., Ortega, L., Sierra, J., Moreno, T. y Prichard, H. (1997): Ni Cu (PGM) mineralization associated with mafic and ultramafic rocks: the recently discovered Aguablanca ore deposit, SW Spain. En: *Mineral deposits: research and exploration* (Ed. Papunen, H.). Balkema, Rotterdam, 463-466.

Montero, P., Salman, K., Bea, F., Azor, A., Exposito, I., Lodeiro, F., Martinez Poyatos, D. y Simancas, F. (2000): New data on the geochronology of the Ossa Morena Zone, Iberian MassifVariscan Appalachian dynamics: The building of the Upper Paleozoic basement. En: *Galicia 2000*. Abstracts: 136-138.

Ortega, L., Lunar, R., García Palomero, F., Moreno, T. y Prichard, H.M. (2002): Características geológicas y mineralógicas del yacimiento de Ni Cu EGP de Aguablanca (Badajoz). *Boletín Sociedad Española Mineralogía*, 25: 57-78.

Tornos, F., Casquet, C., Galindo, C., Velasco, F. y Canales, A. (2001): A new style of Ni Cu mineralization related to magmatic breccia pipes in a transpressional magmatic arc, Aguablanca, Spain. *Mineralium Deposita*, 36 (7): 700-706.

The metallogenic evolution of the Ossa-Morena Zone

La evolución metalogenética de la Zona de Ossa Morena

F. Tornos[1], C. M. C. Inverno[2], C. Casquet[3], A. Mateus[4], G. Ortiz[5], V. Oliveira[6]

[1] *Instituto Geológico y Minero de España. Azafranal 48-50 37002 Salamanca, Spain (f.tornos@igme.es)*
[2] *Instituto Geológico e Mineiro, Estrada Portela-Zambujal, Ap. 7586, 2720 Alfragide, Portugal and CREMINER (carlos.inverno@igm.pt)*
[3] *Dpt. Petrología, Universidad Complutense de Madrid 28040 Madrid, Spain (casquet@geo.ucm.es)*
[4] *Dep. Geologia, Fac. Ciências, Univ. Lisboa, Ed. C2, Piso 5, Campo Grande, 1749-016 Lisboa, Portugal (amateus@fc.ul.pt)*
[5] *Instituto Geológico y Minero de España. Ríos Rosas 23 28003 Madrid, Spain (g.ortiz@igme.es)*
[6] *Instituto Geológico e Mineiro, Rua Frei Amador Arrais, 39, 7800 Beja, Portugal*

Abstract

The Ossa-Morena Zone contains abundant ore deposits and showings for the most part formed during the Cadomian and the Variscan orogenic cycles, and the intermediate rifting and stable platform stages. Despite major tectonic dismembering during Variscan rejuvenation which masked older geologic features, Cadomian mineralisation is comparable to active arc-related ore deposits, i.e., volcanic-hosted massive sulphides, barite and Zn-Pb SEDEX deposits and some minor porphyry copper-like mineralisation. Post-Cadomian Early Paleozoic ore deposits are scarce. Most are iron oxide stratabound deposits probably related to the Early Cambrian rifting volcanism. Variscan tectonic, metamorphic and magmatic activity led to the formation of very different types of mineralisation, including syn-metamorphic and perigranitic base metal-bearing veins, small volcanic-hosted polymetallic massive sulphide deposits, iron oxide replacements and skarns, magnetite and Cu-Ni magmatic ore bodies and Sn-W veins and replacements. Orogenic Au mineralisation is of imprecise age and could be either Variscan or Cadomian. Relatively low temperature Late Variscan hydrothermal activity is believed to be responsible for the formation of abundant Pb-Zn- and Cu-dominated lodes in different geological settings, Hg replacements and uranium-bearing veins.

As a whole, the diverse Variscan metallogenesis of the OMZ is interpreted as a vertical continuum in a continental crust undergoing transpressional strain. During the Variscan cycle, the OMZ first was an active continental margin –and magmatic arc-, that evolved into a collided zone after amalgamation to the South Portuguese Zone terrane. Furthermore, the recently discovered large mafic-ultramafic body set in the middle crust, probably played a key role in Variscan metallogenesis.

Keywords: Ore deposits, transpression, orogenic rejuvenation, Ossa-Morena Zone, Iberia

Resumen

La Zona de Ossa Morena se caracteriza por la abundancia de depósitos e indicios minerales pertenecientes a los ciclos orogénicos Cadomiense y Varíscico, así como a las etapas intermedias de *rifting* y plataforma estable. A pesar del desmembramiento producido por la orogénesis Varíscica, que enmascara los rasgos geológicos más antiguos, la mineralización Cadomiense reúne muchas de las características de las ligadas a arcos magmáticos en bordes de placa, tales como la formación de sulfuros masivos asociados a rocas volcánicas, depósitos sedimentario-exhalativos de barita y Zn-Pb y pequeños pórfidos cupríferos. Los depósitos minerales de edad Paleozoico Inferior son escasos, destacando sólo las mineralizaciones estratoides de óxidos de hierro relacionadas con el vulcanismo del Cámbrico inferior. La actividad tectónica y magmática ligadas a la orogenia Varíscica dieron lugar a una gran variedad de estilos y tipos de mineralización, incluyendo venas de Zn-Pb-Cu sin-metamórficas y peri-plutónicas, pequeños sulfuros masivos asociados a rocas magmáticas, remplazamientos y skarns de óxidos de hierro, mineralizaciones magmáticas de hierro y Ni-Cu y venas/remplazamientos de Sn-W perigraníticos. Hay algunas mineralizaciones de oro en relación con zonas de cizalla que puede ser

Cadomienses o Varíscicicas. Finalmente, en relación con la actividad hidrotermal tardi- a post-Varíscica tuvo lugar la formación de abundantes filones con Pb-Zn, remplazamientos con Hg y venas de uranio.

En conjunto, la diversidad de la metalogénesis Varíscica de la Zona Ossa Morena se interpreta como un continuo vertical de procesos, en un contexto de deformación regional transpresiva. La Zona Ossa Morena durante el ciclo Varíscico comenzó siendo un margen continental activo (con arco magmático), que evolucionó hacia una zona de colisión, una vez amalgamada al mismo la Zona Surportuguesa. Además, el cuerpo de máfico-ultramáfico recientemente descubierto en la corteza media, en toda la Zona Ossa Morena, debió de jugar un importante papel en la metalogénesis Varíscica.

Palabras clave: Depósitos minerales, Transpresión, Rejuvenecimiento orogénico, Zona Ossa Morena, Iberia

Resumo

A Zona de Ossa Morena contém abundantes jazigos e ocorrências mineiras, principalmente formados durante os ciclos orogénicos Cadomiano e Varisco e durante os estádios intermédios de "rifting"e de plataforma estável. Apesar do forte desmembramento tectónico, as mineralizações Cadomianas assemelham-se nas suas características às tipicamente geradas por processos mineralizantes em arcos insulares activos, com formação de jazigos de sulfuretos maciços encaixados em rochas vulcânicas, jazigos de barita e jazigos SEDEX e alguma mineralizacão menor assemelhável à do tipo pórfiro cuprífero. Os jazigos minerais do Paleozóico Inferior são escassos e incluem principalmente alguma mineralizacão estratóide de óxidos de ferro. A actividade tectónica, metamórfica e magmática Varisca levou à formação de tipos de jazigos muito diferentes, incluindo veios de metais básicos sin-metamórficos e perigraníticos, pequenas jazidas de sulfuretos maciços polimetálicos em rochas vulcânicas, corpos de substituição e skarns de óxidos de ferro, jazigos magmáticos de magnetite e de Cu-Ni, e veios e corpos metassomáticos de Sn-W. A mineralização mesotermal de Au é de idade controversa, podendo ser Varisca ou Proterozóica. Finalmente, atribui-se à actividade hidrotermal Varisca tardia, de temperatura relativamente baixa, papel determinante na formação dos abundantes veios predominantemente de Pb-Zn ou Cu em diferentes enquadramentos geológicos, de corpos de substituição de Hg e de veios com urânio. De forma geral, a pouco comum metalogénese Varisca é interpretada como resultado da forte influência exercida pelos efeitos estruturais multi-escala ditados pela tectónica oblíqua, em conjunto com uma actividade magmática relevante.

Palavras-chaves: Jazigos minerais, Transpressão, Rejuvenescimento orogénico, Zona de Ossa Morena, Iberia.

1. Introduction

The Ossa-Morena Zone (OMZ) is the Iberian Massif geotectonic unit that displays the greatest variety of types of mineralisation as well the largest number of ore deposits and showings (>650). It includes a wide range of commodities such as iron, lead-zinc, copper, gold, silver, antimony, nickel, manganese, tungsten, mercury, barite, variscite, uranium and coal. They formed by very different processes in distinct geological settings, ranging from deep mesothermal veins to stratiform exhalative deposits (Table 1).

Despite this diversity, the OMZ was of relatively minor mining importance with only few economically significant deposits discovered to present (Table 2). The Azuaga-Berlanga ore field was an important world leading Pb producer in the second half of the 19th century (c.) and the first half of the 20th c. and significant iron mining took place in the central OMZ during the middle 20th c. Additionally, minor production of copper, gold, zinc, tungsten, tin, uranium and barite took also place. First evidence of mining comes from the Argaric and Iberian cultures that worked some small Cu-Ag veins *circa* 2000 BC. The Roman Empire systematically exploited many of the outcropping mineralisation, including Pb-Ag veins, iron in Jerez de los Caballeros, the Cu-(Au) veins of Sultana, Abundancia, Encinasola and Llerena areas (Domergue, 1987), the Cu

massive ore in Tinoca and Azeiteiros (Campo Maior), Cu veins in Salvação do Índio (Azaruja) and probably also Fe in Monges. After the Roman period, little evidence exists of extensive mining except in the 16th c., when some Pb and Cu veins were worked. In 1848 the systematic exploitation of the Azuaga-Berlanga ore field started, initiating a renewed mining interest in the area. Many mines were opened in the following years that persisted until 1940-45. In the same period, several Cu lodes and iron ores were also exploited in Portugal, namely in the Sousel-Barrancos region; mining activity was extended to very rich supergene Zn ores at Vila Ruiva. Tungsten-tin deposits were worked in Spain during the first half of the 20th century, and iron oxide deposits were mined extensively till the sixties in Portugal and the 1980´ in Spain. In the last 20 years there has been a renewed interest in the metallogenic potential of the OMZ and new deposits have been discovered. It is worth noting that most of the recently discovered deposits are 'unusual', because they are only represented by a few examples and belong to uncommon deposit types. Also, the reappraisal of some long known deposits has shown that they can be classed among types which have only been recently defined in the literature.

Recently discovered and evaluated deposits include Puebla de la Reina and Nava Paredón (Cu-Zn-Pb, VHMS), Oropesa (Sn, replacement), Aguablanca (Ni-Cu, magmatic hosted) or Algueireiras-Nave de Grou-Mosteiros
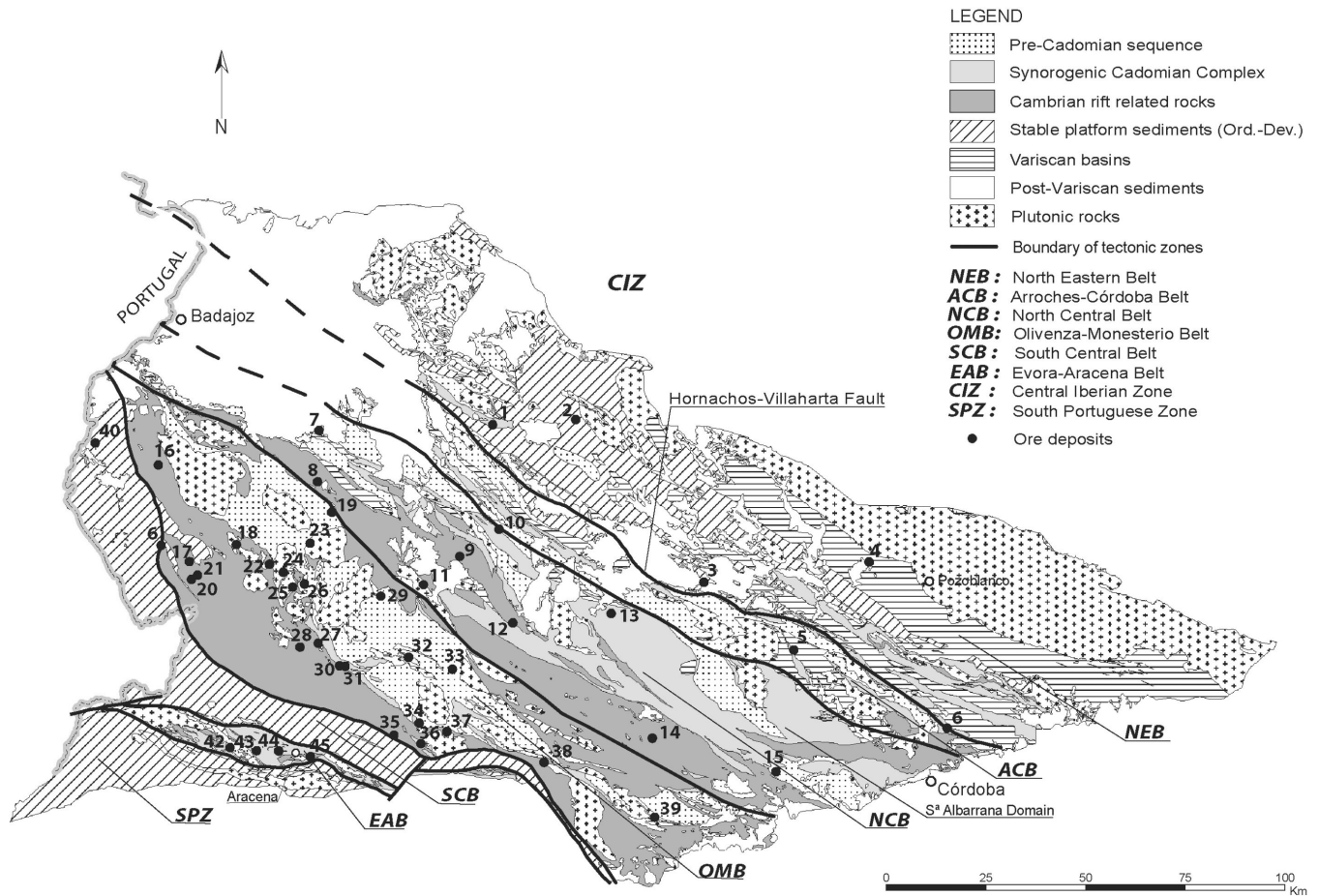
Fig. 1.- Figure 1. Synthetic geologic map of the Ossa-Morena Zone in Spain showing the metallogenic belts and the location of the major deposits and districts described in the text. Deposits and occurrences: 1. Puebla de la Reina (Cu-Zn-Pb); 2.- San Nicolás (W-(Sn-Bi)); 3.- Oropesa (Sn); 4.- El Soldado (Pb-(Zn-Ag)); 5.- Nava Paredón (Zn-Cu-Pb); 6.- Los Arenales-Cerro Muriano (ba-fl-F-(Zn-Pb-Ag)); 7.- Santa Marta (Pb-Zn-(Ag); 8.- Alfredo (Fe); 9.- Mariquita-Sultana (Hg-(Cu-Pb-Ba)); 10.- Retín (Zn-Pb); 11.- Calzadilla de los Barros (Cr); 12.- Llerena (barite); 13.- Azuaga-Berlanga ore field (Pb-(Ag-Zn)); 14.- Cerro del Hierro (Fe); 15.- Sierra Albarrana (U-(REE)); 16.- Las Herrerías (Fe-(Cu)); 17.- Oliva-Zahínos (Mn); 18.- La Bóveda (Fe); 19.- Abundancia (Cu); 20.- Mari Juli (W-(Bi-Au)); 21.- Virgen de Gracia (W); 22.- La Bilbaína (Fe-(Cu-Au)); 23.- Monchi (Fe-(Co-REE-U)); 24.- Colmenar-San Guillermo-Santa Justa (Fe-(Cu)); 25.- Bismark (Fe); 26.- La Berrona (Fe); 27.- La Valera (Fe); 28.- Los Eloys (Fe); 29.- La Hinchona (Cu); 30.- Chocolatero (Au); 31.- Guijarro (Au); 32.- Monesterio (Cabra Alta) (U-(Ni-Co)); 33.- Pallarés (Cu-Ba); 34.- Sultana (Cu-(Au-Bi)); 35.- Cala (Fe-(Cu)); 36.- Teuler (Fe); 37.- Aguablanca (Ni-(Cu-PGE)); 38.- Cazalla de la Sierra (Fe); 39.- Constantina-Huéznar (Au); 40.- Novillero (Fe-(Cu)); 41.- Villanueva del Fresno (Cabra Baja) (U-REE); 42.- Aroche (wollastonite) 43.- Maria Luisa (Cu-Zn-(Pb)); 44.- Fuenteheridos (Zn-Pb-Ag); 45.- Aracena (Zn-Pb-Ag-Ba).

Fig. 1.- Mapa geológico sintético de la Zona Ossa Morena en su parte española, mostrando la división en zonas metalogenéticas y la localización de los principales depósitos y distritos citados en el texto. Depósitos e indicios: 1. Puebla de la Reina (Cu-Zn-Pb); 2.- San Nicolás (W-(Sn-Bi)); 3.- Oropesa (Sn); 4.- El Soldado (Pb-(Zn-Ag)); 5.- Nava Paredón (Zn-Cu-Pb); 6.- Los Arenales-Cerro Muriano (ba-fl-F-(Zn-Pb-Ag)); 7.- Santa Marta (Pb-Zn-(Ag)); 8.- Alfredo (Fe); 9.- Mariquita-Sultana (Hg-(Cu-Pb-Ba)); 10.- Retín (Zn-Pb); 11.- Calzadilla de los Barros (Cr); 12.- Llerena (barite); 13.- Azuaga-Berlanga ore field (Pb-(Ag-Zn)); 14.- Cerro del Hierro (Fe); 15.- Sierra Albarrana (U-(REE)); 16.- Las Herrerías (Fe-(Cu)); 17.- Oliva-Zahínos (Mn); 18.- La Bóveda (Fe); 19.- Abundancia (Cu); 20.- Mari Juli (W-(Bi-Au)); 21.- Virgen de Gracia (W); 22.- La Bilbaína (Fe-(Cu-Au)); 23.- Monchi (Fe-(Co-REE-U)); 24.- Colmenar-San Guillermo-Santa Justa (Fe-(Cu)); 25.- Bismark (Fe); 26.- La Berrona (Fe); 27.- La Valera (Fe); 28.- Los Eloys (Fe); 29.- La Hinchona (Cu); 30.- Chocolatero (Au); 31.- Guijarro (Au); 32.- Monesterio (Cabra Alta) (U-(Ni-Co)); 33.- Pallarés (Cu-Ba); 34.- Sultana (Cu-(Au-Bi)); 35.- Cala (Fe-(Cu)); 36.- Teuler (Fe); 37.- Aguablanca (Ni-(Cu-PGE)); 38.- Cazalla de la Sierra (Fe); 39.- Constantina-Huéznar (Au); 40.- Novillero (Fe-(Cu)); 41.- Villanueva del Fresno (Cabra Baja) (U-REE); 42.- Aroche (wollastonite) 43.- Maria Luisa (Cu-Zn-(Pb)); 44.- Fuenteheridos (Zn-Pb-Ag); 45.- Aracena (Zn-Pb-Ag-Ba).

and Chocolatero-Guijarro (Au, orogenic). The only mine currently (2002) in production is Cala (Fe-skarn), operated by PRESUR SA. Moreover, the recently discovered Aguablanca deposit will start its operation soon.

Despite the economic interest, little scientific work has still been done on the OMZ ore deposits, a fact which contrasts with the major effort done at clarifying its stratigraphy, structure, metamorphism and magmatic record. In this work, we present an overview of its major mineral deposits, including for the first time both the Portuguese

Metal association	Morphology	Host and related rocks	Style	Age	Examples
I. North Eastern Belt (NAB)					
Zn-Cu-Pb	Stratabound	Calc-alkaline, bimodal volcanic and sedimentary rocks	vhms	U. Proterozoic	Puebla Reina
W-(Bi-Sn)	Veins	Shales. Epizonal peraluminous leucogranites and pegmatites	intra-&perigranitic veins	U.Carboniferous	San Nicolás
Bi-(Co-Ni)	Veins	Sandstones & shales adjacent to epizonal leucogranites	perigranitic veins	U.Carboniferous	Espiel
Cu-(Zn-Pb-Ag)	Veins	Shales & sandstones adjacent to peraluminous epizonal biotite granites	intra-&perigranitic veins	U.Carboniferous	El Soldado, Las Morras
Sn	Stratabound, veins	Shales, sandstones, limestones. Veins in quartzites.	perigranitic replacement	U.Carboniferous	Oropesa
U	Veins	Granitoids	veins	Late Variscan-Alpine	Los Pedroches
II. Arronches-Córdoba Belt (ACB)					
Cu-(-Pb)	Disseminated, stratabound	Felsic migmatitic metavolcanics and gneisses	vhms?	Proterozoic	Tinoca, Azeiteiros
Zn-Pb	Stratiform	Shales and sandstones	sedex	Proterozoic?	Usagre
Au	Veins, stockworks	Metasediments & metavolcanic rocks	orogenic gold	Prot? Variscan?	S.Martinho, ANM
Zn-Cu-Pb-(Au)	Stratabound	Calc-alkaline, bimodal high K volcanic and related sedimentary rocks	vhms	E.Carboniferous	Nava Paredón
Fe	Stratiform	Rhyolites in calc-alkaline bimodal high K volcanic rocks	exhalative	E.Carboniferous	Las Berazas
Zn-(Pb-Cu)	Stratabound	Calcic skarns in carbonate rocks, calc-silicate hornfelses	skarn	U.Carboniferous	Los Arenales
Pb-Zn-(Ag)	Veins	Gneisses	shear-related veins	Late Variscan	Azuaga-Berlanga
Ba-F-(Zn-Pb-Ag)	Veins	Granitoids	basement-cover veins	U.Carboniferous – Permian?	Cerro Muriano
III. North Central Belt (NCB)					
Cr	Irregular	Serpentinites	alpine podiform	Proterozoic	Calzadilla
Cu	Irregular & veins	Calc-alkaline epizonal quartz-monzonites	porphyry	U.Proterozoic	Ahillones
Ba	Stratiform	Limestones, volcaniclastic shales	sedex	U. Proterozoic	Llerena
Cu-Zn-Pb	Irregular	Volcanosedimentary sequence	?	Cambrian	
Cu, Ba	Veins	Schists	syn-tectonic veins	Variscan	Pallarés
Fe	Tabular	Gabbro	magmatic	Variscan?	Alter do Chão
U-REE	Irregular	Syn-metamorphic granitic pegmatites	pegmatites	Carboniferous	Sierra Albarrana, Villanueva del Fresno
W (-Sn)	Veins & greisen	Granites	intragranitic veins & replacements	Variscan	Santa Eulália
Hg-(Pb-Cu-Ba-Au)	Stratabound, irregular, veins	Limestones, shales	epithermal replacements	Variscan	Mariquita
Fe	Strata bound	Limestones	skarns	Varican(?)	Alagada
Zn-Pb	Veins	Limestones	periplutonic veins	Varican(?)	Torre das Figueiras
IV. Olivenza-Monesterio Belt (OMB)					
Fe	Stratabound	Volcaniclastic sub-alkaline to alkaline dacites	(sub)-exhalative	Cambrian	Bilbaina, Bóveda, Bismark
Mn	Stratabound, veins	Volcaniclastic sub-alkaline to alkaline dacites	(sub)-exhalative	Cambrian	Zahínos
Fe	Irregular	Dacites with pervasive albitisation	replacement	Cambrian-Variscan?	Berrona, Alfredo
Au	Veins, irregular	Deformed metavolcaniclastic rocks	orogenic gold	Variscan	Guijarro, Chocolatero, Constantina-Hueznar
Cu, Zn-Pb	Veins	Shales, sandstones	syn-tectonic veins	Variscan	Hinchona
Ni-(Cu-PGE)	Pipe	Mafic & ultramafic cumulates, calc-alkaline gabbros	ultrabasic-related	Variscan	Aguablanca

Commodity	Style	Host rocks	Process	Age	Examples
Fe-(Cu-Au)	Stratabound, Irregular	Limestones, granitoids, gneisses	replacement	Variscan?	Colmenar, Monchi
Fe-(Cu-Au)	Stratabound, irregular	Limestones, calc-silicate hornfelses, diorites to leucogranites	skarn	Variscan	Cala, Teuler
Vermiculite	Irregular	Dolostones with magnesial skarn	skarn	Variscan	Garrenchosa
Cu-(Au-Bi)	Veins	Shales, calc-silicate hornfelses, calc-alkaline tonalites	peri-&intragranitic veins	Variscan	Sultana, Abundancia
W-(Sn-Bi-Au)	Veins, irregular	Epizonal peraluminous monzonites to leucogranites	peri-&intragranitic veins & greisens	Variscan	Virgen de Gracia, Mari Juli
Au	Veins	Peraluminous calc-alkaline epizonal leucogranites	intragranitic veins	Variscan	Burguillos
U-(Ni-Co)	Veins	Migmatitic gneisses	basement cover veins	Post Variscan	Cabra Alta
V. South Central Belt (SCB)					
Cu, P, Fe-Mn	Stratiform	Black shales	early diagenetic	Ordovician-Silurian	Aparis, Novillero
Cu, Zn-Pb, Fe	Veins	Shales, sandstones and turbiditic sedimentary rocks	late-tectonic veins	Late to post-Variscan	Defesa das Mercés
Cu	Disseminations, veins	Felsic sub-volcanic intrusives and related breccias	?	Silurian?	
U-REE	Disseminations, veins	Albitic leucogranites	magmatic	Variscan	Villanueva del Fresno
VI. The Evora-Aracena Belt (EAB)					
Fe	Massive, stratabound	Retrograded amphibolites and metalimestones	vhms+skarn?	L.Cambrian-Ordovician, Variscan?	Monges, Orada
Zn-(Cu-(Pb-Ag))	Stratiform (stratabound?)	Metavolcanic-sedimentary sequence with abundant metadolostones	vhms, sedex-Irish type?	Proterozoic-L. Cambrian?	Enfermarias, Maria Luisa, Aracena, Fuenteheridos
Au-Cu-(Pb)	vhms	Metasedimentary and metavolcanic rocks	mesothermal	Proterozoic? Variscan?	Chaminé-Casas Novas-Braços
Au-Bi	Veins, stockworks	Marbles adjoining Beja Igneous Complex	skarn	Variscan	Alvito
Fe	Massive, irregular	Metalimestones, calc-silicate hornfelses	skarn	Variscan	Aracena
Fe-Zn	Stratabound	Limestones	skarn	Variscan	
wollastonite	skarn	Schists	metamorphic	Variscan	
graphite	Irregular			Variscan	
Cu	Veins, diaclase infillings	Quartz-diorite intrusions, aplite-pegmatite veins, and mica schists	periplutonic veins	Variscan	Azaruja
Cu	Veins	Metavolcanic-sedimentary sequence (Ordovician?)	late-tectonic veins	Late to post-Variscan	Rui Gomes
VII. S. Cristovão-Beja-Serpa Belt (SCBSB)					
Fe-Ti-V	Irregular masses	Gabbros of the Beja Igneous Complex	magmatic	U. Devonian?	Odivelas
Cu-(Ni)	Veins, stockworks	Gabbros of the Beja Igneous Complex	late-magmatic	U. Devonian?	Castelo Ventoso
Cu-(Ag-Au)	Veins, stockworks	Porphyry rocks of the Beja Igneous Complex	periplutonic veins. epithermal!?	Carboniferous?	Caeirinha
Sb, Cu(As-Au)	Veins	Metasedimentary rocks	late-tectonic veins	Late to post-Variscan	Ventosa
VIII. Beja Acebuches Ophiolite Complex (BAOC)					
Cr	Disseminations, bands	Strongly serpentinised and metamorphosed peridotites	magmatic	Devonian?	Mombeja-Ferr. Alentejo
Ni-Cu-(Co)	Disseminations, bands	Deformed and metamorphosed wehrlite-troctolite rocks	magmatic	Devonian?	Palmeira
Cu	Disseminations, bands	Carbonatized domains of regional shear zones	syn-tectonic veins	Variscan	Mombeja

Table 1.- Major styles of mineralisation in the Ossa-Morena Zone
Tabla 1.- Principales tipos de mineralización en la Zona de Ossa Morena

and the Spanish ones. Also, an integrated model of ore evolution in time and space is proposed.

General features of the geology of OMZ will not be repeated here because they are reviewed in detail elsewhere in this volume. In this work, the southern boundary of the OMZ is taken to be the major structural contact with the Pulo de Lobo Terrane and the South Portuguese Zone (Figs 1 and 2). The northern boundary is set to be the Pedroches batholith and its westward extension in Portugal. Mineral deposits located between the Tomar-Córdoba Shear Zone (TCSZ) and the Pedroches batholith are included here because they show lead isotope signatures similar to those of the OMZ and distinct to those the Central-Iberian Zone (Tornos and Chiaradia, 2004).

The metallogeny of the OMZ is a record of the different geological processes related with a complex geodynamic evolution since the Cadomian through the Variscan orogenic cycles (Quesada *et al.*, 1987; Eguíluz *et al.*, 2000, and references therein). In this context the OMZ represents an exceptional place to test how magmatic and hydrothermal systems evolved through time, and to ascertain the effects that orogenic rejuvenation had on old metallic provinces.

The division of the OMZ which is followed here, into ore belts parallel to the trend of the orogenic belt is based on Oliveira (1986) and Locutura *et al.* (1990), with some modifications. The reference list includes the more significant papers published in the last ten years and some key earlier references. For a more complete overview the reader is referred to the earlier general overview of Locutura *et al.* (1990) and the metallogenic synthesis of Thadeu (1965), Schermerhorn (1981), Quesada *et al.* (1987) and IGME (2004).

2. Ore deposits description

The distribution of ore deposits and showings shows a clear pattern consisting of successive WNW- ESE-trending ore belts (Figs 1 and 2), modified after Oliveira (1986) and Locutura *et al.* (1990), and that broadly coincide with the major tectono-metamorphic domains (e.g., Apalategui *et al.*, 1990). The description of the ore deposits is organised into eight ore belts. Only the most significant styles of mineralisation and individual deposits are discussed here. Deposits within each belt are ordered according to known or supposed age.

2.1. North Eastern Belt (NEB)

This metallogenic belt occupies the NE part of the OMZ, between the Pedroches batholith and the Hornachos-Villaharta Fault (Fig. 1). This domain is characterised by a Paleozoic sedimentary sequence with Central Iberian Zone affinities which overlies a Proterozoic sequence typical of the OMZ. Shallow marine Carboniferous synorogenic basins are abundant in the area (Gabaldón *et al.*, 1985). A variety of mineral deposits occur, mainly hydrothermal veins related to the Pedroches batholith.

Volcanic-hosted Zn-Cu-Pb mineralisation (Upper Proterozoic-Lower Cambrian)

The **Puebla de la Reina** (1; Fig.1) deposit represents a typical Cu-Zn-Pb volcanic- hosted massive sulphide orebody (Conde *et al.*, 2001). It was discovered by the IGME in 1981 and consists of several stratiform lenses up to 9 m thick and 150 m long set in syn-Cadomian felsic volcaniclastic sandstones and massive dacites, with minor massive andesites, shales and limestones. The footwall and hanging wall of the deposit show a pervasive hydrothermal alteration which is strongly dependent on the type of protolith. Felsic volcanic rocks are chloritized and sericitized and strongly silicified adjacent to the orebody. Disseminated sulphides are common in the altered zones. Mafic rocks only show irregularly distributed chloritization. The mineralisation consists of pyrite, chalcopyrite, sphalerite and galena, with trace amounts of tetrahedrite and arsenopyrite, besides minor carbonates, quartz and illite. The absence of both a stringer zone and of preserved sedimentary structures, along with some textural evidence suggest that the mineralisation resulted from hydrothermal replacement of the volcanics. Conde *et al.* (2001) argued that the process involved mixing of a deep hot metal-bearing fluid with sub-surficial waters which carried reduced sulphur of marine derivation. Fluids were focused along extensional structures and major permeable/reactive horizons, largely vitriclast-rich and porous volcaniclastic sandstones.

These deposits probably formed in an arc or back-arc setting (Sánchez Carretero *et al.*, 1990) and share many features with those of Kuroko-type, i.e., the bimodal-felsic type of deposits (Barrie and Hannington, 1999).

W(-Bi-Sn) veins related to epizonal leucogranites (Late Variscan)

In the southern margin of the Pedroches batholith there are some bodies of leucogranite that show related tin-tungsten mineralisation (Ovtrach and Tamain, 1977). Cassiterite, wolframite and scheelite with accessory molybdenite and bismuth minerals occur disseminated in quartz-muscovite-topaz greisens. Perigranitic pegmatites are also found, with cassiterite, wolframite, scheelite and REE-bearing minerals.

The **San Nicolás** (2, Fig.1) leucogranitic cupola and the enclosing Devonian shales are host to a vein field consist-

Name	Substance	Age	Size & grade	Situation	Reference
Puebla de la Reina	Cu-Zn-Pb	Pr	0.5 Mt @ 1.6%Cu, 11.0%Zn, 1.2%Pb, 32 g/t Ag	Evaluated	Conde et al. (1999)
San Nicolás	W-(Sn-Bi)	V	0.36 Mt @ 3% WO_3, and 0.25% Bi	Mined (1912-1990)	Gumiel (1988)
Oropesa	Sn	V	18 Mt @ 0.28%Sn	Evaluated	Locutura et al. (1990)
El Soldado	Pb-(Zn-Ag)	V	2 Mt	Mined	Ovtrach & Tamain (1977)
Nava Paredón	Zn-Cu-Pb	V	0.25 Mt @ 2%Cu, 10.9%Zb, 4.7%Pb, 183 g/t Ag	Explored	Tornos et al. (2000)
Alfredo	Fe	C	2.3 Mt @ 54%Fe	Mined (1959-1968)	Dupont (1979)
Mariquita-Sultana	Hg-(Cu-Pb-Ba)	V	0.11 Mt @ 5-7%Hg, 2%Cu	Mined (1631-1971)	Tornos & Locutura (1989)
Calzadilla de los Barros	Cr	Pr	<0.03 Mt, 25.1%Cr	Explored	Arriola et al. (1981)
Llerena	ba	C	0.7 Mt 50%barite	Mined (1970-1990?)	Miras (1991)
Azuaga-Berlanga ore field	Pb-(Ag-Zn)	V		Mined (1848-1950)	
Cerro del Hierro	Fe	post V	50-52%Fe	Mined	
Sierra Albarrana	U-(REE)	V	12 Mt	Mined	González del Tánago (1991)
Las Herrerías	Fe-(Cu)	C	12 Mt @ 44%Fe, 0.28%Cu	Mined	IGME (1994)
La Bóveda	Fe	C	43.9%Fe	Mined (-1982)	Dupont (1979)
Oliva de la Frontera (Mari Juli,Virgen de Gracia)	W-(Bi-Au)	V		Mined (-1970)	Gumiel et al. (1987)
La Bilbaína	Fe-(Cu-Au)	C	7.85 Mt @ 52.5%Fe; 0.11%Cu	Mined (1910-1968)	Dupont (1979)
Monchi	Fe (Co-REE-U)	C-V	66%Fe	Mined (1953-1978)	Arribas (1963)
Colmenar-S.Guillermo-Sta Justa	Fe-(Cu)	C-V	31 Mt @ 35.3%Fe	Mined (1910-1978)	Dupont (1979), Sanabria (2001)
La Berrona	Fe	V?	23.6 Mt@ 24.8%Fe	Evaluated	IGME (1994)
Cabra Alta (Monesterio)	U-(Ni-Co)	post V	0.065 Mt @ 1.5% U_3O_8	Mined (1956-1965)	Arribas (1963)
Sultana	Cu-(Au-Bi)	V	<1 Mt 3.15% Cu, 15 g/t Au	Mined (1903-1919)	Tornos & Velasco (2003)
Cala	Fe-(Cu)	V	50 Mt @ 40%Fe, 0.4%Cu	Working (1901-)	Velasco & Amigó (1981)
Teuler	Fe	V	3 Mt	Mined	Vázquez (1989)
Aguablanca	Ni-(Cu-PGE)	V	31 Mt @ 0.62%Ni, 0.5%Cu	Feasibility	Tornos et al. (2001)
Aroche	wollastonite	V	1.8 Mt @ 22.3%wo	Evaluated	IGME (2002)
Maria Luisa	Cu-Zn-(Pb)	Pr	1.5 Mt @0.8%Cu, 3.0%Zn, 0.5%Pb, 50 g/t Ag	Mined (-1979)	Vázquez (1972)
Fuenteheridos	Zn-Pb-Ag	Pr?	4.0 Mt @ 2.0%Zn, 0.2%Pb, 80 g/t Ag	Evaluated	Fernandez Caliani et al. (1989)
Aracena	Zn-Pb-Ag-ba	Pr?	2-3%Zn, 0.4%Pb, 50 g/t Ag	Explored	Arribas et al. (1990)
Tinoca	Cu-(Pb)	Pr	0.025 Mt @ 2.5-5%Cu	Incipiently mined (1907-1934)	Oliveira (1986); Beck (1997)
Defesa das Mercês	Cu	S?	480 t (total exploited ore)	Mined (1896-1898)	SIORMINP (2002)
S. Martinho-Portalegre	Au	Pr? V?	1-2.5 g/t Au	Explored	Oliveira et al. (1995, 2001), Inverno (1997)
Monges	Fe	C?-V	1-2 Mt @ 30-66% Fe	Incipiently mined (1865-1905)	Goinhas & Martins(1986); Carvalho (1976)
Orada	Fe	O?-V	2 Mt @ 40%Fe	Mined (1955-1971)	Carvalho (1971, 1976)
Alvito	Fe	V	0.7 Mt @ 44%Fe	Mined (1884-1929)	Carvalhosa & Zbyszewski (1972), Carvalho (1976)
Enfermarias	Zn,Pb(Ag-Sb-Au)	C?	0.6 Mt @ 2.6% Zn, 0.8%Pb	Prospect	Oliveira & Matos (1992)
Chaminé-Casas Novas-Braços	Au-As-Bi	Pr? V?	4.45 Mt @ 2.81ppm Au	Evaluated	Ribeiro et al. (1993), Inverno (1997), Faria (1997)
Odivelas	Fe-Ti-V	D?	<10%TiO2; < 1% V_2O_5	Prospect	Silva (1945); Jesus (2002)
Castelo Ventoso	Cu-(Ni)	D?	<0.14%Cu, 0.02%Ni	Prospect	Jesus (2002)
Mombeja-Ferr. Alentejo	Cr	D?	<0.1% Cr (in bands)	Prospect	Mateus & Figueiras (1999 a,b)
Mombeja	Cu	V	<1.5%Cu	Prospect	Mateus et al. (1998c)
Caeirinha	Cu(-Ag-Au?)	V?	<1.5%Cu	Prospect	Relvas (1987)
Ventosa	Sb,Cu(As-Au)	V	<30% Sb; < 1% Cu	Prospect	Mateus et al. (1998c)
Alagada	Fe	V	1.82 Mt @ 27%Fe	Prospect	Gonçalves & Assunção (1970)
Santa Eulalia	Sn-(W-F)	V	0.12 Mt of alluvial/elluvial ore	Prospect	Thadeu & Aires-Barros (1973), Oliveira (1986)
Aparis	Cu	Late-post V	0.02 Mt @ 2.75%Cu	Mined	SFM Internal Reports (1951, 1965)

Table. 2.- Tonnages and grades of the most significant ore deposits C: Cambrian; D: Devonian; O: Ordovician; Pr: Proterozoic; S: Silurian; V. Variscan;. Total tonnage includes estimated extracted + resources. Grades in % except Au and Ag in ppm. py: pyrite; wo: wollastonite

Tabla. 2.- Tonelaje y leyes de los depósitos minerales más importantes de Ossa Morena.

ing of several wolframite-bearing quartz veins up to 50 cm thick. Aside from wolframite they contain significant amounts of cassiterite, scheelite, pyrite and chalcopyrite with quartz, muscovite, fluorite and topaz (Gumiel, 1988). Rocks near the vein field underwent pervasive greisenisation and tourmalinisation that was particularly intense in the granite.

Sn replacements (Late Variscan)

A Sn-bearing stratabound replacive mineralisation was recently discovered in **Oropesa** (3; Fig.1), (Locutura *et al.*, 1990). It is a rather large orebody (ab. 18 Mt @ 0.28% Sn with 8 Mt @ 0.4% Sn and up to 1% Cu). The mineralisation is surrounded by a large halo of pervasively hydrothermally altered rocks and is close to N-S subvertical faults. Host rocks consist of strongly silicified Late Carboniferous felsdpatic sandstones, slates, conglomerates and limestones that were deposited in a pull-apart basin, a geological setting similar to that of Nava Paredón massive sulphides (see below). Ore minerals, including arsenopyrite, cassiterite and chalcopyrite occur in veins, stockworks or disseminations. No feeder zone has been recognised at Oropesa. It could be however represented by the abundant tin-rich (up to 11% Sn) quartz veins set in the nearby Ordovician basement, here consisting of quartzites and shales. However, the two orebodies are separated by a fault. A hidden granitic cupola was probably the source of metals, fluids and heat, in an scheme similar to that of Renison Bell in Tasmania (Patterson *et al.*, 1981).

Cu-Zn-Pb(-Ag) veins in granites (Variscan)

These veins are set within or near the Pedroches batholith, and constitute one of the largest vein ore fields in Europe. As a whole, the vein field displays a normal metal zoning with Cu veins inside the pluton (mostly biotite granites), and Pb-Zn(-Ag) veins near the contact or within the host Lower Carboniferous shales and sandstones (Ovtrach and Tamain, 1977). Pb-Zn veins are very abundant in the **Linares-La Carolina** district, in the easternmost exposures of the batholith and outside the limits of the Ossa-Morena Zone. Some major veins also occur in the southern part of the batholith.

Trends of vein swarms are WNW-ESE, NNE-SSW, NE-SW and E-W, and are probably related to normal and dextral strike slip faults (Asensio *et al.*, 1997). The veins consist of quartz, carbonates (ankerite-calcite), chalcopyrite or galena-sphalerite, and always contain pyrite.

The more significant mines on the south of the batholith are **El Soldado-Las Morras** (4; Fig.1) group, set in Carboniferous turbidites (Culm Group) that show contact metamorphism probably due to a hidden granite cupola. The veins are short but thick, with an "echelon" arrange-

ment and NE-SW and NNE-SSW trends. Hydrothermal breccias and cockade structures are common. This group has produced more than 2 Mt ore (Ovtrach and Tamain, 1977).

These veins are apparently related to the granites and metal zoning probably resulted from thermal gradients set up during the cooling of the batholith. Fluid inclusion data (Asensio *et al.*, 1997) and geochemical considerations suggest that hydrothermal fluids probably were meteoric and that metals were scavenged from the regional sedimentary rocks and the granites. Fluid flow was enhanced by regional fracturing in late Variscan times. These veins are hardly distinguished from the barite-fluorite (-Zn-Pb-Ag) veins of the nearby Arronches-Córdoba Belt which could be as young as Early Alpine (see below).

Bi(-Co-Ni) veins and shear zones (Variscan)

South of the Pedroches batholith some poorly known quartz-carbonate veins exist that are hosted by Carboniferous turbidites near to leucogranite bodies. The veins trend is N20-45ºE, and they are 300-1200 m long and 4-30 cm thick. Ore zones within the veins are lenses about 4 m thick. The ore consists of native bismuth, bismuthinite, calcite and quartz, as well as minerals belonging to the Cu-Pb-Sn-W-Ni-Co-As-Ag system (Vázquez, 1989).

Uranium vein mineralisation (Late Variscan-Alpine)

Uranium-bearing quartz veins are found in the easternmost part of this belt, within or near the Pedroches batholith. The veins show a polyphase filling with quartz, chalcopyrite and pyrite as primary minerals, and a superimposed low-T alteration (chlorite-sericite-quartz). Most of the uranium mineralisation (pitchblende, coffinite and abundant oxidised species) was laid down during a late oxidising stage (Arribas, 1964) of unknown age. The uranium mineralisation formed by reduction of meteoric fluids at depth (down to 200 m). Pitchblende intergrowths with sulphides address to a protracted hydrothermal activity with shifts in the redox boundary.

2.2 The Arronches-Córdoba Belt (ACB)

This belt includes the Tomar-Córdoba Shear Zone (Fig.1) (e.g., Apalategui *et al.*, 1990) as well as the neighbouring regions, north and south of it. In the Portuguese part of the OMZ this zone is equivalent to the Arronches-Campo Maior (Au, Cu, Pb, (Ag)) belt of Oliveira (1986). The major structural feature of this belt is a first order shear zone, believed to be a Cadomian cryptic suture by some authors (Abalos *et al.*, 1991; Quesada *et al.*, 1991), that underwent protracted activity during the Paleozoic. The Tomar-Córdoba shear zone exerted a strong control on sedimentation,

magmatic activity, metamorphism and structural evolution of the area.

Volcanic-hosted massive sulphides (Proterozoic)

NW of Campo Maior, the **Tinoca** and **Azeiteiros** (2; Fig. 2) volcanic-hosted massive sulphide Cu mineralisation was mined since Roman times. They are hosted by Proterozoic rocks -a gneiss-migmatitic complex-, within the Tomar-Córdoba Shear Zone. At Tinoca, a stratiform mineralisation 1000 m long and 55 m thick, is set in amphibole- and/or biotite-bearing felsic migmatitic gneisses. Mineralisation consists of (semi-)massive magnetite with interstitial chalcopyrite and pyrite. Moreover, disseminations or irregular veins of chalcopyrite, pyrite and magnetite are set in a granoblastic quartz-rich rock. Felsic metavolcanic rocks (felsic gneiss) are interpreted as the mineralisation footwall. Both mineral assemblages at Tinoca are set in rocks that underwent silicification, chloritization and muscovitization, and also contain accessory sphalerite, argentiferous galena and gold (commonly above 0.5 g/t Au).

The Azeiteiros semi-massive and disseminated chalcopyrite and pyrite mineralisation (2.2% Cu) occurs in a 20-40 m thick, N110-120ºE-trending shear zone and is hosted in magnetite-bearing meta-rhyolites adjacent to amphibolites (Oliveira, 1986; Beck, 1997; SIORMINP, 2002).

Sedimentary-exhalative Zn-Pb mineralisation in the Azuaga Formation (Proterozoic?)

Some intriguing Zn-Pb stratiform mineralisation (**Retín** and some nearby prospects) occurs in the allegedly Late-Proterozoic syn-orogenic (Cadomian) Azuaga Formation. This formation consists of several thousand metres of a monotonous low-grade metamorphosed flysch sequence (Quesada *et al.*, 1987). The mineralisation consists of small lenses of massive sphalerite with minor galena and traces of chalcopyrite, pyrite and pyrrhotite with some barite, hosted by weakly chloritized schists of the flysch sequence. Discontinuous beds of volcano-sedimentary calc-alkaline rocks as well as of garnet-bearing Mn-rich quartzites - probable exhalites- are also found within the flysch sequence (Urbano, 2001, pers. com.). Veinlets and disseminations of sphalerite and galena and, sometimes, chalcopyrite, are common in these rocks.

High Zn/Cu ratios, the relationship to fine-grained siliciclastic sediments and the absence of a stringer zone all suggest that this type of mineralisation could be sedimentary-exhalative (Locutura *et al.*, 1990). Lead isotope ratios suggest sources with high U/Pb ratios, typical of terranes with a long-lived upper crustal evolution; model ages are Upper Neoproterozoic (Tornos and Chiaradia, 2004).

Orogenic gold mineralisation (Proterozoic? Variscan ?)

Orogenic gold mineralisation occurs in the Portalegre area, in **S. Martinho** (4; Fig.2) and **Algueireiras-Nave de Grou-Mosteiros** (A-N-M) (72; Fig. 2), south and north of the Tomar-Cordoba Shear Zone, respectively. Both styles of mineralisation are found near small shear zones within the pre-orogenic (Cadomian) Serie Negra sequence and underwent amphibolite and greenschist facies regional metamorphism, respectively. Gold mineralisation occurs typically in the transition metasedimentary/metavolcanic rocks, namely quartz-biotite slates and schists/amphibolites (and amphibolite gneisses) or felsic metavolcanic rocks. Small felsic-intermediate porphyritic intrusions and felsic-intermediate metavolcaniclastic rocks are commonly present close to the gold mineralisation. Hydrothermal alteration consists of silicification, chloritization, sericitization and carbonatization. The last is pervasive in the case of A-N-M where Fe-dolomite, accompanied by disseminated fuchsite, alters felsic metavolcaniclastic rocks. The mineralisation is found as disseminations, quartz veins, veinlets and stockworks, and can also be stratabound. It consists primarily of pyrite and pyrrhotite, with variable amounts of arsenopyrite; other accessory minerals include löllingite, chalcopyrite, gold, ilmenite, realgar, barite and tourmaline. Grade is 1-2.5 g/t Au at S. Martinho and not above 1 g/t Au at A-N-M (Inverno *et al.*, 1995; Inverno, 1997).

At **S. Martinho** (4), two gold generations were recognised; the first is related to early quartz I veinlets parallel to foliation containing arsenopyrite, pyrite, chalcopyrite and gold I. This low-Au mineralisation was deposited from metamorphic fluids, either aqueous-carbonic (H_2O-CO_2-CH_4), low saline (avg. 10 wt% NaCl equiv.) with Th of 245-521ºC fluids or lower temperature (Th = 112-162 ºC), H_2O-NaCl-$Ca(Mg)Cl_2$ fluids, with 1-18 wt% NaCl equiv. salinity. Quartz II discordant veinlets contain a later generation of arsenopyrite, pyrite and chalcopyrite with trace proportions of löllingite, pyrrhotite and gold II. This main gold mineralisation is interpreted as related with the circulation of magmatic, late stage hypersaline (32-62 wt% NaCl equiv.) H_2O-NaCl (also Mg/K/Fe chlorides, $CaCO_3$) fluids, homogenising between 270 and over 550 ºC (Oliveira, 2001; Oliveira *et al*, 2001a and 2001b).

Volcanic-associated Zn-Cu-Pb(-Au) and iron oxide mineralisation (Lower Carboniferous)

The Carboniferous sedimentary rocks of this belt are restricted to WNW-ESE-trending pull-apart basins. They constitute a siliciclastic-carbonate sequence deposited in a shallow marine to continental environment (Gabaldón *et al.*, 1985). Bimodal, high K calc-alkaline volcanic rocks
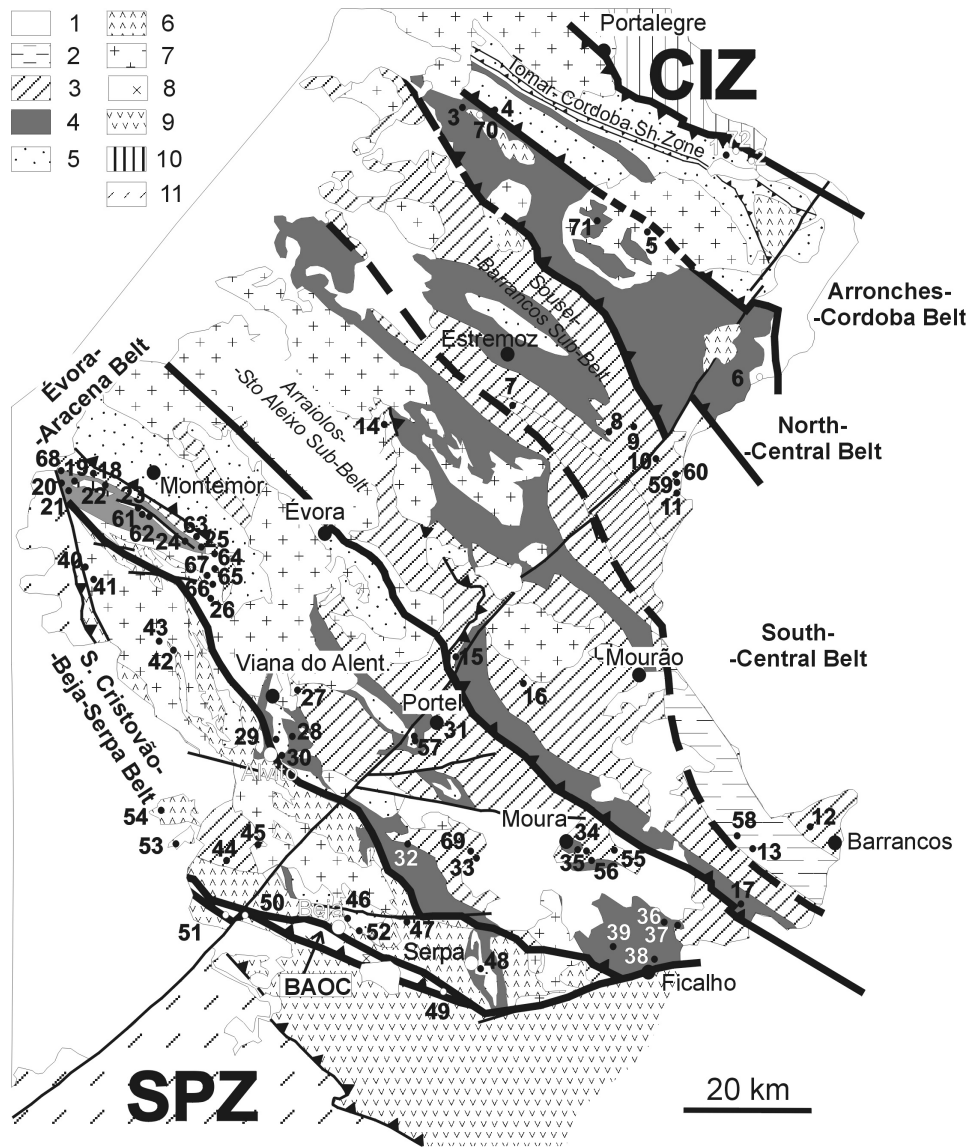
Fig. 2.- Synthetic geologic map of the Ossa-Morena Zone in Portugal showing the metallogenic belts and the location of the major deposits and districts described in text. Adapted from Geological Map of Portugal, scale 1:500000, 1992 – J.T. Oliveira and E. Pereira, compilers. Geology: 1. Cenozoic sedimentary cover. 2. Metasedimentary sequences of Late Devonian age. 3. Metasedimentary and metavolcanic sequences of Ordovician-Silurian age. 4. Metasedimentary (including metadolostones) and metavolcanic sequences of Cambrian age. 5. Metasedimentary and metavolcanic sequences of Proterozoic age. 6. Gabbros (and diorites) and ultramafic rocks (Lower Paleozoic to Variscan). 7. Undifferentiated Variscan and Late-Variscan granitoid rocks. Oceanic exotic Terranes: 8. Beja-Acebuches Ophiolite Complex (BAOC). 9. Pulo do Lobo Group (metasedimentary and metavolcanic rocks). 10. Central-Iberian Zone metasedimentary rocks. 11. South Portuguese Zone metasedimentary and metavolcanic rocks. Deposits and occurrences: *Arronches-Cordoba belt*: 1 - Balôco (Pb); 2 - Tinoca/Azeiteiros (Cu(Pb)); 4 - S. Martinho (Au(As)); 72 – Algueireiras-Nave de Grou-Mosteiros (Au). *North Central belt*: 3 - Alter do Chão (Zn, Cu, Ba);; 5 – Sta. Eulália (Sn, W); 6 – Alagada (Fe); 70 – Alter do Chão-Este (Fe, V); 71 – Torre das Figueiras (Monforte) (Zn, Pb). *South Central belt: a) Sousel-Barrancos sub-belt*: 7 – Mostardeira (Cu); 8 – Miguel Vacas (Cu); 9 – Zambujeira (Cu); 10 – Bugalho (Cu); 11 – Mociços (Cu); 12 – Defesa das Mercês (Cu); 13 – Aparis (Cu); 58 – Botefa (Cu); 59 – Urmos (Cu); 60 – Minancos (Cu); *b) Arraiolos-Sto. Aleixo sub-belt*: 14 – Azaruja (Cu); 15 – Monte do Trigo (Cu); 16 – Reguengos (Cu); 17 – Sto. Aleixo (Cu). *Évora-Aracena belt*: 18 - Courela do Conde (Cu); 19 - Safira (Cu, As, Au); 20 – Courelinha (Cu); 21 – Palmas (Sb, Au); 22 - Gouveia (As, Cu, Au); 23 - Monges (Fe, Py); 24 – Nogueirinha (Fe, Py); 25 – Chaminé (Au, As (Bi)); 26 – Alcalainha (Cu); 27 – Sobral/Ganhoteira (Cu); 28 – Água de Peixes (Pb, Zn); 29 – Alvito (Fe); 30 – Alvito (Cu); 31 – Portel-Algares (Zn, Cu, Pb); 32 – Vale de Pães (Fe); 33 – Orada (Fe); 34 – Enfermarias (Zn, Cu, Pb); 35 – Sto. André (Fe); 36 – Preguiça (Pb, Zn); 37 – Vila Ruiva (Zn, Pb); 38 – Ficalho (Pb, Zn); 39 – Louzeiras (Pb, Sb, Ag); 55 – Rui Gomes (Cu); 56 – Carrasca (Fe, Zn (Pb)); 57 – Portel-Balsa (Zn, Pb (Ag)); 61 – Monfurado (Au); 62 – Banhos (Au (As)); 63 – Casas Novas (Au, As (Bi)); 64 - Ligeiro (Au); 65 – Caras (Au, As); 66 – Braços (Au, As); 67 – Covas (Au, As); 68 – Caeira (Au (Cu)); 69 – Azenhas (Fe); *S. Cristóvão-Beja-Serpa belt*: 40 – Corte Pereiro (Cu, Pb, Zn); 41 – Caeirinha (Cu, Pb, Zn); 42 – Alcáçovas (Entre Matas) (Cu); 43 – Alcáçovas (V. Nogueira) (Cu); 44 – Asseiceiras (Cu); 45 – Peroguarda (Cu, Fe); 46 – Corujeiras (Fe); 47 – Baleizão (Cu); 48 – Serpa (Cu); 52 – Ventosa (Sb, Cu (As, Au)); 53 – Castelo Ventoso (Cu (Ni)); 54 – Odivelas (Fe, Ti, V); *BAOC*: 49 – Palmeira (Ni, Cu (Co)); 50 – Mombeja-Ferr. Alentejo (Cr); 51 – Mombeja (Cu).

→

(Sánchez Carretero *et al.*, 1990) are scarce and confined to some magmatic alignments within the Benajarafe-Matachel basin. Despite the high metallogenic potential of this type of geological setting, ore deposits are rare in this basin and equivalent ones in the OMZ. The major deposit is **Nava Paredón** (5; Fig.1) a polymetallic volcanic-hosted massive sulphide deposit that was mined by the Romans and rediscovered by the IGME in the late 1970´ (Baeza *et al.*, 1981). Recent work (Tornos *et al.*, 2000) has shown that the mineralisation occurs at a well-defined stratigraphic horizon, between pervasively devitrified massive rhyolites and the overlying immature-derived polymictic mass flows. The age of the lithostratigraphical sequence is Upper Tournaisian to Lower Visean (Gabaldón *et al.*, 1985; Sánchez Carretero *et al.*, 1990). Rhyolites are thought to form subaerial to shallow marine domes whilst the overlying volcaniclastic sedimentary rocks probably formed in a fault scarp during syn-sedimentary faulting and deepening of the basin.

Rhyolites show a pervasive hydrothermal alteration consisting of texturally destructive silicification, sericitization and K-alteration synchronous to devitrification; hydrothermal dolomite can be locally important. These altered rocks contain abundant disseminated sulphides and are enriched in Cu and Au but a clear stringer system has not been found. The lowermost volcaniclastic rocks underwent equivalent alteration as the rhyolites. Upwards in the sequence, chloritization, silicification and K-alteration become more irregular.

The massive sulphides occur in five, 1 to 4 m thick lenses, with grades of about 30-35% Zn+Pb, 1.6% Cu, 600 g/t Ag and 1.9 g/t Au, that are enclosed in highly altered rhyolites. The mineralisation is dominantly sphalerite and galena, with minor amounts of pyrite, chalcopyrite, Ag-bearing tetrahedrite, pyrrhotite, bornite, bismuthinite, boulangerite and native gold. A semi-massive to disseminated mineralisation occurs in the volcaniclastic unit above. Here, sulphides, in the more altered zones, selectively replaced some of the silicate fragments or make up the cement of conglomerates and sandstones. The grades here are about 9% Zn+Pb and 2% Cu.

Sulphur isotope values ($\delta^{34}S$) of sulphides range from -0.2 to 6.5‰. Disseminated pyrite in the altered footwall has close to 0‰ values, while overlying massive sulphides have values of 1.3 to 6.5‰. This suggests that sulphur in the stockwork was mainly of igneous origin, probably leached out from the host rhyolites. Massive sulphides sulphur shows however a significant sedimentary component, and was probably derived from the biogenic reduction of seawater in an open system. Lead isotope signature of sulphides ($^{206}Pb/^{204}Pb = 17.93$-$17.95$; $^{207}Pb/^{204}Pb = 15.54$-$15.57$; $^{208}Pb/^{204}Pb = 38.10$-$38.18$; Tornos and Chiaradia, 2004) suggests an evolution close to the average growth curve and well below that of the radiogenic massive sulphides of the Iberian Pyrite Belt (Marcoux, 1998).

Geologic and geochemical features suggest that massive sulphides formed underneath the seafloor, both replacing reactive glassy rhyolites and cementing poorly consolidated sediments, at depths of more than 100 m, probably near syn-sedimentary faults (Tornos *et al.*, 2000). Deep fluids, carrying metals probably leached out from the rhyolites, but with low sulphur contents, were focused into the fault zones. Mixing of these upwelling fluids with sulphur-bearing strata-contained waters confined to the major lithologic contacts, led to sulphide deposition.

In the same area as Nava Paredon, there also exist some

Fig. 2.- Mapa geológico sintético de la Zona Ossa Morena en Portugal, mostrando los cinturones metalogénicos y la situación de los principales distritos y depósitos minerales descritos en el texto. Adaptado del Mapa Geológico de Portugal, escala 1:500.000, 1992 – compilado por J.T. Oliveira y E. Pereira. Geología: 1. Cobertera sedimentaria cenozoica. 2. Secuencia metasedimentaria del Devónico Superior. 3. Secuencias metasedimentaria y metavolcánica del Ordovícico-Silúrico. 4. Secuencias metasedimentaria (incluyendo metadolomías) y metavolcánica del Cámbrico. 5. Secuencias metasedimentaria y metavolcánica del Proterozoico. 6. Gabros (y dioritas) y rocas ultramáficas (Paleozoico Inferior a Varíscico). 7. Rocas graníticas indeferenciadas de edad Varíscica y tardi-Varíscica. Terrenos oceánicos exóticos: 8. Complejo ofiolítico Beja-Acebuches (BAOC). 9. Grupo Pulo do Lobo (rocas metasedimentarias y metavolcánicas). 10. Zona Centro Ibérica, rocas metasedimentarias. 11. Zona Sudportuguesa, rocas metasedimentarias y metavolcánicas. Depósitos e indicios minerales: *Arronches-Cordoba belt*: 1 - Balôco (Pb); 2 - Tinoca/Azeiteiros (Cu(Pb)); 4 - S. Martinho (Au(As)); 72 – Algueireiras-Nave de Grou-Mosteiros (Au). *North Central belt*: 3 - Alter do Chão (Zn, Cu, Ba);; 5 – Sta. Eulália (Sn, W); 6 – Alagada (Fe); 70 – Alter do Chão-Este (Fe, V); 71 – Torre das Figueiras (Monforte) (Zn, Pb). *South Central belt: a) Sousel-Barrancos sub-belt*: 7 – Mostardeira (Cu); 8 – Miguel Vacas (Cu); 9 – Zambujeira (Cu); 10 – Bugalho (Cu); 11 – Mociços (Cu); 12 – Defesa das Mercês (Cu); 13 – Aparis (Cu); 58 – Botefa (Cu); 59 – Urmos (Cu); 60 – Minancos (Cu); *b) Arraiolos-Sto. Aleixo sub-belt*: 14 – Azaruja (Cu); 15 – Monte do Trigo (Cu); 16 – Reguengos (Cu); 17 – Sto. Aleixo (Cu). *Évora-Aracena belt*: 18 - Courela do Conde (Cu); 19 - Safira (Cu, As, Au); 20 – Courelinha (Cu); 21 – Palmas (Sb, Au); 22 - Gouveia (As, Cu, Au); 23 - Monges (Fe, Py); 24 – Nogueirinha (Fe, Py); 25 – Chaminé (Au, As (Bi)); 26 – Alcalainha (Cu); 27 – Sobral/Ganhoteira (Cu); 28 – Água de Peixes (Pb, Zn); 29 – Alvito (Fe); 30 – Alvito (Cu); 31 – Portel-Algares (Zn, Cu, Pb); 32 – Vale de Pães (Fe); 33 – Orada (Fe); 34 – Enfermarias (Zn, Cu, Pb); 35 – Sto. André (Fe); 36 – Preguiça (Pb, Zn); 37 – Vila Ruiva (Zn, Pb); 38 – Ficalho (Pb, Zn); 39 – Louzeiras (Pb, Sb, Ag); 55 – Rui Gomes (Cu); 56 – Carrasca (Fe, Zn (Pb)); 57 – Portel-Balsa (Zn, Pb (Ag)); 61 – Monfurado (Au); 62 – Banhos (Au (As)); 63 – Casas Novas (Au, As (Bi)); 64 - Ligeiro (Au); 65 – Caras (Au, As); 66 – Braços (Au, As); 67 – Covas (Au, As); 68 – Caeira (Au (Cu)); 69 – Azenhas (Fe); *S. Cristóvão-Beja-Serpa belt*: 40 – Corte Pereiro (Cu, Pb, Zn); 41 – Caeirinha (Cu, Pb, Zn); 42 – Alcáçovas (Entre Matas) (Cu); 43 – Alcáçovas (V. Nogueira) (Cu); 44 – Asseiceiras (Cu); 45 – Peroguarda (Cu, Fe); 46 – Corujeiras (Fe); 47 – Baleizão (Cu); 48 – Serpa (Cu); 52 – Ventosa (Sb, Cu (As, Au)); 53 – Castelo Ventoso (Cu (Ni)); 54 – Odivelas (Fe, Ti, V); *BAOC*: 49 – Palmeira (Ni, Cu (Co)); 50 – Mombeja-Ferr. Alentejo (Cr); 51 – Mombeja (Cu).

semi-massive lenses of pyrite with stockworks and gossan outcrops (Las Erillas).

Minor stratabound iron oxide mineralisation also occurs in the rhyolitic domes that host the massive sulphide orebodies (Baeza *et al.*, 1978). It consists of some metre-thick lenses of massive hematite which overlie pervasively chloritized rhyolites. This mineralisation is interpreted as contemporaneous to the massive sulphides, but formed through exhalative processes in an oxidant basin. Nearby magnetite and hematite-rich sandstones probably represent the dismantling products of the iron oxide mineralisation.

Barite-fluorite(-Zn-Pb-Ag) veins (Late Variscan?)

These veins are of the same age and genesis as those of the Pedroches region (North Eastern Belt) referred to above, but are characterised by higher fluorite and/or barite contents. They can be grouped into several vein ore districts, the most significant being **Los-Arenales-Cerro Muriano** (NW Córdoba; 6, Fig.1), the syn-Cadomian Ahillones pluton and nearby host rocks and those in the Variscan Villaviciosa-Ojuelos-La Coronada plutonic-volcanic complex. The first ore district consists of several veins located east of Los Arenales intrusion, in an area of about 8x2 km²; the mineralisation here is related to large alpine faults with NE-SW, N-S and WNW-ESE trends, that probably reactivated earlier Variscan structures. The mineral assemblage consists of fluorite with trace amounts of pyrite, pyrrhotite, chalcopyrite, tetrahedrite, sphalerite and galena, disseminated or crustiform in quartz-chalcedony, fluorite and calcite. The N-S veins show sulphides concentrations, that are not found in the other vein systems (Delgado *et al.*, 1978). The largest veins (up to 2.3 km long) are Perseverancia and Chaparral, on a WNW-ESE trend. Locally, the fault zone can be 30-120 m thick and hosts several fluorite shots up to 3.5 m-thick (Delgado *et al.*, 1978). Furthermore, there exist some barite-rich veins with minor sphalerite, pyrite and galena. Aside to extensive silicification, especially when the host rock is highly deformed, hydrothermal alteration also produced sericitization. In the Pedroches batholith region, barite-bearing veins akin to those described here apparently formed in the shallowest part of vertically zoned vein system with Cu- and Zn-Pb-rich zones at depth.

Fluorite-barite deposition took probably place by fluid mixing in open fractures of deep hot reduced fluids that had interacted with basement rocks, and oxidised brines of surficial origin. Modelling suggests that mixing of such fluids can produce a vertical zoning of hydrothermal minerals with quartz in the bottom, fluorite in the intermediate zone and barite in the uppermost part of the system (Tornos *et al.*, 1991). Sulphides would precipitate at any depth, but particularly in the quartz zone. Veins of this type can form by perigranitic hydrothermal activity, but can also be the consequence of regional hydrothermal events related to faulting, and independent of magmatism. In fact, in the Iberian Peninsula, veins of this type have been dated as either Late Variscan, Mesozoic (Spanish Central System - Galindo *et al.*, 1994; Pyrenees - Johnson *et al.*, 1996) or even Cenozoic (Roig and Canals, 1994). Absence of well constrained ages for the Arronches-Córdoba Belt veins precludes a correct interpretation.

Fluid inclusion data obtained by Asensio *et al.* (1997), show that fluids involved in these systems were rather hot (145-380ºC) and low saline (1-8 wt % NaCl equiv.). Few fluid inclusions with low homogenisation temperatures but high salinities (up to 33 wt % NaCl equiv.) are consistent with mineral deposition by fluid mixing.

Zn(-Pb-Cu) calcic skarns (Late Variscan)

Near **Los Arenales-Cerro Muriano** (6; Fig.1), Late Variscan subvolcanic leucogranite and related porphyritic dykes, there exists some base metal mineralisation (Zn-(Pb-Cu)). It is found in skarn-type replacements in interbedded limestones, dolostones, calc-silicate hornfels and schists of Lower Cambrian age. The prograde skarn minerals are either calcic (idocrase-grossular) or magnesian (diopside-humite) depending on protolith. They were subsequently replaced by amphibole, epidote, calcite, magnetite, fluorite, sphalerite, chalcopyrite and galena with traces of many other sulphides and sulphosalts (Delgado *et al.*, 1978). These skarns share many features with distal Zn-rich type of skarns (Einaudi *et al.*, 1981). The granite nearby was epizonal and water- and volatile-rich, as suggested by miarolitic cavities and the presence of abundant tourmaline and fluorite.

Pb-Zn(-Ag) quartz veins (Late Variscan)

As referred to above, the **Azuaga-Berlanga** ore field (13; Fig.1), was one of the leading lead producers of the world, standing as the most significant historical mineralisation in OMZ. Here, there literally exist hundreds of small mining workings in short and thick quartz-carbonate lensoidal veins within a NW-SE-trending corridor, roughly coincident with the Tomar-Córdoba Shear Zone. The veins developed in the more competent rocks of the shear zone, such as ultramylonites, gneisses, quartzites and amphibolites, all of Proterozoic age (e.g., Abalos *et al.*, 1991 and references therein). However they are discordant to the shear zone trend suggesting that they formed during brittle reactivation of the latter in late Variscan times (Upper Carboniferous). The mineralisation occurs in highly discontinuous veins, about 40-500 m long and 0.5-3 m thick, that trend N20-45ºE, N70-80ºE and N120-130ºE. Host rocks to the vein system show a restricted but pervasive K-feld-

spar-type and sericite-quartz-type alteration. Vein mineral assemblage consists of galena and sphalerite with minor amounts of pyrite, chalcopyrite, Ag-bearing tetrahedrite, linneite, pyrargirite, pyrrhotite and some sulphosalts in a gangue of quartz, calcite and some barite and fluorite that can be locally abundant. Veins exhibit rather monotonous textures typical of the epithermal environment, including vuggy crustiform infillings and hydrothermal breccias with fragments of hydrothermally altered host rocks supported by quartz and carbonates with cockade texture. Chacón *et al*. (1981) briefly studied these orebodies. Fluid inclusions are low salinity and homogenise at temperatures below 200ºC. All the evidence suggests that hydrothermal flow was episodic and that was accompanied by generalised boiling in a shallow environment. These veins share structural and mineralogical features with the adularia-sericite type of epithermal systems. Nevertheless, there is no metal zoning and no relationship whatsoever with igneous rocks could be established. Only at **Santa Marta** (7; Fig. 1), where a small Late Variscan granodioritic intrusion exists, nearby veins might be plutonic related.

Lead isotope data (Tornos and Chiaradia, 2004) show that the metals were probably scavenged from rocks with an average Ossa Morena composition. However, veins near the Santa Marta intrusion show a pristine less radiogenic signature, suggesting that more juvenile lead was involved in this case. Lead isotope signatures show depletion in $^{207}Pb/^{206}Pb$ relative to equivalent mineralisation types of the Iberian Variscan Belt, and plot near the field of Variscan feldspars; this suggests that the age of mineralisation is pre-Mesozoic and probably Late Carboniferous-Early Permian, an approximation consistent with the age of the late movements along the Tomar-Córdoba Shear Zone.

In Portugal the galena-bearing quartz veins of Balõco might be equivalent to this type of mineralisation.

2.3 The North Central Belt (NCB)

This large belt includes the region comprised between the Arronches-Córdoba Belt and the northern flank of the Olivenza-Monesterio antiform. This region includes the Albarrana Domain and the North Central Belt of the Apalategui *et al*. (1990) subdivision of the OMZ. In Portugal it is equivalent to the Alter do Chão-Elvas belt of Oliveira (1986).

Ophiolite-related chromitites (Proterozoic)

Small (<10 km^2) bodies of serpentinites are found as small tectonic slices within the Malcocinado synorogenic formation near **Calzadilla de los Barros** (Badajoz; 11; Fig. 1). These rocks are interpreted as corresponding to olistoliths of alpine-type ophiolites within large andesitic

volcaniclastic mass flows (Arriola *et al*., 1981; IGME, 1985). They consist of strongly retrograded harzburgites consisting of serpentine and talc with minor chlorite, magnetite and carbonates. They preserve some remnants of primary pyroxene, amphibole and olivine. Chromitites occur as decametric sized monotonous, semi-massive lenses less than 1.5 m thick, made of coarse-grained (>2 mm) Cr-spinel with cumulate textures. The two known showings have been systematically explored with negative results. Only one small lens was found, with 25.1% Cr and 0.4% Ni. Maximum values of Au, Pd and Pt are 1.7 g/t, 0.03 g/t and 0.01 g/t, respectively. Geological evidence suggests that they are Alpine-type chromitites (Arriola *et al*., 1981).

Sediment-hosted copper (Upper Proterozoic)

Some scarce copper mineralisation, including chalcopyrite, pyrite and bornite, is found as disseminations or concentrated in organic matter-rich layers within the lenses of black quartzite of the Serie Negra (Neoproterozoic). These rocks also show high geochemical background values of lead and zinc and are perhaps enriched in gold. These ore showings are anecdotal and probably represent minor metal concentrations in anoxic sediments. They have been traditionally interpreted as the source of gold and other metals for the vein-like deposits found nearby (Canales and Matas, 1992).

Porphyry copper mineralisation (Upper Proterozoic)

Small subvolcanic intermediate intrusions, mostly quartz-monzonites, interpreted as deep equivalents of the Cadomian synorogenic volcanic complex, host small copper occurrences (e.g., Ahillones-Los Parrados, El Mosquil). Chalcopyrite, pyrite and minor magnetite occur as disseminations, in stockworks or large quartz lodes within the intrusions. The host granitoids have a pervasive hydrothermal alteration, with replacement of the primary mineral assemblage by quartz, sericite, chlorite and epidote, besides minor carbonates and barite. This mineralisation has been interpreted as broadly equivalent to porphyry copper deposits (Locutura *et al*., 1990), and formed in the same volcanic arc as the afore-mentioned massive sulphide deposits. The hydrothermally altered host rocks could be equivalent to the propylitized rocks found in porphyry-like systems, but no more intense alteration products have been described.

Stratabound sedex barite (Upper Proterozoic)

Stratabound barite mineralisation occurs near **Llerena** (12; Fig.1) in the Spanish part of the NCB. It is hosted by the syn-orogenic (Cadomian) Neoproterozoic-Lower Cambrian Loma del Aire Fm., broadly equivalent to

the Malcocinado Fm. It consists here of fine-grained sandstones, siltites, shales and limestones overlain by Cambrian limestones. This mineralisation probably represents the largest concentration of barite in Spain and was extensively studied by Poole *et al*. (1990), Miras (1991) and Hernández and Miras (1993). The mineralisation occurs as: a) stratabound massive to laminated barite, 1-3 m thick and some kilometres long, including scarce galena, chalcopyrite, cinnabar and pyrite as well as trace amounts of quartz, illite and ankerite-siderite; it is locally associated with cherts; b) equivalent horizons in limestones and shales, 1-2 m thick and less laterally extensive; the host carbonate rocks have significant amounts of barite as disseminations and nodules; c) karstic infillings of unknown age in the limestones, with iron oxides, illite, quartz and some pyrite and chalcopyrite; and d) NE-SW to ENE-WSW-trending near-vertical veins of massive barite crosscutting all previous rock types as well as Cadomian and Variscan granitoids; in these veins barite coexists with quartz, fluorite, carbonate and some sulphides. Barite-rich veins are typically located near both the Cadomian Ahillones granitoid and many other metamorphic and plutonic rocks of the area.

The relation to limestones and fine-grained volcaniclastic sedimentary rocks suggests that the stratabound barite deposits formed in low temperature (<150ºC), oxidised, iron- and manganese-poor brine pools at shallow to intermediate depths, due to the up-flow of hot deep brines, that mixed with seawater in a rather quiescent setting, as suggested by the presence of shales, well bedded barite and stratiform cherts.

Cu-Zn-Pb mineralisation related to volcanic rocks (Early Cambrian?)

Small Cu, Pb and Zn occurrences (e.g., **Alter do Chão;** 3, Fig. 2) associated with intermediate to felsic Early Cambrian metavolcanic rocks (incl. breccias), are also known from this belt (Oliveira, 1986).

U and REE in syn-metamorphic pegmatites (Variscan)

Complex pegmatites of granitic composition with uranium and rare earth mineralisation are found in the **Sierra Albarrana -Villaviciosa de Córdoba** area (Fig.1), where they form large pegmatite fields. Pegmatites which are for the most part of the muscovite type (muscovite, quartz, feldspar) (Ortega *et al*., 1992) form irregular to massive internally zoned veins some hundred metres long and less than 3 m thick, parallel to the Variscan structures. These veins show complex relationship to the host rocks, with the pegmatite accessory mineralogy controlled by the metamorphic grade; those located within the internal, high grade metamorphic core of the Sierra Albarrana Domain

have a complex mineral assemblage including tourmaline, uraninite, brannerite, beryl, garnet, sulphides, xenotime, Nb-tantalite, allanite, complex phosphates, monazite and zircon (González del Tánago, 1991; González del Tánago *et al*., 1991; Ortega *et al*., 1992). These pegmatites have been interpreted as para-autochthonous pegmatites formed by partial melting of the host rocks (e.g., Ortega *et al*., 1992).

W(-Sn) greisen and vein-like mineralisation (Variscan)

The subvolcanic, Late Variscan **Santa Eulália** (5; Fig. 2) granitic massif (309-290 Ma), hosts, mostly within the non-porphyritic inner facies of the massif central monzonite, a subvertical N40º to 50ºW-trending swarm of quartz veins with greisenised (including fluorite) selvages. Quartz veins, up to 15 cm thick, exhibit cassiterite, wolframite, scheelite, base metal sulphides, arsenopyrite, pyrite, muscovite, fluorite and apatite. Cassiterite, with minor sulphides, predominates in the SE whilst wolframite (ferberite) and sulphides are more abundant in the NW. Moreover, small greisens formed at the intersection of N40º to 50ºW and NE-SW-trending fractures contain exclusively cassiterite and scheelite as ore minerals. Alluvial and elluvial deposits containing cassiterite and ilmenite, and subsidiary wolframite and rare earth minerals were mined in the same area (Thadeu and Aires-Barros, 1973; Gonçalves *et al*., 1975; Inverno, 1975; Oliveira, 1986).

Magmatic-related magnetite mineralisation (Variscan)

A distinct iron mineralisation occurs immediately east of Alter do Chão (70; Fig. 2), in the NW body of the mafic-ultramafic Alter do Chão (Lower Paleozoic?) massif, in the form of a 1400 m-long, gabbro-hosted, semi-massive magnetite layer, with 0.5% V_2O_5 (Beck, 1996), genetically analogous to the magmatic vanadiniferous magnetite deposits of the Bushveld Complex.

Iron skarns (Variscan?)

In Portugal, the Early Cambrian carbonates host the **Alagada** (Porto Xico) iron skarn (27-40% Fe) in its contact with the Elvas Variscan(?) granite, near the north-western tip of the OMB (6; Fig 2). This deposit, 400 m long and 2.7-9.5 m thick, is covered by 10 m of Quaternary alluvium. It consists dominantly of magnetite lenses parallel to bedding, with pyrite, pyrrhotite and scheelite as minor minerals (Gonçalves and Assunção, 1970; Oliveira, 1986; SIORMINP, 2002).

Shear- and vein-hosted Cu and barite mineralisation (Variscan)

In the **Pallarés** area (33; Fig.1) there is a large N-S, 10 km long and 3-5 km wide, brittle-ductile shear zone/fault between the Cadomian Pallarés granodioritic pluton and

the host Neoproterozoic siliciclastic metasedimentary rocks. The latter are black schists and minor quartzites and ortho-amphibolites. The rocks within this structure underwent strong syn-tectonic hydrothermal silicification and sericitization postdating a major cataclastic event. Quartz-dolomite-barite veinlets with disseminated chalcopyrite and galena, are common within and near the fault zone.

Accomodation of strike-slip faulting around the Pallarés granodiorite generated a dilational zone that promoted major hydrothermal activity. However, the absence of effective ore-forming processes inhibited the precipitation of significant amounts of sulphides that occur mostly in N45ºE-trending tensional fractures or as replacements in the nearby limestones (IGME, 2004).

Zn-Pb quartz veins (Variscan?)

Zn-Pb sulphide mineralisation associated with milky-quartz veins hosted in the Early Cambrian carbonate rocks are known in several Portuguese areas, although they remain to be investigated. That is, for instance, the case of mineralised veins at Torre das Figueiras (Monforte) developed in the contact zone with the Santa Eulália granitic massif (Oliveira, 1986).

Epithermal Hg-(Pb-Cu-Ba-Au) replacements in limestones (Variscan)

A small ore field characterised by a complex epithermal mineralisation (Hg-Pb-Ba-Cu-Sb) is found near Usagre. Thick chert-rich black limestones with minor slaty intercalations of Lower Cambrian age are host to the mineralisation, which seems to be related to WNW-ESE strike slip faults, which in turn enclose diabase and Late Variscan porphyry dykes. The mineralisation is younger than dykes. Sulphides, either massive or disseminated, occur as irregular or stratabound masses always surrounded by a halo of pervasively silicified rock.

The most important deposit of this type is at **Mariquita** mine (9; Fig. 1), an Hg-rich deposit worked intermittently from the Middle Age to 1971. The mineralisation is found as discordant massive bodies, up to 3 m thick. Cinnabar is associated with pyrite, Hg-rich sphalerite, chalcopyrite, Hg-rich tetrahedrite, galena, realgar and, locally, gold with ankerite, barite and quartz. The ore formed at temperatures between 250 and 320º C involving brines with 19-24 wt% NaCl equiv. (Tornos and Locutura, 1989). It is remarkable that host limestones contain a stratabound barite mineralisation that includes galena and traces of mercury, and that could well be the source of the epithermal ore metals. This type of hydrothermal mineralisation formed at very low depths after significant exhumation of the orogen. Regional faults focused both convective heat flow and small magma intrusions, which in turn promoted replacement of

limestones and fracture fillings at places of strong fluid-carbonate interaction and/or mixing with surficial oxidised waters.

2.4 The Olivenza-Monesterio Belt (OMB)

This is the most diverse metallogenic belt and corresponds to the long known Olivenza-Monesterio antiform. This structure wedges out toward Portugal. A Proterozoic basement consisting mainly of shales and black quartzites of the Serie Negra is exposed in the core of the antiform and is overlain by an Early to Middle Cambrian succession of platform sediments –mainly carbonates- and volcanics. A key feature of this belt is the presence of abundant intrusions of different age (Cadomian and Variscan) and tectonic setting (Quesada *et al.*, 1987; Sánchez Carretero *et al.*, 1990).

Iron oxide deposits related to felsic magmatism (Lower Cambrian)

Discontinuous lenses up to 100 m long and 3-8 m thick of stratabound to stratiform iron oxide ores are found interbedded with hydrothermally altered massive dacites and volcaniclastic rocks of Lower to Middle Cambrian age. These volcanics overlie Early Cambrian massive limestones (Dupont, 1979). Most showings are located in the western part of the Olivenza-Monesterio antiform (e.g., **La Bóveda**, **Bilbaína, Las Herrerías, Bismark**; Fig.1). The ore lenses consist of massive to banded magnetite with some pyrite and chalcopyrite and trace amounts of arsenopyrite, galena, tetrahedrite, pyrrhotite and gold; fluorite can be locally important. The volcanics show pervasive hydrothermal and /or metamorphic alteration consisting mainly of actinolite, albite, quartz, chlorite and sericite. When the host rock to the mineralisation is the Early Cambrian limestone, ores bodies are concordant or discordant and consist of magnetite and siderite. Tourmalinites –probably exhalites- are locally found interbedded with the volcaniclastic rocks (e.g., **La Bóveda,** (18; Fig. 1)). Small mafic and felsic intrusive bodies can be locally common.

These deposits have long been interpreted as broadly syngenetic and resulting from exhalative submarine processes (Dupont, 1979; Locutura *et al.*, 1990). Major orebodies such as la **Bilbaína** (22; Fig. 1) and **Bóveda** probably formed slightly underneath the seafloor by the early diagenetic replacement of the volcanic and carbonate rocks. However, some of the deposits of the Valuengo area (Bismark) might have been formed as true sediments by the exhalation of reduced low temperature (<150ºC) hydrothermal fluids ponding into shallow oxidised third order basins (Tornos *et al.*, 2003). Sm-Nd isotope composi-

tion of magnetite from the **Bilbaína** mine have provided an age of ca.500 Ma and εNd_i values of -3.7 to 0.0, suggesting that relatively juvenile Nd was involved in the ore forming fluids (Darbyshire *et al.*, 1998). Moreover preliminary sulphur isotope values ($\delta^{34}S$= +3.6 - +12.4‰) suggest that sulphur was mostly derived from the thermo-reduction of seawater sulphate to H_2S with a minor but variable input of biogenically derived sulphide in an open system.

Scattered plugs of leucotonalite/dacite some tens of metres in diameter, could be the roots of the volcanics (e.g., La Valera, Los Eloys; Coullaut *et al.*, 1980). They show pervasive albitisation and brecciation, with tonalite/dacite fragments cemented by coarse-grained magnetite. Magnetite can also occur here either as massive ore, breccia fragments or disseminated in the altered host rock. Late replacements and veining including pyrite, chlorite, ankerite, fluorite and adularia are common.

Magnetite can also occur as disseminations (30-50% volume) within fine-grained volcaniclastic rocks. Moreover, evidence of detrital magnetite seems to be locally addressed (e.g., Aurora, Feria) by preserved structures within the ore, that might be sedimentary (e.g., ripple marks or graded bedding) . These showings could correspond to the erosion products of the primary ores.

As a whole, the Coullaut *et al.* (1980) model for these ores seems still to be valid. The leucotonalite / dacite plugs were the feeder conduits whilst the stratabound and stratiform orebodies represent lateral hydrothermal (sub-)exhalative and redeposited deposits.

Subsequent Variscan deformation and metamorphism modified some of the original features of this mineralisation. This is the case at the Bilbaína mine. This mine is near the western contact of the Brovales pluton and both are within a major syn-plutonic shear zone (Fig. 2). The mineralisation shows high temperature ductile deformation, accompanied by replacement of tremolite by talc and of hematite by magnetite. The combination of shearing and proximity to the pluton probably is the cause of copper and gold enrichment (up to 2.9 g/t Au; IGME, 2004) relative to that of other nearby deposits. In fact, textural evidence suggests that most of the sulphides and related gold precipitated during at this stage.

A last type of Fe-oxide ore consists of clays and iron oxide that fill paleo-karsts in limestones such as at the Cerro del Hierro Mine; karstification age is unknown.

Iron oxide deposits associated with albite granite stocks (Cambrian?, Variscan?)

Some large Fe-oxide deposits (e.g., La Berrona, Alfredo) are found within albite granite epizonal intrusions of unknown age and are thus apparently independent of volcanism. These plutons are elongated and roughly concordant and can crosscut thrusts (e.g., to the east of the Valuengo area; IGME, 1980). Often show weak foliation. Geochemically however these felsic rocks are similar to the Early to Middle Cambrian volcanics (Dupont, 1979). One case is **La Berrona** deposit (26; Fig. 1) which is a flat near cylindrical body within a foliated albite granite (IGME, 1980). The mineralisation has sharp but irregular replacive contacts towards the host rock and consists of albite, actinolite-hornblende, ferrosalite, carbonates, quartz and apatite with massive, semi-massive and banded magnetite and minor pyrite, pyrrhotite and chalcopyrite.

The **Alfredo** mine (8; Fig. 1) is a different case. It is located in the SW part of the Feria pluton which consists of massive fine-grained hastingsite syenites and albite granites (Dupont, 1979). The mineralisation, for the most part magnetite, is found within the albite granites and in the host Early Cambrian shales and limestones. The main orebody is stratiform and overlies the carbonate rocks a few hundred meters from the pluton. Lens-shaped orebodies are also found within the pluton. Moreover stockworks, breccias and dykes are common both within the granite and in the host rocks (Dupont, 1979). Minerals accompanying magnetite are hematite, actinolite-tremolite, ankerite, albite and quartz with traces of pyrite and chalcopyrite. The pluton has been dated at 311±15 Ma (K-Ar, whole rock; Dupont, 1979), i.e., Upper Carboniferous, which opens the possibility that at least stockworks, breccias and dykes might be of this same age or younger.

Manganese stratabound mineralisation (Cambrian)

In the **Olivas-Zahinos** area (17, Fig. 1), southwest of the main Cambrian volcanic exposures, there outcrop some volcanic-related ore deposits containing abundant Mn mineralisation. They were described by Ruiz de Almodóvar and Galán (1984) and Jiménez Millán *et al.* (1992), who recognised a wide variety of Mn-bearing hydrothermal assemblages including spessartine-bearing quartzites (cuticules) presumably derived from Mn-rich exhalites, thin (<1 cm) continuous layers of braunite and haussmanite, Mn-bearing jasper lenses and abundant showings of Mn oxides cementing or replacing volcaniclastic rocks; barite is fairly abundant and trace amounts of base metals are also common. Iron oxide mineralisation is restricted to some lenses of magnetite and hematite. The mineralisation is probably related to diffuse, low temperature exhalation of deep fluids into unconsolidated seawater-saturated rocks. The enrichment of Mn relative to Fe can result from differential oxidation of a deep ascending fluid, manganese being transported under more oxidising conditions than iron. West of the Oliva–Zahinos area some Cu-Zn-Pb occurrences probably represent a more reduced, H_2S-rich depositional environment.

Variscan regional metamorphism led to recrystallisation of manganese minerals, giving rise to a complex association of secondary minerals such as rhodonite, pyroxmanganite, tephroite or piamontite (Jimenéz Millan *et al.*, 1992).

Orogenic gold mineralisation (Variscan)

Gold mineralisation was recognised during a regional geochemical survey by PRESUR SA in the central OMZ (Coma *et al.*, 1988; Canales and Matas, 1992). The mineralisation is found within major Variscan SSW-verging WNW-ESE thrusts and shear zones tens of kilometres long and tens of metres wide. Several gold anomalies were discovered, the more representative being those in the **Guijarro** and **Chocolatero** areas (30 & 31; Fig. 1) (Canales and Matas, 1992) within the Monesterio thrust, which is a major structure in the Olivenza – Monesterio Belt (Quesada, 1992). Gold enrichment is found at the intersections of the thrust with black shales of the Tentudía Formation (Neoproterozoic) or with shales, metasandstones, metavolcaniclastic rocks and subvolcanic metadacites and metarhyolites of the Cadomian synorogenic complex (Malcocinado Formation).

Richest zones are hydrothermal breccias, minor brittle-ductile N-135-E shear zones and N-S to N-60-E extensional fractures, particularly their intersections. Mineralised zones show pervasive sericitization and chloritization and irregular but intense, sometimes texturally destructive silicification, with local tourmalinisation, albitisation and K-feldspar growth. Sulphides are scarce. Arsenopyrite and traces of pyrite, pyrrhotite and chalcopyrite with submicroscopic gold are disseminated in the more altered rocks or are related to vein quartz. Magnetite concentrations can be of local importance (Canales, 2000, pers.comm.).

Gold showings similar to those of the Guijarro – Chocolatero area, are also found in the **Constantina – Hueznar** area, in the easternmost Olivenza – Monesterio Belt (nº 29; Fig. 1). They are found within a WNW-ESE shear band about 15 km long (Ordoñez *et al.*, 1992; Urbano, 1994) and are hosted by subvolcanic gabbros and gabbrodiorites of the Cadomian synorogenic volcanic complex or by shales and slates. In the first case gold is found in thin quartz veins, with carbonate and silicic alteration products, and in highly sheared and altered (epidote-sericite-quartz-chlorite-amphibole) rocks. In the second case, the mineralisation occurs in NNE-SSW thick quartz veins only. In both cases the ore assemblage includes minor sulphides, pyrite, arsenopyrite, pyrrhotite and chalcopyrite.

Preliminary research suggests that these gold deposits might be of economic interest (Canales and Matas, 1992). The high Au/Ag ratio (ab. 0.1), the low sulphide content and the geological setting are similar to those of the gold-only or orogenic gold veins located in metamorphic orogenic belts (e.g, Hogdson, 1989; 1993; Kerrich and Wymann, 1990), that formed at intermediate to shallow crustal depths (Groves, 1993). The mineralisation was probably laid down from hydrothermal/metamorphic fluids that leached disseminated gold contained in the Proterozoic sequence. Precipitation was probably caused by fluid depressurisation and immiscibility in extensional fractures.

Syn-metamorphic Cu and Pb-Zn veins (Variscan)

Small Cu and Pb-Zn lodes are widespread in the Serie Negra of the Olivenza – Monesterio Belt. They occur as subvertical veins less than a hundred metres long and a metre thick, filled by quartz with massive and brecciated textures, and disseminated chalcopyrite, galena and sphalerite. Hydrothermal alteration was negligible in the host shales/slates and restricted to local silicification. Most veins are concentrated near the Monesterio migmatitic core.

A special case is **La Hinchona** quartz – siderite vein (29; Fig.1), NW of Monesterio and close to the Salvatierra granodiorite to tonalite pluton. This is the largest known deposit of this category, about 0.5 km long and up to 2 m thick. A complex hydrothermal history is recorded by this vein that includes several stages of brecciation and vein infilling, from high temperatures down to epithermal ore precipitation. An early assemblage of arsenopyrite, pyrrhotite and pyrite, was replaced by chalcopyrite and, later on, by sphalerite, galena and tetrahedrite. Minor amounts of gold seem related to late low temperature silica (jasper).

The Cu and Pb-Zn veins display an apparently zoned distribution, Pb-Zn veins east of the pluton and Cu veins west of it. The current model involves circulation of hydrothermal/metamorphic fluids during Variscan times, that leached metals from the host metasedimentary rocks and precipitated the ore by simple cooling and fluid mixing. No evidence of boiling has been found. Differences between Cu and Pb-Zn veins are probably due to contrasting precipitation temperatures, chalcopyrite forming in the deeper and hotter parts of the system and galena and sphalerite in the shallower and cooler ones.

Ni-(Cu-PGE) in mafic to ultramafic intrusions (Variscan)

The **Aguablanca** Ni-Cu magmatic mineralisation is hosted by mafic and ultramafic rocks of the Aguablanca stock (37; Fig.1). This orebody was found in 1993 after the recognition of a strong stream geochemical anomaly. Its discovery represented a milestone in the mining exploration of the area, since no previous major Ni mineralisation had ever been found in SW Europe. Rio Narcea Recursos SA is currently evaluating the deposit and the exploitation

is scheduled to start in late 2004.

The Aguablanca stock contacts with the Santa Olalla Main Pluton (SOMP), a Variscan high-K, calc-alkaline reversely zoned intrusion formed by diorites tonalites and granodiorites (Casquet *et al.*, 2001; Tornos *et al.*, 2001). The SOMP was dated at 332±3 Ma ($^{207}Pb/^{206}Pb$ zircon age; Montero *et al.*, 2000) and 354 ± 17 Ma (Rb-Sr whole rocks; Casquet *et al.*, 1999). The Aguablanca stock consists of mafic rocks, namely (quartz-)diorites, gabbros and gabbronorites. Isotope geochemistry of the Aguablanca rocks is consistent with that of the SOMP, suggesting that they were consanguineous and broadly contemporaneous (Casquet *et al.*, 2001). However, dating of the Aguablanca stock and the mineralisation was unsuccessful because of a strong crustal contamination and hydrothermal alteration (see below). Host rocks to the SOMP and the Aguablanca are Late Proterozoic to Early Cambrian dark shales (Serie Negra), limestones, volcanic rocks and sandstones, that underwent high-grade contact metamorphism near the intrusions. Limestones were converted into marble and skarn, largely barren garnet-rich skarns (Casquet, 1980). Relics of an earlier coarse-grained plagioclase-amphibole/ pyroxene igneous rock (dioritoid) are locally found along the contacts of limestones with the plutons. These rocks probably formed by assimilation of limestones by dioritic magma (Casquet, 1980). Skarns and dioritoid are barren.

The Ni-(Cu-PGE) ore is found in a breccia pipe hosted by mafic rocks of the Aguablanca stock. The pipe is subvertical and ellipsoidal in cross section. It consists of heterometric fine- to coarse-grained fragments of ultramafic rocks (ortho- and clinopyroxenites and minor peridotites), gabbros-gabbronorites and fragments of the plutons host rocks (limestones, skarns, hornfels) supported by a gabbroic and gabbronoritic matrix (Barren Breccia). However, in the pipe core, the breccia is supported by sulphides (Ore Breccia). Massive orebodies with subordinate silicate inclusions (coarse-grained pyroxenites) are also found in the pipe core. The metallic assemblage consists of intercumulus to massive pyrrhotite, chalcopyrite and pentlandite. Disseminated mineralisation is found in the Barren Breccia and in the host mafic rocks. No spatial zoning of the Ni/Cu ratios was recognised but the Ore Breccia and the massive sulphides have significantly higher Ni grades that the disseminated mineralisation.

Widespread hydrothermal alteration, which can be locally intense, converted the magmatic silicates into clinoamphibole, sericite, phlogopite, talc and epidote and also led to recrystallisation of the sulphides.

As a whole, the deposit shares many of the features of magmatic-hosted Ni-Cu deposits, but is located in a calc-alkaline gabbroic stock in an active margin setting. Very few deposits of this type have been described to date.

Isotope (Nd, Sr and S) and trace elements geochemistry suggest that juvenile magmas intruded into the upper crust during oblique subduction of an oceanic crust (the Acebuches Ophiolite) previous to accretion of the South Portuguese terrane to the OMZ . An intracrustal magma chamber formed where combined assimilation and fractional crystallisation processes took place leading to sulphide magma immiscibility and silicate magma diversification and stratification (Casquet *et al.*, 1999; Tornos *et al.*, 2001; Casquet *et al.*, 2001). Sulphur was added to the melt through assimilation of organic sulphur-rich rocks, probably from the Serie Negra. The relatively radiogenic lead isotope signatures (Tornos and Chiaradia, 2004), and the Au/Au* values (Tornos *et al.*, 2001) reinforce this interpretation. Sulphide magma sunk to the bottom of the chamber and was subsequently intruded along with the mafic and ultramafic cumulates to form the Aguablanca stock. The intrusion was probably favoured by tectonic structures such as the nearby strike-slip Cherneca fault.

Alternative models have been proposed to explain the Aguablanca Ni-(Cu-PGE) mineralisation. Lunar *et al.* (1997) and Ortega *et al.* (2001) suggested that the Aguablanca stock is an old, pre-Variscan layered complex that was verticalised during the Variscan orogeny. Quesada *et al.* (2002) invoked a skarn process, and Marcoux *et al.* (2002) described it as a massive sulphide.

Shear zone and plutonic-related iron-rich Feox(Cu-Au) skarns and replacements (Variscan)

Most orebodies of this category are found in the region including the Burguillos, Brovales and Cala areas, NE and SE of the Jerez de los Caballeros township. Here skarn-type, stratiform and vein-type magnetite mineralisation is found, although not exclusively, along the contacts of Variscan plutons with Early Cambrian metasedimentary and metavolcanic rocks. Emplacement depth of the plutons was about 1.5 - 3 km (Velasco and Amigó, 1981; Casquet and Tornos, 1991). Variscan igneous rocks range in composition from gabbros to granodiorites and have ages of 352±4 Ma to 332±3 Ma (Dallmeyer *et al.*, 1995; Casquet *et al.*, 1998; Pin *et al.*, 1999; Montero *et al.*, 2000).

The most important iron mines are of this type. This is the case of the **Monchi** mine (23; Fig. 1), at the western contact of the Burguillos del Cerro plutonic complex and the **Santa Barbara** and **El Colmenar** mines (Cuervo *et al.*, 1996; Sanabria, 2001), at the eastern contact of the Brovales pluton (24; Fig. 1). Another large magnetite mineralisation is still mined at **Cala** (35; Fig. 1), adjacent to the small Cala granite outcrop (Velasco and Amigó, 1981). Skarns are common at these localities but are small. The long alleged relationship between skarn-forming processes and magnetite is nowadays being reconsidered.

Skarns formed in general by replacement of limestones and calc-silicate hornfelses (exoskarns). Most are calcic Fe-skarns. A case is the skarn at the Santa Barbara mine. Here a small (ferro-)salite-grandite exoskarn is variably replaced by a retrograde assemblage of actinolite-hornblende, minor epidote, scapolite and plagioclase (Casquet, 1980, Casquet and Velasco, 1978; Velasco and Amigó, 1981; Casquet and Tornos, 1991; Cuervo *et al.*, 1996). The ore, consisting of magnetite with minor amounts of pyrite, chalcopyrite, other sulphides (pyrrhotite and bornite) and ilvaite, is intergrown with the retrograde skarn. Late sulphide-bearing chlorite + quartz + calcite veins are common. Endoskarns developed on plutonic rocks are small and consist either of a garnet skarn, or more commonly a low-T actinolite + epidote + feldspar assemblage. Skarns and skarn-type magnetite bodies are of local extent compared to the large stratiform magnetite bodies mined at the same localities referred to above. They consist almost exclusively of magnetite, with some accessory pyrite (Table 1).

The **Cala** mine (35; Fig. 1) is a remarkable case of this type of mineralisation. The mine lies at the fault contact of a small (<1 km^2 on outcrop) biotite granite stock (Casquet and Velasco, 1978; Velasco and Amigo, 1981) with Early Cambrian carbonate rocks and calc-silicate hornfelses. A metasomatic wollastonite zone developed on limestones away from the tectonic contact, followed by an inner grandite zone. In turn, calc-silicate rocks were replaced by a pyroxene skarn. Dolostones remained unaltered. No significant endoskarn has been recognised. The mineralisation occurs as two subvertical lenses (Vázquez *et al.*, 1980) within the grandite zone and near the faulted contact with the granite. These lenses probably formed at dilatational structures within the fault. The ore consists of coarse-grained magnetite intergrown with actinolite, and late pyrite and chalcopyrite; the copper concentrate has about 4 g/t Au. A retrograde skarn of actinolite, epidote and calcite is locally found away from the fault. Major faults as in the case of Cala, were important controls in ore deposition as they focused most of the regional fluid flow. At the Cala mine the close spatial association of ore and garnet skarn has long been taken as a proof for a common origin. However, barren garnet skarns are widespread in the area (e.g., Casquet and Velasco, 1978; Casquet, 1980). Some small copper-rich skarns distal to the iron ones have also been recognised in the area (IGME, 2004).

The **Teuler** deposit 4 km SE of Cala (36; Fig. 1), is the only known magnetite mineralisation related to a magnesian skarn. Magnetite, with accessory pyrite and chalcopyrite, is interbedded with vermiculite and serpentine in a sort of contorted rhythmic layering. The orebody is stratiform and lies within marbles and calc-silicate rocks. Sills

and dykes of biotite leucogranite are widespread.

Another apparently fault controlled mineralisation is found at the **Sta Barbara - El Colmenar** group of mines, at the western contact of the Brovales pluton (24; Fig. 1). Here, aside to the Santa Bárbara skarn, referred to above, there is a discontinuous stratiform mineralisation, about 2 km long and 2-20 m thick, strikingly different from the volcano-sedimentary and skarn-related ores. The assemblage consists of banded to massive actinolite, magnetite and albite with minor proportions of adularia, ferrosalite, biotite, quartz, carbonates and titanite (Cuervo *et al.*, 1996). The more internal zone consists of massive coarse-grained magnetite with interstitial actinolite, ilvaite and sulphides, including chalcopyrite, pyrite, pyrrhotite, millerite and cobaltite, besides significant amounts of titanite, allanite, zircon and apatite. The mineralisation is replacive on felsic volcaniclastic and volcanic rocks, calc-silicate hornfels and limestones of Early Cambrian age, and is older than skarns. Sm-Nd dating of magnetite (334±32 Ma; Darbyshire *et al.*, 1998) and preliminary lead isotope data (Tornos and Chiaradia, 2004), are consistent with a Variscan age for the ore-forming process. The Sta Barbara – El Colmenar mineralisation is but one of a string of magnetite lenses that extend eastward away from the Brovales pluton (e.g., Sta Justa, El Soldado, Aurora or Bismark mines) at an apparently similar stratigraphic position. This has long led to discussion about the exact origin of this mineralisation, either skarn (Coullaut, 1979; Cuervo *et al.*, 1996) or volcanic-related (Vázquez and Fernández Pompa, 1976; Dupont, 1979). However the Variscan age of magnetite and textural evidence speaks in favour of a tectonically controlled hydrothermal replacement.

The **Monchi** Mine (NE of the Burguillos pluton; 23, Fig. 1) exploited five high-grade (66% Fe) magnetite lenses some tens of metres long and few metres thick located at the contact between calc-alkaline granodiorites and diorites of the Burguillos del Cerro plutonic complex and the host pelitic hornfelses, marbles and calc-silicate rocks. This contact is a major syn-magmatic shear zone (Casquet *et al.*, 1998). The ore lenses consist of massive magnetite-vonsenite and minor ilvaite. The ore is foliated and variably recrystallised at places. Moreover it can be found as enclaves within the granodiorite. Fine grained uraninite-bearing allanite-rich hedenbergite-plagioclase rocks are also found at this mine. These rocks are stratiform and apparently independent of magnetite lenses; their significance remains uncertain. They are brecciated and injected by K-feldspar + amphibole ± axinite ± quartz pegmatite veins. Discordant veins of massive, coarse-grained magnetite with actinolite-hornblende constitute a late generation of magnetite ore. Metallic minerals at the Monchi and nearby mines, are scarce and irregularly distributed.

They are however unusual. We record here the following: pyrrhotite, cobaltite, chalcopyrite, pyrite, arsenopyrite, Co-gersdorffite, safflorite, löllingite and bismuthinite, molybdenite, scheelite and gold. Allanite from a fine grained hedenbergite-rich rock was dated by the U-Pb method at 338±1.5 Ma (Casquet *et al*.,1998). This age is consistent with that of the Burguillos pluton and other calc-alkaline intrusions in the area (350-330 Ma).

As a whole, most of the deposits in this district share geologic features with the hydrothermal iron oxide (Cu-Au) (U-REE) style of mineralisation (e.g., Hitzman *et al*., 1992), including the widespread presence of an albite-actinolite-magnetite hydrothermal assemblage, the variable but relatively high contents of scapolite, apatite, fluorite and B-bearing minerals (vonsenite, axinite, tourmaline), and the close association with major crustal discontinuities (Tornos *et al*., 2003). No fluid inclusion data are available, but few oxygen isotope data from magnetite and amphibole (Cuervo *et al*., 1996; Spiro and Tornos, unpub. data) suggest that the ore precipitated at high temperatures (>500°C) from isotopically heavy fluids ($\delta^{18}O_{SMOW}$ between 9 and >12‰) of probably magmatic or metamorphic origin. Galindo *et al*. (1995) and Darbyshire *et al*. (1998) reported Nd and Sr isotope data for magnetite from El Colmenar mine. However the interpretation is not straightforward. εNd_i and $^{87}Sr/^{86}Sr_i$ values of -7.6 to -4.5 and 0.7093-0.7137, respectively, probably represent those of the ore-forming fluid and suggest a crustal source for part of the metals in solution.

Most iron oxide mineralisation referred to above have low and irregular Cu-Au contents (Table 2); in fact, high-grade Cu-Au deposits in the OMZ are only found away from the ironstones (see below). However, significant Cu-Au grades are also found within stratiform magnetite deposits in shear zones or adjacent to Variscan granitoids (Bilbaína, Colmenar, Cala). This suggests that earlier magnetite acted as a geochemical trap for Cu – Au transported by late hydrothermal fluids, probably of igneous origin.

Vermiculite related to Mg-skarns (Variscan)

Small forsterite and diopside/spinel Mg-skarn developed at the contact of Early Cambrian dolomitic marbles with gabbros of the Aguablanca stock, at La Garrenchosa. Vermiculite formed by low temperature alteration of earlier phlogopite-rich veins within the skarn (Velasco *et al*., 1981). Size of vermiculite crystals can be up to 20 cm.

Cu(-Au-Bi) veins (Variscan)

Quartz - ankerite - chalcopyrite veins are scarce in the OMZ, and are restricted to two small ore fields, NE of the Burguillos pluton and N of the Santa Olalla del Cala pluton, respectively. These veins can host minor amounts of

Zn-Pb sulphides.

The Burguillos ore field is represented by the large **Abundancia** Mine (19; Fig.1), and some nearby lodes. The veins (NNE-SSW trending) are hosted by black shales and sandstones of the Late Precambrian Serie Negra, within the contact metamorphic aureole of the Burguillos del Cerro pluton. Veins consist of quartz and dolomite with chalcopyrite and variable amounts of calcite, pyrite, arsenopyrite, tennantite, sphalerite, gersdorfitte and freibergite. Hydrothermal brecciation and other features indicative of boiling are common (Tornos and Velasco, 2002). $\delta^{34}S$ values near 0 ‰, suggest that sulphur source was nearby igneous rocks.

Sultana mine, NW of the Santa Olalla pluton (34; Fig.1), probably is the richest gold deposit in Spain with an average grade near 3.1% Cu and 15 g/t Au, with ore shoots of up to 800 g/t Au (Tornos and Velasco, 2002). The deposit consists of a Late Variscan, low to moderately dipping (20 to 60°W) N160°E vein system with an *en échelon* pattern, hosted by Variscan tonalites and Late Precambrian to Early Cambrian calc-silicate hornfels, schists and metavolcanic rocks. The ore is mostly chalcopyrite, bismuthinite and maldonite, together with an assemblage of quartz, ankerite and sericite; vein selvages exhibiting strong sericitizacion and ankeritization, and local tourmalinisation are well developed. Fluid inclusion studies indicate that hydrothermal fluids were complex H_2O-CO_2-CH_4-NaCl-$CaCl_2$-KCl brines with salinities up to 30 wt % NaCl equiv. (Velasco *et al*., 1995), that underwent several stages of immiscibility. Deposition temperature of the Cu-Au assemblage was 290-380°C. $\delta^{18}O$ values of quartz and carbonates (+4.7 - +7.5‰) suggest equilibrium with deep fluids (Tornos and Velasco, 2002); the heavy sulphur isotope signatures ($\delta^{34}S$ = 10.4-15.6 ‰) are indicative of sulphur leaching from the host sedimentary rocks. The ore assemblage (Cu-Bi-(Au-Te)) and fluid composition of the Sultana veins are strikingly similar to those reported from Tennant Creek (Australia), where Cu-Au ores are hosted by an iron formation (Zaw *et al*., 1994; Stoltz and Morrison, 1994). This suggests that the Sultana deposit might be correlated with the late Cu-Au stage of the ironstones at shear zones and granite contacts.

A key question is why, in spite of many similarities, the gold content is larger at Sultana mine whilst Abundancia mine is barren. Sulphur and lead isotope data suggest that in both cases metals were derived from the same sources, probably the Serie Negra shales and igneous rocks near the vein systems. The cause probably lies in the process of polyphase immiscibility of saline CO_2-rich fluids, only recognised in Sultana.

Leucogranite-related W(-Bi-Au) veins (Variscan)

Veins of this type are scattered over a large area near Oliva de la Frontera; however only two mines came into operation, the Virgen de Gracia and Mari Juli. Veins are hosted by Early Paleozoic volcanic and siliciclastic rocks. No large plutonic bodies outcrop; however the presence of contact metamorphic effects, hydrothermal alteration and granitic dykes suggest the existence of a hidden intrusion (Ruiz de Almodóvar *et al.*, 1984; Gumiel *et al.*, 1987).

At **Virgen de Gracia** mine (21; Fig.1), quartz veins are subhorizontal as in Panasqueira (Portugal), where they formed by decompression consequent to crystallisation of an underlying granite (Kelly and Rye, 1979). At **Mari Juli** mine (20; Fig. 1) however, quartz veins are small and subvertical. Alluvial deposits related to the vein field have produced up to 6 kg/m^3 WO$_3$.

Vein filling consists of quartz and some muscovite (at the veins edge), tourmaline and siderite. Wolframite is found at the selvages and chalcopyrite, pyrite, arsenopyrite, molybdenite, fahlore, bismuthinite and enargite in the vein cores; at Mari Juli mine veins are richer in scheelite, and contain some gold. Host rocks are strongly tourmalinised and greisenised. When host rock to the veins is a mafic rock then scheelite instead of wolframite is found.

The La Bazana pluton, few kilometres East of this vein field is remarkable on this respect. It is formed by muscovite bearing granites. Zones of intense greisenisation, with up to 4% WO$_3$, are found near the pluton´s edge (Coma *et al.*, 1988). It is tempting to correlate the La Bazana granitic event with the W(-Bi-Au) veins.

Leucogranite-related gold veins (Variscan)

In the Burguillos area swarms of tourmaline-bearing muscovite peraluminous leucogranites cross-cut the gabbroic to granodioritic Burguillos plutonic massif and the tonalitic Brovales pluton. They were emplaced at moderate depths (3.5 km) and underwent pervasive albitic alteration associated with Au-bearing sulphide-poor quartz veins (Bachiller *et al.*, 1997). Fluids responsible for this alteration were moderate to highly saline brines in the H$_2$O-CO$_2$-NaCl-KCl-CaCl$_2$-FeCl$_2$ system. High salinities and high δ^{18}O values (9.5-11.2‰) of the fluids suggest that they were magmatic in origin.

Uranium veins (Post-Variscan)

Some uranium deposits, such as **Monesterio** (Cabra Alta) (32; Fig. 1), are found along late- to post-Variscan fractures. Quartz-carbonate veins contain uranium (pitchblende), nickel (nickelite) and cobalt (smaltite-chloantite) along with safflorite, millerite and pyrite, with minor chalcopyrite and pyrite (Arribas, 1962b). The mineralisation

disappears at depths over 60 m. Host migmatitic gneisses underwent pervasive low temperature alteration (chloritization, sericitization and silicification).

2.5 South Central Belt

This belt (Barrancos- Hinojales Domain of Apalategui *et al.*, 1990) is characterised by the presence of a tightly folded thick sedimentary sequence of Ordovician to Devonian age deposited in a stable continental basin. Igneous rocks are poorly represented in Spain but are more abundant in Portugal. Regional metamorphism is low-grade. The boundaries with the neighbouring belts are a south-verging thrust to the north and a longitudinal strike-slip fault to the south. In Portugal this belt has been subdivided into the northern Sousel-Barrancos sub-belt and the southern Arraiolos-Sto. Aleixo sub-belt (Oliveira, 1986) (Fig.2).

Stratabound Fe-Mn, Cu and P prospects (Early Paleozoic)

Few stratabound prospects of oolitic iron oxides are found in small tectonic slices of this belt within a strongly imbricated area near **Cazalla de la Sierra** (38; Fig.1), and west of Cala, in Spain. Rocks are shales and sandstones of Early Ordovician age (Gutierrez Marco *et al.*, 1984). The mineralisation, up to 1 m thick and of regional extent, shares many features with other stratigraphically equivalent mineralisation of Iberia. The ore assemblages consists of goethite and hematite but, in contrast with other deposits, do not contain magnetite or siderite. As elsewhere, ore genesis is correlated with the Lower Ordovician transgression and resulted from accumulation of iron oxides in small oxidised and shallow third order basins.

Scattered stratabound, centimetre thick concentrations of copper sulphides (chalcopyrite and covellite) and pyrite occur in the footwall of some quartzite layers of Silurian age. They are overlain by shales, black lidites and some felsic volcaniclastic beds that host lenses of chalcopyrite, pyrite, barite and manganese oxides. Few variscite replacements and veins are also scattered within the Silurian black shales in close association with chert and lidite beds (Moro *et al.*, 1992). Replacement of the latter by variscite was early diagenetic and related to low temperature exhalative processes. Uranium also occurs locally within the black shales.

Iron- and base metal-bearing veins (Variscan)

The key metallogenic characteristic of the Sousel-Barrancos sub-belt in Portugal is the presence of abundant quartz and carbonate-bearing veins with N-S, ENE-WSW, NNE-SSW and WNW-ESE trends. They were mined extensively during the 19th century and first decades of the

20th century (Rhoden, 1956; Gomes et al., 1959; Mendes, 1967; Barros, 1968; Gaspar, 1968, Cerveira, 1972, 1975; Oliveira, 1984, 1986; Mateus et al., 1983). The old mines of **Aparis** (13; Fig. 2), **Botefa** (58), **Miguel Vacas** (8), **Mociços** (11), **Urmos** (59), **Minancos** (60), **Bugalho** (10), **Zambujeira** (9) and **Mostardeira** (7) are the biggest deposits of this type in Portugal. In Spain, the **Novillero** mine (40; Fig.1) is the more outstanding example. The veins are mainly near-vertical and related to strike slip faults trending NNW-SSE or, more commonly, NNE-SSW to NE-SW. They are composed of polyphase, variably brecciated, hydrothermal quartz + carbonate (ankerite, siderite and/or calcite) + chalcopyrite + pyrite ± tetrahedrite/tennantite ± arsenopyrite ± sphalerite ± galena ± barite infillings; they are usually hosted by thick and monotonous metasedimentary sequences with shales, greywackes and sandstones that underwent very restricted hydrothermal alteration. These veins do not show evident relationship to intrusions of any kind and are interpreted as a result of intense hydrothermal activity of Variscan age that remobilised sedimentary-diagenetic disseminations of metals in the host rocks. The precipitation along faults took place via boiling, cooling or fluid mixing processes at rather low temperatures (<250ºC) and depths. Supergene enrichment is common, leading to the development of mineral associations composed of iron (hydr-)oxides, malachite/azurite, cuprite, liebethenite, atacamite, chrysocolla and covellite.

There is a second group of mineralisation represented by the **Defesa das Mercês** old mine (12; Fig. 2). Here, chalcopyrite, pyrite and local gold (Defesa das Mercês-Ordem Lírio) occur as disseminations or represent an important part of the mineral infillings shown by different arrays of veinlets and veins within felsic subvolcanic intrusions and related breccias, although it is also possible to identify late, brecciated quartz-calcite lodes along strike slip faults trending from NW-SE to NE-SW (Silva, 1949; Oliveira, 1982).

Cu veins (Variscan)

Several Cu mineralisation occurrences, **Azaruja** (14; Fig.2), **Monte do Trigo** (15), **Reguengos** (16), and **Sto. Aleixo** (17), exist in the western part of this belt, i.e., the Arraiolos-Sto. Aleixo sub-belt in Portugal. Sto. Aleixo consists of a chalcopyrite-bearing quartz vein hosted in Silurian spilites (Carvalho and Oliveira, 1992). The remaining occurrences are set in syn- to post-Variscan quartz-dioritic intrusions, microgranite dykes and aplite-pegmatites veins usually emplaced in Cambrian-Early Ordovician? schists. The mineralisation consists of 0.4-1.5 m-thick, decametric (rarely hectometric), NW-SE -trending quartz veins within the intrusions or as masses infilling diaclases and fractures in microgranite dykes and aplite-

pegmatite veins. Host rocks show a variable sericitization. Ore minerals are chalcopyrite, pyrite, occasionally galena and/or sphalerite. Calcite and barite are, at places, gangue minerals in the quartz veins (Goinhas and Martins, 1988). Zones of supergene enrichment with malachite, azurite and chalcocite were targets of Roman mining in Salvação do Índio (Azaruja). The development of the low-grade, primary Cu mineralisation seems to be related to the felsic-intermediate plutonism (Oliveira, 1986)

U in albite leucogranites (Variscan)

Rare albite-tourmaline gneisses and albite leucogranites (aplites) with some U, are found east of Villanueva del Fresno. Host rocks are thermally metamorphosed Ordovician metapelites of the Terena syncline. Contact metamorphism is probably related to a hidden intrusion. Ore mineral is davidite which is found along with pyrite and titanite in an aplite dyke, some tens of metres long and less than 1 m thick, hosted by tourmalinised and albitised gneisses (Arribas, 1963).

2.6. The Évora-Aracena Belt

This metallogenic belt, together with the S. Cristóvão-Beja-Serpa belt in Portugal, corresponds to the Évora-Aracena Domain of Apalategui *et al.* (1990), one of the major and more complex tectono-metamorphic areas of the OMZ. The geological formations belonging to this area have a rather unique stratigraphic sequence that is not easy to correlate with that of other areas of the OMZ (Crespo, 1987, 1989). It consists mostly of a Proterozoic-Lower Paleozoic succession containing schists (Riphean?) overlain by carbonate rocks and a bimodal metavolcanic sequence. The age of the last two is controversial and could be from Upper Proterozoic, and related with the synorogenic Cadomian sequence, to Early Silurian (Crespo, 1989, Oliveira *et al.*, 1991).

The belt includes significant stratabound Cu, Zn, Pb and magnetite orebodies, forming the so-called Magnetite-Zinc Belt (Schermerhorn, 1981; Oliveira, 1986). Most of these deposits show a strong tectonic deformation, often leading to complex imbricate sequences. The recognition and characterisation of the textural relationships, primary mineral assemblages, hydrothermal alteration and original relationships with the host rocks are therefore very difficult. However, according to the present state of knowledge it is possible to distinguish several stratiform and stratabound mineralisation types among other deposit types.

Magnetite-bearing Cu-Zn stratiform/ stratabound mineralisation (Lower Paleozoic? Variscan?)

Different iron oxide deposits, **Monges** (Montemor-o-Novo), **Orada** (Pedrógão) **and Vale de Pães** (Cuba) are

known in this belt. They are commonly hosted in Early Cambrian-Ordovician? amphibolites associated with marbles and metavolcanic rocks of the same age. They contain strongly recrystallised (syngenetic or epigenetic?) disseminated and massive, stratiform (or stratabound) ores composed of magnetite and sulphides (pyrrhotite + pyrite ± chalcopyrite ± sphalerite). Magnetite is dominant in Orada, Vale de Pães and in the upper part of Monges and, although abundant, subordinate to pyrrhotite and pyrite in the deeper levels of Monges. The mineralisation was mined in **Monges** and **Orada**, as well as in other adjacent but minor orebodies (Silva, 1945; Neiva, 1952; Carvalho, 1971; Carvalho *et al.*, 1971; Goinhas and Martins, 1986). The **Algares de Portel-Balsa** deposit is an equivalent mineralisation but is characterised by the presence of abundant sphalerite as well as the presence of many accessory phases such as galena, cubanite, different sulphosalts and arsenopyrite (Gaspar, 1967; Goinhas, 1971a; Carvalho, 1988).

The Early Cambrian (?) Monfurado Formation is the setting for the **Monges** deposit (23; Fig.2), already mined by the Romans. It is hosted by intermediate-basic and felsic metavolcanic and metalimestones, all folded in a Variscan anticline. The mineralisation, either stratiform or disseminated, is mainly hosted by amphibolite and amphibolite gneiss and, in the shallowest levels of the mine, by skarns formed on the interbedded limestones due to the intrusion of the syn-tectonic Variscan Escoural quartz-diorites. The ore assemblage includes magnetite, pyrite and pyrrhotite, and subsidiary chalcopyrite, sphalerite and sulphosalts. Iron-rich gossans occur on surface. Initial resources of the superficial portion (to 10 m depth) were about 1-2 Mt, with 30-66% Fe, 3.3-19% SiO_2 and 0.2-0.8% S. Mineralisation is known down to a depth of at least 200 m. The mineralisation is interpreted as syngenetic exhalative associated with Cambrian mafic volcanic rocks but modified by metamorphism and metasomatism induced by Variscan intrusions (Silva, 1948; Carvalho, 1976; Goinhas and Martins, 1986).

The **Orada** deposit (33; Fig. 2) occurs in an equivalent sequence of Ordovician(?) mafic and felsic metavolcanic rocks with some metalimestone lenses that overly the Cambrian metadolostones. The volcanic rocks (amphibolite or amphibolite gneiss) are the prime host of lenticular or disseminated mineralisation. Some of it also occurs in skarns formed as a product of contact metasomatism of the limestones related to the intrusion of the nearby two-mica, calc-alkaline, late-Variscan Pedrógão granite (308±4 Ma; biotite age). Mineralisation of this type can be traced along 6 km, in up to 10 m-thick and 100 m-long (max. 250 m) lenses. Specifically at Orada, 2 Mt of magnetite-pyrite ore

was mined out of three main ore lenses. Accessory phases include pyrrhotite as well as hematite, calcite, chlorite, epidote, quartz, amphiboles and serpentinised olivine. Ore contains 39-46% Fe, 6-18% SiO_2, 2.5-4.5% CaO and is almost devoid of P (0.01-0.02%) an S (0.01-0.2%), but at places sulphides are abundant and the sulphur content is over 20% S. The genesis would have been similar to that of the Monges deposit (Carvalho, 1971; Carvalho, 1976).

In the equivalent **Vale de Pães** hidden deposit (32; Fig. 2), 17 km to the west of Orada, the magnetite mineralisation is hosted in the same Ordovician(?) amphibolite and amphibolite gneiss, associated with metavolcanic rocks and minor metadolomites and biotitic schist, intruded by Variscan(?) felsic-intermediate plutonic rocks. Mineralisation in the mafic metavolcanic rocks is either massive or disseminated and contains dominant magnetite and subsidiary pyrite and pyrrhotite, and minor epidote, quartz and carbonate. The deposit, that almost reaches the surface and extends to a depth of 180 m, contains 8.5 Mt with average grade of 42% Fe, 19% SiO_2 and 0.6-5.2% S. The genesis was similar to that of Orada (Carvalho, 1976; Oliveira, 1986).

As mentioned above, the current genetic model envisaged for this iron mineralisation involves contact metamorphism and metasomatism of previous syngenetic exhalative mineralisation, due to the intrusion of Variscan igneous rocks. However, a different origin was recently proposed for the iron mineralisation at Azenhas, near the Orada deposit (Mateus *et al.*, 1999a). At **Azenhas** (69; Fig. 2), where minor magnetite orebodies were incipiently mined (Carvalho *et al.*, 1971), recent studies (Matos *et al.*, 1998; Mateus *et al.*, 1999a) have shown that they occur exclusively within strongly metasomatized and imbricated sequences of amphibolite slices, immediately underneath a major WNW-ESE thrust zone. Here, carbonate and calc-silicate rocks (Lower Cambrian?) also occur but form a relatively narrow band apparently confined to another important near-horizontal thrust zone. The mineralisation comprises: 1) massive, fine- to medium-grained ores within non-carbonatised amphibolites; 2) banded, medium- to coarse-grained ores within carbonatised rock domains; and 3) brecciated ores, caused by late deformation of the massive ore near strike slip faults. Magnetite prevails in all these kinds of ores, with interstitial domains infilled usually by tremolite, often partly replaced by lizardite-amesite ± carlosturanite aggregates. Chemically, the ores have less than 62.50% Fe_2O_3 (as total iron), 15.03-21.31% SiO_2 and very low P_2O_5 contents (< 0.04%). Disseminated pyrite, pyrrhotite and chalcopyrite also occur but always along late fractures developed after magnetite formation. As a genetic mechanism, the rise of oxidising aqueous fluids,

subsequently CO_2 enriched, under a significant reverse temperature gradient provided by the tectonic superposition of amphibolites over a relatively cold (lower greenschist facies) autochthonous sequence, would promote iron ore deposition.

This style of iron mineralisation is also found in Spain, mostly in the eastermost Aracena massif. However, some minor iron oxide-bearing deposits are found near the Zn-Cu-(Pb) massive sulphides (see below). They seem to be related to hydrothermal submarine replacements eventually associated with an important, epigenetic dolomitisation process of unknown age.

Zn-Cu-(Pb) volcanic-hosted massive sulphides (Proterozoic? –Cambrian?)

Some Late Proterozoic?-Cambrian? volcano-sedimentary sequences host a second style of mineralisation. It consists of stratiform massive sulphides chiefly composed of pyrite and sphalerite with variable proportions of galena and tetrahedrite. These ores occur almost exclusively within metavolcanic and metacarbonatic horizons belonging to thick volcano-sedimentary sequences, that are affected by strong, although heterogeneous, hydrothermal alteration.

In the Moura-Ficalho area, different Zn-Pb(-Ag-Sb-Au) deposits are known, namely those of Preguiça, Vila Ruiva, Carrasca, Sto André and Enfermarias (Goinhas, 1971b; Oliveira, 1986; Oliveira and Matos, 1992). The **Preguiça** (36; Fig.2) and **Vila Ruiva** (37) deposits correspond to very rich secondary Zn-ores located in metadolostones of Lower Cambrian age, due to strong *in situ* oxidation and supergene enrichment processes on previous sulphide mineralisation. Equivalent metadolostones host the **Carrasca** (56) prospect but only small amounts of disseminated sphalerite and galena were recognised (Aalten and Steenbruggen, 1997). Drilling in the eighties intersected the **Sto André** (35) and **Enfermarias** (34) orebodies, with Zn, Cu, Pb, Ag and Au contents up to 17.53%, 2.88%, 2.75%, 384 ppm and 3.2 ppm, respectively (Oliveira and Matos, 1992). The **Sto. André** orebody, showing somewhat different characteristics, is enclosed in the Ordovician metavolcanic-marble sequence and exhibits a very wide hydrothermal siderite alteration halo with abundant disseminated pyrite and arsenopyrite.

The **Enfermarias** orebody, hosted by a Lower Cambrian metavolcanic-metadolostone sequence, comprises massive and disseminated mineralisation that records a very long and complex evolution (Barroso, 2002, Martins, 2002). The rock sequence drilled at Enfermarias consists of felsic to intermediate-mafic metavolcanic rocks interbedded with silicate-bearing marbles, metadolostones, and different layers of metasomatic rocks. Primary mineralisation occurs mainly in strongly chloritized intermediate-mafic

metavolcanics as semi-massive to massive lenses subparallel to the metamorphic banding; the ore assemblage consists mostly of pyrite and sphalerite with minor amounts of galena, chalcopyrite, magnetite, arsenopyrite and sparse Ag-bearing tetrahedrite (Barroso, 2002; Martins, 2002). The sphalerite, magnetite, arsenopyrite and most pyrite are pre-metamorphic and show evidence of strong recrystallisation and deformation.

The introduction of galena, chalcopyrite and Ag-bearing tetrahedrite, as well as the crystallisation of most of the gangue-forming minerals (actinolite-tremolite, talc, serpentine, biotite and chlorite), took place during the retrograde Variscan metamorphism. Late massive aggregates of magnetite and pyrite developed in metasomatic rocks, mostly consisting of chlorite/serpentine, actinolite/tremolite and talc, are related with late near-horizontal shear zones. The origin of this mineralisation is ascribable to the circulation of oxidised aqueous-carbonic fluids, progressively focussed along near-horizontal structural corridors after the Variscan deformation-metamorphic peak. These fluids were also responsible for partial remobilisation of the primary sulphide assemblage, and for late input of metals (Pb, Cu, Ag, As and Sb) in the system. Finally, there are quartz, chlorite, pyrite, chalcopyrite and pyrrhotite cementing fault breccias and infilling late veins; they are related to near-vertical strike slip fault zones and are interpreted as recording the effects of an independent Cu ore-forming system superimposed to a main, pre-existing, Zn-Pb(-Ag) geochemical halo.

The clear spatial relationship between the primary sulphide mineralisation and the metavolcanic rocks, the sub-parallelism between the sulphide layering and the metamorphic banding, and the preservation of some evidence for the pre-existence of a Fe-Mn carbonate halo around ore strongly suggest that the Enfermarias can be an example of a stratiform (and syngenetic?) deposit with miscellaneous characteristics of SEDEX and Irish-type categories, particularly if the silicate-bearing marbles are envisaged as metamorphic products of dolomitic shaly rocks. In this context, it is worth noting that the fabrics of the metadolostones hosting the nearby Carrasca prospect are polymodal and have red luminescence, usually taken as indicative of continuous nucleation from a chemically homogeneous fluid in a system with high water/rock ratio (Aalten and Steenbruggen, 1997). The O and C stable isotope data suggest that the dolomitisation process took place at low temperatures (40-55ºC), involving seawater as the main fluid type (Aalten and Steenbruggen, 1997). It is not clear yet, however, what is the chronological relationship between the dolomitisation process and the earlier mineralising events in the Enfermarias system.

The **María Luisa** mine is near Aracena (43; Fig.1) and is

set in medium to high grade metamorphosed and deformed volcaniclastic rocks. This metavolcaniclastic unit some 1500 m thick, includes metarhyolites and metadacites with basicity increasing upwards (Crespo, 1989). The age of this sequence is unknown because of structural complications. It might be older than marble beds which are correlated with the regional Early Cambrian carbonates. This possibility is consistent with a syn-Cadomian age for the volcaniclastic complex. On the contrary, Crespo (1989) proposed that the metavolcanic sequence overlies the marble beds and that in consequence it could be as young as Silurian . Recent lead isotope model ages however suggest that the mineralisation is Cadomian; in consequence the host rocks probably are a syn-Cadomian volcanic sequence (Tornos and Chiaradia, 2004).

In detail the mineralisation at María Luisa is hosted in quartz-sericite schists (probably altered metavolcaniclastic rocks) with some intercalations of amphibolites, calc-silicate hornfelses and metalimestones (Florido, 1993) that were strongly chloritized, silicified and skarnified. The orebody consists of several stacked lenses trending N120-140ºE. Underlying the ore lenses there is a small stockwork, with vein-like and disseminated mineralisation, affected by chloritization. Vázquez (1972) distinguished two types of ores: an early syngenetic ore, consisting of pyrite, arsenopyrite and sphalerite with minor magnetite occurs in the footwall and is overprinted by a late ore with magnetite, pyrrhotite, arsenopyrite, pyrite, sphalerite, chalcopyrite and galena with minor cubanite, tetrahedrite and bornite. The existence of a skarn-like assemblage (pyroxene, actinolite, epidote) in association with the second type of ore, suggests that this ore is probably metasomatic and the product of an hydrothermal activity related either to the Variscan metamorphism or to some small epizonal dioritic to quartz-dioritic stocks and dykes of unknown age that occur nearby. The strong deformation precludes any clear genetic interpretation for the first type of ore. However, the widespread evidence of replacement suggests that these massive sulphides formed by sub-seafloor processes. In fact, there exist also lenses of meta-exhalites with jasper and Mn-bearing minerals (pyrolusite, braunite, rhodonite) probably equivalent to the sulphides but formed in a more oxidised and cooler environment

Sulphur isotope data of sulphides from María Luisa range between 13 and 19.5 ‰ (Conde and Tornos, unpub. data), indicating that the source of sulphur is neither magmatic nor biogenic, but possibly resulting from the leaching of the host rocks, and ultimately derived from the thermo-reduction of seawater sulphate.

Some Zn-Pb-Ag-barite stratiform mineralisation is also found at Aracena east of Maria Luisa mine, along the contact between the felsic metavolcaniclastic sequence and the thick marble unit (Guillou, 1967; Fernández Caliani *et al.*, 1989; Arribas *et al.*, 1990). Some poorly known mineralisation within zones of silicified marble consist of galena, sphalerite and pyrite. Most of the ore at Aracena is interpreted by these authors as related to silicified carbonatic lenses that display syn-sedimentary brecciation and are interbedded with pervasively chloritized and silicified volcanic rocks. The mineralisation here occurs as disseminations, veinlets and semi-massive bodies including galena, barite, pyrite and sphalerite with lesser amounts of pyrrhotite and freibergite; barite-galena are more abundant in the silicified limestones. Guillou (1967) quotes a regional zonation with Cu and Ag in the core and Zn and magnetite in the outer zone.

Arribas *et al*. (1990) have stated that syn-sedimentary faults, slumps and neptunian dykes can be recognised at Aracena, in support for a syngenetic to early diagenetic model for the mineralisation. In this hypothesis, the ore formed in a sub-tidal environment by exhalative processes on the seafloor. This mineralisation is probably equivalent to the Maria Luisa mine, but has Pb-enriched zones and minor proportions of chalcopyrite. Moreover, the volcanic influence is lacking at Aracena.

Differences between the Maria Luisa and Aracena orebodies can be attributed to different depositional environments and temperatures, lower at Aracena. In this perspective, the Zn-Pb-barite deposits of Aracena probably represent a (sub-)exhalative mineralisation deposited in a tectonically unstable oxidising carbonate-dominated platform, probably through direct precipitation and shallow diagenetic replacement of the carbonates. The reaction of deep reduced H_2S-bearing brines with sulphate-rich alkaline waters at rather low temperatures (<150ºC) should promote the precipitation of sphalerite, galena and barite.

Some of these deposits, specially those hosted in carbonate rocks, show effects of strong supergene alteration that may be responsible for a significant metal reconcentration, as is the case of Ag in **Fuenteheridos** or Zn in Preguiça and Vila Ruiva gossans, that rendered these deposits economic in the past.

As a whole, these volcanic-related deposits share many features with those of Puebla de la Reina (see above). Lead isotope data suggest that they are broadly contemporaneous and of Upper Proterozoic-Lower Cambrian age. Moreover they are consistent with derivation of the metals from two different sources, i.e., a crustal reservoir, that could correspond to an evolved continental crust similar to that of the Central-Iberian Zone, and a more primitive source, probably mafic magmas generated by the Cadomian subduction (Tornos and Chiaradia, 2004). The tectonic setting of these massive sulphides might thus have been be a syn-Cadomian magmatic arc-basin system.

Orogenic gold mineralisation (Proterozoic? Variscan?)

Orogenic gold mineralisation occurs along 35 km in the NW sector (Montemor-o-Novo) of this belt. It has general characteristics, including the host rocks and the age (Proterozoic Escoural Formation), the alteration and the mineralisation similar to those of the Portalegre area gold deposits. At places, calc-silicate/skarnoid rocks and thin granite dykes can host minor mineralisation (Inverno, 1997). The gold concentrations occur in the vicinity of the Montemor-o-Novo NW-SE shear zone, and are hosted by sheared metamorphic rocks affected in part by a high grade metamorphism (Pereira *et al*., 2002).

According to Ribeiro *et al*. (1993) and Ribeiro (1994), gold mineralisation of **Chaminé-Casas Novas** (63; Fig.2) occurs in veins and lenses of variable thickness, developed within a major, near-vertical, NNW-SSE turning to N-S shear zone that affects mainly biotite schists of Proterozoic age. The mineralised structures consist of centimetre-wide quartz + arsenopyrite veinlets intersecting high grade decimetre- to metre-wide quartz veins parallel to the cleavage and often showing digitations into the country rocks. In the latter structures, three main stages of mineral deposition were identified. The first one comprises the development of quartz ± tourmaline ± ankerite + arsenopyrite + löllingite ± maldonite ± bismuth ± pyrrhotite ± pyrite. The second is responsible for the deposition of quartz + chlorite + ankerite + arsenopyrite + gold ± chalcopyrite ± pyrite, and the third stage involves the precipitation of quartz + chlorite + marcasite + covellite. The host rocks record the effects of intense hydrothermal alteration, particularly strong silicification and chloritization besides incipient sericitization and erratic dissemination of pyrite and arsenopyrite. These textural-chemical transformations confirm the epigenetic nature of the mineralising process and document well the polyphase character of fluid/rock interactions under decreasing temperature conditions between *ca.* 400ºC and 200ºC.

A total resource of 4.45 Mt at avg. 2.81 g/t Au is known in this area, 60% of which from the main deposits, Chaminé (1.2 Mt), Casa Novas (1.7 Mt) and Braços (0.1 Mt), 30% from nearby deposits (Banhos, Ligeiro, Caras and Covas) and the remainder from other deposits and occurrences in the area (Faria, 1997).

The 150 m-long, 25 m-thick **Braços** deposit (66), grading avg. 5 g/t Au, consists mostly of a silicified zone located along the thrust contact between Proterozoic schists with a sequence dominated by quartz-feldspar porphyritic intrusive rocks, amphibolites (and amphibolite gneisses) and felsic metavolcanic rocks. The eastern end of the deposit is disrupted by a normal late-Variscan N-S fault. Chlorite, either in quartz veins or in host rocks, and pervasive Fe-dolomite? alteration are at places present in the mineralised zones. Gold (at times visible) is accompanied by pyrite, arsenopyrite, löllingite, chalcopyrite, galena and barite (Inverno, 1997; SIORMINP, 2002).

In the western portion of this Montemor-o-Novo gold mineralised area, close to the Ferreira-Ficalho thrust, gold-bearing quartz vein mineralisation is also hosted in the same Proterozoic Escoural Formation. Here, the gold mineralisation is related to stibnite (e.g., **Palmas**; 21; Fig. 2) or pyrite and base metal sulphides, mostly chalcopyrite (e.g., **Caeira**; 68) (Goinhas and Martins, 1986). Some gold mineralisation, in quartz veins and disseminations, also occurs in silicified schists, felsic-intermediate metavolcanic and calc-silicate rocks of the Cambrian Monfurado Formation (central part of the area), accompanied by dominant pyrite (e.g., **Monfurado**; 61) (Faria, 1997).

Iron-rich skarns (Variscan)

Along with the skarn-like replacements superimposed to the mafic volcanic-related magnetite mineralisation (see above) there are some massive, calcic and magnesian iron-rich skarns, chiefly developed along the contact of marbles with diorite-gabbro intrusions of the Beja Igneous Complex (Silva, 1945; Neiva, 1952). The small **Alvito** iron deposit (29; Fig.2) occurs in Early Cambrian metalimestones in contact (through a N-S thrust) with diorites of the syn-Variscan Cuba gabbro-diorite. The mineralisation consists of irregular masses and stratiform lenses of magnetite with serpentine, olivine, asbestos, chlorite, garnet, diopside, amphibole and idocrase, or even calcite and dolomite. Pyrite, pyrrhotite, chalcopyrite, and rare galena also occur at places. There is a resource of 0.7 Mt at 44% Fe, 17% SiO_2 and 1.5% S. Though skarn development through metasomatism appears to be the main metallogenic process, it has been proposed that prior to it a volcanogenic process would have concentrated metals in Cambrian (?) volcanic rocks of the area (Silva, 1948; Carvalhosa and Zbyszewski 1972; Carvalho, 1976; SIORMINP, 2002)

Magnetite and sphalerite-rich skarnoids (Variscan?)

In the Aracena massif there are some small sphalerite-magnetite stratabound orebodies enclosed in skarn-like assemblages including garnet, pyroxene, clinoamphibole and epidote. They are probably bimetasomatic skarns formed by the reaction of metamorphic fluids with calc-silicate hornfels.

Wollastonite skarns (Variscan?)

Large lenses, up to 6-8 km long and 1 km wide, of calcic skarns with massive wollastonite are found in the Aroche area (Huelva) within the Aracena Metamorphic Band. They formed by the replacement of high grade marbles, interbedded with calc-silicate hornfelses, schists and different types of orthogneisses of Upper Proterozoic-Lower

Cambrian age. Discordant veins of leucogranite and quartz probably related to nearby Variscan granite and gabbro plutons were probably at the origin of these replacements (Fernández *et al*., 2002).

Graphite in metamorphic rocks (Variscan?)

In the proximity to the wollastonite mineralisation but interbedded with the amphibolite gneisses, quartzites marbles and calc-silicate hornfels, there exist some graphite-bearing lenses that were probably the product of high-grade metamorphism of organic matter-rich layers (Rodas *et al*., 2000). Small minable high-grade orebodies are located in veins or shear zones that transected the stratabound mineralisation.

Cu veins (Variscan)

There are several old mines and prospects that worked Cu- and Co-As-bearing lodes controlled by strike slip fault zones (Oliveira, 1986); minor Co-As occurrences with arsenopyrite and safflorite are found nearby. At **Rui Gomes** (55; Fig.2), the main mined lodes are heterometric tectonic breccias containing heterolithic fragments cemented by late and coarse-grained aggregates of siderite + ankerite ± calcite ± quartz, locally enriched in chalcopyrite and pyrite. The development of these epigenetic lodes is ascribable to the hydrothermal activity correlative of Late-Variscan strike slip faults formation and/or reactivation.

2.7. S. Cristóvão-Beja-Serpa Belt

The geological background of the S.Cristóvão-Beja-Serpa belt is largely dominated by the Beja Igneous Complex (BIC), a wide curved intrusive belt that can be followed for *ca*. 100 km in the westernmost domain of the OMZ southern border in Portugal, resulting from important synorogenic, Variscan magmatic activity developed from Frasnian-Famennian to Late Visean times. This belt can be divided into three major units: 1) the Beja Gabbroic Complex (BIC), mainly consisting of olivine-bearing gabbroic rocks, bordered by heterogeneous diorites resulting from variable extents of magma mixing or crustal assimilation at the margin of the intrusion; 2) the Cuba-Alvito Complex, comprising mostly granodiorites, diorites and gabbros; and 3) the Baleizão Porphyry Complex, a late, epizonal intrusion that includes different types of porphyry rocks (Andrade, 1974, 1983; Perroud *et al*. 1985; Santos, 1990; Santos *et al*., 1990; Dallmeyer *et al*., 1993; Quesada *et al*., 1994). The main known mineralisation is intimately related to the magmatic differentiation path (e.g. Fe-Ti-V), magma mixing and/or crustal assimilation processes (e.g. Cu(-Ni)) and the emplacement/cooling of late porphyry

intrusions (e.g. Cu(-Ag-Au?)). Other, minor, mineralisation includes Fe-skarns (e.g. **Corujeiras;** 46; Fig.2) and Sb-Cu-(As-Au) veins (e.g. **Ventosa;** 53) related to the development and further reactivation of Late-Variscan strike slip faults (Mateus *et al*., 1998b). These prospects are similar to those found around or within the Variscan plutonic complexes in the Olivenza-Monesterio Belt.

Fe-Ti-V mineralisation (Variscan)

This mineralisation is well characterised in the **Odivelas** (54; Fig. 2) area. Detailed geological studies (Silva *et al*. 1970, Andrade 1983, Santos *et al*. 1990, Mateus *et al*., 2001b; Jesus, 2002) show that the outcropping rocks in the westernmost part of BIC are quite diverse and often layered, forming two main Series that show normal polarity and a gradual contact. The lower magmatic sequence embraces three main groups of layers. The lower group comprises essentially olivine leucogabbros, within which layers and lenses (and/or blocks?) of troctolitic rocks and of cumulates (olivine melanogabbros, wehrlites and websterites) can be recognised, besides irregular bodies of massive accumulations of coarse-grained magnetic oxides. These bodies, irregular in shape, at approximately right angles to the regional layering and of considerable size (up to an estimated 50 tons each - Silva, 1945), are mainly composed of vanadium-bearing titanomaghemite, ilmenite, and accessory maghemite (Mateus *et al*., 2001b, Jesus, 2002). The research carried out also shows that the magnetic anomalies are not limited to the small area surveyed for iron ores in 1944 (Silva, 1945) and that the mineralised bodies are quite enriched in titanium and vanadium (up to 10.05% of TiO_2 and up to 0.99% of V_2O_5); this interpretation agrees with the results previously obtained by Fonseca (1999) and Gonçalves *et al*. (2001) concerning the available geophysical and soil geochemistry data, respectively. No accurate reserve estimates are presently available.

Cu(-Ni) veins and stockworks (Variscan.)

Work recently carried out in the Odivelas-Ferreira do Alentejo area enabled the identification and the preliminary characterisation of a Cu(-Ni) mineralising system within the upper, outcropping layered gabbroic Series (Mateus *et al*., 2001a; Jesus, 2002). This Series consists mostly of olivine-pyroxene leucogabbros, olivine leucogabbros and gabbros that are strongly metasomatized and massive pyrrhotite+chalcopyrite+pyrite±pentlandite aggregates fill up anastomosed centimetre-thick vein arrays. The available whole-rock analysis data show that Cu and Ni contents of the massive sulphide aggregates may reach up to 14000 and 1500 ppm, respectively; no other in-

formation is presently available. The development of this type of mineralisation is envisaged as a result of late fluid circulation within the fractured gabbroic Series, probably during the late stages of their cooling.

Cu(-Ag-Au?) epithermal systems (Variscan)

Epithermal mineralisation related to the late magmatic activity of BIC is known but poorly characterised in detail. The most important mineral occurrences are **Corte Pereiro** (40; Fig. 2), **Caeirinha** (41) and **Alcáçovas** (42) (*e.g.* Oliveira, 1986; Relvas, 1987; Massano, 1988; Mateus *et al.*, 1998b). These mineralising systems are characterised by several superimposed and crosscutting stages of pervasive fracturing and hydrothermal circulation and contain minor, but significant amounts, of Ag and in a few exceptional cases, also Au, Bi, Cu, Pb and Zn.

Sb-Cu(-As-Au?) veins (Variscan)

As referred to in Mateus *et al.* (1998b), the Ventosa prospect is representative of the mineralisation related to hydrothermal activity triggered by late reactivation of shear zones and/or by the development of Late Variscan strike slip fault zones. In this prospect, the lodes are controlled by a relatively complex array of structures that are subsidiary to a major WNW-ESE left-lateral shear zone. They are hosted in silicified metamorphic rocks, which sometimes show sulphide (pyrite)-rich disseminations. The ores, randomly distributed within a polyphase hydrothermal quartz-carbonate assemblage, comprise stibnite and tetrahedrite, as well as significant amounts of pyrite, arsenopyrite and berthierite and accessory amounts of chalcopyrite, marcasite and gudmuntite, famatinite-stibioluzonite, aurostibite, chalcostibite, chalcocite and covellite; poorly crystallised Sb and/or Fe-Sb oxides (such as schafarzikite and tripuhyite), besides kermesite and hematite/goethite, are the main products of ore weathering.

2.8. The Beja-Acebuches Ophiolite Complex

The Beja-Acebuches Complex (BAOC) is an extremely dismembered ophiolite sequence incorporated in the Variscan South Iberian Suture. The lower and intermediate sections of BAOC, to be found essentially in Portugal, comprise respectively peridotites (mainly harzburgites) and gabbroic rocks (gabbro-gabbronorites and minor troctolites). The upper sections of BAOC, well represented in Spain, consist essentially of amphibolites derived from basaltic lavas of tholeiitic nature; deep marine sediments and examples of sheeted dike complexes are almost absent (Munhá *et al.*, 1986, 1989; Crespo, 1989; Quesada *et al.*, 1994).

Cr mineralisation (Variscan)

Cr-spinel is an important accessory mineral phase in all of the metaperidotites and metawehrlites/troctolites included in BAOC, for which the whole-rock Cr content goes up to 3620 ppm. In the seventies, the Serviço de Fomento Mineiro drilled several, although very thin, banded chromitites within strongly serpentinised metaperidotites belonging to the Ferreira do Alentejo-Mombeja ultramafic domain. It is also worth noting that the PGE contents of BAOC peridotites are quite low (Mateus and Figueiras, 1999a, b).

Ni-Cu(-Co) sulphide dissemination (Variscan)

BAOC metagabbroic rocks comprise most times accessory amounts of sulphides, usually forming tiny and randomly distributed aggregates of irregular morphology, mainly consisting of pyrrhotite + pyrite ± chalcopyrite. Microscopic sulphide aggregates appear, however, to be characteristic of ilmenite-free rocks, namely of the metatroctolites found at **Palmeira** (49; Fig. 2) (Guadiana Valley), whose Ni+Cu+Co content average is in the order of 1050 ppm (Mateus *et al.*, 1998a). In these variably serpentinised rocks, sulphides occur: 1) as randomly disseminated irregular millimetric globules of pentlandite (and/or bravoite) + pyrrhotite ± chalcopyrite ± mackinawite; 2) as pentlandite (and/or bravoite) + pyrrhotite ± heazlewoodite aggregates within magnetite fringes surrounding altered Cr-spinel; and 3) as fine aggregates of bravoite within weakly disseminated awaruite ± pyrite. The sulphides are interpreted as magmatic.

Cu sulphide disseminations (Variscan)

Polyphase hydrothermal activity along WNW-ESE shear zones led to the development of silica-carbonate infillings and of prominent alteration halos in the mafic and ultramafic host rocks (Mateus *et al.*, 1999b). Usually, the hydrothermal precipitates exhibit variable amounts of disseminated sulphides (mainly pyrite ± chalcopyrite ± sphalerite) or of their weathering products, besides several generations of carbonates. With few exceptions, the whole-rock base metal contents are typically low (< 500 ppm, on average). It should be noted, however, that the only real evidence for historical attempts of mineral exploitation in BAOC is represented by the abandoned trial workings for Cu in western **Mombeja** (50; Fig. 2) village, which are located along the hydrothermal infillings of a WNW-ESE shear zone adjoining strongly carbonatized ultramafic rocks (Mateus *et al.*, 1998c); in this particular case, Cu and Zn contents may reach 1.5% and 1200 ppm, respectively.

3. Discussion and conclusions

Ore deposits in the Ossa-Morena Zone can be grouped into very different types, some of them unusual worldwide. This is chiefly the result of a complex tectono-metamorphic evolution that gave rise to a variety of geological settings where very different ore-forming systems set in. Three main factors are responsible of this particular complex evolution. The first is the position of the OMZ between two contrasting terranes, the Central-Iberian Zone to the north and the South Portuguese Zone to the south. Both terranes experienced a different evolution. The South Portuguese Zone is characterised by a long-lived crustal evolution with minor orogenic input, whilst the OMZ is a polyphase terrane that behaved as an active magmatic arc during Cadomian and Variscan times (Quesada *et al*., 1987; Quesada *et al*., 1991; Eguiluz *et al*., 2000). The second key factor concerns the transpressional type of deformation that existed during the Cadomian orogeny (Liñán and Quesada, 1990), and particularly during the Variscan orogeny. Most present-day large structural features are Variscan; however many of them are rejuvenated older structures. This is the case of the many longitudinal transcrustal, W-E to WNW-ESE-trending faults that strongly controlled sedimentation, magmatism and hydrothermal activity since the Late Proterozoic (Quesada *et al*., 1987). These structures have probably controlled the deposition of many ore deposits in OMZ, as they focused magmatism, heat flow and hydrothermal activity particularly at local extensional zones such as pull-apart structures and releasing bends (Tornos *et al*., 2002). The third factor, has only been recently brought to light. Deep reflection seismic sounding (Simancas *et al*., 2003) has shown that a *ca.* 5 km thick body with the geometry of a sill exists at 10-15 km depth, underneath most of the Ossa-Morena Zone. Because of seismic properties and geometrical considerations this body is probably formed by mafic and ultramafic rocks and has to be of Variscan age. Many metallogenetic features of the OMZ might be related to this hidden mafic to ultramafic body. Its existence had been anticipated by Casquet *et al.* (2001) and Tornos *et al.*, (2001) on the basis of geochemical and textural evidence from the Aguablanca stock and related Cu (-Ni) mineralisation. It might also be the explanation for the [207]Pb-depleted lead isotope signatures which are characteristic of the OMZ (Tornos and Chiaradia, 2004).

3.1. Metallogenic evolution

Pre-Cadomian metallogenesis

The Pre-Cadomian metallogenesis is not significant. In fact, only few deposits undoubtedly associated with Prot-

erozoic ore-forming processes have been recognised. This is the case of some chromite-rich ultrabasic rocks and stratiform Cu deposits within the Serie Negra. This scarcity of mineralisation older than the Cadomian orogenesis has to be attributed to the strong deformation and dismembering of the pre-Cadomian terranes, which have not still been recognised in the OMZ, and to the fact that most of the rocks of the Cadomian cycle were deposited in a rather stable setting where hydrothermal processes are uncommon.

Mineral deposits of the Cadomian orogenesis

The OMZ was the site of a Cadomian magmatic arc formed during the southwards subduction of the Iberian Autochthonous Terrane (Central-Iberian Zone), which preceded collision with the OMZ (Sánchez Carretero *et al*., 1990; Quesada *et al*., 1991). Despite major tectonic dismembering, general features of a typical Andean-type magmatic arc have been claimed by Sánchez Carretero *et al.*(1990), particularly a calc-alkaline andesite-dacite volcanism and plutonism. Ore deposits clearly associated with this orogeny and the related magmatic activity are scarce. Although the partly submarine magmatic arc and related back arc basin had to be favourable settings for the development of a wide variety of ore-forming systems, no major deposits have been found to date. The more significant mineralisation consists of small (sub-)exhalative deposits. These include volcanic-hosted massive sulphides (Puebla de la Reina), sedex barite mineralisation (Llerena) and rare porphyry copper deposits (Ahillones). The Tinoca and Azeteiros deposits, hosted in felsic migmatitic gneisses, could be equivalent to the Puebla de la Reina mineralisation, but underwent higher grade metamorphism. No epithermal mineralisation has been recorded, as it would be expected on behalf of the abundant volcanic and subvolcanic rocks. A sedex-like mineralisation was recognised in the foreland basin, but is restricted to a small area (Retín).

Abundant Fe and Cu-Zn volcanic-hosted and Pb-Zn-Ag mineralisation exists both in the Evora-Aracenal Belt and the North Eastern Belt that bear many similarities, among other the stratigraphical setting and the lead isotope signatures. However, the age of these deposits is still unknown. Geological reasoning suggests that they could be Upper Proterozoic to Silurian. If this mineralisation were not related to the Cadomian magmatic arc, an equivalent tectonic setting had to exist at some other time during the Lower Paleozoic in the Evora-Aracena and North Eastern belt domains.

In the absence of absolute ages, it can be questioned whether orogenic gold mineralisation hosted in Proterozoic terrains formed during pre-Cadomian, Cadomian or Variscan times.

The post-Cadomian rifting stage

This stage is characterised by a (sub-)alkaline bimodal epizonal plutonism, and volcanism, and the formation of ubiquitous (sub-)exhalative iron deposits. Some small manganese-bearing orebodies also formed under more oxidising conditions. These deposits are variable from truly exhalative to sub-exhalative replacive and deeper metasomatic ones.

The stable platform stage

Only some minor ores without relevant economic interest can be related to this stage. They include several stratiform Cu, Pb and Fe-Mn oxide concentrations, probably linked to local exhalative or diagenetic processes. A few Cu concentrations closely associated with the Ordovician-Silurian volcanism can also be included within this style of mineralisation.

Mineral deposits related to the Variscan orogeny

Ore-forming events related in time and space to the Variscan magmatism, led to the formation of most of the ore deposits in the OMZ. Most are set within pull-apart structures, major shear bands and faults and plutons of variable composition (Tornos *et al.*, 2002).

A key feature of the OMZ is the absence of a preserved significant Early Carboniferous volcanism. Moreover, Variscan syn-orogenic basins (e.g., Los Santos de Maimona basin of Visean age, Rodriguez *et al.*, 1992; El Guadiato basin of Visean-Serpukhovian age, Cozar and Rodriguez, 1999; among others, Gabaldón *et al.*, 1985) are not typical arc or back arc basins but, instead, seem to be narrow strike-slip fault related basins, mostly filled with shallow marine to continental sedimentary sequences. Synorogenic basins are the preferential loci for the volcanic-hosted massive sulphides deposits (e.g, Barrie and Hannington, 1999; Large and Blundell, eds., 2000); however, in Southwest Iberia most Variscan massive sulphides formed only in pull-apart basins located in the allochthonous South Portuguese Zone terrane (Iberian Pyrite Belt). The OMZ basins are almost devoid of submarine exhalative deposits. Only the Nava Paredon deposit, some minor prospects and several occurrences of iron oxide mineralisation occur in the OMZ.

Syn-metamorphic probably Variscan (and/or Proterozoic?) gold and base metal mineralisation is widespread in the OMZ. Gold deposits and prospects share many features with "orogenic gold", i.e., sulphide-poor, quartz-bearing veins and disseminations, such as mineral assemblages, hydrothermal type of alteration and fluid composition. They are known from the Montemor-o-Novo, Portalegre and Guijarro-Chocolatero areas. This gold mineralisation is always related to major shear zones and thrusts that crosscut the syn-Cadomian metavolcanic sequence or metasedimentary/metavolcanic rocks of the Late Proterozoic Serie Negra.

Minor regional structures were also controls to the abundant Cu, Fe and Pb-Zn syn-metamorphic veins, usually hosted in black shales belonging to either the Serie Negra or Ordovician-Silurian terrains. They are interpreted as the result of metal remobilisation from proto-concentrations by means of circulating metamorphic fluids and subsequent precipitation along local extensional zones. Re-deposition of metals was probably controlled by system temperature, with chalcopyrite forming at higher temperatures than sphalerite, galena and iron oxides. The deepest syn-metamorphic mineralisation is represented by anatectic pegmatites.

Variscan intrusions, dated between 350 and 330 Ma, i.e., Early Carboniferous, consist of a continuous spectrum of metaluminous rocks from gabbros to monzogranites, and minor peraluminous granites. They form large, usually epizonal, roughly zoned plutons (e.g., Casquet, 1980; Pons, 1982; Sánchez Carretero *et al.*, 1990). A Ni-(Cu) magmatic mineralisation was recently discovered in the mafic cumulates of the Aguablanca stock. It probably resulted from combined crustal assimilation (of the Serie Negra) and fractional crystallisation processes in a predicted deep magma chamber (Casquet *et al.*, 2001; Tornos *et al.*, 2001). This chamber might be correlated with the recently discovered, probably mafic to ultramafic body (Simancas *et al.*, 2003), which apparently spreads under most of the OMZ, in the middle crust. The Aguablanca deposit seems to be rather unique in that it is one of the few syn-orogenic Ni (-Cu) orthomagmatic deposits worlwide described so far. The Beja igneous complex is rather similar to Aguablanca and other Olivenza – Monesterio Belt plutons. It contains irregular and small Fe-Ti-V and Cu-(Ni) mineralisation that formed by processes similar to those invoked for Aguablanca. Some epithermal Cu(-Ag-Au?) prospects in the S.Cristóvao-Beja-Serpa Belt might be also related to late intrusions of the Beja igneous complex.

Early Cambrian carbonate rocks adjacent to the plutons can be host to typical calcic iron-rich skarns. However, the relative contribution of skarn-type metasomatism to the formation of iron oxide deposits has long been debated. Since Cambrian carbonates are overlain by volcanics that contain allegedly exhalative Fe ores, the question as to whether some large stratiform orebodies are Cambrian or Variscan remains open. However, systematic isotope data of magnetite from some of those orebodies (Galindo *et al.*, 1995; Darbyshire *et al.*, 1998) suggest that magnetite achieved isotope equilibrium with nearby Variscan igneous rocks. This in turn implies that fluids involved were

equilibrated with the igneous rocks. An earlier stage of shear zone-related actinolite-albite alteration (with magnetite) similar to the hydrothermal iron oxide stage of the Fe-ox (Cu-Au) deposit type, has been advocated by Tornos *et al.* (2003). This iron oxide mineralisation might be indicative of a vertical magmatic-hydrothermal continuum.

Gold-copper mineralisation is related in space to the metaluminous plutons. This includes Cu-Bi-Au veins, Au-only disseminations within leucogranites, and reconcentration along shear bands. This mineralisation is always younger than the iron oxide type. Furthermore iron oxide were a preferential host rock for the Au-Cu ores. In fact, oxidised environments destabilise thiosulphide complexes, such as those of Cu, Bi and Au, but not chloride complexes, such as Zn, Pb or Ag.

Late orogenic peraluminous granodiorites to granites with poorly constrained ages between 310 and 280 Ma, are related to a different style of mineralisation. Cu-Pb-Zn perigranitic veins display intra- and peri-plutonic zoning with respect to the biotite granite type of the Pedroches plutonic massif (Ovtrach and Tamain, 1977). However, there is no evidence as to the involvement of igneous fluids in these systems. The pluton probably acted as a heat source only. Reduced meteoric water was involved in large convective cells around the pluton. The metals were leached out from the host rocks and precipitated in a temperature-dependent concentric pattern, with chalcopyrite in the inner part and galena in the outer part. The presence of barite and fluorite veins in the district suggests that mixing with cool, oxidising meteoric waters took also place near the surface.

Younger peraluminous leucogranites display characteristic hydrothermal alterations. Tungsten-rich vein fields are found near outcropping or hidden, granitic cupolas in the Pedroches, San Nicolás, La Bazana and Oliva de Frontera areas. They are similar to those found elsewhere in the Iberian Variscan Belt (Tornos and Gumiel, 1992). These vein systems are representative of different depths, from deep systems as at La Bazana, to veins related to hidden granites, such as those at Oliva de la Frontera. Distal Zn-rich skarns, bismuth-rich veins and Sn replacements might also be related to these late leucogranites.

Late Variscan wrench faulting and associated felsic-mafic magmatism were probably responsible for replacive and vein-like mineralisation in the Usagre area. Assemblages of Hg-, Sb-, As-, Pb- and Ba-bearing minerals, fluid inclusion data and regional alteration patterns, resemble those of epithermal deposits. Probably synchronous to the former are the widespread Pb-Zn veins near or within the Tomar-Córdoba Shear Zone. They formed from low temperature (<250º C) convective meteoric waters. Heat was apparently furnished by small intrusive bodies within the shear zone.

The Late Variscan –or younger- hydrothermal activity apparently unrelated to igneous activity of any kind is well established. Metals were extracted from either sedimentary-diagenetic disseminations in host rocks or earlier concentrations, and deposited along fault segments of variable direction through boiling, cooling or fluid mixing processes at rather low temperatures (<250ºC) and depths. The main metal associations of this stage are Cu(Zn-Pb) and Sb-Cu(-As-Au).

The post-Variscan hydrothermal activity

The onset of the Alpine rifting led to fracture reactivation and renewed hydrothermal activity. Minor barite and uranium vein-like mineralisation were formed at this stage.

3.2. Tectonic environment: A vertical continuum in an oblique setting

The strong dismembering induced by Variscan tectonics precludes any interpretation of the original relationship between the different pre-Variscan deposits. However, the study of the Variscan metallogenesis shows that there is a straightforward link between oblique tectonics and ore-forming processes. Such a relation of mineral deposits to transpressional deformation was first documented by Sanderson *et al.* (1991) north of the Tomar-Córdoba Shear Zone and has been recently proposed for the OMZ and South Portuguese Zone by Tornos *et al.* (2002).

In fact, it is possible to envisage a rather continuous vertical evolution of the hydrothermal systems during Variscan times. The common link between most of the Variscan mineralisation is its relation to extensional crustal domains associated with strike slip zones, including pull-apart basins and structures in the shallow portion of the system (approx. less than 1-3 km depth), or more subtle structures, such as bending zones, in the lowermost system counterparts. As a whole, the different mineralisation styles define a continuum from deep pegmatites and orogenic-type gold-only veins and replacements to exhalative massive sulphide or oxide deposits. Following a theoretical model, the deep pegmatites should be overlain by the orogenic-type gold deposits and the Cu, Pb-Zn and Fe syn-metamorphic veins. The epizonal metaluminous magmatism is related to skarn, iron oxide replacements, Ni-(Cu) magmatic pipes and Cu-Au mineralisation, while the peraluminous magmatism is associated with different base metal veins, W-Sn, greisens and replacements. Finally, the shallow hydrothermal systems should include epithermal-like Hg replacements and Pb-Zn veins, besides (sub)-exhalative massive sulphides and iron oxides.

3.3. The alternating mineralising zones

Perhaps the more intriguing feature of OMZ is the existence of several alternating Zn-Pb(-Cu) and Fe(-Cu) NW-SE to WNW-ESE belts some hundred km long and about 10-50 km wide, that are subparallel to the main Variscan structures. The North Eastern Belt, is characterised by a complex metallogeny, with very different styles of mineralisation, including Zn-Cu-Pb volcanic-hosted massive sulphides, Sn replacements and perigranitic W-(Sn), Cu, Zn-Pb, Bi-(Co-Ni) and barite-fluorite veins, all formed at small depths. Lead isotope data (Tornos and Chiaradia, 2004) suggest that metals were scavenged from a crustal source with an isotopic signature intermediate between those of the OMZ and the Central-Iberian Zone. This mixed signature was expected from geological models (e.g., Quesada *et al.*, 1987). Thus, the Obejo-Valsequillo-Puebla de la Reina Domain has a typical OMZ basement, overlain by a Paleozoic sequence similar to that of the Central-Iberian Zone. The Arronches-Córdoba Belt contain Zn-Pb mineralisation, both as stratabound deposits of Proterozoic age as veins. Moreover significant orogenic gold mineralisation also occurs in the Portuguese part of this belt. Zn-Pb mineralisation is also common in the North Central Belt, largely as veins. The Olivenza-Monesterio Belt shows the largest variety of ore deposits of the OMZ. Most of the Fe-(Cu) orebodies of the area are found within this belt, including pre-Variscan and Variscan volcano-sedimentary ores, Variscan skarns, karst fillings and veins. Remarkable is the existence of syn-orogenic orthomagmatic Ni (-Cu) deposits related to the Variscan magmatic arc plutons. The South Central Belt contains few ore deposits, particularly stratabound Fe-Mn, Cu and P prospects. The Évora-Aracena Belt is dominated again by Zn-Pb-(Cu)-bearing orebodies, but orogenic-type Au mineralisation also occurs. Cu, along with other metals (Ni, Ag, Au, ...) regains importance in the S. Cristóvão-Beja-Serpa Belt. Finally Cr and Cu disseminations (along with Ni and Co) are of local importance in the Acebuches Ophiolite Belt.

Locutura *et al.* (1990) interpreted that differences among the ore belts reflected crustal heterogeneities within the OMZ. However, recent lead isotope data do not show significant differences among the various metallogenic belts (Tornos and Chiaradia, 2004). In consequence other variables had to play a role in explaining metal diversification. These might include variations in the composition of the metal reservoir, that could not be traced by lead isotopes, and distinct P-T conditions of transport and precipitation of the metals, Cu mineralisation usually forming at higher temperature than Zn-Pb ores.

The OMZ represents a somewhat unique group of different metallogenic belts, with a non-conventional metallogenesis and zoning that cannot be easily explained on the basis of current geotectonic ore evolution models. The pre-Variscan metallogenesis can be tentatively explained on the basis of an Andean-type active continental margin with a magmatic belt and related basin. This was followed by post-orogenic extension. However, Variscan metallogenesis although related again to a magmatic arc setting is dramatically different. Variscan mineral deposits include peculiar hydrothermal iron oxide, magmatic Ni-(Cu) or Sn replacements, but scarce volcanic-hosted massive sulphide deposits. According to the present state of knowledge, this metallogenesis in an active magmatic arc can only be satisfactorily explained by invoking dominant strike slip deformation and synchronous magma emplacement (Tornos *et al.*, 2002). A distinct geological feature of Variscan age is the deep, probably mafic and ultramafic body, recognised through seismic work all beneath the OMZ (Simancas *et al.*, 2003). It probably played a significative role in the genesis of some ore deposits, particularly some Fe orebodies and Cu-(Ni) mineralisation in the Olivenza-Monesterio Belt and San Cristovao-Beja-Serpa Belt. Why this hidden body was intruded in the middle crust during Variscan orogenesis is still uncertain. A transpressional regime of deformation during Variscan orogeny was characteristic in the OMZ both during subduction and further collision with the South Portuguese Zone.

References

Aalten, A., Steenbruggen. A. (1997): *Syngenetic mineralization and dolomitization in the Carrasca prospect, south-east Portugal*. MSc thesis, Institute of Earth Sciences, Univ. Utrecht, Utrecht, Netherlands.

Abalos, B., Gil Ibarguchi, J. I., Eguiluz, L. (1991): Cadomian

subduction/collision and Variscan transpression in the Badajoz Cordoba shear belt, southwest Spain. *Tectonophysics*, 199: 51-72

Andrade, A. S. (1974): Sur l'age des orthogneiss d'Alcáçovas (Alentejo) et des filons (basiques et acides) que les recoupent. *Mem. Not. Museu Lab. Mineral. Geol. Univ. Coimbra*, 18: 29-36.

Andrade, A. S. (1983): *Contribuition à l'analyse de la suture Hercyniènne de Beja (Portugal), perspectives metallogéniques*. Ph.D. thesis, INLP, Univ. Nancy, Nancy, France.

Apalategui, O., Eguiluz, L., Quesada, C. (1990): Ossa-Morena Zone: Structure. In: E. Martinez and R. D. Dallmeyer (eds.) *Pre-Mesozoic Geology of Iberia*, Springer Verlag, 280-291.

Arribas, A. (1962a): Mineralogía y metalogenia de los yacimientos españoles de uranio: Burguillos del Cerro (Badajoz). *Estudios Geológicos*, 28: 173-192.

Arribas, A. (1962b): Mineralogía y metalogenia de los yacimientos españoles de Uranio: Monesterio (Badajoz). *Notas Comunicaciones IGME*,70: 47-69.

Arribas, A. (1963): Mineralogía y metalogenia de los yacimientos españoles de uranio: Los indicios con davidita de Villanueva del Fresno (Badajoz). *Estudios Geológicos*, 19: 33-51

Arribas, A. (1964): Mineralogia y metalogenia de los yacimientos españoles de uranio: Cardeña (Córdoba). *Notas Comunicaciones IGME*, 76: 45-78.

Arribas, A., Bechstadt, T., Boni, M. (1990): Stratabound ore deposits related to synsedimentary tectonics: South west Sardinia (Italy) and Sierra de Aracena (Spain); a comparision. *Geologische.Rundschau*, 79-2: 373-386.

Arriola, A., Cueto, L., Fernández, J., Garrote, A. (1981): Serpentinitas y mineralizaciones asociadas en el Proterozoico Superior de Ossa Morena. *II Reunión Grupo Ossa Morena*, 137-145.

Asensio, B., Sierra, J., Arribas, A. (1997): Exploration implications of large temperature and salinity variations in Cu-bearing vs barren quartz veins in Sierra Morena, Spain. *Abstracts XIV ECROFI*, Nancy, Francia, 14-15.

Bachiller, N., Casquet, C., Galindo, C., Quílez, E. (1997): Hydrothermal alterations in leucogranites from the Burguillos del Cerro intrusive complex (Badajoz, SW Spain)- Evidence for pulsatile mixing of igneous and meteoric fluids. In: H. Papunen (ed.) *Mineral deposits: research and exploration*, Balkema, Rotterdam: 605-608.

Baeza, L., Ruiz, C., Ruiz, M., Sánchez, A. (1981): Mineralización exhalativo sedimentaria de sulfuros polimetálicos en la Sierra Morena Cordobesa (España). *Boletín Geológico Minero*, 92-3: 203-216.

Baeza, L., Ruiz, C., Ruiz Montes, M. (1978): Presencia de formaciones volcanosedimentarias y mineralizaciones de hierro asociadas en el eje magmático La Coronada-Villaviciosa (Córdoba). *Boletín Geológico Minero*, 89-5: 431-437.

Barrie, C.T., Hannington, M.D. (1999): Classification of volcanic-associated massive sulfide deposits based on host rock composition. In: C. Y. Barrie, M. D. Hannington (eds.) *Volcanic associated massive sulfide deposits: Processes and examples in modern and ancient settings*, Reviews Economic Geology, 8: 1-11.

Barros, J. (1968): Jazigo cuprífero de Aparis. Relatório interno S.F.M. dos trabalhos efectuados entre 1959 e 1964, Lisboa, Portugal (internal, non-published report).

Barroso, M. (2002): Caracterização mineralógica e textural das mineralizações sulfuretadas da jazida de Enfermarias (Moura, Portugal). M.Sc. Thesis, Univ. Lisboa, Lisboa, Portugal, 208 p.

Beck, J. (1996): Report for IGM of Outokumpu exploration in Alter do Chão-Elvas area in 1996 and program for 1997: Madrid, Outokumpu Base Metals Oy, 56 p. (16 annexes).

Beck, J. (1997): Report for IGM of Outokumpu exploration in Alter do Chão-Elvas area in Febr.-Aug. 1997: Madrid, Outokumpu Base Metals Oy, 21 p. (8 annexes).

Canales, A., Matas, J. (1992): Anomalías de Au en el flanco Sur del Anticlinorio de Olivenza-Monesterio. In: I. Rábano, J. C. Gutierrez Marco (eds.) *Libro de Resúmenes. VIII Reunión de Ossa Morena*, 53.

Carvalho, D. (1971): Observações sobre os jazigos de ferro da área Pedrógão-Orada. *Proc. 1st Congresso Hispano-Luso-Americano de Geologia Económica*, Madrid-Lisboa, 1, 519-537.

Carvalho, D. (1976): Les gisements de fer du Portugal. In: *Iron Ore Deposits of Europe*. Hannover, 255-260.

Carvalho, D., Goinhas, J., Oliveira,V., Ribeiro, A. (1971): Observações sobre a geologia do Sul de Portugal e consequências metalogenéticas. *Est. Notas e Trab. Serv. Fom. Min*., 20: 153-199.

Carvalho, D., Oliveira, V. (1992): Recursos minerais metálicos. In: J T. Oliveira (ed.). Notícia Explicativa da Folha 8 da Carta Geológica de Portugal, escala 1:200.000, p. 81-83.

Carvalho, J. P. L. (1988): Contribuição para o estudo dos jazigos de Algares de Portel e Balsa (Portel, Alentejo). Provas de Aptidão Pedagógica e Capacidade Científica, Dep. Geologia da Faculdade de Ciências da Univ. Lisboa, Lisboa, Portugal.

Carvalhosa, A. B., Zbyszewski, G. (1972): Notícia explicativa da carta geológica nº 40-C (Viana do Alentejo), escala 1: 50000: Lisboa, Serviços Geológicos de Portugal, 24 p.

Casquet, C. (1980): *Fenómenos de endomorfismo, metamorfismo y metasomatismo en los mármoles de la Rivera de Cala (Sierra Morena)*. Ph.D. Thesis, UCM: 295 p.

Casquet, C., Eguiluz, L., Galindo, C., Tornos, F., Velasco, F. (1998): The Aguablanca Cu-Ni(PGE) intraplutonic ore deposit (Extremadura, Spain). Isotope (Sr, Nd, S) constraints on the source and evolution of magmas and sulfides. *Geogaceta*: 24, 71-74.

Casquet, C., Galindo, C., Darbyshire, D.P.F., Noble, S.R., Tornos, F. (1998): Fe-U-REE mineralization at Mina Monchi, Burguillos del Cerro, Spain: age and isotope (U-Pb, Rb-Sr and Sm-Nd) constraints on the evolution of the ores. Proceedings GAC-MAC-APGGQ Quebec 98 Conference, 23, A28.

Casquet, C., Galindo, C., Tornos, F., Velasco, F. (2001): The Aguablanca Cu-Ni ore deposit (Extremadura, Spain), a case of synorogenic orthomagmatic mineralization: Isotope composition of magmas (Sr, Nd) and ore (S). *Ore Geology Reviews*, 18: 237-250.

Casquet, C., Tornos, F. (1991): Influence of depth and igneous geochemistry on ore development in skarns: The Hercynian

Belt of the Iberian Peninsula. In: A. Augusthitis (ed) *Skarns, their petrology and metallogeny*, Athens, 555-591.

Casquet, C., Velasco, F. (1978): Contribución a la geología de los skarns cálcicos en torno a Santa Olalla de Cala (Huelva-Badajoz). *Estudios Geológicos*, 34: 399-405.

Cerveira, A. (1972): As minas de cobre de Miguel Vacas. Relatório nº1, EMIL – Emp. de Mineraçao SARL, Porto, Portugal (internal, non-published report).

Cerveira, A. (1975): Ante-projecto para entrada em exploração da Mina de cobre de Vila Viçosa ou de "Miguel Vacas". Relatório 2, EMIL – Emp. de Mineraçao SARL, Porto, Portugal (internal, unpublished report).

Chacón, J., Herrero, J.M., Velasco, F. (1981): Las mineralizaciones de Zn-Pb de Llera (Badajoz). *I Congreso Español Geología*, 2: 447-455.

Coma, F., Alberdi, T., Matas, J., Pérez, H., Vaquero, A. (1988): Estado de la investigación sobre las mineralizaciones de oro en el anticlinorio Olivenza-Monesterio. Actas VIII Congreso Internacional Minería Metalurgia.

Conde, C., Tornos, F., Baeza, L. (2001): Los sulfuros masivos cadomienses de Puebla de la Reina (Badajoz). *Boletín Sociedad Española Mineralogía*, 24-A: 153-154.

Coullaut, J.L. (1979): Geología y metalogenia del criadero de San Guillermo Colmenar, Jerez de los Caballeros, Badajoz. *I Curso Rosso de Luna*, IGME: 1-20.

Coullaut, J.L., Babiano, F., Fernández, J. (1980): Mineralizaciones de hierro del Soroeste de España. Mina La Valera. Jornadas Sidero Metalúrgicas Huelva, 97-108.

Cozar, P., Rodriguez, S. (1999): Evolución sedimentaria del Carbonifero Inferior del área del Guadiato. *Boletín Geológico y Minero,* 110: 663-680.

Crespo, A. (1987): El macizo de Aracena (macizo Iberico meridional): Propuesta de división sobre la base de nuevos datos estructurales y petrográficos. *Boletín Geológico Minero*, 98-4: 507-515.

Crespo, A. (1989): *Evolución geotectónica del contacto entre la Zona de Ossa Morena y la Zona Surportuguesa en las Sierras de Aracena y Aroche (Macizo Iberico Meridional): un contacto mayor en la Cadena Hercínica Europea.* Ph.D.Thesis, Univ. Sevilla, Spain.

Cuervo, S., Tornos, F., Spiro, B., Casquet, C. (1996): El origen de los fluidos hidrotermales en el skarn férrico de Colmenar-Santa Bárbara (Zona de Ossa Morena). *Geogaceta*, 20-7: 1499-1500.

Dallmeyer, R.D., Fonseca, P.E., Quesada, C., Ribeiro, A. (1993). ^{40}Ar/^{39}Ar mineral age constraints to the tectonothermal evolution of the Variscan Suture in SW Iberian. *Tectonophysics*, 222: 177-194.

Dallmeyer, R.D., García Casquero, J.L., Quesada, C. (1995): ^{40}Ar/^{39}Ar mineral age constraints on the emplacement of the Burguillos del Cerro Igneous Complex (Ossa-Morena Zone, SW Spain). *Boletín Geológico Minero*, 106: 203-214.

Darbyshire, D.P.F., Tornos, F., Galindo, C., Casquet, C. (1998): Sm-Nd and Rb-Sr constraints on the age and origin of magnetite mineralization in the Jerez de los Caballeros iron district of Extremadura, SW Spain. ICOG-9, *Chinese Science Bulletin*, 43: 28.

Delgado, M., Pascual, E., Fenoll, P. (1978): A geological and metallogenic study of some occurrences of magnetite and sulphides in Sierra Morena (NNW of Córdoba, Spain). *Estudios Geológicos*, 34: 461-474.

Domergue, C. (1987): *Catalogue des mines et des fonderies antiques de la Peninsule Iberique*. Publ.Casa Velazquez, serie archeologie,VIII, 2 tomes.

Dupont, R. (1979): *Cadre geologique et metallogenese des gisements de fer du sud de la province de Badajoz (Sierra Morena Occidentale-Spagne)*. Ph.D.Thesis Inst.Nat. Polyt. Lorraine.

Eguíluz, L., Gil Ibarguchi, J.I., Abalos, B., Apraiz, A. (2000): Superposed hercynian and cadomian orogenic cycles in the Ossa-Morena Zone and related areas of the Iberian Massif. *Geological Society America Bulletin*, 112-9: 1398-1413.

Einaudi, M. T., Meinert, L. D., Newberry, R. J. (1981): Skarn deposits. In: B. Skinner (ed) *Economic Geology, 75 anniversary volume*, 317-391.

Faria, A.F. (1997): Report for IGM of Potuglobal gold exploration in Montemor-o-Novo area in Jan.-Jun. 1997: Montemor-o-Novo, Portuglobal-Moriminas, 13 p. (7 annexes).

Fernández Caliani, J. C., Moreno Ventas, I., Miras, A., Requena, A. (2002): Nódulos de wollastonita en mármoles de alta temperatura de la banda metamórfica de Aracena (Huelva): ¿Origen metamórfico o metasomático? *Boletin Sociedad Española de Mineralogia*, 25A: 31-32.

Fernández Caliani, J.C., Requena, A., Sáez, R., Ruiz De Almodóvar, G. (1989): Las mineralizaciones de Pb-Zn asociadas a rocas carbonatadas en el sector de Fuenteheridos, Huelva. *Studia Geol.*, 4: 7-15.

Florido, P. (1993): *Síntesis geológica y minera de la mina Maria Luisa*. Informe interno ITGE, 17 p.

Fonseca, P. (1999): *Prospecção geofísica por métodos magnéticos de componente vertical e total em Odivelas- Ferreira do Alentejo*. Relatório preliminar de projecto, DPMM – IGM, Lisboa, Portugal (internal, non-published report).

Gabaldón, V., Garrote, A., Quesada, C. (1985): El Carbonífero Inferior del Norte de la Zona de Ossa Morena (SW de España). *Proceedings X Congreso Geología Carbonífero*, IGME, 173-185.

Galindo, C., Darbyshire, F., Tornos, F., Casquet, C., Cuervo, S. (1995): Sm-Nd geochemistry and dating of magnetites: A case study from an Fe district in the SW of Spain. In: J. Pasava, B. Kribek, K. Zak (eds.) *Mineral Deposits: From their origin to environmental impacts*, Balkema, Rotterdam, 41-43.

Galindo, C., Tornos, F., Darbyshire, D.P.F., Casquet, C. (1994): The age and origin of the barite-fluorite (Pb-Zn) veins of the Sierra del Guadarrama (Spanish Central System): a radiogenic (Nd, Sr) and stable isotope study. *Chemical.Geology.*, 112: 351-364.

Gaspar, O. (1967): Micrografia dos sulfuretos de Algares de Portel e sua contribuição para o esclarecimento da génese desta ocorrência. *Est. Notas e Trab. Serv. Fom. Min.*, XVIII (1-2): 237-251.

Gaspar, O. (1968): O jazigo de cobre de Aparis. *Est. Notas e Trab. Serv. Fom. Min.*, XVIII (3-4): 253-290.

Goinhas, J. A C. (1971a): Jazigos de Algares e Balsa (Portel). *Proc. 1st Congresso Hispano-Luso-Americano de Geologia Económica*, Madrid-Lisboa, 1: 89-94.

Goinhas, J. A. C. (1971b): Minas de Vila Ruiva e Preguiça. *Proc. 1ˢᵗ Congresso Hispano-Luso-Americano de Geologia Econó-mica*, Madrid-Lisboa, 1: 78-84.

Goinhas, J. A. C., Martins, L.M.P. (1986): Área metalífera de Montemor-o-Novo – Casa Branca (Baixo Alentejo, Portugal). *Estudos, Notas e Trabalhos Serviço Fomento Mineiro*, 28: 119-148.

Goinhas, J. A. C., Martins, L.M.P. (1988): Alguns trabalhos de prospecção desenvolvidos no maciço de Èvora (Áreas de Vimeiro-Azaruja, S. Marcos do Campo e Mourão): *Estudos, Notas e Trabalhos Serviço Fomento Mineiro*, 30: 89-109.

Gomes, A., Barros, J., Araújo, C. (1959): *O jazigo de cobre de Aparis*. Relatório interno S.F.M. dos trabalhos efectuados entre 1956 e 1958, Lisboa, Portugal (internal, non-published report).

Gonçalves, M.A., Mateus, A., Oliveira, V. (2001): Geochemi-cal anomaly separation by multifractal modeling. *Journal Geochemical Exploration*, 72: 91-114.

Gonçalves, F., Assunção, C. T. (1970): Notícia explicativa da carta geológica nº 37-A (Elvas), escala 1:50000. Lisboa, Ser-viços Geológicos de Portugal, 50 p.

Gonçalves, F., Zbyszewski, G., Coelho, A.V.P. (1975): Notícia Explicativa da carta geológica nº 32-D (Sousel), escala 1: 50000: Lisboa, Serviços Geológicos de Portugal, 49 p.

González del Tánago, J. (1991): Las pegmatitas graníticas de Sierra Albarrana (Córdoba,España): Minerales con boro y fósforo. *Boletín Sociedad Española de Mineralogía*, 14-1: 54-55.

González del Tánago, J., Peinado, M., Brändle, J.L. (1991): Contribución al estudio de las pegmatitas graníticas de Sierra Albarrana (Córdoba, España): Minerales con elementos raros. *Boletín Sociedad Española de Mineralogía*,14-1: 105-106.

Groves, D. I. (1993): The crustal continuum model for late-Ar-chean lode-gold deposits of the Yilgarn block, Western Aus-tralia. *Mineralium Deposita*, 28-6: 366-374.

Guillou, J. (1967): Situation et zonalité de mineralisations sul-furees dans un complexe volcano-sedimentaire (Cambrien de la Sierra Morena, Espagne). *C.R. Acad. Sci. Paris*, 264: D885-887

Gumiel, J. C. (1988): *Estudio geológico y metalogénico de la mineralización de W-Sn-Bi-Mo asociada a la cúpula granítica de San Nicolás (Valle de la Serena, Badajoz)*. Unpublished M.Sc.Thesis, Universidad Complutense Madrid, 221 p.

Gumiel, P., Lunar, R., Sierra, J., López, J. A. (1987): Contri-bución al conocimiento de las mineralizaciones de W, Bi del distrito de Oliva de la Frontera (Badajoz). *Revista Materiales Procesos Geológicos*, I: 229-248.

Gutierrez Marcos, J. C., Lunar, R., Amorós, J. L. (1984): Los depósitos de hierro oolítico en el Ordovícico de España. *I Congreso Español Geologia*, II: 501-525.

Hernández, M. J., Miras, A. (1993): Geochemistry and minera-logenesis of the barite deposits in southwestern Spain. In: P. Fenoll, J. Torres, F. Gervilla(eds.) *Current Research in geolo-gy applied to ore deposits*, 683-686.

Hitzman, M. W., Oreskes, N., Einaudi, M. T. (1992): Geological characteristics and tectonic setting of Proterozoic iron-oxide (Cu-U-Au-REE) deposits. *Precambrian Research*, 58: 241-287

Hodgson, C.J. (1989): The structure of shear related, vein type gold deposits: A review. *Ore Geology Reviews*, 4: 231-273.

Hodgson, C. J. (1993): Mesothermal lode gold deposits. In: R. V. Kirkham, W. D. Sinclair R.I. Thorpe, J. M. Duke (eds.) *Mineral Deposit Modeling*, Geol.Soc.Canada Spec Paper 40: 635-678.

IGME (1980): Hoja Geológica 1/50000 núm.875 Jerez de los Caballeros Serie MAGNA.

IGME (1985): *Investigación de cromitas en la reserva de Calza-dilla de los Barros (Badajoz)*. Internal Report IGME, 11142.

IGME (1994): Mapa Metalogenético de España escala 1/200000, hoja nº67-68, Cheles-Villafranca de los Barros IGME.

IGME (2002): Inventario Nacional de Wollastonita IGME, 180 p.

IGME (2003): Mapa Metalogenético de Extremadura IGME-Junta de Extremadura (in press).

Inverno, C.M.C. (1975): Introdução ao estudo da área da Folha +70/-72 (Região de Santa Eulália-Barbacena), na escala de 1:5000. Relatório de Estágio Científico (5º ano), Faculdade Ciências, Univ. Lisboa, 40 p.

Inverno, C. M. C. (1997): A few gold prospects in Ossa-More-na Zone, Portugal. In: Estudos sobre a Geologia da Zona de Ossa Morena (Maciço Ibérico). *Livro de Homenagem ao Prof. Francisco Gonçalves*, Dep. Geociências da Univ. Évora, Évo-ra, Portugal, 283-292.

Inverno, C. M. C., Martins, L. M. P., Viegas, L. F. S., Oliveira, D. P. S. (1995): Eugeosyncline-type ("mesothermal") gold mineralization in Alter do Chão-Arronches, NE. Alentejo, Portugal. *Geological Society of America (GSA) Abstracts with Programs*, 27(6): p. A-66.

Jesus, A. P. (2002): *Fe-Ti-V mineralizations and sulphide occu-rrences in gabbroic rocks of the Beja Igneous Complex (Odi-velas – Ferreira do Alentejo)*. M.Sc. Thesis, Univ. Lisboa, Lisboa, Portugal.

Jiménez Millan, J., Ruiz de Almodóvar, G., Velilla, N. (1992): Litologías manganesíferas del área central de Ossa Morena (SW de Badajoz). *Geogaceta*, 12: 46-49.

Johnson, C.A., Cardellach, E., Tritlla, J., Hanan, B.B. (1996): Cierco Pb-Zn-Ag vein deposits: isotopic and fluid inclusion evidence for formation during the mesozoic extension in the Pyrenees of Spain. *Economic Geology*, 91-3: 497-506.

Kelly, W.C., Rye, R. O. (1979): Geologic, fluid inclusion and stable isotope studies of the tin- tungsten deposits of Panas-queira, Portugal. *Economic Geology*, 74: 1721-1819.

Kerrich, R., Wyman, D.A. (1990): The geodynamic setting of mesothermal gold deposits: an association with accretionary tectonic regimes. *Geology*, 18: 882-985.

Large, R.R., Blundell, D.L. (eds.) (2000): *Database on Global VMS districts*. CODES-GEODE, 179 p.

Liñán, E., Quesada, C. (1990): Ossa-Morena Zone: Stratigraphy, rift phase (Cambrian). In: E. Martinez, R. D. Dallmeyer (ed.) *Pre-Mesozoic Geology of Iberia*, Springer Verlag, 259-266.

Locutura, J., Tornos, F., Florido, P., Baeza, L. (1990): Ossa-Mo-rena Zone: Metallogeny. In: E. Martinez, R. D. Dallmeyer (ed) *Pre-Mesozoic Geology of Iberia*, Springer Verlag, 321-332.

Lunar, R., García Palomero, F., Ortega, L., Sierra, J., Moreno, T., Prichard, H. (1997): Ni-Cu-(PGM) mineralization associa-ted with mafic and ultramafic rocks: the recently discovered

Aguablanca ore deposit, SW Spain. In: H. Papunen (ed.) *Mineral deposits: research and exploration*, Balkema, Rotterdam, 463-466.

Marcoux, E. (1998): Lead isotope systematics in the giant massive sulphide deposits in the Iberian Pyrite belt. *Mineralium Deposita*, 33/1-2: 45-58.

Marcoux, E., Pascual, E., Onezime, J. (2002): Hydrothermalisme ante-Hercynien en Sud-Iberie: apport de la geochimie isotopique du plomb. *C.R. Geoscience*, 334: 259-265.

Martins, R. (2002): *Caracterização dos processos metassomáticos correlativos da recristalização e deposição de sulfuretos na jazida de Enfermarias (Moura, Portugal)*. M.Sc. Thesis, Univ. Lisboa, Portugal.

Massano, C. (1988): *Mineralizações do tipo epitermal em pórfiros da região de Alcaçovas*. Relatório de Estágio Científico, Departamento de Geologia da Faculdade de Ciências da Univ. Lisboa, Lisboa, Portugal.

Mateus, A., Araújo, A., Matos, J. (1999a): Análise estrutural e caracterização mineralógico-geoquímica da mina de ferro de Azenhas II (Pedrógão, Zona de Ossa Morena). *5ª Conferência Nacional do Grupo de Geologia Estrutural e Tectónica*, Vila Real, Portugal: 58-65.

Mateus, A., Figueiras, J. (1999a): Chemical composition of Cr-spinels in deformed and metamorphosed ultramafic/mafic complexes from Portugal; can it be used as an ore-guide for Ni-Cu sulphide mineralizations? *Actas II Congreso Ibérico de Geoquímica, XI Semana de Geoquímica, Lisboa, Portugal*: 255-258.

Mateus, A., Figueiras, J. (1999b): Chondrite-normalised PGE patterns of deformed and metamorphosed peridotites from Portugal. *Actas II Congreso Ibérico de Geoquímica, XI Semana de Geoquímica, Lisboa, Portugal*: 269-272.

Mateus, A., Figueiras, J., Gonçalves, M.A., Fonseca, P. (1998a): Sulphide disseminations in metatroctolites of the Beja-Acebuches Ophiolite Complex; their genesis and geological meaning. *Comun. Inst. Geol. e Mineiro*, 84(2): F7-F10.

Mateus, A., Figueiras, J., Gonçalves, M.A., Fonseca, P. (1999b): Evolving fluid circulation within the Variscan Beja-Acebuches Ophiolite Complex (SE, Portugal). *Ofioliti*, 24: 269-282.

Mateus, A., Jesus, A. P., Conceição, P., Oliveira, V., Rosa, C. (2001a): Natureza mineralógica e geoquímica das mineralizações sulfuretadas em gabros do Complexo Ígneo de Beja; algumas questões relativas à sua génese. *Actas VI Congresso de Geoquímica dos Países de Língua Portuguesa, XII Semana de Geoquímica*, Faro, Portugal: 125-129.

Mateus, A., Jesus, A. P., Oliveira, V., Gonçalves, M. A., Rosa, C. (2001b): Vanadiferous iron-titanium ores in gabbroic series of the Beja Igneous Complex (Odivelas, Portugal); remarks on their possible economic interest. *Est., Notas e Trab. Inst. Geol. e Mineiro*, 43: 3-16.

Mateus, A., Matos, J. X., Rosa, C., Oliveira, V. (2003): Cu-ores in quartz-carbonate veins at Estremoz-Alandroal and Barrancos-Santo Aleixo regions (Ossa-Morena Zone): A result of Late-Variscan hydrothermal activity? *Actas do VI Congresso Nacional de Geologia, Cîencias da Terra (Univ. Nova Lisboa),* Volume Especial V, p. 80 (CD-ROM F90-F93).

Mateus, A., Oliveira, V., Gonçalves, M. A., Figueiras, J., Fonse-

ca, P., Martins, L. (1998b): General assessment on the metallogenetic potential of the Iberian Terrane southern border. *Est., Notas e Trab. Inst. Geol. e Mineiro*, 40: 35-40.

Mateus, A., Waerenborgh, J. C., Figueiras, J., Gonçalves, M. A., Fonseca, P. (1998c): Mineralizações em metais preciosos na Zona de Ossa Morena (ESE-SE de Portugal). Projecto PBICT/P/CTA/2112/95 do Programa de Investigação Científica e Tecnológica, Fundação para a Ciência e Tecnologia, Portugal, Relatório Final.

Matos, J., Araújo, A., Mateus, A. (1998): Cartografia de detalhe e controlo estrutural das mineralizações na região de Pedrógão-Orada. *4ª Conferência Anual do Grupo de Geologia Estrutural e Tectónica, Porto, Portugal, Geologos*, 2: 101-104.

Meinert, L.D. (1993): Skarns and skarn deposits. In: P. Sheahan, M. E. Cherry (eds.) *Ore deposit models*, vol.II, Geoscience Canada reprint series 6: 117-134

Mendes, F. (1967). *Interesse económico da Mina de Aparis*. Relatório interno, Direcção Geral de Minas e Serviços Geológicos, Lisboa, Portugal (internal, non-published report).

Miras, A. (1991): *Geoquímica y mineralogénesis de los depósitos de barita de Badajoz y Sevilla (Zona central de Ossa Morena)*. Ph.D.Thesis, Univ. Sevilla, 481 p.

Montero, P., Salman, K., Bea, F., Azor, A., Expósito, I., Lodeiro, F., Martínez Poyatos, D., Simancas, F. (2000): New data on the geochronology of the Ossa-Morena Zone, Iberian Massif. *Variscan Appalachian dynamics: The building of the Upper Paleozoic basement.* Galicia 2000. Abstracts.

Moro, M. C., Gil Agero, J. M., Cembrabos, M. I., Pérez del Villar, L.,Fernández, A., Hernández, E. (1992): Características de las mineralizaciones de variscita asociadas a los materiales silúricos del sinforme de Terena, Encinasola (provincia de Huelva). Comparación con los de la provincia de Zamora. *Boletín Sociedad Española Mineralogía*, 15: 79-90.

Munhá, J., Oliveira , J. T., Ribeiro, A., Oliveira, V., Quesada, C., Kerrich, R. (1986): Beja-Acebuches ophiolite; characterization and geodynamic significance. *Maleo*, 2(13): 31.

Munhá, J., Ribeiro, A., Fonseca, P., Oliveira, J. T., Castro, P., Quesada, A. C. (1989): Accreted terranes in Southern Iberia: Beja-Acebuches ophiolite and related oceanic sequences. *28th Int. Geol. Cong. (Washington, U.S.A.), Abstracts with programs*, 2: 481-482.

Neiva, J. M. C. (1952): Les mineraux de fer portugais. *Est. Notas e Trab. Serv. Fom. Min.*, 7: 281-293.

Oliveira, D. P. S. (2001): *The nature and origin of gold mineralization in the Tomar Cordoba Shear Zone, Ossa-Morena Zone, east central Portugal*. PhD thesis, University of the Witwatersrand, Rep. South Africa, 351 p.

Oliveira, D. P. S., Robb, L. J., Inverno, C. M. C. (2001a): The São Martinho gold occurrence, NE Ossa-Morena Zone, Portugal. In: Piestrzynki *et al.*, *Mineral Deposits at the Beginning of the 21st Century: Lisse*, Balkema (Swets and Zeitlinger), Proceedings of the 6th Biennal SGA-SEG Meeting, Kraków, Poland, Aug. 2001, p. 791-793.

Oliveira, D. P. S., Shepherd, T., Naden, J., Yao, Y. (2001b), Evidence for a late magmatic gold remobilising event in a mesothermal temperature setting at São Martinho, NE Ossa-Morena Zone, Portugal. In: F. Noronha, A. Dória, A. Guedes

(eds.) *Abstracts of XVI ECROFI European Current Reseach On Fluid Inclusions*, Porto, May 2001: Depto. Geologia, Faculdade de Ciências do Porto, Memória 7: 349-351.

Oliveira, J. T., Oliveira, V., Piçarra, J. M. (1991): Traços gerais da evolução tectono-estratigráfica da Zona de Osa Morena em Portugal. *Cuad. Lab. Xeol. Laxe*, 16: 221-250.

Oliveira, V. (1984): Rochas ígneas e recursos minerais. In: J.Perdigâo, J. T. Oliveira, A. Ribeiro (cords.) Notícia Explicativa de Folha nº 44-B (Barrancos) da Carta Geológica de Portugal, escala 1:50.000: Lisboa, Serviços Geológicos de Portugal.

Oliveira, V. (1984): Contribuição para o conhecimento geológico-mineiro da região do Alandroal-Juromenha (Alto Alentejo). *Est. Notas e Trab. Serv. Fom. Min.*, 26 (1-4): 103-126.

Oliveira, V. (1986): Prospecção de minérios metálicos a sul do Tejo. *Geociências-Revista da Univ. de Aveiro*, 1(1-2): 15-22.

Oliveira, V., Matos, J. (1992): Enquadramento geológico-mineiro da Jazida de Enfermarias (Faixa Magnetítico-Zincífera, Sector SW da Zona de Ossa Morena). In: I. Rábano, J.C. Gutiérrez-Marco (eds.) *VII Reunion del Grupo de Ossa Morena, Cáceres, España, Libro de Resúmenes*: 114-115.

Ordoñez, J.L., Molina, J., Urbano, R. (1992): Prospección de oro asociado a zonas de cizalla, Constantina, Sevilla. *Actas III Congreso Geología España*: 3, 405-409.

Ortega, L., Lunar, R., García Palomero, F., Moreno, T., Prichard, H. M. (2001): Removilización de minerales del grupo del platino en el yacimiento de Ni-Cu-EGP de Aguablanca (Badajoz) *Boletín Sociedad Española Mineralogia*, 24-A: 175-176.

Ortega, M., Fenoll, P., Garrote A. (1992): Los yacimientos de pegmatitas de Sierra Albarrana y otras áreas metamórficas del norte de la provincia de Córdoba. In: *Recursos Minerales de España*, CSIC, Textos Univ., 15: 471-486.

Ovtrach, A., Tamain, G. (1977): Tectonique, migration des centres chaudes et mineralisations dans le sud de la meseta iberique (Espagne). In: *Les roches plutoniques dans leurs rapports avec les gites mineraux*, Masson et cie., Paris, 191-211.

Patterson, D.J., Ohmoto, H, Solomon, M. (1981): Geological setting and genesis of cassiterite-sulfide mineralization at Renison Bell, Western Tasmania. *Economic Geology*, 76: 393-438.

Pereira, M. F., Silva, J. B., Chichorro, M. (2002): Field guide to Cadomia-2002 Workshop – The Cadomian basement of the Ossa-Morena Zone (Iberian Massif) in Northeast and West Alentejo, Portugal: Univ. Évora, 50 p.

Perroud, H., Bonhommet, N., Ribeiro, A. (1985): Paleomagnetism of Late Paleozoic igneous rocks from southern Portugal. *Geophysical Research Letters*, 12: 45-48.

Pin, C., Liñán, E., Pascual, E., Donaire, T., Valenzuela, E. (1999): Late proterozoic crustal growth in Ossa Morena: Nd isotope and trace element evidence from the Sierra de Cordoba volcanics. *XV Reunion Geologia Oeste Peninsular*, 215-218.

Pons, J. (1982): *Un modele d'evolution de complexes plutoniques: Gabbros et granitoides de la Sierra Morena Occidentale (Espagne)*. Ph.D. These, Trav. Lab. Geol. Petrol. Univ. P. Sabatier, Tolouse, 451pp.

Poole, F. G., Moro, M. C., Lopera, E., Arribas, A. (1990): Setting and origin of stratiform barite and associated rocks of the Hercynian orogen in Western Spain. *Abstracts VIII IAGOD*, Ottawa (Canadá), A21-A22.

Quesada, C. (1992): Evolución tectónica del Macizo Ibérico (una historia de crecimiento por acrecencia sucesiva de terrenos durante el Proterozoico Superior y Paleozoico). In: J. C. Gutierrez Marco, J. Saavedra, I. Rábano (eds.) *Paleozoico Inferior de Ibero-América*, Junta de Extremadura, 173-192

Quesada, C., Bellido, F., Dallmeyer, R. D., Gil Ibarguchi, I., Oliveira, T. J., Pérez Estaun, A., Ribeiro, A. (1991): Terranes within the Iberian Massif: Correlations with West Africa sequences. In: R. D. Dallmeyer (ed) *The West African orogens and circum atlantic correlations*, Springer Verlag, 162-194.

Quesada, C., Bellido, F., Gabaldon, V., Sanchez, T., Cueto, L.A. (2002): Definición y evaluación de guías geológicas y geofísicas para la exploración de materias primas minerales en el sector central de la Zona Ossa Morena en Extremadura. Final Report, FEDER-CICYT (1FD97-1177) project, IGME.

Quesada, C., Florido, P., Gumiel, P., Osborne, J., Larrea, F., Baeza, L., Ortega, C., Tornos, F., Sigüenza, J. (1987): *Mapa Geológico Minero de Extremadura*. Junta de Extremadura, 131 p.

Quesada, C., Fonseca, P., Munhá, J., Oliveira, J.T., Ribeiro, A. (1994): The Beja-Acebuches Ophiolite (Southern Iberian Variscan fold belt): geologic characterization and geodynamic significance. *Boletín Geologico y Minero*, 105: 3-44.

Relvas, J.M.R.S. (1987): *Alteração hidrotermal na área da Mina da Caerinha (Sta Susana): perspectiva metalogenética*. Relatório de Estágio Científico, Departamento de Geologia da Faculdade de Ciências da Univ. Lisboa, Lisboa, Portugal.

Rhoden, H. (1956): *Copper mines of the Barrancos region*. Relatório interno, Serviço de Fomento Mineiro, Lisboa, Portugal (internal, non-published report).

Ribeiro, C. (1994): *Estudo metalogenético da mineralização aurífera do Escoural (Évora)*. Provas de Aptidão Pedagógica e Capacidade Científica, Dep. Geociências da Univ. Évora, Évora, Portugal.

Ribeiro, C., Mateus, A., Barriga, F. J. A. S. (1993): Gold mineralizations of the Escoural area (Montemor, Évora, Portugal): a progress report. *Comun. XII Reunião de Geologia do Oeste Peninsular*, Évora, Portugal, 1: 215-226.

Rodas, M., Luque, F. J., Barreneceha, J. F., Fernández Caliani, J. C., Miras, A., Fernández Rodríguez, C. (2000): Graphite occurrences in the low pressure/high temperature metamorphic belt of the Sierra de Aracena (southern Iberian Massif). *Mineralogical Magazine*, 64-5: 801-814.

Rodriguez, S., Arribas, M.E., Comas-Rengifo, M. J., de la Peña, J. A., Falces, S., Kullmann, J., Gegundez, P., Legrand-Blain, M., Martinez-Chacón, M. L., Moreno-Eiris, E., Perejón, A., Sanchez, J. L., Sanchez-Chico, F., Sarmiento, G. (1992): Análisis paleontológico y sedimentológico de la cuenca carbonifera de los Santos de Maimona (Badajoz). *Coloquios de Paleontología,* 44: 1-303.

Roig, A., Canals, A. (1994): Caracterización de las condiciones de formación de Mina Berta (F-Pb-Zn) (Cadenas Costero Catalanas): datos mineralógicos y de inclusiones fluidas. *Boletín Sociedad Española de Mineralogía*, 17-1:194-195.

Ruiz de Almodóvar, R, G., Galán, E. (1984): Mineralizaciones de manganeso hierro del SW de Badajoz (Ossa Morena). *1er Congreso Español Geología*, II: 643-657.

Ruiz de Almodóvar, G., Galán, E., Pascual, E. (1984): Las rocas plutónicas del sector NW del anticlinorio de Olivenza Monesterio y su posible relación con mineralizaciones de Sn-W. *Publ. Mus. Lab. Mineral. Geol.Coimbra*, 98: 243-258.

Sanabria, R. (2001): *Caracterización y evolución de las mineralizaciones ferríferas y de los skarns del Coto Minero San Guillermo, Jerez de los Caballeros (Badajoz)*. M. Sc. Thesis Universidad Complutense de Madrid, 97 pp

Sánchez Carretero, R.., Eguíluz, L., Pascual, E., Carracedo, M. (1990): Ossa-Morena Zone: Igneous rocks. In: E. Martinez, R. D. Dallmeyer (eds), *Pre-Mesozoic Geology of Iberia*, Springer Verlag, 292-313.

Sanderson, D. J., Roberts, S., Mcgowan, A., Gumiel, P. (1991): Hercynian transpressional tectonics at the southern margin of the Central Iberian Zone, west Spain. *Journal. Geological Society London*, 148: 893-898.

Santos, J.F. (1990): *Petrologia do sector oeste da Unidade de Odivelas (Maciço de Beja)*. M.Sc. Thesis, Univ. Aveiro, Aveiro, Portugal.

Santos, J. F., Andrade, S. A., Munhá, J. (1990): Magmatismo orogénico Varisco no limite meridional da Zona de Ossa Morena. *Comun. Serv. Geol. Portugal*, 76: 91-124.

Schermerhorn, L. J. G. (1981): Framework and evolution of hercynian mineralization in the Iberian Meseta. *Leiden Geologische Mededelingen*, 52: 23-56.

Silva, J. M. (1945): Notas acerca do depósito de ferro de Odivelas. *Est. Notas e Trab. Serv. Fom. Min.*, 1: 286-292.

Silva, J. M. (1948): Gisements de fer du Sud du Portugal. *Est. Notas e Trab. Serv. Fom. Min.*, 4(1): 31-42.

Silva, J. M., (1949): Considerações sobre as formações cupríferas da regiâo de Barrancos. *Estudos, Notas e Trabalhos Serviço Fomento Mineiro,* 5, (1-2), p. 23-43.

Silva L.C., Quadrado, R., Ribeiro L. (1970): Nota prévia sobre a existência de uma estrutura zonada e de anortositos no maciço gabro-diorítico de Beja. *Bol. Mus. Lab. Min. Geol. Univ. Lisboa*, 11: 223-232.

Simancas, F., Carbonell, R., González Lodeiro, F., Perez Estaun, A., Juhlin, C., Ayarza, P., Kashubin, A., Azor, A., Martinez Poyatos, D., Almodovar, G. R., Pascual, E., Saez, R., Exposito, I. (2003): Crustal structure of the transpressional Variscan orogen in SW Iberia: SW Iberia deep seismic reflection profile (IBERSEIS). *Tectonics,* 22 (doi:10.1029/2002TC001479).

SIORMINP (2002): Sistema de Informação de Ocorrências e Recursos Minerais Portugueses: Lisboa, Instituto Geológico e Mineiro.

Stolz, A.J., Morrison, R.S. (1994): Proterozoic igneous activity in the Tennant Creek region, Northern Territory, Australia, and its relationship to Cu-Au-Bi mineralisation. *Mineralium Deposita*, 29-3: 261-274.

Thadeu, D. (1965): Notícia Explicativa da Carta Mineira de Portugal, escala 1:500000: Lisboa, Serviços Geológicos de Portugal, 46 p.

Thadeu, D, Aires-Barros, L. (1973): Influence du milieu et du processus de mise en place sur les gisements stanno-wolframitiques de Santa Eulália et de Góis (Portugal). In: *Les Roches Plutoniques dans leurs Reports avec les Gîtes Minéraux*, Paris, Masson et Cie.

Tornos, F., Baeza, L., Galindo, C. (2000): The Nava-Paredon orebody (SW Spain): a replacement massive sulfide in a shallow subaqueous setting. In: Gemmell,J.B., Pongratz,J. (eds.), *Volcanic environments and massive sulfide deposits, Program and Abstracts*, CODES, 215-216.

Tornos, F., Casquet, C., Galindo, C. (2003): Hydrothermal iron oxide (-Cu-Au) mineralization in SW Iberia: Evidence for a multiple origin. *Proceedings 7th Biennial SGA Meeting "Mineral Exploration and Sustainable Development"*, Athens.

Tornos, F., Casquet, C., Galindo, C., Velasco, F., Canales, A. (2001): A new style of Ni-Cu mineralization related to magmatic breccia pipes in a transpressional magmatic arc, Aguablanca, Spain. *Mineralium Deposita*, 36-7: 700-706.

Tornos, F., Casquet, C., Locutura, J., Collado, R. (1991): Fluid inclusion and geochemical evidence for fluid mixing in the genesis of Ba-F (Pb-Zn) lodes of the Spanish Central System. *Mineralogical Magazine*, 55: 225-234.

Tornos, F., Casquet, C., Relvas, J., Barriga, F., Sáez, R. (2002): Transpressional tectonics and ore deposit formation:The southwestern margin of the Iberian Variscan Belt:. In: D. Blundell, F. Neubauer, A. von Quadt (eds), *The timing and location of major ore deposits in an evolving orogen*. Geological Society, London, Special Publications 206: 179-198.

Tornos, F., Chiaradia, M. (2004): Plumbotectonic evolution of the Ossa-Morena Zone (Iberian Peninsula): Constraints from ore lead isotopes. *Economic Geology* (in press.).

Tornos, F., Gumiel, P. (1992): El wolframio y estaño: aspectos económicos y metalogénicos. *Recursos Minerales de España*, CSIC, Textos Univ.15: 379-394.

Tornos, F., Locutura, J. (1989): Mineralizaciones epitermales de Hg en Ossa Morena (Usagre, Badajoz). *Boletín Sociedad Española Mineralogía*, 12: 363-374.

Tornos, F., Velasco, F. (2002): The Sultana orebody (Ossa-Morena Zone, Spain): Insights into the evolution of Cu-(Au-Bi) mesothermal mineralization. *Abstracts GEODE Study Centre*, Grenoble, 25-28 Oct 2002.

Urbano, R. (1994): Exploración minera de yacimientos de oro por el Instituto Tecnológico Geominero de España. *Boletín Geologico y Minero*, 105-6: 537-549.

Vázquez, F. (1972): Génesis de la Mina Maria Luisa, La Nava (Huelva). Una mineralización zonada. *Boletín Geológico Minero*, 83-4: 377-386.

Vázquez, F. (1989): Mineral deposits of Spain. In *Mineral Deposits of Europe*, The Institution of Mining and Metallurgy, 4/5, 105-196.

Vázquez, F., Arteaga, R., Schemerhorn, J. J. (1980): Depósitos minerales del SO de la Península Ibérica. *Boletín Geológico Minero*, 91-2: 293-342.

Vázquez, F., Fernández Pompa, F. (1976): *Contribución al conocimiento geológico del SW de España en relación con la prospección de magnetitas*. Memorias Instituto Geológico y Minero de España, 89, 130 p.

Velasco, F., Amigó, J. M. (1981): Mineralogy and origin of the skarn from Cala (Huelva, Spain). *Economic Geology*, 76: 719-727.

Velasco, F., Casquet, C., Ortega, M., Rodriguez, J. (1981): Indicio de vermiculita en el skarn magnésico (aposkarn flogopíti-

co) de La Garrenchosa (Sta. Olalla, Huelva). *Boletín Sociedad Española Mineralogía*, 2: 135-149.

Velasco, F., Tornos, F., Pesquera, A., Peña, A. (1995): Metamorphic hydrothermal fluids in tonalite-hosted copper-gold vein mineralization. Mina Sultana (Cala, Huelva, Spain). *Boletín Sociedad Española Mineralogía*, 18-1: 263-264.

Zaw, K. M., Huston, D. L., Large, R.R., Mernagh, T., Hoffmann, C. F. (1994): Microthermometry and geochemistry of fluid inclusions from the Tennant Creek gold-copper deposits: implications for ore deposition and exploration. *Mineralium Deposita*, 29-3: 288-300.

The iron oxide -(Cu-Au) Deposits of SW Iberia

Fregenal-Burguillos-Cala District: Lat. 38°18' N, Long. 6°40' W

F Tornos [1], C. Casquet [2], L Rodriguez Pevida [3], & F Velasco [4]
[1] Instituto Geológico y Minero de España, c/Azafranal 48, 37002 Salamanca, Spain
[3] Facultad de Geología. Universidad Complutense de Madrid. 28040 Madrid, Spain
[2] Rio Narcea Nickel SA, Avda. Estación 22, 06300 Zafra, Badajoz, Spain
[4] Universidad del País Vasco, Facultad de Ciencias, Campus de Leioa, Apdo. 644. 48080 Bilbao, Spain

Producing mining district: Cala mine. Extensive exploration is taking place in the area.

Mining: Underground and open pit

Metals: Cu, Au, Fe

Past production: The iron production has been concentrated in 15 mines (1910-2003). Copper-gold production was only minor and concentrated in the Sultana mine (1903-1919) or as byproduct of iron ores. Equivalent Cu ores (no gold) in Abundancia Mine.

Total resources: >180 Mt @ 25-66%Fe and 0.11-0.4%Cu. Gold grades very irregular. Cu-Au ores about 1 Mt, 3.15%Cu, 15 g/t Au (Sultana)

Type: Iron oxide-rich endmember of iron-oxide-Cu-Au mineralization (IOCG). Cu-Au-rich ores as independent veins or as Au-Cu-rich zones in iron oxide deposits.

Morphology and alteration: Stratabound to lensoidal, locally discordant. The ironstone is related with: (a) structurally controlled albite-actinolite-salite alteration; (b) albite-actinolite rocks in the contact of albitite and host limestone and shale; (c) magnetite-vonsenite replacements; (d) massive calcic and magnesial skarn in roof pendants on the granitoids. Mineralized endoskarn are uncommon.

About 30% of ironstone is skarn and the remainder is related to albite-actinolite-salite replacement. Cu-Au ores occur as: (a) Cu-(Bi-Au) quartz-ankerite veins with sericite-albite-tourmaline-carbonate alteration. (b) Cu-(Au)-rich replacements on ironstone, associated with late amphibole, quartz and carbonates; (c) quartz veins with disseminated gold in late orogenic peraluminous granite (Tornos et al., 2003).

Age of mineralization: Lower Carboniferous, 350-330 Ma based on U-Pb and Sm-Nd dating of ores (Casquet et al., 1998).

Ore minerals: Magnetite, chalcopyrite, maldonite, native gold, bismuthinite, garnet.

Nature of host rocks: Calcsilicate hornfels, limestone and dolostone, schist and volcanic rocks of Late Neoproterozoic-Early Cambrian age (600-520 Ma) adjacent to Variscan (350-330 Ma) quartz-diorite to granodiorite.

Banded magnetite ore with sulphides hosting boudins of actinolite-(albite) rock. Colmenar
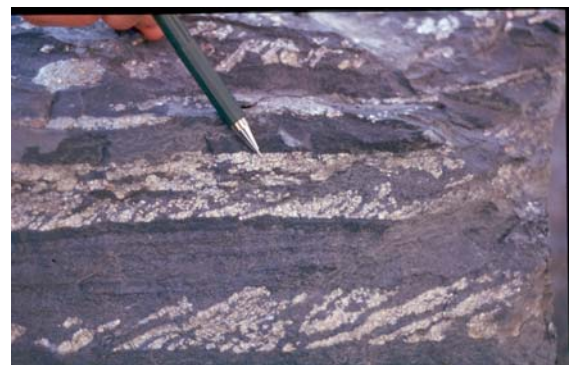
Magnetite ore replaced by pyrite along tensional planes. Cala Mine.

Isotope geochemistry of the iron ore suggest that the mineralization took place by reaction of the Ca-Al-bearing rocks by deep hot (>500ºC) volatile (B, F, P)-rich, saline, Na-Ca-Fe fluids having high

isotopic oxygen signatures ($\delta^{18}O$=9-12‰) had led to the formation of extensive zones of albite-actinolite-magnetite-(salite) replacement. The Cu-Au fluids are thought to have similar chemical and isotopic compositions but lower temperatures (290-420ºC) and behaved fluid unmixing or reaction with the ironstone (Tornos and Velasco, 2002). The sulphur seems to be scavenged from the host rocks ($\delta^{34}S$=11-20‰).

The formation of these unusual ores is interpreted as related with the intrusion at midcrustal levels of a mafic sill during the Variscan regional transpressional tectonics. Crustal delamination along the basal detachment and intrusion of the dyke produced extensive crust-magma interaction, crustal melting and widespread dehydration of sedimentary rocks. Large amounts of deep fluids and coetaneous metaluminous granitoids ascended along WNW-ESE to N-S transcrustal faults leading to the observed mineralization and related granitoids (Tornos & Casquet, in press).
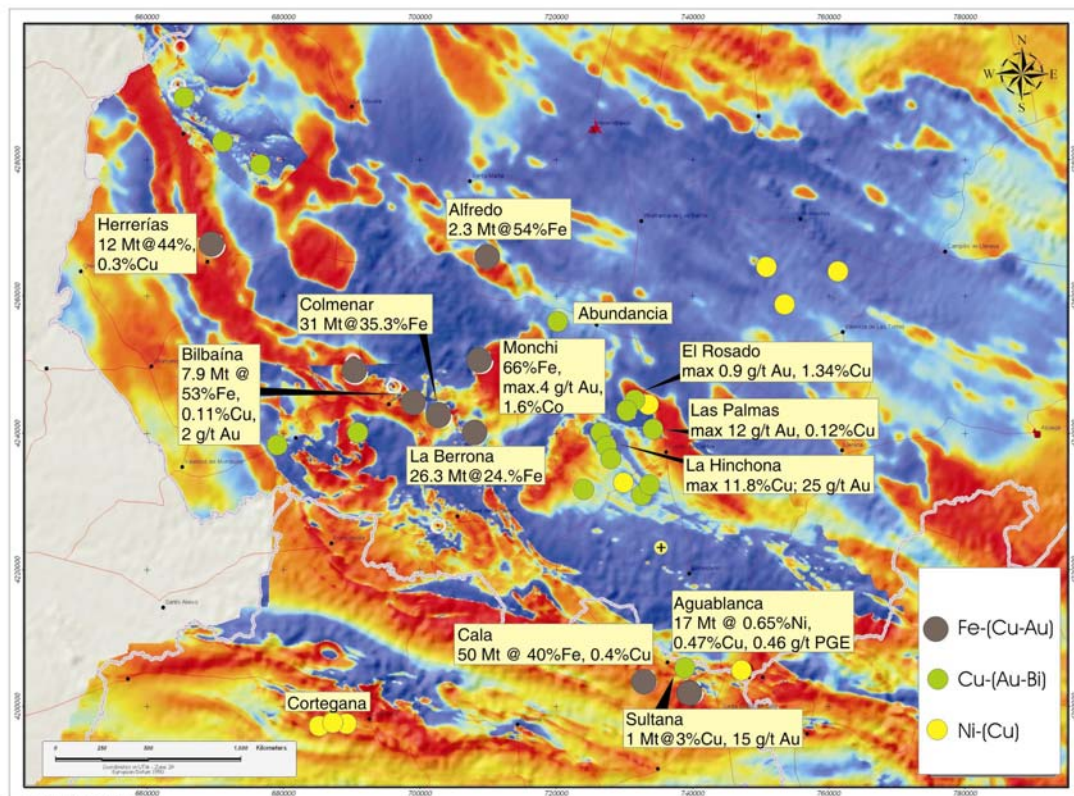
Airbone magnetic map of the central Spanish Ossa Morena Zone showing the location of major iron-oxide, Cu-(Au) and Ni-(Cu) mineralization.

References:

Casquet, C., Galindo, C., Darbyshire, D.P.F., Noble, S.R., & Tornos,F., 1998. Fe-U-REE mineralization at Mina Monchi, Burguillos del Cerro, Spain: age and isotope (U-Pb, Rb-Sr and Sm-Nd) constraints on the evolution of the ores. *Proceedings GAC-MAC-APGGQ Quebec 98 Conference*, **23**, A28

Tornos, F., & Casquet, C., 2004. A new scenario for related IOCG and Ni-(Cu) mineralisation: the relationship with giant mid-crustal mafic intrusion, Variscan Iberian Massif. *Terra Nova* (in press).

Tornos, F., Casquet, C., & Galindo, C., 2003. Hydrothermal iron oxide (-Cu-Au) mineralization in SW Iberia: Evidence for a multiple origin. In: Eliopoulos, D.G., et al. (eds.), *Mineral Exploration and Sustainable Development*, Millpress Rotterdam, 395-398

Tornos, F., & Velasco, F., 2002. The Sultana orebody (Ossa Morena Zone, Spain): Insights into the evolution of Cu-(Au-Bi) mesothermal mineralization. Abstracts GEODE Study Centre, Grenoble, 25-28

ARTICLE

The Aguablanca Ni–(Cu) sulfide deposit, SW Spain: geologic and geochemical controls and the relationship with a midcrustal layered mafic complex

**Fernando Tornos · Carmen Galindo · César Casquet ·
Luis Rodríguez Pevida · César Martínez ·
Enrique Martínez · Francisco Velasco ·
Alexander Iriondo**

Abstract The Aguablanca Ni–(Cu) sulfide deposit is hosted by a breccia pipe within a gabbro–diorite pluton. The deposit probably formed due to the disruption of a

Editorial handling: B. Lehmann

F. Tornos (✉)
Instituto Geológico y Minero de España,
Azafranal 48,
37001 Salamanca, Spain
e-mail: f.tornos@igme.es

C. Galindo · C. Casquet
Departamento Petrología, Universidad Complutense Madrid,
28040 Madrid, Spain

L. Rodríguez Pevida
Río Narcea Nickel,
Avda Estación 22,
06300 Zafra, Spain

C. Martínez · E. Martínez
Río Narcea Recursos, Mina de Aguablanca,
41250 El Real de la Jara, Spain

F. Velasco
Departamento Mineralogía-Petrología, Universidad País Vasco,
48080 Leioa, Spain

A. Iriondo
Centro de Geociencias, Universidad Nacional Autónoma de México,
Querétaro 76230, Mexico

A. Iriondo
Department of Geological Sciences,
University of Colorado at Boulder,
Boulder, CO 80309, USA

partially crystallized layered mafic complex at about 12–19 km depth and the subsequent emplacement of melts and breccias at shallow levels (<2 km). The ore-hosting breccias are interpreted as fragments of an ultramafic cumulate, which were transported to the near surface along with a molten sulfide melt. Phlogopite Ar–Ar ages are 341–332 Ma in the breccia pipe, and 338–334 Ma in the layered mafic complex, and are similar to recently reported U–Pb ages of the host Aguablanca Stock and other nearby calc-alkaline metaluminous intrusions (ca. 350–330 Ma). Ore deposition resulted from the combination of two critical factors, the emplacement of a layered mafic complex deep in the continental crust and the development of small dilational structures along transcrustal strike-slip faults that triggered the forceful intrusion of magmas to shallow levels. The emplacement of basaltic magmas in the lower middle crust was accompanied by major interaction with the host rocks, immiscibility of a sulfide melt, and the formation of a magma chamber with ultramafic cumulates and sulfide melt at the bottom and a vertically zoned mafic to intermediate magmas above. Dismembered bodies of mafic/ultramafic rocks thought to be parts of the complex crop out about 50 km southwest of the deposit in a tectonically uplifted block (Cortegana Igneous Complex, Aracena Massif). Reactivation of Variscan structures that merged at the depth of the mafic complex led to sequential extraction of melts, cumulates, and sulfide magma. Litho-geochemistry and Sr and Nd isotope data of the Aguablanca Stock reflect the mixing from two distinct reservoirs, i.e., an evolved siliciclastic middle-upper continental crust and a primitive tholeiitic melt. Crustal contamination in the deep magma chamber was so intense that orthopyroxene replaced olivine as the main mineral phase controlling the

early fractional crystallization of the melt. Geochemical evidence includes enrichment in SiO_2 and incompatible elements, and Sr and Nd isotope compositions ($^{87}Sr/^{86}Sr_i$ 0.708–0.710; $^{143}Nd/^{144}Nd_i$ 0.512–0.513). However, rocks of the Cortegana Igneous Complex have low initial $^{87}Sr/^{86}Sr$ and high initial $^{143}Nd/^{144}Nd$ values suggesting contamination by lower crustal rocks. Comparison of the geochemical and geological features of igneous rocks in the Aguablanca deposit and the Cortegana Igneous Complex indicates that, although probably part of the same magmatic system, they are rather different and the rocks of the Cortegana Igneous Complex were not the direct source of the Aguablanca deposit. Crust–magma interaction was a complex process, and the generation of orebodies was controlled by local but highly variable factors. The model for the formation of the Aguablanca deposit presented in this study implies that dense sulfide melts can effectively travel long distances through the continental crust and that dilational zones within compressional belts can effectively focus such melt transport into shallow environments.

Keywords Nickel · Magmatic sulfide deposits · Sulfide immiscibility · Aguablanca · Spain

Introduction

Most magmatic Ni–Cu deposits occur in greenstone belts, stable cratons, or rifted intraplate areas and are hosted by Mg-rich igneous rocks such as komatiite, picrite, anorthosite, or basalt-gabbro. Orebodies are located within stratiform magmatic complexes, sills, or lava flows or occur as subvertical bodies in the underlying feeder zones (Naldrett 1999). Only a few deposits, usually subeconomic, have been described in orogenic settings (see Naldrett 1989, 1999, 2004 for reviews). Thus, active continental margins have been considered as zones of minor interest for nickel exploration. This is probably the reason why the suboutcropping deposit of Aguablanca was not discovered until 1993 when a regional stream geochemical survey detected a major Cu–Au anomaly within a gossan with only a few ancient trenches. Further drilling by Rio Tinto Minera and PRESUR led to the definition of an orebody that was acquired by Rio Narcea Recursos SA in 2001. Estimated proven and probable reserves are 15.7 Mt grading 0.66% Ni, 0.46% Cu, and 0.47 g/t PGE. Total ore mined in 2005 was 997,000 t with the production of 5,381 t of nickel and 4,888 t of copper. The deposit has been mined in an open pit since 2004, and there is no indication that the grade diminishes with depth. Underground mining is expected to start in early 2007 (http://www.rionarcea.com).

The orebody is hosted by the intermediate to mafic Aguablanca Stock, which is one of a number of metaluminous

Variscan intrusions in SW Iberia (Fig. 1). The surrounding area contains different types of ore deposits and showings, including IOCG (Iron oxide–copper–gold) mineralization, iron-rich skarns, and Cu–(Au–Bi) veins (Tornos et al. 2004).

The immediate area near the orebody has been the subject of major research. The plutonic and the sedimentary host rocks were described by Velasco (1976), Casquet (1980, 1982), Casquet and Velasco (1978), Eguíluz et al. (1989), and Bateman et al. (1992, 1994). After the discovery of the deposit, several studies have been published, mainly dedicated to the mineralogy of the ore (Lunar et al. 1997; Bomati et al. 1999; Ortega et al. 1999–2002, 2004; Martín Estévez et al. 2000; Piña et al. 2005), the nature of the fragments in the breccia (Piña et al. 2004), and the geology, the geochemistry, and the origin of the deposit (Casquet et al. 1999, 2001; Tornos et al. 1999– 2002a). The latter contributions have shown that this deposit is remarkable in that it is the first case of a significant synorogenic magmatic Ni–(Cu) deposit related to calc-alkaline plutonism recorded to date. We in this study attempt to summarize our current geological and geochemical understanding of the Aguablanca deposit and its host rocks, placing the formation of the orebody into the regional framework of transpressional deformation during Variscan times and proposing relationships with sills emplaced deep into the crust. The comparison with an outcropping dismembered part of one of these deep sills (Cortegana Igneous Complex) gives clues on the overall evolution of these systems.

General geologic context

The Aguablanca orebody is located in the northeastern zone of the Santa Olalla Plutonic Complex, within the southernmost part of the Ossa Morena Zone of the Variscan Belt of Iberia (Fig. 1). The Ossa Morena Zone underwent a complex geodynamic evolution (see Quesada et al. 1991; Eguíluz et al. 2000, and references therein for reviews) with a Neoproterozoic Cadomian basement reworked by the Variscan orogeny. The Cadomian orogeny resulted from the subduction and subsequent collision of the exotic Ossa Morena terrane with the autochthonous Iberian terrane in the Late Neoproterozoic to Early Cambrian while the Variscan orogeny resulted from the oblique collision of the South Portuguese terrane with the southern margin of the Iberian Massif in the Devonian to Early Carboniferous. The Ossa Morena Zone hosts a wide suite of igneous rocks related to the two orogenies and to an intermediate rift-related pulse of Cambrian–Ordovician age (Sanchez Carretero et al. 1990; Eguíluz et al. 2000; Galindo and Casquet 2004). Variscan plutonism is volumetrically dominant and consists of calc-alkaline metaluminous composite intrusions ranging in
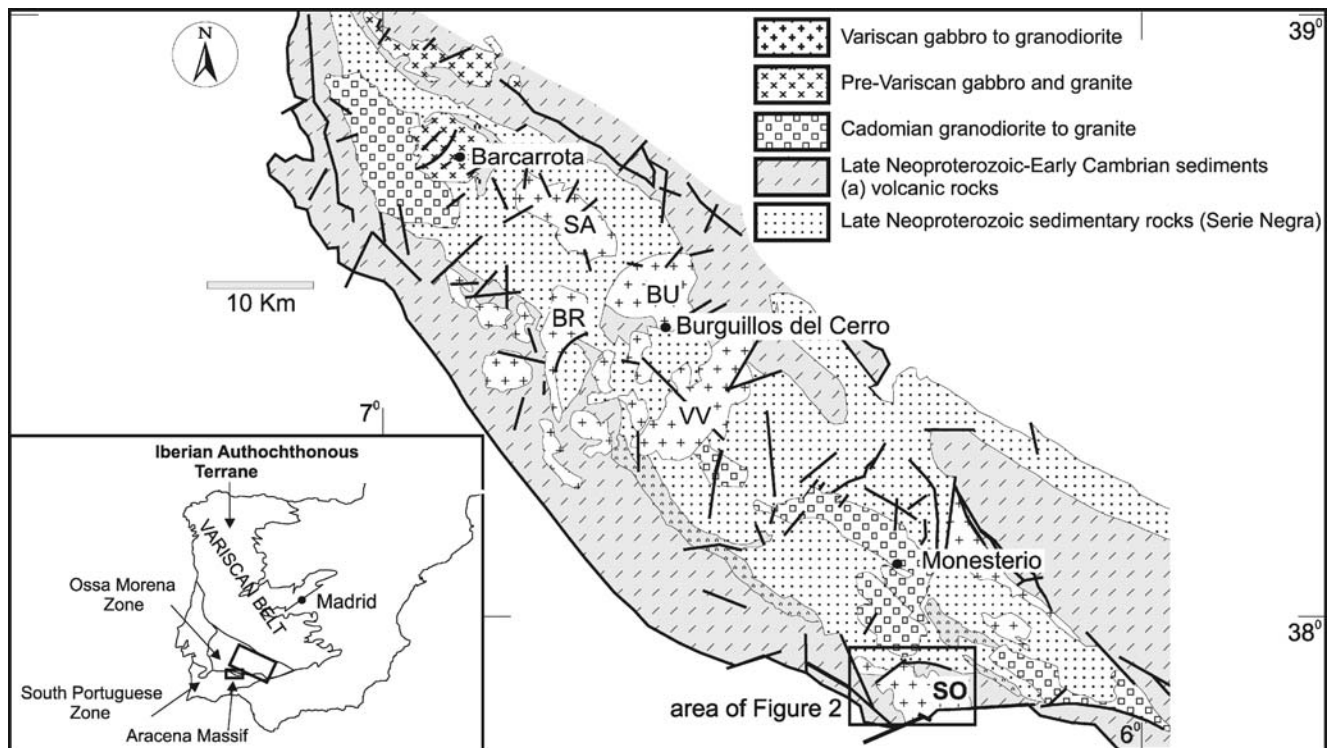
Fig. 1 Geology of the Central Part of the Ossa Morena Zone (Olivenza-Monesterio antiform) showing the major Variscan intrusions of the area. *BR* Brovales, *BU* Burguillos, *SA* Salvatierra, *SO* Santa Olalla Plutonic Complex, *VV* Valencia del Ventoso. The *inset* shows the location of the Ossa Morena Zone in the Variscan Belt of Iberia

composition from gabbro to granodiorite and minor peraluminous granite (Fig. 1).

During the Variscan deformation, the Ossa Morena Zone underwent thick-skinned deformation with the development of south-verging longitudinal fold-and-thrust zones that involved both the Cadomian basement and the Palaeozoic sedimentary cover. There are abundant contemporaneous and younger strike-slip faults. All these structures show evidence of formation in a transpressional setting in response to oblique subduction and played a major role in focusing magma ascent and pluton formation (Quesada et al. 1987; Tornos et al. 2005).

A major Variscan feature of the Ossa Morena Zone is the Olivenza-Monesterio antiform, where the Santa Olalla Plutonic Complex is located, of which the Aguablanca Stock and other intrusions are part (Fig. 1). Neoproterozoic rocks crop out in the core of this structure and consist of gray schist, quartzite, and graywacke with intercalated ortho-amphibolite (Serie Negra). Late Neoproterozoic to Middle Cambrian rocks unconformably overlie the Serie Negra and consist of syn-Cadomian calc-alkaline volcanic and subvolcanic rocks interbedded with graywacke, quartzite, limestone, and slate. Both sequences are overlain by a thick passive to rifted-margin sequence of limestone, siliciclastic metasedimentary rocks, and alkaline to subalkaline volcanic rocks of Early to Middle Cambrian age.

A second domain of interest in the Ossa Morena Zone is the Aracena Massif, which is a high-T low-P metamorphic belt located adjacent to the exotic South Portuguese terrane (Fig. 1). It includes a strained thick sequence of peraluminous gneiss with interbedded quartzite, pyroxene-bearing gneiss, ortho-amphibolite, limestone, and calc-silicate hornfels. This sequence is probably equivalent to the Late Neoproterozoic/Middle Cambrian sequence recognized elsewhere in the central and northern Ossa Morena Zone (Crespo 1991; Giese et al. 1994; Castro et al. 1999). The Aracena Massif hosts abundant bodies of mafic and ultramafic rocks remarkably similar to those of the Aguablanca Stock.

Recent seismic-reflection work has shown the existence of a 1-5-km-thick high-velocity zone at about 10 to 15 km depth throughout the Ossa Morena Zone where the large Variscan thrusts and faults are interpreted to be rooted (IRB, Iberian Reflective Body; Simancas et al. 2003; Carbonell et al. 2004). The more likely interpretation is that the reflector represents a large sill-like structure of mafic–ultramafic rocks intruded during the Variscan times (Simancas et al. 2003). In detail, the IRB seems to be formed by several tens of lensoidal plutonic bodies separated by conductive graphite-rich shale, likely belonging to the Serie Negra (Pous et al. 2004; Tornos and Casquet 2005), and forming a layered magmatic complex similar in size to the Kunene or Bushveld complexes (Tornos et al. 2005). In this hypoth-

esis, the Aracena Massif represents an exhumed middle-lower crust section where dismembered parts of the magmatic complex crop out (Simancas et al. 2003; Tornos and Casquet 2005).

An alternative interpretation of the reflector has been proposed by Pous et al. (2004), relying on a hypothetical preferred orientation of graphite flake concentrations along the basal thrust. However, the coincidence with regional magnetometric data, the widespread low $^{207}Pb/^{206}Pb$ ratios of sulfides in the Ossa Morena Zone (Tornos and Chiaradia 2004), and the igneous geochemistry (Casquet et al. 2001) lend much support to the first hypothesis. Juvenile magmas probably intruded within a crustal decoupling zone, a major middle crust detachment, in response to oblique ridge collision at the Devonian–Carboniferous boundary (Tornos and Casquet 2005).

The Santa Olalla Plutonic Complex

The Santa Olalla Plutonic Complex is located in the southernmost Olivenza-Monesterio antiform and has intrusive contacts except in its southern part, where it ends abruptly against the Zufre Fault, which constitutes the limit between the Ossa Morena and South Portuguese Zones (Fig. 2).

The host rocks of the Santa Olalla Plutonic Complex underwent Variscan low-grade metamorphism before the plutonism (Casquet and Velasco 1978), and they belong to the Late Neoproterozoic to Middle Cambrian sequence. The Plutonic Complex reached its final emplacement level after the main thrusting and folding phase of the Variscan orogeny and produced an aureole of contact metamorphism about 2 km wide, which is only recognized south of the Cherneca Fault. Temperatures within the aureole attained values of the hypersthene hornfels facies (ca. 750°C) near the contact with the Aguablanca Stock, resulting in local partial melting. A depth of 1.7 to 3.5 km (0.5–1 kbar) was inferred for its emplacement from metamorphic mineral equilibria (Casquet 1980). Widespread garnet-pyroxene± magnetite skarn and minor magnesian skarn were formed by replacement of the marble and calc-silicate rocks before final emplacement of the Aguablanca Stock (Casquet and Velasco 1978; Casquet 1980).

The Santa Olalla Plutonic Complex includes the Santa Olalla Main Pluton, which is a large funnel-shaped intrusion with an apophysis to the NW, and the smaller Aguablanca Stock located in the northeastern part (Table 1, Fig. 2). The Main Pluton shows reverse compositional zoning with monzogranite and granodiorite in the center, tonalite in the middle, and amphibole-bearing quartz diorite in the edge (Velasco 1976; Casquet 1980; Casquet et al. 2001). U–Pb dating shows that the Santa Olalla Main

Pluton and the Aguablanca Stock were broadly coeval. Ages of 332±3 Ma (Montero et al. 2000; U–Pb zircon, Kober method), 341±3 Ma (Romeo et al. 2004; U–Pb zircon, conventional), and 347±3.4 Ma (Spiering et al. 2005; U–Pb zircon, SHRIMP) are recorded for the Santa Olalla Main Pluton. The Aguablanca Stock, in turn, has yielded absolute ages of 338.6±0.8 Ma (Romeo et al. 2004) and 344±1.1 Ma (Spiering et al. 2005). With the exception of the 332±3.4 Ma value, the age sets for the two plutons are quite similar, although those of Spiering et al. (2005) are older by some 5 Ma. Geochemically and chronologically, the Santa Olalla Plutonic Complex is equivalent to other nearby intrusions such as Burguillos (336±1.6 to 338±1.3 Ma, Dallmeyer et al. 1995; 338±1.5 Ma, Casquet et al. 1998) and Brovales (340±7 Ma, Montero et al. 2000) (Fig. 1).

The Aguablanca Stock

The Aguablanca Stock is a small (ca. 10 km^2) and highly heterogeneous intrusion. The outer contacts are both concordant and discordant, and the internal architecture of the stock is interpreted as a half bell jar (Tornos et al. 2001). Moreover, detailed mapping suggests that the roof of the intrusion is close to the present erosion level as evidenced by the presence of roof pendants of skarnified marble and calc-silicate hornfels.

The intrusion consists of a dominant unit of medium-grained hornblende-biotite diorite and quartz diorite (Diorite Unit; Table 2, Fig. 3). These rocks are similar to the quartz diorite that forms the outer ring of the Santa Olalla Main Pluton (Casquet 1980). They have an inequigranular subeuhedral texture, locally subophitic, and consist of 2 to 3-mm-sized crystals of weakly zoned plagioclase of intermediate composition (an$_{46-51}$), diopside–augite, actinolitic hornblende, and biotite–phlogopite (Mg/Fe=2.3; Casquet 1980). Accessory minerals include quartz and trace amounts of apatite, pyrrhotite, and zircon.

The Gabbronorite Unit crops out in the northern part of the Aguablanca Stock. It consists for the most part of medium-grained massive gabbronorite with lesser amounts of pyroxene gabbro and norite in an approximate 2:1:1 ratio. A 10-m interval of faint layering resulting from modal and textural changes defined by alternating plagioclase- and mafic-rich centimeter-sized layers can be observed. Sub-horizontal veins of pegmatitic gabbro and scapolite (Cl-rich meionite)-hedenbergite are locally present. The contact with the Diorite Unit is apparently gradational. At the contact with the host metasedimentary rocks, there is a discontinuous and up to 5- to 6-m-thick margin of fine-grained, phlogopite-rich gabbro (Contact Gabbro; Table 2).

Pyroxene occurs as unzoned crystals of between 0.5 and 3 mm, locally exhibiting a glomero-porphyritic disposition.

Fig. 2 Geologic map of the Santa Olalla Plutonic Complex. Modified from Casquet (1980) and ITGE (1990). Grid in UTM coordinates. An interpretative cross section (b–b′) is exposed below showing the likely existence of two feeder zones for the intrusions. *zf* Zufre Fault, *cf* Cherneca Fault, *gsz* Garrenchosa Shear Zone, *SOMP* Santa Olalla Main Pluton, *AS* Aguablanca Stock, *gn* Gabbronorite Unit and breccia, *du* Diorite Unit, *ag* Aguablanca Mine, *s* Sultana Cu–(Au) Mine
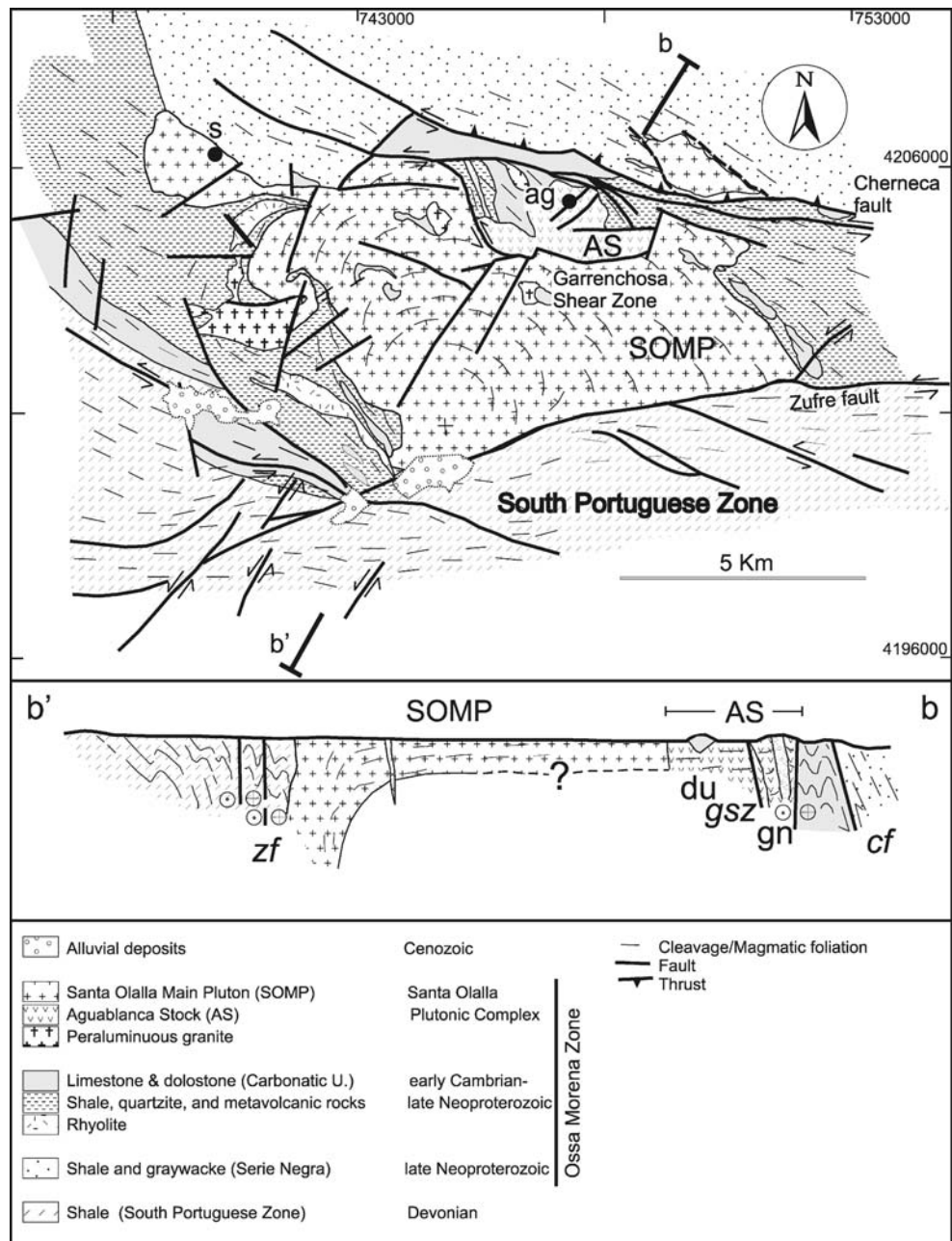
Orthopyroxene is poikilitically included in the larger clinopyroxene crystals, suggesting that its crystallization began earlier than that of clinopyroxene. The orthopyroxene composition is rather monotonous (en$_{78–92}$) and shows low NiO contents (0.01–0.06 wt%) (see Electronic supplementary material). Clinopyroxene has a more variable composition (diopside and Mg–augite) and has similar low NiO contents (<0.12 wt%). Plagioclase phenocrysts show normal zoning with cores of variable composition between an$_{56}$ and an$_{90}$ (bytownite–labradorite) and rims of oligoclase–andesine (an$_{24–35}$). Olivine is very scarce and only occurs as scattered anhedral unzoned grains mantled by plagioclase and pyroxene. Phlogopite (X_{phlog}, 0.49–0.70)

and clinoamphibole (magnesiohornblende-actinolite) occur as interstitial 0.5- to 2-mm-sized anhedral crystals along with quartz (Fig. 4a). Accessory igneous minerals are ilmenite, rutile, pyrrhotite, and apatite. The pegmatitic gabbro consists of actinolite-hornblende, diopside, and oligoclase (an$_{16–24}$) and minor quartz, muscovite, titanite, allanite, and apatite.

The Aguablanca Stock has abundant xenoliths of the host rocks, ranging in size from centimeters to several meters, particularly garnet-pyroxene skarn and pelitic and calc-silicate hornfels. There are fairly abundant but small peraluminous microenclaves that contain oligoclase, biotite, spinel, cordierite, corundum, sillimanite, and K-feldspar.

Table 1 Major lithologic units of the Santa Olalla plutonic complex, SW Spain

Intrusion & intrusive unit	Occurrence	Composition	Mineralogy	Texture	Hydrothermal alteration	Age (Ma)
Santa Olalla Main Pluton						
	Large (km-sized) ellipsoidal intrusion with reverse zonation. Subtle subhorizontal magmatic foliation	Monzogranite–granodiorite in the core grading to tonalite and diorite and Q-diorite in the rim	plag, bt, amph, Q, kf (ap, zr, ilm, rut). Only accessory sulfides (po)	Massive, granular, medium- to coarse-grained	Negligible	332±3[a] 341±3[2] 347.0±3.4[3]
Aguablanca Stock						
Diorite Unit	Dominant in the stock. Subhorizontal magmatic foliation	Bt-, amph-bearing diorite, and Q-diorite	plag, cpx, amph, bt (Q, ap, zr). Scarce sulfides disseminated and in veinlets	Massive, granular, coarse- to medium-grained. Local subophitic textures	Minor. Sericitization plag. Replacement px by amph. Most sulfides of hydrothermal origin	338.6±0.8[b]
Gabbro–norite Unit	Located in the N area of the Stock. Gradual contacts. Subhorizontal to subvertical magmatic foliation	Norite, gabbronorite, and pyroxenitic gabbro	opx, cpx, plag (bt, amph, ol, Q, ilm, rut, ap, sp). Sulfides disseminated, patches and veinlets forming locally significant mineralization	Massive, medium-grained. Local cumulates	Intermediate. Local texturally destructive. Sericitization plag. Replacement px by amph. Endoskarn. Some hydrothermal mineralization	344.0±1.1[c] 338.2±1.7[d] 338.2±3.0[d]
Breccia pipe	Hosted by the Gabbro–norite Unit forming a subvertical pipe with gradual contacts	Heterometric fragments of pyroxenitic and accessory peridotitic cumulates. Fragments of host rocks. The fragments are usually unmineralized	opx, cpx, bt, amph (plag, ol, sp). Sulfides massive and disseminated. Abundant veinlets	Dominant cumulates (ultramafic). Fragments randomly oriented but local flow textures	Extensive. Local texturally destructive. Sericitization plag. Replacement px by amph. Endoskarn	335±2[d]
Barren breccia	Usually external zone of the breccia pipe	Fragments of the breccia pipe cemented by rocks of the Gabbro–norite Unit			Extensive. Local texturally destructive. Sericitization plag. Replacement px by amph. Endoskarn	
Ore breccia	Internal zone of the breccia pipe	Fragments of the breccia pipe cemented by sulfides with more accessory gabbro–norite			Irregular recrystallization of magmatic sulfides	
Massive sulfides	Included in the ore breccia as large, randomly distributed masses	Massive–semimassive sulfides with disseminated pyroxene crystals			The pyroxenes are only slightly altered. Widespread retrogradation of magmatic sulfides	
Cortegana Complex						
	Large sills in the Aracena Massif	Highly heterogeneous tonalite–diorite with norite–gabbro and ol–websterite, lherzolite, dunite, orthopyroxenite. Minor harzburgite, troctolite, and wehrlite	ol, opx, cpx, bt, amph (plag, sp). Abundant disseminated sulfides	Dominant cumulates in the mafic–ultramafic rocks. Coarse-grained	Widespread evidences of major fluid circulation	321.5±33[d] 336.2±1.7[d]

amph Clinoamphibole, ap apatite, bt biotite, cpx clinopyroxene, ilm ilmenite, kf K-feldspar, ol olivine, opx orthopyroxene, plag plagioclase, po pyrrhotite, Q quartz, rut rutile, sp spinel, zr zircon

[a] Montero et al. (2000) (U–Pb)
[b] Romeo et al. (2004) (U–Pb)
[c] Spiering et al. (2005) (U–Pb)
[d] This study

Table 2 Representative chemical analyses of samples from the Aguablanca Stock and the Cortegana Complex

	AG-207-2 Breccia ore	AG-156	AG-159	AG-160	AB-37 Gabbronorite Unit	AG-97	SO-32	AG-85	AG-213	SO-57 Diorite Unit	SO-56d	TE-4 Cortegana Complex	TE-12	TE-9
	Pyroxenite		Norite		Gabbronorite		Gabbro		Contact Gabbro	Diorite		Norite	Gabbro	Websterite
SiO_2	50.88	52.44	53.67	52.64	53.25	53.46	51.80	53.60	52.09	55.00	57.10	51.60	53.36	46.20
Al_2O_3	14.00	7.71	7.24	9.17	10.22	8.10	13.00	9.95	13.70	15.00	15.60	14.11	14.32	6.48
FeO_t	5.94	10.84	9.62	9.34	8.04	8.96	7.94	8.14	5.94	7.45	6.31	9.51	6.93	14.02
MnO	0.15	0.20	0.19	0.18	0.19	0.22	0.16	0.18	0.12	0.16	0.12	0.17	0.14	0.25
MgO	11.12	17.64	18.69	16.98	17.50	19.13	14.00	15.92	13.59	7.69	5.59	11.93	9.70	24.78
CaO	12.24	6.74	6.12	7.01	7.04	6.08	8.71	6.65	8.75	6.76	6.07	7.68	10.11	3.67
Na_2O	1.59	1.07	1.09	1.46	1.15	0.98	1.64	1.44	1.75	3.22	3.49	1.27	2.55	0.61
K_2O	0.62	0.48	0.59	0.65	0.54	0.56	0.52	0.74	0.89	1.49	2.40	0.54	0.55	0.39
TiO_2	0.37	0.36	0.32	0.50	0.24	0.36	0.58	0.33	0.32	0.82	0.72	0.21	0.23	0.32
P_2O_5	<0.05	0.02	0.02	0.07	0.02	0.03	0.04	0.09	0.02	0.13	0.12	<0.05	0.03	<0.05
S	(*)	0.27	0.05	0.09	0.06	0.09	(*)	(*)	(*)	(*)	(*)	(*)	0.69	(*)
LOI	2.49	1.32	1.38	0.96	0.93	1.13	0.93	2.41	2.18	0.62	0.93	1.93	1.33	2.72
Total	99.87	99.23	99.23	99.27	99.38	99.43	99.55	99.69	99.63	98.57	98.66	100.20	100.47	101.20
Rb	32	17	22	21	22	22	25	31	36	59	81	16.7	13	10
Sr	347	173	154	213	219	170	319	260	278	318	339	289	214	124
Ba	256	121	144	160	98	129	211	174	206	494	594	98	110	86
V	40	191	131	164	108	128	204	125	97	186	188	119	194	65
Cr	609	1410	1473	1252	1176	1394	880	1110	1084	510	250	4.05	211	118
Co	79	75	60	61	63	68	58	64	64	9	31	108	38	147
Ni	1888	539	454	431	419	525	292	348	444	202	78	366	173	1190
Cu	1158	177	60	67	66	122	66	61	407	68	85	175	85	154
Zn	33	56	70	57	54	66	93	73	38	108	75	76	44	78
Y	27	11	10	15	7	10	12	12	10	10	40	49	13	8
Nb	<0.6	2.2	2.2	2.8	1.4	2.1	10.0	2.4	1.2	14.0	30.0	2.5	<10	1.1
Zr	35	23	17	22	17	19	39	57	38	128	169	53	58	27
Pb	21	3	8	5	10	7	3	5	10	9	32	3	<10	4
U	2.2	0.51	0.68	0.50	0.44	0.49	0.50	0.87	1.3	1.40	1.50	<0.1		<0.1
Th	<1	1.40	2.09	1.53	1.31	1.58	1.10	3.12		4.20	10.00	<1		<0.8
La	9.8	5.9	6.2	7.7	4.9	5.8	7.6	8.4	7.2	25.1	25.9	13.6		2.6
Ce	18.9	13.6	13.5	18.0	10.2	13.0	17.0	17.5	14.0	51.0	52.0	24.4		5.8
Pr	2.6	1.7	1.7	2.3	1.2	1.6		2.1	1.6			3.3		0.7
Nd	12.7	7.3	7.0	10.9	4.6	6.4	9.0	8.4	6.7	21.0	25.0	12.5		3.0
Sm	3.5	1.9	1.7	2.8	1.1	1.5	2.1	2.0	1.5	4.3	5.1	3.7		1.0
Eu	1.1	0.5	0.4	0.7	0.4	0.4	0.7	0.6	0.4	1.4	1.1	0.4		0.3
Gd	3.9	1.9	1.7	2.6	1.0	1.5		2.0	1.4			4.8		0.9
Tb	0.6	0.3	0.3	0.4	0.2	0.2	0.5	0.3	0.2	0.7	0.7	0.9		0.2
Dy	3.8	1.9	1.6	2.6	1.1	1.5		2.1	1.2			6.0		1.0
Ho	0.8	0.4	0.4	0.6	0.3	0.3		0.4	0.1			1.3		0.2
Er	2.1	1.1	1.0	1.5	0.8	0.9		1.3	0.7			4.2		0.6
Tm	0.3	0.2	0.2	0.2	0.1	0.2		0.2	0.1			0.9		0.1
Yb	1.7	1.1	1.1	1.4	0.8	0.9	1.3	1.40	0.8	2.5	2.6	5.6		0.8
Lu	0.3	0.2	0.2	0.2	0.1	0.1	0.2	0.2	0.1	0.4	0.4	0.9		0.1

Analysis IGME

LOI Loss on ignition

All Fe as FeO_t

(*) Included in LOI

Major elements in weight percent (wt%); trace elements in parts per million (ppm)

Fig. 3 Detailed premining geologic map of the Aguablanca orebody. Modified from Tornos et al. (2001) and Spiering et al. (2005). Grid in UTM coordinates
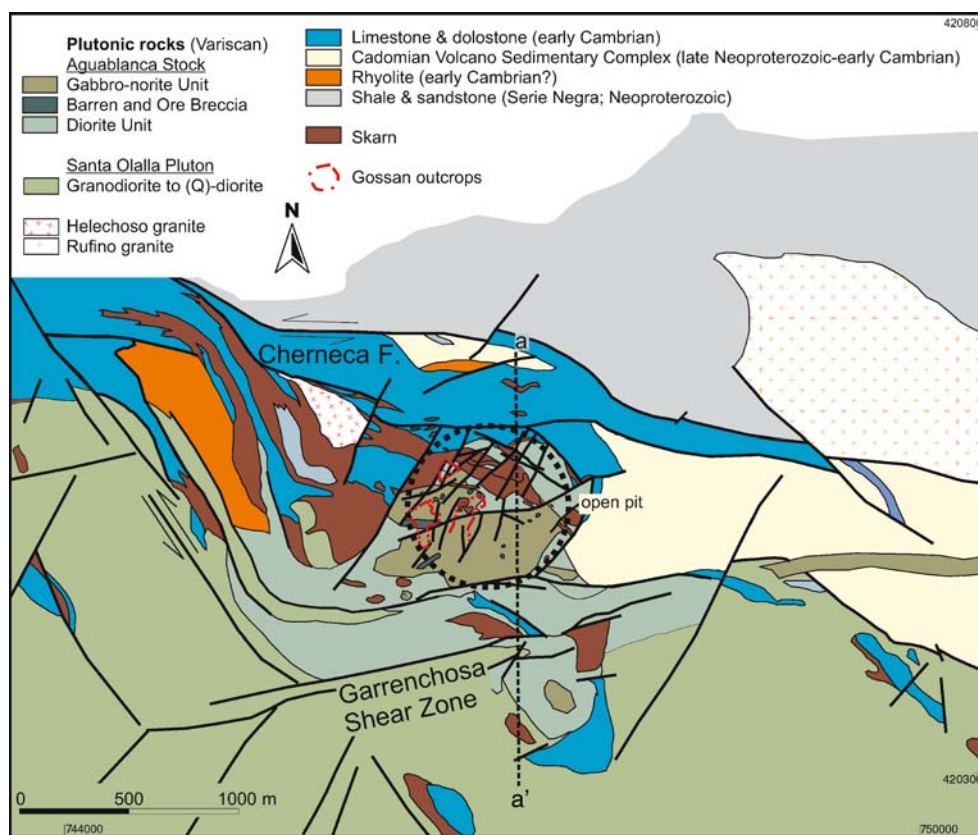
Spinel forms clusters of green euhedral crystals included in plagioclase. Electron microprobe (EPMA) analyses show that it is a ferriferous aluminum spinel (FeO_t=19.9–22.7 wt%) characterized by low Cr (<0.05 wt% Cr_2O_3), Ni (<0.31 wt% NiO), and Ti (<0.1 wt% TiO_2) contents. This composition, the absence of plagioclase rims, and the relationship with peraluminous assemblages strongly suggest that the spinel phase corresponds to insoluble relicts of assimilated xenoliths. The spinel composition differs from those of igneous spinel in magmatic Ni–Cu deposits (Barnes and Tang 1999) but is similar to that recognized in the Voisey's Bay Ni–(Cu–Co) deposit where assimilation of crustal pelitic material was important (Kerr and Ryan 2000; Li and Naldrett 2000).

The Gabbronorite Unit, as well as to a lesser extent the Diorite Unit, also contains irregularly distributed centimeter-sized ellipsoidal enclaves of sulfide-bearing pyroxenite that is equivalent to those of the breccia pipe which is described below.

Application of the geothermometer based on the enstatite-diopside solvus (Bertrand and Mercier 1985) in the Gabbronorite Unit yields consistent values between 940 and 1,120°C. For these temperatures, the pyroxene geobarometry (Nimis 1999) indicates pressures of 4.3 to 5.7 kbar. P–T values recorded here probably correspond to those of the differentiating magma chamber that underlies the Santa Olalla Plutonic Complex (see below).

The Aguablanca orebody

The Ni–(Cu) Aguablanca deposit consists of two E–W steeply northward dipping ellipsoidal orebodies hosted by the Gabbronorite Unit (Figs. 3, 5 and 6). The southern orebody is the largest one, with a surface of approximately 360×300 m^2, and has been traced down to a depth of 550 m. The northern orebody is significantly smaller, 300×100 m^2, and extends downward for at least 160 m. The extension below these ore zones is not well understood due to the limited amount of deep drill holes but it seems that they grade into a gently dipping high-grade mineralized zone (1 wt% Ni) averaging 30–70 m in thickness (Spiering et al. 2005).

Four types of ore have been distinguished: ore breccia, massive sulfides, disseminated ore, and patchy ore. Ore breccia and massive sulfides are only found in the southern orebody, whereas the northern orebody includes patchy and disseminated ores. The relationships among the different types of ore are obscure because most of the contacts are tectonic (Figs. 5 and 6). The pattern that emerges in the southern orebody is one of a telescoped arrangement, with disseminated and patchy ore in an outer disposition and pipe-like breccia bodies and massive sulfides as inner lenses.

Most of the ore (50–60%) occurs as disseminations in rocks belonging to the Gabbronorite Unit. Sulfides (5–20% of the rock volume; 0.1–10 mm in size) are interstitial to plagioclase and pyroxene and intergrown with phlogopite and

Fig. 4 Photographs of the host rocks and mineralization at Aguablanca and Cortegana. **a** Norite with cumulus texture and abundant intercumulus phlogopite. Sample AG-135. *Scale bar*: 1 mm. **b** Ore breccia. Fragments of fine-grained pyroxenite (*dark gray*) supported by massive sulfides and some coarse-grained gabbro to norite. **c** Semimassive sulfides made up of pyrrhotite, chalcopyrite, and pentlandite. They have abundant, unevenly dispersed crystals of ortho- and clinopyroxene and irregular intergrowths of coarse-grained gabbro to norite. This rock and the sulfides are interpreted as derived from immiscible melts. *Scale bar*: 3 cm. **d** Ore breccia. Fragments of fine-grained pyroxenite (*px*) and serpentinite (*serp*) supported by irregularly mixed sulfides and gabbronorite (*gn*). The pyroxene crystals tend to concentrate near the fragments. *Scale bar*: 1 cm. **e** Sheared calcitic marble with highly strained garnet-rich skarn within the Cherneca Fault. **f** Cortegana Igneous Complex. Intercumulus pyrrhotite in pyroxenite. *Scale bar*: 2 cm. **g** Orbicular gabbro forming the lowermost part of the Cortegana Igneous Complex. *Scale bar*: 3 cm. **h** Anatexite in the footwall of the Cortegana Igneous Complex
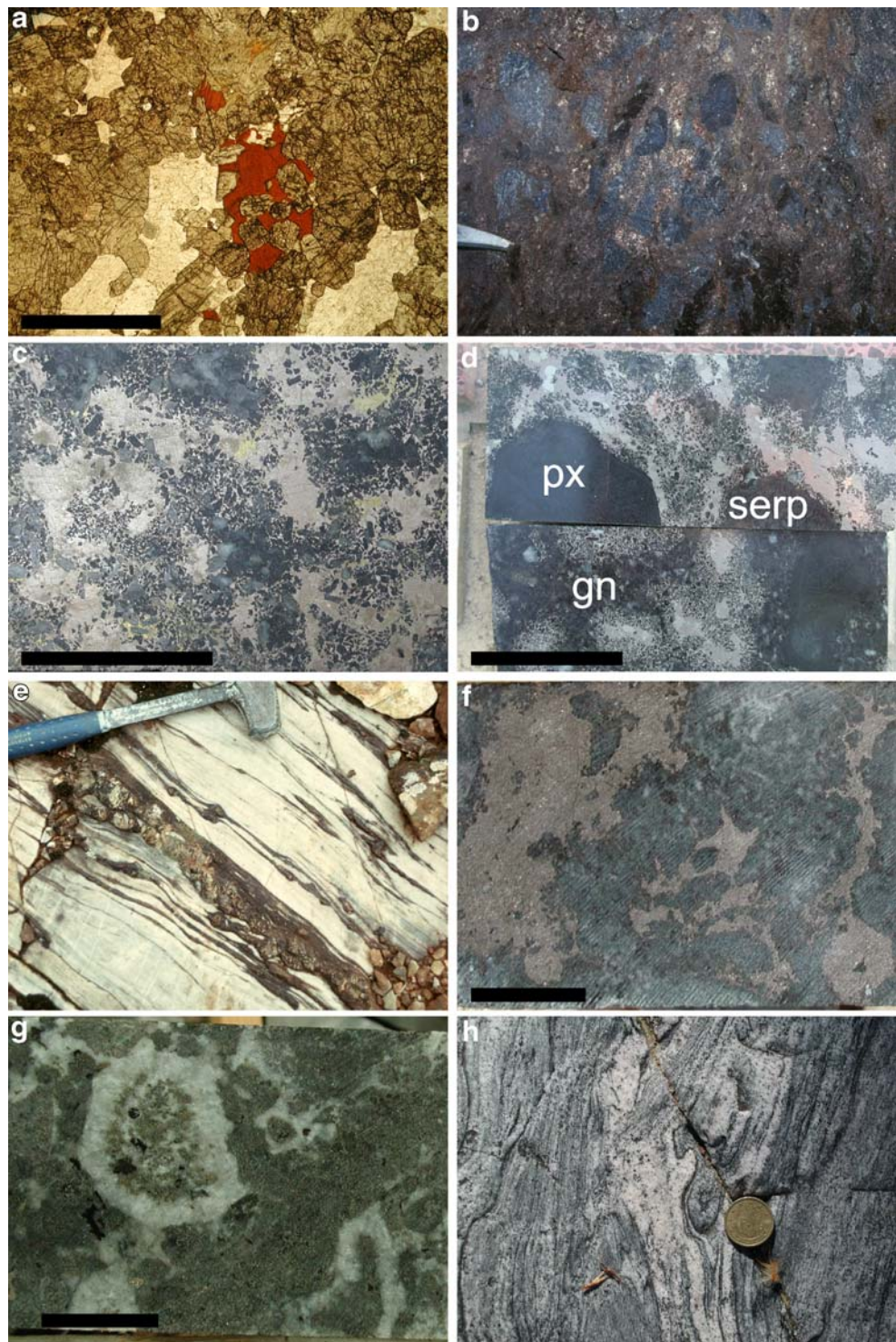
amphibole. The grades are up to 1% Ni+Cu, and the Ni/(Ni+Cu) ratio is close to 0.3–0.5. Patchy ore is similar to the disseminated ore, although the sulfides occur in dispersed blebs about a centimeter in diameter. It comprises 20–35% of the total ore volume and has irregular grades, usually below 0.7% Cu+Ni. Moreover, the Gabbronorite Unit also includes scattered meter-sized lenses of massive sulfides (Fig. 7).

Ore breccia and massive sulfides comprise 15–20% of the total orebody volume. Copper grades are equivalent to those of disseminated and patchy ore but there is an up to fivefold enrichment in Ni, which is usually higher than 1% (Ortega et al. 2004). Because of their genetic and economic importance, the ore breccia and the massive sulfides are described in detail below.

Fig. 5 Interpretative N–S cross section (a–a′ in Fig. 3) of the Aguablanca orebody showing the distribution of the mineralization. Modified from Spiering et al. (2005)
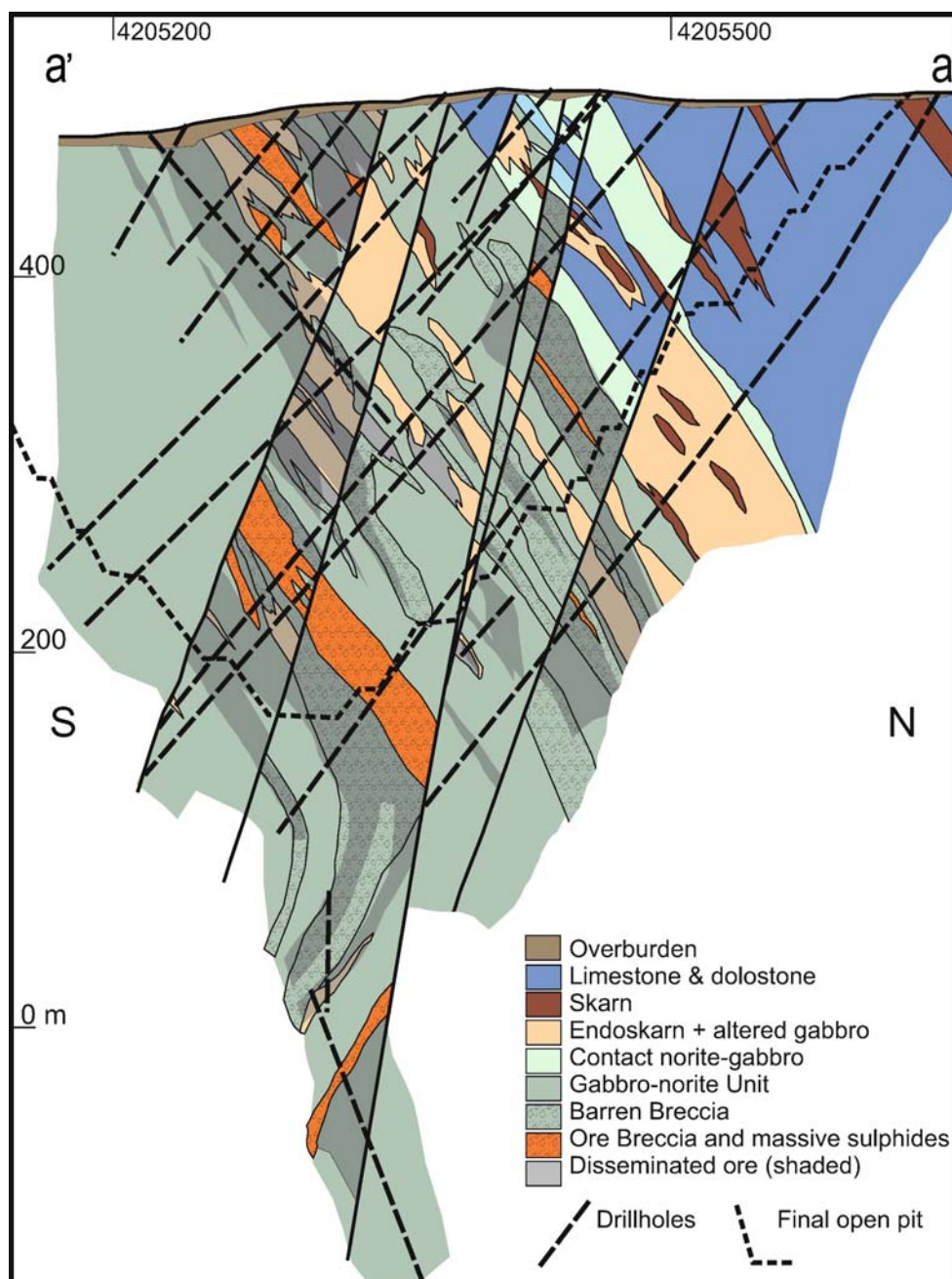
As a whole, the orebody has a Ni/(Cu+Ni) ratio of 0.43. This ratio is equivalent to that of other gabbro-hosted deposits like Voisey's Bay (0.45–0.75; Naldrett 1999). Cu and Ni show a positive correlation ($r=0.78$), a feature probably inherited from a liquid monosulfide solution and unlikely to result from Cu input during later hydrothermal alteration. Cobalt has a positive but weak correlation with Ni and Cu ($r=0.04$–0.07).

The Ni and Cu contents and the Ni/(Ni+Cu) ratio are quite variable throughout the orebody, and no vertical or horizontal chemical zonation is evident. Also, there is no increase in grade or change in the style of mineralization toward the contact with the host rocks; in fact, the rocks adjacent to the contact, including the skarn, are usually barren, and only a few bodies of massive magnetite or pyrrhotite are found. No metasomatic ore, similar to that described at Jinchuan by Chai and Naldrett (1992), has been found in the host rocks or within the xenoliths in the Aguablanca Stock.

Breccias and massive sulfides

The breccia bodies are discontinuous and have a pipe-like geometry with a roughly elliptical, up to 30×10 m², section. The lenses are roughly parallel to the stock contact

Fig. 6 Plan of the 485-m level of the Aguablanca mine showing the relationships between the different orebodies and faults
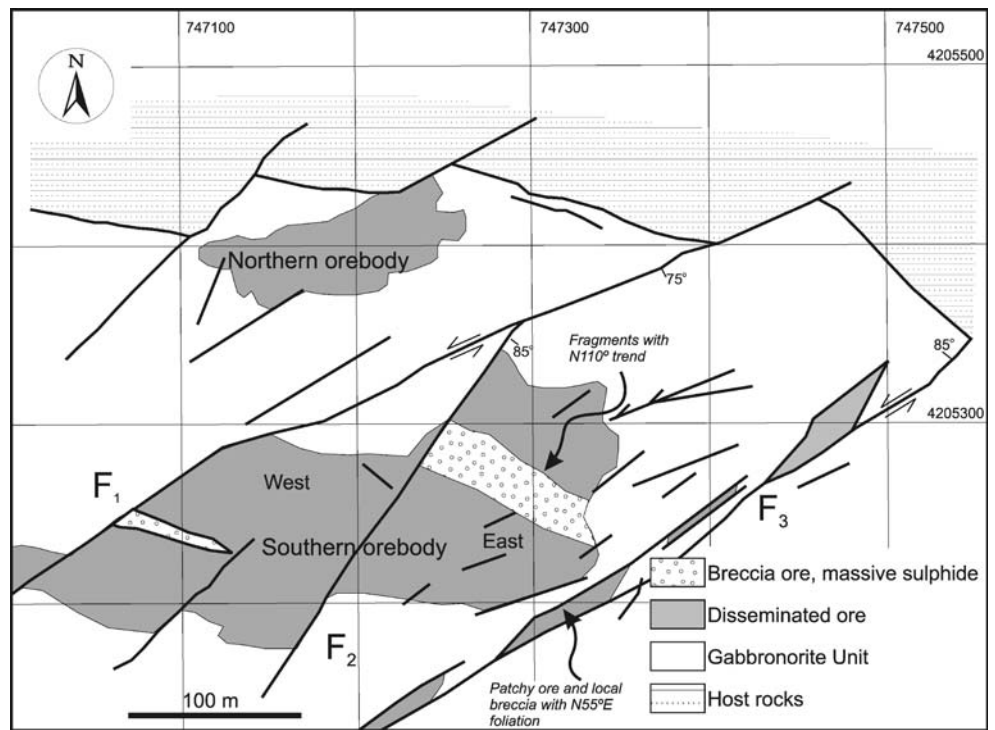
(N100–120°E) and dip 45–80°NE (Fig. 5). The breccia consists of poorly sorted heterolithic subangular to subrounded fragments supported dominantly by sulfides (ore breccia) or by gabbronorite (barren breccia) (Figs. 4b–d and 8). The barren breccia dominates in the northern orebody, while ore breccia is restricted to the southern orebody.

The proportion of fragments is very variable. There are rocks with evenly dispersed fragments to fragment-supported breccias with fragments forming up to 60–70% of the total rock volume. Their size is usually between 1 and 20 cm, but sporadic clasts up to some meters across can be found. Reaction rims are uncommon, and the fragments show sharp contacts with the supporting matrix.
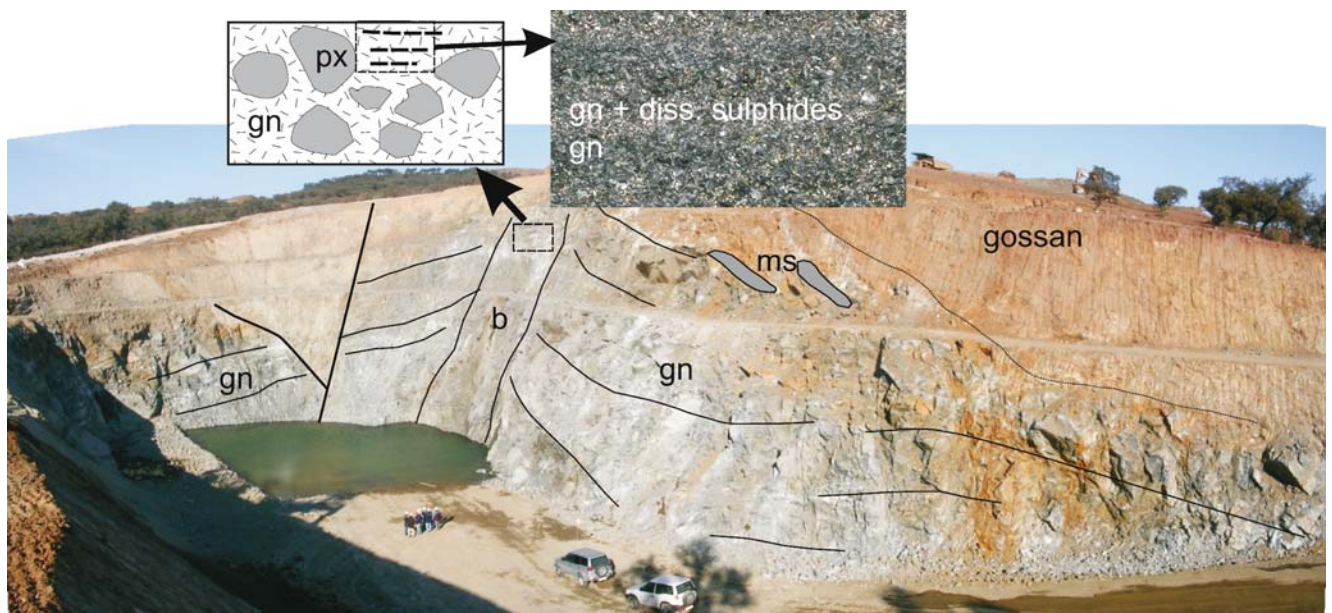
Fig. 7 Crosscutting relationships between the Gabbronorite Unit and the breccia in the northern orebody. The breccia (*b*) dissected the Gabbronorite Unit (*gn*), verticalizing the originally subhorizontal magmatic layering. The Gabbronorite Unit hosts some lenses of massive sulfides (*ms*). The uppermost part of the breccia bodies show centimeter-sized subhorizontal cumulate textures with pyroxenite fragments (*px*) supported by gabbronorite with disseminated ore

Fragments include:

(a) fine-grained (0.05–0.5 mm) massive pyroxenitic ortho-cumulate with no signs of internal deformation. The pyroxenite consists of subeuhedral to euhedral orthopyroxene (en$_{76-79}$; NiO<0.1 wt%) and clinopyroxene (diopside-augite) in variable proportions with only minor plagioclase and abundant intercumulus phlogopite and clinoamphibole (fluor–ferroedenite to magnesiohornblende). The pyroxenite fragments are poor in sulfides, and only little low-Ti magnetite and pyrrhotite occur.

(b) Host rock xenoliths, including calcic and magnesian skarns, pelitic and calcsilicate hornfels, and minor marble.

(c) Fine-grained gabbro, similar to the Contact Gabbro of the Aguablanca Stock.

(d) Rare peridotite fragments that consist of forsteritic olivine (fo$_{86-93}$; NiO=0.01–0.18 wt%), sometimes poikilitically included in orthopyroxene, and Mg-rich phlogopite (X_{phlog}=0.61–0.83). Olivine crystals surrounded by a kelyphitic rim of clinopyroxene, plagioclase, and spinel were described by Lunar et al. (1997).

(e) Serpentinite consisting of reniform to nodular serpentine with interstitial chlorite and Ti- and V-poor magnetite, graphite, and pyrrhotite. The intercumulus texture of the magnetite and sulfides suggests that these enclaves are altered peridotitic cumulates and are not retrograded magnesian skarn.

(f) Rare plagioclase-rich fragments, composed of subhedral plagioclase (an$_{95-100}$); the origin of these rocks is unknown and could well be a true anorthosite or a plagioclase-rich endoskarn similar to that found in the immediate vicinity of the stock. Piña et al. (2004) have also mentioned fragments of olivine-bearing gabbro and troctolite that have not been found in this study. The first two types of fragments account for more than 95% of the total clasts in the breccia. The barren breccia includes abundant fragments of partially digested host rock, while the ultramafic fragments dominate in the ore breccia.

The supporting groundmass of the breccia consists of either massive sulfides or coarse-grained gabbronorite with disseminated sulfides. Both sulfides and silicates are irregularly intergrown as centimeter- to meter-sized irregular masses with curved irregular to cuspated contacts that are unlikely for fragments and strongly suggest the presence of immiscible sulfide and silicate magmas (Fig. 8).

Massive sulfides occur as meter-sized lenses within the breccia and consist of coarse-grained pyrrhotite–pentlandite with irregular masses and veins of chalcopyrite and only evenly dispersed fragments. Dispersed in the massive sulfides, preferentially near the fragment margins, there are abundant millimeter-sized euhedral crystals of orthopyroxene (en$_{74-87}$; NiO<0.1 wt%) and diopside-augite in addition to some plagioclase and phlogopite. These pyroxene crystals are typically unoriented but have developed a glomeroporphyritic texture. However, they locally define a flow banding wrapping large fragments. These rocks are called leopardite in mine terminology.

The pipe-like morphology of the breccia bodies, the crosscutting relationships with the host Gabbronorite Unit, the polymictic nature of the fragments, and the presence of steeply dipping magmatic flow banding are all consistent with a highly dynamic mechanism of intrusion.

Figure 7 shows the crosscutting relationships between the different units in the NE area of the orebody. They show that the breccias are younger than the gabbronorite hosting the disseminated ore. The subhorizontal layering in the Gabbronorite Unit gradually displays steepness toward the barren breccia of the northern orebody, showing that the breccia disrupted an already layered but still ductile gabbronorite. Crosscutting relationships between the Diorite and Gabbronorite Units are unclear but the presence of enclaves of the latter in the diorite suggests that the Diorite Unit is younger than the Gabbronorite Unit.

Breccias similar to those of the Aguablanca deposit are fairly common in magmatic Ni–(Cu) deposits. They have been interpreted as zones of incomplete assimilation of the host rocks, sometimes in erosional channels in the footwall of magmatic complexes (e.g., Sudbury; Lightfoot et al.
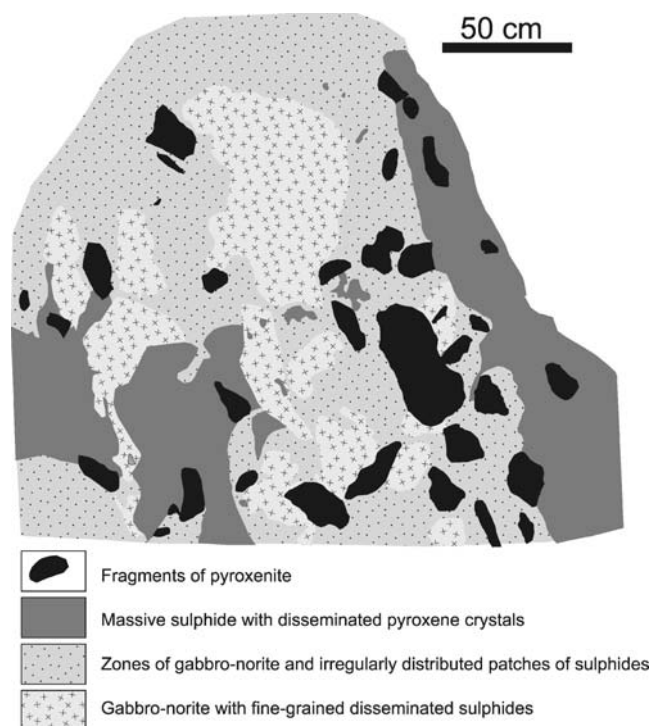
Fig. 8 Sketch highlighting the relationships between the gabbronorite and sulfide cement in the breccia

1997b), as collapse breccias in the top of intrusions (Noril'sk; Naldrett 1992) or as feeder zones to overlying plutons (e.g., Voisey's Bay; Ryan 2000). The spatial relationships with the host rocks and the relative timing make the breccia at the Aguablanca deposit somewhat similar to the Composite Gabbro or the Ovoid Conduit of Voisey's Bay, characterized by its subvertical morphology and the presence of gabbro with disseminated mineralization that is crosscut by the massive sulfides (Kerr and Ryan 2000). However, an uncommon feature of the breccia at the Aguablanca deposit is the relatively xenolith-poor character if compared with those described elsewhere.

The magmatic ore assemblage

The main sulfide mineralization intergrown with primary magmatic silicates shows two superimposed mineral assemblages. An earlier assemblage of massive pyrrhotite with inclusions of pentlandite and chalcopyrite (stage I) was variably replaced by later coarse-grained chalcopyrite, pyrrhotite, and pentlandite (stage II). Stage I pyrrhotite occurs as 0.2–3 mm (exceptionally 5 mm) anhedral grains; XRD spectra of this pyrrhotite display an irregular crest instead of the typical 102 peak. This pattern is consistent with partial retrogradation of hexagonal pyrrhotite to a monoclinic phase during subsolidus reequilibration (Arnold 1969). Pyrrhotite exsolved pentlandite in droplets or, more frequently, in 50- to 100-μm-sized flames (Fe/Ni=0.96–1.08) along grain boundaries or within microfractures. As for many other equivalent systems, this early assemblage is interpreted as having formed through the exsolution of a monosulfide solid solution (Fe, Ni, Cu)$_{1-x}$ S$_x$ during the early crystallization of a parental sulfide melt (e.g., Chai and Naldrett 1992; Ebel and Naldrett 1996).

However, most of the economic mineralization seems to be younger. Here, chalcopyrite, pyrrhotite, and pentlandite occur as coarse-grained aggregates (1–5 mm) that replaced early pyrrhotite or formed independent intercumulus or massive facies. Chalcopyrite occurs as subrounded grains that locally include small grains of cubanite, euhedral cobaltite, magnetite, and graphite. Pyrrhotite, lacking exsolved pentlandite, occurs as coarse grains interlocked with pentlandite and, to a lesser extent, with chalcopyrite. Pentlandite (Fe/Ni=0.8–1.2) occurs as inclusion-free, highly fractured independent grains between coetaneous pyrrhotite and chalcopyrite, or as veins within the latter. Evolution from early pyrrhotite-rich ores to later chalcopyrite-rich ones is typical of magmatic Cu–Ni deposits and is an expected consequence of fractional crystallization of sulfide melts (e.g., Naldrett 1989). The scarcity of Co-bearing minerals suggests that most of the Co is in the pentlandite lattice.

The relative timing of the magmatic mineralization can be established from petrographic relationships. Orthopyroxene and olivine are usually devoid of sulfide inclusions but are usually rimmed by sulfides; symplectitic intergrowths of pyrrhotite–orthopyroxene occur only locally. Moreover, the presence of abundant droplets of pyrrhotite in clinopyroxene suggests that sulfide immiscibility took place synchronously with the crystallization of orthopyroxene but predated the crystallization of clinopyroxene.

Abundant subhedral to anhedral magnetite occurs during intercumulus phase to pyroxene but earlier than the sulfides. Magnetite is Ti-rich (up to 1.2 wt%; see Electronic Supplementary Material) and locally carries exsolved ilmenite needles. Similar Ni-, Cr-, and Al-poor magnetite has been reported at Sudbury (Barnes and Tang 1999). Some ilmenite crystals are also observed but their relationship in the paragenetic sequence is not fully understood.

The sulfides exhibit a subtle deformation, and pyrrhotite and pentlandite show tectonic twinning and brecciation near major faults only.

Hydrothermal and supergene alteration

The Aguablanca Stock underwent an irregular but pervasive polyphase hydrothermal alteration. Most of the rocks show a subtle alteration with irregular replacement of primary mafic minerals by phlogopite (X_{phlog}, 0.68–0.74) and actinolite/magnesiohornblende (Fe/Fe+Mg, 0.07-0.52; see Electronic supplementary material) and of plagioclase by sericite, calcite, and chlorite.

However, alteration is particularly intense near the faults and lithologic contacts, predominantly affecting the plagioclase-bearing rocks, with the texturally destructive assemblage of clinoamphibole, biotite, clinozoisite (X_{ep}=0.02–0.03), quartz, and sulfides. Typical trace minerals are apatite, titanite, and zircon. The proportion of hydrothermal sulfides is quite variable, ranging from semimassive to disseminations or veinlets in altered gabbronorite. The sulfide assemblage is dominated by coarse-grained chalcopyrite and pyrite with only random inclusions of pyrrhotite and sphalerite. Bravoite and mackinawite are present as small grains, the latter replacing pentlandite. There is a characteristic late assemblage of magnetite–pyrite–graphite.

Ortega et al. (1999, 2004) have carried out an extensive study of the platinum group-bearing minerals and related phases. In Aguablanca, these minerals are found as grains of between 1 and 15 μm (exceptionally up to 45 μm) and consist of Pd- and Pt-bearing tellurides usually associated with Ag and Bi tellurides and native gold. The location of these minerals in fractures or on grain edges of pyrrhotite and pyrite strongly suggests that they are of hydrothermal origin and probably related to the retrograde alteration of

the magmatic sulfides, by which PGE contained as solid solution became liberated. This is consistent with the proton-microprobe studies of Czamanske et al. (1992) that show that early, high-temperature chalcopyrite and pentlandite can host significant amounts of Pd and Pt. A hydrothermal origin for the discrete PGE minerals in Cu–Ni deposits has been postulated by several authors (e.g., Mathez and Peach 1989).

A later hydrothermal event gave rise to irregular masses and veins of calcite, chlorite (clinochlore-pycnochlorite), phengite, talc, tremolite, quartz and sulfides, typically pyrite, chalcopyrite, mackinawite, and marcasite.

The hydrothermal alteration at Aguablanca is similar to that described elsewhere in magmatic Ni–(Cu) deposits (e.g., Ripley 1990), which has been interpreted as the major cause of Cu (Ripley et al. 1993) and PGE redistribution (e.g., Mathez 1989; Stumpfl 1993).

Supergene alteration is intense in the shallow part of the orebodies, with development of an earthy and soft goethite-, chlorite-, and clay-rich gossan up to 8–16 m in depth with grades up to 1% Ni; at near fractures, this supergene alteration reaches to depths of up to 60–80 m (Suarez et al. 2005). Incipient supergene alteration has altered pyrrhotite and pyrite to marcasite, magnetite to hematite, and chalcopyrite to chalcocite and covellite. Perhaps the most important aspect is the partial replacement of pentlandite by fine-grained violarite along grain edges and fractures. PGE minerals seem to be also concentrated in the supergene zone (Ortega et al. 2004).

The structural setting

Besides earlier Variscan folding and thrusting of the host sequence (Casquet 1980), the more important structures in the area are longitudinal strike-slip faults. The Santa Olalla Plutonic Complex is bounded by two first-order left-lateral strike-slip faults, i.e., the Cherneca Fault to the north and the Zufre Fault to the south (Figs. 1 and 2). The Cherneca Fault is associated with secondary antithetic faults that delimit blocks with a bookshelf geometry (Tornos et al. 2002b). A third structure, the Garrenchosa Shear Zone is found between the Santa Olalla Main Pluton and the Aguablanca Stock (Figs. 2 and 3), but mapping shows that it represents an anastomosing segment of the Cherneca Fault. The Garrenchosa Shear Zone includes a complex array of ENE–WSW sinestral shear zones that turn to the NNW–SSE west of the Aguablanca Stock. In detail, the Cherneca Fault and the Garrenchosa Shear Zone define an elongated structure 3 km long and up to 1.5 km wide, which hosts the Aguablanca Stock (Fig. 3). Mapping also shows that the regional cleavage and bedding of the host rocks generally wrap around the Aguablanca Stock, with dips between 50 and 70° outward.

The Santa Olalla Main Pluton displays gentle magmatic foliation that is subhorizontal or gently dipping inward. In the Aguablanca Stock, the foliation is less prominent but is also subhorizontal and trending N50 to N95°E. However, it changes to near vertical dips approaching the breccia bodies (Figs. 2 and 7), where both the flow banding in the massive sulfides and the orientation of the breccia fragments trace a subvertical magmatic foliation.

The Aguablanca Stock is densely fractured; however, the fractures do not extend away from the pluton into the host rocks. The more significant faults are subparallel to the Cherneca Fault, having strikes of N90–110°E and dips of 60° or more to the NE. The location of the orebodies seems to be controlled by left-lateral N35–55°E trending faults with steep dips (Fig. 6). Synthetic NW–SE trending faults, with a staircase geometry and 10 to 30-m spacing, branch out from the Cherneca Fault. Finally, there are WNW–ESE faults with dips close to 45°S; they seem to displace the mineralization at depth toward the south.

As a consequence of faulting, most contacts are tectonic, distorting the original morphology of the orebodies (Figs. 3, 5 and 6). Ongoing operation shows that three major strike-slip faults, the denominated F_1 to F_3, limit the mineralized area. F_1 and F_3 trend N50–60°E and dip steeply; F_1 marks the NW limit of the southern orebody, while F_3 bounds the SE limit. F_2 is a N40°E trending fault that splits the southern orebody in two different zones denominated west and east (Fig. 6). The F_3 structure hosts several ore pockets in extensional jogs indicating that it was active during the ore-forming process and controlled the emplacement of the orebodies.

Geochronology of the orebody

The age of the Aguablanca Stock and the hosted orebody has been one of the more controversial points for the regional geology, with implications to both the genetic interpretation of the deposit and mineral exploration models.

Two phlogopite concentrates, one from the gabbronorite cement from the ore breccia (AG-38) and another from a gabbro in the Gabbronorite Unit (AG-68), were selected for $^{40}Ar/^{39}Ar$ dating. Both rock samples contain abundant phlogopite that forms 1 to 3-mm-sized aggregates interstitial to plagioclase and pyroxene. Because the closure temperature for the diffusion of Ar is ca. 400°C, i.e., lower than the crystallization temperature of silicate magmas and the ore, $^{40}Ar/^{39}Ar$ dating of phlogopite provides minimum ages.

Phlogopite concentrates were irradiated for 50 h in packages KD32 and KD37 at the TRIGA reactor at the U.S. Geological Survey in Denver. Hornblende from the McClure Mountain Syenite (MMhb-1) with an age of 519.4±2.5 Ma (Alexander et al. 1978; Dalrymple et al. 1981) was used as a monitor mineral. The mineral concentrates were analyzed at

the USGS Argon Thermochronology Laboratory in Denver on a VG Isotopes Model 1200 B Mass Spectrometer fitted with an electron multiplier using the $^{40}Ar/^{39}Ar$ step-heating method of dating. For additional information on both analytical procedures and data reduction, see Kunk et al. (2001). We used the decay constants recommended by Steiger and Jäeger (1977). Plateau ages are identified when three or more contiguous steps in the age spectrum agree in age, within the limits of analytical precision, and contain more than 50% of the $^{39}Ar_K$ released from the sample. Average ages were calculated in the same manner as plateau ages except where contiguous steps do not agree. The $^{40}Ar/^{39}Ar$ step-heating values are listed in Table 3 and presented in Figs. 9 and 10.

The age spectrum for phlogopite AG-38 is fairly concordant but does not define a plateau. However, an isochron age of 335.0±2 Ma ($^{40}Ar/^{36}Ar_{initial}$=220±48; MSWD=0.63; 100% of total $^{39}Ar_K$ gas) was obtained. The age spectrum for phlogopite AG-68 is also fairly concordant but also does not define a plateau. However, a statistically well-constrained isochron age of 338.2±3.0 Ma was retrieved ($^{40}Ar/^{36}Ar_{initial}$=461±97; MSWD=0.47; 100% of total $^{39}Ar_K$ gas). Both phlogopite ages are coincident within the error limits between 335 and 337 Ma; thus, the age interval of coincidence probably corresponds to the age of cooling of the pluton and orebody below ca. 400°C.

These phlogopite Ar–Ar ages are consistent with the U–Pb zircon crystallization ages for the igneous rocks (Romeo et al. 2004; Spiering et al. 2005). Whole-rock K–Ar dating of the Gabbronorite Unit by Casquet et al. (1999) yielded two ages (325 and 307 Ma) that are significantly younger than the phlogopite Ar–Ar ages, suggesting that significant hydrothermal overprint occurred after the crystallization of the plutons.

Mafic–ultramafic intrusions of the Cortegana Igneous Complex

Bodies of mafic and ultramafic plutonic rocks, formerly mapped as "diorite", are widespread in the Aracena Massif. As quoted above, these intrusions probably correspond to exhumed portions of a deep magmatic complex located below the Ossa Morena Zone.

In the Cortegana area (Fig. 11), plutonic rocks, grouped in the Cortegana Igneous Complex, form lenses concordant with the subhorizontal foliation in the host migmatite (Fig. 4h). The lenses can be up to 600 m thick and are mainly composed of gabbro and norite. They host several, up to 100–150 m thick, units of ultramafic rocks, including olivine websterite, lherzolite, dunite, and orthopyroxenite; harzburgite, troctolite, and wehrlite are also found. Anorthosite locally occurs in the footwall of the ultramafic

bodies. A contact zone, 15–300 m thick, consists of tonalite to diorite with abundant diffuse remnants of incompletely digested host rock. This outer hybrid contact facies grades into orbicular (quartz)-diorite and tonalite (Fig. 4g) and the innermost gabbro–norite. All the igneous rocks are coarse-grained, show a subhorizontal magmatic layering and cumulus textures, and have abundant intercumulus phlogopite and amphibole; xenoliths of skarn and of calc-silicate and pelitic hornfelses are common. Moreover, graphite is locally abundant and probably derived from the digestion of the graphite-bearing black quartzite interbedded in the Neoproterozoic metasedimentary sequence (Rodas et al. 2000). Hydrothermal alteration is pervasive and has produced an irregular retrograde mineral assemblage. All rocks are crosscut by aplitic to pegmatitic dykes of trondhjemitic composition, which probably represent partial melts derived from the host migmatite.

Recent exploration work by Rio Narcea SA (Spiering et al. 2005) has recognized several mineralized zones within the ultramafic cumulates. Mineralization consists of pyrrhotite and chalcopyrite with minor amounts of pentlandite. Bulk grades are low, near 0.16% Ni and 0.08% Cu, but there are narrow intervals with higher grades reaching up to 1.4% Ni and 0.2% Cu. The PGE contents are also very low at about 2–6 ppb combined PGE.

Phlogopite $^{40}Ar/^{39}Ar$ chronology

Two concentrates of phlogopite from quartz-diorite (TEJ-3) and websterite (ZOM-23) from the Cortegana Igneous Complex were dated by the $^{40}Ar/^{39}Ar$ method following the procedure described above (Table 3).

Sample TEJ-3, which is heterogeneous and shows evidence of interaction with the host migmatite, shows a disturbed age spectrum (Fig. 9). However, an isochron age of 321.5±32.6 Ma ($^{40}Ar/^{36}Ar_{initial}$=4,039±4,214; MSWD=0.06; 70.6% of total $^{39}Ar_K$ gas) was obtained. Sample ZOM-23 yielded a plateau age of 336.2±1.7 Ma (steps B through D; 58% of $^{39}Ar_K$). This age is supported by the less precise isochron age of 328.1±6.3 Ma. Both phlogopite ages record minimum ages for the crystallization of the igneous rocks and their sulfide mineralization in the Cortegana Igneous Complex and are within error of those found for the Aguablanca Stock. Because peak–metamorphic conditions in the Aracena Massif were attained between 342 and 328 Ma (hornblende $^{40}Ar/^{39}Ar$ ages; Dallmeyer et al. 1993; Castro et al. 1999), we infer that mafic/ultramafic magmatism in the Aracena Massif took place synchronously with the high-T low-P postorogenic metamorphism and was broadly coeval with the emplacement of the Santa Olalla Plutonic Complex at epizonal levels.

The synmetamorphic emplacement of the Cortegana Igneous Complex is evidenced by concordance of the

Table 3 ^{40}Ar/^{39}Ar step-heating data for phlogopite separates from Aguablanca and Cortegana, SW Spain

Step	T (°C)	^{39}Ar of total (%)	Radiogenic yield (%)	^{39}Ar$_k$ (mol × 10^{-12})	$\frac{^{40}Ar^*_k}{^{39}Ar_k}$	Apparent K/Ca	Apparent K/Cl	Apparent age (Ma)	Error (Ma)
(a) AG-38. Phlogopite. J=0.012248±0.50%. Wt.=2.5 mg. #36KD32									
A	1,000	5.6	95.7	0.01592	16.432	31.1	17	330.8	±2.0
B	1,050	7.1	98.8	0.02033	16.552	33.4	18	333.0	±1.7
C	1,100	6.4	99.0	0.01844	16.580	21.6	17	333.5	±1.9
D	1,150	9.2	99.2	0.02647	16.768	15.3	17	337.0	±1.1
E	1,200	14.9	99.5	0.04278	16.797	24.5	17	337.5	±0.8
F	1,250	29.4	99.7	0.08420	16.660	89.0	19	335.0	±0.5
G	1,300	27.4	99.8	0.07867	16.595	37.6	20	333.8	±0.4
Total gas		100.0	99.3	0.28681	16.647	47.0	18	334.8	
(b) AG-68. Phlogopite. J=0.012328±0.50%. Wt.=2.4 mg. #34KD32									
A	1,000	7.3	96.0	0.01816	17.049	29.2	16	344.1	±1.2
B	1,050	7.0	98.7	0.01743	16.901	23.3	18	341.4	±1.8
C	1,100	7.4	99.3	0.01835	17.019	15.5	17	343.6	±1.9
D	1,150	12.0	99.1	0.02984	17.014	13.9	17	343.5	±1.1
E	1,200	23.9	99.6	0.05927	16.793	40.7	18	339.4	±0.5
F	1,250	30.7	99.9	0.07617	16.680	61.4	21	337.4	±0.4
G	1,300	11.6	99.7	0.02890	16.496	29.6	22	334.0	±1.1
Total gas		100.0	99.3	0.24814	16.793	38.6	19	339.4	
(c) TEJ-3. Phlogopite. J=0.011726±0.50%. Wt.=7.9 mg. #23KD37									
A	1,000	15.1	98.3	0.1154	17.704	12.5	54	340.3	±0.8
B	1,050	9.0	98.9	0.0690	18.045	12.3	55	346.3	±0.9
C	1,100	11.4	99.0	0.0871	18.718	11.1	53	358.0	±0.8
D	1,150	18.5	993	0.1410	18.741	9.6	56	358.4	±0.6
E	1,175	14.6	99.4	0.1119	18.049	12.3	62	346.3	±0.5
F	1,200	14.6	99.5	0.1113	17.784	13.5	26	341.7	±0.5
G	1,225	11.5	99.5	0.0881	17.614	13.0	43	338.7	±0.6
H	1,250	5.3	98.7	0.0402	17.377	6.6	60	334.6	±0.9
Total gas		100.0	99.1	0.7639	18.076	11.6	50	346.8	
(d) ZOM-23. Phlogopite. J=0.011726±0.50%. Wt.=8.0 mg. #27KD37									
A	1,000	15.9	98.9	0.1435	17.684	46.4	53	339.4	±0.47
B	1,050	13.5	99.3	0.1218	17.555	24.0	63	337.7	±1.47
C	1,100	23.7	99.8	0.2138	17.537	545	68	337.4	±0.43

D	1,150	20.7	99.9	0.1862	17.420	30.0	69	335.3	±0.34
E	1,175	9.9	98.9	0.0894	17.084	13.8	65	329.4	±1.20
F	1,200	9.4	99.3	0.0852	17.180	10.2	22	331.1	±0.77
G	1,225	6.8	997	0.0616	17.199	5.3	38	331.4	±0.61
Total gas		100.0	99.5	0.9015	17.437	32.5	58	335.6	

Ages calculated assuming an initial $^{40}Ar/^{36}Ar=295.5\pm0$. All precision estimates are at the one-sigma level of precision. Ages of individual steps do not include error in the irradiation parameter J. No error is calculated for the total gas age.

(a) Isochron information: $[^{40}Ar/^{36}Ar]_i=220\pm48$; steps A–G with 100% of $^{39}Ar_K$. Isochron age: 335 ± 2.0 Ma; MSWD=0.63;

(b) Isochron information: $[^{40}Ar/^{36}Ar]_i=461\pm97$; steps A–G with 100% of $^{39}Ar_K$. Isochron age: 338.2 ± 3.0 Ma; MSWD=0.47;

(c) Isochron information: $[^{40}Ar/^{36}Ar]_i=4,093\pm4,214$; steps A–G with 70.6% of $^{39}Ar_K$. Isochron age: 321.5 ± 32.6 Ma; MSWD=0.06;

(d) Isochron information: $[^{40}Ar/^{36}Ar]_i=1,329\pm557$; steps A–G with 100% of $^{39}Ar_K$. Isochron age: 328.1 ± 6.3 Ma. Plateau age: 336.2 ± 1.7 Ma with 57.9% of gas on plateau in 1,050 through 1,150 steps; MSWD=0.76;

igneous bodies with the migmatite foliation, the thorough mixing with migmatite at the contacts, and the location of the igneous rocks in the high-grade core of the Aracena Massif, with the metamorphic grade quickly diminishing outward (Crespo 1991). The maximum metamorphic P–T conditions for the Aracena Massif (>920 to 1,000°C; 4 to 6 kbar), identified by Patiño Douce et al. (1997) and Diaz-Azpiroz et al. (2004), are also consistent with the metamorphism being directly related to the intrusion of mafic magmas.

West of the Aracena Massif is the large synmetamorphic Beja Igneous Complex, which comprises layered olivine–hypersthene gabbro, quartz diorite, troctolite, and anorthosite and contains Fe–Ti–V oxide concentrations and Cu–(Ni) disseminations similar to those of Aguablanca and Cortegana (Mateus et al. 2001). Amphibole $^{40}Ar/^{39}Ar$ ages of ca. 352 to 338 Ma were recorded for the regional metamorphism (Dallmeyer et al. 1993). These ages overlap with those found for Aracena and Aguablanca, strengthening the idea that mafic–ultramafic magmatism, sulfide ore formation, and high-T low-P regional metamorphism were largely coeval (Fig. 10).

Geochemistry of the igneous host rocks

Representative chemical analyses of rocks from a database of fifty three samples from the Santa Olalla Plutonic Complex are shown in Table 2. Analyses were carried out at the laboratories of the Instituto Geológico y Minero de España (IGME) by XRF for major and trace elements except Na_2O that was measured by AAS. Rare earths and Y were measured by ICP-MS-TOF.

Rocks showing petrographic evidence of pervasive hydrothermal alteration or having significant sulfur content (>0.3 wt% S) were excluded from the database. For calculations, the analyses have been recalculated on a S- and water-free basis and normalized to 100 wt%; all sulfur is assumed to be in the form of pyrrhotite and, thus, an equivalent proportion of iron has been subtracted from the total sum. Complementary data can be found in Casquet et al. (2001) and in the Electronic supplementary material.

The Aguablanca Gabbronorite Unit

The less altered rocks of the Gabbronorite Unit are characterized by high silica contents (48.0–57.3 wt% SiO_2; average 52.3 wt%) but are slightly depleted in FeO_t (6.0–16.5 wt%; average 8.8 wt%) and TiO_2 (0.23–0.83 wt%; average 0.49 wt%), CaO (6.1–14.3 wt%; average 7.6 wt%), alkalis (specially Na_2O), and Al_2O_3 (7.2–17.3 wt%; average 10.8 wt%) as well as in Y, Ce, and Eu compared to average basalt (e.g., Middlemost 1985). Total REE content is low

Fig. 9 ^{40}Ar–^{39}Ar age spectra diagrams for step-heating experiments of phlogopite mineral separates from the Aguablanca deposit (AG-38 and AG-68) and the Cortegana prospect (TEJ-3 and ZOM-23)
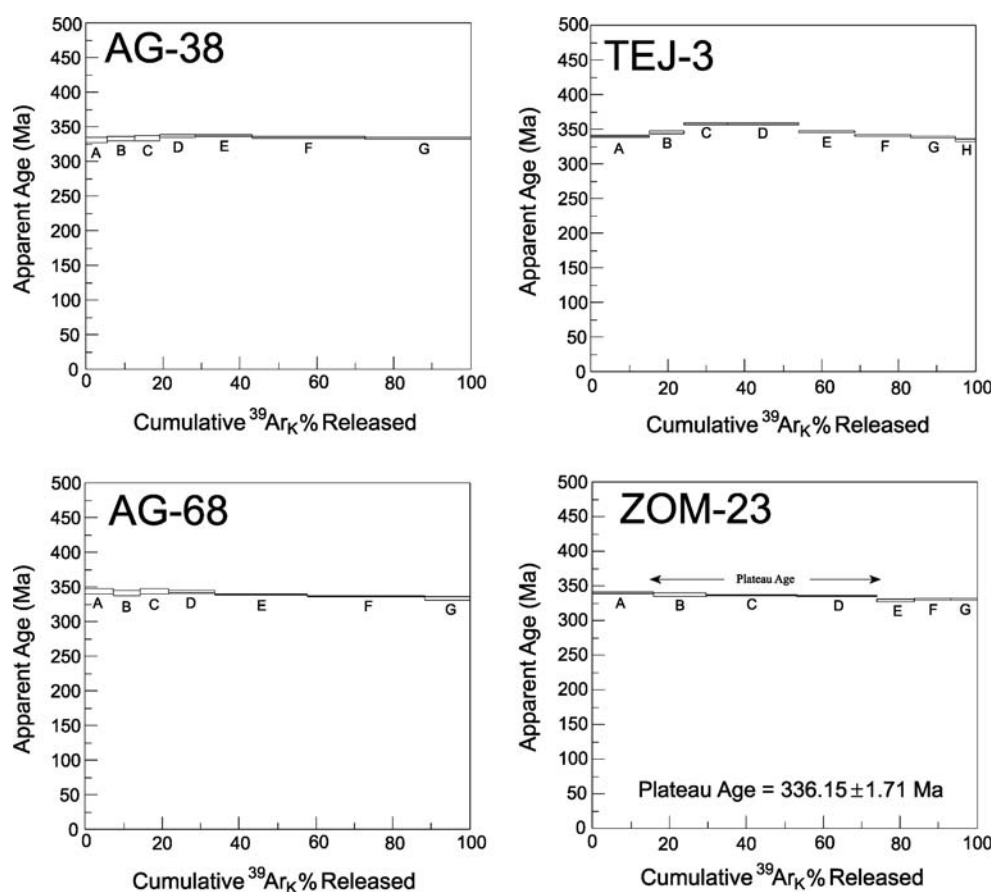
(5–57 ppm), but the rocks have relative enrichment in LREE ([La/Sm]$_{MN}$=0.53–3.1; average 2.3; [La/Yb]$_{MN}$= 0.6–7.5; average 4.1). The Mg number (Mg#, atomic Mg/ Mg+Fe) varies between 0.38 and 0.54. As a whole, the samples are broadly similar to the silica- and magnesium-rich basalt of Hoatson and Sun (2002).

Most of the rocks of the Gabbronorite Unit have geochemical features of cumulates, such as high MgO (8.3–19.1 wt%), Ni (96–927 ppm), and Cr (670–1,504 ppm) contents (Casquet et al. 2001), but cumulate textures are uncommon. The composition of the Contact Gabbro and the fact that the outcropping rocks were close to the roof of the intrusion (Casquet 1980) make it unlikely that such a geochemical pattern was controlled by in situ accumulation; more likely, it is a feature inherited from a deep source. Different explanations include: (a) a parental MgO-rich magma; (b) formation of an olivine/pyroxene cumulate and subsequent remelting; (c) major assimilation of amphibolite or dolostone; (d) plagioclase fractionation and concomitant Fe–Mg enrichment; and (e) a deep stratified magma chamber. Most of these alternatives are at odds with the geochemical and geological features, and (e) is the most likely possibility, i.e., a chemical and density gradient in a magma chamber. More dense and mafic melt should accumulate in the bottom of the chamber,

whereas more felsic magmas should concentrate in the upper part, as has been described by Beard and Day (1988) for the Smartville Complex, USA, or by Cawthorn and Kruger (2004) for the Mount Ayliff intrusion, South Africa.

The composition of the Contact Gabbro is probably the best approximation to the magma that formed the Gabbronorite Unit because it is interpreted to be a chilled margin without syncrystallizational modifications. Its composition is close to that of the average Gabbronorite Unit but is slightly enriched in Al$_2$O$_3$, CaO, K$_2$O, Rb, Sr, Ba, and U and depleted in FeO, Cr, Nb, and Y (Table 2 and Figs. 12, 13, 14 and 15).

Most of the rocks plot on linear trends on Pearce element ratio diagrams (Fig. 12). The Al/Ti vs Ca/Ti and Si/Ti vs (Fe+Mg)/Ti ratios define straight lines with good correlation, which overlap with the orthopyroxene control line as calculated from the average orthopyroxene composition in the Gabbronorite Unit. In these plots, only four samples could arguably be related to olivine fractionation. Most of the rocks belonging to the Gabbronorite Unit plot in the norite field of the CaO–MgO diagram (Fig. 13), in between the tie lines of the composition of orthopyroxene and plagioclase. These geochemical trends are consistent with the petrographic observation that the Gabbronorite Unit
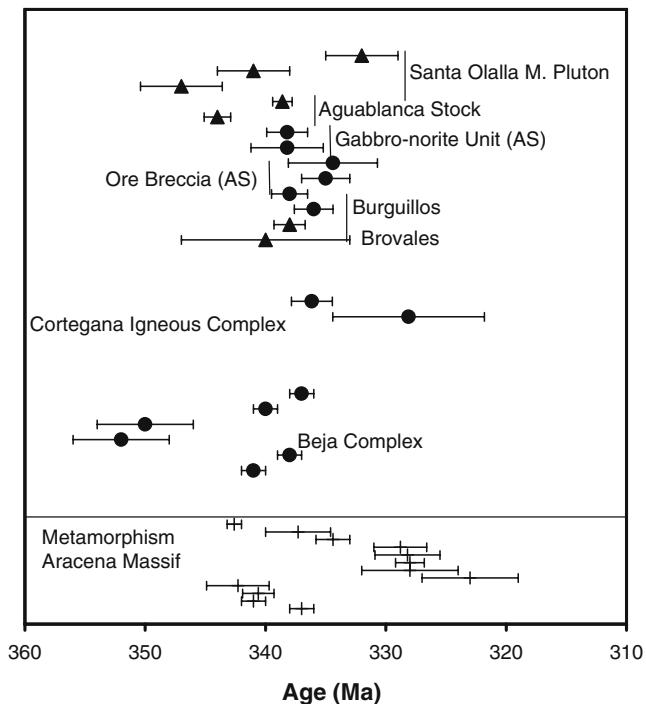
Fig. 10 U–Pb (*triangles*) and Ar–Ar ages (*circles*) of metaluminous plutonic rocks of the Ossa Morena Zone. Data from Garcia Casquero (1995), Casquet et al. (1998), Pin et al. (1999), Montero et al. (2000), Romeo et al. (2004), Spiering et al. (2005), and this study. For comparison, Ar–Ar ages of the regional metamorphism in the Aracena Massif are also included (Dallmeyer et al. 1993; Castro et al. 1999). *AS* Aguablanca Stock

always has higher proportions of orthopyroxene than clinopyroxene.

The Aguablanca Diorite Unit and the Santa Olalla Main Pluton

Rocks of the Diorite Unit and the Santa Olalla Main Pluton show neither petrographic nor chemical evidence of cumulus processes. They are geochemically different from the Gabbronorite Unit, having higher SiO_2, REE, Ba, Y, Nb, Th, Zr, Ba, V, and TiO_2 but lower Cr, Co, and MgO contents. These rocks are metaluminous with SiO_2 contents between 50 and 70 wt%, K_2O up to 4.7 wt%, and low Cr values (<280 ppm; average 173 ppm). The REE content is high, averaging 173 ppm, and the rocks are also variably enriched in LREE ([La/Sm]$_{MN}$=1.5–9.6; average 3.9; [La/Yb]$_{MN}$=3.0–29.4; average 10.5). Incompatible elements show a greater range than in the Gabbronorite Unit. The K_2O content, usually above 2 wt%, and the low FeO_t+TiO_2 contents are typical of a high-K_2O calc-alkaline magmatic trend (Fig. 14). In fact, the overall trend plots on the calc-alkaline field of the FeO/MgO–SiO_2 and FeO–Na_2O+K_2O–MgO diagrams (not shown); the TiO_2 content is below that of tholeiitic magmas.

Rocks belonging to the Diorite Unit and the Santa Olalla Main Pluton are geochemically similar, but in most binary diagrams, the compositions do not overlap, indicating that there is a compositional gap between both intrusive units. This is probably due to the different evolution within independent magma chambers.

Evidence for extensive contamination in a shallow magma chamber

Crustally contaminated mafic magmas are typically enriched in SiO_2, K_2O, Rb, Ba, Th, and LREE and usually have low TiO_2 contents (Lightfoot et al. 1990; Li et al. 2000). They tend to have high Th/Yb, La/Sm, La/Nb, Th/Nb, and La/Yb ratios reflecting the high LILE/HFSE ratio (Fig. 15), which usually correlates with high SiO_2 (Lightfoot et al. 1990; Li et al. 2000). Condie (2003) has also used the Ce/Yb, Sm/Nd, and Gd/Yb ratios to monitor crustal contamination. La/Nb >1.4, [La/Sm]$_{MN}$ >1.5, and Th/Ce >0.05 are typical of rocks with significant crustal contamination. Other variables such as the MgO, TiO_2, or Ce contents reflect the degree of fractional crystallization (Lightfoot et al. 1990; Li et al. 2000). Thus, the La/Sm ratio vs the MgO or Th/Nb can trace the role of fractional crystallization vs magma mixing or crustal contamination (e.g., Lesher et al. 2001). As can be seen in Fig. 15, the decrease in MgO due to accumulation of pyroxene and/or olivine is accompanied by an increase in La/Sm ratios, indicating that an AFC (assimilation-fractional crystallization) process is the more likely mechanism of magma evolution at Aguablanca. Furthermore, fractional crystallization alone is not consistent with the large variation in the Th/Nb and La/Sm ratios, which indicates that considerable crustal contamination occurred. The dominance of orthopyroxene and the increase of Gd/Yb with changing La/Sm (Fig. 15) exclude variable degrees of partial melting of a homogeneous melt as the dominant evolutionary mechanism. The Th/Nb ratio of rocks from the Gabbronorite Unit and the Diorite Unit–Santa Olalla Main Pluton are similar (0.03–1.73 vs 0.18–1.22) and usually well above the primitive mantle values (0.12), indicating that the proportion of contaminated material is high but variable (Fig. 15). Low Sr/Y ratios, usually less than 35, suggest that the magma equilibrated with a plagioclase-rich but garnet- and amphibole-poor reservoir, i.e., middle to upper crustal environment (Defant and Drummond 1990).

Trace element and REE spider diagrams (Pearce 1996) normalized to primitive mantle (McDonough and Sun 1995) are shown in Fig. 16. The average values for the Santa Olalla Plutonic Complex show an overall enrichment in LILE (Rb, K), Th, and LREE and are strongly depleted in more compatible Cr. The moderately incompatible elements (Ti, V, Sr, Y, Zr, Ce, and Eu) show variable enrichment
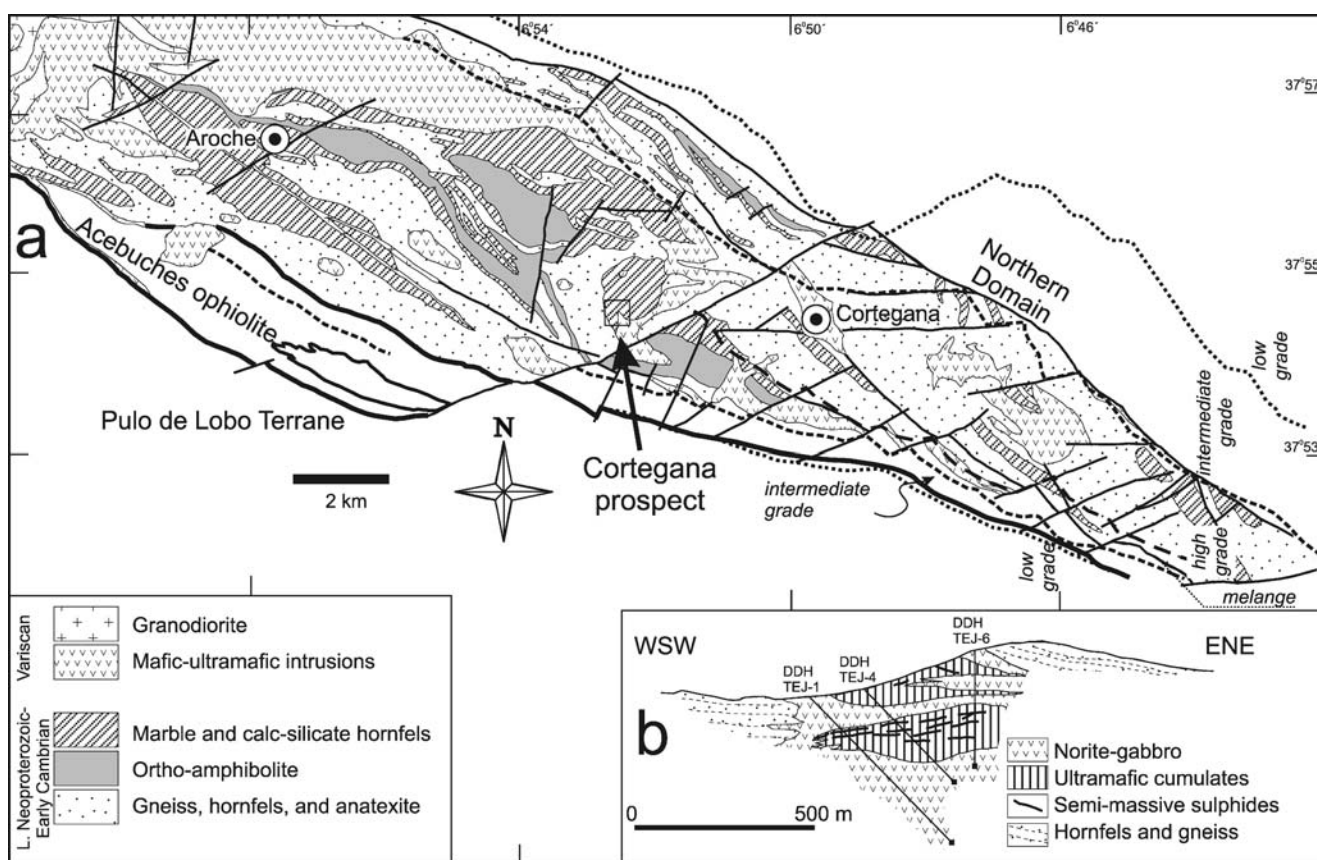
Fig. 11 Geologic setting of the central Aracena Massif showing the location of the Cortegana Igneous Complex. **a** Schematic geologic map, based on IGME (1983), with the metamorphic isograds of Crespo (1991). **b** Cross section of the Cortegana prospect based on drill-hole information of Rio Narcea Nickel (unpublished)

between 1 and 50, and Nb has a variable behavior. These values, bracketed between primitive mantle and upper continental crust (Taylor 1995), are typical of mature magmatic arcs with major crustal contamination. The ultramafic cumulates and the Gabbronorite Unit show less pronounced anomalies than the Diorite Unit and the Santa

Olalla Main Pluton, which have a pattern similar to that of the middle-upper crust. A simplified binary mixing model allows to estimate that the Gabbronorite Unit has incorporated about 20–25% of crustal material, whereas the Santa Olalla Main Pluton has more than 60–80% of crustal contamination.
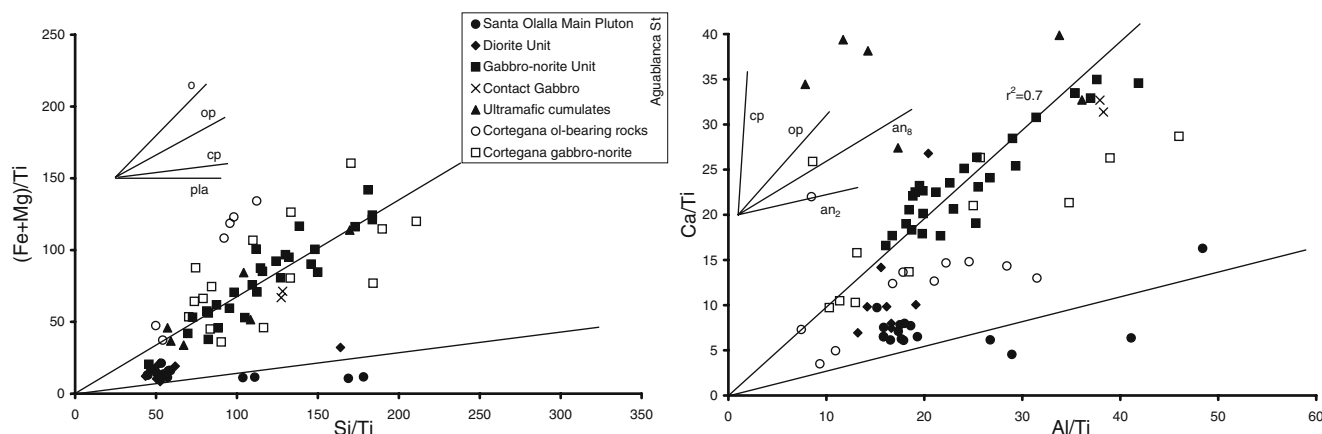
Fig. 12 Pearce element Ca/Ti vs Al/Ti and (Fe+Mg)/Ti vs Si/Ti diagrams showing that the evolution of the Santa Olalla magmatic sequence was controlled by the fractional crystallization of orthopyroxene except the more acid terms that are controlled by plagioclase. The fractionation curves of ortho- and clinopyroxene are calculated for the average composition of these minerals in the Gabbronorite Unit. Based on James et al. (2002)

Fig. 13 CaO–MgO diagram showing the composition of the analyzed rocks. Tie lines limiting fields are only estimative. *Small x, circles*, and *crosses* represent the composition of individual plagioclase, orthopyroxene, and clinopyroxene within the Aguablanca Stock. *PUM* Average composition of the Primitive Upper Mantle, *UC* average composition of the Upper Crust. *Legend as in Fig.* 12
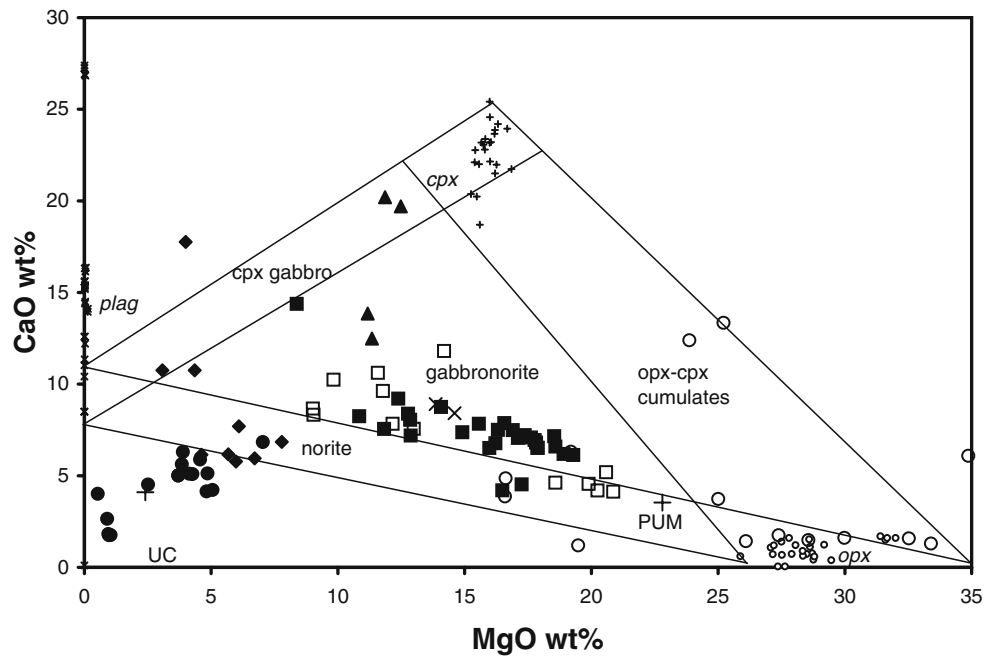
Rocks of the Santa Olalla Plutonic Complex are significantly enriched in REE, particularly in LREE, and have steep REE profiles with a systematic enrichment in ΣREE from the ultramafic cumulates to the Gabbronorite Unit, the Diorite Unit, and the Santa Olalla Main Pluton. This is accompanied by an increase in the LREE content, with average $[La/Yb]_{MN}$ values of 4.1 in the Gabbronorite Unit, 8.7 in the Diorite Unit, and 11.2 in the Santa Olalla Main Pluton (Fig. 16). The weak negative Eu anomaly (Eu/Eu* 0.8–0.9) and the high Sm/Nd and La/Yb ratios in the more mafic rocks are consistent with orthopyroxene fractionation and absence of plagioclase-rich cumulates. Within the Diorite Unit and the Santa Olalla Main Pluton, the negative Eu/Eu* anomaly (Eu/Eu* 0.5–0.6) is more

pronounced confirming that plagioclase fractionation played a major role in the evolution of these rocks.

All rocks analyzed show evidence of contamination or accumulation and, accordingly, the chemical composition of the primitive magma cannot be inferred with certainty. The closest approximation to the MgO content of the parental magma can be estimated following the procedure of Makkonen (1996). Rare olivine (fo$_{86-87}$) found in the breccia fragments is interpreted as the earliest accumulated mineral. Using a K_D of 0.33 (Makkonen 1996), the magma may have been near 12 wt% MgO. Similarly, orthopyroxene compositions are consistent with olivine compositions, and the earliest orthopyroxene accumulated from parental magmas of 12 wt% MgO, with the latest orthopyroxene forming from a magma with 6.2 wt% MgO.
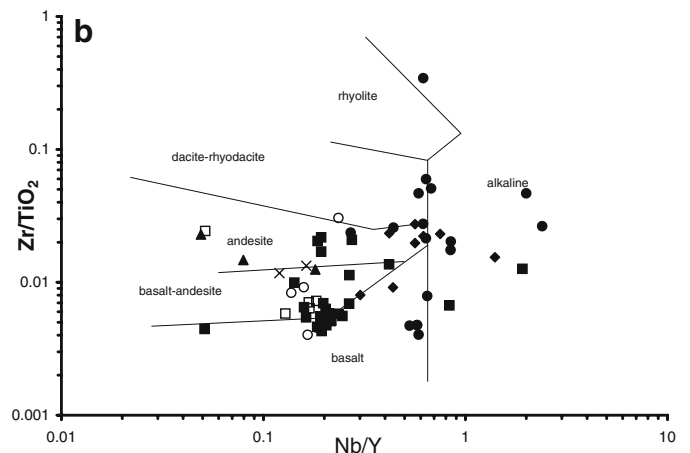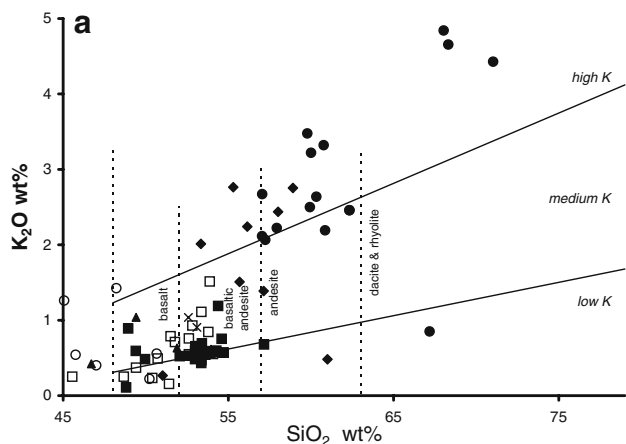
Fig. 14 Harker SiO$_2$–K$_2$O and Nb/Y vs Zr/TiO$_2$ (Winchester and Floyd 1977) diagrams. Note that most of the Gabbronorite Unit and the ultramafic rocks are cumulates and, thus, the chemical compositions do

not correspond to the original magma. The low K$_2$O contents are probably due to this feature. *Legend as in Fig.* 12
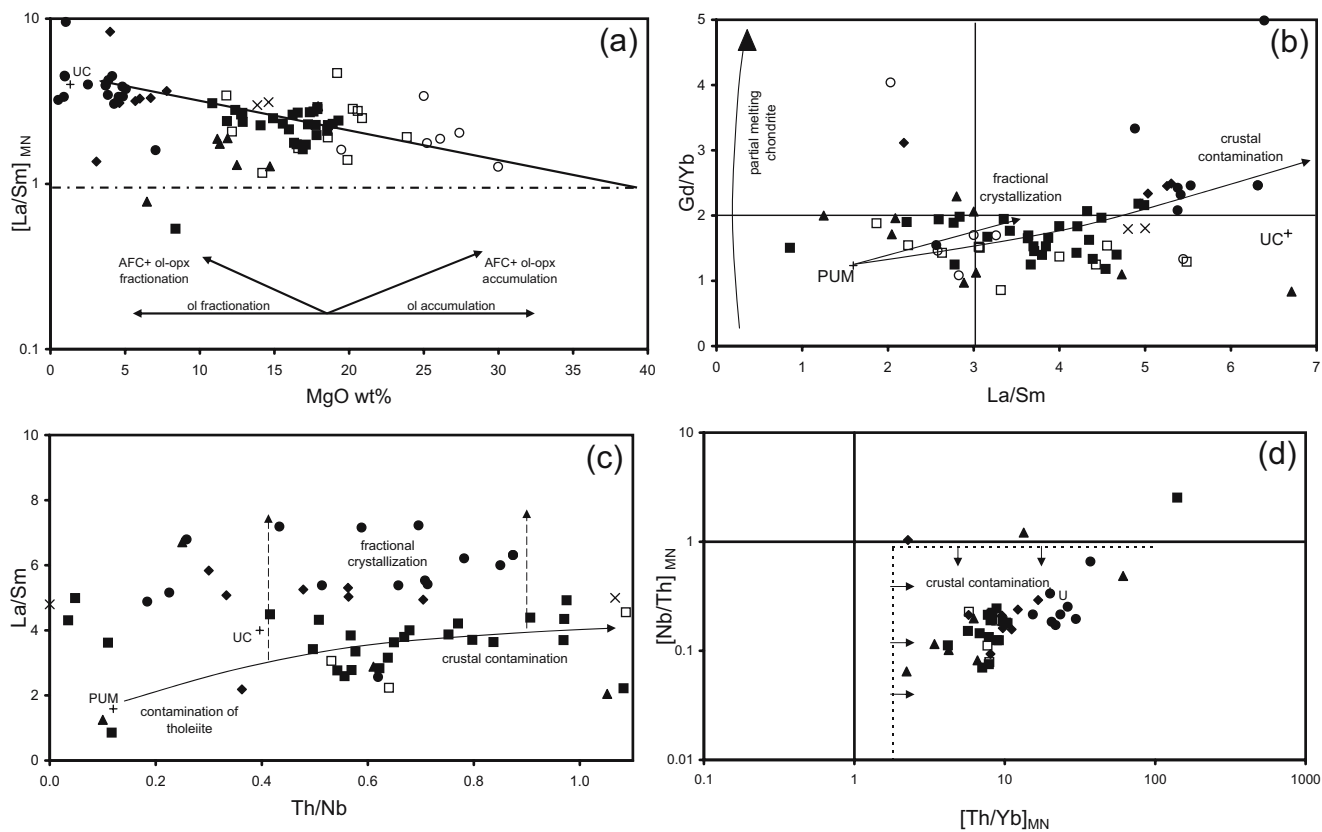
Fig. 15 Trace-element discriminant diagrams. **a** MgO% vs [La/Sm]$_{MN}$ diagram (Lesher et al. 2001). The trend is consistent with an evolution controlled by an AFC process involving fractionation pyroxene and/or olivine. **b** La/Sm vs Gd/Yb and **c** Th/Nb vs La/Sm diagrams (Lightfoot et al. 1990; Li et al. 2000). Fractional crystallization alone is not able to produce the large spread in La/Sm ratios and major crustal contamination synchronous or followed by fractional crystallization is needed to explain the variation in the La/Sm ratio. **d** [Nb/Th]$_{MN}$ vs [Th/Yb]$_{MN}$ diagram showing the estimated field for crustally contaminated magmas. The *line* represents likely minimum contamination as estimated from Condie (2003). *UC* Upper Crust as calculated from Taylor (1995) except La/Sm that is from Rudnick and Fountain (1995), *PUM* Primitive Upper Mantle as calculated from McDonough and Sun (1995). *Legend* as in Fig. 12
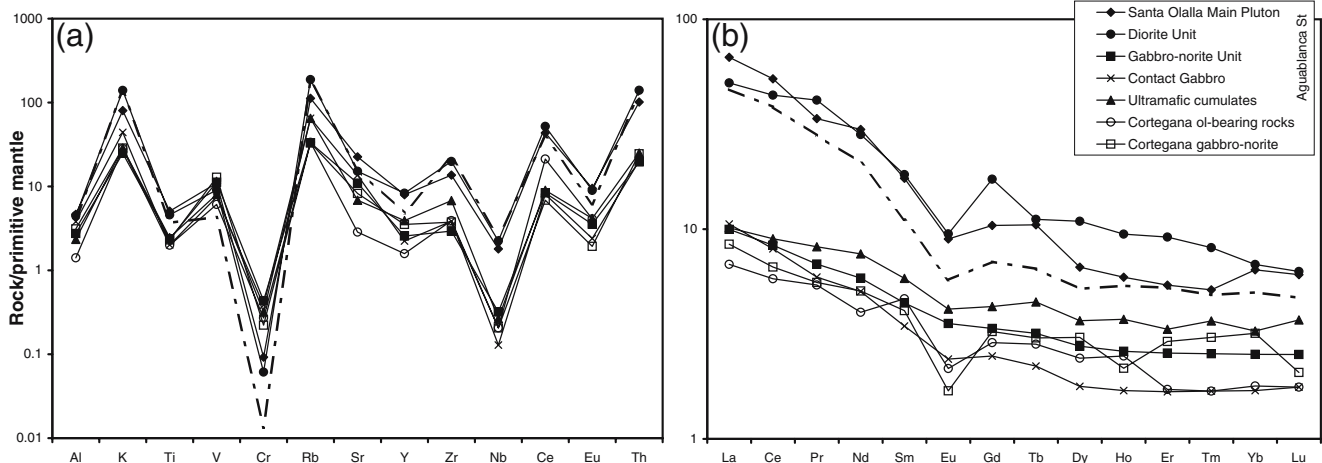
Fig. 16 Spider diagrams for more relevant elements and rare earth elements for the average values of the Santa Olalla Plutonic Complex and Cortegana Igneous Complex. Ol-bearing rocks of the Cortegana Igneous Complex include lherzolite, troctolite, harzburgite, wehrlite, and dunite. Data normalized to the Primitive Upper Mantle of McDonough and Sun (1995). The *dash-point lines* are the average values for the upper crust as calculated by Taylor (1995)

The rocks of the Cortegana Igneous Complex

Rocks of the Cortegana Igneous Complex are geochemically broadly similar to those of the Aguablanca Stock (Figs. 12, 13, 14, 15 and 16). However, the mafic rocks at Cortegana are depleted in MgO and FeO_t and enriched in CaO and K_2O with respect to Aguablanca, probably reflecting the interaction with quartz–feldspar-rich rocks. This is also reflected in the pronounced negative Eu anomaly (Eu/Eu* 0.55). Only the olivine-rich rocks are more primitive, as reflected by their low SiO_2 and Al_2O_3 contents and high Mg#.

Strontium and neodymium isotope composition

Rb–Sr and Nd–Sm isotope data were obtained from 17 whole-rock samples from the Santa Olalla Plutonic Complex and the Cortegana Igneous Complex (Table 4 and Fig. 17). Analytical methods are as in Casquet et al. (2001). In addition, 11 whole-rock Sr and Nd isotope data from the Santa Olalla Plutonic Complex by Casquet et al. (2001) were also included in the dataset. Initial Sr and Nd compositions were calculated at a reference age of 340 Ma (Table 4). Epsilon-Nd (εNd_{340}) values were calculated after Ludwig (1993).

Whole-rock $^{87}Sr/^{86}Sr_{340}$ ratios range from 0.7017 to 0.7106, and $^{143}Nd/^{144}Nd_{340}$ ratios range from 0.5118 to 0.5127. However, if one pyroxenite sample is excluded (AB-102), the ranges of Sr and Nd isotope ratios reduce significantly to 0.7059–0.7106 and 0.5118–0.5125, respectively. Values of εNd_{340} range from −8 to +9, but if the AB-102 pyroxenite is excluded, all values are negative and between −8.0 and −3.2 (Table 4).

Isotope data are best shown on $^{87}Sr/^{86}Sr_{340}$ vs Rb/Sr and $^{143}Nd/^{144}Nd_{340}$ vs Sm/Nd plots (Fig. 17a,b). This type of diagram allows the discrimination of magmatic differentiation and other processes such as crustal assimilation or magma mixing. By combining information, three groups of rocks can be distinguished.

The first group corresponds to the Santa Olalla Main Pluton and the Aguablanca Diorite Unit. The ranges of $^{87}Sr/^{86}Sr_{340}$ and $^{143}Nd/^{144}Nd_{340}$ values are small, 0.7085–0.7106 and 0.51179–0.51190, respectively. The Rb/Sr and Sm/Nd ratios of the group range from ca. 0.03 to 0.54 and ca. 0.18 to 0.23, respectively.

The second group includes the Gabbronorite Unit and most of the pyroxenite fragments from the breccia. This group is, on average, isotopically more primitive than the first group. The ranges of Sr and Nd isotope ratios are also small, 0.7065–0.7084 and 0.51187–0.51196, respectively. Pyroxenite AB-102 has the most primitive composition with an initial Sr isotope ratio of 0.70171 and an initial Nd

isotope ratio of 0.51267. Rb/Sr and Sm/Nd ratios within this group are between 0.06 and 0.9, and 0.19 and 0.36, respectively.

The third group consists of the Cortegana samples. Initial Sr isotope ratios are between 0.7046 and 0.7074, i.e., generally more primitive than those of the other two groups. The initial Nd isotope ratios are between 0.51181 and 0.51204, and the Rb/Sr and Sm/Nd ratios range from 0.06 to 1.81 and 0.28 to 0.4, respectively.

Most samples have initial $^{87}Sr/^{86}Sr$ ratios higher than 0.7050 and negative εNd values, confirming that a significant proportion of continental crust has been added to a basaltic magma. Moreover, in rocks belonging to the Santa Olalla Plutonic Complex, the uniform Sr and Nd isotope ratios and the relatively large range of Rb/Sr and Sm/Nd values within each group (Fig. 17a,b) imply that magmatic variability was the result of either differentiation or mixing of isotopically similar consanguineous magmas. In the Cortegana rocks, the Sr and Nd isotope composition and the Rb/Sr and Sm/Nd values suggest mixing between isotopically different sources.

However, chemical diversification within the Gabbronorite Unit and pyroxenite cumulates probably resulted from mixing between isotopically homogeneous pyroxene cumulate and Rb-rich interstitial magma in different proportions. An increase in the ratio of groundmass/pyroxene crystals resulted in an increase of the Rb/Sr ratio which can be as high a 0.89 in pyroxenite AG-72, without modifying the Sr (and Nd) isotope composition.

Pelitic and calc-silicate rocks equivalent to those around the Aguablanca Stock have variable $^{87}Sr/^{86}Sr_{340}$ ratios, but most are between 0.7104 and 0.7119 with Rb/Sr ratios of 0.11 to 0.73 (Darbyshire et al. 1998). In Fig. 17a, pyroxenite cumulates and rocks belonging to the Gabbronorite Unit plot between these values and depleted mantle. The same holds true for the Nd isotope composition (Fig. 17b).

Figure 17c is a εSr–εNd plot that includes additional data on other metaluminous plutons from the Ossa Morena Zone. All rocks, besides the anomalous pyroxenite sample AB-102, have subchondritic εNd and superchondritic εSr values and define a classical crust–mantle mixing trend. Large-scale crustal contamination is clearly indicated for the Santa Olalla Main Pluton and Aguablanca Stock, while the Cortegana Complex displays a lower degree of crustal contamination.

The Cortegana rocks define an apparently contradictory trend of decreasing $^{87}Sr/^{86}Sr$ and $^{143}Nd/^{144}Nd$ values with increasing Rb/Sr and Sm/Nd ratios (Fig. 17a,b). One likely end member lies on the mixing line between the depleted mantle basaltic source and regional supracrustal rocks and is isotopically more juvenile than parental magmas of the Santa Olalla Main Pluton and the Aguablanca Stock. A second likely end member remains puzzling because it had higher Rb/Sr and Sm/Nd ratios. The samples closer to this

Table 4 Radiogenic isotope data of igneous rocks

		Rb (ppm)	Sr (ppm)	$^{87}Rb/^{86}Sr$	$^{87}Sr/^{86}Sr$	$^{87}Sr/^{86}Sr_{340\ Ma}$	$\varepsilon\ Sr_{340\ Ma}$	Sm (ppm)	Nd (ppm)	$^{147}Sm/^{144}Nd$	$^{143}Nd/^{144}Nd$	$^{143}Nd/^{144}Nd_{340\ Ma}$	$\varepsilon Nd_{340\ Ma}$
Aguablanca Stock													
AB-102	Pyroxenite	1.0	5.0	0.5785	0.704506	0.701707	−34	0.4	1.1	0.2199	0.513155	0.512665	+9.0
AG-72	Pyroxenite	120.0	135.0	2.5746	0.718956	0.706496	+34	0.6					−6.5
AG-207-1	Pyroxenite	56.1	153.7	1.0560	0.713354	0.708243	+59	2.7	12.0	0.1369	0.512173	0.512123	−4.6
AG-207-2	Pyroxenite	28.9	334.1	0.2504	0.709629	0.708417	+61	2.4	9.5	0.1545	0.512308	0.512279	−6.5
AG-207-4	Pyroxenite	19.6	117.6	0.4834	0.710765	0.708426	+62	4.4	20.2	0.1328	0.512163	0.512146	−5.8
AG-207-5	Pyroxenite	48.7	226.7	0.6217	0.711314	0.708305	+60	2.9	12.5	0.1399	0.512217	0.512172	−6.0
AG-97	Gabbronorite	21.6	146.3	0.4277	0.710009	0.707939	+55	2.1	8.1	0.1524	0.512236	0.511897	−5.7
AG-5	Gabbro	20.2	256.0	0.2281	0.709387	0.708283	+60	1.3	5.3	0.1440	0.512230	0.511909	
C-12	Diorite	109.4	294.2	1.0763	0.715820	0.710611	+93						
C-5	Diorite	104.8	268.2	1.1317	0.714350	0.708873	+68	5.5	27.0	0.1240	0.512160	0.511884	−6.2
Santa Olalla Main Pluton													
C-18	Q-diorite	10.8	415.5	0.0752	0.709660	0.709296	+74	22.0	99.3	0.1338	0.512149	0.511851	−6.9
AG-82	Granodiorite	128.1	359.0	1.0335	0.715559	0.710557	+92	11.3	61.6	0.1107	0.512040	0.511793	−8.0
Cortegana Complex													
TE-4	Norite	16.7	288.5	0.1675	0.708197	0.707387	+47	3.7	12.5	0.17894	0.512439	0.512040	−3.2
TEJ-7	Olivine–websterite	16.0	110.2	0.4201	0.707921	0.705888	+25	1.0	3.5	0.17272	0.512411	0.512026	−3.4
TEJ-9	Olivine–websterite	10.1	123.8	0.2360	0.707065	0.705923	+26	1.0	3.0	0.20151	0.512486	0.512037	−3.2
TEJ-11	Harzburgite							3.2	8.3	0.23307	0.512334	0.511815	−7.6
ZOM-23	Lherzolite	38.0	21.0	5.2468	0.730020	0.704626	+8	2.0	5.0	0.24181	0.512441	0.511903	−5.8

Analyses CAI Geochronology and Isotope Geochemistry, Universidad Complutense Madrid. Errors (2σ) are 0.01% (Sr) and 0.006% (Nd). Chemical analysis of the rocks in Table 2, Casquet et al. (2001), and the Electronic supplementary material
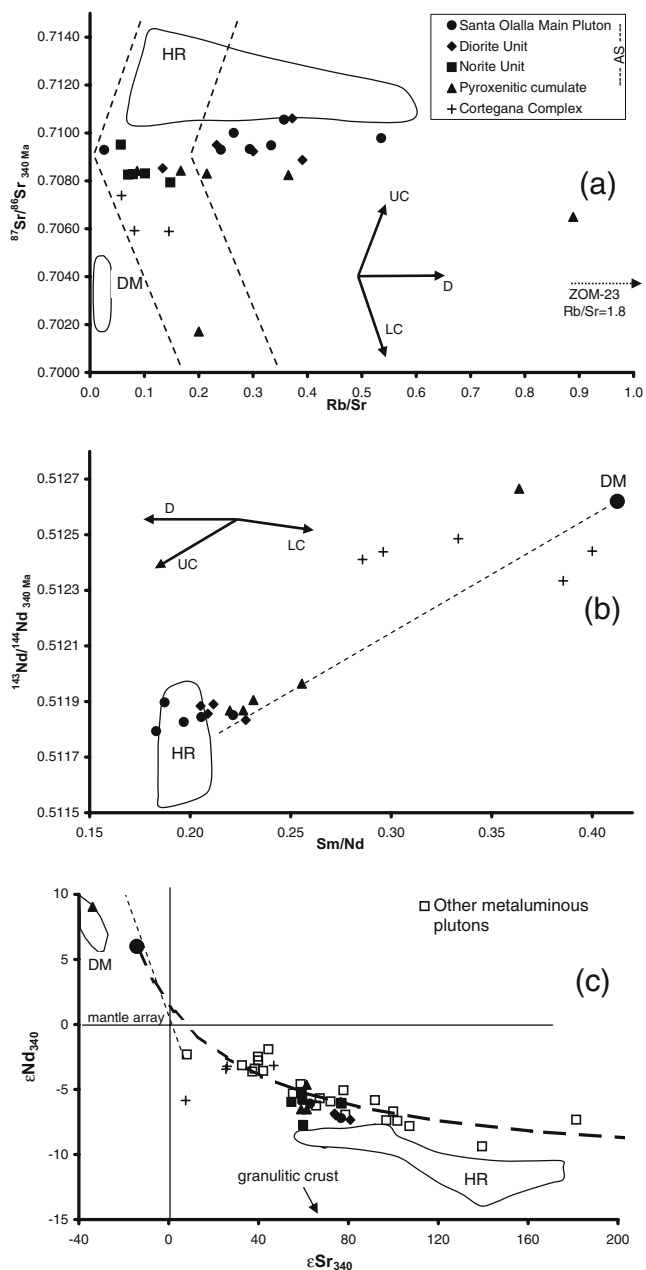
Fig. 17 Rb/Sr–^{87}Sr/^{86}Sr, Sm/Nd–^{143}Nd/^{144}Nd, and εSr–εNd plots of rocks of the Aguablanca Stock, adjacent plutonic rocks, and host rocks of late Neoproterozoic–middle Cambrian age (Galindo et al. 1995; Darbyshire et al. 1998; Casquet et al. 2001). *DM* represents the Sr and Nd isotope compositions of the average depleted mantle at the age of formation (Leeman and Dasch 1978; Fauré 1986; McDonough and Frey 1989; Workman and Hart 2005). The field HR includes the composition of the host rocks to the Santa Olalla Pluton (Galindo et al., unpublished data). *D* represents the differentiation trend with increase in plagioclase and depletion in olivine and pyroxene, while *UC* and *LC* show the likely trend of evolution during mixing with average upper crustal and lower crustal rocks, respectively. Most of the analyzed rocks plot on a mixing curve between a juvenile magma and the host metasedimentary rocks

second hypothetical end member are ZOM 23, with an ^{87}Sr/^{86}Sr$_{340}$ ratio of 0.7046 and an ^{143}Nd/^{144}Nd$_{340}$ of 0.51190, and TEJ 11 (not analyzed for Sr), with an ^{143}Nd/^{144}Nd340 ratio of 0.51181. No candidates for this crustal contaminant member have been recognized so far in the area, and its geological implications remain unknown. The high Rb/Sr ratio is compatible with a granitic magma or a pelitic rock, a feature consistent with the low Nd isotope ratio (see Rollinson 1993), but the low Sr isotope ratio points toward a depleted source. High Sm/Nd values might be explained by melting reactions involving garnet. A low crustal metapelite can concentrate intermediate and heavy REE with high Sm/Nd ratios that increase with pressure (Bea et al. 1997). Thus, garnet bearing low crustal felsic continental could be a suitable source for the Cortegana mafic–ultramafic rocks second end member. Field evidence suggests that mixing between juvenile magmas and the host migmatite took place at or near the emplacement level (Fig. 4h). There are published Sr isotope composition data for the Cortegana migmatite (Castro et al. 1999) and Sr and Nd isotope data for late peraluminous leucogranite of likely deep migmatitic origin in the Olivenza-Monesterio antiform (Bachiller 1996). Only Los Molares migmatite (Rb/Sr: 7.2, ^{87}Sr/^{86}Sr$_{340}$: 0.7038; Castro et al. 1999) and one leucogranite (Sample Bp2; Rb/Sr: 12, ^{87}Sr/^{86}Sr$_{340}$; 0.7052, Sm/Nd=0.35, ^{143}Nd/^{144}Nd$_{340}$: 0.5120; Bachiller 1996) approach the isotopic characteristics of the second end member.

Lead isotope ratios of pyrrhotite are consistent with the Nd and Sr isotope data. Four analyses range between 17.935 and 18.068 (^{206}Pb/^{204}Pb), 15.566 and 15.602 (^{207}Pb/^{204}Pb), and 38.159 and 38.252 (^{208}Pb/^{204}Pb) (Marcoux et al. 2002; Tornos and Chiaradia 2004). These values plot slightly below the calculated growth curve of the area (μ=9.7; Nägler 1990) that is broadly similar to the average crustal growth curve of Stacey and Kramers (1975) and well above the mantle curve (Doe and Zartman 1979). This indicates that most of the lead was derived from a rather uranogenic source, i.e., the host metasedimentary rocks. Because the average lead content of upper crustal rocks is well above that of the mantle and lower crust, minor crustal contamination of juvenile magmas can significantly modify the primary lead isotope signature. The Aguablanca Stock apparently underwent larger crustal contamination than other equivalent systems, like Voisey's Bay (Amelin et al. 2000) where the μ values are always lower than 8.0.

Discussion and genetic model

The unusual geologic setting of the Aguablanca deposit has given place to different genetic hypotheses. The earliest models suggested a magmatic stratiform mineralization

style located in a zoned pre-Variscan sill equivalent to Sudbury or Noril'sk, and then tilted to vertical position during the Variscan orogeny (Lunar et al. 1997). This hypothesis relies mainly on the comparison with other magmatic Ni–Cu deposits, presumed geopetal structures found in drill core, chemical zonation (Ortega et al. 2000), and on the recognition of an isoclinally folded magmatic layering (Ortega et al. 2002). This hypothesis, however, is at odds with the more recent geochronological data that show that the Aguablanca Stock is of Variscan age (ca. 340–335 Ma) (Casquet et al. 1999, 2001; Romeo et al. 2004; Spiering et al. 2005). Moreover, structural and geological evidence indicates that the orebody consists of a discordant magmatic breccia pipe within a mafic stock (Tornos et al. 1999, 2001; Casquet et al. 2001). The combination of the available geological and geochemical data suggests that two concurrent events were involved in the development of the Aguablanca deposit (Figs. 18 and 19).

Stage I: development of a deep differentiated magma chamber

The presence of a deep magma chamber below the Aguablanca orebody was inferred by Tornos et al. (1999, 2001) and Casquet et al. (2001) and has been recently confirmed by geophysical studies (Simancas et al. 2003). Moreover, geological, geochemical, and geochronological evidence strongly suggests that the Cortegana Igneous Complex is an exhumed part of this deep igneous complex.

The magmatic variability of the Santa Olalla Plutonic Complex can be interpreted as resulting from the AFC evolution of a basaltic parental melt in a crustal magma chamber. The Gabbronorite Unit was formed by the early contamination of REE, Sr, and LILE-depleted primitive melt with more evolved material, very likely continental

crust, with later fractionation of orthopyroxene. Such a process is consistent with the evolution from basalt with tholeiitic composition to calc-alkaline basalt-andesite. Further fractional crystallization of hornblende and plagioclase formed the Santa Olalla Main Pluton and the Diorite Unit of the Aguablanca Stock. The geochemical data show that contamination and fractional crystallization were synchronous but highly variable processes (Casquet et al. 2001). The geochemistry of the igneous rocks is consistent with their derivation from a stratified magma chamber. Due to density contrasts, immiscible sulfide melt would pond near the footwall along with pyroxenitic and norite-gabbro cumulates below a more evolved residual magma.

At Aguablanca, evidence for widespread crustal assimilation includes the high orthopyroxene/olivine ratio, the presence of inclusions of Al-rich minerals, the abundance of host-rock xenoliths, the enrichment in silica and incompatible elements, and the crustal isotopic signatures of Nd, Sr, S (see below), and Pb. All these features preclude magma mixing or incorporation of country rock sulfur through metamorphic devolatilization as the principal cause for sulfide immiscibility. Crustal contamination is a common feature of rocks hosting magmatic Ni–(Cu) deposits such as Noril'sk (Lightfoot et al. 1990), Voisey's Bay (Amelin et al. 2000; Li and Naldrett 2000), Sudbury (Lightfoot et al. 1997a), Kalatongke (Shengao et al. 2003), or the Juva district (Makkonen 1996), as well as other layered complexes such as Bushveld (Davies et al. 1980). However, the degree of contamination seems to be much higher in Aguablanca than in many other magmatic nickel deposits. For example, at Voisey's Bay, the Th/Nb ratio is up to 0.8 (Li et al. 2000), whereas in Aguablanca, the Norite Unit has ratios up to twice as high. The compositional similarity between the Contact Gabbro and the Gabbronorite Unit shows that most
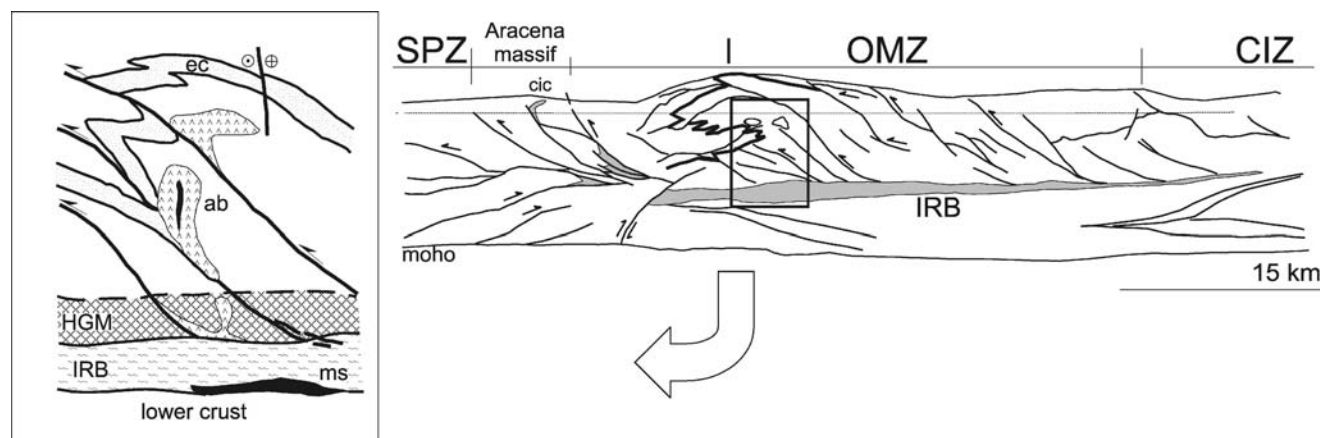
Fig. 18 Cross section of the continental crust in the Ossa Morena Zone showing the relationships between the deep-layered complex (IRB, IBERSEIS Reflective Body) with stratiform Ni–(Cu) mineralization (*ms*) and the metaluminous plutonism with Aguablanca-like ore deposits (*ab*). The Cortegana Igneous Complex (*cic*) probably corresponds to a dismembered part of the IRB body. Section based on Simancas et al. (2003) and Tornos and Casquet (2005). *c* Early–Middle Cambrian sediments, *HGM* zone of high-grade metamorphism adjacent to the deep magmatic complex, *SPZ* South Portuguese Zone, *OMZ* Ossa Morena Zone, *CIZ* Central Iberian Zone
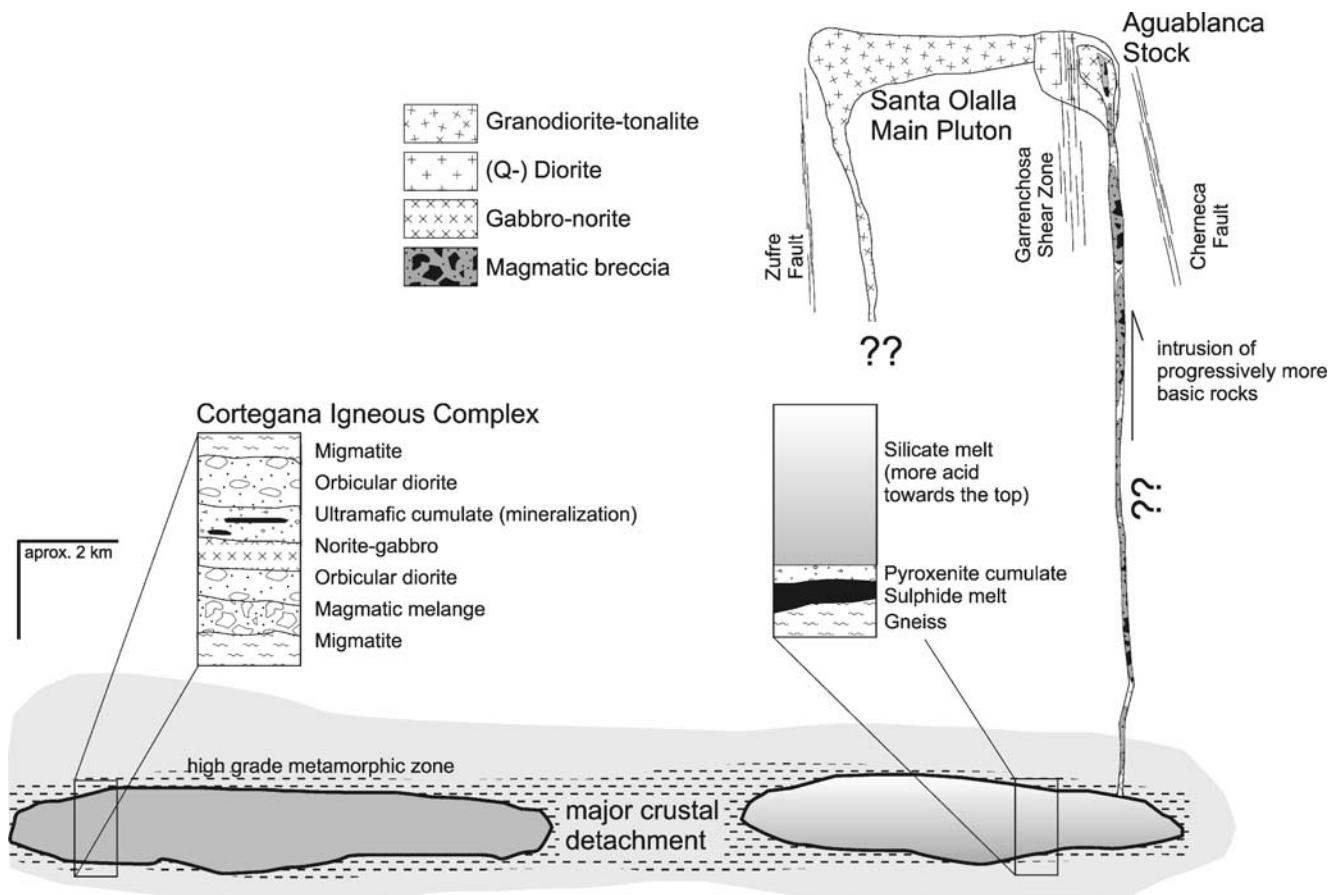
Fig. 19 Proposed genetic model for the Ni–(Cu) magmatic deposits of the Ossa Morena, including the autochthonous Cortegana prospect, the allochthonous Aguablanca orebody, and a hypothetical stratiform mineralization that forms the protore of the Aguablanca deposit

AFC processes took place at depth before the emplacement of the Aguablanca Stock.

The most likely candidate for the crustal end member contaminant is the Late Neoproterozoic to Middle Cambrian siliciclastic sequence that forms the bulk of the Aracena Massif and dominates the basement of the Ossa Morena Zone. In fact, in the Olivenza-Monesterio area, Late Neoproterozoic slate with 0.1–2 wt% sulfur (Nägler 1990; Schäfer 1990, and unpublished data) hosts abundant small stratabound concentrations of chalcopyrite and bornite with traces of gold (Tornos et al. 2004). The relatively high Cu and Au contents of the Aguablanca ore could well be due to the assimilation of larger amounts of such a crustal component.

Contamination was an early process that took place before the crystallization of olivine, leading to early orthopyroxene crystallization and inhibiting the formation of major peridotite. This contamination did not take place in the magmatic conduits, as has been suggested for Voisey's Bay or Noril'sk (Li et al. 2000, 2001), but rather in a deep-seated magma chamber as proposed for Noril'sk by Lightfoot and Keays (2005). Textural evidence indicates that sulfide immiscibility was synchronous with orthopyroxene and always before clinopyroxene crystallization.

The homogeneous sulfur isotope values of the Aguablanca ore, from +7.1 to +7.8‰ (Casquet et al. 2001), point toward a homogeneous sulfur composition during the ore-forming process. Mass balance considerations assuming that $\delta^{34}S$ of the uncontaminated primitive magmas was between −3 to +2‰ and that of the country rocks was 14–21‰ (Tornos and Velasco 2002) suggest that up to 30% of the sulfur was of external derivation to the magma.

The depth of the magma chamber at ca. 340 Ma was between 12 and 19 km, as estimated from the present depth of the IRB body plus the inferred depth of intrusion of the Aguablanca Stock (Casquet 1980). Pressure estimates obtained from mineral equilibria geobarometry in the Gabbronorite Unit (4.3–5.7 kbar) record pressures that probably correspond to those of the deep magmatic complex and agree with the depth estimation above. These values are consistent with the lithostatic pressure of about 4–6 kbar, i.e., 12–18 km depth, obtained by Patiño Douce et al. (1997) and Díaz-Azpiroz et al. (2004) for the Aracena metamorphism.

The geology of the Aracena Massif and the geophysical data (Simancas et al. 2003) show that the deep magmatic complex is highly discontinuous and composed of several

tens of subhorizontal sills and irregular intrusions that likely evolved differently depending on the size, nature of the host rocks, temperature of intrusion, and degree of assimilation. This is consistent with the differences between the Santa Olalla Plutonic Complex and the Cortegana Igneous Complex that suggest that rocks cropping out in the Cortegana Complex are not exact equivalents to the deep intrusion underlying Aguablanca. Below Aguablanca, the intrusion of a voluminous batch of mafic magma into middle to upper crust was able to digest significant amounts of sedimentary wallrocks. The high surface ratio would favor wallrock–magma interaction and immiscibility of a sulfide melt from the parental silicate magma. The fine grain size suggests quick crystallization of pyroxene. However, at Cortegana, the presence of coarse-grained olivine and pyroxene-bearing heterogeneous rocks with abundant remnants of partially digested host rock suggests that assimilation was less effective. In fact, only sporadic sulfide blebs are found. Four $\delta^{34}S$ determinations from Cortegana yielded values of −0.1, +0.4, +2.4, and +3.1‰. These values are significantly more heterogeneous and depleted in ^{34}S than those of Aguablanca and consistent with a lower degree of contamination, a different source for sulfur or less efficient homogenization of sulfur from different sources.

Metaluminous magmatism in the Ossa Morena Zone took place in between 350 and 330 Ma, a short time span if compared with the Variscan subduction and collision that probably took place between the Early Devonian and the Late Carboniferous (ca. 416–300 Ma; Eguíluz et al. 2000). This suggests that metaluminous magmatism was not directly controlled by subduction and, instead, related with the large-scale intrusion of the deep magmatic complex into the middle crust. This deep magmatic complex was interpreted as being emplaced during a short extensional stage in the development of the subduction-related magmatic arc (Simancas et al. 2003). However, the structural relationships of the Santa Olalla Plutonic Complex strongly suggest that it was intruded during a compressional stage and favored by crustal delamination induced by left-lateral transpressional deformation (Tornos and Casquet 2005).

Stage II: upwelling and final emplacement

The emplacement of the Aguablanca Stock took place in a small subvertical pull-apart structure. Such small dilational structures can effectively focus overpressured magmas and fluids to shallow depths (Saint Blanquat et al. 1998; Sanderson and Zhang 1999). Recently, Tornos and Casquet (2005) have suggested that magma tapping from the deep-seated magma chamber took place along structures rooted in the deep magmatic complex. This model implies ascent of sulfide melt for a distance of between 8.5 and 17 km. Ascent of such dense magma is difficult to envisage unless it is assumed that small extensional structures within transpressional settings can channelize small amounts of overpressured dense magmas. In any case, only a small proportion of the total generated sulfide melt should arrive to the surface, and the existence of other magma chambers at intermediate depth is likely. Such staging chambers have been described as critical in the shallow emplacement of magmas (e.g., Jahoda et al. 1989; Saint Blanquat et al. 1998), in mesothermal gold deposits (Roberts et al. 1991; Matthai et al. 1995), in epithermal gold (Tosdal and Nutt 1998), in volcanic- and shale-hosted massive sulfide deposits (Gauthier et al. 1994), and in porphyry copper districts (Unrug et al. 1999), but there are few evidences that they controlled the formation of Ni–Cu sulfide deposits.

The foliation within the Santa Olalla Plutonic Complex suggests that there were two major feeder zones (Fig. 2). One is marked by the breccia pipes, which probably intruded both the Diorite and Gabbronorite Units. However, the foliation suggests the existence of another independent feeder zone located southward, below the Santa Olalla Main Pluton, and near the Zufre Fault. If that holds true, the Aguablanca Stock and the Santa Olalla Main Pluton represent cogenetic and broadly synchronous intrusions but developed from different feeder zones and magma chambers.

At Aguablanca, the crosscutting relationships and the orientation of the magmatic foliation suggest that successive melt batches were brought to the near surface. Available data suggest that the first magma to be tapped was the Gabbronorite Unit, immediately followed by the emplacement of the breccia pipe. The Diorite Unit, hypothetically derived from the uppermost part of the magma chamber, was probably the youngest phase. This overall intrusion scheme is broadly similar to that proposed by Beard and Day (1988) for the Smartville Complex (Northern California), where they describe the emplacement of a zoned pluton as due to the episodic intrusion of magma derived from an inferred stratified magma chamber, where differentiation and fractional crystallization took place.

Pyroxenite dominates in the breccia fragments, indicating that it probably occurred as an already crystallized cumulate in the bottom of the magma chamber but perhaps underlain by a dense sulfide melt. Overpressuring and rock failure disrupted the chamber, driving the cumulates, host rock fragments, and sulfides upward. Due to its lower viscosity, the sulfide melt could effectively separate from the silicate system and squeeze upward, concentrating in large massive sulfide blebs and in the cement of the more internal zones of the breccia, which forcefully ascended to the present position with the sulfide melt acting as a lubricant. In this context, the barren breccia and the disseminated and patchy ores probably represent the product of turbulent and variable mixing between the gabbro–noritic magma, the already crystallized cumulates, host rocks, and the sulfide melt.

Many of the Variscan metaluminous intrusions of the Ossa Morena Zone, particularly in the Olivenza-Monesterio antiform, are similar to the Aguablanca Stock. They are dominantly composed of intermediate to mafic rocks and have different types of cumulates. What seems to make Aguablanca different is the degree of crustal contamination. For example, the large Burguillos Plutonic Complex consists of a core of layered cumulates (olivine-rich harzburgite, lherzolite, olivine-bearing websterite, and melanogabbro–norite) and two outer units of diorite and tonalite composition, respectively (Pons 1982; Garcia Casquero 1995; Casquet and Galindo 2004). The Sr isotope composition at the crystallization age of 338 Ma (Dallmeyer et al. 1995; Casquet et al. 1998) ranges from 0.7047 to 0.7069. The initial εNd isotope composition is in the range of −2.4 to −3.7 (Casquet and Galindo 2004). These values are more primitive than those of the Santa Olalla Plutonic Complex and suggest a smaller degree of contamination by continental crust for the Burguillos magmas.

The Aguablanca deposit is probably the largest of a group of numerous but small synorogenic Ni–(Cu) deposits that occur in Phanerozoic arcs (Caledonides, Appalachians, North-western Cordillera, and Lachlan belt) and include Las Aguilas, Argentina (Skirrow and Sims 1999), Vakkerlien, Norway (Thompson et al. 1980), Moxie, USA (Thompson 1984), the Juva district in Finland (Makkonen 1996; Papunen 2003) or Kalatongke, China (Shengao et al. 2003), but these are only locally related with large breccia pipes (Giant Mascot, Canada; Metcalfe and McClaren 2003). The major difference of Aguablanca with these deposits is the degree of crustal contamination that seems to be much more important in Aguablanca. Probably, the unusual magmatotectonic setting and the intrusion of a large mafic body high into the crust favored abnormal crustal contamination and sulfide immiscibility.

Conclusions

The Aguablanca Ni–(Cu) deposit is related to a magmatic breccia pipe hosted by a small epizonal mafic stock that is part of a large metaluminous calc-alkaline igneous province of Variscan age dated at ca. 350–330 Ma. The deposit is interpreted as having formed in a two-stage process, which included: (a) early intrusion of a primitive tholeiitic magma along a major subhorizontal discontinuity at midcrustal depths, which evolved into a layered mafic–ultramafic complex through AFC processes; and (b) subsequent rise of magmas along small transcrustal dilational structures to upper crustal levels. Geologic relationships, Ar–Ar geochronology, and radiogenic isotope geochemistry demonstrate that part of that deep magmatic complex presently crops out in the southern-most Ossa Morena Zone (Cortegana Igneous Complex).

There is strong evidence for major contamination of the basaltic magma by sulfide-bearing crustal rocks, as traced by systematic enrichment in SiO_2 and incompatible elements, increase in $^{87}Sr/^{86}Sr$ and depletion in $^{143}Nd/^{144}Nd$ ratios, and crustal $\delta^{34}S$ and Pb isotope signatures. These data are consistent with the predominance of orthopyroxene instead of olivine in cumulate rocks and the presence of host-rock xenoliths within the intrusion. The degree of crustal contamination was probably significantly larger than in many other equivalent systems. Magma–crust interaction and immiscibility of a sulfide-rich melt were early processes and promoted by the style of intrusion in the middle crust dominated by the injection of abundant but small sills and the formation of a superheated zone. Melt stratification took place within the magma chamber and was responsible for the zonation of the Aguablanca Stock and cumulate-like geochemistry of the more mafic rocks. Comparison between the orebodies at Aguablanca and Cortegana strongly suggests that the degree and mode of crust–magma interaction was critical for mineralization. Small and/or cool intrusions were not able to effectively digest the host rock, promoting only minor mineralization. However, superheated intrusions facilitated the assimilation of large amounts of crustal material and effective homogenization, probably in a highly dynamic magma chamber.

The data presented in this study confirm that economic Ni–(Cu) sulfide deposits can form in calc-alkaline complexes developed in active-margin settings. The formation of the Aguablanca deposit required the confluence of three factors: (1) development of a deep magmatic complex with major assimilation of host rocks, (2) existence of trans-crustal channelways to the upper crust, and (3) over-pressured ascent of sulfide-silicate melt to a shallow emplacement level. Superposition of these processes seems to be rare and probably explains why this style of mineralization is so unusual.

The above model implies that dense sulfide melts can travel from deep midcrustal to shallow environments if the appropriate geodynamic context favors such reinjection.

References

Alexander EC, Mickelson GM, Lanphere MA (1978) Mmhb-1: a new ^{40}Ar/^{39}Ar dating standard. In: Zartman RE (ed) Short papers of the Fourth International Conference, Geochronology, Cosmochronology, and Isotope Geology, vol 78-701, pp 6-81

Amelin Y, Li C, Valeyev O, Naldrett AJ (2000) Nd–Pb–Sr isotope systematics of crustal assimilation in the Voisey's Bay and Mushuau intrusions, Labrador, Canada. Econ Geol 95:815–830

Arnold RG (1969) Pyrrhotite phase relations below 304°C. Econ Geol 64:405–419

Bachiller N (1996) Las alteraciones hidrotermales de los leucogranitos del Complejo intrusivo de Burguillos del Cerro (Badajoz). Edad, geoquímica y modelo de procedencia y evolución de los fluidos. Master Thesis, Universidad Complutense de Madrid, Madrid

Barnes SJ, Tang Z (1999) Chrome spinels from the Jinchuan Ni–Cu sulfide deposit, Gansu province, People's Republic of China. Econ Geol 94:343–356

Bateman R, Martin MP, Castro A (1992) Mixing of cordierite granitoid and pyroxene gabbro, and fractionation, in the Santa Olalla tonalite (Andalucia). Lithos 28:111–131

Bateman R, Rosa JD, de la Castro A (1994) Mineral chemical disequilibrium and hybridization in the Santa Olalla Pluton, Spain. Bol Soc Esp Mineral 17:83–84

Bea F, Montero P, Garuti G, Zaccarini F (1997) Pressure-dependence of rare earth element distribution in amphibolite- and granulite-grade garnets. A LA-ICP-MS study. Geostand Newsl 21:253–270

Beard JS, Day HW (1988) Petrology and emplacement of reversely zoned gabbro–diorite plutons in the Smartville Complex, Northern California. J Petrol 29:965–995

Bertrand P, Mercier JC (1985) The mutual solubility of coexisting ortho- and clinopyroxene: toward the absolute geothermometer for the natural system? Earth Planet Sci Lett 76:109–122

Bomati O, Ortega L, Lunar R, Sierra J, Moreno T, Garcia Palomero F (1999) Distribución de sulfuros de N–Cu–Fe y de minerales del grupo del platino en la mineralización intramagmática de Aguablanca (Badajoz): Implicaciones genéticas. Bol Soc Esp Mineral 22-A:19–20

Carbonell R, Simancas F, Juhlin C, Pous J, Pérez Estaún A, Gonzalez Lodeiro F, Muñoz G, Heise W, Ayarza P (2004) Geophysical evidence of a mantle-derived intrusion in SW Iberia. Geophys Res Lett 31:L11601–L11604

Casquet C (1980) Fenómenos de endomorfismo, metamorfismo y metasomatismo en los mármoles de la Rivera de Cala (Sierra Morena). Doctoral thesis, Universidad Complutense, Madrid, p 295

Casquet C (1982) Metamorfismo de contacto en el borde N del plutón de Santa Olalla de Cala con especial enfasis en las rocas carbonatadas. Rev R Acad Cienc Exactas Fis Nat Madr 76:334–363

Casquet C, Galindo C (2004) El magmatismo Varisco de la Zona de Ossa Morena. In: Geología de España, Vera JA (eds) Sociedad Geológica España-Instituto Geológico y Minero de España, Madrid, pp 194–199

Casquet C, Velasco F (1978) Contribución a la geología de los skarns cálcicos en torno a Santa Olalla de Cala (Huelva-Badajoz). Estud Geol 34:399–405

Casquet C, Galindo C, Darbyshire DPF, Noble SR, Tornos F (1998) Fe–U–REE mineralization at Mina Monchi, Burguillos del Cerro, Spain: age and isotope (U–Pb, Rb–Sr and Sm–Nd) constraints on the evolution of the ores. Abstracts GAC-MAC-APGGQ, Quebec, p A28

Casquet C, Eguiluz L, Galindo C, Tornos F, Velasco F (1999) The Aguablanca Cu–Ni (PGE) intraplutonic ore deposit (Extremadura, Spain). Isotope (Sr, Nd, S) constraints on the source and evolution of magmas and sulfides. Geogaceta 24:71–74

Casquet C, Galindo C, Tornos F, Velasco F (2001) The Aguablanca Cu–Ni ore deposit (Extremadura, Spain), a case of synorogenic orthomagmatic mineralization: isotope composition of magmas (Sr, Nd) and ore (S). Ore Geol Rev 18:237–250

Castro A, Fernandez C, El Hmidi H, El Biad M, Diaz M, Rosa J, Stuart F (1999) Age constraints to the relationships between magmatism, metamorphism and tectonism in the Aracena metamorphic belt, southern Spain. Geol Rundsch 88:26–37

Cawthorn RG, Kruger FJ (2004) Petrology and Ni–Cu–PGE potential of the Insizwa Lobe, Mount Ayliff Intrusion, South Africa. Can Mineral 42:303–324

Chai G, Naldrett AJ (1992) Characteristics of Ni–Cu–PGE mineralization and genesis of the Jinchuan Deposit, Northwest China. Econ Geol 87:1475–1495

Condie KC (2003) Incompatible element ratios in oceanic basalts and komatiites: tracking deep mantle sources and continental growth rates with time. Geochem Geophys Geosyst 4:1–28

Crespo A (1991) Evolución geotectónica del contacto entre la Zona de Ossa Morena y la Zona Surportuguesa en las Sierras de Aracena y Aroche (Macizo Ibérico Meridional): un contacto mayor en la Cadena Hercinica Europea. Ediciones Universidad Granada, Granada, p 327

Czamanske GK, Kunilov VE, Zientek ML, Cabri LJ, Likhachev AP, Calk LC, Oscarson RL (1992) A proton microprobe study of magmatic sulfide ores from the Noril'sk-Talnakh district, Siberia. Can Mineral 30:249–287

Dallmeyer RD, Fonseca PE, Quesada C, Ribeiro A (1993) ^{40}Ar/^{39}Ar mineral age constraints for the tectonothermal evolution of a Variscan Suture in SW Iberia. Tectonophysics 222:177–194

Dallmeyer RD, Garcia Casquero JL, Quesada C (1995) ^{40}Ar/^{39}Ar mineral age constraints on the emplacement of the Burguillos del Cerro Igneous Complex (Ossa Morena Zone, SW Spain). Bol Geol Min 106:203–214

Dalrymple GB, Alexander EC, Lanphere MA, Kraker GP (1981) Irradiation of samples for ^{40}Ar/^{39}Ar dating using the Geological Survey TRIGA reactor. U.S. Geological Survey Professional Paper 1176, p 55

Darbyshire DPF, Tornos F, Galindo C, Casquet C (1998) Sm–Nd and Rb–Sr constraints on the age and origin of magnetite mineralization in the Jerez de los Caballeros iron district of Extremadura, SW Spain. Chin Sci Bull (Suppl) 43:28

Davies G, Cawthorn RG, Barton JM Jr, Morton M (1980) Parental magma to the Bushveld Complex. Nature 287:33–35

Defant MJ, Drummond MS (1990) Derivation of some modern arc magmas by melting of young subducted lithosphere. Nature 347:662–665

Diaz Azpiroz M, Castro A, Fernández C, López S, Fernández Caliani JC, Moreno-Ventas I (2004) The contact between the Ossa Morena and the South Portuguese zones. Characteristics and significance of the Aracena metamorphic belt, in its central sector between Aroche and Aracena (Huelva). J Iber Geol 30:23–52

Doe BR, Zartman RE (1979) Plumbotectonics, the phanerozoic. In: Barnes HL (ed) Geochemistry of hydrothermal ore deposits, 2nd edn. Wiley, New York, pp 22–70

Ebel DS, Naldrett AJ (1996) Fractional crystallization of sulfide ore liquids at high temperature. Econ Geol 91:607–621

Eguiluz L, Carracedo M, Apalategui O (1989) Stock de Santa Olalla de Cala (Zona de Ossa Morena, España). Stud Geol Salmant 4:145–157

Eguiluz L, Gil Ibarguchi JI, Abalos B, Apraiz A (2000) Superposed Hercynian and Cadomian orogenic cycles in the Ossa Morena

Zone and related areas of the Iberian Massif. Geol Soc Amer Bull 112:1398–1413

Fauré G (1986) Principles of isotope geology, 2nd edn. Wiley, New York, p 589

Galindo C, Darbyshire F, Tornos F, Casquet C, Cuervo S (1995) Sm–Nd geochemistry and dating of magnetites: A case study from an Fe district in the SW of Spain. In: Pasava J, Kribek B, Zak K (eds) Mineral Deposits: from their origin to environmental impacts, vol. Balkema, Rotterdam, pp 41–43

Galindo C, Casquet C (2004) El magmatismo Pre-varisco de la Zona de Ossa Morena. In: Vera JA (ed) Geología de España. SGE/IGME, Madrid, pp 190–194

Garcia Casquero JL (1995) Intrusión múltiple y cuerpos ígneos politípicos: El Complejo Igneo de Burguillos del Cerro, un macizo diorítico zonado en el basamento varisco de la Península Ibérica. Bol Geol Min 106:379–398

Gauthier M, Chartrand F, Trottier J (1994) Metallogenic epochs and metallogenic provinces of the Estrie-Beauce region, Southern Quebec Appalachians. Econ Geol 89:1322–1360

Giese U, Walter R, Winterfeld C (1994) Geology of the southwestern Iberian Meseta II. The Aracena Metamorphic Belt between Almonaster La Real and Valdelarco, Huelva province (SW Spain). Neues Jahrb Geol Palaontol Abh 192:333–360

Hoatson DM, Sun SS (2002) Archean layered mafic–ultramafic intrusions in the West Pilbara Craton, Western Australia: a synthesis of some of the oldest orthomagmatic mineralizing systems in the world. Econ Geol 97:847–872

IGME (1983) Mapa Geológico de España, hoja 916, Aroche. Instituto Geológico y Minero de España, Madrid, p 53

ITGE (1990) Mapa Geológico de España a escala 1/50.000 núm. 918 (Santa Olalla de Cala). Instituto Tecnológico Geominero de España, Madrid, p 46

Jahoda R, Andrews JR, Foster RP (1989) Structural controls of Monterroso and other gold deposits in NW Spain—fractures, jogs and hot jogs. Trans Inst Min Metall 98:b1–b6

James RS, Easton RM, Peck DC, Hrominchuk JL (2002) The East Bull Lake intrusive suite: remnants of a ~2.48 Ga large igneous and metallogenic province in the Sudbury area of the Canadian Shield. Econ Geol 97:1577–1606

Kerr A, Ryan B (2000) Threading the eye of the needle: lessons from the search for another Voisey's Bay in Labrador, Canada. Econ Geol 95:725–748

Kunk MJ, Winick JA, Stanley JO (2001) ^{40}Ar/^{39}Ar age-spectrum and laser fusion data for volcanic rocks in west central Colorado. U.S. Geological Survey Open-File Report 01-472, pp 1–94

Leeman WP, Dasch EJ (1978) Strontium, lead and oxygen isotopic investigation of the Skaergard intrusion, east Greenland. Earth Planet Sci Lett 41:47–59

Lesher CM, Burnham OM, Keays RR, Barnes SJ, Hulbert L (2001) Trace element geochemistry and petrogenesis of barren and ore-associated komatiites. Can Mineral 39:673–696

Li C, Naldrett AJ (2000) Melting reactions of gneissic inclusions with enclosing magma at Voisey's Bay, Labrador, Canada: implications with respect to ore genesis. Econ Geol 95:801–814

Li C, Lightfoot PC, Amelin Y, Naldrett AJ (2000) Contrasting petrological and geochemical relationships in the Voisey's Bay and Mushuau intrusions, Labrador, Canada: implications for ore genesis. Econ Geol 95:771–799

Li C, Naldrett AJ, Ripley EM (2001) Critical factors for the formation of a nickel-copper deposit in an evolved magma system: lessons from a comparison of the Pants Lake and the Voisey's Bay sulfide occurrences in Labrador, Canada. Miner Depos 36:85–92

Lightfoot PC, Keays RR (2005) Siderophile and chalcophile metal variations in flood basalts from the Siberian Trap, Noril'sk Region: implications for the origin of the Ni–Cu–PGE sulfide ores. Econ Geol 100:439–462

Lightfoot PC, Naldrett AJ, Gorbachev NS, Doherty W, Fedorenko VA (1990) Geochemistry of the Siberian Trap of the Noril'sk area, USSR, with implications for the relative contributions of crust and mantle to flood basalt magmatism. Contrib Mineral Petrol 104:631–644

Lightfoot PC, Keays RR, Morrison GG, Bite A, Farrell KP (1997a) Geochemical relationships in the Sudbury igneous complex: origin of the main mass and offset dykes. Econ Geol 92:289–307

Lightfoot PC, Keays RR, Morrison GG, Bite A, Farrell KP (1997b) Geologic and geochemical relationships between the contact sublayer, inclusions and the main mass of the sudbury igneous complex: a case study of the whistle mine embayment. Econ Geol 92:647–673

Ludwig KR (1993) ISOPLOT: a plotting and regression program for radiogenic isotope data. Version 2.82. USGS Open File Report 91-445, pp 1–45

Lunar R, Garcia Palomero F, Ortega L, Sierra J, Moreno T, Prichard H (1997) Ni–Cu–(PGM) mineralization associated with mafic and ultramafic rocks: the recently discovered Aguablanca ore deposit, SW Spain. In: Papunen H (ed) Mineral deposits: research and exploration. Balkema, Rotterdam, pp 463–466

Makkonen HV (1996) 1.9 Ga tholeiitic magmatism and related Ni–Cu deposition in the Juva area, SE Finland. Bull Geol Surv Finl 386:101

Marcoux E, Pascual E, Onezime J (2002) Hydrothermalisme ante-Hercynien en Sud-Iberie: apport de la geochimie isotopique du plomb. Compte Rendu Academie Sciences Paris Geosciences 334:259–265

Martín Estévez JR, Ortega L, Lunar R, García Palomero F (2000) Características texturales y geoquímicas de la pirita en la mineralización intramagmática de Ni-Cu-PGE de Aguablanca (Badajoz). Cuad Lab Xeol Laxe 25:107–110

Mateus A, Jesus AP, Oliveira V, Gonçalves MA, Rosa C (2001) Vanadiferous iron–titanium ores in Gabbroic Series of the Beja Igneous Complex (Odivelas, Portugal): remarks on their possible economic interest. Estud Notas Trab Inst Geol Min 43:3–16

Mathez EA (1989) Interactions involving fluids in the Stillwater and Bushveld complexes: observations from the rocks. In: Whitney JA, Naldrett AJ (eds) Ore deposition associated with magmas. Rev Econ Geol 4:167–180

Mathez EA, Peach CL (1989) The geochemistry of the platinum-group elements in mafic and ultramafic rocks. In: Withney JA, Naldrett AJ (eds) Ore deposition associated with magmas. Rev Econ Geol 4:33–44

Matthai SK, Henley RW, Bacigalupo-Rose S, Binns RA, Andrew AS, Carr AR, French DH, McAndrew J, Kavanagh ME (1995) Intrusion related, high temperature gold-quartz veining in the Cosmopolitan Howley metasedimentary rock-hosted gold deposit, N Territory, Australia. Econ Geol 90:1012–1045

McDonough WF, Frey FA (1989) REE in upper mantle rocks. In: Lipin B, McKay GR (eds) Geochemistry and mineralogy of rare earth elements. Rev Miner 21:99–145

McDonough WF, Sun SS (1995) The composition of the earth. Chem Geol 120:223–253

Metcalfe P, McClaren M (2003) The Pacific nickel complex: profile of an environment for magmatic Ni-Cu deposits in a transpressive continental margin setting. In: GAC-MAC Annual Meeting, Vancouver 2003, session SS14

Middlemost EAK (1985) Magmas and magmatic rocks. Longman, London, p 266

Montero P, Salman K, Bea F, Azor A, Exposito I, Lodeiro F, Martinez Poyatos D, Simancas F (2000) New data on the geochronology of the Ossa Morena Zone, Iberian Massif. In: Variscan-Appalachian dynamics: the building of the Upper Paleozoic basement. Galicia 2000, A Coruña, Spain

Nägler T (1990) Sm–Nd, Rb–Sr and common lead isotope geochemistry on fine-grained sediments of the Iberian Massif. Ph.D. thesis, Swiss Federal Institute Technology Zurich, 139 pp. Swiss Federal Institute Technology, Zurich, p 139

Naldrett AJ (1989) Magmatic sulfide deposits. Oxford University Press, London, UK, p 186

Naldrett AJ (1992) A model for the Ni–Cu–PGE ores of the Noril'sk region and the application to other areas of flood basalt. Econ Geol 87:1945–1962

Naldrett AJ (1999) World class Ni–Cu–PGE deposits: key factors in their genesis. Miner Depos 34:227–240

Naldrett AJ (2004) Magmatic sulfide deposits: geology, geochemistry and exploration. Springer, Berlin Heidelberg New York, p 727

Nimis P (1999) Clinopyroxene geobarometry of magmatic rocks: part 2: structural geobarometers for basic to acid, tholeiitic and mildly alkaline magmatic systems. Contrib Mineral Petrol 135:62–74

Ortega L, Moreno T, Lunar R, Prichard H, Sierra J, Bomati O, Fisher P, Garcia Palomero F (1999) Minerales del grupo del platino y fases asociadas en el depósito de Ni–Cu–(EGP) de Aguablanca, SW España. Geogaceta 25:155–158

Ortega L, Lunar R, Garcia Palomero F, Martin Estevez JR (2000) Evidencias de fraccionamiento en el yacimiento intramagmático de Ni–Cu–EGP de Aguablanca (Badajoz). Cuad Lab Xeol Laxe 25:111–114

Ortega L, Lunar R, Garcia Palomero F, Moreno T, Prichard HM (2001) Removilización de minerales del grupo del platino en el yacimiento de Ni–Cu–EGP de Aguablanca (Badajoz). Bol Soc Esp Mineral 24-A:175–176

Ortega L, Lunar R, García Palomero F, Moreno T, Prichard HM (2002) Características geológicas y mineralógicas del yacimiento de Ni–Cu–EGP de Aguablanca (Badajoz). Bol Soc Esp Mineral 25:57–78

Ortega L, Lunar R, Garcia Palomero F, Moreno T, Martin Estevez JR, Prichard HM, Fisher PC (2004) The Aguablanca Ni–Cu–PGE deposit, Southwestern Iberia: magmatic ore-forming processes and retrograde evolution. Can Mineral 42:325–350

Papunen H (2003) Ni–Cu sulfide deposits in mafic–ultramafic orogenic intrusions—examples from the Svecofennian areas, Finland. In: Eliopoulos DG et al (ed) Mineral exploration and sustainable development. Millpress Rotterdam, Rotterdam, pp 551–554

Patiño Douce AE, Castro A, El-Biad M (1997) Thermal evolution and tectonic implications of spinel–cordierite granulites from the Aracena Metamorphic Belt, Southwest Spain. GAC-MAC Annual Meeting, Ottawa, Abstracts volume 22, p A113

Pearce JA (1996) User's guide to basalt discrimination diagrams. In: Wyman DA (ed) Trace element geochemistry of volcanic rocks. Applications for massive sulphide exploration. Geol Assoc Can Short Course 12:79–114

Pin C, Liñan E, Pascual E, Donaire T, Valenzuela E (1999) Late Proterozoic crustal growth in Ossa Morena: Nd isotope and trace element evidence from the Sierra de Cordoba volcanics. XV Reunion Geologia Oeste Peninsular, Abstracts volume, pp 215–218

Piña R, Lunar R, Ortega L, Gervilla F, Alapieti T, Martínez C (2004) Origen de los fragmentos máficos-ultramáficos de la brecha mineralizada del yacimiento de Ni-Cu-EGP de Aguablanca (Badajoz). Macla (Madrid) 2:19–20

Piña R, Gervilla F, Ortega L, Lunar R (2005) Geochemistry and mineralogy of platinum-group elements in the Aguablanca Ni–Cu deposit (SW Spain). In: Törmanen TO, Alapieti T (eds) Platinum group elements—from genesis to beneficiation and environmental impact. 10th International Platinum Symposium, Oulu, Finland, pp 215–218

Pons J (1982) Un modele d'evolution de complexes plutoniques: Gabbros et granitoies de la Sierra Morena Occidentale (Espagne).

Doctoral thesis. Laboratoire Geologie Petrologie, Université Paul Sabatier, Tolouse, p 451

Pous J, Muñoz G, Heise W, Melgarejo JC, Quesada C (2004) Electromagnetic imaging of Variscan crustal structures in SW Iberia: the role of interconnected graphite. Earth Planet Sci Lett 217:435–450

Quesada C, Florido P, Gumiel P, Osborne J, Larrea F, Baeza L, Ortega C, Tornos F, Sigüenza J (1987) Mapa Geológico Minero de Extremadura. Junta de Extremadura, Direccion General Industria, Energia y Minas, p 131

Quesada C, Bellido F, Dallmeyer RD, Gil Ibarguchi I, Oliveira TJ, Perez Estaun A, Ribeiro A (1991) Terranes within the Iberian Massif: correlations with West Africa sequences. In: Dallmeyer RD (ed) The West African orogens and Circum-Atlantic correlations. Springer, Berlin Heidelberg New York, pp 267–294

Ripley E (1990) Platinum group element geochemistry of Cu–Ni mineralization in the basal zone of the Babbit Deposit, Duluth Complex, Minnesota. Econ Geol 85:830–841

Ripley EM, Butler BK, Taib NI, Lee I (1993) Hydrothermal alteration in the Babbitt Cu–Ni deposit, Duluth Complex: mineralogy and hydrogen isotope systematics. Econ Geol 88:679–696

Roberts S, Sanderson DJ, Dee S, Gumiel P (1991) Tectonic setting and fluid evolution of auriferous quartz veins from La Codosera area, Western Spain. Econ Geol 86:1012–1022

Rodas M, Luque FJ, Barrenechea JF, Fernandez Caliani JC, Miras A, Fernandez Rodriguez C (2000) Graphite occurrences in the low pressure/high temperature metamorphic belt of the Sierra de Aracena (southern Iberian Massif). Mineral Mag 64:801–814

Rollinson H (1993) Using geochemical data: evaluation, presentation, interpretation. Longman, Essex, p 352

Romeo I, Lunar R, Capote R, Dunning GR, Piña R, Ortega L (2004) Edades de cristalización U–Pb en circones del complejo ígneo de Santa Olalla de Cala: implicaciones en la edad del yacimiento de Ni–Cu-EGP de Aguablanca (Badajoz). Macla (Madrid) 2:29–30

Rudnick RL, Fountain DM (1995) Nature and composition of the continental crust—a lower crustal perspective. Rev Geophys 33:267–309

Ryan B (2000) The Nain Churchill boundary and the Nain plutonic suite: a regional perspective on the geologic setting of the Voisey's Bay Ni–Cu–Co deposit. Econ Geol 95:703–724

Saint Blanquat M, Tikoff B, Teyssier C, Vigneresse JL (1998) Transpressional kinematics and magmatic arcs. In: Holdsworth RE, Strachan RA, Dewey JF (eds) Continental transpressional and transtensional tectonics. Geol Soc Lond Spec Vol 135:327–340

Sanchez Carretero R, Eguiluz L, Pascual E, Carracedo M (1990) Ossa Morena Zone: igneous rocks. In: Martinez E, Dallmeyer RD (eds) Pre-Mesozoic geology of Iberia. Springer, Berlin Heidelberg New York, pp 292–313

Sanderson DJ, Zhang X (1999) Critical stress localization of flow associated with deformation of well-fractured rock masses, with implications for mineral deposits. In: McCaffrey KJW, Lonergan L, Wilkinson JJ (eds) Fractures, fluid flow and mineralization. Geol Soc Lond Spec Vol 155:69–81

Schäfer HJ (1990) Geochronological investigations in the Ossa Morena Zone, SW Spain. Doctoral thesis. Swiss Federal Institute Technology, Zurich, p 153

Shengao Y, Zhaochiong Z, Denghong W, Bailin C, Lixin H, Gang Z (2003) Kalatongke magmatic copper–nickel sulfide deposit. In: Mao J, Goldfarb RJ, Seltmann R, Wang D, Xiao W, Hart CRJ (eds) Tectonic evolution and the metallogeny of the Chinese Altay and Tianshan, pp 131–151

Simancas JF, Carbonell R, Gonzalez Lodeiro F, Perez Estaun A, Juhlin C, Ayarza P, Kashubin A, Azor A, Martínez Poyatos D, Ruiz Almodovar G, Pascual E, Saez R, Expósito I (2003) Crustal structure of the transpressional Variscan orogen of SW Iberia:

SW Iberia deep seismic reflection profile (IBERSEIS). Tectonics 22:1962–1974

Skirrow RG, Sims JP (1999) Genesis and setting of intrusion hosted Ni–Cu mineralization at Las Aguilas, San Luis province, Argentina: implications for exploration of an Ordovician arc. Explor Min Geol 8:1–20

Spiering ED, Rodriguez Pevida L, Castelo JM, Garcia Nieto J, Martinez C (2005) Aguablanca: a new nickel mine in a potential new Ni/Cu and IOCG belt of southern Spain and Portugal. Proceedings Geological Society Nevada. Symposium 2005

Stacey JS, Kramers JD (1975) Approximation of terrestrial lead isotope evolution by a two stage model. Earth Planet Sci Lett 26:207–221

Steiger RH, Jäeger E (1977) Subcommission on geochronology: convention on the use of decay constants in geo- and cosmo-chronology. Earth Planet Sci Lett 36:359–363

Stumpfl EF (1993) Fluids: a prerequisite for platinum metals mineralization. In: Fenoll P, Torres J, Gervilla F (eds) Current research in geology applied to ore deposits, Granada, pp 15–21

Suarez S, Velasco F, Yusta I (2005) Caracterización química y mineralógica de suelos en el yacimiento magmático Ni–Cu de Aguablanca, Badajoz (España). Bol Soc Esp Mineral 3:201–202

Taylor SRM (1995) The geochemical evolution of the continental crust. Rev Geophys 33:241–265

Thompson JFH (1984) Acadian synorogenic mafic intrusions in the Maine Appalachians. Am J Sci 284:462–483

Thompson JFH, Nixon F, Siversten R (1980) The geology of the Vakkerlien nickel prospect, Kvikne, Norway. Bull Geol Soc Finl 52:3–21

Tornos F, Casquet C (2005) A new scenario for related IOCG and Ni–(Cu) mineralisation: the relationship with giant mid-crustal mafic intrusion, Variscan Iberian Massif. Terra Nova 17:286–290

Tornos F, Chiaradia M (2004) Plumbotectonic evolution of the Ossa Morena Zone (Iberian Peninsula): tracing the influence of mantle–crust interaction in ore forming processes. Econ Geol 99:965–985

Tornos F, Velasco F (2002) The Sultana orebody (Ossa Morena Zone, Spain): insights into the evolution of Cu–(Au–Bi) mesothermal mineralization. In: Blundell DJ (ed) GEODE Study Centre, Grenoble, p 17

Tornos F, Casquet C, Galindo C, Canales A, Velasco F (1999) The genesis of the Variscan ultramafic-hosted magmatic Cu–Ni deposit of Aguablanca, SW Spain. In: Stanley et al (eds) Mineral deposits: processes to processing. Balkema, Rotterdam, pp 795–798

Tornos F, Casquet C, Velasco F, Galindo C, Canales A (2000) Las mineralizaciones de Cu–Ni de Aguablanca: un caso inusual de mineralizacion discordante en rocas ultrabásicas (PICG n°427). Temas Geol Min 30:183–191

Tornos F, Casquet C, Galindo C, Velasco F, Canales A (2001) A new style of Ni–Cu mineralization related to magmatic breccia pipes in a transpressional magmatic arc, Aguablanca, Spain. Miner Depos 36:700–706

Tornos F, Casquet C, Galindo C, Velasco F, Canales A (2002a) The Aguablanca Ni–Cu orebody (Ossa Morena Zone, SW Spain): geologic and geochemical features. Bol Soc Esp Mineral 25:99–116

Tornos F, Casquet C, Relvas J, Barriga F, Saez R (2002b) The relationship between ore deposits and oblique tectonics: the SW Iberian Variscan Belt. In: Blundell D, Neubauer F, von Quadt A (eds) The timing and location of major ore deposits: an evolving orogen. Geol Soc Lond Spec Publ 204:179–198

Tornos F, Inverno C, Casquet C, Mateus A, Ortiz G, Oliveira V (2004) The metallogenic evolution of the Ossa Morena Zone. J Iber Geol 30:143–180

Tornos F, Casquet C, Relvas J (2005) The metallogenesis of transpressional orogens: the Variscan of SW Iberia. Ore Geol Rev 27:133–163

Tosdal RM, Nutt CJ (1998) Formation of sedimentary rock-hosted (Carlin-type) Au deposit of the Carlin Trend along an Eocene accommodation zone. Geological Society of America Abstracts with Programs, vol 30

Unrug R, Haranczyk C, Chocyk JM (1999) Eastern Avalonian and Armorican–Cadomian terranes of Central Europe and Caledonian-Variscan evolution of the polydeformed Krakow mobile belt; geological constraints. Tectonophysics 302:133–157

Velasco F (1976) Mineralogía y metalogenia de las skarns de Santa Olalla (Huelva). Doctoral thesis, Universidad del Pais Vasco, Bilbao

Winchester JH, Floyd PA (1977) Geochemical discrimination of different magma series and their differentiation products using immobile elements. Chem Geol 20:325–343

Workman RK, Hart SR (2005) Major and trace element composition of the depleted MORB mantle. Earth Planet Sci Lett 231:53–72

The relationship between large deep mafic sills, crustal contamination and the formation of Ni-(Cu) and IOCG deposits

Fernando Tornos, Jorge Carriedo
Instituto Geológico y Minero de España. Azafranal 48. 37001 Salamanca (Spain)

Francisco Velasco
Universidad del País Vasco,48080 Leioa, Spain

Carmen Galindo, César Casquet
Universidad Complutense, 28040 Madrid, Spain

ABSTRACT: The Ossa Morena Zone (SW Iberia) hosts an unusual suite of ore deposits, including magmatic Ni-(Cu) and IOCG mineralization. These deposits are interpreted to have a relationship to a deep mafic sill intruded in the middle crust. Interaction of mafic magmas with crustal rocks produced immiscible sulphide-rich melts and water-rich melts. The latter exsolved large amounts of Fe- and CO_2-rich brines that were responsible for widespread albite-actinolite alteration and IOCG mineralization.

KEYWORDS: Geochemistry, Ni, Cu, Au, Fe, mafic sills

1 INTRODUCTION

In the Ossa Morena Zone (OMZ, SW Iberia), magmatic Ni-(Cu) and iron oxide-copper-gold (IOCG) deposits are contemporaneous with voluminous metaluminous calc-alkaline magmatism of Variscan age. This magmatism is related to the oblique collision between Gondwana and an exotic terrane, represented by the South Portuguese Zone, in late Devonian-Carboniferous times. Classical models suggest that most of the magmas formed overlying a subducting slab in a scheme somewhat similar to that of Pacific-like convergent margins. However, the area lacks significant volcanism and porphyry and epithermal deposits suggesting that the classical subduction-related magmatism and metallogenesis cannot be applied here.

Below the OMZ there is a deep (10-15km) seismic reflector (IRB) (Simancas *et al* 2003). It probably corresponds to a giant but discontinuous basaltic sill intruded during Variscan times along a detachment zone in the middle crust, and in which many of the structures of the area are rooted. This large intrusion probably controlled both the Variscan magmatism and ore-forming processes in the area (Tornos & Casquet 2005). This magmatic body only crops out in the southernmost OMZ (Aracena-Beja Massif, Fig. 1). Our interpretation is that the IRB controlled Variscan magmatism and hydrothermal circulation, leading to the unusual association of ore deposits.

2 GEOLOGIC SETTING AND ORE DEPOSITS

The geology of the OMZ includes a thick sequence of dark slate, quartzite and amphibolite (Serie Negra) overlain by a syn-Cadomian orogenic sequence of calc-alkaline andesite-rhyolite volcanic rocks, slate and limestone (late Neoproterozoic-early Cambrian) and limestone, slate, sandstone and alkaline-tholeiitic bimodal volcanic rocks belonging to a rift related sequence of Cambrian age. Younger sediments are scarce and are only found in the cores of synclines or in grabens. Magmatic rocks are related to both the Cadomian and Cambrian events, but the more voluminous magmatism is that related to the Variscan orogeny. These plutonic rocks occur as discrete epizonal plutons ranging in composition from ultrabasites to granite but the most common rock types by far are diorite to tonalite.

The area is rich in albite-bearing magmatic rocks. They occur as subvolcanic stocks representing the roots of the Cambrian volcanic systems but are also related to the Variscan rocks.

Variscan deformation in the OMZ is dominated by thick-skinned thrusts and large faults, all of which have an important lateral displacement suggesting that deformation took
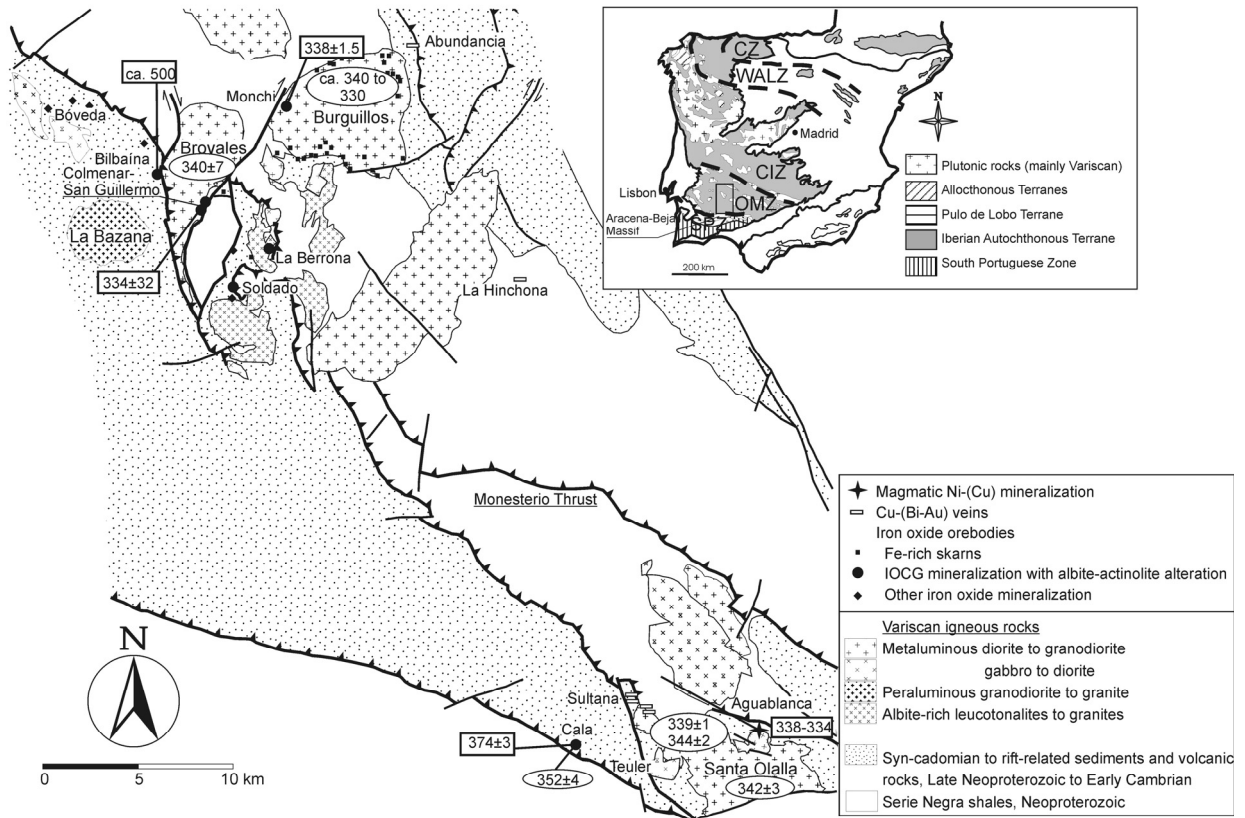
Figure 1. Geologic setting of the most significant Ni-Cu and IOCG deposits of the Ossa Morena Zone, showing the ages of individual deposits and related metaluminous plutonic rocks (in ellipses). Data from Romeo *et al.* (2006), Stein *et al.* (2006) and the compilation of Tornos & Casquet (2005). Modified from Tornos & Casquet (2005).

place in an overall left-lateral transpressive setting (Quesada 1991).

The OMZ hosts several hundreds of showings that have made it a leading producer of Pb, Zn and Fe. Nowadays, exploration is mainly focused on Ni-Cu magmatic ores and IOCG deposits.

Ni-(Cu) showings are common in both the Cadomian and Variscan plutonic rocks of the OMZ, but the most remarkable deposit is Aguablanca. This deposit is located in a subvertical, highly discontinuous, irregular body in which massive sulphides cement fragments of ultramafic rocks. This high-grade ore is surrounded by gabbro to norite with disseminated sulphide ore. Fragments in the breccia are heavily dominated by pyroxenite, and only sporadic fragments of other compositions are found. They include host rocks, skarns and some olivine-rich ultramafic rocks. This deposit is in-

terpreted to have formed via the disruption of a deep, layered magmatic complex by injection of molten sulfides to epizonal levels, through a localized pull apart structure in the overall compressive setting (Tornos *et al* 2006). Lithogeochemistry and isotope geochemistry trace a major crustal contamination that obliterates the original juvenile values of the magmatic rocks. High $^{87}Sr/^{86}Sr$ (0.708-0.710) and low $^{143}Nd/^{144}Nd$ (0.512-0.513) values are accompanied by typical crustal signatures of $\delta^{34}S$ (7.4‰), Pb (μ, 9.6-9.8) and Os (γOs, 40-65) (Casquet *et al* 2001; Tornos & Chiaradia 2004; Mathur *et al unpub. data*).

Iron oxide deposits, although not large, are widespread in the OMZ. Some of them are exhalative in the Cambrian sequence but others ones are clearly replacive and share many features with the IOCG style of mineralization. They are replacive with respect to the late Neoproterozoic-early Cambrian synorogenic sequence, mainly interbedded calc-silicate rocks and slate; where carbonate rocks are present, they develop large calcic and magnesian skarns. As a whole, they show a vertical zonation. Deep Cu-Au-poor magnetite-rich systems (Colmenar, Berrona, Monchi) are associated with albite-actinolite alteration, and adjacent to

albite-rich magmatic rocks. Shallow systems (Cala) are richer in Cu-Au, have a biotite-sericite-chlorite-ankerite alteration and are apparently unrelated to intrusions. In both cases, the mineralization shows a major tectonic control (Tornos & Casquet 2005; Carriedo *et al* 2007).

Fluid inclusion and isotope data show that fluids related with the IOCG deposits are very heterogeneous, always hypersaline and sometimes enriched in CO_2-CH_4, and underwent complex processes of unmixing-mixing. Fluids in the deep systems are characterized by relatively heavy $\delta^{18}O$ values (9-15‰) and δD (-35 to -30‰) signatures within the metamorphic field but close to magmatic values. In shallow systems they show O-D values that indicate mixing with surficial waters. However, all Nd (ϵNd, -8 to -4; Tornos & Casquet 2005), Pb (μ, 9.6-9.9; Tornos & Chiaradia 2004) and Os (γOs, 380; Stein *et al* 2006) isotopic values are indicative of a large crustally-derived component. Sulphur ($\delta^{34}S$, 3.6 to 20‰) is also mostly derived from the host metasedimentary sequence.

Dating of hydrothermal and magmatic rocks (in progress) shows that most of them are contemporaneous. Variscan mineralization ranges in age from *ca.* 374 to 340 Ma while magmatic rocks are near 340 Ma (342-338; see a compilation in Tornos *et al* 2005 and Romeo *et al* 2006). These ages are also equivalent to those of the mineralization at Aguablanca (Spiering *et al* 2005; Romeo *et al* 2006) and those of the deep sill (336±2 Ma; Tornos *et al* 2006). However, there is not always a direct relationship between magmatism and mineralization. For example, Re-Os dating of magnetite at the Cala orebody show that at least some of the magnetite mineralization predated by the adjacent plutonic rocks some 20 Ma (Stein *et al* 2006).

3 ORE FORMING PROCESSES IN THE OMZ

Geological and geochemical data on mineralization and related rocks in the OMZ suggest a scenario in which the intrusion of the mafic sill had a critical influence on the ore forming systems. Crustal contamination of deep mafic magmas intruded in the middle crust is responsible of the formation of both IOCG and magmatic Ni-(Cu) deposits in the OMZ. Intrusion of juvenile magmas into water-bearing low grade metamorphic slate produced widespread
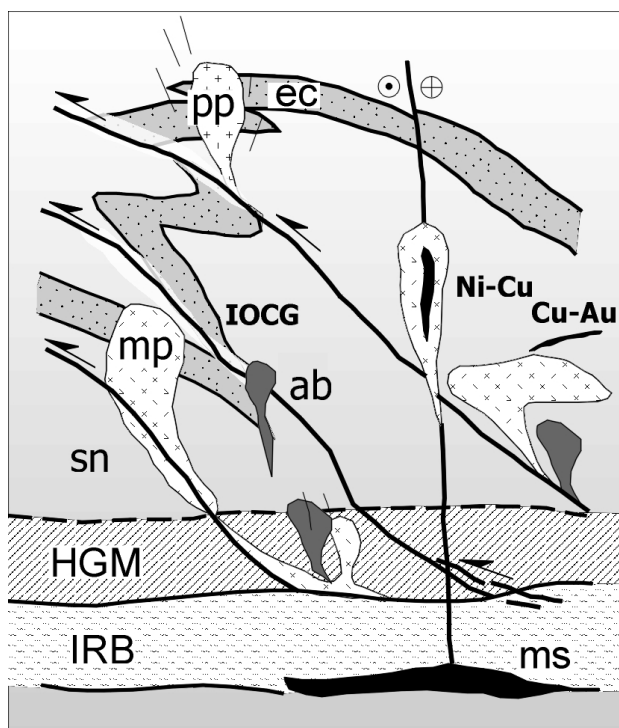
Figure 2. Sketch of the genetic relationships between metaluminous magmatism (mp), IOCG deposits and related albite-actinolite alteration (IOCG) and Ni-Cu magmatic mineralization, including both deep stratiform protore (ms) and epizonal breccias (Ni-Cu). IRB is the deep magmatic complex and HGM is the high grade metamorphic zone adjacent to the IRB. Sn is the metasedimentary Serie Negra, ec, the late Neoproterozoic-early Cambrian metasediments, pp the late Variscan peraluminous magmatism and ab, albitite. Modified from Tornos *et al.* (2005).

dehydration of the metamorphic rocks but water-enrichment in the magma was accompanied by assimilation of large amounts of host rocks.

The contamination was so intense that geochemical signatures of mafic-intermediate rocks are controlled by those of the crustal rocks. Contamination favored the formation of sulphide-rich magmas, the protore of the Aguablanca orebody. However, it also promoted the formation of fluid-rich mafic intermediate magmas that exsolved hypersaline, iron-rich and CO_2-bearing brines. These brines were probably responsible for sodic autometasomatism and formation of albitite on igneous rocks, widespread albite-actinolite-magnetite hydrothermal alteration and related mineralization (Fig. 2).

4 CONCLUSIONS

The intrusion of the IRB controlled the metallogenic evolution of the OMZ. It inhibited the formation of intermediate, relatively dry, calc-

alkaline magmas but favored the formation of highly contaminated more basic and water-rich magmas. These magmas intruded along major crustal discontinuities to shallow levels and exsolved large amounts of hypersaline, usually CO_2-bearing, brines that formed large IOCG-like hydrothermal systems. Crustal contamination also favored immiscibility of sulphide-rich magmas, which used the same channel ways as silicate melts and hydrothermal fluids to ascend to shallow levels in the crust.

Deep sills perhaps similar to those forming the IRB system can be common in transpressional settings, substantially modifying the heat flow, magmatic regime and mineralization in converging terranes. A magmatic-hydrothermal system similar to that proposed here could be important in other IOCG-rich provinces. However, the intense deformation and metamorphism that has affected Proterozoic terranes has probably masked the original relationships.

ACKNOWLEDGEMENTS

REFERENCES

Carriedo J, Tornos F, Velasco F, Galindo C, Tornos F (2007) Complex structural and hydrothermal evolution of IOCG deposits: The Cala deposit, SW Iberia. *This volume*

Casquet C, Galindo C, Tornos F Velasco F (2001) The Aguablanca Cu-Ni ore deposit (Extremadura, Spain), a case of synorogenic orthomagmatic mineralization: Isotope composition of magmas (Sr, Nd) and ore (S). *Ore Geology Reviews* 18: 237-250.

Romeo I, Lunar R, Capote R, Quesada C, Dunning GR, Piña R, Ortega L (2006) U-Pb age constraints on Variscan magmatism and Ni-Cu-PGE metallogeny in the Ossa Morena Zone (NW Iberia). *Journal Geological Society London* 163: 837-846.

Simancas JF, Carbonell R, Gonzalez Lodeiro F, Perez Estaun A, Juhlin C, Ayarza P, Kashubin A, Azor A, Martínez Poyatos D, Ruiz Almodovar G, Pascual E, Saez R, Expósito I (2003) Crustal structure of the transpressional Variscan orogen of SW Iberia: SW Iberia deep seismic reflection profile (IBERSEIS). *Tectonics* 22: 1962-1974.

Quesada C (1991) Geological constraints on the Paleozoic tectonic evolution of tectonostratigraphic terranes in the Iberian Massif. *Tectonophysics* 185: 225-245.

Spiering ED, Rodriguez Pevida L, Castelo JM, Garcia Nieto J, Martinez Chaparro C (2005) Aguablanca: a new nickel mine in a potential new Ni/Cu and IOCG belt of southern Spain and Portugal. *Geological Society of Nevada Symposium 2005:* Window to the World: Reno, Nevada.

Stein H, Markey R, Carriedo J., Tornos F. (2006) Re-Os evidence for the origin of Fe-oxide-(Cu-Au) deposits in SW Iberia at the Frasnian-Famennian boundary. *Geochimica Cosmochimica Acta - Goldschmidt Conference Abstracts* 2006, 18: A612.

Tornos F, Casquet C (2005) A new scenario for related IOCG and Ni-(Cu) mineralisation: the relationship with giant mid-crustal mafic intrusion, Variscan Iberian Massif. *Terra Nova* 17: 286-290.

Tornos F, Chiaradia M (2004) Plumbotectonic evolution of the Ossa Morena Zone (Iberian Peninsula): Tracing the influence of mantle-crust interaction in ore forming processes. *Economic Geology*: 99: 965-985.

Tornos F, Galindo C, Casquet C, Rodríguez Pevida L, Martínez C, Martínez E, Velasco F, Iriondo A (2006) The Aguablanca Ni-(Cu) magmatic deposit (SW Spain). Geologic and geochemical controls and the relationship with deep magmatic layered complexes. *Mineralium Deposita* 41: 737-769.

LOS YACIMIENTOS DE OXIDOS DE HIERRO Y MINERALIZACIONES DE COBRE-ORO ASOCIADAS DEL SO PENINSULAR: UN MODELO VERTICAL DE EVOLUCIÓN

J. Carriedo y F. Tornos

Instituto Geológico y Minero de España. IGME, c/ Azafranal 48, 1ºA, 37001, Salamanca.

INTRODUCCIÓN

La Zona de Ossa Morena (SO de la Península Ibérica) se caracteriza por la abundancia de mineralizaciones de óxidos de hierro, a veces con contenidos importantes de cobre-oro. Con unas reservas originales estimadas de unas 180 Mt, estos depósitos han sido intensamente trabajados durante el s. XX, quedando actualmente en producción intermitente la mina de Cala (Huelva). Sin embargo, los localmente elevados contenidos en cobre y oro y la reciente alza en el precio de los metales hacen que actualmente la zona sea un objetivo minero de importancia.

Las mineralizaciones se concentran en dos bandas de dirección NO-SE situadas en ambos flancos del antiforme de Olivenza-Monesterio y generalmente encajadas en una secuencia volcanosedimentaria de edad Neoproterozoico Superior-Cámbrico Medio relacionada con una etapa de rift que sucedió al arco magmático cadomiense (Quesada, 1991; Eguíluz et al., 2000). Las mineralizaciones se encuentran preferentemente en los niveles volcánicos o carbonatados, generalmente cerca de rocas ígneas cámbricas y/o Variscas o grandes accidentes tectónicos, como es el Cabalgamiento de Monesterio (Tornos y Casquet, 2005).

El estudio detallado de los depósitos más significativos muestra que hay diversos estilos de mineralización. Estos incluyen tanto mineralizaciones estratiformes/estratoides de edad Cámbrico Inferior-Medio como depósitos epigenéticos de edad Varisca y posiblemente relacionados por fenómenos complejos de removilización-reconcentración. El hecho de que las rocas encajantes sean las mismas en ambos tipos de estilos dificulta la interpretación global, pero la geocronología confirma que hay mineralizaciones pertenecientes a las dos etapas (Darbyshire et al., 1998; Casquet et al., 1998).

DEPÓSITOS VOLCANOSEDIMENTARIOS ESTRATIFORMES

Estos depósitos se encuentran intercalados en la serie volcanosedimentaria cámbrica como cuerpos estratiformes localizados en el contacto entre pizarra y arenisca volcanoclástica félsica y el horizonte regional de caliza suprayacente (Bilbaína, La Bóveda) o dentro de las rocas volcanoclásticas (Las Herrerías, Aurora-Las Galerías?). La mineralización está compuesta por magnetita con cantidades a veces significativas de barita y hematites, presentando un bandeado concordante con la estratificación; localmente es posible reconocer probables estructuras sedimentarias tales como *ripple marks* o laminación paralela o cruzada. La mineralización alterna con niveles de exhalitas silíceas. Local-mente, la caliza asociada está remplazada por masas de siderita. Las rocas infrayacentes pueden tener una intensa alteración a albita-cuarzo y un stockwork enriquecido en pirita. Aunque son mineralizaciones generalmente pobres en Cu-Au, la mineralización de Herrerías tiene contenidos apreciables de calcopirita, bien asociada a la magnetita, bien diseminada en la roca volcanoclástica intercalada. Esta mineralización parece ser siempre posterior a la de óxidos de hierro y controlada por fracturas Variscas.

DEPÓSITOS DE REEMPLAZAMIENTO

Esta misma secuencia del Cámbrico Inferior-Medio engloba también a un segundo tipo de mineralización, pero de carácter reemplazante. Estos depósitos suelen estar relacionados con rocas ígneas o zonas de cizalla y fracturas de carácter regional. Se distinguen varios tipos de mineralización:

· Mineralizaciones de magnetita localizadas en la facies retrógrada de skarns cálcicos o magnésicos en el contacto entre las rocas plutónicas y la caliza y dolomía Cámbrica, tal como es el caso de los depósitos situados alrededor de los plutones de Burguillos, Aguablanca o Teuler (Casquet y Tornos, 1991). Una paragénesis primaria, rica en andradita o diópsido-salita en los skarns cálcicos o de forsterita en los magnésicos, fue remplazada por clinoanfíbol y epidota o serpentina, respectivamente. Estas mineralizaciones suelen ser ricas en pirita pero tienen cantidades muy accesorias de cobre-oro.

· Depósitos de magnetita en el contacto de plutones albíticos, en los que la mineralización está ligada a zonas de albita-magnetita(-actinolita-fluorita) remplazando a rocas detríticas y carbonatadas cerca de los plutones; los contenidos en cobre-oro son relativamente bajos. Estas mineralizaciones se encuentran preferentemente en el entorno de los plutones de albitita de edad desconocida situados en el entorno del Domo de Valuengo (e.g., La Berrona, El Soldado).

· Los depósitos en relación con bandas de cizalla presentan una gran variedad mineralógica pero tienen muchos rasgos en común. Así, en la mina Monchi (Casquet et al., 1998) la mineralización de magnetita-vonsenita está asociada a una roca de hedenbergita-allanita que aparece como enclaves dentro de la tonalita-granodiorita del borde y es anterior a una pegmatita alcalina rica en axinita. El depósito de Colmenar-Santa Bárbara ha explotado unas bandas de magnetita-albita-actinolita que remplazan a esquisto, rocas de silicatos cálcicos y mármol cerca del contacto con el plutón Varisco de Brovales y que son el equivalente metamórfico de la serie volcanosedimentaria del
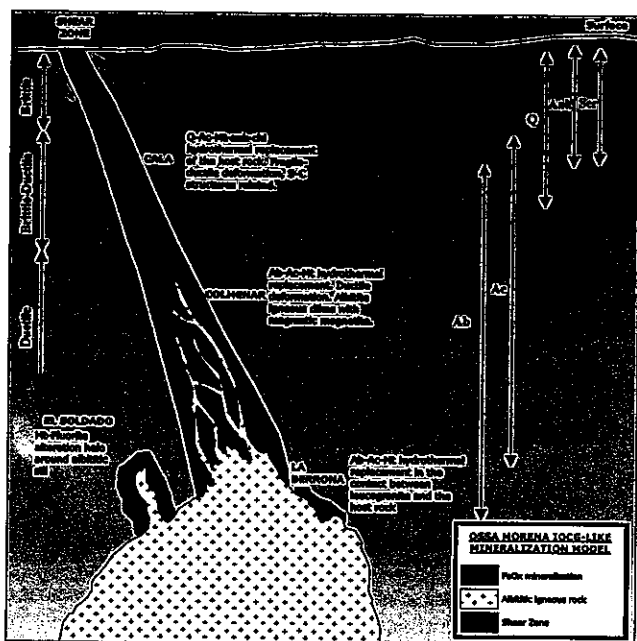
Figura 1: Modelo interpretativo de los yacimientos reemplazativos en la zona de Ossa Morena, mostrando el zonado vertical.

Cámbrico Inferior-Medio (Cuervo et al., 1996; Sanabria et al., 2005). Estas rocas están cortadas por diques de albita-magnetita. El depósito de Cala se encuentra en un encuadre geológico similar, cerca del contacto de una granodiorita Varisca afectada por una intensa alteración potásica. La mineralización principal parece ser anterior a esta intrusión y está relacionada con una gran zona de alteración desarrollada en una pequeña estructura de *pull-apart*. La mineralización se encuentra como lentejones subverticales de dirección NO-SE y formados por ankerita, cuarzo, clinoanfíbol y magnetita que remplazan a pizarra, rocas de silicatos cálcicos y mármol. Localmente se observa albita residual (Carriedo et al., 2006).

Los contenidos en sulfuros son muy variables. Mientras que en Cala la pirita y calcopirita son relativamente abundantes, en Colmenar hay cantidades accesorias de pirita, calcopirita, millerita y pirrotita y en Monchi solo hay cantidades anecdóticas de löellingita, pirrotita, cobaltita, arsenopirita y otros sulfuros. Todas estas mineralizaciones remplazan a una secuencia rica en mármoles y, por ello, los skarns son relativamente frecuentes. Sin embargo, no toda la mineralización está ligada a éstos. Generalmente suelen ser independientes de la mineralización principal, desarrollando solo un pequeño skarn retrógrado con proporciones variables de magnetita.

La edad de estas mineralizaciones de reemplazamiento parece ser Varisca, tal como sugieren las relaciones con plutones y bandas de cizalla de esa edad, así como los datos geocronológicos preliminares (Casquet et al., 1998).

CARACTERIZACIÓN DE LOS DEPÓSITOS

Numerosos depósitos reemplazativos de hierro con proporciones variables de cobre y oro de la Zona de Ossa Morena reúnen muchas de las características de los depósitos de tipo Iron Oxide-Copper-Gold (Hitzman et al., 1992), tales como la relación con cizallas transcrustales, la asociación con una alteración alcalina rica en albita-actinolita, el enriquecimiento en minerales típicamente enriquecidos en volátiles (F, P, Cl, B) y la relación con la circulación de fluidos hidrotermales salinos

y de derivación profunda (Tornos y Casquet, 2005; Tornos et al., 2005). Al igual que en otros distritos similares, la mineralización de hierro parece estar asociada a la removilización de concentraciones anteriores.

La interpretación global de los depósitos de reemplazamiento sugiere la existencia de una cierta zonación vertical (Figura 1). Así, los depósitos más profundos serían los directamente relacionados con las albititas y caracterizados por una asociación de albita-magnetita-(actinolita-fluorita), tales como La Berrona o El Soldado. La mineralización de El Colmenar estará formada a profundidades intermedias; en ella, las albititas son accesorias pero la alteración dominante es de tipo albita-actinolita. Finalmente, la parte más somera del sistema estaría representada por la mina de Cala, en la que no se han observado albititas y la alteración de albita-actinolita está remplazada por una de cuarzo-ankerita-actinolita-magnetita. El intervalo de profundidades al que se desarrolla el sistema no se conoce pero es probable que no supere los 1000-1500 m.

CONCLUSIONES

Excepto en contados casos, los depósitos de tipo IOCG se localizan en terrenos arcaicos o proterozoicos muy deformados, por lo que sus relaciones con los procesos magmáticos e hidrotermales son oscuras. La Zona de Ossa Morena representa un área de gran interés para definir las relaciones de estas mineralizaciones con procesos geológicos regionales. Las características geológicas de las mineralizaciones de hierro-(cobre-oro) de Ossa Morena parecen estar controladas por su situación dentro de una zonación vertical, dando lugar a distintos estilos de mineralización según su profundidad de formación.

AGRADECIMIENTOS

REFERENCIAS

Carriedo, J., Tornos, F., Velasco, F. y Terrón, A. (2006).. Geogaceta (en prensa).

Casquet, C., Galindo, C., Darbyshire, D.P.F., Noble, S.R., Tornos, F. (1998). Fe-U-REE mineralization at Mina Monchi, Burguillos del Cerro, Spain: age and isotope (U-Pb, Rb-Sr and Sm-Nd) constraints on the evolution of the ores: Proceedings GAC-MAC-APGGQ Quebec 98 Conference, 23, A28.

Casquet, C. y Tornos, F. (1991). Influence of depth and igneous geochemistry on ore development in skarns: The Hercynian Belt of the Iberian Peninsula: 'Skarns, their petrology and metallogeny', Augusthitis ed.,Athenas, pp.555-591.

Cuervo, S., Tornos, F., Spiro, B. y Casquet, C. (1996). Geogaceta, v. 20-7, 1499-1500.

Darbyshire, D.P.F., Tornos, F., Galindo, C. y Casquet, C. (1998). ICOG-9, Chinese Science Bulletin, 43 sup., 28.

Eguiluz, L., Gil Ibarguchi, J.I., Abalos, B., and Apraiz, A.. (2000): Geologic Society America Bulletin, v. 112, p. 1398-1413.

Quesada, C. (1991). Tectonophysics, v. 185, p. 225-145.

Sanabria, R., Casquet, C., Tornos, F. y Galindo, C. (2005). Geogaceta, v. 38, p. 223-227.

Tornos, F., y Casquet, C. (2005). Terra Nova, v. 17, p. 286-290.

LA RELACIÓN ENTRE INTRUSIONES LAMINARES PROFUNDAS Y LA MINERALIZACIÓN DE AGUABLANCA: LAS ROCAS INTRUSIVAS DE CORTEGANA (HUELVA)

F. Tornos [1], C. Galindo [2], C. Casquet [2], L. Rodríguez Pevida [3] y A. Iriondo [4]

[1] Instituto Geológico y Minero de España, Azafranal 48, 37002 Salamanca

[2] Dpto. Petrología, Universidad Complutense de Madrid, 28040 Madrid

[3] Río Narcea Nickel,06300 Zafra, Badajoz

[4] Centro de Geociencias, Universidad Nacional Autónoma de México, Querétaro, México

INTRODUCCIÓN

El depósito de Ni-(Cu) de Aguablanca (Badajoz) se localiza en una pipa magmática de edad Varisca y es producto de la removilización de un complejo estratiforme profundo parcialmente consolidado a favor de una pequeña estructura extensional de tipo *pull-apart* en un orógeno mayoritariamente transpresivo (Casquet et al., 2001; Tornos et al., 2001). Este modelo preliminar se ha visto confirmado por las dataciones radiométricas realizadas en la mineralización y rocas encajantes (Romeo et al., 2004; Tornos et al., 2004; Spiering et al., 2005) y también por la detección de un cuerpo denso y reflectivo de 1-5 km de potencia a unos 10-15 km de profundidad y localizado bajo la mayor parte de la Zona de Ossa Morena (IRB; Simancas et al., 2003), que posiblemente corresponda a un complejo magmático laminar discontinuo pero de gran extensión lateral.

La mayor parte del cuerpo reflector no aflora y, por lo tanto, no es posible determinar sus características y si realmente corresponde a una roca ígnea. Sin embargo, los cortes geológicos propuestos por Simancas et al. (2003) y Tornos et al. (2005) sugieren que el Macizo de Aracena, situado en el sur de la Zona de Ossa Morena, es un trozo de corteza media-inferior que ha sido levantado y en el que es posible reconocer restos desmembrados de este complejo magmático laminar. En este trabajo presentamos datos geológicos, geoquímicos y geocronológicos de las rocas intrusivas de la zona de Cortegana (Huelva) y de las mineralizaciones asociadas, mostrando que estas rocas pueden ser parte del complejo magmático profundo y discutiendo sus relaciones con las rocas encajantes de la mineralización de Aguablanca.

GEOLOGÍA DEL COMPLEJO PLUTÓNICO DE CORTEGANA

El Macizo de Aracena es un terreno metamórfico situado entre las zonas Sudportuguesa y de Ossa Morena. Su parte septentrional incluye una secuencia continental de posible edad Neoproterozoico Superior-Cámbrico Inferior similar a la que se encuentra en la central y septentrional de la Zona de Ossa Morena, pero afectada por un metamorfismo de alta temperatura-baja presión. La zona meridional está dominada por una secuencia oceánica muy deformada (Ofiolita de Beja-Acebuches) (e.g., Crespo, 1991; Quesada et al., 1994). En el primer caso, la serie consiste en una potente unidad de gneis peralumínico

muy deformado intercalado con corneana pelítico y con intercalaciones de cuarcita, gneis piroxenítico, ortoanfibolita, caliza y roca de silicatos cálcicos (Giese et al. 1994, Castro et al. 1999). En las zonas más internas hay abundantes intrusiones de rocas máficas y ultramáficas que, a grandes rasgos, son geoquímicamente muy similares al magmatismo metalumínico Varisco de la Zona de Ossa Morena.

Estas rocas plutónicas son especialmente abundantes en las cercanías de Cortegana, donde forman cuerpos lentejonares de hasta 600 m de potencia (Complejo Plutónico de Cortesana) subconcordantes con la foliación de la roca encajante, que es casi horizontal. Están formados mayoritariamente por gabro y norita de grano grueso. Incluyen lentejones discontinuos de ortoacumulado ultramáfico de grano grueso, websterita olivínica, lherzolita, dunita y ortopiroxenita; hay cantidades más accesorias de harzburgita, troctolita y wehrlita. Muy localmente hay cantidades accesorias de anortosita. Todas estas rocas tienen abundante flogopita y clinoanfíbol intercumular. En todas las rocas ígneas son frecuentes los enclaves de skarn, roca de silicatos cálcicos, corneana pelítica y migmatita, pero lo son especialmente en su zona marginal. De hecho, a lo largo del contacto con la migmatita y corneana pelítica encajante hay una zona híbrida muy heterogénea de entre 15 y 300 m de potencia formada por diorita y tonalita con abundantes restos parcialmente asimilados de roca encajante y abundantes facies orbiculares. En estas rocas el grafito puede ser muy abundante; se interpreta como derivado de la asimilación de cuarcita rica en grafito e intercalada en la secuencia metasedimentaria Neoproterozoica (Rodas et al., 2000). Todas estas rocas están afectadas por una intensa pero irregular alteración hidrotermal que ha retrogradado la paragénesis primaria. Apesar de estar en la zona de mayor grado metamórfico y con migmatización generalizada, las rocas ígneas no están afectadas por el metamorfismo regional, cuyas condiciones máximas (>920 to 1000°C; 4 to 6 kbar) han sido establecidas por Patiño Douce et al. (1997) y Diaz-Azpiroz et al. (2004). A 340 Ma su profundidad de intrusión se estima entre 12 y 19 km, que es similar a la calculada para el metamorfismo (12-18 km profundidad).

Los trabajos de exploración minera realizados por Río Narcea han reconocido varias zonas mineralizadas dentro de los acumulados ultramáficos (Spiering et al., 2005). La mineralización aparece de forma intercumular

o remplazando a los minerales magmáticos y está formada fundamentalmente por pirrotita y calcopirita con pequeñas cantidades de pentlandita. Los contenidos medios en la zona investigada son de cerca del 0.16%Ni y 0.08%Cu, aunque puntualmente se han obtenido valores de 1.36% Ni y 0.2% Cu. El contenido en platinoides es bajo, 2-6 ppb. Sin embargo, las La relación Cu/Ni del cumulado mineralizado (0.53) es significativamente mayor que en el depósito de Aguablanca.

Al Oeste del Macizo de Aracena se encuentra el Complejo Ígneo de Beja, que incluye gabro con olivino-hiperstena, cuarzo-diorita, troctolita y anortosita, muchas veces con facies de acumulado, y que tiene concentraciones de óxidos de Fe-Ti-V y diseminaciones de Cu-(Ni) (Mateus et al., 2001).

EDAD DE LA INTRUSIÓN Y MINERALIZACIÓN

Dos concentrados de flogopita de una cuarzo-diorita de la zona de contacto (TEJ-3) y una websterita de la zona central (ZOM-23) han sido datados por el método 40Ar/39Ar. La muestra TEJ-3 ha dado una edad de isócrona de 321.5 ± 32.6 Ma, cuya imprecisión probablemente refleja la interacción existente en el margen del cuerpo intrusivo entre las rocas máficas y el encajante. La muestra ZOM-23 ha dado una edad plateau de 336.2 ± 1.7 Ma y una edad de isócrona menos precisa de 328.1 ± 6.3 Ma. Ambas edades probablemente reflejan la edad mínima de la cristalización de las rocas ígneas y mineralización asociada en el Complejo Plutónico de Cortegana.

Este Complejo Plutónico fue sincrónico con el metamorfismo regional, tal como indica la concordancia de los cuerpos ígneos con la foliación regional, la presencia de facies de mezcla en la zona marginal de la intrusión y la relación de estos cuerpos intrusivos con las zonas de mayor grado metamórfico (Tornos et al., 2005). Este metamorfismo ha sido datado por 40Ar/39Ar entre 342.6 ± 0.6 y 328 ± 1.2 Ma (Dallmeyer et al., 1993; Castro et al., 1999) y, por lo tanto, parece razonable asumir que estuvo directamente ligado a la advección de calor magmático, tal como ocurre en las cercanías de muchas intrusiones laminares profundas (Pirajno, 2000). A su vez, estas edades son similares a las del emplazamiento del Complejo Ígneo de Beja (Dallmeyer et al., 1993) en ambientes profundos y del Complejo Plutónico de Santa Olalla y la formación de la mineralización de Aguablanca en niveles epizonales.

GEOQUÍMICA DE LAS ROCAS ÍGNEAS

El Complejo Plutónico de Cortegana es geoquímicamente similar al Stock de Aguablanca (Casquet et al., 2001), con contenidos de SiO2 entre 38.43 y 69.72% y Mg# entre 0.14 y 0.67, mostrando una tendencia calcoalcalina. Solo las rocas ricas en olivino son más primitivas que las del Stock de Aguablanca. Los contenidos en elementos traza son también similares sugiriendo un origen común para el magma y un grado de contaminación crustal equivalente. Sin embargo, las rocas de Cortegana están empobrecidas en MgO y FeOt y enriquecidas en CaO y K2O, probablemente reflejando la interacción con una roca más cuarzo-feldespática. Esto también se refleja en una pronunciada anomalía negativa en Eu (Eu/Eu* ≈ 0.55).

Los isótopos de Sm-Nd y Rb-Sr muestran igualmente la existencia de procesos de mezcla similares a los de Aguablanca, pero con una tendencia muy distinta. Así, hay un empobrecimiento en las relaciones $^{86}Sr/^{87}Sr$ y $^{143}Nd/^{144}Nd$ ligados al incremento en Rb/Sr y Sm/Nd, respectivamente. Un término extremo de este proceso de mezcla podría ser una roca intermedia entre el manto empobrecido y rocas de la corteza superior, pero isotópicamente más primitivo que los magmas del Stock de Aguablanca. El segundo término extremo se caracteriza por unas elevadas relaciones Rb/Sr y Sm/Nd e hipotéticamente podría corresponder a rocas pertenecientes a una corteza inferior continental. Hay evidencias de campo que indican que los procesos de mezcla tuvieron lugar en o cerca del nivel de emplazamiento y la geoquímica de algunas de las rocas de la zona (Bachiller, 1996; Castro et al., 1999) es consistente con este modelo.

DISCUSIÓN Y CONCLUSIONES

Las evidencias geológicas, geoquímicas y geocronológicas son consistentes con la hipótesis de que las rocas del Complejo Plutónico de Cortegana pertenecen al complejo magmático laminar que subyace bajo la Zona de Ossa Morena.

Tanto la geología del Macizo de Aracena como los datos geofísicos indican que el complejo magmático laminar era muy discontinuo y formado por varias decenas de sills subhorizontales e intrusiones irregulares que probablemente evolucionaron diferentemente dependiendo de su tamaño, naturaleza de la roca encajante, temperatura de intrusión y grado de asimilación de las rocas encajantes. Estas variables han condicionado la geología y geoquímica de las distintas unidades magmáticas, aún a escala local. Las diferencias isotópicas sugieren que la cámara magmática bajo el Stock de Aguablanca es distinta al Complejo Plutónico de Cortegana. Probablemente, bajo Aguablanca, la intrusión de un volumen significativo de magma sobrecalentó la roca encajante y fue capaz de asimilar cantidades significativas de roca de caja, perteneciente a la corteza media. La interacción dio lugar a la inmiscibilidad de un magma sulfurado que se separó del fundido silicatado y que evolucionó mediante procesos AFC desde una composición toleítica primitiva a una de tendencia calcoalcalina. El tamaño de grano fino en Aguablanca se interpreta como debido a la supersaturación rápida del piroxeno durante la cristalización magmática. En Cortegana, el tamaño de grano grueso de los acumulados se interpreta como debido a una cristalización lenta a partir de diversos pulsos magmáticos. En la sección estudiada los acumulados quedaron aislados de la roca de caja por rocas de carácter intermedio que son las que han sufrido la contaminación crustal. Por lo tanto, y a escala local, no se produjo homogeneización isotópica del azufre ni desarrollo de un volumen significativo de magma sulfurado inmiscible. Por ello, las zonas más favorables para el desarrollo de mineralizaciones son aquellas en las que el magma poco evolucionado tuvo un alto grado de interacción con las rocas encajantes.

AGRADECIMIENTOS

BTE2003-290. Agradecemos la ayuda y comentarios de Francisco Velasco, Jorge Carriedo, Carmen Conde, Lorena Luceño y Casimiro Maldonado.

REFERENCIAS

Bachiller, N. (1996). Tesis Licenciatura, Universidad Complutense de Madrid (inédito).
Casquet, C., Galindo, C., Tornos, F., y Velasco, F. (2001). Ore Geology Reviews, 18, 237-250.
Castro, A., Fernandez, C., El-Hmidi, H., El-Biad, M., Diaz, M., Rosa, J., y Stuart, F. (1999). Contributions Mineralogy
Petrology, 88, 26-37
Crespo, A. (1991). Tesis Doctoral. Ediciones Universidad Granada, Granada. 327 pp.
Dallmeyer, R.D., Fonseca, P.E., Quesada, C., y Ribeiro, A. (1993). Tectonophysics, 222, 177-194
Diaz Azpiroz, M., Castro, A., Fernández, C., López, S., Fernández Caliani, J.C., y Moreno-Ventas, I. (2004). Journal
Iberian Geology, 30, 23-52.
Giese, U., Walter, R., y Winterfeld, C. (1994). Neues Jahrbuch fur Geologie und Palaontologie, Abhandlungen, 192-
3, 333-360.
Mateus, A., Jesus, A.P., Oliveira, V., Gonçalves, M.A., y Rosa, C. (2001). Estudos Notas e Trabalhos Instituto

Geologico Mineiro, 43, 3-16.
Patiño Douce, A.E., Castro, A., y El-Biad, M. (1997). GAC-MAC Annual Meeting, Ottawa, Abstracts Volume 22, p A113
Pirajno, F. (2000). Kluwer Academic Pub., Dordrecht, 556 pp.
Quesada, C., Fonseca, P. E., Munhá, J., Oliveira, J. T., y Ribeiro, A. (1994). Boletin Geologico Minero, 105, 3-49.
Rodas, M., Luque, F. J., Barrenechea, J. F., Fernandez Caliani, J. C., Miras, A., y Fernandez Rodriguez, C. (2000).
Mineralogical Magazine, 64, 801-814.
Romeo, I., Lunar, R., Capote, R., Dunning, G.R., Piña, R., y Ortega, L. (2004). Macla, 2, 29-30
Simancas, J. F., Carbonell, R., Gonzalez Lodeiro, F., Perez Estaun, A., Juhlin., C., Ayarza, P., Kashubin, A., Azor, A.,
Martínez Poyatos, D., Ruiz Almodovar, G., Pascual, E., Saez, R., y Expósito, I. (2003). Tectonics, 22, 1962-1974.
Spiering, E.D., Rodriguez Pevida, L., Castelo, J.M., Garcia Nieto, J., y Martinez, C. (2005). Proceedings Geological
Society Nevada. Symposium 2005.
Tornos, F., y Casquet, C. (2005). Terra Nova ,17, 286-290.
Tornos, F., Casquet, C., Galindo, C., Velasco, F., y Canales, A. (2001). Mineralium Deposita, 36, 700-706.
Tornos, F., Casquet, C., y Relvas, J. (2005). Ore Geology Reviews, 27, 133-163.

Estudio petrológico y geoquímico de las vulcanitas de los afloramientos de El Pimpollar, extremo nororiental de la Zona Surportuguesa

Petrological and geochemical study of the volcanic rocks of "El Pimpollar" out-crops, northeastern sector of the South-Portuguese Zone, Spain

F. Bellido [1], A. Díez Montes [1] y G. Ortiz [2]

[1] Instituto Geológico y Minero de España, C/ La Calera, nº 1, 28760-Tres Cantos. Madrid. f.bellido@igme.es
[2] Instituto Geológico y Minero de España, C/ Ríos Rosas, nº 23, 28003-Madrid

ABSTRACT

The Lower Unit of "El Pimpollar" volcanic outcrop (South-Portuguese Zone) is mainly composed of submarine dacites and andesites, with some subordinate basalts and trachyandesites. All these volcanic materials have intraplate affinities. The more basic rocks have alkaline character and show some differences with the equivalent vulcanites of the Iberian Pyrite Belt.
The rhyolites of the Upper Unit are very rich in K and have geochemical characteristics intermediate between the silica rich igneous rocks related with volcanic arcs or collisional orogens. These rhyolitic rocks are different from other volcanic rocks with similar SiO_2 content of the Iberian Pyrite Belt.
The volcanic suite has a post-Middle-Visean age and its two units extruded in different tectono-sedimentary environments.

Key words: South-Portuguese Zone, volcanism, geochemistry, El Pimpollar

Introducción

En la Zona Surportuguesa (ZSP, Lotze, 1945) afloran principalmente materiales del Devónico Medio al Carbonífero Superior. En su mitad N se localiza la Faja Pirítica Ibérica (FPI), constituida por secuencias volcánicas y series volcanosedimentarias, en las que se encuentran importantes depósitos de sulfuros masivos, y en su extremo nororiental se sitúan los afloramientos volcánicos de El Pimpollar. Inicialmente estos materiales se habían correlacionado con las vulcanitas pérmicas de la cuenca del Viar (Martín Escorza y Rivas Ponce, 1973), aunque posteriormente Simancas (1983) los estudia con más detalle y los relaciona con el vulcanismo de la FPI, asignándoles una edad Viseense Superior.

En el borde oriental, el afloramiento de El Pimpollar está recubierto por los sedimentos detríticos de la Cuenca del Viar, a los que Simancas (1983) atribuye una edad Autuniense (Pérmico Inferior).

El borde S está determinado por una falla normal con cierto componente de desgarre que tiene una dirección aproximada N 70ºE y que pone en contacto a los materiales de la Cuenca de El Pimpollar con las rocas plutónicas del Batolito de la Sierra Norte.

Las investigaciones geológicas realizadas en la zona de El Pimpollar, han sido fruto del estudio previo de los mapas aeromagnético y radiométrico realizados por el IGME para el estudio de la Faja pirítica Ibérica, que pusieron de manifiesto la presencia de importantes anomalías magnéticas, y en la radiación gamma natural del K. La geometría de esta última anomalía se puede observar en la figura 1.

Los materiales volcánicos más antiguos identificados en los afloramientos de El Pimpollar corresponden a bloques y cantos de andesitas que se encuentran como clastos en los sedimentos bajo las vulcanitas masivas.

La Unidad Inferior está constituida principalmente por vulcanitas submarinas de composición dacítica y andesítica que representan la masa principal del afloramiento volcánico de El Pimpollar y que pueden presentar estructuras masivas o brechoides.

En los niveles inferiores de la Unidad Superior se encuentran tobas y brechas volcanosedimentarias con gran proporción de componentes líticos y minerales de origen riolítico. También en estos niveles se encuentran ignimbritas y brechas soldadas riolíticas.

El cuerpo riolítico principal está compuesto por rocas porfídicas masivas y es el causante de la fuerte anomalía positiva de

K que se observa en la cartografía radiométrica del afloramiento de El Pimpollar.

Descripción petrográfica de los materiales volcánicos.

En la Unidad Inferior se encuentran vulcanitas cuyas composiciones varían entre andesitas y dacitas. Se trata de rocas que en la gran mayoría de los casos tienen texturas porfídicas, con fenocristales de plagioclasa y en menor proporción de clinopiroxeno, pudiendo aparecer también anfíbol y cuarzo en algunas muestras. Como minerales accesorios se encuentran: magnetita, circón, apatito y biotita.

Las rocas masivas tienen texturas porfídicas, con matriz microcristalina afieltrada o traquitoide, con orientación fluidal.

En los tipos brechoides, los clastos son angulosos y en la mayoría de los casos sus composiciones y texturas son muy semejantes a las de las vulcanitas masivas. La matriz tiene una composición que generalmente es similar a la de los clastos, con fragmentos angulosos de cristales, líticos y vidrios volcánicos, de tamaño muy variable. Estas rocas brechoides proceden de la fragmentación de domos y coladas submarinas durante su efusión.
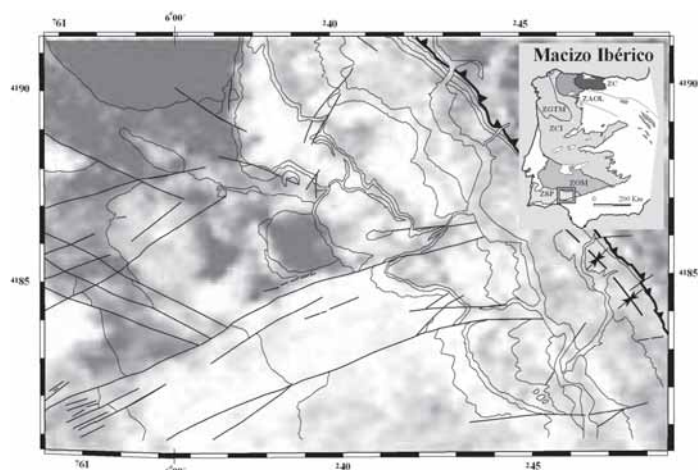
También se encuentran con carácter mucho más restringido rocas más básicas, de composición basáltica o traquiandesítica que pueden tener fenocristales de olivino, plagioclasa y clinopiroxeno en una matriz con textura subofítica-intersertal, formada por listones subidiomorfos de plagioclasa, con clinopiroxeno y vidrio intersticial. La mineralogía accesoria está compuesta esencialmente por opacos.

Estas rocas presentan un grado de alteración variable y están afectadas por carbonataciones, albitizaciones, cloritizaciones, y epidotizaciones que suelen afectar con mayor intensidad a los minerales ferromagnesianos, que con frecuencia están totalmente sustituidos por productos secundarios.

El tipo de vulcanitas ácidas más abundante en los afloramientos de El Pimpollar, son riolitas porfídicas masivas, que forman parte de un domo. Estas rocas tienen abundantes fenocristales de pequeño tamaño de cuarzo y de feldespato potásico (originalmente sanidina). Los fenocristales tienen hábitos idiomorfos, subredondeados o ameboides por efecto de la corrosión magmática, sobre todo los de cuarzo. También pueden encontrarse, en algunos casos, pequeños fenocristales de biotita cloritizada. Como minerales accesorios pueden encontrarse biotita, magnetita, circón, apatito y ocasionalmente fluorita.

En menor proporción, también se encuentran tobas y brechas riolíticas que en algunos casos tienen carácter ignimbrítico. Los componentes minerales fundamentales son feldespatos alcalinos y cuarzo, que pueden encontrarse como fragmentos muy angulosos o como cristales idiomorfos o afectados por la corrosión.

Una gran proporción de los componentes líticos de estas rocas está representada por pequeños fragmentos de vidrio muy angulosos ("shards") que se encuentran aplastados, soldados y desvitrificados,

constituyendo una matriz muy compacta en la que se aprecian en algunos casos flameados y microbandeados que pueden estar afectados por pliegues de flujo. En algunas muestras se encuentran fragmentos cuarzo-feldespáticos con texturas simplectíticas o micropegmatíticas que corresponden a rocas subvolcánicas.

Con carácter restringido se encuentran microbrechas y tobas riolíticas de origen volcanosedimentario, con clastos angulosos y subredondeados de líticos volcánicos (entre los que se encuentran a veces vidrios perlíticos) y clastos monominerales (cuarzo, plagioclasa y feldespato potásico), algunos clastos metamórficos (filitas, cuarcitas y pizarras). Estos clastos están empastados por una matriz detrítica de grano fino y de composición cuarzo-feldespática que presenta un cierto grado de recristalización y cementación hidrotermal.

Caracterización geoquímica de las vulcanitas de El Pimpollar.

Con el fin de establecer su caracterización geoquímica y su correlación con los materiales volcánicos de los sectores más occidentales de la Faja Pirítica Ibérica, se han realizado en los laboratorios del IGME 13 análisis químicos de roca total de las vulcanitas representativas del afloramiento de El Pimpollar.

Los elementos mayores se han determinado mediante fluorescencia de rayos X (XRF) sobre pastillas fundidas con tetraborato de litio. El Na y el Mg se han determinado por absorción atómica (AAS) tras fusión de las muestras con metaborato de litio. La pérdida al fuego se ha realizado por calcinación a 950ºC.

La mayoría de los elementos traza, se han determinado por XRF en pastilla prensada con el programa PROTRACE, mientras que el Y y las REE se han determinado por ICP-MS.

Las rocas analizadas tienen una variabilidad composicional que se extiende desde basaltos hasta riolitas, predominando las rocas dacíticas y andesíticas. En el diagrama de Winchester y Floid (1977. Fig. 2A), puede observarse la distribución de las muestras analizadas en este trabajo en los distintos campos composicionales definidos en el mismo. También se ha representado en este diagrama el campo de variación de las rocas volcánicas de la Faja.Pirítica Ibérica, con un sombreado gris. El extremo más básico está representado por basaltos, que son bastante escasos y que corresponde a coladas submarinas intercaladas entre las andesitas y dacitas. Estos basaltos son subsaturados en SiO_2 (Ne normativos) y tienen afinidad alcalina.

Dentro del grupo andesítico-dacítico, la roca más básica, es metalumínica y se proyecta en el campo alcalino, mientras que las más ácidas son peralumínicas y se proyectan en el campo subalcalino.

El extremo más ácido del conjunto volcánico estudiado corresponde a riolitas potásicas y peralumínicas. No obstante, se ha encontrado una riolita sódica (K_2O/Na_2O=0,38) que tiene un carácter peralumínico más débil que el resto de las riolitas estudiadas y se proyecta en el campo de las comenditas-pantelleritas (Fig. 2A).

Al comparar estos materiales con las vulcanitas de la Faja Pirítica Ibérica (Fig. 2A), se observa que la mayor parte de las rocas de El Pimpollar se proyectan dentro del campo de variación de esta región volcánica, aunque los materiales más básicos tienen un carácter más alcalino. También la riolita sódica se sitúa fuera del campo de variación normal de las vulcanitas de la FPI.

Los espectros de REE de las rocas dacítico-andesíticas y del basalto, normalizados a la composición condrítica (Fig. 2B), son relativamente similares. No obstante, los tipos más básicos presentan fraccionamientos más bajos, con relaciones La/Yb$_n$ medias del orden de 2,5 y carecen de anomalías negativas de Eu, mientras que las rocas dacíticas tienen fraccionamientos más elevados (La/Yb$_n$ H" 3,9) y pequeñas anomalías negativas de Eu. Estas últimas rocas tienen contenidos de LREE superiores a los de las vulcanitas básicas de la FPI.

La vulcanita basáltica de El Pimpollar, tiene unas relaciones Ba/Nb, Zr/Hf, Ti/Zr y K/Rb bastante diferentes a las medias de las vulcanitas básicas de la FPI y presenta algunas semejanzas con los basaltos de tipo E-MORB y OIB (Fig. 2E, Tabla I), si bien la relación Zr/Hf es muy superior y la relación K/Rb es bastante inferior en la vulcanita de El Pimpollar.

Las riolitas potásicas tienen unos espectros de REE normalizados al condrito muy homogéneos con fraccionamientos débiles de las LREE y prácticamente nulos de las HREE (Fig. 2C). Las relaciones medias La/Yb$_n$ son aproximadamente de 1,5 y tienen fuertes anomalías negativas de Eu con relaciones Eu/Eu*$_n$ de hasta 0,23. Al comparar los espectros de estas vulcanitas con los de las riolitas de la FPI se observa que sus contenidos de LREE son inferiores, mientras que los de HREE se encuentran dentro del campo de variación de aquellas. Estas riolitas tienen unas relaciones Ba/Nb, La/Nb, Th/U, La/Sm, La/Yb, P/Ce y K/Rb sensiblemente diferentes a las de las riolitas de la FPI (Fig. 2F, Tabla I), que en principio permiten pensar en la hipótesis de una génesis diferente para ambos grupos de riolitas.

La riolita sódica tiene mayores contenidos y un fraccionamiento más elevado de LREE que las riolitas potásicas, mientras que para las HREE, el fraccionamien-
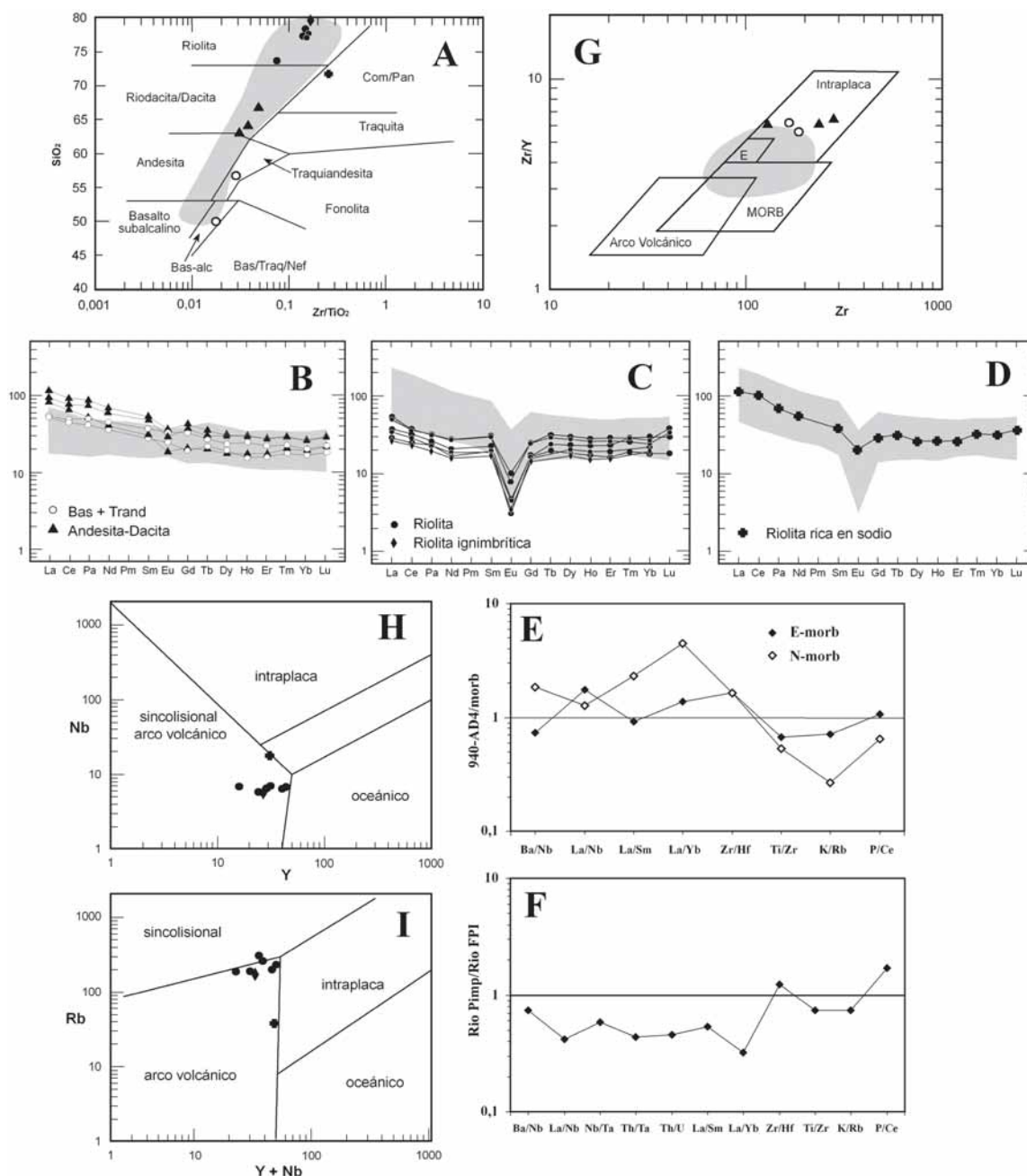
Fig. 2. A/ Proyección de las rocas volcánicas analizadas en el diagrama de Winchester y Floyd (1977). B, C, D/ Diagramas de REE de las rocas volcánicas de la Unidad Inferior (B); riolitas ricas en K (C); riolita rica en Na (D). (Normalizadas al condrito, Sun y McDonough, 1989). E/ Relaciones interelementales del basalto 940-AD-4. Normalizadas los basaltos E-MORB y N-MORB. F/ Relaciones interelementales de la media de las riolitas ricas en K normalizadas a la media de las riolitas de la FPI. G/ Proyección de las vulcanitas de la Unidad Inferior en el diagrama de caracterización tectónica de Pearce y Norry (1979). H, I/ Proyección de las riolitas de "El Pimpollar" (Unidad Superior), en los diagramas de caracterización tectónica de Pearce *et al.* (1984).

Fig. 2.- A/ Plot of the analyzed volcanic rocks in the Winchester & Floyd (1977) diagram. B, C, D/ REE diagrams of volcanic rocks of the Lower Unit (B); K rich rhyolites (C); Na rich rhyolite (D). (Chondrite normalized, Sun and McDonoug, 1989). E/ Element ratios of 940-AD-4 basalt. (E-MORB and N-MORB normalyzed). F/ Element ratios of the average K-rich rhyolites. (Average FPI rhyolites normalized). G/ Plot of the Lower Unit volcanic rocks of "El Pimpollar" in the tectonic discrimination diagram of Pearce and Norry (1979). H, I/ Plot of the "El Pimpollar" rhyolites (Upper Unit), in the tectonic discrimination diagram of Pearce et al. (1984).

	Pimpollar media de riolitas	Pimpollar riolita rica en Na	Pimpollar Basalto 940-AD4	Pimpollar Andesitas y dacitas
Ba/Nb	36,3	17,4	5,05	17,4-119,6
La/Nb	1,38	1,54	1,41	1,59-4,26
Nb/Ta	6,25	44,75	-	-
Th/Ta	6,21	27,75	-	-
Th/U	2,10	4,62	-	-
La/Sm	2,50	4,67	2,22	3,0-4,26
La/Yb	2,21	5,02	3,70	4,50-6,22
Zr/Hf	38,2	48,7	59,7	34,8-45,9
Ti/Zr	6,61	3,96	55,40	20,7-35,9
K/Rb	243	557	293	307-444
P/Ce	13,55	1,81	44,8	8,85-29,12

Tabla I.- Principales relaciones interelementales

Table I.- Main interelement ratios

to es prácticamente nulo y similar al de aquellas (Fig. 2D). Esta vulcanita tiene una anomalía negativa de Eu bastante débil y un contenido total de REE superior al de las riolitas potásicas de El Pimpollar, situándose su espectro dentro de los límites de variación de las riolitas de la FPI.

Esta roca tiene unas relaciones Ba/Nb, Th/U, La/Sm, La/Yb, Ti/Zr, P/Ce y K/Rb bastante diferentes de las de las riolitas potásicas de El Pimpollar, y estas mismas relaciones son también claramente diferentes de las medias de las riolitas de la FPI (Tabla I).

Las vulcanitas de la Unidad Inferior de El Pimpollar, se proyectan en el campo del magmatismo intraplaca en el diagrama Zr-Zr/Y de Pearce y Norry (1979. Fig. 2G). En este diagrama, el campo de variación de las vulcanitas básicas de la Faja Pirítica Ibérica tiene su centro de gravedad entre los campos de los basaltos MORB y los intraplaca. Las rocas más básicas de esta unidad se localizan en los límites del mismo y dentro del campo de intraplaca.

En el diagrama de caracterización geotectónica Y-Nb de Pearce *et al.* (1984. Fig. 2H), las riolitas de El Pimpollar se proyectan en el campo de las asociaciones magmáticas sin-colisionales o de arco volcánico, pudiéndose observar que la riolita sódica se separa del conjunto y tiende a situarse junto al límite de las asociaciones magmáticas intraplaca. Esta situación vuelve a repetirse en el diagrama Rb frente a Y+Nb de los mismos autores (Fig. 2I), apreciándose nuevamente que la riolita rica en Na se separa del conjunto, que se sitúa junto a la divisoria de los campos de los magmatismos intraplaca y sin-colisionales.

Discusión y conclusiones

El estudio de las vulcanitas de los afloramientos de El Pimpollar y de los materiales sedimentarios relacionados con ellos pone de manifiesto la existencia de dos episodios volcánicos principales, entre los que verosímilmente se ha producido un importante cambio en la tectónica regional que ha inducido profundos cambios en la cuenca sedimentaria y en la naturaleza del magmatismo.

Los materiales del primer evento volcánico (Unidad Inferior) son predominantemente de composición dacítico-andesítica con proporciones subordinadas de rocas basálticas o riolíticas y su efusión se ha producido en un medio submarino relativamente profundo en el que se registra sedimentación de rocas silíceas radiolaríticas.

Con posterioridad a la llegada a la cuenca de aportes de sedimentos clásticos muy gruesos, relacionables con "debris flows" que contienen clastos de calizas de edad Viseense Medio y gran cantidad de clastos de pizarras y metacuarcitas, se produce un evento volcánico riolítico (Unidad Superior), en cuyos tramos básales se encuentran depósitos volcano-sedimentarios e ignimbríticos que posiblemente se han formado en condiciones muy superficiales o localmente subaéreas.

Entre los materiales más básicos del primer episodio volcánico se encuentran basaltos que tienen afinidad alcalina y mayor relación La/Yb que los de la FPI. Estos basaltos tienen cierta semejanza con los basaltos de tipo E-MORB. Las rocas dacíticas y andesíticas tienen contenidos superiores de LREE y elevadas dispersiones en muchas de las relaciones interelementales más características (La/Nb, K/Rb, P/Ce).

El conjunto de materiales de este primer episodio volcánico presenta afinidades intraplaca de acuerdo con los criterios del diagrama de discriminación de Pearce y Norri (1979).

Las riolitas ricas en K del episodio volcánico superior presentan relaciones La/Nb inferiores a las de las basaltos, andesitas y dacitas de la Unidad Inferior, lo que en principio apoya la hipótesis de que su génesis es independiente de la evolución petrogenética del conjunto intermedio-básico de El Pimpollar. Estas riolitas potásicas presentan también bastantes diferencias con el quimismo de las riolitas de los sectores más occidentales de la FPI, tanto con respecto a los contenidos de LREE como a las relaciones entre los elementos incompatibles más característicos. Esta Unidad Superior riolítica es asignable a ambientes de arco volcánico o sin-colisionales según los diagramas de caracterización geotectónica por criterios geoquímicos de Pearce *et al* (1977).

La cronología de los episodios volcánicos de El Pimpollar, así como sus características petrológicas y geoquímicas permiten estimar que corresponden a unos eventos volcánicos que son tardíos y posiblemente independientes con respecto a la actividad magmática principal de la Faja Pirítica Ibérica. Los variaciones petrológicas y geoquímicas que se registran entre el episodio magmático inferior y el superior del afloramiento de El Pimpollar pueden estar relacionadas con una etapa de cambios importantes en el régimen tectónico y sedimentario.

Agradecimientos

Referencias

Eversen, N.M., Hamilton, P.J. y O'Nions (1978). *Geochimica et Cosmochimica Acta,* 42, 1199-1212

Martín Escorza, C. y Rivas Ponce, A. (1973). *Mapa Geológico de España 1:50.000, hoja nº940 (Castilblanco de los Arroyos).* IGME.

Lotze, F. (1945). *Geotektonische Forschungen*, 6, 78-92 (Traducido en: *Publicaciones Extranjeras de Geología de España*, 5, 149-166).

Pearce, J.A., Harris, N.B.W. y Tindle, A.G. (1984). *Journal of Petrology*, 25, 956-983.

Pearce, J.A. y Norry, M.J. (1979). *Contributions to Mineralogy and Petrology*, 69, 33-47.

Simancas, F. (1983). *Geología de la extremidad oriental de la Zona Sudportuguesa*. Tesis Doctoral, Univ. de Granada, 439 p. (Inédita).

Sun, S.S. y McDonough, W.F. (1989). En: *Magmatism in ocean basins*. (A.D. Saunders y M.I. Norry, Eds.). Geological Society of London Special Publication, 42, 429-448.

Taylor, S.R. y McLennan, S.M. (1985). *The Continental Crust: its Composition and evolution*. Blackwell, Oxford, 312p.

Winchester, J.A. y Floyd, P.A. (1977). *Chemical Geology*, 20, 325-343.

Geology and lithogeochemistry of the unique Las Cruces VMS deposit, Iberian Pyrite Belt.

C. Conde & F. Tornos
Instituto Geológico y Minero de España, Azafranal 48, 37002 Salamanca, Spain.

M. Doyle
Cobre Las Cruces, Gerena, Sevilla, Spain

ABSTRACT: The Las Cruces deposit is a unique example of supergene enriched massive sulphide deposit in the Iberian Pyrite Belt (IPB). This massive sulphide, is the most easterly in the IPB hosted in shales and fine grain volcanoclastic rocks within the lower Volcano-Sedimentary (VS) Complex. Detailed lithostratigraphic study identifies four units. The footwall comprises a dacitic dome interbedded with sandstone and shale, at the bottom, where the primary mineralization is developed. The hanging wall is formed of three main units, consisting of a complex sequence of volcanoclastic breccias and sandstone, alternating with siltstone and shale, including a pumice-rich breccia. The chemostratigraphic results show a composition between rhyodacite and basalt-andesite with a calc-alkaline affinity. There is no significant geochemical difference within the entire sequence suggesting a unique magmatic pulse. Lastly, the geochemical analysis of the hosted shale suggests local anoxic conditions prevailed during massive sulphide formation.

KEYWORDS: Las Cruces, VHMS, IPB, lithogeochemistry, supergene, gossan, massive sulphide

1 INTRODUCTION

Las Cruces mine hosts the southeasternmost massive sulphide deposit of the IPB. It is the only deposit located within the Guadalquivir Cenozoic basin and is covered by a thick sequence of Neogene marls. The orebody occurs as lenses within the lower part of Volcanic-Sedimentary Complex (VS Complex) (Conde *et al* 2003), the late Devonian-early Carboniferous sequence that hosts all the massive sulphide deposits of the IPB.

The deposit was discovered in 1994 by Riomin Exploraciones S.A. (a subsidiary company of Río Tinto) after a geophysical campaign in the extension of the IPB below Cenozoic sediments. INMET Mining Corporation is currently the owner of the project and the mine is expected to produce the first concentrates in late 2007. The main feature of the Las Cruces deposit is the presence of a pristine zone of supergene alteration that caps the massive sulphides. In all the other deposits of the IPB, supergene enrichment zones have been systematically eroded and/or mined. Supergene enrichment makes Las Cruces one of the richest copper deposits worldwide. The estimated total pre-mining reserves are 30.2 Mt @ 1.15% Cu,

1.19% Pb, 3.51% Zn, 21g/t Ag and 0.3g/t Au for the primary massive sulphides, 16 Mt @ 6.9% Cu, 0.25% Zn and 0.76%Pb for the supergene cementation zone and 1.7 Mt @ 115 g/t Ag and 4.3 g/t Au for the gossan.

Previous work has dealt with a detailed study of mineralization (Knight 2000) or else focused on the mining project (Doyle *et al* 1998, Norris 2001). In this abstract we present the first conclusions of an ongoing study of the geology and geochemistry of the deposit. The work deals with the stratigraphy and the geochemistry of the host sequence and the results are based on the detailed logging of 12 drill-holes, a petrographic study, and the analysis of representative samples of the host rocks, including both volcanic and sedimentary rocks.

2 GEOLOGICAL SETTING

The primary mineralization of the Las Cruces massive sulphide deposit has a lensoidal morphology, dipping of 45° to the N (Doyle *et al* 1998). Mineralization is hosted by shale and fine grain volcanoclastic rocks of the lower VS Complex. Detailed study of the host sequence shows that it occupies the same stratigraphic position of nearby deposits of Aznalcóllar and

Los Frailes (Conde *et al* 2003). In this area, the VS Complex is formed of massive volcanic rocks (domes and sills), volcanoclastic breccia and arenite, interbedded with shale and chemical sediments (chert and jasper). Felsic volcanic rocks dominate (dacite and rhyolite) but andesitic and basaltic-andesitic flows and sills are also present in the stratigraphic sequence.

3 LITHOSTRATIGRAPHY OF THE LAS CRUCES DEPOSIT

The host rocks of the deposit can be grouped into four main units (Fig. 1).

The footwall (>300m) consists of a porphyritic dacite dome with associated hyaloclastite and hydrothermal breccias along the margins. These rocks grade upwards into crystal-rich sandstone and dark shale, the latter hosting the primary mineralization (Fig. 1). Rocks beneath the massive sulphides have been affected by a pervasive but highly irregular hydrothermal alteration, consisting of chloritization, sericitization and silicification. The more altered rocks host a mineralized stockwork similar to that found in other deposits of the IPB.

The hanging wall consists of a complex sequence (450-600m) of felsic and intermediate volcanic rocks, including lava, debris flow and pumice-rich breccia alternating with siltstone and shale, which dominate the upper part of the sequence. In the hanging wall, three units can be distinguished. The basal unit, capping the massive sulphides, includes dark shale alternating with epiclastic argillite and arenite. The intermediate unit is a thick package made up of heterogeneous breccias and rich-crystal sandstone (debris flow); here there is a single layer containing pumice rich fragments that has been traced over the whole area (Conde e*t al.* 2003). The uppermost part of the hanging wall is composed of shale and felsic volcanoclastic rocks. A characteristic unit of massive dacite that could either is flow or a sill locally caps these rocks. The hanging wall units show a weak to moderate hydrothermal alteration (chloritization, sericitization, silification, and carbonatization).In the area around Las Cruces these Palaeozoic rocks are capped by about 150m of Neogene conglomerate, sand and marl (Fig. 1).

Both U-Pb isotopic (Barrie *et al* 2002) and palynological (Oliveira *et al* 2004) dates of the host rocks at Las Cruces show that the massive sulphides formed during the late Strunian (late Devonian) and contemporaneously with most
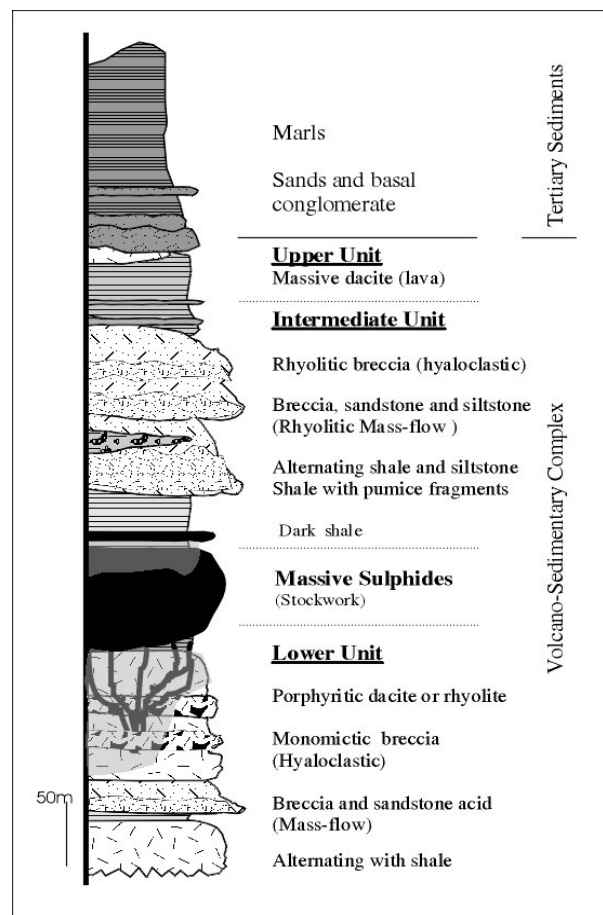
Fig. 1. Summary lithologic column of the Las Cruces ore deposit.

of the shale-hosted massive sulphide deposits of the southern IPB (Tornos 2006).

In detail, the massive sulphides occurs as stratiform massive and semi-massive sulphides, an irregular copper-rich stockwork, and a zone of supergene alteration including both a cementation zone and an overlying gossan (Knight 2000). The primary massive sulphides are very similar to those found in other deposits of the IPB. They are dominated by fine grained, massive to banded, pyrite with local enrichments in sphalerite, chalcopyrite and galena. These massive sulphides show local sedimentary structures such as parallel lamination, as well as a characteristic layer near the footwall and made up of syn-sedimentary breccias with fragments of massive sulphide, shale, chert and jasper. Furthermore, there are evidences of stratiform sulphates being replaced by pyrite (Tornos 2006). All these features indicate that the primary mineralization was exhalative onto the seafloor, probably within a third order anoxic basin.

The secondary mineralization occurs as veins and breccias at the top of the massive sul-

phides and has produced a systematic enrichment in copper and depletion in zinc. The mineralogy of the secondary zone includes chalcocite, covellite, bornite, and enargite.

4 LITHOGEOCHEMICAL

48 samples (25 volcanic rocks and 23 shale) from drillcore were analysed by XRF and ICP techniques for major and trace elements. The shale was also analyzed for total organic carbon and sulphur.

Since many of the rocks show a pervasive alteration, discrimination between lithological groups has been predominantly based on elements traditionally regarded as immobile (Al_2O_3, TiO_2 and Zr) (MacLean & Barret, 1993; Barret & MacLean, 1999) .

The volcanic rocks have been plotted in the standard discriminating diagram SiO_2 vs. Zr/TiO_2. They range in composition between rhyodacite and basalt-andesite without major gaps (Fig 2). The magmatic affinity has been tracked using the La-Yb diagram of Barret & MacLean (1999). La and Yb contents of 7-30 ppm and 1-3 ppm, respectively, define a calc-alkaline trend. The TiO_2% vs. Zr and Nb/Zr ratios identifies only one group of volcanic rocks with no major differences, suggesting that all the sequence is derived from a unique magmatic pulse with no dramatic chemical changes.
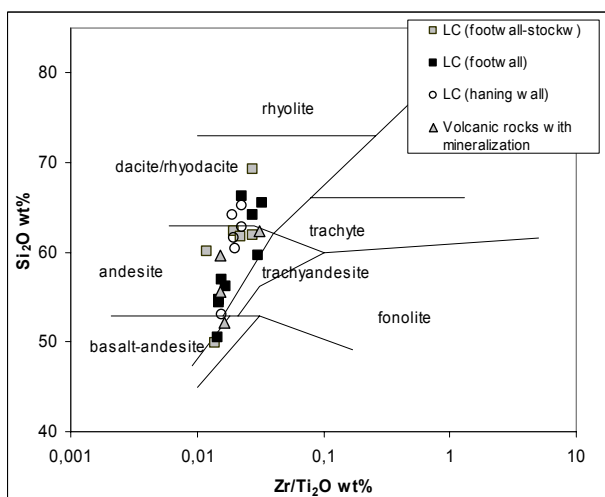
Fig.2. SiO_2 vs. Zr/TiO_2 discrimination diagram for the volcanic rocks in Las Cruces deposit (Wincherter & Floyd 1977)

The chondrite-normalized REE spidergram for felsic and intermediate rocks show similar patterns for all REE except for Eu. The intermediate rocks show either no Eu anomaly or else a positive one whilst the dacite and rhyolite-dacite patterns have no a clear negative Eu
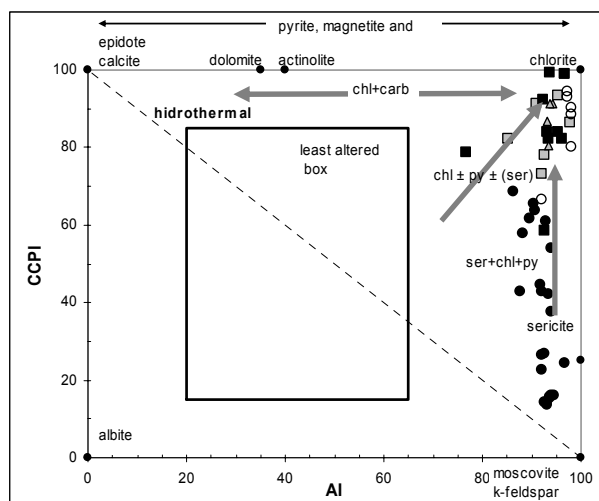
Fig.3. Alteration box plot showing volcanic rocks and shale (filled circles). (AI, Ishikawa alteration index; CCPI, chlorite-carbonite-pyrite index)

anomaly. This may indicate difference in the plagioclase composition. However, this is not reflected in the other REE. This observation, together with the equivalent spidergram for the felsic and mafic rocks, suggests that these rocks have been significantly altered rather than having magmatic sources (Mitjavila *et al* 1997).

The degree of hydrothermal alteration can be assessed using the alteration box plot of Large *et al* (2001). The data confirm that both the footwall and the hanging wall are affected by hydrothermal processes but only the footwall rocks plot into the chl ± py ± (ser) field (Fig 3).

As indicated above, shale is a rather significant component of the whole sequence and the immediate host rock to the orebody. Mineralized shale is enriched in elements typically present in anoxic settings (*e.g.* V, Cr, Mo and W). The Mn-Fe-V and V/(V+Ni) rates show that this hosted shale are plotted in the anoxic field (0.73-0.89 avg. V/V+Ni). However, the redox conditions change in the barren shale above the massive sulphides where sub-oxic to oxic conditions are established. These different features confirming the evidence found in other massive sulphide deposits of the IPB that the mineralization is related to local anoxic conditions (Tornos *et al* 2003).

5 DISCUSSION AND CONCLUSION

The detailed geological and geochemical studies of the host sequence of Las Cruces massive sulphide deposit show that both the ore horizon and the environment of formation were the same as for neighbouring Aznalcóllar and Los Frailes deposits. The host unit is a complex

volcanosedimentary sequence composed of coherent dacite to andesite with associated hyaloclastite, interbedded with volcanoclastic sandstone, siltstone and thick shale units. The lithogeochemical results show that all the volcanic rocks belong to a single sequence showing no major chemical change. The geochemistry also suggests that shale which hosts the primary massive sulphides was deposited in an anoxic setting.

ACKNOWLEDGEMENTS

REFERENCES

Conde C, Tornos F, Fernández J, Doyle M (2003) Encuadre estratigráfico de los sulfuros masivos de la parte suroriental de la Faja Pirítica: Aznalcóllar-Los Frailes, y Las Cruces. *Bol. Soc. Mineralogía*, 26-A: 161-162.

Barret TJ, MacLean WH (1999) Volcanic sequences, lithogeochemistry and hydrothermal alteration in some bimodal volcanic-associated massive sulphide systems. *Reviews in Economic Geology*, 8: 101-131.

Barrie CR, Amelin Y, Pascual E (2002) U-Pb geochronology of VMS mineralization in the Iberian Pyrite Belt. *Mineralium Deposita* 37: 684-703

Doyle M, Moissey C, Sharp G, (1998) Discovery of the Las Cruces massive sulphide deposit, Andalucia, Spain. *Pathways'98 Extended Abstracts. Society of Economic Geologist, Denver:* 108-110.

Knight FC (2000) The mineralogy, geochemistry and genesis of the secondary sulphide mineralization the Las Cruces deposit, Spain. *PhD. University of Wales, Cardiff.*

Large RR, Gemmell JB, Paulick H, Huston DL (2001) The alteration box plot: A simple approach to understanding the relationship between alteration mineralogy and lithogeochemistry associated with volcanic-hosted massive sulphide deposit. *Economic Geology* 96: 957-971.

Mac Lean WH, Barret TJ (1990) Lithogeochemical techniques using immobile elements. *J Geochem Explor* 48: 109-133.

Mitjavila J, Martí J, Soriano C (1997) Magmatic evolution and tectonic setting of the Iberian Pyrite Belt volcanism. *Journal of Petrology,* 38: 727-755.

Oliveira JT, Pereira Z, Carvalho P, Pacheco N, Korn D (2004) Stratigraphy of the tectonically imbricated lithological succession of the Neves Corvo mine area, Iberian Pyrite Belt, Portugal. *Mineralium Deposita* 39: 422-436.

Tornos F, Conde C, Solomon M. Spiro B (2003) Effects of oxic/anoxic seafloor on the formation and preservation of shale-hosted massive sulphides, Iberian Pyrite Belt. In: Eliopoulos et al. (eds) *Mineral exploration and sustainable development.* Millpress, Rotterdam, pp 191-194.

Tornos F (2006) Enviroment of formation and styles of volcanogenic massive sulphides: Iberian Pyrite Belt. *Ore Geology Reviews,* 28: 259-307.

Wincherter JA, Floyd PA (1977) Geochemical discrimination of different magma series and their differentiation products using immobile elements. *Chemical Geology*, 20: 325-343.

Caracterización geológica de los afloramientos de El Pimpollar, extremo nororiental de la Zona Surportuguesa

Geological characterization of "El Pimpollar" colcanic and sedimentary rocks, northeastern sector of the South-Portuguese Zone, Spain

A. Díez Montes [1], **F. Bellido** [1], **P. Cózar** [2] **y V. Monteserín** [3]

[1] Instituto Geológico y Minero de España, C/ La Calera, 28760-Tres Cantos, Madrid. f.bellido@igme.es
[2] Instituto de Geología Económica CSIC-UCM, UEI y Departamento Paleontología, Facultad de Ciencias Geológicas, C/ José Antonio Novais, nº 2, 28040-Madrid. pcozar@geo.ucm.es
[3] Instituto Geológico y Minero de España, C/ Ríos Rosas, 28020-Madrid. v.monteserin@igme.es

ABSTRACT

Two volcanic units can be distinguished in the "El Pimpollar" outcrop (eastern South-Portuguese Zone). The Lower Unit is composed mainly of submarine dacites and andesites, with some subordinated basalts and trachyandesites. The Upper Unit is composed of massive rhyolites, with volcano-sedimentary and volcanoclastic deposits towards the base.
Radiolaritic sediments interbeded with the andesites and dacites show that these volcanic rocks extruded in a relatively deep marine basin.
The upper part and top of the Lower Volcanit Unit includes some diamictic layers related with mass-transport processes. Some of these diamictic layers contain limestone pebbles and blocks with middle Visean microfossils. These sedimentary deposits mark possibly the beginning of a tectonic event that was responsible for the destruction of a carbonate platform, and for severe changes in the tecto-sedimentary environment.

Key words: *South-Portuguese Zone, volcanism, El Pimpollar, middle-Visean*

Introducción

La Zona Surportuguesa (ZSP, Lotze, 1945) constituye el extremo meridional del Macizo Ibérico y en ella afloran principalmente materiales cuya edad se extiende desde el Devónico Medio al Carbonífero Superior. En su mitad norte se encuentra la Faja Pirítica Ibérica (FPI), constituida por secuencias volcánicas y series volcano-sedimentarias, a las que se asocian importantes depósitos de sulfuros masivos que constituyen una de las mayores provincias metalogenéticas del mundo. En su extremo nororiental se encuentran los afloramientos volcánicos de El Pimpollar (Fig. 1), que son el objeto de estudio de este trabajo.

Inicialmente, estos materiales se habían correlacionado con las vulcanitas pérmicas de la Cuenca del Viar (Martín Escorza y Rivas Ponce, 1973), aunque posteriormente Simancas (1983) los estudia con más detalle y les relaciona con el vulcanismo de la FPI, asignándoles una edad Viseense Superior según criterios paleontológicos.

El límite oriental del afloramiento de El Pimpollar está constituido por los sedimentos detríticos de la Cuenca del Viar, a los que Simancas (1983) atribuye una edad Autuniense (Pérmico Inferior) y para los que Díez Montes *et al.* (1997) establecen dos megasecuencias.

El borde S está definido por una falla normal con componente de desgarre que tiene una dirección aproximada N 70ºE y que pone en contacto los materiales de la Cuenca de El Pimpollar con las rocas plutónicas del Batolito de la Sierra Norte.

Características litoestratigráficas y descripción de los materiales

El afloramiento de El Pimpollar se localiza en el sector NE de la Hoja de Castilblanco de los Arroyos y está constituido fundamentalmente por rocas volcánicas andesítico-dacíticas, a techo de las que se encuentran diversas intercalaciones de sedimentos detríticos, sin continuidad aparente. Sobre este conjunto volcánico y sedimentario se encuentra un domo riolítico que en su base tiene algunos lentejones poco importantes de depósitos volcanoclásticos y volcanosedimentarios de composición riolítica. Estos materiales volcánicos se encuentran en aparente conformidad (Díez Montes *et al.*, 1997) sobre una su-

cesión de pizarras y areniscas atribuidas al grupo devónico P-Q.

Los niveles sedimentarios situados inmediatamente bajo las vulcanitas en el borde occidental del afloramiento de El Pimpollar están representados principalmente por una sucesión de lutitas verdosas con intercalaciones de areniscas, que pueden constituir alternancias rítmicas. En algunos niveles se encuentran capas de areniscas desmembradas y también en algunos casos aparecen incluidos en los sedimentos, cantos y bloques de vulcanitas andesíticas que pueden alcanzar tamaños superiores a 1 m.

En el borde suroriental del afloramiento, que está determinado por una falla normal, con dirección aproximada N 70ºE, también pueden observarse los sedimentos infrayacentes a las vulcanitas. En esta zona, se encuentra un conjunto de pizarras grises con algunos niveles morados y alternancias pizarroso-limolítico-arenosas, afectadas por la intrusión de algunos sills de vulcanitas félsicas con las que presentan contactos peperíticos. En alguna de las brechas peperíticas se encuentran radiolarios junto con componentes sedimentarios y volcanoclásticos. De forma discontinua

se han observado lentejones de pizarras negras.

Sobre los materiales anteriores se encuentran vulcanitas submarinas de composición intermedia que constituyen la Unidad Inferior del afloramiento volcánico de El Pimpollar. Las rocas predominantes en este conjunto son andesitas y dacitas de color gris verdoso oscuro, porfídicas, con matriz afanítica y con abundantes fenocristales de plagioclasa de tamaños milimétricos y fenocristales de minerales ferromagnesianos en menor proporción. Estas vulcanitas pueden presentar estructuras masivas o brechoides y pertenecen a domos o coladas submarinas que están afectadas por brechificaciones hidroclásticas en sus zonas externas. Las variedades brechoides tienen con frecuencia un aspecto bastante masivo, pero la observación en detalle pone de manifiesto que están constituidas por abundantes fragmentos angulosos de andesitas porfídicas, empastados por una matriz fragmentaria de composición muy similar (Fig. 2A). En la mayoría de los casos estas brechas son de carácter monomíctico, pero en algunos casos se encuentran fragmentos volcánicos que pueden ser de distinta procedencia.

Entre las vulcanitas brechoides pueden encontrarse intercalaciones de sedimentos que en general son de escasa potencia y continuidad lateral. Las más importantes y significativas se encuentran en los tramos superiores del conjunto volcánico andesítico-dacítico y una de ellas está constituida por una serie de capas diamictíticas que tienen una potencia conjunta de unos 3-4 m y contiene abundantes cantos y bloques de calizas bioclásticas (Fig. 2B).

Por encima de estas diamictitas se encuentra una capa de roca silícea radiolarítica de color negro, de unos 50 cm de potencia (Fig. 2C), y sobre ella aparecen nuevamente vulcanitas porfídicas andesítico-dacíticas, entre las que se intercala un nivel de diamictitas en el que se encuentran algunos bloques angulosos de calizas que pueden alcanzar tamaños próximos a 1m y que contienen restos de crinoides.

A escasos metros por encima de estas intercalaciones sedimentarias, se encuentran una serie de depósitos caóticos de diamictitas, con abundantes clastos de rocas metamórficas (pizarras y metacuarcitas principalmente) y con proporciones variables de clastos de vulcanitas. La matriz de estas diamictitas es de naturaleza microbrechoide o pelítica, de color verdoso-amarillento y está esquistosada, siendo la proporción entre matriz y clastos bastante variable.

En posición estratigráfica equivalente, también se encuentran diversos lentejones y capas de escasa continuidad lateral de sedimentos detríticos más finos, representados por alternancias rítmicas de lutitas, limolitas y areniscas grises y negruzcas con laminaciones paralelas, y niveles de grauvacas y tobas volcanosedimentarias que marcan el techo de la unidad volcánica dacítico-andesítica y la base de la unidad riolítica de El Pimpollar.

En otras zonas de los afloramientos volcánicos inferiores, se han localizado algunas pequeñas intercalaciones de sedimentos, que posiblemente están situados a distintos niveles. Así, por ejemplo, en el extremo noroccidental, en el collado del Risco del Blanquillo, se encuentra una sucesión de espesor métrico constituida por lutitas negras con restos vegetales, silexitas, y lutitas blancas de aspecto cinerítico.

Los niveles inferiores asociados a la unidad volcánica riolítica, se encuentran con frecuencia sobre las diamictitas o sobre sedimentos pelítico-arenosos y están representados por tobas y brechas volcanosedimentarias de color blanquecino-grisáceo, con gran proporción de componentes líticos y minerales de origen riolítico. También, en relación con estos afloramientos se encuentra algún nivel de tobas soldadas y de ignimbritas de composición riolítica.

El cuerpo riolítico principal tiene un afloramiento de forma subcircular con un diámetro próximo a 1,5 km y constituye el resalte topográfico de la Sierra Bajosa. Los materiales que lo forman, son bastante homogéneos y corresponden fundamentalmente a riolitas porfídicas masivas, de colores grises verdosos o rosáceos claros, en las que localmente se observan bandeados que pueden estar afectados por pliegues de flujo.

Estas riolitas tienen pequeños y abundantes fenocristales (1-4 mm) de feldespatos y de cuarzo y una matriz afanítica muy abundante. Con frecuencia presentan disyunción o lajeado grosero en capas subparalelas de 10 a 50 cm de potencia. Este afloramiento riolítico corresponde, a un domo que se apoya sobre
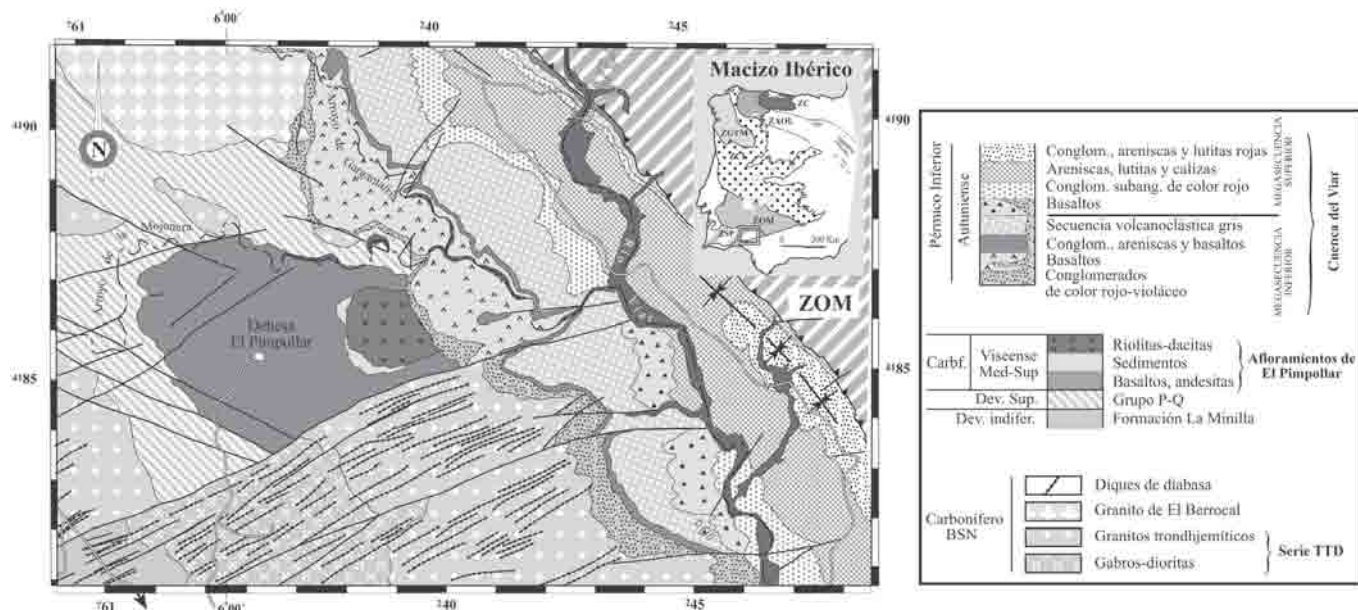

Fig. 1.- Mapa geológico de la zona de "El Pimpollar".

Fig. 1.- Geologic map of "El Pimpollar" zone.

un pequeño espesor de materiales volcanosedimentarios y volcanoclásticos que pueden asociarse a los primeros estadios eruptivos de la Unidad Superior. Este domo riolítico es el responsable de la importante anomalía positiva en K que se pone de manifiesto en la cartografía radiométrica del afloramiento de El Pimpollar.

También se encuentran algunos afloramientos riolíticos dispersos en la masa principal de vulcanitas andesíticas de El Pimpollar, entre los que el más importante corresponde a un pequeño pitón situado a aproximadamente a 1,5 km al N de las casas del cortijo de El Pimpollar. Este afloramiento forma un resalte de sección subcircular constituido por riolitas masivas de color verdoso, que están constituidas por una masa soldada de fragmentos de cristales y de vidrio con textura de tipo "shard" y que puede corresponder a un conducto de salida de materiales riolíticos "proto-ignimbríticos" (Fig. 2D).

En el extremo occidental del afloramiento de vulcanitas de la Unidad Inferior, se han observado localmente argilificaciones, oxidaciones y movilizaciones de óxidos de hierro y silicificaciones que podrían estar relacionadas con la emersión pérmica.

Datos paleontológicos

Simancas (1983) considera que los materiales volcánicos de El Pimpollar son concordantes con los materiales infrayacentes, que corresponderían al Grupo P-Q. Este autor encuentra un nivel inferior de rocas carbonatadas que está constituido por "grainstone bioclásticos", que está intercalado entre secuencias HCS en el techo del Grupo P-Q, y otros niveles superiores intercalados entre las vulcanitas andesítico-dacíticas, que corresponderían a parches pararrecifales.

El estudio del contenido faunístico permite atribuir a estos niveles calcáreos una edad Viseense Superior, aunque Simancas (1983) no detalla de qué niveles proceden los fósiles datados, entre los que se encuentran taxones devónicos y carboníferos.

Teniendo en cuenta estas observaciones, los carbonatos de El Pimpollar podrían corresponder a dos episodios bien diferenciados. Los de edades devónicas corresponderían a niveles carbonatados situados en el techo de la secuencia del P-Q, y los de edades viseenses a las intercalaciones en las vulcanitas.

Las muestras que se han estudiado en este trabajo pertenecen a los depósitos diamictíticos con clastos calcáreos que se
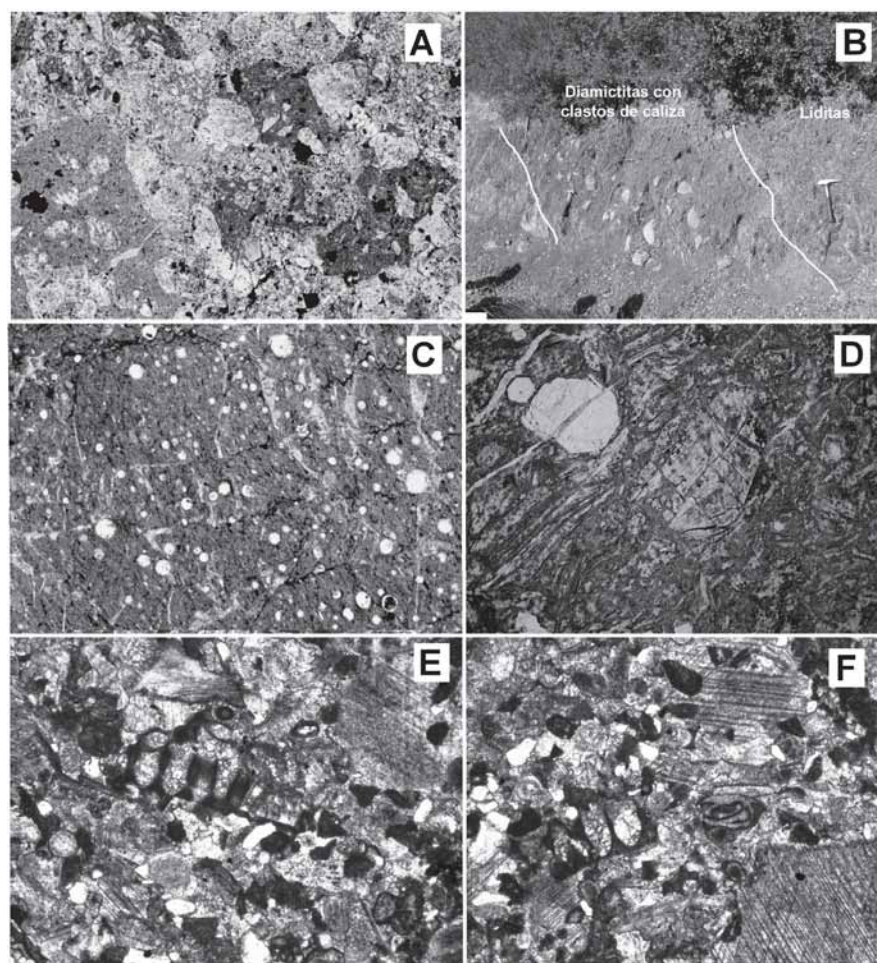
Fig. 2.- A) Aspecto textural de la matriz de una brecha andesítica de la Unidad Inferior (NP x 2,5). B) Afloramiento de diamictitas con clastos de calizas. Capa de radiolaritas negras en el lado derecho de la fotografía. C) Aspecto microscópico de las radiolaritas del afloramiento representado en la figura 2B (NP x 10). D) Riolita ignimbrítica. Cristales idiomorfos de cuarzo y de feldespato potásico en una matriz compuesta por "shards" soldados y desvitrificados. (NP x 5). E, F) Aspecto microscópico de clastos de calcarenitas bioclásticas procedentes de las diamictitas del afloramiento representado en la figura 2B. Se observan restos de crinoides, *Koninckopora tenuiramosa*, *Endothyra* sp. y *Archaeodiscus* sp. (estado involuto).

Fig. 2.- A) Textural aspect of the matrix of an andesitic breccia of the Lower Unit (PPL x 2,5). B) Outcrop of diamictites with limestone clasts. A black radiolarite layer appears in the righ side of the picture. C) Microscopic view of the radiolarites shown in figura 2B (PPL x 10). D) Ignimbritic Rhyolite. Idiomorphic quartz and K-feldspar crystals in a devitrified welded shards matrix (PPL x 5). E, F) Microscopic aspect of a limestone clast of the diamictites shown in the Fig 2B. Crinoids fragments, **Koninckopora tenuiramosa,** *Endothyra sp. and* **Archaeodiscus** *sp. (involutus stage) can be observed (PPL x 10).*

encuentran a techo del nivel andesítico-dacítico (Fig. 2E y 2F). Los foraminíferos que se han identificado son: Forchiinae, *Pseudoammodiscus volgensis*, *Endothyra* spp., *Uralodiscus* sp., Lituotubellinae (indet.), *Eoparastaffella* sp., *Mediocris mediocris*, *Viseidiscus* sp., *Earlandia* sp.(aff. *E. Elegans*) y *Globoendothryra* sp. Todos estos foraminíferos muestran una dispersión entre el Viseense Inferior y medio, aunque pudiendo alcanzar alguno de ellos el Viseense Superior. No obstante, los foraminíferos más significativos que se ha encontrado pertenecen al género *Archaediscus*, del que se han en-

contrado muchos ejemplares, tanto en estado "*involutus*" como "*concavus*". Este último estado se alcanza en niveles equivalente al Viseense Medio.

Las algas que se han encontrado son: *Koninckopora tenuiramosa* y *Koninckopora inflata*, ambas con la pared bilaminar, que corresponden al Viseense. Además, en la matriz se puede observar la presencia de abundantes palaeoberesélidos, en concreto *Kamaenella tenuis*, cuyo acme comienza a partir del Viseense Medio.

Por lo tanto, los datos paleontológicos obtenidos en este trabajo, permiten asig-

nar con alto grado de certeza una edad Viseense Medio a los clastos calcáreos de las diamictitas intercaladas en los tramos superiores de las vulcanitas andesítico-dacíticas de "El Pimpollar".

Discusión y conclusiones

La secuencia de procesos geológicos registrados por los materiales volcánicos y sedimentarios de los afloramientos de "El Pimpollar" pone de manifiesto la implantación de un vulcanismo submarino en una cuenca con sedimentación siliciclástica fina pelítico-arenosa.

Los materiales volcánicos de la Unidad Inferior están constituidos fundamentalmente por un conjunto de andesitas y dacitas, masivas o brechoides, que corresponden a domos y coladas submarinas afectados por fragmentación debido a su extrusión subacuática. Este conjunto es bastante monótono y masivo, y únicamente se encuentran en él escasas y poco importantes intercalaciones de sedimentos, sin continuidad lateral.

Esta relativa homogeneidad, y la ausencia de estructuración estratoide y de superficies importantes de discontinuidad, es debida posiblemente a que los procesos eruptivos que han generado este conjunto volcánico se han producido en un intervalo de tiempo relativamente corto.

Así mismo, la existencia de sedimentos silíceos de origen orgánico (radiolaritas y pizarras silíceas con radiolarios) a muro y a techo de estas vulcanitas, pone de manifiesto que los procesos sedimentarios y volcánicos referidos, se han producido en un ambiente marino relativamente profundo.

En los tramos terminales del conjunto andesítico-dacítico se encuentran una serie de intercalaciones diamictíticas que corresponden a aportes masivos de sedimentos muy heterométricos y que marcan un importante cambio en las condiciones tectónicas del entorno regional. La presencia de cantos y bloques de calizas bioclásticas en estos niveles diamictíticos profundos, se debe a la desestabilización y destrucción de una plataforma carbonatada de edad Viseense Medio, cuya situación geográfica se desconoce.

El aporte de estos sedimentos diamictíticos a la cuenca, marca posiblemente el comienzo de un proceso de crisis tectónica y somerización de la cuenca, que se corresponde con el fin del episodio de vulcanismo andesítico-dacítico de "El Pimpollar". En los niveles diamictíticos superiores no se encuentran clastos carbonatados, siendo casi exclusivamente los componentes gruesos de origen metamórfico (pizarras y metacuarcitas).

La unidad andesítico-dacítica tiene una edad post-Viseense Medio, evidenciada por los datos paleontológicos procedentes de los depósitos clásticos intercalados en sus tramos superiores, que marcan el fin de este vulcanismo y el comienzo de una etapa de crisis tectónica.

Sobre este conjunto sedimentario, cuya potencia es poco importante, se encuentran una serie de depósitos de tobas y brechas riolíticas volcanosedimentarias y volcaniclásticas (alguno de carácter ignimbrítico) que se han formado en un ámbito poco profundo y posiblemente con zonas emergidas. Estos materiales se encuentran en la base de un domo formado por riolitas porfídicas masivas que constituye la Unidad Superior del afloramiento volcánico de "El Pimpollar".

Estos eventos volcánicos son claramente posteriores a la actividad volcánica principal de la Faja Pirítica Ibérica.

En el extremo occidental del afloramiento volcánico de "El Pimpollar" se han observado localmente alteraciones sobre las vulcanitas de la Unidad Inferior que podrían estar relacionadas con la emersión pérmica.

Agradecimientos

Referencias

Díez Montes, A., Leyva Cabello, F., Matas González, J. y Muñoz del Real, J.L. (1997). *Revisión y actualización del Mapa Geológico de España 1:50.000, hoja nº 940 (Castilblanco de los Arroyos)*. IGME, inédito.

Lotze, F. (1945). *Geotektonische Forschungen*, 6, 78-92 (Trad. en: *Publicaciones Extranjeras de Geología de España*, 5, 149-166).

Martín Escorza, C. y Rivas Ponce, A. (1973). *Mapa Geológico de España 1:50.000, hoja nº 940 (Castilblanco de los Arroyos)*. IGME.

Simancas, F. (1983). *Geología de la extremidad oriental de la Zona Sudportuguesa*. Tesis Doctoral. Univ. de Granada, 439 p. (Inédita).

Geología y estructura de la Mina de Río Tinto (Faja Pirítica Ibérica, España)

Geology and structure of Rio Tinto Mine (Iberian Pyrite Belt, Spain)

D. Mellado [1], E. González Clavijo [1,2], F. Tornos [1] y C. Conde [1].

[1] Instituto Geológico y Minero de España. Oficina de Proyectos de Salamanca. C/ Azafranal 48. 37001 Salamanca.
[2] Dirección actual: INETI, Departamento de Geología, Ap. 7586, 2720-866, Amadora, Portugal.
d.mellado@igme.es; emilio.clavijo@ineti.pt; f.tornos@igme.es; c.conde@igme.es.

ABSTRACT:

The Rio Tinto mining district is regarded as the largest volcanogenic massive sulphide district worldwide, but its geologic and structural setting remains poorly disclosed. The mineralized sequence includes a lower unit of interbedded mafic volcanics, shale and conglomerate overlain by a felsic dome-sill complex. The massive sulphides occur within the felsic rocks, either as exhalative deposits on the top or as replacive masses within the volcaniclastic rocks.
The present review has a special aim on structural geology bearing up a genetic model update for the ore. Regional thin-skinned tectonic was clearly identified as the leading Variscan structural style in the district. Several stocked units bounded by thrust-faults display normal polarity on structural and sedimentary criteria basis. Reconstruction of the palaeogeography prior to the tectonic stacking reveals a very extensive mineralizing system.

Key words: Río Tinto, Massive Sulphide, Iberian Pyrite Belt, South-Portuguese Zone.

Introducción

El distrito minero de Río Tinto es uno de los ocho depósitos gigantes de sulfuros masivos de la Faja Pirítica Ibérica y quizás la mayor concentración de sulfuros masivos en la corteza terrestre, con más de 400 Mt de sulfuros masivos y unos 2000 Mt de stockwork de baja ley. Se ha explotado interrumpidamente desde siglo VIII a.c. hasta la actualidad, marcando un importante hito en la historia de la minería mundial.

A pesar de su importancia histórica y minera, existen pocos trabajos recientes dedicados a la interpretación de su geología, estructura y metalogenia (e.g., Williams, 1934; Rambaud, 1969; García Palomero, 1980; Boulter, 1993; Tornos, 2005). En este trabajo se presentan los primeros resultados de un estudio geológico y estructural del distrito minero, comparando los resultados con otros trabajos de carácter más regional (e.g., Silva *et al.,* 1990; Quesada, 1998; Onézime *et al.*, 2002).

Encuadre geológico

La Zona Sud-Portuguesa (ZSP) es la unidad más meridional, en las coordenadas actuales, del segmento Ibérico del Macizo Varisco (Fig. 1). Se trata de un terreno exótico acrecionado al autóctono ibérico como un cinturón de pliegues y cabalgamientos de vergencia suroeste (Silva *et al.*, 1990; Quesada, 1998) y con un grado metamórfico bajo. La Faja Pirítica Ibérica, su unidad más septentrional, es una banda de más de 250 Km de largo y 75 Km de anchura máxima, donde se han localizado más de 80 yacimientos de sulfuros masivos y más de 300 de manganeso.

Desde un punto de vista estratigráfico, la Faja Pirítica presenta rocas sedimentarias e ígneas de edad Devónico Superior–Carbonífero. Se pueden diferenciar tres unidades litoestratigráficas, que de muro a techo, son el Grupo de Filitas y Cuarcitas (Grupo PQ), el Complejo Volcano-Sedimentario (CVS) y el Grupo Culm (Schermerhorn, 1971). En este periodo los ambientes evolucionan desde una plataforma estable (Grupo PQ) hasta una cuenca antepaís sinorogénica, con la deposición del flysch (Grupo Culm) en un surco que se desplaza hacia el sur siguiendo el avance de la orogenia Varisca (Silva *et al*., 1990; Quesada, 1998). El desarrollo de cuencas de tipo *pull-apart* durante las etapas más tempranas de la colisión oblicua facilitó el ascenso de un vulcanismo predominantemente dacítico con proporciones más accesorias de basalto, riolita y andesita a unas subcuencas, con depósitos pizarrosos y de rocas químicas, como jaspe y sulfuros masivos.

Las estructuras de deformación presentes en la Faja Pirítica tradicionalmente se han agrupado en tres fases principales de deformación (Quesada, 1998; Onezime *et al.*, 2002; Soriano *et al.*, 2002). En una primera fase, se generan pliegues vergentes al sur asociados a cabalgamientos, que son sincrónicos con el metamorfismo. Las estructuras de segunda fase son las predominantes en la Faja Pirítica y consisten en pliegues y cabalgamientos vergentes al sur, subparalelos a los de primera fase. La interferencia con los pliegues D_1 homoaxiales, produce lineaciones de intersección de dirección E-O. La tercera fase se caracteriza por la presencia de un despegue que desplaza los materiales sinorogénicos hacia el sur, disponiéndolos sobre la unidad de cabalgamientos que imbrican al Grupo PQ y al CVS.

Litoestratigrafía del área de Río Tinto

Las unidades estratigráficas definidas en el área de Río Tinto corresponden a materiales del Complejo Vulcano-Sedimentario y Grupo Culm, no habiéndose observado los materiales del grupo PQ. La secuencia litológica simplificada se muestra en la figura 2. Los criterios tectónicos y sedimentarios observados en las distintas unidades indican siempre una polaridad normal de las mismas.
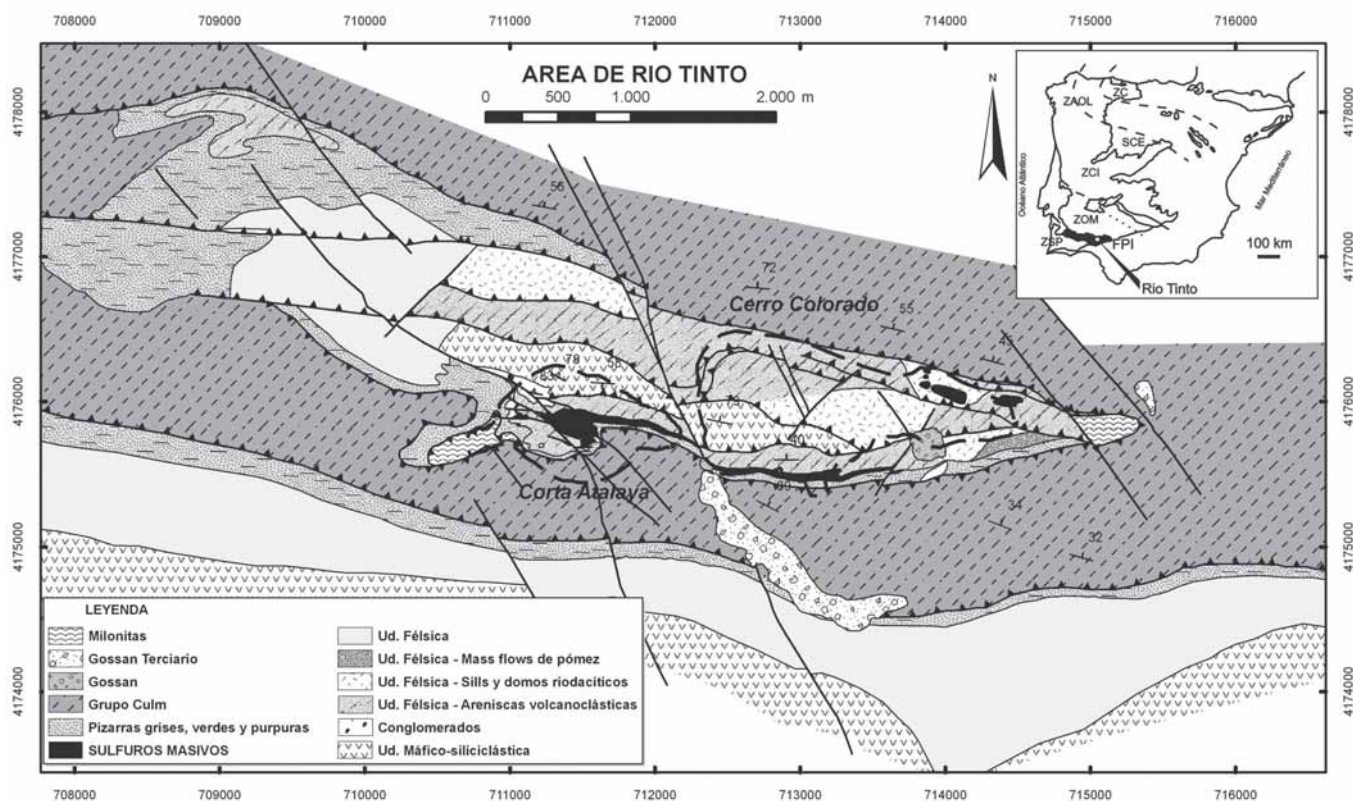
Fig. 1.- Mapa geológico del área de Río Tinto.

Fig. 1.- Geologic map of Río Tinto area.

En la base de la columna estratigráfica aparece una Unidad Máfico-siliciclástica, formada por intercalaciones de pizarra y basalto, éste último constituido por coladas con *pillow lavas* locales. También se distinguen dos tipos de rocas intrusivas, diques y *sills* subvolcánicos máficos, con desarrollo de estructuras peperíticas en sus contactos (Boulter, 1993) y en algunos casos, metamorfismo de contacto. En la parte superior de esta unidad dominan las areniscas volcanoclásticas de derivación básica. Esta unidad aflora en una banda continua de dirección este-oeste en el Antiforme de Cerro Colorado (Fig. 1) (García Palomero, 1980) y es similar a la que se encuentra en la parte sur del gran Sinforme de Río Tinto, concordante sobre el Grupo PQ. Geoquímicamente las rocas volcánicas tienen composiciones basalto-andesíticas. Boulter *et al.* (2004) encuentran una diferencia geoquímica entre las rocas volcanoclásticas máficas y los cuerpos masivos, basándose en los análisis de los elementos traza (Ti/Nb). Hacia el techo de esta unidad, aumenta la proporción de rocas sedimentarias, apareciendo en Corta Atalaya un nivel de conglomerado pizarroso (García Palomero, 1980) matriz-soportado, con cantos dominantes de pizarra y, en menor medida, de rocas volcánicas félsicas y máficas. Dentro de él hay concentraciones locales de sulfuros que

reemplazan preferentemente a algunos clastos de naturaleza variable. La granulometría, forma y disposición de los cantos del conglomerado parece indicar un transporte mínimo.

Sobre la unidad descrita aparece una Unidad Félsica, generalmente separada de la anterior por estructuras tectónicas, aunque localmente se han observado contactos intrusivos de las facies masivas. Está formada por una sucesión muy homogénea de rocas volcánicas de composición dacítica a riodacítica. Aunque suelen mostrar una intensa alteración hidrotermal que ha borrado muchas de las estructuras, es posible diferenciar rocas volcanoclásticas poco estructuradas acumuladas probablemente por procesos de *mass flow* y equivalentes a hialoclastitas transportadas. Tienen cristales y fragmentos de cuarzo y plagioclasa en una matriz de grano fino. También se han reconocido (cripto-) domos de rocas masivas e hialoclastitas y diques subvolcánicos de la misma composición; en conjunto, la Unidad Félsica parece corresponder a un complejo de domos submarinos intruidos o interestratificados en depósitos pizarrosos. Los contactos de las rocas masivas con las rocas sedimentarias suelen mostrar un borde vítreo y contactos peperíticos. Esta Unidad es químicamente muy homogénea, con una distribu-

ción similar de elementos traza (TiO_2/Al_2O_3 o Zr/Al_2O_3, entre otros) indicando un origen volcánico común.

Sobre el techo de la Unidad Félsica aparece de manera concordante la mineralización. Los sulfuros masivos aparecen como un lentejón (Filón Sur) formado por pirita con cantidades accesorias de calcopirita, esfalerita, galena y trazas de otros sulfuros. La mayor parte de los sulfuros están recristalizados y no se reconocen estructuras primarias. Sólo localmente es posible observar un bandeado sedimentario y venas zonadas relacionadas con las zonas de alimentación. Estos sulfuros masivos se han interpretado como exhalativos y acumulados en una subcuenca anóxica sobre una zona de exhalación de carácter difuso (Solomon *et al.*, 2002; Tornos, 2005).

La unidad sedimentaria superior, denominada Serie de Transición por García Palomero (1980) está formada por pizarras grises con intercalaciones de cinerita félsica y algunas intercalaciones de sedimentos químicos (jaspe). Se sitúa en el mismo nivel estratigráfico que los sulfuros masivos pudiéndose observar las interdigitaciones entre ambas unidades litológicas. En varias zonas de Cerro Colorado y Corta Atalaya las pizarras presentan zonas irregulares de color morado y verde intenso y en las que la coloración no sigue la estratificación.

Fig. 2.- Columna litoestratigráfica general del área de Río Tinto.

Fig. 2.- Litho-stratigrahic general sequence in Río Tinto mine.

La unidad más alta de la zona es el Grupo Culm, que constituye el flysch sinorogénico varisco, en este sector de edad Viseense. Es una serie monótona de pizarra silícea y carbonosa, con tramos donde aparece la secuencia típica de flysch con alternancias de bandas centimétricas de pizarra y grauvaca (García Palomero, 1980; Oliveira, 1983). Siempre presenta un despegue basal que los separa del resto de la secuencia infrayacente, desarrollando una banda de filonita negra que oscila entre 18 y 25 m de anchura.

Las dataciones absolutas y palinológicas indican que la pizarra situada a techo de la Unidad Máfico-siliciclástica se depositó durante el límite Devónico-Carbonífero (Rodríguez *et al.*, 2002). Esta pizarra es, por lo tanto, la encajante de los sulfuros masivos que afloran en la parte meridional de la Faja Pirítica (e.g., González *et al.*, 2002) pero que aquí no presenta mineralización. La Unidad Félsica ha sido datada por el método del U/Pb en 349,76 ± 0,90 Ma. (Barrie *et al.*, 2002) o 347,5 ± 1,5 Ma. (Dunning *et al.*, 2002). Por lo tanto, la pizarra suprayacente es de edad probable Tournaisiense Medio y los sulfuros masivos de Filón Sur ocupan una posición estratigráfica superior al resto de las mineralizaciones equivalentes de la Faja Pirítica.

Las rocas infrayacentes a los sulfuros masivos muestran una alteración hidrotermal generalizada, aflorando las rocas alteradas en la mayor parte del núcleo del antiforme de Cerro Colorado sobre una superficie de unos 8 km² (García Palomero, 1980; Costa, 1996). Las rocas félsicas muestran una intensa sericitización que borra muchas de las estructuras primarias. En las zonas cercanas a fallas o cerca de los sulfuros masivos esta alteración sericítica es reemplazada por una alteración clorítica (+pirita+cuarzo) posterior o por una alteración de cuarzo+pirita aún más interna. Tanto el basalto como la pizarra están reemplazados exclusivamente por una alteración clorítica. Todas estas rocas muestran abundantes sulfuros, bien diseminados, bien formando un *stockwork* que se interpreta como la zona de alimentación de los sulfuros masivos suprayacentes. Este *stockwork* está formado por venillas anastomosadas de sulfuros, fundamentalmente pirita, con cuarzo y algo de clorita. Localmente, tiene contenidos económicos de cobre. Dentro de las rocas félsicas y en zonas localizadas de intensa alteración hidrotermal el stockwork pasa gradualmente a sulfuros semimasivos ricos en esfalerita y calcopirita (masas de Filón Norte, Salomón o Lago). Son rocas de grano grueso, con abundante cuarzo, sericita y clorita intersticiales que se interpretan como producto del reemplazamiento casi total de las rocas volcánicas por sulfuros (Tornos, 2005).

En la zona de la Mesa y al este de la estructura de Río Tinto, existen depósitos sedimentarios de *gossan* transportado por procesos fluviales formados por una estructura de bandas superpuestas de óxi-dos e hidróxidos de hierro con cantos polimícticos incluidos.

Estructura

Estructuralmente, existen dos unidades principales en la mina de Río Tinto. La superior está constituida por los materiales del Grupo Culm, que siempre presentan una estructura de despegue en su base. Bajo este despegue existe un apilamiento de escamas tectónicas imbricadas y vergentes al Sur; cada una de estas escamas presenta en su interior cabalgamientos menores acompañados de pliegues menores también vergentes al Sur. La superficie de despegue que separa las dos unidades tectónicas principales está plegada, igualmente con vergencia al Sur (Fig. 3), formando un antiforme en la zona de Cerro Colorado y el correspondiente sinforme en Corta Atalaya (Fig. 1). Este último proceso de plegamiento ha reaplastado las estructuras anteriores de la unidad imbricada inferior.

Las estructuras de cabalgamiento de la unidad inferior presentan una dirección predominante N100ºE con un buzamiento hacia el norte, concordante con un acortamiento aproximadamente N-S y una propagación de la deformación hacia el sur. En un sector próximo, Soriano (1997) clasifica los cabalgamientos como correspondientes a dos fases sucesivas de deformación, debido a la presencia de cabalgamientos plegados. Localmente hemos observado cabalgamientos menores plegados y cortados por otros cabalgamientos fuera de secuencia dentro de la unidad inferior, pero consideramos que todas estas estructuras se formaron en un proceso compresivo continuo con desarrollo de
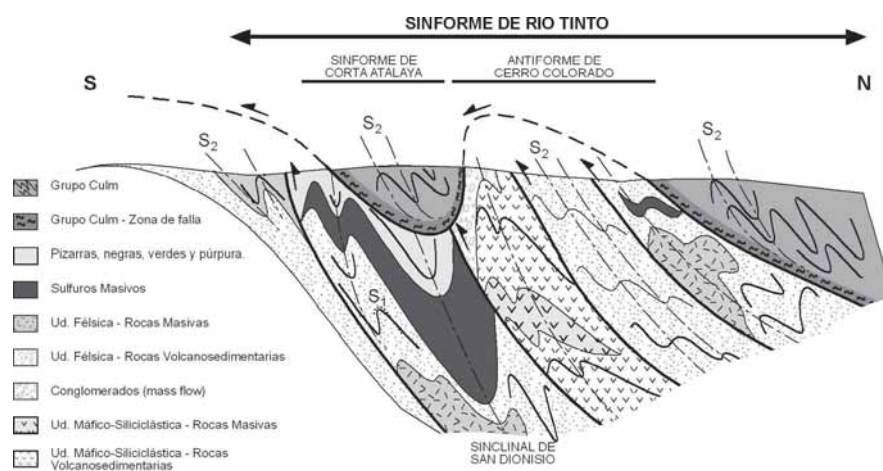

Fig. 3.- Esquema geológico de la estructura de Río Tinto.

Fig. 3.- Cross-section showing structural geology scheme in Río Tinto.

las complejidades típicas de este tipo de tectónica. Los pliegues están asociados a la propagación de estos cabalgamientos y la foliación tectónica principal es paralela al plano axial de los pliegues y ligeramente menos tendida que los cabalgamientos asociados. Esta foliación tiene una disposición predominante N 100° E/60° N y ha sido denominada S_2 debido a la presencia, en algunas charnelas de pliegues menores, de otra foliación tectónica previa, casi paralela a S_0 y crenulada por S_2, por lo que ha sido llamada S_1. Esta primera foliación tectónica debe de corresponder a los primeros eventos del mismo proceso compresivo general y por ello sólo ha quedado preservada en algunas zonas de charnela, siendo imposible identificarla en los flancos, donde ha sido totalmente obliterada por S_2 que tiene en general una orientación paralela.

La foliación tectónica principal (S_2) puede describirse como un clivaje pizarroso bien desarrollado en las rocas sedimentarias y vulcanoclásticas de grano fino; y como un clivaje grosero y anastomosante en las rocas masivas o que previamente habían sufrido alteraciones cloríticas intensas. A escala microscópica se define por la orientación de minerales planares y la orientación de minerales de hábito prismático.

Asociada a las estructuras de cabalgamiento, y posiblemente relacionada con el movimiento de las mismas, aparece una foliación tectónica S_3, que presenta una orientación media N 105°E/60° S, Crenula a la foliación principal y no es tan penetrativa ni continua como S_2. Se dispone paralela al plano axial de trenes de pliegues menores de geometría muy abierta.

De manera más aislada aparecen bandas de pocos metros de anchura con desarrollo de estructuras de tipo kink de planos axiales sub-verticales y dirección N-S.

La principal familia de fracturas presenta una dirección N150-170°E, y su familia conjugada N50-70°E. Ambas tienen una cinemática inversa con cierta componente de desgarre, siendo dextras predominantemente la primera familia y senestras las pertenecientes a la segunda familia, movimientos congruentes con un acortamiento en dirección Norte-Sur. Si bien se observa que estas fallas desplazan a todas las estructuras antes descritas, según Quesada (1998), corresponden probablemente a antiguas estructuras extensionales reactivadas durante la compresión varisca y vueltas a reactivar durante el ciclo Alpino .

Conclusiones

La mina de Río Tinto está situada dentro de una amplia estructura, con materiales del Grupo Culm en su núcleo, tradicionalmente denominada Sinforme de Río Tinto. Dentro de ella existe un domo antiformal elongado que permite el afloramiento de los materiales infrayacentes del CVS, incluyendo los grandes cuerpos de sulfuros masivos y el *stockwork* asociado. La cartografía estructural de este domo revela una importante complejidad, con dos unidades principales separadas por una importante estructura de despegue tectónico que está plegada con vergencia al Sur. Los pliegues principales que forma este despegue son el Antiforme de Cerro Colorado y el Sinforme de Corta Atalaya, visibles en las cortas mineras homónimas. La unidad inferior está constituida por materiales del CVS apilados en un sistema de unidades tectónicamente imbricadas vergentes al Sur, que incluyen la mineralización; estas unidades presentan en su interior pliegues, siendo uno de ellos el apretado sinclinal que forma la masa minera San Dionisio. La unidad superior contiene únicamente materiales del Grupo Culm y tiene un carácter alóctono con origen en un surco sinorogénico situado más al Norte en el momento de su depósito (Viseense).

El CVS de la Unidad Máfico-siliciclástica está formado por una serie alternante de pizarra, coladas de basalto y niveles volcanoclásticos máficos que, localmente y hacia su techo, tiene un nivel de conglomerados. Sobre ella se encuentra una Unidad Félsica que corresponde a un complejo de domo de composición dacítica-riodacítica y *sills* asociados dentro de una cuenca sedimentaria restringida, sobre el que se dispone una unidad de pizarra con exhalitas. Los sulfuros masivos se encuentran tanto en el contacto entre las rocas volcánicas félsicas con la pizarra suprayacente como reemplazando a las primeras.

La reconstrucción paleogeográfica de la cuenca donde se desarrolló el vulcanismo y la mineralización indicaría un sistema mineralizante muy extenso, del que apenas se han preservado los sulfuros masivos en algunas de las unidades tectónicas imbricadas.

Agradecimientos

Referencias

Barrie, C. T. , Amelin, Y. y Pascual, E. (2002). *Mineralium Deposita*, 37, 684-703.

Boulter, C.A. (1993). Geology, 21, 801-804.

Boulter, C.A., Hopkinson, L.J., Ineson, M.G. y Brockwell, J.S. (2004). *Journal Geological Society of London, 161, 103-115*.

Costa, I.M.S.R., (1996). *Efeitos mineralógicos e geoquímicos da alteração mineralizante em rochas vulcânicas félsicas de Rio Tinto (Faixa Piritosa Ibérica, Espanha)*. Dissertação de Mestrado. Univ. de Lisboa, 198 pp.

Dunning, G.R., Díez Montes, A., Matas, J., Martín Parra, L.M., Almarza, J. y Donaire, M., (2002). *Geogaceta*, 32, 127-130.

García Palomero, F. (1980). *Caracteres geológicos y relaciones morfológicas y genéticas de los yacimientos del anticlinal de Rio Tinto*. Instituto de Estudios Onubenses «Padre Marchena». Excma. Diputación de Huelva. 262 pp.

Gonzalez, F., Moreno, C., Saez, R. y Clayton, J. (2002). *Journal Geological Society of London*, 159, 229-232.

Oliveira, J.T. (1983). *Memorias Servicios Geologicos Portugal*, 29, 3-37.

Onézime, J., Charvet, J., Faure, M., Chauvet, M. y Panis, D. (2002). *Journal Structural Geology*, 24, 451-468.

Quesada, C. (1998). *Mineralium Deposita*, 33, 31-44.

Rambaud, F. (1969), *El sinclinal carbonífero de Riotinto (Huelva) y sus mineralizaciones asociadas*. IGME, 299 p.

Rodríguez, R.M., Díez, A., Leyva, F., Matas, J., Almarza, J. y Donaire, M. (2002). Geogaceta, 32, 247-250

Silva, J.B., Oliveira, J.T. y Ribeiro, A. (1990). En: *Pre-Mesozoic Geology of Iberia.* (Dallmeyer y Martínez García Eds.). Spriger Verlag, 348-362.

Solomon, M., Walshe, J.L. y García Palomero, F. (1980). *Transactions-Institution of Mining and Metallurgy. Section B. Applied Earth Science*, 89; 16-24.

Soriano, C. (1997). *Vulcanisme I estructura de la Faja Pirítica Ibérica. Zona Sud-Portuguesa*. Tesis Doctoral, Univ. de Barcelona, 265 pp.

Soriano, C. y Casas, J.M. (2002). *Geological Society of America. Special Paper* 364, 183-197.

Tornos, F. (2005). *Ore Geology Reviews, 28, 259-307*.

Williams, D. (1934). *Transactions Institution Mining Metallurgy, 43, b593-b678*.

REPLY

Javier Sánchez-España · Francisco Velasco
Adrian Joseph Boyce · Fernando Tornos

Reply to the comments by Marignac and Cathelineau on the paper by Sánchez-España et al.: Source and evolution of ore-forming hydrothermal fluids in the northern Iberian Pyrite Belt massive sulphide deposits (SW Spain): evidence from fluid inclusions and stable isotopes (Mineralium Deposita 38: 519–537)

We acknowledge the interest and criticism of Marignac and Cathelineau on our paper on the Iberian Pyrite Belt (IPB) ore-forming fluids, which presented new fluid inclusion and stable isotope data from several deposits (Aguas Teñidas Este, Concepción, San Miguel, San Telmo, Cueva de la Mora) and drew some conclusions about the origin and evolution of these fluids. The discussion of Marignac and Cathelineau affords a welcome opportunity for further discussion on the character of the fluid inclusions (FIs) and origin of the fluids and helps to clarify the relationships, often controversial, between deformation and volcano-sedimentary mineralization in the IPB.

Marignac and Cathelineau question the applicability of our FI and stable isotope data to the main ore forming event of the IPB, postulating that an extended recrystallization (with formation of new minerals) and a pervasive late to post-kinematic fluid percolation geo-

J. Sánchez-España (✉)
Instituto Geológico y Minero de España (IGME),
Rios Rosas, 23, 28003 Madrid, Spain
E-mail: j.sanchez@igme.es

F. Velasco
Dpto. Mineralogía y Petrología, Universidad del País Vasco,
Apdo. 644, Bilbao, Spain
E-mail: nppverof@lg.ehu.es

A. J. Boyce
Scottish Universities Environmental Research Centre,
Scottish Enterprise Technology Park,
G75 0QF East Kilbride, Scotland, UK
E-mail: a.boyce@suerc.gla.ac.uk

F. Tornos
Instituto Geológico y Minero de España (IGME),
C/Azafranal, 48, 1° A, 37001 Salamanca, Spain
E-mail: f.tornos@igme.es

chemically modified the stockworks during Variscan tectono-thermal events. Consequently, they preclude the possibility of the survival of pristine fluids trapped in quartz crystals during the Lower Tournaisian to Middle Visean mineralization processes. Further, they cast doubt upon the primary character of the stable isotope signatures obtained for the stockwork minerals, suggesting these phases would have been re-equilibrated through isotopic exchange during post-kinematic hydrothermal fluid circulation, and/or overprinted by a pervasive post-kinematic mineral formation. Whilst we see merit in their arguments, especially as related to their own research areas, we strongly disagree with their position on our data and interpretation.

The first point to address is that the observations of Marignac and Cathelineau are mainly based on the work of Marignac et al. (2003) on the Tharsis stockwork, with additional information from La Zarza (B. Diagana, unpublished data). The study of Marignac et al. (2003) was carried out on a limited number of samples taken from drillcore in only some of the more gold-enriched and deformed areas of the IPB. For example, at La Zarza and Tharsis, footwall and hanging walls of the massive sulphides are strongly sheared (see for example plate IIID, p. 10 in Leistel et al. 1998, and Fig. 4A-C, p. 154 in Tornos et al. 1998). Obviously, the deformation in these rocks is much more intense than that shown in the stockwork systems of other deposits such as Rio Tinto, San Miguel or Concepción (e.g. plates IIIC-F, p. 10 in Leistel et al. 1998, or Fig. 4A-B, p. 1270 in Sánchez-España et al. 2000). At Tharsis, the existence of several shear bands within the stockwork had already been highlighted by Tornos et al. (1998). In fact, quartz in this stockwork is always related to the Variscan deformation and does not appear to be coeval with the massive sulphides. Thus, it is not surprising that the fluid inclusions never record syn-exhalative hydro-

thermal activity. We therefore consider that using samples taken in strongly deformed rocks and then extrapolating conclusions based on the study of these minerals to all the IPB is not prudent.

Secondly, Marignac and Cathelineau use only two quoted works (Marshall and Spry 2000; Marshall et al. 2000) in support of their arguments on the broader level. These works usually deal with a much higher grade of metamorphism than we see in the IPB, and therefore any extrapolation must be made with caution.

Nonetheless, we do agree with Marignac and Cathelineau that Variscan tectonic events have played a more significant role in the present-day occurrence and configuration of some massive sulphides than has been traditionally considered. This has been observed in deposits of the IPB such as Aguas Teñidas Este (Hidalgo et al. 2001) where distinctive fluids have been observed between the mineralizing and remobilizing stages (G. S. McKee, unpublished data). Notwithstanding, the assumption of a complete obliteration and re-equilibration of the ore-related stockwork minerals by a late to post-metamorphic fluid percolation and new mineral growth, if properly demonstrated, would have profound theoretical consequences, as it would obviously invalidate any contribution to our understanding of IPB ore genesis which involved fluid inclusion and stable isotope studies. We do not believe this to be the case; instead, we view the work of Marignac and Cathelineau as having a very local applicability. From their own observations on Tharsis and La Zarza, and additional data from Nehlig et al. (1998) on the Corta Atalaya stockwork, and from Moura et al. (1997a, b) on Neves-Corvo, they extrapolate their conclusions to the whole IPB, a vast area that comprises more than 80 deposits with considerably different degrees of deformation and structural settings. Moreover, Tornos et al. (1998) and Quesada (1998) have demonstrated in both the Filón Norte (Tharsis) and La Zarza deposits, that complex thrust systems have developed during intense thin-skinned tectonics, strongly localizing deformation. This fact weakens Marignac and Cathelineau's conclusions, as they apparently overlook other mineralizations within these deposits which show much less deformation and overprinting of the pristine textures and primary mineralogy, similar to some deposits included in our work (e.g. San Miguel, San Telmo).

Consequently, we are in strong disagreement with Marignac and Cathelineau's conclusions, and reaffirm the main ideas exposed in our work. Specifically:

1. that selected fluid inclusions really do record the pristine fluids trapped during ore deposition and,
2. that stockwork quartz, chlorite, and sulphides were not systematically re-equilibrated with Variscan fluids, and that consequently, stable isotopes do provide relevant information about ore genesis.

Further, we consider that the idea of a pervasive Variscan fluid percolation through the ore bodies, with total obliteration of the original mineralogy and stable isotope signatures, is an oversimplification of the complex reality of the IPB regional geology.

Below we discuss briefly several relevant aspects proposed by Marignac and Cathelineau as compelling evidence for a generalized superimposition of the Variscan events to the hydrothermal ore-forming stages.

Was the Variscan deformation homogeneous across the whole IPB?

For many years now, a considerable number of authors have proposed a metamorphic SW–NE trend in the IPB, mainly based on petrological arguments (Schermerhorn 1971, 1975; Lécolle 1977; Routhier et al. 1980; Ribeiro and Silva 1983; Munhá 1983; 1990). More recently, the Variscan deformation in the IPB has been interpreted to be channelized along shear zones in which local strain would have been considerably higher than in other areas (Quesada 1998; Tornos et al. 1998). In fact, Tornos et al. (1998) state in their study on the Tharsis deposit (p. 161) that "...*the effect of the Variscan deformation is largely heterogeneous and the tectonic modifications are mostly concentrated along discontinuous, usually metric, deformation bands where phyllonites coexist with strained sulphides*". In fact, sedimentary and diagenetic textures are relatively well-preserved outside these strongly channelized deformation bands (see Fig. 4F-H, p. 154 in Tornos et al. 1998, or Fig. 3A, p. 9 in Velasco et al. 1998). Also, the different rheologic behaviour of the deformed materials in the ore deposits, has allowed the brittle minerals (such as pyrite or quartz) to remain less intensely brecciated and/or deformed than in other areas, as the deformation at the micro-scale was mainly absorbed by the ductile sulphides (sph, cpy, gal). Hence, it is more probable to find little strained quartz containing pristine FIs in the Zn–Pb–Cu-rich facies and/or deposits situated outside the main deformation bands (e.g. San Miguel, San Telmo, Aguas Teñidas Este), than in more pyritic deposits close to or within shear zones (such as Tharsis or La Zarza).

For example, in San Miguel, an in situ and beautifully exposed stockwork underlies the massive mineralization and crosscuts the footwall rhyolite (e.g. plate IIIF, p. 10 in Leistel et al. 1998; Fig. 4A, p. 1270 in Sánchez-España et al. 2000). Here it is possible to distinguish the network of hydrothermal py-chl-qtz veins from the late to post-tectonic, barren quartz veins. Quartz grains from the stockwork veins of this deposit that were selected for FI measurements presented textures that clearly suggested a hydrothermal origin affected by some degree of recrystallization/deformation. This deformation, however, was not so intense as to provoke the implosion of all pristine FIs. On the other hand, this quartz showed a statistically higher density of FIs, and a larger number of isolated and more saline FI than late to post-metamorphic quartz, which usually showed a milky aspect and much less FI presence.

Did all pristine, ore-related fluid inclusions really implode during the Variscan deformation?

Fluid inclusion studies in metamorphosed deposits are always subject to the particular interpretation of the author(s) about critical aspects such as the textural relations between different mineral and/or vein generations. In our study, we recognized the controversial origin of some of our FIs (specially those of type IV), as they showed temperatures and salinities similar to those described by Wipfler and Sedler (1995) for late to post-tectonic quartz veins in the IPB.

The assumption of Marignac and Cathelineau seems to be that Sanchez España et al. (2003) have indiscriminately measured all the FIs taken from inevitably highly deformed rocks. However, the study was based on carefully selected samples and, furthermore, on FIs that did not show any evidence of implosion, leakage or later modification. In fact, the actual results support a primary origin for all of them.

Contrary to Marignac and Cathelineau's ideas, but in agreement with previous FI studies performed in the area (e.g. Bobrowicz 1995; Almodovar et al. 1998; Nehlig et al. 1998), we do believe that the great majority of FIs studied by our group are primary in origin. This assertion is based upon many detailed and careful microscopic examinations of several hundred thin sections and polished blocks from the ore mineralizations, stockwork systems and footwall volcanic rocks of 11 deposits from the northernmost part of the IPB (Sánchez-España 2000). These studies revealed a paragenetic sequence with several stages of crystalline growth for ore sulphides and silicates (including quartz, chlorite, sericite and carbonates) during the hydrothermal, ore-forming event. Although these minerals are usually affected by recrystallization and deformation during the Variscan metamorphism, these events have not masked the original textures, so that the primitive history of mineral replacements during the different thermal stages of hydrothermal deposition can be reconstructed.

The calculations performed by Marignac and Cathelineau concerning the formation temperatures and size of FIs necessary to avoid decrepitation during the Variscan metamorphism are based on contentious assumptions, such as the formation depth of the massive sulphides, the maximum conditions estimated for peak metamorphism or the average salinity for FI. Marignac and Cathelineau present several examples of present day hydrothermal systems in which there is evidence of recharge by seawater and, based on those references, state that all these systems, and thus ancient ones, are recharged by such fluids. However, they do not quote abundant systems fed by saline waters of other origins, for example, Atlantis II, Mid Atlantic Ridge (Delaney et al. 1987; Bortnikov et al. 1997) or Lau Basin (Rona 1988). Furthermore, highly saline fluids are implicated in the formation of ancient massive sulphides such as Mattagami lake (Costa et al. 1983) or Hellyer (Solomon

et al. 2002). In addition, neither the size nor the tectonic environment nor the host rocks and probably the style of mineralization of the IPB deposits are similar to most of the present day systems (e.g. Tornos in press). Our stable isotope data of the stockworks are consistent with those of the massive sulphides and altered host rocks and suggest the percolation of large amounts of ^{18}O-enriched water that variably mixed with seawater (Munhá et al. 1986; Fouillac and Javoy 1988; Lerouge et al. 2001; Tornos in press).

In any case, accepting the statements assumed by these authors in their Figure 1, and considering the FI data provided in our study, the conclusion that emerges from their isochore diagram would be just the opposite to Marignac and Cathelineaús statement that "*many of the pristine fluid inclusions would have decrepitated...*". In fact, they use for their isochore calculations average diameters of 10 and 16 μm for the FIs when, actually, the mean (median) diameter would be around 7 μm for a population of about 300 FIs (from the studied stockworks; p. 524, Table 3). This size would correspond to a critical differential pressure of around 190 MPa. When plotting the limiting isochore for 7 μm FI in Marignac and Cathelineau's Figure 1, this isochore intersects the 1,500 m depth reference line at a temperature of around 250°C. This means that fluid inclusions trapped at temperatures lower than 250°C would have sustained the metamorphic pressure. Consequently, it could be concluded that the great majority of our FIs (which present a range of 120–280°C with a mode peak of 180°C; p. 525, Figs. 3 and 4 in Sánchez-España et al. 2003) would not have imploded during peak metamorphic conditions, as none of them would have exceeded the critical differential pressure. In any case, it is known that the effects of possible implosion/decrepitation of FI by overpressures is not yet completely understood (Van der Kerkholf and Hein 2001) and many exceptions of FI preservation have been described in the literature.

Further, and in contrast with the lack of evidence in support of Marignac and Cathelineau, we point out that other mineral provinces have been subjected to similar levels of deformation and metamorphism during the Variscan, particularly the Irish type base-metal deposits. These deposits also exhibit a similar, though copper poor base-metal and pyrite dominance, with associated quartz in feeder zones. In several in-depth studies of these deposits involving many hundreds of analyses (e.g. Samson 1983; Samson and Russell 1983, 1987; Banks and Russell 1992; Wilkinson 2003), there is very little evidence of significant Variscan overprinting. Instead the inclusions preserve pre-Variscan evidence.

The argument of the late Variscan fluid percolation

Post-kinematic remobilization of ore sulphides (sph, gal, cpy) and gold is a widespread feature of the IPB deposits, as has been previously described (Tornos et al.

1998; Velasco et al. 2000). Marignac and Cathelineau conclude that ".... part of the iron sulphides, most polymetallic sulphides and all gold in the Thars stockwork was introduced at the post-kinematic stage". However, this remobilization cannot account for, at least in the stockworks we studied (Aguas Teñidas Este, San Miguel, Concepción, San Telmo), the presence of all base metal sulphides present in association with pyrite. Also, we have observed the presence of some minerals (e.g. bismuthinite in the stockworks of Aguas Teñidas Este, San Miguel and Concepción), which are not observed within the remobilized ores in the late Variscan veins.

For example, south of Tharsis (Tornos et al. 1998) syn- to post-tectonic pyrite stockwork-like veins hosted by siliciclastic sediments have no related chlorite-rich alteration and show neither gold nor base metal enrichment. Thus, it seems highly unlikely that metamorphic fluids could remobilize at large scale significant amounts of metals. Furthermore, we find no evidence in literature or the field of mineralization that could suggest significant, shear-related remobilization of metals from the massive sulphides, strongly suggesting that the capability of metamorphic fluids to transport metals was minimal. Also, the absence of Au and Bi showings away from the massive sulphides also indicate that these metals were originally in the orebodies and were not introduced late by metamorphic fluids, as proposed by Marignac et al. (2003). In fact, at Tharsis gold occurs primarily as minute inclusions within cobaltite, alloclasite and/or bismuth minerals (Leistel et al. 1998). Tornos et al (1998) have also reported primary gold inclusions in cobaltite from the Tharsis stockwork and other studies (Velasco et al. 2000) point to the relation of gold with various mineral facies, thus suggesting a primary and older origin for gold and not the result of neo-deposition during metamorphic remobilization as suggested by Marignac and Cathelineau.

Further, it is difficult to agree with Marignac and Cathelineau when they say that the late Variscan tectonics and metamorphism was responsible for extensive new mineral formation and isotopic re-equilibration of ore sulphides and even carbonates. Such a pervasive tectono-thermal modification would have implied a generalized percolation through tens of meters of massive sulphides and would have led to widespread mineralization of the shear zones and thrusts close to massive sulphides, which is not observed.

Did ore sulphides and the accompanying chlorite and quartz homogenize isotopically with late Variscan fluids?

It seems intuitively highly unlikely that under low-grade, anchizonal Variscan metamorphic conditions, fluids circulating along shear bands were able to homogeneously re-equilibrate the geochemistry, including the O and S isotopes of large, km-sized stockworks away from the shear zones. Metamorphism of sulphides tends only to homogenize the sulphur isotope values (thus reducing the sulphur isotopic ranges, e.g. Sangster 1971), usually on the mm/cm scales (e.g. Skauli et al. 1992) and, under greenschist conditions, the preservation of the original isotopic fractionations is the rule and not the exception (see, for example, Cook and Hoefs 1997). The homogenization of the $\delta^{34}S$ signatures would imply dissolution and reprecipitation of the sulphides. However, although local remobilization of sulphides has been detected in some places, this mechanism is not commonly observed in the IPB ores.

Micro-textural studies performed by different etching techniques on massive and stockwork ores from the Northern IPB deposits (Sánchez España 2000) indicate that the more ductile sulphides (sph, gal, cpy) had been in most cases affected not only by recrystallization/annealing, but also by plastic deformation, thus suggesting a pre-kinematic origin. The accompanying chlorite and quartz are also normally deformed and show features such as cleavage and micro-folding in the case of chlorite, and granoblastic habit and undulating extinction in the case of quartz. These textures, however, coexist with unequivocally primary diagenetic (framboidal, colloform) textures at the micro-scale.

In fact, under the low-grade conditions assumed for the Variscan metamorphism in the IPB, not only can the primary and metamorphic textures coexist (with minor mineralogical changes), as commonly recognized by several authors through experiments (e.g. McClay and Ellis 1983; Cox 1987; Marshall and Gilligan 1987) or natural observations (Brown 1994; Larocque and Hogdson 1995), but also pristine FIs can be preserved (e.g. Ripley and Ohmoto 1977; Broman 1987; Khin Zhaw and Large 1992; Wilkinson 2003).

Therefore, we believe that the study and interpretation of stable isotopes in these ores can be useful and relate to primary processes, if paragenetically well-characterized samples are selected following detailed microscopic examination, as were the samples analyzed in Sanchez-España et al. (2003). By doing so, Velasco et al. (1998) reported the first in situ laser microprobe analyses of $\delta^{34}S$ for the IPB massive and stockwork ores. This study revealed marked isotopic differences (from −15 to about 5–10‰) among distinct ore facies and minerals, even over very short distances of about 200 μm, which precluded the existence of a wholesale isotopic homogenization of the IPB ores during metamorphism.

The highest $\delta^{34}S$ values are not restricted to coarse-grained sulphides, being also observed in a variety of grain sizes and hydrothermal textures that coexist with pyrite grains showing diagenetic textures and very negative $\delta^{34}S$ (Velasco et al. 1998; Sánchez-España 2000). We have also measured negative $\delta^{34}S$ in recrystallized sphalerite and galena. Thus, it is very difficult to consider that these minerals "...have recorded the post-kinematic hydrothermal event", as stated by Marignac and Cathelineau.

Also, Sanchez-España (2000) reports marked mineralogical differences between stockwork (hydrothermal)

and regional (metamorphic) chlorites in the northern-most IPB deposits, with the latter having significantly higher Fe/(Fe + Mg) ratio. It is therefore assumed that hydrothermal chlorite did not systematically equilibrate, neither chemically nor isotopically, with the late metamorphic fluids, which would have much lower $\delta^{18}O$ and higher δD, as suggested in Figure. 10A (p.534) of our original work.

Considering all this evidence, we state that despite the Variscan tectonics, mineral and isotopic constraints corresponding to the hydrothermal ore-forming stages have been preserved in many cases, allowing the reconstruction of the depositional history by the above-mentioned techniques.

Despite the discussion of Marignac and Cathelineau regarding the problem of re-equilibration of FIs in deformed belts, the uncritical assumption of such statements can lead to the obviously erroneous conclusion that all FI studies, even in slightly metamorphosed areas, only record the very late ones. Thus, all these studies—including those of these authors in orogenic gold systems—should be reinterpreted as only recording late stages.

Conclusions

1. The Variscan deformation which affected the massive ores and host volcanic and sedimentary rocks of the IPB during the Late Visean to Westfalian, was heterogeneous and channelized along shear zones and deformation bands, in which the mineralogical and textural effects of deformation were likely to have been more important than in areas away from these focused deformation zones.
2. Consequently, although Marignac and Cathelineau provide reasonable arguments to support their "tectono-metamorphic view" of effects within two very specific areas of strong deformation, they over-extrapolate their results from these two deposits to the whole metallogenic province.
3. In fact, the geological, mineralogical and isotopic constraints presented in our studies in the Northernmost IPB deposits, preclude a generalized over-printing of mineral assemblages, as well as the implosion of all pristine fluid inclusions during metamorphism and deformation, and the wholesale isotopic homogenization of ores and related materials by late Variscan fluids.
4. Finally, our fluid inclusion and stable isotope results are undoubtedly consistent with a mixed origin for ore fluids involving deep (connate or magmatic) fluids and seawater, in agreement with recent studies performed in other IPB deposits such as Neves-Corvo (Relvas 2000; Moura 2003; Tornos, in press).

References

Almodóvar GR, Sáez R, Pons JM, Maestre A, Toscano M, Pascual E (1998) Geology and genesis of the Aznalcóllar massive sulphide deposits, Iberian Pyrite Belt, Spain. Miner Deposita 33:111–136

Banks DA, Russell MJ (1992) Fluid mixing during ore deposition at the Tynagh base-metal deposit, Ireland. Euro J Mineral 4:921–931

Bobrowicz GL (1995) Mineralogy, geochemistry and alteration as exploration guides at Aguas Teñidas Este, Pyrite Belt, Spain. PhD Thesis, University of Birmingham

Broman C (1987) Fluid inclusions of the massive sulphide deposits in the Skellefte district, Sweden. Che. Geol 61:161–168

Brown D (1994) Low temperature, low pressure deformation and metamorphism of the Vangorda massive sulphide orebody, Yukon, Canada. Miner Deposita 29:330–340

Bortnikov NS, Krylova TL, Bogdanov YA, Vikentyet IV, Nosik LP (1997) The 14°45'N hydrothermal field, Mid-Atlantic ridge: fluid inclusion and sulfur isotope evidence for submarine phase separation. In: Papunen H (eds) Mineral deposits: research and exploration. Balkema, Rotterdam, pp 353–356

Cook NJ, Hoefs J (1997) Sulphur isotope characteristics of metamorphosed Cu-(Zn) volcanogenic massive sulphide deposits in the Norwegian Caledonides. Chem Geol 135:307–324

Costa UR, Barnett RL, Kerrich R (1983) The Mattagami Lake mine Archean Zn-Cu sulfide deposit, Quebec: Hydrothermal coprecipitation of talc and sulfides in a sea floor brine pool - evidence from geochemistry, $^{18}O/^{16}O$ and mineral chemistry. Econ Geol 78:1144–1203

Cox SF (1987) Flow mechanisms in sulphide minerals. Ore Geol Rev 2:133–171

Delaney JR, Mogk DW, Mottl MJ (1987) Quartz cemented breccias from the Mid Atlantic Ridge: samples of a high salinity hydrothermal upflow zone. J Geophys Res 92:9172–9192

Fouillac AM, Javoy M (1988) Oxygen and hydrogen isotopes in the volcano-sedimentary complex of Huelva (Iberian Pyrite Belt): example of water circulation through a volcano-sedimentary sequence. Earth Planet Sci Lett 87:473–484

Hidalgo R, Guerrero V, Pons JM (2001) Geology of the Aguas Teñidas Este mine, Southern Spain. GEODE workshop, October 2001, Aracena, Spain

Khin Zaw, Large RR (1992) The precious metal-rich South Hercules mineralization, western tasmania: a possible subsea-floor replacement volcanic-hosted massive sulphide deposit. Special Issue on Australian VHMS deposits. Econ Geol 87:931–952

Larocque ACL, Hodgson CJ (1995) Effects of greenschist facies metamorphism and related deformation on the Mobrun massive sulphide deposit, Quebec, Canada. Miner Deposita 30:439–448

Lécolle M (1977) La ceinture sudibérique: un exemple de province á amas sulfurés volcano sedimentaires. Thése Univ. Pierre et Marie Curie

Leistel JM, Marcoux E, Thiéblemont D, Quesada C, Sánchez A, Almodóvar GR, Pascual E, Sáez R (1998) The volcanic-hosted massive sulphide deposits of the Iberian Pyrite Belt. Review and preface to the Thematic issue. Miner Deposita 33:2–30

Lerouge C, Deschamps Y, Joubert M, Bechu E, Fouillac AM, Castro JA (2001) Regional oxygen isotope systematics of felsic volcanic; a potential exploration tool for volcanogenic massive sulphide deposits in the Iberian Pyrite Belt. J Geochem Explor 72:193–210

McClay KR, Ellis PG (1983) Deformation and recrystallization of pyrite. Mineral Mag 47:527–538

Marignac C, Bocar D, Cathelineau M, Boiron MC, Banks D, Fourcade S, Vallance J (2003) Remobilisation of base metals and gold by Variscan metamorphic fluids in the south Iberian Pyrite Belt: evidence from the Tharsis deposit. Chem Geol 194:143–165

Marshall B, Gilligan LB (1987) An introduction to remobilization: information and experimental considerations. Ore Geol Rev 2:87–131

Marshall B, Spry PJ (2000) Discriminating between regional metamorphic remobilization and syntectonic emplacement in the genesis of massive sulphide ores. In: Spry PJ, Marshall B, Vokes FM (eds) Metamorphosed and metamorphogenic ore deposits. Rev Econ Geol 11:39–79

Marshall B, Giles AD, Hagemann S (2000) Fluid inclusions in metamorphosed and synmetamorphic (including metamorphogenic) base and precious metal deposits: indicators of ore-forming conditions and/or ore-modifying histories? In: Spry PJ, Marshall B, Vokes FM (eds), Metamorphosed and metamorphogenic ore deposits. Rev Econ Geol 11:119–148

Moura A (2003) Fluids from the Neves Corvo ores. Goldschmidt Conference Abstract 2003, p A310

Moura A, Noronha F, Cathelineau M, Boiron MC (1997a) Fluids from the Neves-Corvo Volcanic Massive Sulphide deposit, Portugal. In: European Current Research on Fluid Inclusions-ECROFI XIV, 1–4 July, CREGU, Nancy, France, pp 220–221 (Abstracts)

Moura A, Noronha F, Cathelineau M, Boiron MC, Ferreira A (1997b) Evidence of metamorphic fluid migration within the Neves-Corvo ore deposits: the fluid inclusion data. SEG Neves Corvo Field Conference. Abstracts and Program, May 11–14, Lisbon, Portugal, p 92

Munhá J (1983) Low grade regional metamorphism in the Iberian Pyrite Belt. Com Serv Geol Port 69:3–35

Munhá J (1990) Metamorphic evolution of the South Portuguese/Pulo do Lobo Zone. In: Dallmeyer RD, Martínez García E (eds) PreMesozoic geology of Iberia. Springer. Berlin Heidelberg New York, pp 363–368

Munhá J, Barriga FJAS, Kerrich R (1986) High ^{18}O ore-forming fluids in volcanic-hosted base-metal massive sulphide deposits: geologic, ^{18}O/^{16}O and D/H evidence for the Iberian Pyrite Belt; Crandon, Wisconsin; and Blue Hill, Maine. Econ Geol 81:530–552

Nehlig P, Cassard D, Marcoux E (1998) Geometry and genesis of feeder zones of massive sulphide deposits : constraints from the Rio Tinto ore deposit (Spain). Miner Deposita 33:137–149

Quesada C (1998) A reappraisal of the structure of the Spanish segment of the Iberian Pyrite Belt. Miner Deposita 33:31–44

Relvas JMRS (2000) Geology and metallogenesis at the Neves Corvo deposit, Portugal. PhD Thesis, University of Lisbon

Ribeiro A, Silva JB (1983) Structure of the South Portuguese Zone. Mem Serv Geol Portugal 29:83–90

Ripley EM, Ohmoto H (1977) Mineralogic, sulphur isotope, and fluid inclusion studies of the stratabound copper deposits at the Raul mine, Peru. Econ Geol 72:1017–1041

Rona PA (1988) Hydrothermal mineralization at oceanic ridges. Can Mineral 26:431–466

Routhier P, Aye F, Boyer C, Lécolle M, Moliére P, Picot P, Roger G (1980) La Ceinture Sud-Ibérique a amás sulfurés dans sa partie espagnole médiane. Mem BRGM no 94:265

Samson IM (1983) Fluid inclusion and stable isotope studies of the Silvermines orebodies, Ireland, and comparison with Scottish vein deposits. Unpublished PhD dissertation, Glasgow, University of trathclyde, 290 p

Samson IM, Russell MJ (1983) Fluid inclusion data from Silvermines base-metal-baryte deposits, Ireland.Trans Inst Mining Metal 92:B67–B71

Samson IM, Russell MJ (1987) Genesis of the Silvermines zinc-lead-baryte deposit, Ireland: Fluid inclusion and stable isotope evidence. Econ Geol 82:371–394

Sánchez-España FJ (2000) Mineralogía y geoquímica de los yacimientos de sulfuros masivos del área septentrional de la Faja Pirítica Ibérica (San Telmo-San Miguel-Peña del Hierro), Huelva, España. PhD Thesis, Universidad del País Vasco

Sánchez-España FJ, Velasco F, Boyce A, Fallick AE (2003) Source and evolution of ore-forming hydrothermal fluids in the northern Iberian Pyrite Belt massive sulphide deposits (SW Spain): evidence from fluid inclusions and stable isotopes. Miner Deposita 38:519–537

Sangster DF (1971) Sulphur isotopes, stratabound sulphide deposits, and Ancient Seas. Soc Mining Geol Japan, Spec. Issue Proc IMA-IAGOD Meeting 70–3:295–299

Schermerhorn LJG (1971) An outline stratigraphy of the Iberian Pyrite Belt. Bol Geol Min 82:239–268

Schermerhorn LJG (1975) Spilites, regional metamorphism and subduction in the Iberian Pyrite Belt: some comments. Geol Mijnbouw 54:23–35

Skauli H, Boyce AJ, Fallick AE (1992) A sulphur isotope study of the Blaekvassli Zn–Pb–Cu deposit, Nordland, North Norway. Miner Deposita 27:284–292

Solomon M, Tornos F, Gaspar OC (2002) Explanation for many of the unusual features of the massive sulfide deposits of the Iberian Pyrite Belt. Geology 30:87–90

Tornos F (2005) Environment of formation and styles of volcanogenic massive sulfides: the Iberian Pyrite Belt. Ore Geol Rev (in press)

Tornos F, González-Clavijo E, Spiro B (1998) The Filón Norte orebody (Tharsis, Iberian Pyrite Belt): a proximal low-temeperature shale-hosted massive sulphide in a thin-skinned tectonic belt. Miner Deposita 33:150–169

Van der Kerkhof AM, Hein U (2001) Fluid inclusion petrography. Lithos 55:27–47

Velasco F, Sánchez-España FJ, Boyce A, Fallick A, Sáez R, Almodóvar GR (1998) A new sulphur isotopic study of some IPB deposits: evidence of a textural control on the sulphur isotope composition. Miner Deposita 33:4–18

Velasco F, Sanchez-España FJ, Yanguas A, Tornos F (2000) The occurrence of gold in the sulphide deposits of the Iberian Pyrite Belt. In: Gemmell B, Pongratz J (eds) Abstract international conference on volcanic environment and massive sulphide deposits, CODES Special publications 3, Tasmania, Australia, pp 221–223

Wilkinson JJ (2003) On diagenesis, dolomitisation and mineralisation in the Irish Zn–Pb orefield. Miner Deposita 38:968–983

Wipfler EL, Sedler IK (1995) Vein mineralizations in the Iberian Pyrite Belt, SW Spain. In: Pasava, et al. (eds) Mineral deposits, proceedings of the 3rd Biennial SGA Meeting, Balkema, pp 405–408

ELSEVIER

Zn–Pb–Cu volcanic-hosted massive sulphide deposits: criteria for distinguishing brine pool-type from black smoker-type sulphide deposition

M. Solomon[a,*], F. Tornos[b], R.R. Large[a], J.N.P. Badham[c], R.A. Both[d], Khin Zaw[a]

[a] Centre of Ore Deposit Research, University of Tasmania, Private Bag 79, Hobart, Tasmania, 7001, Australia
[b] Instituto Geológico y Minero de España, C/Azafranal, 48-50, 37002, Salamanca, Spain
[c] Crockery House, Over Wallop, Stockbridge, S020 8HU, UK
[d] Department of Geology and Geophysics, University of Adelaide, GPO Box 498D, Adelaide, South Australia 5001, Australia

Abstract

Eight Zn–Pb–Cu massive sulphide deposits that appear to have formed on the sea floor (seven in Spain, one in Tasmania) are believed to have been precipitated in brine pools, based on the salinities and temperatures of fluid inclusions in underlying stockworks. Comparing the geological features of these deposits with those of the Zn–Pb–Cu massive sulphide ores of the Hokuroku Basin, Japan, which have formed as mounds from buoyant fluids of low salinity, shows that brine pool deposits have: (1) potentially very large size and tonnage, and high aspect ratio, (2) higher Zn/Cu and Fe/Cu values, (3) no evidence of chimneys, (4) relatively abundant framboidal pyrite and primary mineral banding, (5) reduced mineral assemblages (pyrite-arsenopyrite/pyrrhotite), and minor or rare barite in the massive sulphide, (6) associated stratiform and/or vein carbonates, (7) relatively unimportant zone refining, (8) lack of vertical variation in sphalerite and sulphur isotopic compositions, and (9) evidence of local bacterial sulphate reduction. Application of these criteria to the Rosebery deposit in Tasmania, for which there are no fluid inclusion data, leads to the conclusion that the southern section was deposited as separate lenses in a brine-filled basin or basins. Other potential candidates include Brunswick no. 12 and Heath Steele (Canada), Woodlawn and Captains Flat (New South Wales), Hercules and Que River (Tasmania), and Tharsis and the orebodies at Aljustrel (Spain and Portugal). Recently published fluid inclusion data for Gacun (China) and Mount Chalmers (Queensland) suggest that not all ores deposited from highly saline fluids have reduced mineral assemblages.
© 2004 Elsevier B.V. All rights reserved.

Keywords: Massive sulphides; Criteria; Brine pools

1. Introduction

Discussions concerning the manner of deposition of massive sulphide deposits on the sea floor have been dominated since about 1980 by the results of the multi-disciplinary study of the ores of the Hokuroku

* Corresponding author. Tel.: +61-3-62267208; fax: +61-3-62267662.

E-mail address: Mike.Solomon@utas.edu.au (M. Solomon).

Basin, Japan (Ohmoto and Skinner, 1983), and of research into modern vent activity on the ocean floor (e.g., Scott, 1997). Although massive Zn–Cu deposits were known in the Red Sea brine pools (for example, Scholten et al., 2000), and the geology of a number of ancient deposits indicated some form of basin filling (for example, Solomon, 1981; Green et al., 1981), most massive sulphide interpretations followed the Hokuroku (or "Kuroko") model. This involved building sulphate chimneys by mixing exhaling, hot, buoyant fluids with seawater, followed by their dissolution and collapse to form a mound on the sea floor, which was then modified by subsequent fluid passage (Lydon, 1996; Ohmoto, 1996; Fig. 1). In contrast, the brine-pool type sulphide deposits formed when hot, more saline, fluids became negatively buoyant after mixing with seawater, and were trapped in basins on the sea floor (Fig. 1).

Sato (1972) was the first to apply such reversing behaviour to ore formation. He recognised that for the

Fig. 2. Density–temperature plot to illustrate the effects of mixing brines with 5 and 11 wt.% salinity at 200 bars and 350 °C with seawater at 2 °C and a salinity of 3.2 wt.%. Drawn from Turner and Campbell (1987).

Fig. 1. Two major styles of massive sulphide formation on the sea floor. (A) Mound building by chimney collapse and zone refining of the growing mound (from Lydon, 1996). (B) Mineral depositon by quenching in a brine pool (from Solomon and Khin Zaw, 1997).

ranges of temperature and salinity observed in massive sulphide fluids factors such as heat of reaction and heat capacity could safely be ignored, and that simple mixing calculations between seawater and fluids of different NaCl content and temperature would yield reasonably accurate results for fluid density. He showed that the non-linear behaviour of fluid density with temperature resulted in three fluid types, viz. those that were permanently buoyant (type 1), those that reversed buoyancy and collected in basins (type II), and those that were permanently denser than seawater (type III). McDougall (1984) later modelled the behaviour of fluids entering a brine pool from below, and also from outside the pool, and Turner and Campbell (1987) used the data of Potter and Brown (1977) to calculate curves for mixing seawater and fluids having various salinities and temperatures (Fig. 2), and to define more precisely the boundaries between fluid types I and II. High dilutions are required in the early stages of pool formation (Fig. 2), declining as the basin fills.

Although fluid inclusions studies had shown that type II fluids might be significant in the generation of several orebodies (for example, Large and Both, 1980;

Broman, 1987), sophisticated interpretations were inhibited by uncertainty about the timing or status of the inclusions or the geology. However, the definition of a vein paragenesis in the footwall of the Hellyer

massive sulphide in Tasmania (Gemmell and Large, 1992), and determination of fluid salinities and homogenisation temperatures in inclusions in each vein stage (Khin Zaw et al., 1996), allowed Solomon and

Table 1
Data for the massive sulphide ores of deposits thought to have been formed in brine pools, and others mentioned in the text

Deposit	Size, Mt	Aspect ratio[a]	Zn, wt.%	Pb, wt.%	Cu, wt.%	Ag, ppm	Au, ppm	Zn/Cu	Fe/Cu[b]	Zn+Pb +Cu, Mt	Data source
Brine pool ores											
Hellyer, Tasmania	16.2	7	13.9	7.1	0.4	168	2.5	37	63	3.5	McArthur, 1996
Rio Tinto, Spain	500	30–35	ca. 1.0	ca. 2.0	ca. 1.0	22	0.4	2	43	20	García Palomero, 1990
Masa Valverde, Spain	ca. 92	20	11 Mt at 5 wt.% Pb+Zn						75%=105		Ruiz et al., 2002
			80 Mt at 1.5 wt.% Pb+Zn		0.4		0.1			2.1	
San Telmo, Spain	4		12	0.4	1.2	60	0.8	10	19	0.5	Leistel et al., 1998a
San Miguel, Spain	1.3				3				7	0.03	Leistel et al., 1998a
Aguas Teñidas Este, Spain	10	8	8	2.2	1.1	74		7.3	23?	1.1	Hidalgo et al., 2001
Los Frailes, Spain	70	13	3.9	2.2	0.3	62		13	40?	4.4	Leistel et al., 1998a,b
Aznalcóllar, Spain	161		2.7	1.4	0.4	37	0.5	6.7		7.2	Large and Blundell, 2000
Hokuroku											
Matsumine, Japan	30	5.5	3.6	1	2.4	57	0.5	1.5	8	2.1	Tanimura et al., 1983
Motoyama, Japan	15	6	4.5	0.8	2.2			1.8	9	1.1	Tanimura et al., 1983
Doyashiki, Japan	8.9	3	1.3	0.4	2.3			0.6	7	0.3	Tanimura et al., 1983
Other											
Rosebery, Tasmania	31.7	high	14.3	7.5	0.6	146	2.3	23.8	22	7.1	Pasminco mine staff, pers. comm., 2000
Que River, Tasmania	3.3		13.3	7.4	0.7	200	3.4	19		0.7	McArthur and Dronseika, 1990
Hercules, Tasmania	2.6		16.7	5.2	0.4	159	2.7	42		0.6	Lees et al., 1990
Woodlawn, New South Wales (complex ore only)	8.5	8	12.5	4.7	1.6	88	0.5?	8.1	13	1.6	McKay, 1989
Captains Flat, New South Wales	4	>20	10	6	0.7	55	1.7	14.3	ca. 40?	0.7	Davis, 1975
Brunswick no. 12, New Brunswick	148		9	3.6	0.3	100	0.2	30		19.1	Franklin, 1996
Heath Steele, New Brunswick	33.8		6.3	2.5	0.7	60	0.6	9		3.2	Franklin, 1996
Alexandriska, southern Urals	3.6	6 to 14	5.5		4.4			1.2		0.3	Maslennikov et al., 2000;
Sibaiskoye, southern Urals	110	2 to 4	1.6	0.4				0.2		2.2	Large and Blundell, 2000
Mauk, southern Urals	3	>15	1.7		1.5			1.1		0.1	Large and Blundell, 2000

[a] Maximum length/average thickness. The aspect ratios are only reliable for the Hokuroku, Urals, Woodlawn and Hellyer orebodies.

[b] Fe contents accurate only for Hokuroku ores (Tanimura et al., 1983), Rio Tinto (43%, Williams, 1934), Masa Valverde (75%=42%, Ruiz et al., 2002), Woodlawn (ca. 21%, McKay, 1989), Hellyer (25%, McArthur, 1996) and Rosebery (13%, Pasminco mine staff, pers. comm, 2000).

Khin Zaw (1997) to examine semi-quantitatively the growth of a brine pool, using the modelling developed by McDougall (1984). Subsequently, similar fluids were discovered in stockwork veins of seven massive sulphides orebodies in the Iberian pyrite belt, enabling Solomon et al. (2002) to discuss the generation of brine pools and ore formation in that province. There are thus eight "known" brine-pool type massive sulphide deposits, and they include some of the largest (for example, Rio Tinto, Spain) and richest (for example, Hellyer, Tasmania) of all volcanic-hosted massive sulphide deposits. They all belong to the Zn–Pb–Cu group of volcanic-hosted or volcanic-associated massive sulphide ores (Solomon, 1976; Franklin, 1996), and are believed to have been deposited largely on the sea floor. The Zn–Pb–Cu ores generally occur in volcanic or volcano-sedimentary terrains containing mixed basic and acid compositions, with the latter dominant.

Because most massive sulphide deposits have been deformed and metamorphosed, and material suitable for thermometric studies is uncommon, we attempt here to develop other criteria to distinguish between the Hokoroku and brine-pool styles of ore deposition. We review the major characteristics of Hellyer and the seven Iberian pyrite belt ores for which a brine-pool origin has been proposed from fluid inclusion data (Table 1), and compare them with the ores of the Hokuroku Basin, probably the best understood of the ancient buoyant, or black-smoker, Zn–Pb–Cu types. Where appropriate, we make use of data from massive sulphide ores belonging to the Zn–Cu and Cu types such as those of modern mid-ocean ridges or back-arc basins, and the southern Urals. The manner of deposition on the sea floor can help in assessing the likely range of salinities of the ore-forming fluids, whether or not a basin existed during mineralization, and the likelihood of finding deposits nearby that might have been derived from basin overflow. The distinguishing characteristics are determined empirically, but we also attempt to explain the reasons for the differences. This discussion does not concern those orebodies that formed by subsurface replacement of consolidated or unconsolidated material, such as the Highway-Reward orebody in Queensland, Australia (Doyle, 2001).

The strongest case for sulphide brine-pool deposition is the Hellyer deposit in western Tasmania,

because it is relatively mildly deformed and the feeder veins provide at least a partial fluid paragenesis. The geology of this deposit is discussed separately from the less intensively studied, high-salinity examples in the Iberian pyrite belt. The scarcity of comparable detail in the Iberian pyrite belt is the result of the very early mining (intermittently from Chalcolithic times, Gaspar, 1996), and/or the locally severe Hercynian deformation. The criteria for distinguishing brine-pool- from black-smoker-type deposits that emerge from these comparisons are then applied to the Rosebery deposit in western Tasmania, as an example of those deposits for which there are no fluid inclusion data and an uncertain origin.

2. The geology of the Hellyer deposit

The Hellyer massive sulphide deposit lies within the Mount Read Volcanics, a bimodal suite of calc-alkaline and tholeiitic volcanics of Cambrian age in western Tasmania (Corbett, 1992; Fig. 3). The orebody consisted, before mining, of a single, massive lens of pyrite-sphalerite-galena-arsenopyrite-chalcopyrite (in order of abundance) overlain by a discontinuous barite-sulphide, and a more restricted silica-sulphide cap (McArthur and Dronseika, 1990; McArthur, 1996; Fig. 4, Table 1). Fragments of barite in the overlying clastic rocks (Sharpe, 1991), and the lack of large-scale replacement of footwall rocks at the base of the orebody, show that sulphide deposition took place mainly on the sea floor (McArthur, 1996). By unwinding the Devonian and later deformation, Downs (1993) outlined the shape of the basin in which the orebody grew, and the control over shape by syn-mineralization extensional faults (Fig. 4). Only two thin lenses of volcaniclastic material were shed from the margins during ore deposition, testifying to rapid sulphide deposition (McArthur, 1996; Solomon and Khin Zaw, 1997). Beneath the orebody there is a downward-tapering cone of altered rocks (quartz-chlorite-sericite-carbonate) with a silicified core, the location of which is clearly related to coeval faulting (Fig. 4). The alteration cone is cut by three stages of steeply inclined, quartz-sulphide-carbonate-barite veins, most commonly in the silicified core (Gemmell and Large, 1992); stage 2A veins are cut by stage 2B and both by stage 2C veins. Stage 2A and 2B veins coalesce and merge into
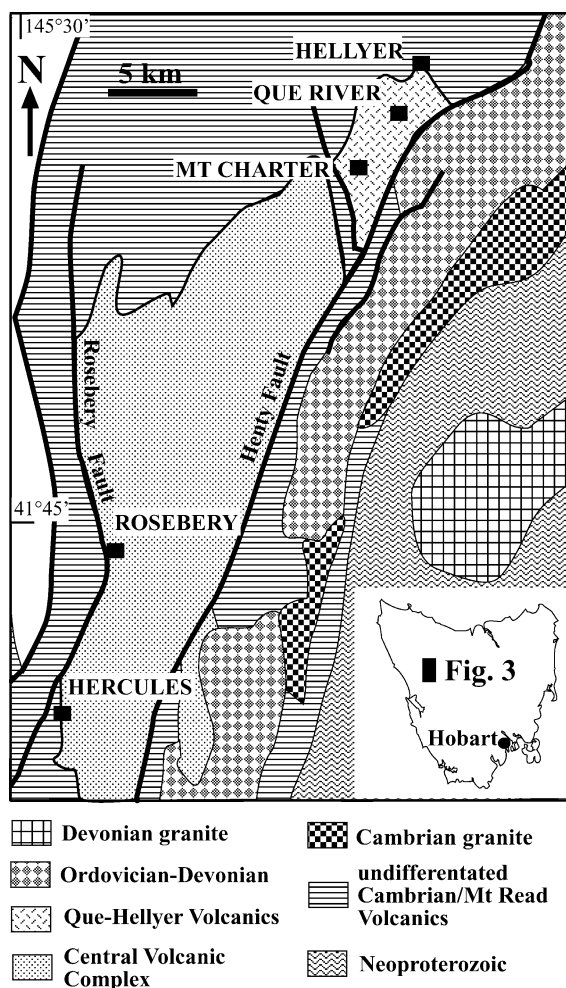
Fig. 3. Map displaying the locations of Hellyer and other deposits in the Mount Read Volcanics that are referred to in the text, from Corbett (1992).

the pyritic base of the deposit (McArthur and Dronseika, 1990), and are thought to be more or less contemporaneous with sulphide deposition (Gemmell and Large, 1992). Stage 2C veins, largely of barite, also cut the massive sulphide ore and merge into the barite cap.

Khin Zaw et al. (1996) found fluid inclusions in the quartz of two of the two syn-mineralization vein stages (2A and 2B), and in barite of the third, final stage. The 2A inclusions occurred on growth zones in crustiform quartz and are clearly primary, while determination of primary origin proved more difficult in

the 2B and 2C veins. As noted by Solomon and Khin Zaw (1997), the stage 2A fluids were of such a high salinity (up to 15 wt.%) that they would have ponded in the basin, and hence so would most of the subsequent fluids (Fig. 5). This conclusion seems inescapable unless it is based on false density–temperature–salinity data, or the fluids of the inclusions do not represent the ore-forming fluids (Solomon and Gaspar, 2001). Upward fluid flow must have preceded
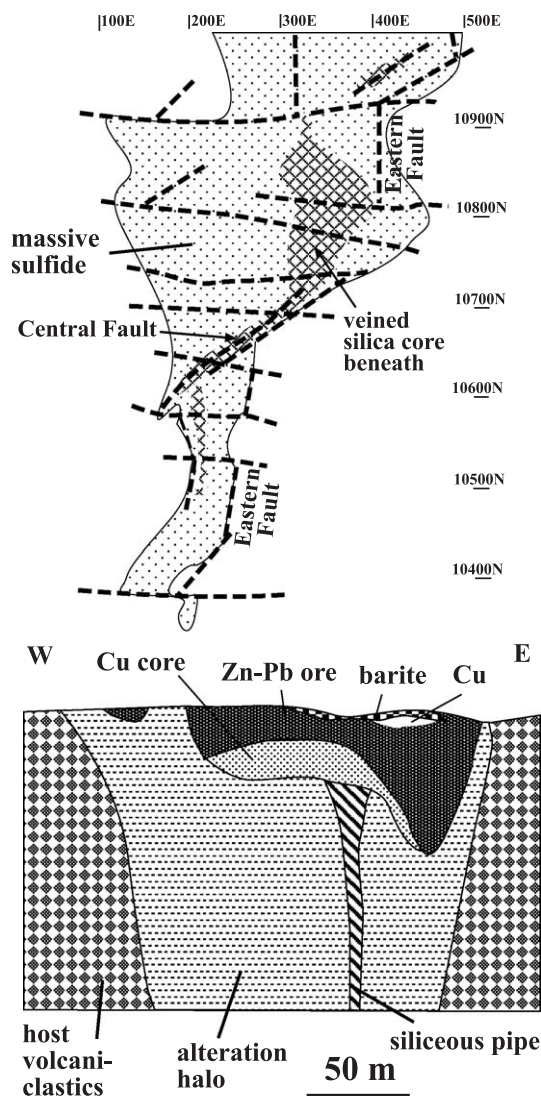
Fig. 4. Plan of the Hellyer massive sulphide orebody and a section at about 10970N, after unfolding by Downs (1993).

stage 2A veining because the veins cut altered rocks in the footwall, but the salinity of the fluids responsible for the alteration, and their ability to precipitate sulphides on the sea floor, are not known. During
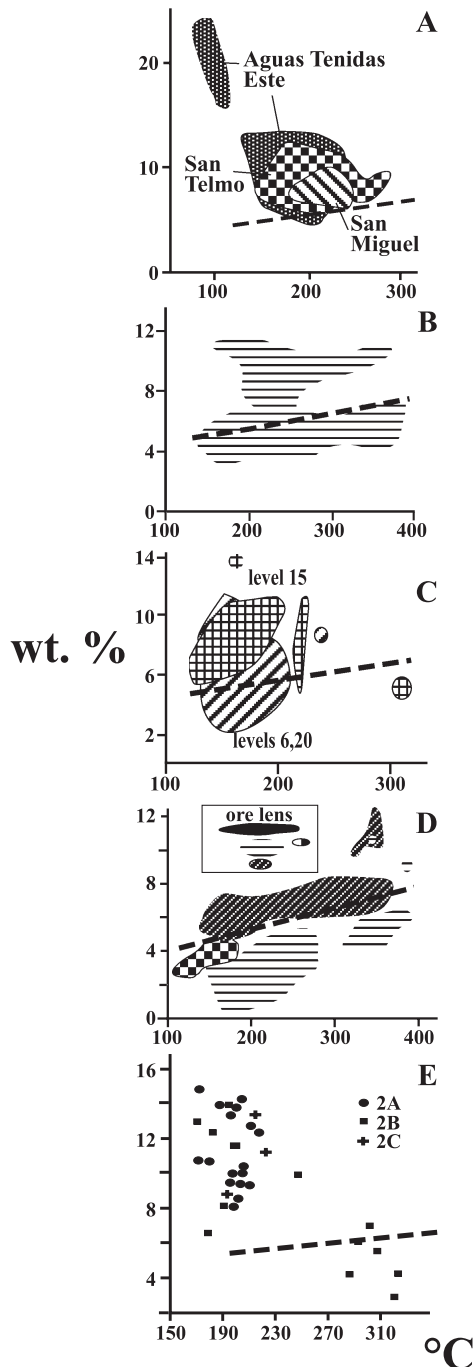
stage 2B a less saline, non-reversing fluid was introduced, but this would most probably have been rendered negatively buoyant as a result of mixing in the pool. Sulphides or their precursors, and subsequently barite, would have been quenched within the brine pool, resulting in build-up of the orebody by sedimentation of very fine particles (Solomon and Gaspar, 2001). Estimating the area of the pool surface enabled Solomon and Khin Zaw (1997), using the modelling of McDougall (1984), to calculate the approximate temperature and salinity of the brine pool at steady state, for various volume fluxes of vent fluid. Modification of the central part of the massive sulphide by late fluids, in a process similar to zone refining in Hokuroku ores, resulted in decreased Zn, Pb and Ag content, and slight Cu enrichment (McArthur, 1996). This zone was described by McArthur and Dronseika (1990) as the footwall depleted zone, and the remainder of the massive sulphide body (~ 60%) as the hanging wall enriched zone, and by Solomon and Khin Zaw (1997) as the Cu core and the Zn–Pb ore, respectively.

3. The geology of the Iberian pyrite belt deposits

The Iberian pyrite belt extends almost from Lisbon to Seville and lies on the tectonic suture between the South Portuguese Zone and the Iberian Massif (Fig. 6). It contains over 80 massive sulphide deposits within a volcano-sedimentary sequence (Leistel et al., 1998a; Carvalho et al., 1999). They commonly consist of several individual lenses that range in size from <1 Mt up to the largest, Rio Tinto, with about 500 Mt (García Palomero, 1990; Table 1), and mostly have a sheet-like form with high aspect ratio (maximum length/average thickness). They are characteristically rich in pyrite, accompanied by sphalerite, galena, chalcopyrite and arsenopyrite ± pyrrhotite,

Fig. 5. Temperature–salinity data from (A) San Miguel, San Telmo and Aguas Teñidas Este (Sánchez-España et al., 2000); (B) Masa Valverde (Toscano et al., 1997a); (C) Rio Tinto (Nehlig et al., 1998); (D) Aznalcóllar and Los Frailes (Almodóvar et al., 1998; Toscano et al., 1997b); (E) Hellyer (Khin Zaw et al., 1996). The inset in Fig. 4D illustrates the location of the inclusion groups (from Almodóvar et al., 1998). The dashed lines separate permanently buoyant fluids (below the lines) from those that would reverse buoyancy on mixing with seawater (from Turner and Campbell, 1987).
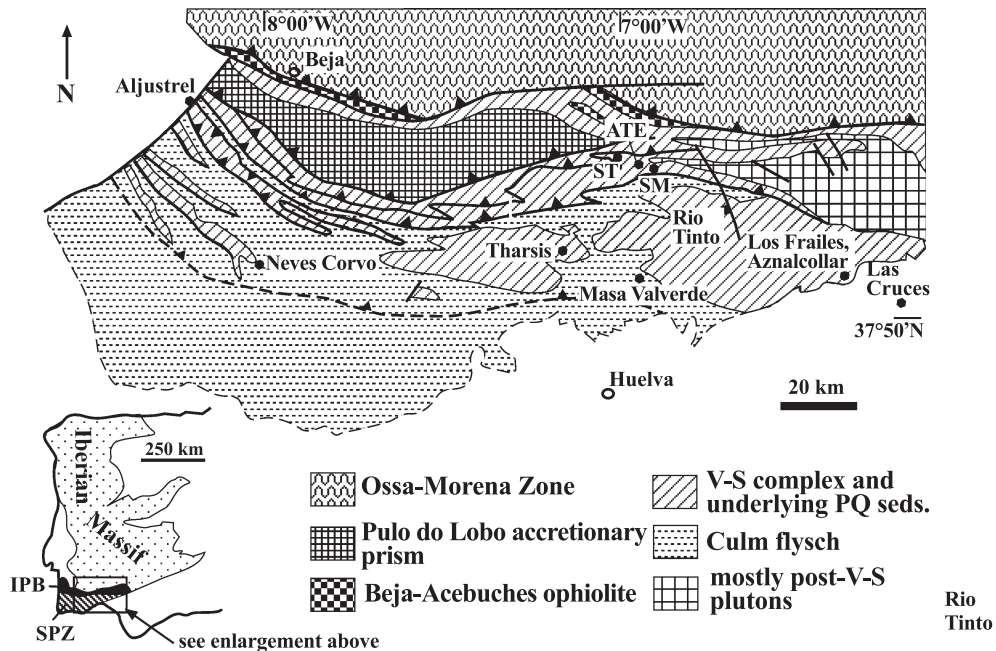
Fig. 6. Simplified geological map of the central and eastern parts of the Iberian pyrite belt, from Leistel et al. (1998a). SPZ: South Portuguese Zone, IPB: Iberian pyrite belt, ST: San Telmo, ATE: Aguas Teñidas Este, SM: San Miguel.

but with Zn and Pb grades that are low compared to those of deposits in other massive sulphide provinces. Barite occurs in veins cutting the massive sulphide and the hanging wall at Rio Tinto (Williams, 1934), and within ore at San Telmo (Mitsuno et al., 1988), but is rare or absent in most deposits. The massive sulphide bodies mostly overlie footwall rocks displaying quartz or quartz-sulphide veining and the effects of associated phyllosilicate-carbonate alteration, while overlying rocks are not, or only weakly, altered, suggesting that ore deposition took place mostly on the sea floor. Sulphide debris flows within the Rio Tinto ores lend weight to this suggestion, which is further supported by the ubiquity of quench textures in the Iberian massive sulphides (Gaspar, 1996; Velasco et al., 1998), the presence of sedimentary textures such as grading in the sulphides at the top of the Tharsis massive sulphide (Tornos et al., 1998) and in the Masa Valverde ore (Ruiz et al., 2002), of grading, banding and slump textures in the Planes-San Antonio and other orebodies at Rio Tinto (Williams, 1934; Williams et al., 1975), and at Aljustrel and Neves Corvo (Gaspar, 1996). A syn-mineralization basin has been postulated for Rio Tinto, based on the local

stratigraphy, the sharp southern cut-off of the massive sulphide in the Atalaya pit, and the relationships of the stockwork zones to the overall form of the sulphide sheet (Solomon et al., 1980; Badham, 1982). It is also tentatively proposed in this paper for Aguas Teñidas Este, based on the wedge shape of the massive sulphide displayed by McKee et al. (2001) and Hidalgo et al. (2001). Lenses of volcanic or sedimentary material occur within some massive sulphide bodies (for example, San Dionisio and Planes at Rio Tinto, Williams, 1934; Williams et al., 1975), but they are relatively rare, suggesting rapid massive sulphide deposition.

Almodóvar et al. (1998) believed that the Los Frailes and Aznalcóllar lenses were replacements of shales, but Allen (2001) found no evidence of replacement after detailed mapping, and concluded that the ore lenses were deposited on the sea floor. Minor sulphide replacement can be seen at the base of the massive sulphide bodies at Tharsis and Rio Tinto, and some feeder pipes on the northern margin of the Rio Tinto field appear to have been totally replaced by pyrite.

Most massive sulphide deposits in the Iberian pyrite belt are underlain by steeply inclined or vertical

stockwork zones, and show various degrees of zone refining, producing chalcopyrite enrichment near the base of the massive sulphide (Marcoux et al., 1998). The quartz of quartz-sulphide veins in the stockwork systems have yielded fluid inclusions with salinities much greater than that of seawater at San Telmo, San Miguel and Aguas Teñidas Este in the north (Sánchez-España et al., 2000), Rio Tinto (Nehlig et al., 1998) and Masa Valverde (Toscano et al., 1997a) in the centre, and Aznalcóllar and Los Frailes (Toscano et al., 1997b; Almodóvar et al., 1998) in the south (Fig. 6). Proof of a primary origin for the inclusions has clearly been difficult in some cases, but many lie on growth zones in quartz crystals (for example, Almodóvar et al., 1998), and the inclusions are notably more saline than fluids associated with the later, Hercynian, deformation (for example, Sánchez-España et al., 2000). In the case of the first three examples, in the north of the belt, virtually all the ore-related inclusion fluids have salinities that would have reversed buoyancy on mixing with seawater, and ponded in basins if they existed (Fig. 5; Solomon et al., 2002). At Rio Tinto and Masa Valverde, some of the fluid inclusion compositions fall below the line dividing reversing-type and buoyant fluids. If these were the earliest fluids they would have behaved as black smokers and been lost to the ocean, but subse-

quent fluids would have ponded. If the low salinity fluids arrived after the brine pools were established they would most likely have mixed with pool fluids and reversed buoyancy, even if on occasions they overshot the brine-seawater interface. At Aznalcóllar and the adjacent Los Frailes lens, the inclusion fluids from deep in the stockwork lie above the reversing line, but immediately beneath the massive sulphides the fluids lie below it (Fig. 5). The distribution patterns of both groups of fluids indicates mixing between saline fluids and seawater. If this situation was maintained throughout the life of the system, then no brine pool would have formed, yet the high aspect ratio of both lenses (Almodóvar et al., 1998) suggests deposition in a basin from dense fluids. More work is clearly required to define further the fluid history.

Tornos and Spiro (1999) suggested that the Tharsis sulphides were deposited in a brine pool, based on the high aspect ratio of the orebodies, the relatively weak hanging wall alteration, and the absence of sulphate or oxidised facies, but there are no fluid inclusion data to support this thesis. However, not all Iberian pyrite belt deposits necessarily formed in brine pools because fluid inclusions in the quartz veins of the Salgadinho stockwork in western Portugal have salinities of ≤ 5.7 wt.% (Inverno et al., 2000), indicating the passage of fluids that would have remained buoyant on entering
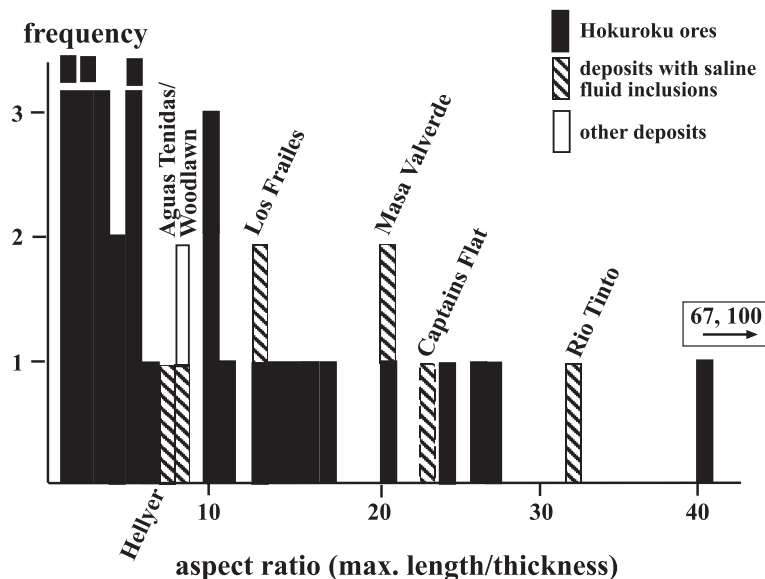
Fig. 7. Variation of aspect ratios (maximum length/average thickness) among the brine pool, Hokuroku and other ores mentioned in the text.

the ocean; no massive sulphide body was found above the stockwork.

4. Characteristics of the Hellyer and Iberian brine pool deposits, and comparisons with ores of the Hokuroku Basin

Many of the features of the deposits described above are listed in Tables 1 and 2, and compared to

typical polymetallic massive sulphide ores of the Hokuroku Basin.

4.1. Shape and size

In the case of brine pool deposits, for a given amount of ore-forming fluid, the shape in plan, the depth and the total area of the basin are obviously important controls over the form and size. For black-smoker-type systems, a basin may assist in preserving

Table 2
Comparisons between Hellyer, Hokuroko and Iberian pyrite belt ores

	Hellyer[a]	Iberian massive sulphide ores with saline stockwork fluids[b]	Hokuroku[c]
Ore types	barite-sulphide ore	no barite ore	Kuroko (black ore) has less barite than Hellyer barite cap, more sulphide
	Zn–Pb ore 15.5% Zn, 8.2% Pb (hangingwall enriched zone)	low Zn and Pb contents	no equivalent
	Cu core 0.48% Cu (footwall depleted zone), pyritic at base	Cu enrichment near base	Oko (yellow ore) has higher Cu, lower Zn and Pb
	veined chloritised and sericitised footwall, with siliceous core, sulphides in veins; uneconomic	veined, sericitised and chloritised footwall, economic at Rio Tinto (~ 1% Cu)	Keiko (siliceous ore): silica and pyrite, chalcopyrite and/or sphalerite in altered host rock; economic in some deposits (e.g. Kosaka)
Textures	framboids and veinlets common, local banding	framboids common, minor banding	framboids, banding and veinlets generally not common
Chimney evidence	none	none	fragments in several deposits
Grain size	variable, sub-micron upward	variable, mostly fine grained where undeformed	more coarsely grained overall
Mineral content of massive sulphide(s)	pyrite>sphalerite>galena>arsen-opyrite>chalcopyrite; no marcasite or barite	pyrite ≫ sphalerite>galena> chalcopyrite>arsenopyrite ± pyrrhotite; little or no marcasite, barite absent or rare in most	Kuroko: barite>sphalerite>galena> pyrite>chalcopyrite; rare marcasite Oko: pyrite ≈ chalcopyrite
fO_2	pyrite-arsenopyrite-stable	pyrite-arsenopyrite-stable	pyrite stable (As in tetrahedrite-tennantite)
FeS content of sphalerite	lower in Cu core than in Zn–Pb ore	variable, non-systematic	higher in Oko than Kuroko, but overall much lower than Hellyer
$\delta^{34}S$ trend in sulphides	increasing upward	no vertical change in massive sulphide (Rio Tinto, Aznalcóllar)	decreasing upward in Shakanai ores
$^{87}Sr/^{86}Sr$ in barite	values more radiogenic than coeval seawater or volcanic rock	no data for deposits with fluid inclusions	values between coeval seawater and volcanic rock
Fauna	bacteria indicated by local isotope fractionation	bacteria indicated by local isotope fractionation	no evidence
Fluid inclusion salinities	up to 15 wt.%	up to 14 wt.%	≤5.5 wt.%

[a] Data for Hellyer from Sharpe (1991), McArthur and Dronseika (1990), Gemmell and Large (1992, 1993), Whitford et al. (1992, 1993), McArthur (1996), Khin Zaw et al. (1996), Solomon and Khin Zaw (1997), Solomon and Gaspar (2001), Solomon et al. (2004).

[b] Data for the Iberian deposits from Almodóvar et al. (1998), Eastoe et al. (1986), Marcoux et al. (1998), McKee et al. (2001), Nehlig et al. (1998), (1998), Sánchez-España et al. (2000), Toscano et al. (1997a,b), Velasco et al. (1998).

[c] Data for Hokuroku ores from Kajiwara (1971), Shimazaki (1974), Urabe (1974), Bryndzia et al. (1983), Eldridge et al. (1983), Kalogeropoulis and Scott (1983), Ohmoto et al. (1983), Kusakabe and Chiba (1983), Pisutha-Arnond and Ohmoto (1983), Tanimura et al. (1983).

the sulphide but other factors are likely to be more important, such as the shape and stability of the ocean floor (the mounds may collapse gravitationally), and the means of preservation (for example, whether covered rapidly or not). Brine pool orebodies can extend well beyond the limits of the feeder pipe or upflow zone, and thereby achieve high aspect ratios, but black smoker types can only extend far from the fluid source by the coalescing of separate mounds, gravitational collapse or erosion. Black smoker types in general have aspect ratios mostly between 3 and 10 (Lydon, 1996), and Hokuroku ores have ratios mostly ≤10 but up to 100 (Tanimura et al., 1983; Table 1). The effects of mound collapse are well illustrated by Zn–Cu deposits in the southern Urals. Intact mounds, such as those at Sibaiskoye, have aspect ratios of 2–4 (Maslennikov et al., 2000; Table 1), but where extended laterally by gravitational collapse the aspect ratios are much higher, for example, the Alexandrinska deposit has ratios of 6–14, and at Mauk the aspect ratio is >15, the original mound having been completely destroyed (Maslennikov et al., 2000). Gravitational collapse may explain some of the high Hokuroku values. Hellyer has an aspect ratio of only 6.7, but the original Rio Tinto body (assuming gossan represents oxidized massive sulphide) has a value in the range 30–35, and Aguas Teñidas Este about 40 (Table 1). Clearly, shape alone cannot be a definitive criterion for distinguishing between buoyant and reversing-type systems, because of the control by basin form and problems of mound collapse, but nevertheless a sulphide lens formed on the sea floor having a high aspect ratio, with no evidence of extension by collapse, and a feeder zone much smaller in area or even outside the area of the deposit, is likely to have formed in a brine pool from negatively buoyant fluids.

Brine pools are able to trap 100% of the metal in the exhalative fluid, provided $\Sigma H_2S \geq \Sigma$metals and the fluid is retained in the pool for long enough to trap the metal content by precipitation of sulphides. In contrast, the depositional efficiency of the Hokuroku hydrothermal systems (i.e. the proportion of metal in the incoming fluids that is retained in the mound) is probably ≪100%. This is because some metal escapes from the mound in the buoyant, black smoker plumes, and only a small percentage of particles quenched in the plume settle onto the growing mound (<3%; Converse et al., 1984). There has as yet been no comparison between the amount of metal arriving at the base of the mound, and that being emitted through the chimneys, so the efficiency of precipitation in the mounds is not known. It may be lowest at the highest temperatures, when thermal buoyancy is at a maximum, and Ba, Zn and Pb are being removed from the lower part of the mound and not necessarily trapped in the upper part. Relative depositional efficiency might account for some of the disparity between the total metal content (Zn + Pb + Cu) of individual Hokuroku orebodies and those of Hellyer and the high-salinity Iberian orebodies (Table 1, Fig. 8), though there may be more fundamental reasons, such as the composition of the fluids. However, that large size and high metal content are not exclusive to brine pool systems is displayed by several of the orebodies in the southern Urals, for example, the four lenses of the Sibaiskoye deposit with total reserves of 110 Mt of 1.57 wt.% Cu and 0.38 wt.% Zn, which formed from buoyant fluids and are largely intact (Herrington and Little, 1999; Prokin and Buslaev, 1999; Large and Blundell, 2000; Maslennikov et al., 2000; Table 1).

4.2. Metal content

In the genetic models of Lydon (1988, 1996) and Ohmoto (1996) for the Hokuroku deposits, the early barite-sphalerite-galena ore (kuroko) grows upward by erection of sulphate (barite, anhydrite)-sulphide chimneys, followed by their collapse onto the sea floor. Later fluids rework, replace, add to, and modify the growing sulphate-sulphide mound. During subsequent elevation of the fluid temperature, the mound is replaced from the base upward by oko, which consists of pyrite and/or pyrite-chalcopyrite assemblages (the zone refining of Eldridge et al., 1983), in most cases yielding a vertically zoned deposit of Zn–Pb ore overlying Cu–Fe ore. Subsequent circulation of seawater probably removes anhydrite from the mound, leaving barite as the only sulphate.

At Hellyer, reworking of the earlier Zn–Pb assemblage in the Cu core resulted in loss of only 3–4% each of Zn and Pb, and increase in Cu from an average 0.34 to 0.48 wt.% Cu (McArthur, 1996). The small increase of Cu may be because much of the late Cu was deposited, mostly as chalcopyrite and tetrahedrite, on the top of the earlier Zn–Pb ore, forming an anomalous, discontinuous zone beneath the barite
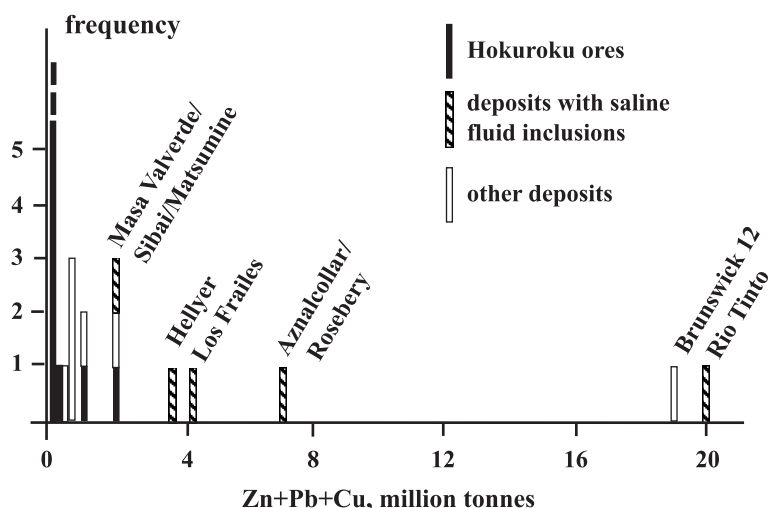
Fig. 8. Variation in metal content (as Zn + Pb + Cu in million of tonnes, from wt.% ore grades and tonnage) among brine pool, Hokuroku and other ores mentioned in the text.

cap with grades >0.5 wt.% Cu (Fig. 4). Only at the base of the massive ore above the siliceous core of the alteration cone was there massive, oko-type, pyrite> chalcopyrite replacement. Late fluids at Hellyer appear to have moved through earlier ore via fractures and fracture networks, precipitating new sulphides in the process and leaving the earlier-formed Zn–Pb ore more or less intact, rather than recrystallising and/or replacing entire assemblages (Solomon and Gaspar,

2001). This may explain in part the much higher Zn/ Cu ratio of Hellyer ore compared to Hokuroku ores, viz. 37 versus 19.2–0.6 (but mostly <10, Tanimura et al., 1983; Fig. 9, Table 1). Their respective oxidation potentials may also play a part, because the Zn/Cu values in a typical massive sulphide-forming fluid in equilibrium with pyrite, sphalerite and chalcopyrite decrease with increasing fO$_2$ (for example, Walshe and Solomon, 1981; Section 4.4).
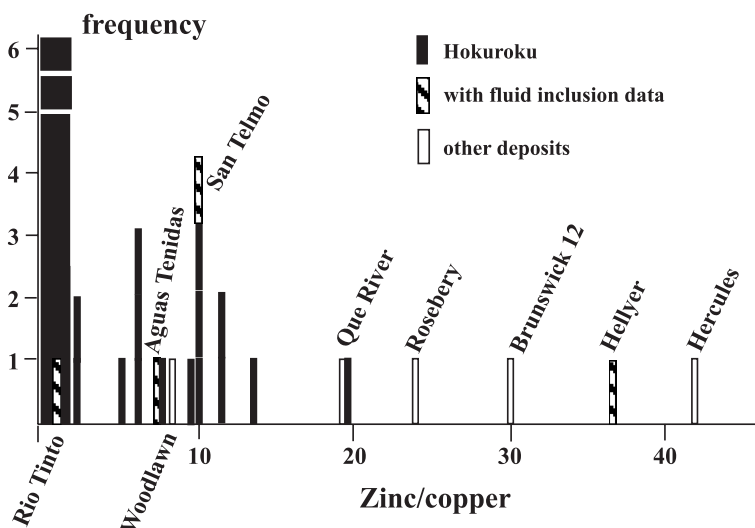
Fig. 9. Variation in Zn/Cu ratios (from wt.% ore grades) among brine pool, Hokuroku and other ores mentioned in the text.

Zone refining in the high-salinity Iberian deposits is also not as pronounced as it is in the Hokuroku ores, Marcoux et al. (1998) describing Cu enrichment only in the basal 1 to 2 m of massive sulphide. However, the Zn/Cu ratio is low, and Tornos et al. (1998) and Solomon et al. (2002) suggested that this reflected low Σ_S/Σ_{metal} values in the ore-forming fluids, resulting in deposition of Cu and Fe minerals but loss from the basins of the more soluble aqueous metal species.

Pre-refining (i.e., early) metalliferous deposition in the Hokuroku ores was dominated by barite, sphalerite and galena, whereas in Hellyer and the high-salinity Iberian ores, pyrite was dominant and barite largely absent. The different mineral contents combined with less intense high temperature zone refining in the brine-pool group mean that its members tend to have higher overall Fe/Cu ratios (Fig. 10, Table 1). This ratio for Hellyer is 63, while the largest ten Hokuroku ores (i.e., >2.5 Mt) average 7.4, plus one highly pyritic, low-grade ore at 41.0 (Tanimura et al., 1983). Fe/Cu data are available only for Rio Tinto (43) and Masa Valverde (105) among the high-salinity Iberian ores but the dominantly pyritic composition, and known Cu grades, result in mostly high estimated Fe/Cu values (Fig. 10). These differences in Fe/Cu may reflect primary variations in fluid composition related to the oxidation potentials of the fluids. For typical massive sulphide fluids at about 300 °C, Fe is more, and Cu less, soluble in solutions lying near the pyrite/arsenopyrite boundary than in solutions approaching the hematite boundary (Walshe and Solomon, 1981). In the calculations for the Mount Lyell ore-forming fluids, the variation in Fe/Cu ratio over the pyrite field is about an order of magnitude, close to the difference outlined above between Hellyer and Hokuroku ores. The different Fe/Cu values may also reflect differences in mode of formation on the sea floor. In the case of the proposed Hellyer brine pool, the exhaling fluid would have mixed with the cool, intra-pool fluid in a turbulent plume, and be effectively quenched. Such cooling could result in increased acidity (for example, see Reed and Spycher, 1985 for equilibrium cooling) but would also result in strong supersaturation of the highly soluble Fe monosulphides, leading to precipitation of pyrite precursors (Solomon and Gaspar, 2001). The main processes forming the Hokuroku-type mounds are probably also cooling, and to a lesser extent, pH increase, following mixing with seawater (Ohmoto et al., 1983). However, the thermal gradients in the mound would be shallower, and extend over a narrower temperature interval, than in the brine pool, with the result that Fe, particularly, is not wholly removed from solution and is partly lost in chimney-related plumes and diffuse flow from the mound surface.

4.3. Textures and grain size

Chimney fragments occur in many Hokuroku orebodies, supporting the concept of growth by chimney collapse and incorporation into the underlying mound (Lydon, 1988; Ohmoto, 1996; Figs. 1 and 11). However, despite the relatively undeformed nature of the Hellyer deposit and almost continuous observations during mining, none have been reported (McArthur, 1996); neither have they been found in any of the Iberian pyrite belt ores, despite focused search (F.J.A.S. Barriga, pers. comm., 2000). The lack of sightings testifies to the absence of sulphate-bearing seawater during massive sulphide growth, because sulphate deposition is an essential step in chimney formation. Evidence that the ambient seawater at Hellyer and in the Iberian pyrite belt contained sulphate is examined below (ore mineral assemblage).

The majority of the sulphide textures observed in the Hellyer and high-salinity Iberian deposits may be found in Hokuroku ores and also in sea-floor mounds at modern spreading centres; typical are microbotryoi-
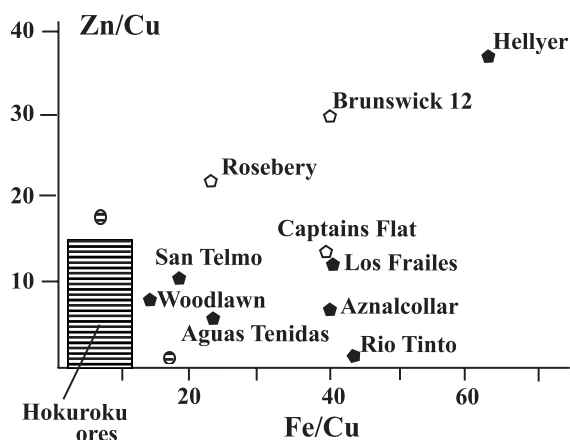

Fig. 10. Fe/Cu versus Zn/Cu (from wt.% ore grades) among brine pool, Hokuroku and other ores mentioned in the text.
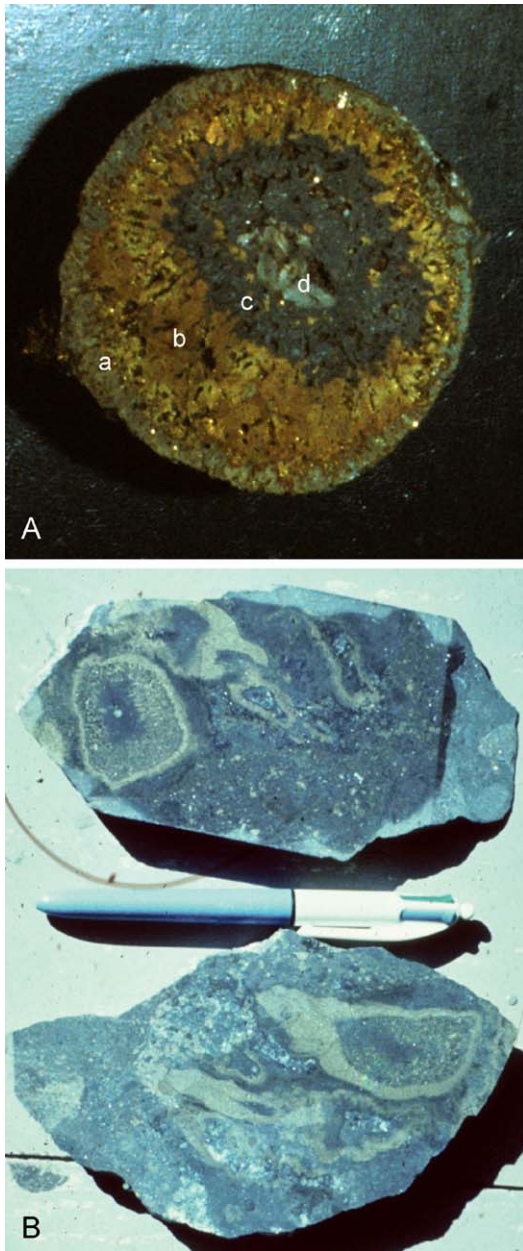
Fig. 11. Examples of chimneys and chimney fragments from Hokuroku ores. Photo A. Slice through a chimney about 10 cm diameter, from a Hokuroku mine; at the Akita museum. Four zones dominated by one mineral, viz. (a) pyrite, (b) chalcopyrite, (c) sphalerite, (d) barite. Photo B. "Tigers eye" samples from Matsumine mine. Pen about 14 cm long. The photographs were taken in 1981 with the assistance of Tetsuro Urabe (University of Tokyo).

dal or reniform, reticulate, bladed, and fibrous textures, all commonly described as "colloform". They result from a high degree of supersaturation consequent upon rapid cooling, and represent the products of early, fast crystal growth (for example, Rimstidt, 1997). However, the brine pool sulphides differ in the frequency of occurrence of framboidal pyrite, and in the presence of mineral banding. Both these textures are present in black-smoker types (for example, Ito et al., 1974; Eldridge et al., 1983), but framboidal pyrites are common in Hellyer ore and widely reported in Iberian deposits, and banding occurs locally in Hellyer and Iberian ores (Williams et al., 1975; McArthur, 1996; Velasco et al., 1998; Solomon and Gaspar, 2001).

For Hellyer, Solomon and Gaspar (2001) suggested that, unlike conditions in black-smoker-type deposits, the formation of fine grained, particulate, metal-sulphur compounds on the sea floor as a result of quenching in the brine pool provided ideal conditions for development of framboidal pyrite from early-formed, possibly amorphous, Fe monosulphides. Whether the framboids formed during the initial quenching in the brine pool, or somewhat later within the sulphide mud, was not made clear. Wilkin and Barnes (1997) concluded that framboid formation involves precipitation of early Fe monosulphides, followed by mackinawite then greigite, and that the mackinawite-greigite transformation proceeds in the solid state in the presence of an oxidant such as O_2. Butler and Rickard (2000), however, found that framboids can form directly from mackinawite, perhaps via a stoichiometric solution process involving oxidation of S^{II} by aqueous H_2S, and that framboidal rather than euhedral form is favoured by rapid nucleation and/or slow crystal growth. The critical energy required to initiate nucleation is inversely related to the degree of supersaturation; the number of crystals formed in a given time is inversely, and the rate of crystal growth directly, related to the diffusion constant (Mullin, 1993). A high degree of supersaturation would follow quenching of the ore-forming fluids to brine-pool temperature, and be further enhanced near the anoxic-oxic boundary at the brine/seawater interface, because of the lower solubility at higher oxidation potential. The less frequent occurrence of framboids in Hokuroku ores fits with the likely shallower gradients of pyrite supersaturation beneath

and within the sulphide mounds and in the chimneys, compared to gradients developed during quenching of hot fluids in a relatively cool brine pool.

Stratiform sulphide mineral banding, with single bands dominated by one or two sulphide minerals, was found near the top of the Hellyer massive sulphide body (McArthur, 1996), consisting mostly of pyrite-rich bands 10 mm or so thick and sphalerite-galena-rich bands, both types of bands being very fine grained (Solomon and Gaspar, 2001). Similar banding has been reported from the Rio Tinto and Masa Valverde massive sulphide ores (Williams, 1934; Ruiz et al., 2002). Differential settling of particles of similar size under gravity alone cannot account for such bands (for example, galena does not form monomineralic bands) but it might do so if combined with different rates of nucleation and crystal growth. Banding in Hokuroko ores appears to be confined to more coarsely grained, fragmental material formed by mound erosion and transport (for example, the Matsumine deposit with high aspect ratio (Ito et al., 1974; Table 1), or the Furutobe mine (Ohmoto and Skinner, 1983).

The generally coarser grain size of the Hokuroku ores compared to the brine pool ores may reflect the greater degree of recrystallisation and reworking of the former during zone refining. Early kuroko (black ore) lies over the vent unless disturbed by gravitational collapse, and hence all or most of the mound is subject to reworking by later fluids. In brine pools, the sedimented sulphides may spread as far as the basin allows, and only that part of the sulphide mass overlying the hydrothermal vent or vents may be affected by zone refining. If the vent lies outside the basin there is unlikely to be any zone refining.

4.4. Ore mineral assemblage

The Hellyer and high-salinity Iberian brine pool deposits are characterised by pyrite-arsenopyrite or pyrite-pyrrhotite assemblages that are not products of metamorphism, i.e., they were derived from relatively reduced, ore-forming fluids. These may have remained reduced even if cooled rapidly by oxic seawater, judging by the lack of marked oxidation in modern sea floor mounds during their formation (excluding subsequent oxidation by sea-floor weathering), but the lack or scarcity of associated barite

suggests that seawater was not involved. Significant Ba enrichment has been reported from the sericitized footwall rocks at Hellyer (Gemmell and Fulton, 2001), Rio Tinto and Masa Valverde (Leistel et al., 1998a), and slight enrichment in the San Miguel, San Telmo and Aguas Teñidas Este deposits (Sánchez-España et al., 2000). If Ba was present in the ore-forming fluids, then mixing with seawater would have resulted in rapid barite precipitation, even at low temperature (Ohmoto, 1996). Note that the barite sulphur at Hellyer has $\delta^{34}S$ values up to 16‰ greater than that of ambient seawater sulphate (Sharpe, 1991). According to McDougall (1984), at steady state in brine pools fed from below there is little or no entrainment across the brine/seawater interface, and the lack of evidence of seawater involvement in the deposits under consideration suggests this condition prevailed for much of the mineralising period. The incoming plume could have broken through the interface and mixed with seawater, and seawater must have been introduced during early development of the pool following mixing and buoyancy reversal, but these processes seem not to have been of sufficient importance to oxidize the pool fluids, or produce significant barite. Diffusion of O_2 across the brine-seawater interface could have contributed to minor oxidation (Solomon and Gaspar, 2001), but would only have become significant well after hydrothermal flow ceased.

Eastoe and Gustin (1996) attempted to explain the lack of barite and evidence of oxidation in many massive sulphide deposits by proposing that the distribution through time of sulphate-free, reduced ores is correlated with periods of widespread ocean anoxia, or in some cases, local anoxic conditions. However, none of the anoxia proposed by these authors or others have been established by independent analysis of the associated sedimentary rocks, and are mostly based on the relative abundance of only moderately carbonaceous sedimentary rocks. Some of the problems associated with establishing anoxia in such terrains were discussed by Solomon (1999), in a reply to the proposition by Goodfellow and Peter (1996) that the Brunswick no. 12 ore was derived from oxygen- and sulphate-free seawater. We suggest that the presence or absence of sulphate in the ore-forming fluids might be most closely dependent on the amount of reductant in the deep footwall, and/or

the length of time for which seawater circulation persisted. That seawater was a major component of the deep fluid systems is suggested by sulphur isotopic compositions of the ore minerals (Gemmell and Large, 1992; Velasco et al., 1998).

In the stratigraphic sequence at Hellyer, there is independent evidence that ambient seawater was oxic. Shales overlying pillow lavas that comprise the hanging wall rocks contain trilobites and sessile benthic graptolites (Solomon and Gaspar, 2001), even though Goddéris et al. (2001) estimated Cambrian atmospheric PO_2 at about 0.1 PAL. In the Iberian pyrite belt, shales in the uppermost part of the volcano-sedimentary host sequence contain radiolarian cherts and jaspers (Leistel et al., 1998b), and the overlying shales and greywackes of the Flysch or Culm Group contain goniatites (Williams, 1934). Parts of the host sequence contain ripple marks and other evidence of shallow water (Oliveira and Quesada, 1998), but these authors assumed that the ores were deposited in adjacent deep-water basins. These data allow anoxic bottom layers in these deeper basins, but such stratification seems unlikely given the coeval volcanic activity in much of the belt. In addition, the shales hosting the Filon Norte ore at Tharsis have "normal" C/S ratios (Tornos et al., 2003), and Tornos and Conde (2003) discovered a worm burrow at the base of the massive sulphide ore. One of us (JNPB) found that, on the southern margin of the basin containing the Atalaya (Rio Tinto) massive sulphide sheet (see Badham, 1982), the sericite-pyrite veins high on the basin rim were overprinted by a descendant epidote-hematite assemblage, leading him to suggest that this level was above the Fe^{3+}/Fe^{2+} boundary—is this the ancient seawater/brine interface? That seawater in the Hokuroku basin was oxic is indicated by the tetsusekiei (hematitic chert) overlying many of the orebodies (Kalogeropoulis and Scott, 1983).

The mineral content of the Hokuroku ores indicates oxidation potentials of the ore-forming fluids that are higher than for Hellyer and the high-salinity Iberian deposits. Arsenopyrite and pyrrhotite, in particular, are not recorded in Hokuroku ores, either in the sulphide mounds or the stockwork zones (Shimazaki, 1974). Higher fO_2 in fluids reaching the sea floor might be explained by subsurface entrainment of seawater. Lu (1983) attributed to such a process the upward decreases in salinity and temperature of fluid

inclusions in the siliceous footwall ore of the Uchinotai East deposits. Slow, equilibrium mixing of entrained seawater and ore-forming fluids in the stockwork zones could decrease fO_2, but rapid mixing could increase it dramatically (Ohmoto et al., 1983). Mixing clearly did not increase the oxidation potential to the level of seawater, but may be the cause of the higher oxidation potential of the Hokuroku fluids. Solomon et al. (in press) showed that rare high $\delta^{34}S$ values in the footwall veins at Hellyer could be the result of partial sulphate reduction of entrained seawater sulphate, but there is no decrease in temperature of salinity of the fluid inclusions with depth, indicating that such entrainment is probably a minor process. Further evidence of at least intermittent entrainment in the seawater-derived carbon in carbonates is seen in the cores of early veins in the Hellyer footwall. Trends of decreasing salinity and temperature in the fluid inclusions from several of the Iberian deposits (Fig. 5) also point to subsurface entrainment of cool seawater and mixing with hot ore-forming fluids.

A mineralogical characteristic of the brine pool deposits that contrasts with modern black-smoker deposits, but not Hokuroku ores, is the lack of marcasite. Marcasite is fairly common in modern mid-ocean ridge sulphide deposits (for example, Graham et al., 1988; Hannington and Scott, 1988), presumably because the related fluids are at very low pH (Von Damm, 1990). It might also be expected at Hellyer, because the lack of feldspar (McArthur, 1996), and the presence of abundant sericite, suggests pH values of <4 at 250 °C, using the average PIXE fluid inclusion data of Khin Zaw et al. (1996). Its absence may reflect the reduced conditions, marcasite requiring $10^{-5}-10^{-6}$ m of oxidized aqueous sulphur species (Benning et al., 2000; Solomon and Gaspar, 2001). A similar point was made by Solomon et al. (2002) for the brine-pool deposits in the Iberian pyrite belt, marcasite being recorded only as absent, trace or rare by Marcoux et al. (1998) and Carvalho et al. (1999). However, the acidities for the Iberian fluids have not been determined, and the common presence of carbonates may indicate that in addition to the low oxidation potential, they were not sufficiently acid. Marcasite is also rare in Hokuroku deposits and this may also reflect a relatively high pH, because Ohmoto (1996) estimated pH values of 4.5 to 5, between about 200 and 300 °C, for fluids in the footwall sericite-

chlorite zone (local kaolinite was attributed to occasional pulses of fluid in which hydration of magmatic SO_2 occurred).

4.5. Sulphur isotopic and mineral composition variation

The Shakanai No. 1 deposit is the only Hokuroku orebody examined in some detail by sulphur isotopic analysis. Kajiwara (1971) showed that there was a small upward decline in $\delta^{34}S$ values through the massive sulphide from pyrite through oko to the top of kuroko; a similar trend was recorded by Bryndzia et al. (1983) in the Uwamuki no. 4 stockwork in passing from yellow siliceous ore to black siliceous ore. This trend could reflect variation in temperature, and/or SO_4^{2-}/H_2S. In contrast, there is no significant change of $\delta^{34}S$ values at Hellyer in passing up the feeder vein system from 500m below the massive sulphide and through the massive sulphide body, but the sulphides show slightly higher $\delta^{34}S$ values in the overlying barite, and significantly higher values in the silica cap. The massive ore averages 6.9‰ the barite-sulphide ore 8.3‰ and the silica-sulphide bodies 12.4‰ possibly due to an increased content of sulphur derived from reduction of seawater sulphate (data from Sharpe, 1991; Gemmell and Large, 1992, 1993; Solomon et al., in press). There is no significant vertical variation in values through the Rio Tinto massive sulphide ore in the Atalaya open pit (Eastoe et al., 1986), and Velasco et al. (1998) reported no vertical variation in the Aguas Teñidas Este and Aznalcóllar deposits.

There is an upward decline in the FeS content of sphalerite from oko to kuroko in several Hokuroku deposits (Urabe, 1974), attributed by Urabe and Sato (1978) to an increasing seawater input into the ore-forming fluid with time, causing a decline in temperature and increasing fS_2. It could also have resulted from temperature and fO_2 gradients within the sulphide mound. For the Hellyer deposit, McArthur (1996) determined that the FeS contents of sphalerite are, on average, lower in the Cu core (3.1 wt.% FeS) than in the Zn–Pb ore (4.9 wt.% FeS), the opposite of the Hokuroku situation. Solomon and Gaspar (2001) suggested that the Cu core values may have developed late in the mineralization history, during passage of fluids with increased SO_4^{2-}/H_2S and lower temperature through the Cu core to the barite cap, where similar FeS contents were found in sphalerite by Sharpe (1991). There is a considerable variation in the FeS contents of the sphalerites in massive sulphide and stockwork veins of the San Telmo, Rio Tinto and Aznalcóllar ores in the Iberian pyrite belt (0.03–11.4 mol%, Leistel et al., 1998c). These authors showed that these sphalerites belong to the Zn–Ag–As–Au association, in which assemblage the sphalerites tend to have lower FeS contents compared to those of the later Co–Bi–Au association (for example, Tharsis and Sotiel, with up to 14 mol% FeS).

4.6. Strontium isotopic composition of barite

Kusakabe and Chiba (1983) found, for the barites of the Fukazawa ores in the Hokuroku Basin, that the $^{87}Sr/^{86}Sr$ values (ca. 0.70695–0.70802) lie between that of seawater (0.7088) and of Miocene volcanic rocks (0.703–0.705). These authors suggested, based on the Sr, S and O isotopic data, that the barite formed by mixing cold, ambient seawater (up to 30%) with a hot fluid containing Ba and both reduced and oxidized sulphur species. In contrast, Whitford et al. (1992, 1993) showed that the $^{87}Sr/^{86}Sr$ values of the Hellyer barites (0.70989–0.71144) are more radiogenic than those of both 500 Ma seawater (ca. 0.7091, Veizer et al., 1999) and the local volcanic rocks (0.7063–0.7080 in clinopyroxene), suggesting that the ore-forming fluids had penetrated deep into radiogenic basement. There is no equivalent data for the brine-pool ores from the Iberian pyrite belt.

4.7. Carbonates

Carbonates in Hokuroku ores occur only in post-ore veins (Ohmoto et al., 1983), but carbonates of various compositions are found in Hellyer and the high-salinity Iberian ores, and/or the altered footwall rocks and stockwork veins. The carbonates vary from deposit to deposit, and include calcite, ferruginous dolomite, rhodochrosite, kutnahorite and siderite (for example, Carvalho et al., 1999). At Hellyer, dolomite occurs in the cores of feeder veins, and stable isotope data indicate that the carbon was derived largely from seawater, possibly with a magmatic or organic carbon component (Solomon et al., in press). In the Iberian brine-pool examples, carbonates occur in ore and

stockwork veins. Though there are no stable isotope data for the brine-pool types, the carbon of the Feitais (Aljustrel) stockwork has strongly negative $\delta^{13}C$ values and is probably largely of organic origin (C. Inverno, pers. comm., 2002), and the less negative values for siderite from Tharsis may indicate a similar origin (Tornos et al., 1998). Carbonates form in modern brine pools in the Gulf of Mexico, derived from oxidation of methane derived from microbial degradation of hydrocarbons (Behrens, 1988). In the Iberian brine-pool deposits, a slight increase in oxidation potential due to subsurface seawater entrainment might be sufficient to produce such oxidation, inducing carbonate precipitation.

4.8. Fauna

The many negative $\delta^{34}S$ values of the Aznalcóllar ore lens, and in a few of the samples of the Aguas Teñidas Este and Hellyer ores, suggest bacterial sulphate reduction of seawater sulphate during ore deposition in some of the high-salinity deposits. No such data have been recorded for the Hokuroku Basin, though bacteria are locally abundant in modern sea floor deposits (Scott, 1997). Specialised, sulphate-reducing, thermophyllic bacteria could have survived in the anoxic, acid brine pools envisaged by Solomon and Gaspar (2001) and Solomon et al. (2002), reducing minor seawater sulphate that was entrained in the footwall, or mixed in plumes that overshot the brine/seawater interface, or surviving from early pool formation.

Although brine pool fluids represent a hostile environment for macrofauna, Tornos and Conde (2003) have described a possible worm burrow at the basal of the Filon Norte (Tharsis) massive sulphide lens, suggesting that macrofauna may have existed in the early phases of mineralization. Enhanced biological activity might be expected around the pool rims, as shown by MacDonald et al. (1990), for example, who described abundant chemosynthetic mussel beds around an inactive, low temperature, hypersaline, anoxic pool (or "pockmark") on the continental shelf of the Gulf of Mexico.

Macrofauna preserved by sulphide replacement have been found in ancient Zn–Cu massive sulphide deposits formed on the sea floor in arc/back-arc environments ranging in age from Tertiary to Silurian

(Little et al., 1998; Herrington and Little, 1999), and are common on modern sea floor deposits (Scott, 1997). They might be expected in the essentially similar environment of the Hokuroku Basin, but have not been reported.

4.9. Summary

The main attributes, other than their fluid salinities, of the inferred Iberian and Hellyer brine pool deposits that help to differentiate them from Hokuroku-type black-smoker deposits appear from the above discussion to be: (1) potentially very large size and tonnage and high aspect ratio, (2) higher Zn/Cu and Fe/Cu values, (3) no evidence of chimneys, (4) relative abundance of framboidal pyrite and primary mineral banding, (5) reduced mineral assemblage (pyrite-arsenopyrite/pyrrhotite) and absence or scarcity of barite in massive sulphide, (6) presence of stratiform and/or vein coeval carbonates, (7) relative unimportance of zone refining, (8) lack of vertical variation in sphalerite and sulphur isotopic compositions, and (9) local evidence of bacterial sulphate reduction in massive sulphide.

5. Applying the criteria—the example of Rosebery

A number of Zn–Pb–Cu volcanic-hosted massive sulphide deposits have some or all of the features of the Hellyer and the high-salinity Iberian deposits, including, for example, Tharsis (Tornos et al., 1998) and those at Aljustrel (Barriga and Fyfe, 1988) in the Iberian pyrite belt; Rosebery, Hercules and Que River (Large et al., 1988; Lees et al., 1990) in Tasmania; Brunswick no. 12 (Luff et al., 1993) and Heath Steele (Hamilton et al., 1993) in the New Brunswick province of Canada; Captains Flat and Woodlawn (Davis, 1975; McKay and Hazeldene, 1987) in New South Wales; and Thalanga in Queensland (Gregory et al., 1990). That some of them may have been deposited in basins from dense fluids has already been suggested, based on various geological features (for example, Solomon, 1981; McKay and Hazeldene, 1987; Gregory et al., 1990; Tornos and Spiro, 1999). The Rosebery deposit is considered in some detail here as an example, because it is among the world's largest in terms of metal content, it is still being mined and its

mode of formation has been the subject of controversy for many years.

5.1. The Rosebery Zn–Pb–Cu–Au–Ag deposit

This deposit lies in the Cambrian Mount Read Volcanics of western Tasmania, about 25 km SSW of Hellyer (Fig. 3, Table 1). It consists of at least sixteen lenses lying within an east-dipping sequence of volcanic and sedimentary rocks (Brathwaite, 1974; Green et al., 1981; Berry and Keele, 1997; Figs. 12 and 13). The ore lenses lie within altered siltstones containing lenses of crystal-rich volcanic sandstone, overlain by grey, carbonaceous shales (the "black slate"), and then dacitic volcaniclastic and volcanic rocks, and underlain by altered, rhyolitic to dacitic volcaniclastic rocks. The strike extent of the "black slate" is approximately that of the ore lenses, suggesting that it might define a basin. Berry and Keele (1997) identified a number of Cambrian, fault-bounded sub-basins within the host rocks, and reported, somewhat optimistically, a "moderate" correlation between these basins and ore occurrences. The rocks underwent a major phase of folding and

faulting in the Devonian, so that the ore sequence lies between two parallel, east-dipping shears, and the ore lenses were disrupted by imbricate, high angle, reverse faults (Brathwaite, 1972; Aerden, 1993; Berry and Keele, 1997). The present discussion relates only to previously published studies, which mostly concern lenses from C to H, and, to a lesser extent, lenses A and B. Green (1983) assumed that the lenses were folded and tentatively unwound the Devonian deformation to reveal high aspect, rather irregular, sulphide sheets. However, later work suggested that they were disrupted by thrusts (Berry and Keele, 1997). Parts of the ore lenses south of about 100 mS have been replaced by pyrrhotite-pyrite and magnetite-biotite-chalcopyrite assemblages, thought to have been derived from reduced, acid fluids emanating from an underlying Devonian granitoid pluton (Brathwaite, 1974; Solomon et al., 1987; Khin Zaw et al., 1999).

The mineral content of the massive sulphide lenses (C to G) is dominated by pyrite, sphalerite, galena, chalcopyrite, and arsenopyrite ($<5\%$). There is no marcasite, but small lenses of hematite, magnetite and pyrite occur within some massive
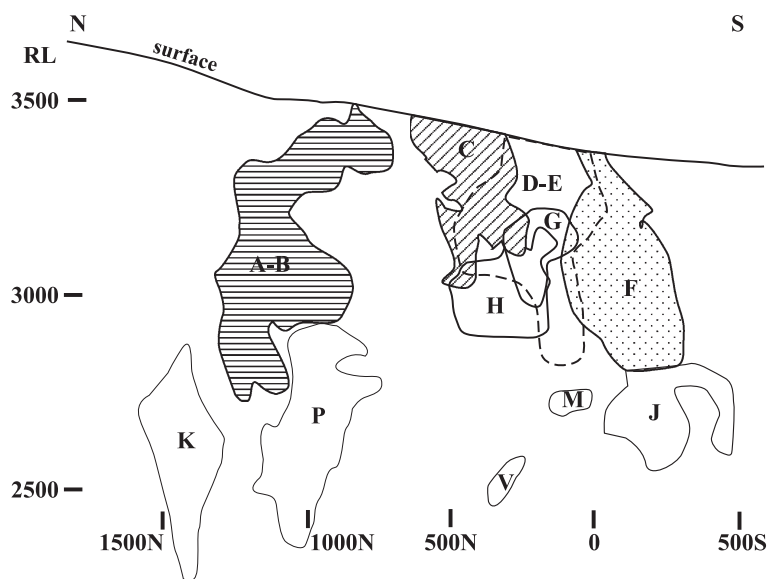
Fig. 12. Outlines of the major ore lenses at Rosebery mine, plotted from a figure by Graves et al. (1997) on a plane dipping at 45°, parallel to the dip of the host rock. No allowance has been made for stretching due to Devonian deformation, though there is a weak down-dip lineation (cf. Berry and Keele, 1997, who assumed that inevitable foreshortening on vertical longitudinal sections was matched by Devonian stretching). Different patterns for the ore lenses are to aid visualization.
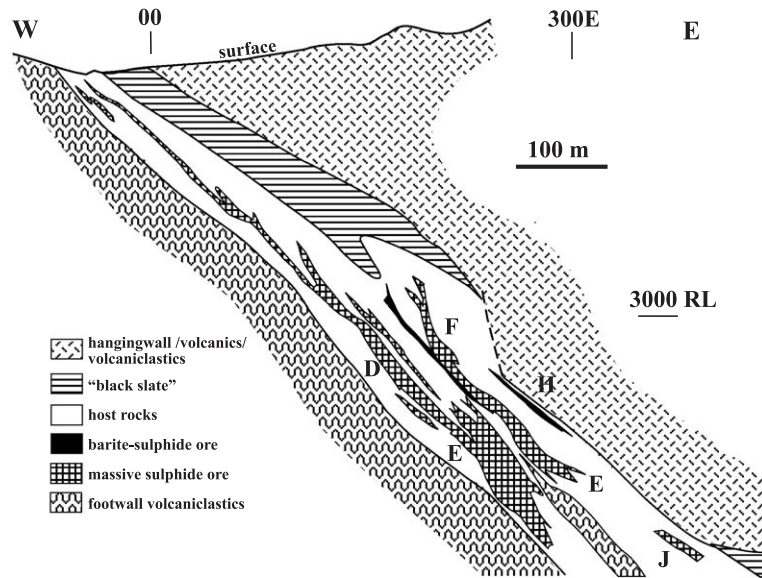
Fig. 13. Cross-section 500N of the Rosebery mine, looking north, from Green (1983).

sulphide lenses. Pyrite-chalcopyrite-rich assemblages lie at the base of several of the massive sulphide lenses, overlain or flanked by pyrite-sphalerite-galena-rich ore (Brathwaite, 1970, 1974; Green, 1983). At the base of some lenses, pyrite-chalcopyrite bands up to several cm thick alternate with phyllo-silicate bands (Brathwaite, 1970; observations by M. Solomon), showing that the Cu-rich ore has not been derived by zone refining of Zn–Pb-rich assemblages. Overlying the massive sulphide lenses, and generally separated from them by siltstone, is a lens (H lens) of barite containing sphalerite and galena. Carbonates (mostly Mn-bearing carbonates such as rhodochrosite and kutnahorite) occur within, and at the strike limits of, the southern massive sulphide lenses (Brathwaite, 1970, 1974; Dixon, 1980; Green et al., 1981; Khin Zaw, 1991). The largest carbonate bodies lie at the orebody margins, and are up to 400 m along strike and 30 m thick, with the greatest thicknesses at the massive sulphide margins, and appear to be primary precipitates contemporaneous with the base metal sulphides. Other carbonates replaced host rocks above and below the ore lenses.

The sulphides were annealed during Devonian deformation but mineral banding was preserved. Individual bands, millimeters to decimeters thick,

may be monomineralic or mixed, but are commonly dominated either by pyrite, or sphalerite and galena, or pyrite and chalcopyrite. The bands are parallel to bedding in the overlying sedimentary rocks but are locally folded within the sulphide lenses. Phyllosilicate minerals dominate in some bands, and Vokes (1983) reported numerous clasts of albite and vein quartz in banded ore from F lens. Few early sulphide textures are visible but Brathwaite (1970) recorded rhythmic concentric, fibrous, and very fine-grained spongy textures, and framboidal pyrites in chert. The barite of H lens commonly displays fine, stratiform banding and fresh, simply twinned albite is a common accessory.

The barite of H lens is clearly younger than the massive sulphide lenses, and with one exception, the $\delta^{34}S$ values of barite sulphur are considerably higher than that of ambient seawater sulphate ($\sim 30\%_0$ Claypool et al., 1980), ranging from $35.5\%_0$ to $41.2\%_0$ and thought by Green et al. (1981) and Green (1983) to have been derived by partial reduction of sulphate during deep convective circulation of seawater in the underlying rocks. A comparable origin for barite at Hellyer was proposed by Gemmell and Large (1992). The isotopic composition of Sr in the barite is similar to that of Hellyer (Whitford et al., 1992).

5.2. Formation of the Rosebery deposit on the sea floor

Brathwaite (1974) followed earlier tentative suggestions of an exhalative origin for the ore lenses A to H (e.g., Solomon et al., 1969), citing their stratiform, sheet-like, and banded nature, primitive textures, and metal zoning. The lack of evidence for more than minor sulphide replacement of the host rocks (for example, disseminated pyrite) provides further support for an exhalative origin. Solomon and Walshe (1979) suggested that the sulphides were sedimented from a plume that had stagnated at the seawater surface, while Green et al. (1981) proposed a derivation by sedimentation into a basin from plumes that at first remained buoyant, but later underwent buoyancy reversal. Huston and Large (1989) favoured zone refining of overlapping sea floor mounds to explain the mineral zonation and gold distribution, but Large (1992) recognised the difficulties in applying the Hokuroku models to Rosebery orebodies. Suggestions by Aerden (1993) that the ores are of syntectonic origin appear to be based on textures interpreted by Berry and Keele (1997) and others as due to local recrystallisation and crystal growth within the lenses during Devonian boudinaging and stretching of the massive sulphide sheets.

For lenses C to H, the following features point to an origin by deposition in a brine pool, in a similar way to that proposed for Hellyer: lack of evidence for massive sulphide deposition by replacement, stratiform layering and mineral banding, presence of albite and other mineral clasts and absence of chimney fragments, presence of coeval carbonates, overall high Zn/Cu and Fe/Cu values, reduced mineral assemblage (except for the minor pyrite-Fe oxide occurrences). Additionally, the S and Sr in barite has similar isotopic values to those of Hellyer barite. However, although the footwall is altered to a sericite-chlorite-quartz-pyrite assemblage and the Co content of pyrite is locally enriched (Green et al., 1981), no obvious feeder pipe for the ore fluids, such as seen at Hellyer, has been found. It is possible that the fluid source(s) lies elsewhere within the mineralised zone, or even outside it. If the latter, then the absence of barite with seawater sulphate compositions, and the minimal Fe-oxide occurrences, suggests that the source mostly lay within the reduced basin.

6. Zn–Pb–Cu brine pools and the oxidation potential of ore-forming fluids

We are unaware of any Zn–Pb–Cu ores with reduced mineral assemblages that have been shown from fluid inclusion data to have been formed from buoyant fluids. If reduced, black smoker-type deposits do exist, then they will provide a much better basis for comparing the features of brine pool-type ores with those of black smoker-type ores. Eastoe and Gustin (1996) implied such a situation for the West Shasta deposits of northern California, accounting for the presence of primary pyrrhotite and lack of barite by assuming anoxic, sulphate-free seawater, but as noted earlier, such an aqueous environment has not been demonstrated. It may be that the lack of reduced black smoker-type Zn–Pb–Cu deposits is the result of oxidation of ore-forming fluids at depth or on the sea floor during entrainment of, and mixing with, ambient seawater, as suggested earlier. From the evidence available to date it might appear that reduced-type Zn–Pb–Cu ores are likely to have formed from saline fluids, but it cannot be said that potentially reversing fluids are necessarily reduced, because recently published data suggest that brine pool deposits can form from oxidized ore-forming fluids. For example, fluid inclusions from the Gacun (Hou et al., 2001) and Mount Chalmers (Large and Both, 1980; Khin Zaw et al., 2003) pyrite-barite deposits extend to high salinities (21 and 13.7 wt.%, respectively), and brine pool deposition has been considered for both deposits. Further investigation into these occurrences might account for the relatively oxidized nature of the fluids, for example, as the result of boiling. As several of the distinguishing criteria developed for this paper relate to the reduced nature of the mineral assemblages involved, the list of criteria for oxidized ores is somewhat shorter, involving only the potentially very large size and tonnage, high aspect ratio, higher Zn/Cu and Fe/Cu values, presence of stratiform and coeval carbonates, no evidence of chimneys, relative abundance of framboidal pyrite and primary mineral banding, relative unimportance of zone refining, lack of vertical variation in sphalerite and sulphur isotopic compositions.

7. Conclusions

Fluid inclusions from quartz in the stockwork zones of the Hellyer and several Iberian massive sulphide deposits strongly suggest that these ores were deposited in brine pools. The ores differ from those of the Hokuroku Basin in having a tendency to larger maximum size and high aspect ratios, high Zn/Cu and Fe/Cu values, reduced mineral assemblages (pyrite-arsenopyrite $\pm$ pyrrhotite) and lack or scarcity of barite in massive sulphide, primary sulphide mineral banding, abundant framboidal textures in pyrite, presence of coeval, stratiform and/or vein carbonates, no upward decline of FeS contents of sphalerite or δ^{34}S values within the massive sulphides, and local evidence of bacterial sulphate reduction.

Most of these criteria apply to the southern ore lenses (A to H) at Rosebery, Tasmania, suggesting that they were also deposited in a brine pool or pools, and the criteria might usefully be applied to other ores such as Brunswick no. 12, Woodlawn and Thalanga. Available data suggest that all reduced, massive sulphide-forming fluids are saline, but not all saline, massive sulphide-related fluids are reduced. That brine pools may develop from more oxidized fluids, is indicated by the high salinities recorded in fluid inclusions from the Gacun and Mount Chalmers deposits.

Volcanic-hosted massive sulphide deposits are present in rocks as old as 3.5 Ga (for example, in the Pilbara, Vearncombe et al., 1995) and as young as the present day (for example, at mid-ocean ridges, Scott, 1997), and both Lydon (1996) and Solomon and Sun (1997) have suggested that the processes of ore formation have not changed substantially in the intervening period. Thus deposits of all ages are potentially brine-pool candidates. However, determinations of depositional origin in Archaean rocks may be made difficult by the special oceanic (and tectonic?) environments of that period (for example, the likely low oxygen and sulphate contents), and the bulk of the criteria outlined above may apply mostly to post-Archaean ores.

It should be emphasized that this discussion only concerns Zn–Pb–Cu-type ores, however, there are members of the Zn–Pb and Cu types that formed, or appear to have formed, in brine pools, including those of the Atlantis II Deep in the Red Sea (Scholten et al., 2000) and Windy Craggy in British Columbia (Peter and Scott, 1993), respectively.

Acknowledgements

References

Aerden, D.G.A.M., 1993. Foliation boudinage control on the formation of the Rosebery Pb–Zn orebody, Tasmania. Journal of Structural Geology 13, 759–775.

Allen, R.L., 2001. Volcanic facies in VHMS districts and their use in reconstructing stratigraphy: an example from Los Frailes-Aznalcóllar, Iberian Pyrite Belt. GEODE Workshop ''Massive sulphide deposits in the Iberian Pyrite Belt: New advances and comparison with equivalent systems''. University of Huelva, Huelva, Spain, pp. 1–3.

Almodóvar, G.R., Sáez, R., Pons, J.M., Maestre, A., Toscano, M., Pascual, E., 1998. Geology and genesis of the Aznalcóllar massive sulphide deposits, Iberian Pyrite Belt, Spain. Mineralium Deposita 33, 111–136.

Badham, J.P.N., 1982. Further data on the formation of ores at Rio Tinto, Spain. Transactions-Institution of Mining and Metallurgy. Section B. Applied Earth Science 91, 26–32.

Barriga, F.J.A.S., Fyfe, W.S., 1988. Giant pyritic base-metal deposits: the example of Feitais, Aljustrel, Portugal. Chemical Geology 69, 331–343.

Behrens, E.W., 1988. Geology of a continental slope oil seep, northern Gulf of Mexico. Bulletin of the American Association of Petroleum Geologists 72, 105–114.

Benning, L.G., Wilkin, R.T., Barnes, H.L., 2000. Reaction pathways in the Fe−S system below 100 °C. Chemical Geology 167, 25−51.

Berry, R.F., Keele, R.A., 1997. Cambrian tectonics and mineralization in western Tasmania. Publications of the Australasian Institute of Mining and Metallurgy 6/97, 13−16.

Brathwaite, R.L., 1970. The geology of the Rosebery ore deposits. Unpublished PhD thesis, University of Tasmania, Hobart, Australia, 218 pp.

Brathwaite, R.L., 1972. The structure of the Rosebery ore deposits, Tasmania. Australasian Institute of Mining and Metallurgy 241, 1−13.

Brathwaite, R.L., 1974. The geology and origin of the Rosebery ore deposit, Tasmania. Economic Geology 69, 1086−1101.

Broman, C., 1987. Fluid inclusions of the massive sulfide deposits in the Skellefte district, Sweden. Chemical Geology 61, 161−168.

Bryndzia, L.T., Scott, S.D., Farr, J.E., 1983. Mineralogy, geochemistry, and mineral chemistry of siliceous ore and altered footwall rocks in the Uwamuki 2 and 4 deposits, Kosaka mine, Hokuroku district, Japan. Economic Geology Monographs 5, 507−522.

Butler, I.B., Rickard, D., 2000. Framboidal pyrite formation via the oxidation of iron(II) monosulfide by hydrogen sulfide. Geochimica et Cosmochimica Acta 64, 2665−2672.

Carvalho, D., Barriga, F.J.A.S., Munhá, J., 1999. The Iberian Pyrite Belt of Portugal and Spain: examples of bimodal siliciclastic systems. Reviews in Economic Geology 8, 385−418.

Claypool, G.E., Holser, W.T., Kaplan, I.R., Sakai, H., Zak, I., 1980. The age curves of sulfur and oxygen isotopes in marine sulfate and their mutual interpretation. Chemical Geology 28, 199−260.

Converse, D., Holland, H.D., Edmond, J.M., 1984. Flow rates in the axial hot springs of the East Pacific Rise (21°N): implications for the heat budget and the formation of massive sulfide deposits. Earth and Planetary Science Letters 69, 159−175.

Corbett, K.D., 1992. Stratigraphic-volcanic setting of massive sulphide deposits in the Cambrian Mount Read Volcanics, Tasmania. Economic Geology 87, 564−586.

Davis, L.W., 1975. Captains Flat lead−zinc orebody. Monograph-Australasian Institute of Mining and Metallurgy 5, 694−700.

Dixon, G., 1980. Geological, mineralogical, and stable isotope studies of the carbonates of the Rosebery ore deposit. Unpublished BSc Hons. thesis, University of Tasmania, Hobart, Australia.

Downs, R.C., 1993. Syn-depositional fault controls on the Hellyer volcanic-hosted massive sulphide deposit. Unpublished M. Econ. Geol. thesis, University of Tasmania, Hobart, Australia. 62 pp.

Doyle, M.G., 2001. Volcanic influences on hydrothermal and diagenetic alteration: evidence from Highway-Reward, Mount Windsor subprovince, Australia. Economic Geology 96, 1133−1148.

Eastoe, C.J., Gustin, M.M., 1996. Volcanogenic massive sulfide deposits and anoxia in the Phanerozoic oceans. Ore Geology Reviews 10, 179−197.

Eastoe, C.J., Solomon, M., Palomero, G.F., 1986. Sulphur isotope study of massive and stockwork pyrite deposits at Rio Tinto, Spain. Transactions-Institution of Mining and Metallurgy. Section A. Mining industry 95, 201−207.

Eldridge, C.S., Barton Jr., P.B., Ohmoto, H. 1983. Mineral textures and their bearing on formation of the Kuroko orebodies. Economic Geology Monograph 5, 241−281.

Franklin, J.M., 1996. Volcanic-associated massive sulphide base metals. In: Ekstrand, O.R., Sinclair, W.D., Thorpe, R.I. (Eds.), Geology of Canadian Mineral Deposits. Geological Survey of Canada, Geology of Canada, vol. 8, pp. 158−183.

García Palomero, F., 1990. Rio Tinto deposits—geology and geological models for their exploration and ore-reserve estimation. In: Gray, P.M.J., Bowyer, G.J., Castle, J.F., Vaughan, D.J., Warner, N.A. (Eds.), Sulphide Deposits—Their Origin and Processing. Institution of Mining and Metallurgy, London, pp. 17−35.

Gaspar, O.C., 1996. Microscopia e petrologia de minérios aplicadas à génese, exploração e mineralurgia dos sulfuretos maciços dos jazigos de Aljustrel e Neves-Corvo Estudos Notas e Trabalhos do Instituto Geológico e Mineiro, Lisbon. 195 pp.

Gemmell, J.B., Fulton, R., 2001. Geology, genesis, and exploration implications of the footwall and hangingwall alteration associated with the Hellyer VHMS deposit, Tasmania, Australia. Economic Geology 96, 1003−1035.

Gemmell, J.B., Large, R.R., 1992. Stringer system and alteration zones underlying the Hellyer volcanic-hosted massive sulfide deposits, northwestern Tasmania. Economic Geology 87, 620−649.

Gemmell, J.B., Large, R.R., 1993. Evolution of a volcanic-hosted massive sulphide hydrothermal system, Hellyer deposit, Tasmania, Australia: sulfur isotope evidence. Resource Geology Special Issue 17, 108−119.

Goddéris, Y., François, L.M., Veizer, J., 2001. The early Paleozoic carbon cycle. Earth and Planetary Science Letters 190, 181−196.

Goodfellow, W.D., Peter, J.M., 1996. Sulphur isotope composition of the Brunswick N. 12 massive sulphide deposit, Bathurst Mining Camp, New Brunswick: implications for ambient environment, sulphur source, and ore genesis. Canadian Journal of Earth Sciences 33, 231−251.

Graham, U.M., Bluth, G.J., Ohmoto, H., 1988. Sulfide-sulfate chimneys on the East Pacific Rise, 11° and 13°N latitudes: Part 1. Mineralogy and paragenesis. Canadian Mineralogist 26, 487−504.

Graves, C.C., Carnie, C.W.A., Hale, C.T., 1997. Rosebery mine exploration—recent successes. Publications of the Australasian Institute of Mining and Metallurgy 6/97, 21−24.

Green, G.R., 1983. Geological setting and formation of the Rosebery volcanic-hosted massive sulphide orebody, Tasmania. Unpublished Ph.D. thesis, University of Tasmania, Hobart, 288 pp.

Green, G.R., Solomon, M., Walshe, J.L., 1981. The formation of the volcanic-hosted massive sulfide ore deposit at Rosebery, Tasmania. Economic Geology 76, 304−338.

Gregory, P.W., Hartley, J.S., Wills, K.J., 1990. Thalanga zinc−lead−copper−silver deposit. Monograph-Australasian Institute of Mining and Metallurgy 14, 1527−1537.

Hamilton, A., Park, A., Moreton, C., 1993. Geology of Heath Steele mines, Bathurst Camp, New Brunswick. In: McCutcheon, S.R., Lentz, D.R. (Eds.), Guidebook to the metallogeny of the Bathurst Camp, Guidebook 4, Annual Field Conference, Geological Society of the Canadian Institute of Mining, 50−65.

Hannington, M.D., Scott, S.D., 1988. Mineralogy and geochemistry

of a hydrothermal silica–sulfide–silicate spire in the caldera of Axial Seamount, Juan de Fuca Ridge. Canadian Mineralogist 26, 603–625.

Herrington, R.J., Little, C.T.S., 1999. Ancient hydrothermal vent communities associated with volcanic-hosted massive sulfide deposits: evidence of seafloor venting. In: Gemmell, B.J., Pongratz, J. (Eds.), Volcanic Environments and Massive Sulfide Deposits. Centre for Ore Deposit Research, University of Tasmania, Hobart, pp. 79–80.

Hidalgo, R., Guerrero, V., Pons, J.M., 2001. Geology of the Aguas Teñidas Este mine, southern Spain. GEODE Workshop: Massive sulphide deposits in the Iberian pyrite belt. New advances and comparison with equivalent systems, Aracena, Field Guide.

Hou, Z.-Q., Khin Zaw, Qu, X.-M., Ye, Q.-T., Yu, J.-J., Xu, M.-G., Fu, D.-M., Yin., X.-K.Origin of the Gacun volcanic-hosted massive sulfide deposit in Sichuan, China: fluid inclusion and oxygen isotope evidence. Economic Geology 96, 1491–1512.

Huston, D.L., Large, R.L., 1989. A chemical model for the concentration of gold in volcanogenic massive sulfide deposits. Ore Geology Reviews 4, 171–200.

Inverno, C., Lopes, C.J.C.D., d'Orey, F.L.C., Carvalho, D., 2000. The Cu (-Au) stockwork deposit of Salgadinho, Cercal, Pyrite Belt, SW Portugal—paragenetic sequence and fluid inclusion investigation. In: Gemmell, J.B., Pongratz, J. (Eds.), Volcanic Environments and Massive Sulfide Deposits. CODES Special Publication 3 Centre for Ore Deposit Research, Hobart, pp. 99–101.

Ito, T., Takahashi, T., Omori, Y., 1974. Submarine volcanic-sedimentary features in the Matsumine Kuroko deposits, Hanaoka mine, Japan. Mining Geology Special Issue 6, 115–130.

Kajiwara, Y., 1971. Sulfur isotope study of the Kuroko-ores of the Shakanai no. 1 deposits, Akita Prefecture, Japan. Geochemical Journal 4, 157–181.

Kalogeropoulis, S.I., Scott, S.D., 1983. Mineralogy and geochemistry of tuffaceous exhalites (tetsusekiei) of the Fukazawa mine, Hokuroku district, Japan. Economic Geology Monographs 5, 412–432.

Khin Zaw, 1991. The effect of Devonian metamorphism and metasomatism on the mineralogy and geochemistry of the Cambrian VMS deposits in the Rosebery-Hercules district, western Tasmania. Unpublished PhD thesis, University of Tasmania, Hobart, Tasmania. 302 pp.

Khin Zaw, S.D., Gemmell, J.B., Large, R.R., Mernagh, T.P., Ryan, C.G., 1996. Evolution and source of ore fluids in the stringer system, Hellyer VHMS deposit, Tasmania, Australia: evidence from fluid inclusion microthermometry and geochemistry. Ore Geology Reviews 10, 251–278.

Khin Zaw, C.G., Huston, D.L., Large, R.R., 1999. A chemical model for the Devonian remobilization process in the Cambrian volcanic-hosted massive sulfide Rosebery deposit, western Tasmania. Economic Geology 94, 529–546.

Khin Zaw, Hunns, S.R., Large, R.L., Gemmell, J.B., Ryan, C.G., Mernagh, T.A.P., 2003. Microthermometry and chemical composition of fluid inclusions from the Mt Chalmers volcanic-hosted massive sulfide deposits, central Queensland, Australia: implications for ore genesis. Chemical Geology 194, 225–244.

Kusakabe, M., Chiba, H., 1983. Oxygen and sulfur isotope composition of barite and anhydrite from the Fukazawa deposit, Japan. Economic Geology Monographs 5, 292–301.

Large, R.R., 1992. Australian volcanic-hosted massive sulfide deposits: features, styles, and genetic models. Economic Geology 97, 471–510.

Large, R.R., Blundell, D. (Eds.), 2000. Database of Global VMS Districts. Centre for Ore Deposit Research, Hobart. 179 pp.

Large, R.R., Both, R.A., 1980. The volcanogenic sulfide ores at Mount Chalmers, eastern Queensland. Economic Geology 75, 992–1009.

Large, R.R., McGoldrick, P.J., Berry, R.F., Young, C.H., 1988. A tightly folded, gold-rich, massive sulfide deposit: Que River mine, Tasmania. Economic Geology 83, 681–693.

Lees, T., Zaw, K., Large, R.R., Huston, D.L., 1990. Rosebery and Hercules copper–lead–zinc deposits. Monograph-Australasian Institute of Mining and Metallurgy 14, 1241–1247.

Leistel, J.M., Marcoux, E., Thiéblemont, D., Queseda, C., Sánchez, A., Almodóvar, G.R., Pascual, E., Sáez, R., 1998a. The volcanic-hosted massive sulphide deposits of the Iberian Pyrite Belt. Mineralium Deposita 33, 2–30.

Leistel, J.M., Marcoux, E., Deschamps, Y., 1998b. Chert in the Iberian pyrite belt. Mineralium Deposita 33, 59–81.

Leistel, J.M., Marcoux, E., Deschamps, Y., Joubert, M., 1998c. Antithetic behaviour of gold in the volcanogenic massive sulphide deposits of the Iberian pyrite belt. Mineralium Deposita 33, 82–97.

Little, C.T.S., Herrington, R.J., Maslennikov, V.V., Morris, N.J., Zaykov, V.V., 1998. The fossil record of hydrothermal vent communities. In: Mills, R.A., Harrison, K. (Eds.), Modern Ocean Floor Processes and the Geological Record. Special Publication-Geological Society of London, vol. 148, pp. 259–270.

Lu, K.I., 1983. Geology and geochemistry of the Uchinotai-East ore deposit, Kosaka mine, Akita Prefecture, Japan. Mining Geology 33, 367–384.

Luff, W.M., Lentz, D.R., van Staal, C.R., 1993. The Brunswick no. 12 and no. 6 mines, Bathurst Camp, northern New Brunswick. In: McCutcheon, S.R., Lentz, D.R. (Eds.), Guidebook to the Metallogeny of the Bathurst Camp, Guidebook 4, Annual Field Conference, Geological Society of Canadian Institute of Mining, 75–105.

Lydon, J.W., 1988. Ore deposit models: 14. Volcanogenic massive sulfide deposits: Part 2. Genetic models. Geoscience Canada 15, 43–65.

Lydon, J.W., 1996. Characteristics of volcanogenic massive sulphide deposits: interpretation in terms of hydrothermal convection systems and magmatic hydrothermal systems. Boletin Geológico y Minero 107, 215–264.

McArthur, G.J., 1996. Textural evolution of the Hellyer massive sulfide deposit. Unpublished PhD thesis, University of Tasmania, Hobart, Australia. 272 pp.

McArthur, G.J., Dronseika, E.V., 1990. Que River and Hellyer zinc–lead–silver deposits. Monograph-Australasian Institute of Mining and Metallurgy 14, 1229–1239.

MacDonald, I.R., Reilly II, J.F., Guinasso Jr., N.L., Brooks, J.M., Carney, R.S., Bryant, W.A., Bright, T.J. 1990. Chemosynthetic mussels at a brine-filled pockmark in the northern Gulf of Mexico. Science 248, 1096–1099.

McDougall, T.J., 1984. Fluid dynamic implications for massive sulphide deposits of hot saline fluid flowing into a submarine depression from below. Deep-Sea Research 31, 145–170.

McKay, W.J., 1989. A study of the geological setting, nature and genesis of the Woodlawn base metal deposit, New South Wales, Australia. Unpublished PhD thesis, Australian National University, Canberra, 273 pp.

McKay, W.J., Hazeldene, R.K., 1987. The Woodlawn Zn–Pb–Cu sulfide deposit, New South Wales, Australia: an interpretation of ore formation from field observations and metal zoning. Economic Geology 82, 141–164.

McKee, G.S., Hidalgo, R., Ixer, R.A., Boyce, A., Guerrero, V., Pons, J.M., 2001. Deposit formation and structural evolution at Aguas Teñidas Este. GEODE Workshop "Massive sulphide deposits in the Iberian Pyrite Belt: New advances and comparison with equivalent systems". University of Huelva, Huelva, pp. 38–39.

Marcoux, E., Moëlo, Y., Leistel, J.M., 1998. Bismuth and cobalt minerals as indicators of stringer zones to massive sulphide deposits, Iberian pyrite belt. Mineralium Deposita 31, 1–26.

Maslennikov, V.V., Zaykov, V.V., Zaykova, E.V., 2000. Paleohydrothermal fields and ore formation conditions at massive sulfide deposits in the Uralian paleoocean. In: Mezhelovsky, N.V., Morozov, A.F., Gusev, G.S., Popov, V.S. (Eds.), Geodynamics and Metallogeny: Theory and Implications for Applied Geology. GEOKART, Moscow, pp. 339–357.

Mitsuno, C., Nakamura, T., Yamamoto, M., Kase, K., Oho, M., Suzuki, S., Thadeu, D., Carvalho, D., Arribas, A., 1988. Geological Studies of the "Iberian Pyrite Belt" with Special Reference to its Genetical Correlation of the Yanahara Deposits and others in the Inner Zone of Southwest Japan University of Okayama, Japan. 300 pp.

Mullin, J.W., 1993. Crystallisation, 3rd edition Butterworth and Heinemann, Oxford, England. 527 pp.

Nehlig, P., Cassard, D., Marcoux, E., 1998. Geometry and genesis of feeder zones of massive sulphide deposits: constraints from the Rio Tinto ore deposit (Spain). Mineralium Deposita 33, 137–149.

Ohmoto, H., 1996. Formation of volcanogenic massive sulfide deposits. Ore Geology Reviews 10, 135–177.

Ohmoto, H., Skinner, B.J. (Eds.), 1983. The Kuroko and Related Volcanogenic Massive Sulfide Deposits. Economic Geology Monograph, vol. 5. 604 pp.

Ohmoto, H., Drummond, S.E., Eldridge, C.S., Pisutha-Arnond, V., Lenagh, T.C., 1983. Chemical processes of ore formation. Economic Geology Monographs 5, 570–604.

Oliveira, J.T., Quesada, C., 1998. A comparison of stratigraphy, structure and palaogeography of the South Portuguese zone and South-west England, European Variscides. Geoscience in South-west England 9, 141–150.

Peter, J.M., Scott, S.D., 1993. Fluid inclusion and light stable isotope geochemistry of the Windy Craggy Besshi-type massive sulfide deposit, northwestern British Columbia. Resource Geology Special Issue 17, 229–248.

Pisutha-Arnond, V., Ohmoto, H., 1983. Thermal history, and chemical and isotopic compositions of the ore-forming fluids responsible for the kuroko massive sulfide deposits in the Hokuroko district of Japan. Economic Geology Monograph 5, 523–558.

Potter, R.W., Brown, D.L., 1977. The volumetric properties of aqueous sodium chloride solution from 0° to 500 °C at pressure up to 2000 bars based on a regression of available data in the literature. U.S. Geological Survey Bulletin 1421C, 1–36.

Prokin, V.A., Buslaev, F.P., 1999. Massive copper–zinc sulphide deposits in the Urals. Ore Geology Reviews 14, 1–69.

Reed, M.H., Spycher, N.F., 1985. Boiling, cooling, and oxidation in epithermal systems: a numerical modelling approach. Reviews in Economic Geology 2, 249–272.

Rimstidt, J.D., 1997. Gangue mineral transport and deposition. In: Barnes, H.L. (Ed.), Geochemistry of Hydrothermal Ore Deposits, 3rd edition Wiley and Sons, New York, pp. 487–515.

Ruiz, C., Arribas, A., Arribas Jr., A., 2002. Mineralogy and geochemistry of the Masa Valverde blind massive sulphide deposit, Iberian Pyrite Belt (Spain). Ore Geology Reviews 19, 1–22.

Sánchez-España, J., Velasco, F., Yusta, I., 2000. Hydrothermal alteration of felsic volcanic rocks associated with massive sulphide deposition in the northern Iberian Pyrite Belt (SW Spain). Applied Geochemistry 15, 1265–1290.

Sato, T., 1972. Behaviours of ore-forming solutions in seawater. Mining Geology 22, 31–42.

Scholten, J.C., Stoffers, P., Garbe-Schönberg, D., Moammar, M., 2000. Hydrothermal mineralization in the Red Sea. In: Cronan, D.S. (Ed.), Handbook of Marine Mineral Deposits. CRC Press, London, pp. 369–395.

Scott, S.D., 1997. Submarine hydrothermal systems and deposits. In: Barnes, H.L. (Ed.), Geochemistry of Hydrothermal Ore Deposits, 3rd edition Wiley and Sons, New York, pp. 797–875.

Sharpe, R., 1991. The Hellyer baritic and siliceous caps. Unpublished Honours BSc thesis, University of Tasmania, Hobart, Australia. 114 pp.

Shimazaki, Y., 1974. Ore minerals of the Kuroko-type deposits. Mining Geology Special Issue 6, 311–322.

Solomon, M., 1976. 'Volcanic' massive sulphide deposits and their host rocks—a review and an explanation. In: Wolf, K. (Ed.), Handbook of Stratabound and Stratiform Ore Deposits, vol. 6. Elsevier, Amsterdam, pp. 21–54.

Solomon, M., 1981. An introduction to the geology and metallic mineral resources of Tasmania. Economic Geology 76, 194–208.

Solomon, M., 1999. Discussion: sulphur isotope composition of the Brunswick no. 12 massive sulphide deposit, Bathurst mining camp, New Brunswick: implications for ambient environment, sulphur source, and ore genesis. Canadian Journal of Earth Sciences 36, 1–5.

Solomon, M., Gaspar, O.C., 2001. Textures of the Hellyer volcanic-hosted massive sulfide deposit, Tasmania—the ageing of a sulfide sediment on the sea floor. Economic Geology 96, 1513–1534.

Solomon, M., Khin Zaw, 1997. Formation of the Hellyer volcanogenic massive sulfide deposit on the sea floor. Economic Geology 92, 686–695.

Solomon, M., Sun, S.-S., 1997. Earth's evolution and mineral resources, with particular emphasis on volcanic-hosted massive sulphide deposits and banded iron formations. AGSO Journal of Australian Geology and Geophysics 17, 33–48.

Solomon, M., Walshe, J.L., 1979. The formation of massive sulfide deposits on the sea floor. Economic Geology 74, 797–813.

Solomon, M., Rafter, A., Jensen, M.L., 1969. Isotope studies on the Rosebery, Mount Farrell and Mount Lyell ores, Tasmania. Mineralium Deposita 4, 172–199.

Solomon, M., Walshe, J.L., Garcia Palomero, F., 1980. Formation of massive sulphide deposits at Rio Tinto, Spain. Transactions of the Institution of Mining and Metallurgy, Section B 89, 16–24.

Solomon, M., Vokes, F.M., Walshe, J.L., 1987. Chemical remobilization of volcanic-hosted sulphide deposits at Rosebery and Mt. Lyell, Tasmania. Ore Geology Reviews 2, 173–190.

Solomon, M., Tornos, F., Gaspar, O.C., 2002. Explanation for many of the unusual features of the massive sulfide deposits of the Iberian pyrite belt. Geology 30, 87–90.

Solomon, M., Gemmell, J.B., Khin Zaw, 2004. The nature and origin of the fluids responsible for forming the Hellyer volcanic-hosted massive sulphide deposit, Tasmania, using stable and radiogenic isotopes and fluid inclusions. Ore Geology Reviews 25, 89–124.

Tanimura, S., Date, J., Ohmoto, H., 1983. Geologic setting of the kuroko deposits: Part II. Stratigraphy and structure of the Hokuroku district. Economic Geology Monographs 5, 24–38.

Tornos, F., Conde, C., 2003. La influencia biogénica en la formación de los yacimientos de sulfuros masivos de la Faja Piritica Ibérica. Geogaceta 32, 235–238.

Tornos, F., Spiro, B., 1999. The genesis of shale-hosted massive sulphides in the Iberian Pyrite Belt. In: Stanley, B.et al., (Ed.), Mineral Deposits: Processes to Processing. Balkema, Rotterdam, pp. 605–608.

Tornos, F., Clavijo, E.G., Spiro, B., 1998. The Filon Norte orebody (Tharsis, Iberian Pyrite Belt): a proximal low-temperature shale-hosted massive sulphide in a thin-skinned tectonic belt. Mineralium Deposita 33, 150–169.

Tornos, F., Conde, C., Solomon, M., Spiro, B., 2003. Effects of oxic/anoxic seafloor on the formation and preservation of shale-hosted massive sulphides, Iberian Pyrite Belt. In: Eliopoulis, D.G.et al., (Ed.), Mineral Exploration and Sustainable Development. Millpress, Rotterdam, pp. 191–194.

Toscano, M., Sáez, R., Almodóvar, G.R., 1997a. Multi-stage fluid evolution in the Masa Valverde stockwork (Iberian Pyrite Belt): evidence from fluid inclusions. SEG Neves Corvo Field Conference, Society of Economic Geology, Lisbon, 11–14.

Toscano, M., Sáez, R., Almodóvar, G.R., 1997b. Evolución do los fluidos hidrotermales en la génesis de los sulfuros masivos de Aznalcóllar (Faja Pirítica Ibérica): evidencias a partir de inclusiones fluidas. Geogaceta 21, 211–214.

Turner, F.J., Campbell, I.H., 1987. Temperature, density and buoyancy fluxes in "black smoker" plumes, and the criterion for buoyancy reversal. Earth and Planetary Science Letters 86, 85–92.

Urabe, T., 1974. Iron content of sphalerite coexisting with pyrite from some Kuroko deposits. Mining Geology Special Issue 6, 377–384.

Urabe, T., Sato, T., 1978. Kuroko deposits of the Kosaka mine, northeast Honshu, Japan—products of submarine hot springs on Miocene sea floor. Economic Geology 73, 161–179.

Vearncombe, S., Barley, M.E., Groves, D.I., McNaughton, N.J., Mikucki, E.J., Vearncombe, J.R., 1978. 3.25 Ga black smoker-type mineralization in the Strelley Belt, Pilbara Craton, western Australia. Journal of the Geological Society (London) 152, 587–590.

Veizer, J., Ala, D., Azmy, K., Bruckschen, P., Buhl, D., Bruhn, F., Carden, G.A.F., Diener, A., Ebneth, S., Godderis, Y., Jasper, T., Korte, K., Pawellek, F., Podlaha, O.G., Strauss, H., 1999. $^{87}Sr/^{86}Sr$, $\delta^{13}C$ and $\delta^{18}O$ evolution of Phanerozoic seawater. Chemical Geology 161, 59–88.

Velasco, F., Sánchez-España, J., Boyce, A.J., Fallick, A.E., Sáez, G.R., Almodóvar, G.R., 1998. A new sulfur isotopic study of some Iberian Pyrite Belt deposits: evidence of a textural control on sulphur isotope composition. Mineralium Deposita 34, 4–18.

Vokes, F.M., 1983. Paragenetical and textural relations in the south end of F-lens (16 level), Rosebery mine. Australian Bureau of Mineral Resources, Geology and Geophysics, unpublished report.

Von Damm, K.L., 1990. Seafloor hydrothermal activity: black smoker chemistry and chimneys. Annual Review of Earth and Planetary Sciences 18, 173–204.

Walshe, J.L., Solomon, M., 1981. An investigation into the environment of formation of the volcanic-hosted Mt. Lyell copper deposits using geology, mineralogy, stable isotopes, and a six-component chlorite solid solution model. Economic Geology 76, 246–284.

Whitford, D.J., Korsch, M.J., Solomon, M., 1992. Strontium isotope studies of barites: implications for the origin of base metal mineralization in Tasmania. Economic Geology 87, 953–959.

Whitford, D.J., Sharpe, R., Gemmell, J.B., 1993. Origin of barite from the Hellyer VHMS deposit, Tasmania: a Sr isotopic study. Abstracts-Geological Society of Australia Series 24, 75.

Wilkin, R.T., Barnes, H.L., 1997. Formation processes of framboidal pyrite. Geochimica et Cosmochimica Acta 61, 323–339.

Williams, D., 1934. The geology of the Rio Tinto mines, Spain. Transactions of the Institution of Mining and Metallurgy 43, 593–640.

Williams, D., Stanton, R.L., Rambaud, F., 1975. The Planes-San Antonio pyritic deposit of Rio Tinto, Spain: its nature, environment and genesis. Transactions of the Institution of Mining and Metallurgy, Section B 84, 73–82.

The relationship between shale and giant massive sulphide deposits: More than a spatial coincidence?

Fernando Tornos
Instituto Geológico y Minero de España. Azafranal 48. 37001 Salamanca (Spain).

Christoph A. Heinrich
Isotope Geochemistry and Mineral Resources, ETH Zürich, CH-8092 (Switzerland).

ABSTRACT: Numerical modeling based on the geology and geochemistry of the massive sulphide deposits of the Iberian Pyrite Belt and their underlying siliciclastic sediments shows that moderately oxidized shale can be the source of metal-rich but sulphide-poor hydrothermal brines. These fluids can migrate long distances through large faults until they find a suitable geochemical trap. Reaction with fluids and rocks rich in H_2S promotes sulphide saturation and the precipitation of large sulphide masses. Thus, the giant massive sulphide deposits of the IPB may have formed by the circulation of normal basinal brines without needing to invoke metal-rich magmatic fluid source.

KEYWORDS: Geochemistry, massive sulphides, Iberia, numerical modeling

1 INTRODUCTION

Genetic models for volcanic and sediment-hosted base metal massive sulphide deposits have been hampered by the problem of finding the source of metals and reduced sulphur. Numerical calculations in these low temperature hydrothermal systems show that reduced sulphur and metals cannot be transported by the same fluid unless unrealistically large amounts of hydrothermal fluids have been involved in the system (Anderson 1975; Sverjensky 1989). Alternative models include: (a) transport of metals by sulphide-poor fluids with later *in situ* addition of reduced sulphur via fluid mixing or reaction with host rocks, and, (b) transport of metals and sulfate by oxidized fluids, with the sulfate being later reduced synchronously with metal deposition (Sverjensky 1989; Cooke *et al* 2000). However, the major problem of the first alternative is where and how such H_2S-depleted fluids are formed. In fact, average reservoirs/metal sources are usually sulphur-rich. This is especially significant in shale-related deposits, where the presumed metal source may have had significant (authigenic?) pyrite.

However, numerical modelling shows that, paradoxically, fluids equilibrated with shale can be quite metal-rich but sulphur poor. We have tested such a model in the Iberian Pyrite Belt (IPB), where there is a direct spatial, genetic and chronological relationship between shale and giant massive sulphide deposits.

2 GEOLOGIC AND METALLOGENIC SETTING

The IPB includes a thick volcaniclastic (is this the PQ plus VS groups or only the VS – not clear) sequence deposited in pull apart structures during the oblique collision between an exotic terrane, nowadays represented by the South Portuguese Zone, and the Iberian Autochthonous Terrane (Silva *et al* 1990) during late Devonian to early Carboniferous. The sequence is rather monotonous and includes several thousand m of siliciclastic sediments (PQ Group) overlain a complex unit with felsic and mafic volcanic rocks interbedded with volcaniclastic rocks, shale and chemical sediments (VS Complex).

The VS Complex hosts a large number of massive sulphide bodies, forming perhaps the largest concentration of sulphides on the earth's crust. The massive sulphides are either interbedded with late Devonian shale as in the southern IPB or as massive to tabular bodies replacing felsic volcanic rocks as in the northern IPB (Tornos 2006). Both styles of mineralization have an underlying stockwork that only locally penetrates into the PQ Group, suggesting that the hydrothermal fluids have equili-

brated (or failed to interact?) with the underlying sediments.

Isotope geochemistry shows that ore forming fluids equilibrated with rocks with a large crustal residence time, very likely the shale and sandstone of the PQ Group. Fluids are characterized by high $\delta^{18}O$ but variable δD signatures, 0-8‰ and -45 to 5‰, respectively, and have radiogenic $^{87}Sr/^{86}Sr$ (0.7073-0.7203), $^{207}Pb/^{206}Pb$ and γOs values. These values are consistent with the derivation of metals and fluids from highly evolved crustal sources. Fluid inclusion data show that hydrothermal fluids were CO_2-poor brines having salinities up to 24 wt% NaCl eq., but usually ranging between 3 and 12 wt% NaCl eq. (see Relvas et al 2001, Munhá et al 2005, Tornos 2006 and references therein). Sulphur isotope values of sulphides are very variable, between -34 and +21‰, and consistent with a dual derivation of the sulphur, from the biogenic reduction of seawater sulfate and from the leaching of the underlying sedimentary sequence (Velasco et al 1998).

Some stockworks below the massive sulphide deposits have an assemblage enriched in sulphur-poor minerals, such as pyrrhotite, tellurides and magnetite, while these minerals are minor or absent in the overlying deposits. This suggests that deep fluids were sulphur-depleted and only mixing with external sulphur can produce large deposits.

Different studies have claimed a derivation of metals and fluids from magmatic sources. The main arguments for such a model are the presence of deep plutonism contemporaneous with massive sulphide formation, the isotopic signatures coupled with the fluid inclusion data (Solomon & Quesada 2003) and the high efficiency of magmatic fluids in the formation of massive sulphides (Yang & Scott 1996). However, the absence of large hydrothermal systems with typical magmatic alteration (e.g., Corbett 2001) suggest that magmatic fluids were minor, if not absent, in the IPB hydrothermal systems.

Barrie & Hannington (1999) have shown that there is a close correlation between the metal ratios in the source rocks and the related massive sulphide deposits. The Cu:Zn:Pb ratio of massive sulphides and of rocks belonging to the PQ Group is very variable but the average, recalculated to total tonnage of the orebodies, is strikingly similar. The ratio in the PQ Group is 28:53:19 while that of the massive sulphides is 25:52:23. This close agreement strongly supports the isotopic and geological results and

confirms that the major source of metals in the IPB is the PQ Group.

3 NUMERICAL MODEL

A numerical model has been constructed assuming the equilibrium of fluids with the PQ Group using the SOLVEQ/CHILLER code (Reed & Spycher 1988) with a modified SOLTHERM database including recent data on
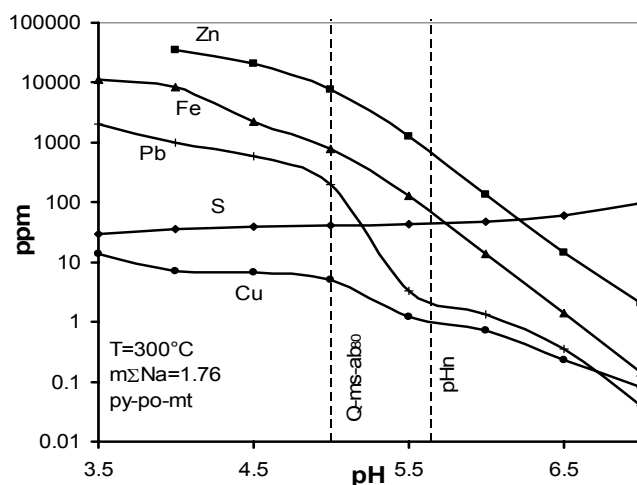

Fig. 1. Solubility of base metals, iron and H_2S in a fluid with a salinity of 9 wt% NaCl equiv. equilibrated with the PQ shale at 300°C at an fO_2 buffered by the pyrite-pyrrhotite-magnetite equilibrium. Except at high pH, the solubility of sulphur is significantly less than that of combined metals

the solubility of base metals. The composition of a fluid equilibrated with the PQ Group has been based assuming equilibration of shale with a fluid having a total salinity of 9%NaCl equiv. The shales of the PQ Group are made up of phengite, quartz chlorite and minor amounts of both plagioclase and K feldspar. Pyrite is a fairly common accessory mineral and locally it is accompanied by traces of magnetite and pyrrhotite. Systematic geochemical sampling has shown that most of the PQ shale has been deposited in an oxic to sub-oxic environment (Tornos et al in press).

This assemblage indicates that fluids were pH buffered by a quartz-feldspar-white mica assemblage - a feature consistent with the absence of large hydrothermal zones below the massive sulphides.

Calculations at different temperatures, pH and redox conditions show that the solubility of the metals is strongly dependant on the fO_2 of the system (Figs. 1 and 2). For example, at 300°C and a pH of 5.0, highly reducing systems (log fO_2 3.5 units below NNO, near C-CO_2

equilibrium) can transport more reduced sulphur (1885 ppm) than combined Cu (1 ppm), Zn (283 ppm), Pb (8 ppm) and Fe (28 ppm). However, at intermediate redox conditions (between the NNO and HM buffers), the solubility of metals increases dramatically to 7 ppm Cu, >10000 ppm Zn, 1000 Pb and 8300 ppm Fe while the solubility of sulphur drops to only 36 ppm.
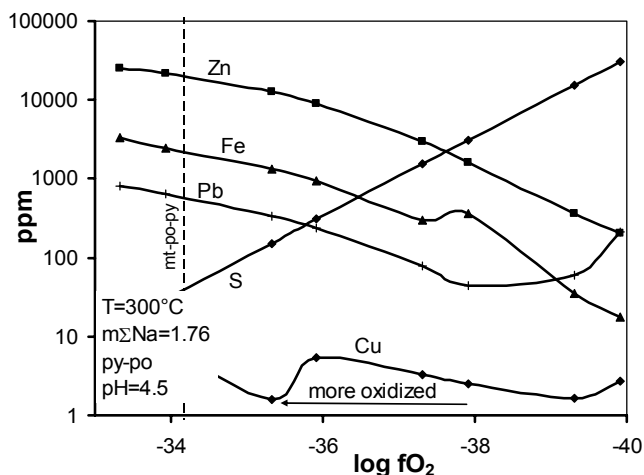

Fig. 2. Solubility of base metals, iron and H_2S at the same conditions that fig. 1 but at a pH of 4.5 and at different redox conditions. In reduced systems the solubility of sulphur is significantly higher than that of metals, inhibiting thus their transport.

Reaction of such a fluid with seawater that has 90% of its sulphate reduced to H_2S leads to the precipitation of massive sulphides with an average base metal content similar to that of many deposits of the IPB. These calculations show that inflow of the hydrothermal fluid in an anoxic bottom with high degree of biogenic reduction of seawater sulphate can produce giant massive sulphide deposits.

Mass balance calculations show that only a small depletion in metals of about 5 ppm of each is needed for forming all the massive sulphides in the IPB. Thus, metal leaching will not have a major geochemical effect on the source rocks.

4 DISCUSSION AND CONCLUSIONS

The numerical results show that fluids equilibrated with weakly oxidized (magnetite-rich but carbon poor) siliciclastic sediments are moderately base metal and iron-rich but sulphur deficient brines. These fluids can travel long distances within sedimentary basins without changing their chemical composition nor leaving a halo of hydrothermal alteration. Only when approaching the seafloor, where major chemical and thermal changes take place, fluids react with the host rocks and mix with seawater producing the stockwork zone. On the seafloor fluid mixing dominates and deposition of massive sulphides takes place.

The formation of giant massive sulphide deposits in the IPB is probably due to the combination of several key factors including the presence of a thick immature siliciclastic sequence that was quickly followed by rifting and related high heat flow. This promoted quick dewatering and channeling of fluids along restricted extensional structures in an overall transpressional regime, promoting high fluid flow. Fluid flow modeling of Conde et al (2005) shows that during the onset of convective hydrothermal circulation during the late Devonian, first batches of fluids vented to the seafloor included most of the basinal water generated by sediment maturation. Venting of these fluids into anoxic bottoms rich in biogenic sulphur lead to the formation of the ore deposits.

This simple model can perhaps be also applied to the genesis of other styles of mineralization such as volcanic-hosted massive sulphides, sedimentary-exhalative ores, Irish-type deposits or even Mississippi Valley ones (e.g., Goodfellow et al 1993; Plumlee et al 1994; Wilkinson et al 2005). Many of these deposits are underlain by a thick (meta-) siliciclastic sequence and some show evidence for the circulation of sulphur-depleted fluids.

ACKNOWLEDGEMENTS

REFERENCES

Anderson G M (1975) Precipitation of Mississippi Valley-type ore fluids. Economic Geolo-gy 70: 937–942.

Barrie, CT, Hannington, MD (1999) Classi-fication of volcanic-associated massive sulphide deposits based on host rock composition. Reviews Economic Geology 8: 2-12.

Conde C, Mathaii S, Geiger S, Tornos F, Herrington R (2005) Heat and fluid modeling of the shale-hosted massive sulphides in the Iberian Pyrite Belt, Spain. Abstracts GAC-MAC-CSPG-CSSS meeting Halifax, 30: 238 p.

Corbett KD (2001) New mapping and interpretations of the Mount Lyell mining district, Tasmania: A large hybrid Cu-Au system with an exhalative Pb-Zn top. *Economic Geology* 96: 1089-1122.

Cooke DR, Bull SW, Large RR, McGoldrick PJ (2000) The importance of oxidized brines for the formation of Australian Proterozoic stratiform sediment-hosted Pb-Zn (Sedex) deposits. *Economic Geology* 95: 1-18.

Goodfellow WD, Lydon JW, Turner RJW (1993) Geology and genesis of stratiform sediment-hosted (sedex) zinc-lead-silver sulphide deposits. In: Kirkham RV, Sinclair WD, Thorpe RI, Duke JM (eds) *Mineral Deposit Modeling, Geological Society Canada Special Paper* 40: 201-251.

Munha J, Relvas JMRS, Barriga FJAS, Concei-çao P, Jorge RCGS, Mathur R, Ruiz J, Tassina-ri CCG (2005) Os isotopes systematics in the Iberian Pyrite Belt. In Mao J, Bierlein F (eds), *Mineral Deposit Research: Meeting the Global Challenge: Beijing,* Springer, 663-666.

Plumlee GS, Leach DL, Hofstra AH, Landis GP, Rowan EL, Viets JG (1994) Chemical reaction path modeling of ore deposition in Mississippi Valley-type Pb-Zn deposits of the Ozark Region, US Midcontinent. *Economic Geology* 89: 1361-1383.

Reed MH, Spycher NF (1988) Chemical modeling of boiling, condensation, fluid-fluid mixing and water rock reaction using programs CHILLER and SOLVEQ. *Abstracts American Chemical Society Symposium, Chemical Mo-deling Aqueous Systems,* 25-30.

Relvas JMRS, Tassinari CCG, Munha J, Barri-a FJAS (2001) Multiple sources for ore for-ming fluids in the Neves Corvo VHMS deposit of the Iberian Pyrite Belt (Portugal): Strontium, Neodymium and Lead isotope evidence. *Mine-ralium Deposita* 36:416-427.

Silva JB, Oliveira JT, Ribeiro A (1990) Structural outline of the South Portuguese Zone. In Dallmeyer RD, Martinez García E. (eds), *PreMesozoic Geology of Iberia.* Springer Verlag, 348-362.

Solomon M., Quesada C. (2003) Zn-Pb-Cu massive sulphide deposits: Brine pool types oc-cur in collisional orogens, black smoker types in backarc and/or arc basins. *Geology* 31: 1029-1032.

Sverjensky DA (1989) The diverse origins of Mississippi Valley-type Zn-Pb-Ba-F deposits. *Chronique Recherche Miniere* 495: 5-13.

Tornos, F (2006) Environment of formation and styles of volcanogenic massive sulphides: The Iberian Pyrite Belt. *Ore Geology Reviews* 28: 259-307.

Tornos F, Solomon M, Conde C, Spiro BF (2006) Formation of the Tharsis massive sulphide deposit, Iberian Pyrite Belt: geological, lithogeochemical and stable isotope evidence for deposition in a brine pool. *Economic Geology,* in press.

Velasco F, Sanchez España J, Boyce A, Fallick AE, Saez R, Almodovar GR (1998) A new sul-phur isotopic study of some Iberian Pyrite Belt deposits: evidence of a textural control on some sulphur isotope compositions. *Mineralium De-posita* 34: 1-18.

Wilkinson JJ, Eyre SL, Boyce AJ (2005) Ore-forming processes in Irish-type carbonate-hosted Zn-Pb deposits: Evidence from mineralogy, chemistry, and isotopic composition of sulphides at the Lisheen mine. *Economic Geology* 100: 63-86.

Yang K, Scott SD (1996) Possible contribution of a metal-rich magmatic fluid to a sea-floor hydro-thermal system. *Nature* 383: 420-423.

MODELIZACIÓN DEL TRANSPORTE DE CALOR Y FLUIDO EN LOS SULFUROS MASIVOS ENCAJADOS EN PIZARRAS DE LA FAJA PIRÍTICA IBÉRICA, ESPAÑA.

C. Conde [1], F. Tornos [1], S. Matthäi [2] y S. Geiger [3]

[1] Instituto Geológico y Minero de España, C/Azafranal, 48, 37001, Salamanca, España.

[2] Dept. of Earth Sciences & Engineering, Imperial College, Prince Consort Road, SW7 2BP Londres, Reino Unido.

[3] Dept of Earth Sciences, Geology and Miner Resources, ETH Zurich Sonneggstr. 5, DH-8092 Zurich, Suiza.

INTRODUCCIÓN

El estudio de los procesos geoquímicos y termodinámicos relacionados con la génesis de los sulfuros masivos es un campo de interés creciente en la investigación de los yacimientos minerales. La simulación mediante modelos numéricos de flujo de fluido y trasporte de solutos permite un mejor entendimiento de los procesos fisicoquímicos que intervienen en los sistemas hidrotermales en los fondos marinos. Sin embargo, pocos son los trabajos orientados a comprender los procesos que han intervenido en la formación de la mayor provincia mundial de sulfuros masivos, la Faja Pirítica Ibérica (FPI) (Barrie et al., 2004; Conde et al. 2005).

La mayoría de los sulfuros masivos gigantes (>100 Mt) de la Faja Pirítica se encuentran en su sector septentrional. Los cuerpos mineralizados encajan en una secuencia félsico-siliciclástica a techo de una potente unidad sedimentaria. La FPI incluye una serie estratigráfica relativamente simple y de edad Devónico Superior-Carbonífero Inferior, en la que se han diferenciado tres unidades. Las rocas más antiguas forman el Grupo Cuarzo-filítico (Grupo PQ). Está formado por una potente serie detrítica (>2000 m) constituida por una alternancia de pizarras y areniscas depositadas en una ambiente de plataforma continental estable. Estratigráficamente por encima está el Complejo Volcano Sedimentario (CVS) formado por una serie heterogénea compuesta por una alternancia de rocas volcánicas, subvolcánicas y volcanoclásticas de carácter bimodal, junto con pizarras y sedimentos químicos. El CVS se depositó en una cuenca de tipo *pull-apart* formada durante la colisión oblicua de la Zona Sur-Portuguesa y el Terreno Ibérico Autóctono durante la orogenia Varisca. La unidad superior, suprayacente a la unidad volcánica, es el Grupo Culm formado por una secuencia tipo flysch constituida por pizarras y grauvacas, producto de la colmatación de la cuenca y posterior inversión tectónica. (Moreno, 1993).

Los depósitos más significativos de la zona sur de la FPI encajan en pizarras oscuras. En algunos casos estas pizarras se localizan directamente por encima del Grupo PQ (e.g., Tharsis) o sobre una unidad félsica con complejos de tipo domo (e.g., Aznalcóllar-Los Frailes, Las Cruces, Sotial, Valverde o Tharsis). Estos sulfuros masivos están caracterizados por su gran tonelaje, el alto contenido en pirita, y la presencia de estructuras sedimentarias que sugieren un probable origen ligado a procesos exhalativos en una cuenca anóxica restringida, tipo *brine pool* (Tornos

et al., en prensa). Estos depósitos parecen ser contemporáneos y limitados a un único nivel estratigráfico de 3 a 4 Ma, datado como Estruniense Superior (González et al., 2002; Oliveira et al., 2002; Pereira et al., 1996). Las propiedades geológicas y geoquímicas sugieren que los fluidos que originaron la mineralización proceden de la maduración diagenética de la unidad detrítica inferior (Grupo PQ), cuya circulación fue acelerada por un alto gradiente geotérmico inducido por la intrusión magmática (Conde et al., 2005; Tornos, 2006).

El objetivo principal de este trabajo es el desarrollo de un modelo de elementos finitos que sea capaz de verificar si el Grupo PQ puede ser la fuente de los metales y del fluido hidrotermal que da lugar a la formación de los sulfuros cmasivos, así como intentar entender porqué estas mineralizaciones se formaron en un lapso tan corto de tiempo.

METODOLOGÍA DE LA MODELIZACIÓN NUMÉRICA

El modelo ha sido construido mediante la simulación de un flujo multi-fase, combinando métodos de elementos finitos y volúmenes finitos que predigan la convección hidrodinámica y termohalina. La realización de este modelo numérico precisa de una serie de consideraciones como son los procesos básicos y las ecuaciones fundamentales que gobiernan la dinámica de fluidos y el transporte de calor. Matemáticamente, los procesos básicos como el flujo de fluido, la transferencia de calor y el transporte de soluto pueden ser descritos mediante la ecuación de continuidad (1) y la ley de Darcy (2):

donde ϕ es la porosidad de la roca, ρ es la densidad de

$$\phi \frac{\partial S_\infty}{\partial t} = -\nabla v_\infty + q_\infty \qquad (1)$$

$$v_\infty = -\lambda_\infty k (\nabla p_\infty - \rho_\infty g) \qquad (2)$$

fluido y S es la saturación de la fase. Y donde la velocidad del fluido viene dada por la ecuación (2), donde λ es el ratio de movilidad relativo a la permeabilidad de la fase (k) y su viscosidad (μ). La permeabilidad en el medio poroso es k, p es la presión del fluido, y g, es la aceleración por gravedad. Para la modelización de nuestro sistema se han tenido en cuenta tres ecuaciones de estado: a. conservación de la masa de fluido, teniendo en

cuenta la fase de líquido y vapor; b. conservación de la masa de soluto, en relación a la conservación de la fracción de masa NaCl en el H_2O; y c. conservación de la energía, definida por la capacidad de calor y conductividad térmica. Estas ecuaciones han sido calculadas en base a los términos de presión de fluidos, temperatura y salinidad.

Las principales ecuaciones de estado que intervienen en la formación de los yacimientos, han sido simultáneamente resueltas mediante el *Complex System Platform (CSP)* (Matthäi *et al.*, 2001), sistema que está orientado a objetos (C++). Este software fue diseñado con el objetivo de resolver numéricamente y al mismo tiempo, las ecuaciones diferenciales de conservación de la masa y energía, pudiendo variar las condiciones fisicoquímicas (permeabilidad, porosidad, salinidad y geometría) que simulan le flujo de calor y fluido en un sistema hidrotermal termohalino (Geiger, 2004).

Modelo hidrogeológico conceptual

La construcción del modelo conceptual está basada en el conocimiento de la características estratigráficas, tectónicas y paleogelógicas de la zona sur de la FPI, que previamente han sido descritas en estudios generales de la zona (Leistel *et al.*, 1998; Mitjavila *et al.*, 1997; Tornos, 2006), así como en trabajos enfocados al estudio concreto de algunos yacimientos. Un aspecto importante para la construcción del modelo numérico es el conocimiento del emplazamiento geotectónico en el momento de formación de las mineralizaciones. Para ello, en este trabajo se ha tenido en cuenta las características paleogeográfica regionales interpretadas a partir del perfil sísmico IBERSEIS (Simancas *et al.*, 2003)

Modelo inicial

El modelo inicial ha sido construido en base a una malla bidimensional de más de 3600 elementos triangulares, que representa un corte geológico simple de dimensiones 20 x 40 km. Litológicamente, el modelo numérico presenta dos unidades: una unidad sedimentaria con una potencia de 3 a 4 km que simboliza el Grupo PQ, y una secuencia heterogénea suprayacente compuesta por rocas volcánicas y sedimentarias (800-1200 m), equivalente al CVS. Este conjunto está afectada por una serie de fallas extensionales y de desgarre, que dan lugar a la formación de zonas relativamente permeables ($10^{-12}m^2$) y que canalizan gran parte del flujo de fluido. Por tanto, la estructura de la cuenca está condicionada por la distribución de estas fallas. En este simple modelo, hemos prefijado una serie de parámetros físicos para el conjunto de elementos triangulares que constituyen una misma unidad sedimentaria. Para el CVS, situado directamente bajo el fondo marino, hemos considerado una permeabilidad de $10^{-15}m^2$. La serie de pizarras y areniscas infrayacentes a la unidad volcánica (Grupo PQ), se asume una permeabilidad relativamente más alta ($10^{-14}m^2$). Otras propiedades físicas de las rocas, como la capacidad calorífica, la conductividad térmica, porosidad y salinidad han sido impuestas según parámetros empleados en otros trabajos hidrodinámicos previos (Allen & Allen, 2004; Bear, 1972; Domenico & Schwartz, 1990; Matthäi *et al.*, 2004; Geiger, 2004).

Las condiciones iniciales y de contorno consideradas en el modelo son: la condición de contorno inferior representa la presencia de un basamento intruido por ro-

cas ígneas, el cual es menos permeable que la unidad sedimentaria superior, y se caracteriza por un alto flujo de calor (85-120 mWm^{-2}). Esta elevada fuente de calor da lugar al desarrollo de un alto gradiente geotérmico en la cuenca. La condición de contorno superior está definida por la superficie del agua marina, con una temperatura de 21°C, una salinidad del 3,2 % peso Na Cl eq., y una presión de 1 atm. Las condiciones iniciales para el conjunto del sistema, asumen que la salinidad, presión de fluidos, temperatura y fuente calorífica son cero. Las simulaciones numéricas han sido calculadas para un tiempo total de 3 Ma.

En el presente trabajo se han postulado dos casos. La primera hipótesis asume que los fluidos en equilibrio con el Grupo PQ tiene una salinidad cero (agua pura), y una condición de contorno inferior con una salinidad del 5 % peso NaCl. En el segundo caso, se ha estudiado la influencia que la variación de salinidad tiene en la dinámica del fluidos de la unidad sedimentaria. Para ello, se toma como condición inicial para la unidad del Grupo PQ una salinidad del 10 % peso NaCl, basada en estudios de inclusiones fluidas previos (Tornos, 2006, y otras referencias citadas en el mismo) y una condición inferior de salinidad del 15 % peso NaCl.

SIMULACIÓN NUMÉRICA Y RESULTADOS

Caso 1

El modelo numérico basado en la circulación de agua pura muestra como resultado principal que la circulación de fluidos es por circulación convectiva y que las primeras celdas se instauran muy rápidamente, a unos 300000 años de comenzar el sistema. Este sistema hidrodinámico condiciona que los primeros fluidos exhalativos sean los más salinos y de mayor temperatura. Después de este estadio inicial, los fluidos ascienden con menor temperatura y salinidad, probablemente como consecuencia de la mezcla convectiva del agua oceánica y fluidos salinos profundos. Durante estas etapas, la distribución de la temperatura y salinidad tienen un patrón similar. En posteriores estadios, el sistema se estabiliza dando lugar a la formación de niveles poco salinos a techo del Grupo PQ. Después del primer millón de años, las plumas de calor son menos vigorosas y por lo tanto, la temperatura con la que los fluidos ascienden es menor (90- 125°C). La modelización también muestra como a través de las fallas se canaliza el ascenso de fluidos hidrotermales y el descenso de agua oceánica, aunque también muestra como se produce la formación de las células convectivas fuera del campo de acción de dichas fallas.

Caso 2

La modelización de la dinámica de un fluido salino muestra aspectos muy diferentes al primer modelo. La simulación revela que la salinidad causa un gran efecto en el régimen térmico y dinámico del sistema, de manera que controla las velocidades de la convección termohalina y la transferencia de soluto. De hecho, parece ralentizar la formación de la circulación convectiva, requiriendo para su desarrollo más del triple de tiempo que en el caso 1, produciendo además células significativamente más pequeñas. Sin embargo, el patrón del ascenso y descenso de fluido y calor es similar al primer caso.
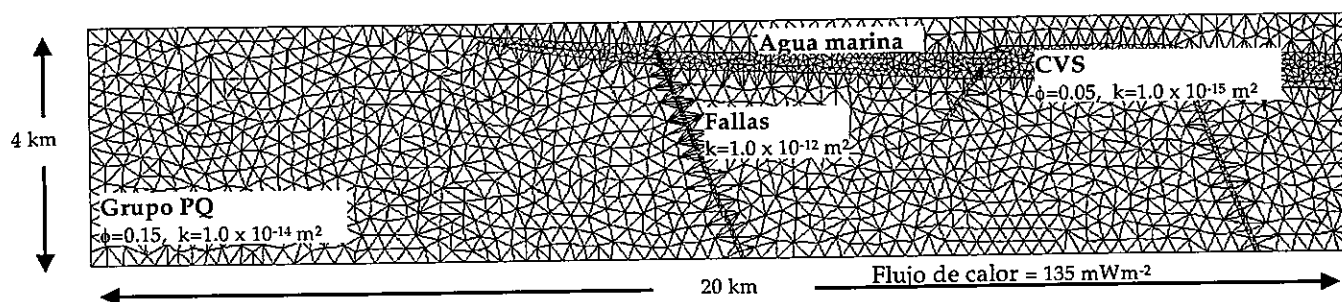
Figura 1: Malla del modelo hidrogeológico de la zona sur de la Faja Pirítica Ibérica.

CONCLUSIONES

La modelización numérica de los procesos hidrogeológicos que dan lugar a la formación de yacimientos de sulfuros masivos de la FPI muestra que el flujo de fluido esta controlado por una circulación convectiva, desestimándose una circulación de fluidos por compactación pura de los sedimentos. Por otro lado, la salinidad parece ser un aspecto crítico en la temporalidad y tamaño de las células convectivas desarrolladas. Los resultados también indican que en el Grupo PQ pueden generarse grandes células convectivas hidrotermales sin necesidad de que haya intrusiones someras. La presencia de fallas controla la distribución de las celdas, aunque su presencia no parece ser crítica en la formación de las células convectivas.

Quizás el resultado más significativo de los modelos numéricos es que estos muestran que los fluidos más salinos y calientes son los que primero ascienden y son exhalados en el fondo marino, tan pronto como se desarrollan las primeras células hidrotermales convectivas. Teniendo en cuenta la relación directa entre la salinidad y la temperatura y la solubilidad de los metales transportados como complejos clorurados, es muy posible que estos flujos canalizados sean los que dieron lugar a los sulfuros masivos gigantes, siempre que los fluidos hidrotermales fueran acumulados en un entorno geológico favorable, como una cuenca de tercer orden. Esto es coherente con la formación de los sulfuros masivos en un intervalo tan corto de tiempo. Los fluidos posteriores serían más fríos y menos salinos, disminuyendo por lo tanto la probabilidad de formación de grandes depósitos.

AGRADECIMIENTOS

REFERENCIAS

Allen, P.A., y Allen J.R.. (2004): Thermal history, In «Basin Analysis. Principles & Applications», P.A. Allen and J.R. Allen, eds Balckwell Publishing, 282-305

Barrie, C.T., Amelin, Y., y Pascual, E. (2002). Mineralium Deposita, 37-8, 684-703.

Barrie, C.T., Cathles, L.M, y Erendi, A. (2004). Eos. Trans. AGU 85(19), Joint Assambly Supple., Abstract V11B-02

Bear, J. (1988). Dynamics of Fluids in Porous Media. Dover Publicatons, Inc. 764 pp.

Domenico, P.A., and Schwartz F. W. (1997). Physical and Chemical Hydrogeology. Willey. New York. 506 pp.

Conde, C., Mathaii, S., Geiger, S., Tornos, F., y Herrington, R. (2005). In Abst. GAC-MAC meeting Halifax 2005, v. 30,

Geiger, S (2004) PhD Thesis, Swiss Federal Institute of Technology Zürich, 233 pp.

Leistel, J. M., Marcoux, E., Thieblemont, D., Quesada, C., Sanchez, A., Almodovar, G. R., Pascual, E., y Saez, R. (1998).

Mineralium Deposita, 33/1-2, 2-30.

Matthäi, S., Geiger, S. y Roberts, S.G. (2001). Eidgenossische Technische Hochschule Zurich, Switzerland.

Mitjavila, J., Marti, J., y Soriano, C.(1997).Journal Petrology, 38-6, 727-755.

Moreno, C. (1993). Journal Sedimentary Petrology, 63-6, 1118-1128.

Oliveira, D. P. S., Poujol, M., y Robb, L. J. (2002). Revista Sociedad Geológica España, 15/1-2, 105-112.

Pereira, Z., Saez, R., Pons, J. M., Oliveira, J. T., y Moreno, C. (1996). Geogaceta, 20-7, 1609-1612.

Quesada, C. (1998). Mineralium Deposita, 33/1-2, 31-44.

Simancas, J. F., Carbonell, R., Gonzalez Lodeiro, F., Perez Estaun, A., Juhlin., C., Ayarza, P., Kashubin, A., Azor, A.,

Martínez Poyatos, D., Ruiz Almodovar, G., Pascual, E., Saez, R., y Expósito, I. (2003). Tectonics, 22-6, 1962-1974.

Tornos, F. (2006). Ore Geology Reviews, 28, 256-307.

Tornos, F. Solomon, M., Conde, C., y Spiro, B., (in press) Economic Geology.

LOS SULFUROS MASIVOS (Cu-Zn-Au) DE LOMERO POYATOS (FAJA PIRÍTICA IBÉRICA): ENCUADRE GEOLÓGICO, ALTERACIÓN HIDROTERMAL Y REMOVILIZACIÓN

F. Velasco [1] y F. Tornos [2]

[1] *Departamento de Mineralogía y Petrología. Universidad del País Vasco, Apdo. 644, 48940 Bilbao*

[2] *Instituto Geológico y Minero de España, Azafranal 48, 37002 Salamanca*

INTRODUCCIÓN

El depósito de Cu-Zn-Au de Lomero Poyatos (Huelva) se encuentra localizado en la parte más septentrional de la Faja Pirítica Ibérica (FPI), dentro de la banda norte donde afloran numerosos depósitos de sulfuros masivos encajados en rocas volcánicas, tales como San Telmo, Confesionarios, Aguas Teñidas, Castillejito, Cueva de la Mora y Monte Romero. Excepto Aguas Teñidas y Castillejito, son depósitos relativamente pequeños (<20 Mt), pero todos presentan leyes elevadas en Cu-Zn-Pb-Ag-Au si se comparan con los depósitos gigantes, ricos en pirita, situados en la zona meridional de la Faja Pirítica (Leistel et al., 1998; Tornos, 2006). La zona se encuentra afectada por un metamorfismo regional de grado muy bajo e intensamente tectonizada con desarrollo de abundantes zonas de cizalla. Los efectos de la deformación incluyen la formación de milonitas con procesos de estiramiento y dislocación del encajante y de las masas de sulfuros (disolución por presión, maclas, deslizamientos, recristalización dinámica, etc.), dando lugar a fenómenos de recristalización y removilización mecánica y química.

Dentro de este conjunto, el depósito de Lomero Poyatos representa un ejemplo inusual ya que se encuentra en una zona donde las rocas volcánicas de composición andesítica muestran una intensa cataclásis y tiene leyes excepcionalmente elevadas en Au. En conjunto, el depósito tiene unos recursos indicados de sulfuros masivos de 4.25 Mt con 5.76 g/t Au, 116.9 g/t Ag, 1.58% Cu, 5.71% Zn y 1.48% Pb, y 11.2 Mt de sulfuros semimasivos con 2.29 g/t Au, 70.8 g/t Ag, 1.26% Cu, 3.02% Zn y 0.98% Pb (Cambridge, 2004). Como otros yacimientos de la FPI presenta una historia larga y compleja. Fue descubierto en 1853, explotado entre los años 1931 y 1991, produciendo un total de 2.6 Mt de pirita. Las zonas enriquecidas en metales base no fueron explotadas durante esta época. En 1980-82 la mina fue evaluada por Indumetal y entre 1982-86 por Billiton. Desde 1999 ha sido explorada para metales preciosos y cobre-zinc por Recursos Metálicos y posteriormente por Cambridge Resources, que han realizado un estudio de viabilidad.

GEOLOGÍA DEL DEPÓSITO DE LOMERO POYATOS

El depósito de Lomero Poyatos se encuentra en la zona norte de la FPI donde el Complejo Volcano Sedimentario está dominado por rocas volcánicas y volcanoclásticas con poca proporción de pizarras. En conjunto, la geología de la zona está dominada por el apilamiento de escamas tectónicas de unos 0.1-2 km de potencia cabalgantes hacia el sur; cada una de estas unidades parece tener una estratigrafía propia, por lo que la correlación entre distintas unidades es difícil. No existen dataciones de este vulcanismo pero por comparación con áreas similares es de edad Tournaisiense-Viseense.

En detalle, el yacimiento se encuentra en una pequeña unidad tectónica de unos 10-80 m de potencia y una extensión lateral de unos 900 km, en contacto tectónico con otras dos unidades en las que dominan las rocas de composición andesítica. La dirección media es N110°E, con un buzamiento de unos 30 a 50°N. La Unidad Inferior tiene una potencia de unos 260 m y está formada dominantemente por andesita volcanoclástica; esta unidad es cabalgante sobre otra en la que dominan las vulcanitas félsicas similares a las que se encuentran a techo de la Mina de Aguas Teñidas Este. En detalle, consiste en brecha y arenisca volcanoclástica monomíctica de derivación proximal entre la que intercalan pequeños niveles dm de lapilli consolidado rico en vidrio y con estructuras perlíticas. Son frecuentes los diques de igual composición. En esta unidad hay zonas irregulares de alteración hidrotermal, caracterizadas por el remplazamiento de los fenocristales de plagioclasa por sericita y cloritización generalizadas. La Unidad Superior está también formada por andesita, aunque dominan las facies masivas que gradan a hialoclastita. La andesita se caracteriza por la presencia de facies vacuolares, otras ricas en enclaves de roca volcánica y otras en las que dominan los agregados glomeroporfídicos no orientados de plagioclasa; en ambos casos quedan restos de una matriz originariamente vítrea y que ahora es microcristalina con microlitos no orientados de plagioclasa con sericita, clorita y cuarzo; se aprecia una alteración clorítica sobre la que se superponen zonas con intenso desarrollo de epidota. Esta unidad se interpreta como una sucesión de domos submarinos. Intruyendo estas rocas hay frecuentes diques de microgabro.

La Unidad Intermedia es la que encaja la mineralización y, a diferencia de las otras, presenta una estratigrafía compleja. Al oeste y cerca de la superficie dominan las litologías de composición más
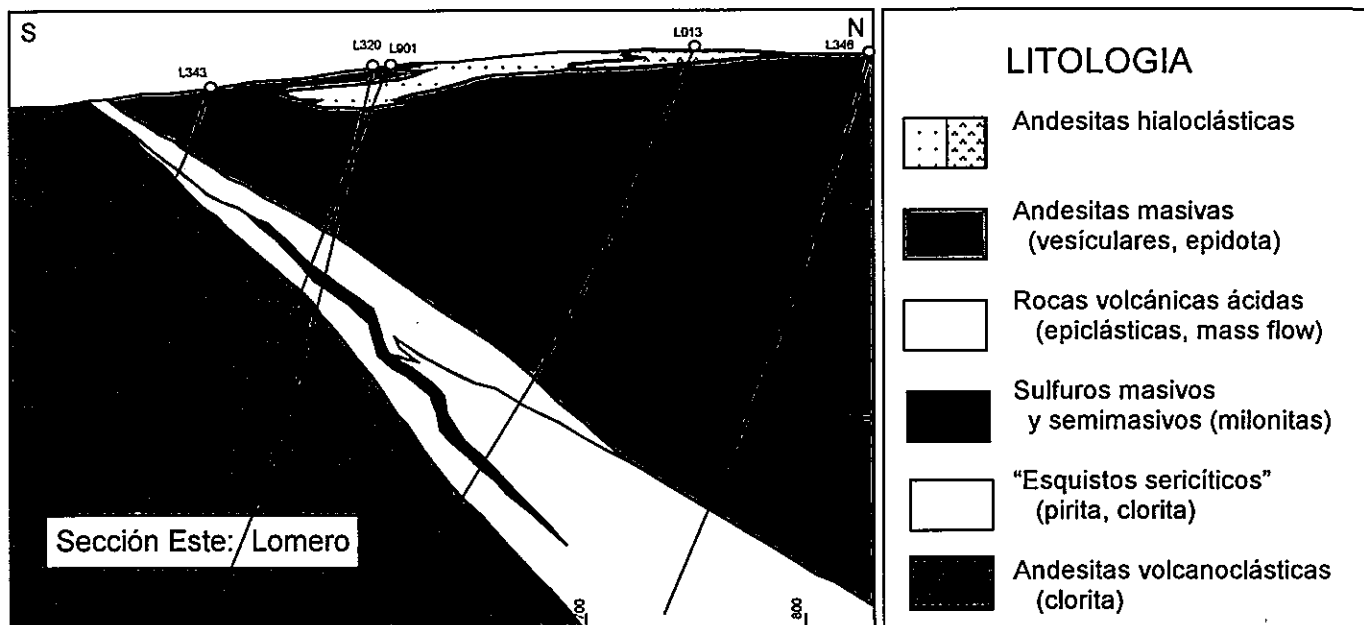
LITOLOGIA

Andesitas hialoclásticas

Andesitas masivas
(vesiculares, epidota)

Rocas volcánicas ácidas
(epiclásticas, mass flow)

Sulfuros masivos
y semimasivos (milonitas)

"Esquistos sericíticos"
(pirita, clorita)

Andesitas volcanoclásticas
(clorita)

Figura 1: Sección esquemática del yacimiento de Lomero-Poyatos en la transversal este
Elaborado a partir de datos de Cambridge Mineral Resources (2004)

ácida, variando de dacita a riolita. Por el contrario, en secciones localizadas al este y en profundidad los sondeos han cortado rocas epiclásticas grises y filonitas, fuertemente deformadas y finamente esquistosadas y con abundante pirita de grano muy fino que probablemente correspondan a zonas de deformación extrema. Estas rocas se presentan muy alteradas hidrotermalmente con cambios graduales de facies entre los extremos volcánicos y sedimentarios. La parte superior de la secuencia ha sido reemplazada parcial o totalmente por los sulfuros masivos, observándose zonas con stockworks de pirita. En la parte central del yacimiento, sin embargo, las litologías observadas parecen corresponder a una brecha volcanoclástica félsica rica en vidrio y quizás pómez. La alteración hidrotermal del conjunto consiste en una intensa sericitización y silicificación, con cloritización subordinada, estando la silicificación directamente asociada a la mineralización. En detalle, esta Unidad Intermedia incluye rocas siempre muy deformadas (tectonitas), con sulfuros masivos alternando como peces tectónicos de potencia hasta decamétrica y longitud hectométrica entre bandas de milonita y ultramilonita, formadas mayoritariamente por cuarzo de grano fino con algo de sericita y muy poca clorita; en estas rocas hay zonas de cloritita rica en pirita que hipotéticamente pueden corresponder a zonas de stockwork totalmente modificadas tectónicamente.

Los contactos entre todas las unidades son siempre tectónicos y jalonados por bandas de milonitas de unos 5-10 m de potencia. En todas las unidades hay un incremento gradual de la deformación hacia los contactos, con desarrollo de una esquistosidad y estructuras de tipo S-C. Esta disposición se observa en la mesoescala, formando las unidades tectónicas una estructura de tipo *ramp and flat*. Las bandas de deformación muestran una oxidación característica, con enriquecimiento en hematites de las bandas más de-

formadas, formación de niveles de jaspe y oxidación de los sulfuros a magnetita.

ZONAS DE ALTERACION DETECTADAS CON SWIR

El estudio por espectrometría portátil de infrarrojo de onda corta (SWIR) de varios perfiles del yacimiento ha permitido identificar y evaluar la extensión lateral y vertical de los diversos tipos de alteración hidrotermal de las rocas encajantes del yacimiento. Este análisis mineralógico, realizado con un equipo PIMA-SP, sobre testigos de sondeo, muestra la existencia de tres zonas de alteración superpuestas, adaptándose *grosso modo* a los cambios litológicos de las Unidades Inferior, Intermedia y Superior, respectivamente. El orden, de muro a techo, señala la existencia de varias zonas: (1) «Zona de clorita» afectando las tres unidades, si bien muestra mayor intensidad alrededor de las zonas próximas a la mineralización; (2) «Zona de sericita», localizada principalmente en la Unidad Intermedia que contiene a la mineralización, con efectos decrecientes en zonas laterales a la mineralización; va acompañada de incipiente paragonitización (18%) y descenso del grado de fengitización de las micas en los niveles de filitas; (3) «Zona de epidota», desarrollada exclusivamente en la Unidad Superior, y más acusada a medida que nos alejamos de la mineralización. Del mismo modo, con esta metodología de carácter prospectivo, es posible diferenciar zonas ricas en esmectitas y halloysita, siempre ligadas a ambientes superficiales y claramente relacionadas con procesos de alteración meteórica («Zona supergénica»).

Las citadas zonas hidrotermales, que aparecen con un marcado carácter *semiconformable* adaptadas a las diversas litologías, permiten localizar y seguir en profundidad la posición del horizonte mineralizado. La distribución de las dos primeras zonas coincide a grandes rasgos con las envolturas concéntricas de alteración hidrotermal alrededor de los stockworks encon-

tradas en otros sulfuros masivos, si bien es rara la aparición distal de una zona propilítica con epidota, además de clorita y sericita.

LOS SULFUROS MASIVOS

En superficie la mineralización aflora en dos lentejones (Lomero y Poyatos), que en profundidad se superponen dando lugar a un único cuerpo mineralizado. Los sulfuros masivos están rodeados por una zona en la que las rocas volcánicas están silicificadas y son ricas en pirita. Los sulfuros están intercrecidos con cuarzo, siderita y poca sericita, con boudines de sulfuros de grano fino de dimensiones cm en bandas miloníticas de grano más grueso y con abundante cuarzo intersticial. Se distinguen varios tipos de menas: (i) polimetálicas («complejo») de grano fino a muy fino, con bandas ricas en sulfuros de metales base alternando con otras de pirita. Tiene una importante foliación tectónica que rodea lentes y clastos de pirita; (ii) menas de pirita masiva, mostrando cierta foliación marcada por la presencia de intercalaciones de cuarzo y clorita; (iii) menas «cobrizas» (relativamente escasas), dominadas por pirita pero ricas en calcopirita y cobres grises que reemplazan y rellenas las microfracturas de la pirita.

Tanto en los sulfuros masivos como en los semimasivos el mineral dominante es pirita, con cantidades a veces significativas de esfalerita, calcopirita, cobres grises (tetraedrita-tenanntita) y galena. Como minerales accesorios aparecen arsenopirita, pirrotita, magnetita, barita y oro. La distribución de los sulfuros parece sugerir una cierta zonación, con una zona enriquecida en cobre el centro del depósito y un enriquecimiento en zinc y plomo hacia los márgenes este y oeste (Cambridge, 2004). La pirita es el mineral principal (entre 60 y 100%), exhibe hábitos muy variables, desde agregados coloformes (relictos) a microcristales cúbicos, y cristales subautomorfos zonados de grano medio a grueso con signos de intensa cataclasis. Le sigue en abundancia la esfalerita, formando agregados xenomorfos de grano fino, reemplazados por galena y calcopirita. El oro aparece como pequeños granos discretos en ambientes de bajo *stress* (preferentemente sombras de presión): adheridos a bordes de cristales de pirita, rellenando microfisuras en fenoclastos de pirita y/o asociado a la calcopirita y galena que actúa de matriz. El tamaño de estos granos de oro varía entre 1-2 y 75 micras (media de 15 micras) mostrando invariablemente composiciones ricas en Ag y Hg, lo que obligan a caracterizarlos como aleaciones Au-Ag-Hg (aprox. Au40Ag50Hg10). Estos valores coinciden con las características de las fases ricas en oro de Sotiel, Zarza y otros yacimientos de la FPI (Velasco et al. 2000).

Durante el metamorfismo regional estos sulfuros han sufrido una importante recristalización, concomitante con un proceso de deformación frágil en el caso de la pirita y dúctil para el resto de las menas. Las evidencias texturales, principalmente *pressure solution*, *annealing, grain boundary sliding* y formación de maclas indican el desarrollo de gradientes locales de deformación y recristalización, probablemente controlados por la proximidad a las zonas de cizalla. El resultado más evidente ha sido la aparición de texturas bandeadas y laminaciones que deben ser descritas como típicamen-

te miloníticas (protomilonitas y milonitas ss) con claras evidencias de flujo cataclástico. Al final de esta etapa, el relleno de microfracturas desarrolladas en pirita por las fases removilizadas (e.g., calcopirita, sulfosales, galena) demuestra la aparición de fenómenos hidrotermales tardíos (sin- a post-metamórficos) responsables de la aparición de fases discretas de oro (aleaciones Au-Ag-Hg).

GEOQUÍMICA DE LAS ROCAS ÍGNEAS

La geoquímica de elementos asumidos como inmóviles (Al, Ti, Y, Zr, Nb) permite caracterizar las distintas unidades volcánicas y establecer relaciones entre ellas a pesar de la alteración hidrotermal y deformación superimpuesta (e.g., Barrett et al., 2001). En el caso de Lomero Poyatos, las relaciones entre estos elementos muestran que la Unidad Superior está formada por dos unidades geoquímicamente diferentes caracterizadas por contenidos en Y y Zr muy distintos, lo que sugiere que provienen de un mismo magma pero con distinto grado de fraccionamiento. A pesar de ser petrográficamente similar, la Unidad Inferior es geoquímicamente muy distinta a las dos facies de la Superior, con menores contenidos en TiO_2 y Zr, sugiriendo que no proviene de la erosión de las anteriores sino de otra unidad volcánica independiente. La Unidad Intermedia guarda muchas similitudes geoquímicas con las rocas volcánicas que incluyen los sulfuros masivos de Aguas Teñidas, confirmando que esta unidad es probablemente una lámina tectónica que originariamente pertenecía al vulcanismo félsico que engloba los sulfuros masivos de la zona.

DISCUSIÓN Y CONCLUSIONES

El depósito de Lomero Poyatos se localiza en una zona en la que el vulcanismo es predominantemente andesítico. Sin embargo, la geología de detalle muestra que la mineralización está encajada en rocas volcanoclásticas félsicas ricas en vidrio y similares, a las que encajan otros sulfuros masivos de la zona más septentrional de la FPI (Tornos, 2006). Por ello, parece lógico suponer que el vulcanismo andesítico fue independiente de la mineralización y que ésta ha quedado laminada como una unidad exótica entre otras dos unidades tectónicas. La deformación de las rocas volcánicas alteradas y de los sulfuros masivos asociados es probablemente la responsable de la removilización y reconcentración hidrotermal de los sulfuros más dúctiles junto con el oro, que se han enriquecido en zonas más deformadas del depósito, dejando pirita masiva en las zonas centrales. Este proceso se revela como muy efectivo y capaz de dar lugar a zonas con altas leyes en metales base y oro. La extensión de estos mecanismos de deformación y recristalización al conjunto de los sulfuros masivos es responsable de la formación de bandeados de carácter milonítico que, a su vez, evidencian episodios de deformación asistidos por fluidos. Muchas de estas texturas ocasionalmente han sido interpretadas como texturas deposicionales primarias.

A pesar de la deformación superimpuesta, el depósito de Lomero Poyatos reúne muchas de las características geológicas de los sulfuros masivos formados por remplazamiento de rocas volcánicas reactivas y/o po-

rosas, tales como la ausencia de estructuras sedimentarias, la existencia de una aureola de alteración alrededor de los sulfuros masivos o la presencia de barita.

Este trabajo se enmarca en un proyecto sobre la geología del SO Ibérico, financiado por el IGME y por DGI-FEDER (BTE2003-290). Agradecemos la ayuda y comentarios de Bill Sheppard, Sergio Tenorio, Raúl Hidalgo, Víctor Guerrero y Carmen Conde.Agradecemos a Colin Andrew y Cambridge Mineral Resources el habernos facilitado el acceso a los sondeos y a la información existente sobre el depósito. Este trabajo es una contribución al proyecto del PICG 502 «Comparación Global de Sulfuros Masivos»

REFERENCIAS

Barrett TJ, MacLean, W. H. y Tennant, S. C. (2001). Economic Geology, 96, 1279-1305

Cambridge Mineral Resources (2004) http://www.cambmin.co.uk

Leistel, J.M., Marcoux, E., Thieblemont, D., Quesada, C., Sanchez, A., Almodóvar, G.R., Pascual, E., Saez, R. (1998). Mineralium Deposita, 33, 2-30.

Tornos, F. (2006). Ore Geology Reviews, 28, 259-307.

Velasco, F. Sánchez-España, J. Yanguas, A. Tornos, F. (2000). In: Volcanic environments and Massive Sulfide Deposits, Gemmell, J.B. and Pongrats, J. (eds), Codes and SEG, Univ. Tasmania, 221-223.

Shale basins, sulfur-deficient ore brines and the formation of exhalative base metal deposits

Fernando Tornos [a],*, Christoph A. Heinrich [b]

[a] *Instituto Geológico y Minero de España, c/Azafranal 48, 37001 Salamanca, Spain*
[b] *Isotope Geochemistry and Mineral Resources, Department of Earth Sciences, ETH Zurich, Clausiusstrase 25, CH-8092 Zurich, Switzerland*

Abstract

The massive sulfide deposits of the Iberian Pyrite Belt are interbedded with felsic volcanic rocks and shale, and underlain by several thousand meters of siliciclastic sedimentary rocks known as the PQ Group. Isotope geochemistry and regional geology are both consistent with equilibration of the ore-forming fluids with the PQ Group, prior to ore deposition near the former seafloor. The average Cu:Zn:Pb ratio of the PQ Group rocks (ca. 26:55:19) is similar to the weighted average of all the massive sulfide orebodies combined (ca. 25:52:23).

The genetic relationship between massive sulfide deposits and a siliciclastic sedimentary metal source is explained here by a thermodynamic model, proposing that mildly reducing redox conditions imposed by equilibration with the sedimentary rocks are most critical for the formation of an effective ore-forming fluid. Relatively metal-rich but organic-poor pyrite-bearing shale undergoing dewatering of saline pore fluids is an effective source for the generation of sulfur-deficient but relatively iron and base metal-rich brines. Thus, we propose that the giant deposits of the Iberian Pyrite Belt owe their existence not to exceptionally metal-enriched (e.g., magmatic) fluids, but to the existence of a fairly ordinary but large metal source in reactive siliciclastic sediments, combined with an underlying igneous heat source and a particularly efficient mechanism of sulfide precipitation by mixing with H_2S-rich fluids at or near the seafloor.

Essentially similar mineral equilibria are imposed when saline fluids are buffered by typical continental basement rocks. Leaching of retrograde minerals and possibly residual salts from their magmatic or metamorphic prehistory is expected to generate similar, variably metal-rich but relatively sulfide-deficient fluids. Thus, the existence of mildly reducing rocks can be the dominant chemical control in the source of fluids generating many volcanogenic, Irish-type or sedex deposits, many of which are known to precipitate their metal load in response to biogenic sulfide addition at the ore deposition site.
© 2007 Published by Elsevier B.V.

Keywords: Iberian Pyrite Belt; Volcanogenic massive sulfides; Sedex deposits; Geochemical modeling; Metal solubility

1. Introduction

One of the most controversial aspects of the genesis of sediment- and volcanic-hosted stratabound hydrothermal mineralization is the source of fluids and metals and the physical and chemical conditions of material

* Corresponding author. Tel.: +34 923 265009; fax: +34 923 265066.
E-mail addresses: f.tornos@igme.es (F. Tornos), heinrich@erdw.ethz.ch (C.A. Heinrich).

transport. Solubility considerations suggest that metals and reduced sulfur cannot be transported together in sufficiently high concentrations in a mildly acid to neutral fluid at temperatures below about 350°C. Unrealistically high volumes of fluid and long lived convection systems would be required to form a significant deposit (Anderson, 1975; Sverjensky, 1989; Solomon and Heinrich, 1992; Spirakis and Heyl, 1995). Thus, it seems a prerequisite that effective metal-transporting fluids must be poor in reduced sulfur (e.g., Plumlee et al., 1994; Kyle and Saunders, 1996; Anderson et al., 1998). Two main alternatives have been proposed, including (a) the transport of metals and sulfur by different solutions that later mix, or (b) the joint transport of metals with sulfate, which is later reduced in the depositional environment (e.g., Sverjensky, 1989; Plumlee et al., 1994; Spirakis and Heyl, 1995; Hinman, 1996; Cooke et al., 2000).

Geochemical studies and comparison with present-day submarine hydrothermal systems have shown that many seafloor hydrothermal systems are related with the convective circulation of heated seawater that acquires metals from volcanic and basement rocks (Bischoff and Dickson, 1975; Francheteau et al., 1979; Reed, 1983) whereas some deposits formed in active arc settings show evidences of input of magmatic fluids carrying significant amounts of metals (e.g., Urabe, 1987; de Ronde, 1995; Yang and Scott, 1996, 2005).

In this work we present a new thermodynamic and conceptual argument, suggesting that there is a genetic relationship between giant massive sulfides and the presence of underlying thick shaly sequences or their metamorphic equivalents. Intuitively, diagenetic fluids equilibrated with pyrite-bearing shale might be expected to be sulfur-rich and unable to transport large amounts of metals. However, thermodynamic modeling shows that moderately saline fluids are able to leach large amounts of metals from such sediments, because the H_2S content of the fluid is buffered to low levels by the moderately reducing mineral assemblages that characterize the sedimentary rocks. Calculated metal solubility and the estimated quantity of shaly sediments are adequate to produce the deposits by single-pass fluid expulsion from the basin, after underplating by magmatic rocks or by incipient convection driven by the resulting elevated geothermal gradient (Conde et al., 2005; Tornos, 2006).

2. Geological and geochemical aspects of the Iberian Pyrite Belt

The Iberian Pyrite Belt (IPB) is the world's largest province of volcanogenic massive sulfides. About 1700–2000Mt of massive sulfides are known to be hosted mainly by nine giant deposits (> 100Mt: Neves Corvo, Aljustrel, La Zarza, Rio Tinto, Tharsis, Aznalcóllar-Los Frailes, Masa Valverde, Sotiel-Migollas and Aguas Teñidas), plus tens of smaller orebodies (see Leistel et al., 1998; Tornos, 2006; Fig. 1). Some authors have emphasized that the IPB shares some features more typical of sedex ore provinces than volcanogenic ones (Saez et al., 1996).

The IPB is interpreted to have formed in a synorogenic, continental marine basin during the oblique collision of the South Portuguese Zone and Gondwana during Variscan times. Transpressional tectonics formed large pull-apart basins, accompanied by crustal thinning, magma underplating, high heat flow and intrusion of igneous rocks (e.g., Silva et al., 1990; Quesada, 1992). The massive sulfides are hosted by the Volcanic Sedimentary Complex (VS Complex), a late Devonian to early Carboniferous sequence of dominantly felsic volcanic and volcaniclastic rocks, interbedded with mafic volcanics, shale and chemical sediments. The VS Complex overlies the Phyllite–Quartzite (PQ) Group, a several km thick sequence of shale with accessory quartz-rich to arkosic sandstone of Famennian age and deposited in a stable epicontinental platform. The basement to these rocks is not known due to later trust tectonics but probably consisted of thinned continental crust. The original total thickness of the PQ Group is also unknown but the most detailed studies suggest that is well above 2000m (Moreno et al., 1986; Mantero et al., 2005). Geophysical studies (Simancas et al., 2003) indicate that the present upper to middle crust below the IPB is dominated by rocks that are physically similar to the PQ Group. The uppermost PQ Group includes rocks indicative of basin destabilization and compartmentalization in individual sub-basins, such as coastal, delta-related or continental siliciclastic sediments or reef-like carbonatic rocks (Moreno et al., 1996).

Siliciclastic rocks of the PQ Group are dominated by quartz, phengitic muscovite and chlorite with plagioclase (oligoclase–albite) and K-feldspar always present in smaller amounts. Pyrite and ilmenite (replaced by rutile) are widely dispersed along with traces of pyrrhotite, magnetite and chalcopyrite. Sulfur content in the shale is between 0.04 and 9.3%, averaging 1.5%S. The organic carbon content of most rocks is low (< 0.3–1.2wt.%). Where visible, carbon occurs as minute dispersed flakes adjacent to phyllosilicates or interstitial to detrital grains.

The massive sulfides are mostly composed of pyrite with lesser sphalerite, galena and chalcopyrite and several tens of accessory phases (e.g., Marcoux and Leistel,
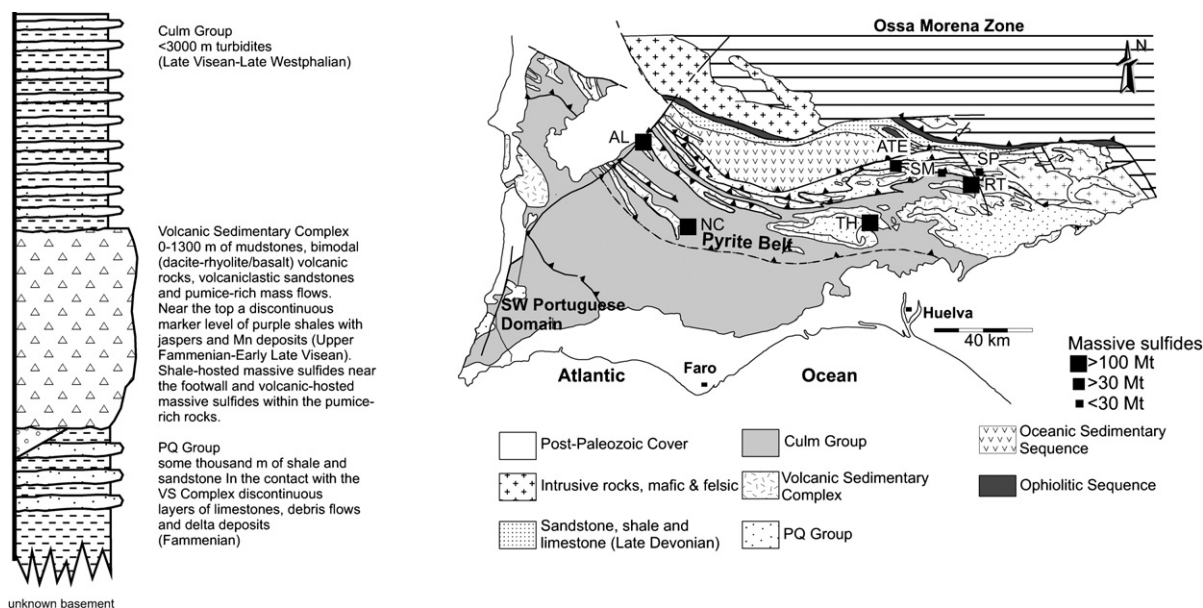
Fig. 1. Geological setting of the South Portuguese Zone showing the location of the Iberian Pyrite Belt and the most significant volcanic-hosted massive sulfide deposits. The stratigraphic column is of the Iberian Pyrite Belt. AL: Aljustrel; ATE: Aguas Teñidas Este; NC: Neves Corvo; RT: Rio Tinto; SM: San Miguel; SP: San Platón; TH: Tharsis. Modified from Tornos (2006).

1996). There are two main groups of deposits: (a) large stratiform pyrite-rich deposits probably, which formed in anoxic brine pools within shale of the lowermost VS Complex (Solomon et al., 2002; Tornos et al., in press); and (b) replacive deposits within felsic volcanic rocks, formed during the early diagenesis of porous and reactive pumice- or glass-rich volcaniclastic lithologies in the shallow subsurface beneath the seafloor (Tornos, 2006). Barite is absent in the shale-hosted deposits but fairly common in the volcanic-hosted ones. Stockworks, exposed to a maximum known depth of about 400m, underlie most of the massive sulfides and are best developed in deposits hosted by volcanic rocks. Where stockwork zones extend into the PQ Group they are present as irregular to stratabound zones of chlorite-rich alteration grading laterally and downwards into unaltered shale. This indicates that the ascending fluids were close to chemical equilibrium with the underlying siliciclastic rocks before they reached the environment of sulfide deposition.

Hydrothermal fluids trapped as inclusions in stockwork veins are aqueous and have salinities exceeding that of seawater, up to 30wt.% $NaCl_{eq.}$, but mostly in the 3 to 12wt.% range (Almodovar et al., 1998; Nehlig et al., 1998; Sánchez España et al., 2003; Moura, 2005). Sulfur isotope values vary widely (−38 to +22‰; Velasco et al., 1998; Tornos, 2006) and are consistent with a dual origin for the reduced sulfur: some derived from a deep sulfide source via leaching from underlying rocks or thermochemical reduction of seawater sulfate, and some derived by biogenic reduction of seawater sulfate, added in the environment of ore deposition. The range in $\delta^{34}S$ is largest in the shale-hosted deposit, inferred to be deposited at the sediment–water interface, and somewhat more homogeneous and positive in the replacive deposits hosted by volcaniclastic rocks (Tornos, 2006). Sulfur carried by the deep fluids was isotopically more homogenous with a $\delta^{34}S$ value near 8‰. The isotopic signature of the reduced sulfur derived by biogenic reduction of seawater is highly variable and mainly depends on the closed or open nature of the system, and the scale and degree of mixing (Ohmoto, 1986). Highly heterogeneous sulfur isotope values indicate that about half of the total sulfur now present within the massive sulfides was added in situ near the seafloor (Tornos, 2006), but this fraction may have been even higher if sulfide derived by partial sulfate reduction had became homogenized prior to massive sulfide precipitation. Ore mineral assemblages and the geologic setting also suggest that the deep fluids were reduced, and certainly did not have high $SO_4^=/H_2S$ ratios like the evaporite-derived hydrothermal fluids in the McArthur Basin of northern Australia (Hinman, 1996; Cooke et al., 2000).

The studies of Marcoux et al. (1996) and Leistel et al. (1998) show that stockworks in the IPB have a different mineral assemblage than the overlying massive sulfides.

This is especially evident in the Tharsis deposit, where the stockwork is enriched in pyrrhotite, cobaltite, arsenopyrite, sulfosalts and tellurides. This assemblage contrasts with the virtual absence of these minerals and the predominance of pyrite in the overlying massive sulfides (Marcoux et al., 1996; Tornos et al., 1998), indicating that the ascending fluids were relatively sulfide-poor and became sulfidized when they entered the ore depositional environment. Sulfur-depleted but metal-rich hydrothermal fluids have also been quoted in several sediment-hosted base metal deposits such as Navan (Anderson et al., 1998), the MVT deposits of the Ozark region (Plumlee et al., 1994) or some modern oceanic hydrothermal systems (Kyle and Saunders, 1996). The detailed isotopic study of Fallick et al. (2001) at the Navan deposit (Ireland) shows that the deep metal-bearing carrying fluids were depleted in reduced in sulfur and 90% of the reduced sulfur was acquired in situ by biogenic reduction of seawater sulfate.

3. Metal ratios in sediments and deposits

Before addressing a general thermodynamic model for sulfur-deficient ore fluids, we present a new data set for the composition of the proposed metal source rocks in IPB, providing at least permissive evidence that metal quantities and even metal ratios in the underlying sedimentary package were adequate for ore formation. Compilation of geochemical analyses of 89 widely distributed and apparently unaltered samples of shale and sandstone of the PQ Group (Appendix A) shows that this sequence contains quite variable metal concentrations and ratios, but covers the typical range of global shale averages (Turekian and Wedepohl, 1961; Carmichael, 1989: 45–57 ppm Cu, 80–95 ppm Zn and 20 ppm Pb). Metal contents of the PQ Group are, on average, 6.0% FeO_t (2.3–12.3%; $\sigma = 3.5\%$), 39 ppm Cu (3–473 ppm; $\sigma = 57$ ppm), 79 ppm Zn (13–238 ppm; $\sigma = 36$ ppm) and 29 ppm Pb (4–514 ppm; $\sigma = 74$ ppm). These average base metal ratios (Cu:Zn:Pb, 26:55:19) match almost exactly the integrated weighted metal grade in all massive sulfides and related stockworks combined (25:52:23; Leistel et al., 1998; Tornos, 2006) (Fig. 2). Statistical analysis using the 25 and 75 percentile shows similar metal ratios (24:64:12) despite the variability of individual bulk-rock analyses and the metal grades of single deposits, indicating that this match is not a mere coincidence. The close correspondence,
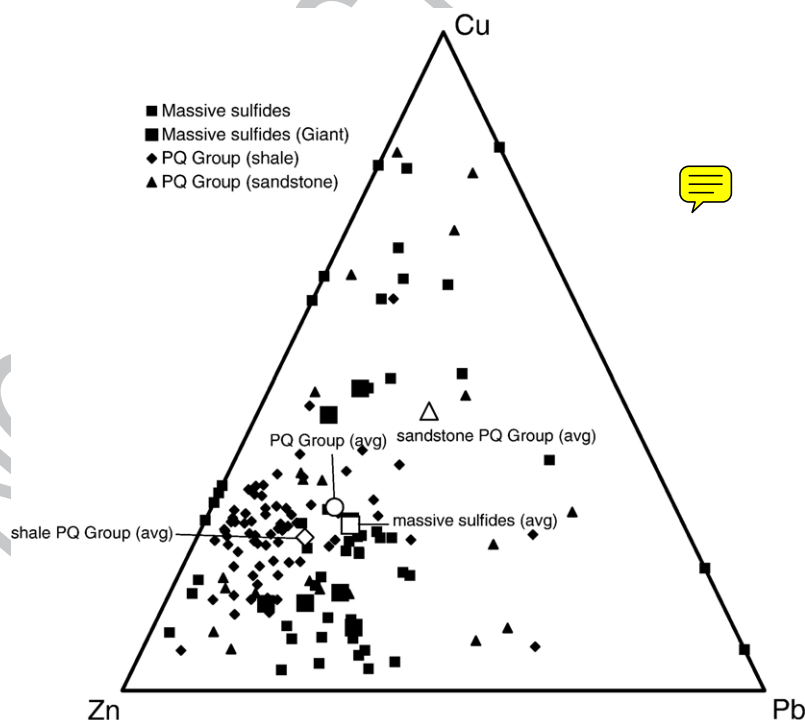

Fig. 2. Metal proportions in sediments of the Phyllite–Quarztite Group and in the massive sulfide deposits of the Iberian Pyrite Belt. The Cu–Zn–Pb ratio of the bulk of the massive sulfides is calculated weighted by the total tonnage of the orebodies. Data from Leistel et al (1998) and Tornos (2006).

even within an order-of-magnitude, may indicate that the metal ratios in the massive sulfides are partly controlled by the metal abundance in the underlying rocks. Barrie and Hannington (1999) observed a similar correlation in other massive sulfide provinces, and interpreted it as a consequence of the inheritance of metals from the basement rocks of each region.

All isotopic data are permissive of equilibration of fluids with the PQ Group and possible derivation of metals from these sedimentary rocks, but they do not exclude crustal magmas. Most $\delta^{18}O$ and δD fluid values are between 0 and 8‰ and −45 to 5‰, respectively. These values are consistent with fluids derived either from a magmatic source (Sánchez España et al., 2003) or from the equilibration at low fluid/rock ratio with (meta-) sedimentary rocks (Fouillac and Javoy, 1988; Tornos, 2006), that later mixed with seawater near the seafloor. The $^{87}Sr/^{86}Sr$ ratios of hydrothermal carbonate are moderately high (0.7073–0.7109, locally up to 0.7203; Tornos, 2006) and suggest mixing of seawater with a radiogenic source that could well be the PQ Group or an underlying basement with similar isotopic composition. Limited $^{87}Sr/^{86}Sr$ data of the PQ Group ($^{87}Sr/^{86}Sr_i$, 0.7113–0.7171; Tornos, 2006) are consistent with such a model. The lead and osmium isotope signatures also indicate that the source of these metals was homogeneous and of crustal derivation (Marcoux, 1998; Mathur et al., 1999; Relvas et al., 2001; Munhá et al., 2005; Tornos, 2006).

4. Solubility constraints on the fluid source

In this section we show that the mineralogical characteristics of the sedimentary rocks of the PQ Group are thermodynamically consistent with effective metal leaching by common crustal fluids, and that the sedimentary package can therefore be the dominant source of the ore metals in the massive sulfide deposits of the IPB. Calculation of multicomponent solubilities using experimental thermodynamic data and geological constraints from the IPB provides important new constraints, compared with previously published arguments based on the solubility of individual sulfide minerals. The SOLVEQ/CHILLER package (Reed, 1998) and an updated SOLTHERM database including the thermodynamic data of Liu and McPhail (2005) were used to predict the composition of a hydrothermal fluid in equilibrium with shale at 350 to 100°C and its behavior during cooling and fluid mixing. The model fluid had a salinity of 9wt.% NaCl eq. and was assumed to be in equilibrium with the mineral assemblage of the PQ Group shale (Table 1). Chlorite is a common phase within the shale, but its thermodynamic data are not

Table 1				t1.1
Conditions of numerical calculation for the Figs. 3 to 5				t1.2
	Deep fluid (ppm)		Reduced seawater[a]	t1.3
T°C		325°C	2°C	t1.4
SiO_2	Equilibrated with quartz	638	0	t1.5
$\sum Na$	Defined by salinity	29,258	10,752	t1.6
$\sum K$	KFMASH buffer	13,626	390	t1.7
$\sum Al$	KFMASH buffer	7.8	0	t1.8
$\sum H_2S$	py–po equilibrium	56	2410	t1.9
$\sum SO_4^-$	From mt–py–po equilibrium	13.8	2680	t1.10 Q1
$\sum Fe$	py–po equilibrium	316	0.00006	t1.11
$\sum Cu$	Saturation in chalcopyrite	28	0.00045	t1.12
$\sum Zn$	Zn:Pb:Cu ratio in rock (see text)	53	0.00065	t1.13
$\sum Pb$	Zn:Pb:Cu ratio in rock (see text)	16	0.00045	t1.14
$\sum Ba$	Assumed	10	0	t1.15
pH	KFMASH buffer	4.93	7.8	t1.16
fO_2	mt–py–po equilibrium	$10^{-32.2}$ [b]	10^{-78} [b]	t1.17
fS_2		$10^{-10.5}$ [b]	10^{-17} [b]	t1.18

[a] Partially based on Scott (1992) assuming that 90% of all the sulfate has been reduced to H_2S and pyrite is stable.   t1.19

sufficiently well known to provide a rigorous constraint on fluid composition. The presence of quartz, two feldspars and muscovite suggests that the aK^+ and the pH of the fluids were close to this common crustal rock buffer (Hemley et al., 1992; Yardley, 2005). The absence of large zones of hydrothermal alteration within the PQ Group is also consistent with the assumption that hydrothermal fluids were close to equilibrium with siliciclastic rocks until they approached the seafloor, where there are steep chemical gradients due to fluid mixing and rapid temperature variation.

Calculations were performed between rather low fO_2 near graphite saturation (3.5 log fugacity units below NNO) and intermediate fO_2 conditions (NNO and pyrite–pyrrhotite–magnetite, PPM). In such mildly acidic and moderately reduced systems, sulfur and iron solubilities are internally constrained by excess iron sulfides and oxides (and/or chlorite) and vary strongly with temperature. At low fO_2 (with graphite present in the extreme case) the concentration of reduced sulfur in the fluid is always higher than those of combined metals, which are correspondingly low. Thus, cooling of such a highly reduced fluid and reaction with the same host rocks will always lead to base metal sulfide saturation within hydrothermally altered rocks, leading to dispersed mineralization before the fluids reach the seafloor. At mildly reducing conditions in equilibrium with pyrite–pyrrhotite–magnetite (PPM; Fig. 3) sulfide concentration are much lower, and the amounts of metals that can
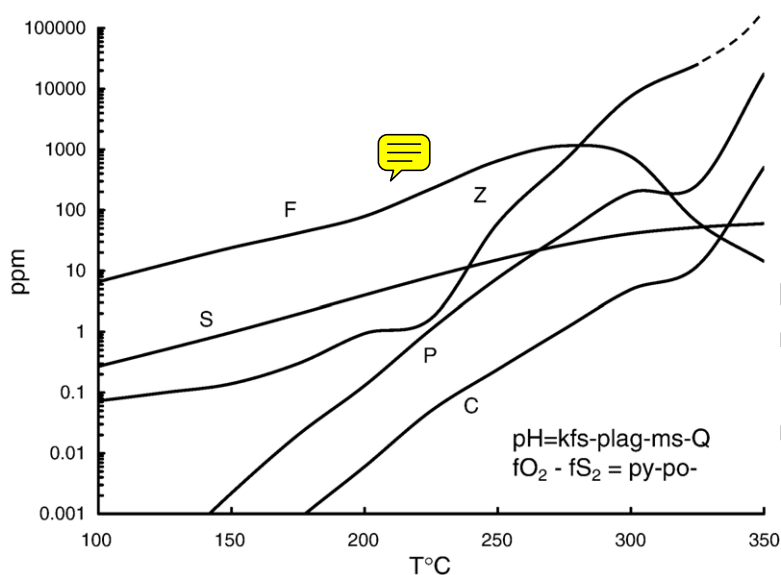
Fig. 3. Base metal and sulfur solubility as a function of temperature between 350 and 100°C at a pH buffered by the mineral assemblage observed in the sedimentary rocks, for a total salinity of 9wt.% NaCl equivalent and the fO_2–fS_2 conditions defined by the pyrite–pyrrhotite–magnetite equilibria. Base metal solubilities are calculated in equilibrium with excess sphalerite, galena and chalcopyrite. Mineral abbreviations are in www.unige.ch/sciences/terre/mineral/fontbote/opaques.

be leached by the fluid are correspondingly higher. In general, the more oxidized and the more alkaline the solution is in the multicomponent system, the higher are the base metal solubilities and the lower the reduced sulfur content. At redox conditions near and above the hematite–magnetite buffer, sulfate species become the main sulfur form, defining the fluid environment proposed by Cooke et al. (2000) for base metal transport in sediment-hosted deposits overlying oxidized sequences like at McArthur River (Australia).

At 300°C, a fluid equilibrated with feldspar-bearing shale at fS_2 and fO_2 close to the PPM buffer can transport 8300 ppm Fe, more than 10000 ppm Zn, 1000 ppm Pb and 7 ppm Cu, but will contain only 36 ppm S as H_2S, if saturation with the respective sulfide minerals is assumed (Fig. 4). Dominant metal-transporting aqueous complexes include mostly chloride complexes such as $FeCl_4^-$ and $FeCl_2^-$ (Fe), $CuCl_2^-$ and $CuCl_3^=$ (Cu), $ZnCl_4^=$ (Zn) and $PbCl_3^-$, $PbCl_4^=$ and $PbCl_2$ (Pb). The solubility of metals increases dramatically with increasing temperature, and copper, in particular, cannot be leached significantly from the proposed source rocks at temperatures below 300–325°C.

Calculations show that co-transported sulfur is therefore only able to precipitate a small proportion (< 1%) of the metals contained in the fluid. This sulfide deficiency of the hydrothermal fluid is suggested to be critical for

the formation of the exhalative deposits, because it favors large-distance transport of metals up to a site where the fluid encounters an external source of reduced sulfur, e.g., a H_2S-rich anoxic basin or brine pool, surficial water carrying reduced sulfur, or a sulfide-rich rock.

The correspondence in metal ratios between the IPB deposits and the PQ Group shale implies that the hydrothermal fluids were metal-undersaturated at source, at least in lead and zinc. Otherwise, the (Zn + Pb)/Cu ratio should increase with increasing equilibration (i.e., rock/fluid ratio) of the fluid with a galena + sphalerite + chalcopyrite bearing source rock, to values well above those of the PQ Group (≫ 250) but below those of the massive sulfides (< 30). Assuming that the Cu:Zn:Pb ratio in the fluid was mainly controlled by the metal proportion in the source rock, the likely average deep fluid in the IPB at 300–325°C, having a pH close to 5 and an fO_2 and fS_2 near the PPM buffer, should transport between 64 and 750 ppm Fe but only 41–52 ppm H_2S. For these conditions, the solubility of copper is strongly dependent on temperature, ranging from 5 ppm at 300°C to 28 ppm at 325°C. Corresponding Zn and Pb contents will then be 10–60 and 4–23 ppm, respectively.

Mixing of such a mildly reduced sulfide-deficient ore fluid in the site of deposition with fluids having excess H_2S would effectively precipitate sulfides. Mixing with seawater in which most of the sulfate has been biogenically reduced to H_2S will lead to both cooling
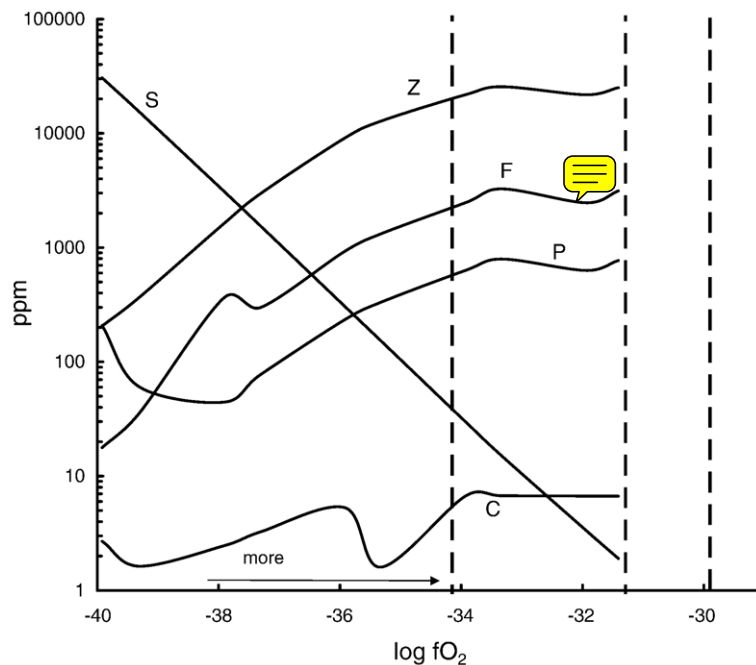
Fig. 4. Reduced sulfur (S) and metal solubility in a shale-buffered reservoir at 300°C showing the strong dependence on the redox conditions. Calculations performed at a constant pH of 4.5 and the fS_2 controlled by the pyrite–pyrrhotite equilibrium. The $H_2S:SO_4^=$ boundary is that defined by equal molalities of reduced and oxidized sulfur species.

and an increase of the sulfide content in the fluid mixture, resulting in supersaturation of all metals and the deposition of the massive sulfides. Fig. 5 shows the reaction of a deep fluid equilibrated at 325°C with the PQ shale, and subsequent mixing with cool seawater that has 90% of its sulfate reduced to H_2S.

Numerical modeling shows that mineral assemblages are predicted to be dominated by pyrite with lesser chalcopyrite (up to 3–4%), sphalerite (max. 9%) and galena (max. 2%). These results closely match the observed assemblage and ore grades in the pyrite-rich orebodies of the IPB. The highest base metal grades are generated during the initial stages of mixing, while at a higher degree of mixing the assemblage is increasingly dominated by pyrite. In these Mg–Al-free model calculations, the main precipitated gangue mineral is quartz. This would be partly substituted by chlorite in nature, where pure colloidal silica is known to be lost to the water column due to the sluggish rate of nucleation of quartz or its amorphous counterpart (Mottl and McConachy, 1990). Minor K-feldspar or muscovite, and carbonate (dolomite, calcite or ankerite) are also predicted to precipitate.

Barite only forms at very high proportions of seawater to deep fluid and requires that the Ba content of

the deep fluid or the $SO_4^=/H_2S$ ratio are higher than those assumed here (> 10ppm and > 0.1, respectively). In present-day anoxic bottom waters, less than 30% of the total sulfate becomes reduced by biological activity (see Goodfellow et al., 2003), and barite-free massive sulfides can only form in extremely anoxic settings, such as brine pools. A significant increase of the proportion of sulfate in the depositional site would lead to widespread precipitation of barite. This indicates that the barite-poor deposits of the IPB precipitated from very $SO_4^=$-poor systems or that all the Ba was extracted from the fluid prior the site of deposition. In fact, white micas within the stockwork zones of the IPB show major enrichment in Ba (Costa, 1996).

Cooling without admixing of reduced sulfur will lead to the precipitation of chlorite, chalcopyrite and a smaller proportion of pyrite (±quartz) but will never reach galena or sphalerite saturation. Chalcopyrite enrichment in the stockworks (Leistel et al., 1998) is probably related to such a process, since most of the total copper contained in the fluid precipitates by cooling from 350 to 300°C, utilizing the small amount of H_2S in the sediment-equilibrated fluid. The conceptually simplified local-equilibrium calculations of Figs. 4 and 5 would predict that Cu should be precipitated during the earliest cooling
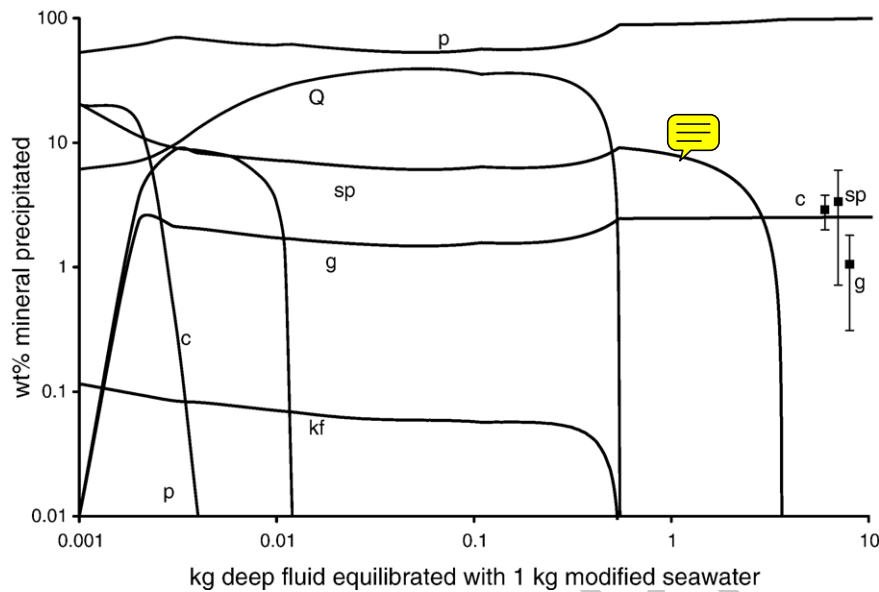
Fig. 5. Plot showing the predicted weight proportion of minerals precipitated due to mixing of a deep basinal brine equilibrated with the PQ Group at 325°C (Fig. 3) with seawater having 90% of its sulfate reduced to H_2S (modified seawater) in an anoxic seafloor. Average base metal sulfide content and its variation (2σ) calculated from weighted average ore grade for the whole of the Iberian Pyrite Belt, is indicated for comparison.

steps after the fluid leaves the rock-buffered source region, thereby separating Cu from Zn–Pb mineralization. The fact that the fluids obviously reach the chalcopyrite-rich but low-fS_2 (pyrite + pyrrhotite + arsenopyrite) stockwork environment beneath the Zn and Pb-bearing massive sulfide deposits requires that the fluids ascended by fast and focused flow under adiabatic conditions. This aspect of the hydrothermal systems in the IPB is similar to observations from mid-ocean ridge black smokers, which indicate that fluid focusing leads to near-isothermal fluid ascent (see Jupp and Schultz, 2000). Structurally focused saline fluids tend to become more acid upon cooling, due to limited interaction with feldspathic wall rocks, which will partially counteract early chalcopyrite precipitation far below the stockwork zone of the deposits.

5. Discussion

5.1. The role of magmatism

The deposits of the IPB are usually classified as volcanogenic massive sulfide deposits, on account of their association with coeval volcanoclastic rocks (Carvalho et al., 1997; Leistel et al., 1998). Some authors have therefore suggested a magmatic origin for saline fluids and metals within the IPB (e.g., Solomon and Quesada, 2003) or at least to the unusual Sn–Cu-rich ores at Neves Corvo (Relvas et al., 2001, 2006), in analogy with volcanogenic deposits associated with submarine arc or back-arc magmatism elsewhere (Yang and Scott, 1996). Although a magmatic fluid source has been recognized in several recent and ancient systems (Yang and Scott, 1996, 2005; Hannington, 1999; Galley, 2003; de Ronde et al., 2005), there is little or no evidence that magmatic fluids were an essential ingredient for ore formation in the IPB. The proposed evidence for magmatic fluids is circumstantial and probably driven by hydrological, mineralogical and tectonic considerations, rather than by geochemical or geological evidence, which merely indicates that the magmatism provided an essential heat source. Acid alteration typical of submarine magmatic-hydrothermal systems (advanced argillic or magnetite–chlorite–apatite assemblages; e.g., Corbett, 2001) or replacement zones formed by subseafloor mixing of magmatic fluids with seawater (Gemmell et al., 2004) are absent beneath the IPB deposits. None of the deposits is spatially associated with shallow intrusions and no specific plutons showing evidence for magmatic fluid exsolution have ever been identified in the region. Furthermore, vein systems or large hydrothermal haloes associated with the interaction of magmatic fluids with the PQ Group have never been described (cf. Large et al., 1996; Corbett, 2001; Galley, 2003). Extensive stable and

radiogenic isotope studies do not conclusively show a significant magmatic component (Barriga, 1990) and all the isotope signatures can be explained by derivation of fluids and metals from shale or a basement of continental derivation. The observed high $\delta^{18}O_{fluid}$ values interpreted as magmatic (Barriga, 1990; Sánchez España et al., 2003) can equally well be explained as reflecting the circulation of isotopically exchanged connate or metamorphic water. Original magmatic signatures could be masked due to isotope exchange with the sedimentary rocks during upflow. However, interaction of a magmatic fluid traveling along a structure through the upper crust and equilibrating with it – in order to produce isotopic equilibrium – is likely to leave some geological signal in the form of major hydrothermal alteration or mineralization.

5.2. The high tin contents at Neves Corvo

Another argument proposed for the presence of magmatic fluids is the high tin grade in Neves Corvo (Relvas et al., 2006). Tin is a common but minor metal present in volcanogenic (Kidd Creek; Hennigh and Hutchinson, 1999) and sedex deposits (Sullivan; Hamilton et al., 1983). Cassiterite commonly occurs as inclusions in sphalerite in many IPB deposits (Marcoux and Leistel, 1996). Analyses of selected ore samples presented by Leistel et al. (1994) show grades of up to 0.7% Sn in Río Tinto, 0.2% in Aznalcóllar, 0.13% in Romanera, 3% in Sierrecilla and 0.02% in Sotiel. Although Sn grades as high as 13% are found at Neves Corvo (Relvas et al., 2002), such Sn-rich orebodies are small (ca. 2Mt) compared with the total tonnage of the massive sulfides there (219Mt; Tornos, 2006). Therefore, the average Sn grade of Neves Corvo, if taken relative to the total of massive sulfides, is probably comparable to that of other IPB deposits and quite similar to some sediment-hosted deposits with no recognized magmatic input, such as Sullivan (Hamilton et al., 1983).

The locally high Sn contents of Neves Corvo ores may reflect a highly efficient mechanism of cassiterite precipitation, rather than extremely Sn-rich fluids. Mildly reducing saline fluids of any origin are ideal for transporting Sn^{2+} chloride complexes, and Heinrich (1990) already predicted that mixing of similar fluids with oxidized seawater could lead to the formation of rich exhalative Sn deposits. At Neves Corvo, precipitation of the high-grade stratiform Sn ore predates that of the massive sulfides (Relvas et al., 2001). We suggest that this might record the transition from early cassiterite precipitation by venting of initial batches of S-poor basinal fluid into sulfate-bearing oxic seawater, followed by the main stage of massive sulfide mineralization after an anoxic brine pool had been established.

5.3. Fluids derived from dewatering of siliciclastic sequences?

The model that best accounts for the geological and geochemical features of the massive sulfides in the IPB involves the flow of basinal brines expelled from or circulating through the PQ Group, in a scheme similar to that envisaged for many sedimentary-exhalative deposits (e.g., Goodfellow et al., 1993; Large et al., 2005). The IPB was a particularly efficient ore-forming environment, because high heat flow enhanced metal solubility (especially Cu), facilitated fluid-rock equilibration and acted as a heat engine driving fluid advection. Accelerated diagenetic maturation and single-pass dewatering alone can release enough fluid and leach enough metals to form large orebodies (Lydon, 1983). Mass balance estimates, assuming that the PQ Group has a minimum volume of 100x100km and is 2km thick, indicate that the sedimentary sequence underlying the massive sulfide deposits of the Iberian Pyrite Belt contains at least 200 times the total metal contained in the orebodies. These are minimum values as the basin may have been much larger. Thus, only a small fraction of the metals contained in the PQ Group (< 0.5%) needs to be extracted in order to form the orebodies. As a result, the average metal content of the sediments as analyzed today is not significantly depleted and the correspondence of metal budgets did not suffer any systematic disturbance by the hydrothermal process. Diagenetic maturation of a volume of $100 \times 100 \times 2$ km of sediment originally consisting of 80% clay and 20% sand can release between 7.2×10^{12} to 1×10^{13} m^3 of fluid, as calculated using the parameters of Garven and Freeze (1984). This fluid volume is about 10 times larger than required for the formation all massive sulfides of the IPB using the fluid-chemical parameters computed above. Single-pass dewatering of the PQ Group basin is therefore entirely adequate to explain the IPB deposits, perhaps followed later by open-system convection (Conde et al., 2005). Both modes of fluid flow are ultimately driven by high thermal gradients caused by the widespread intrusion of igneous rocks. Although those magmas could have contributed a component of magmatic fluid to the ore-forming hydrothermal system, there is neither clear evidence nor any fluid-chemical necessity. Diagenetic maturation and compaction of shaly sequences can build up the fluid overpressures needed for vigorous upflow of connate fluids (Fowler and Anderson, 1991; Caritat and Baker, 1992; Bolas et al., 2004; Garavito, 2006).

5.4. The origin of salinity

While fairly ordinary sediments are adequate as a source of all ore-forming components in the IPB deposits, an elevated salinity of the fluids is decisive for the model to work. High salinities are required both for chemical and hydrological reasons. Copper solubility, a limiting chemical parameter in the efficiency of our transport model, increases almost with the square of the chloride concentration. Depending on estimated exhalation temperature (100–350°C; Tornos et al., 1998), the hydrothermal fluids have to be between 3 and more than 10 times more saline than the ambient seawater, to remain negatively buoyant and generate the stratiform deposits in brine pools (Solomon et al., 2002).

Fluids with salinities up to 32wt.% NaCl eq. are widespread in evolved sedimentary basins (Sverjensky, 1984; Sheppard, 1986; Hanor, 1994; Nesbitt and Muehlenbach, 1994; Gleeson et al., 2003; Yardley, 2005). The origin of such saline connate brines is controversial and several hypotheses have been proposed. They include the presence of evaporated seawater trapped in the pores of a shaly sediment (Leach et al., 2001) or dissolution of dispersed evaporites (Hanor, 1994) The original pore fluid in the PQ Group sediments may have high salinities due to deposition in a moderately evaporative closed basin. This is consistent with the fact that SW Iberia was located in subequatorial latitude during late Devonian times (Stampfli and Borel, 2002) and with local evaporite layers in limestone within the uppermost PQ Group (Tornos, 2006). Other processes invoked for significantly increasing the chlorine content of seawater trapped in the sediments include shale membrane filtration (Graf, 1982; Garavito, 2006), diagenetic maturation of Cl-rich illite to white mica with concomitant release of Cl (Michalik, 1997) or diagenetic hydration of clastic minerals to sheet silicates (Gleeson et al., 2003). The exact mechanism for the IPB is not known, but any of these processes involve intimate interaction of pore fluids with the sedimentary rocks on the mineral grain scale, which is the one essential requirement for the fluid source process proposed here.

5.5. Application to other metal provinces

The presented model is applicable to siliciclastic basins in other important metal provinces (Bathurst camp: Goodfellow et al., 2003; the Selwyn and Rhenic basins or the Sullivan deposit: Goodfellow et al., 1993) but also to fluids equilibrated with any other pyrite-bearing, mildly reduced rocks. Continental basement composed of quartz–feldspathic metamorphic rocks and granitoids has a similar dominant mineralogy and thus may buffer fluids contributing to the formation of Pb–Zn deposits in overlying carbonate basins, such as Mississippi Valley Type deposits (Plumlee et al., 1994). In particular, the multicomponent mineral equilibria shown in this paper are directly applicable to the current model for the Irish Pb–Zn–(Cu) deposits (Russell et al., 1983; Wilkinson et al., 2005). Direct geological and isotopic tracing shows that these deposits form by initial interaction of evaporated seawater with basement rocks below a major unconformity, followed by their expulsion into a exhalative to diagenetic precipitation environment characterized by biogenic or abiotic sulfide generation in an epicontinental carbonate basin. Although the geology, hydrology and driving forces are entirely different, the decisive fluid-chemical controls on ore formation may be the same in the Irish and Iberian base metal deposits.

6. Summary and conclusions

The composition of the siliciclastic sediments underlying the massive sulfides in the Iberian Pyrite Belt probably controlled the metal ratios and buffered the H_2S content of the ore-forming fluids to a relatively low level. Sediment-equilibrated, sulfide-deficient hydrothermal fluids are interpreted to be critical for the ore-forming process, because they allow transport of significant concentrations of Cu, Pb and Zn, given the intermediate fO_2 and mildly acid pH imposed by the source rock. Large pyrite-rich orebodies are deposited where the H_2S-deficient ore fluids encounter a source of external sulfide near the sediment–water interface. Our model implies that the exceptional metal endowment of the IPB is the result of the specific depositional and thermal evolution of a sedimentary basin, comprising the following essential ingredients: (1) a suitable source rock package of sediments with a relatively constant mineralogical composition characterized by the presence of disseminated sulfides but little or no organic carbon, (2) a highly elevated thermal gradient at the base of the sedimentary package, which accelerated diagenesis and promoted rapid expulsion of metalliferous brines and, (3) a highly efficient chemical trap for concentrated precipitation of massive sulfides by addition of sulfide near the sediment–water interface, derived by biogenic or thermogenic reduction of seawater sulfate. This model may apply to other sediment- or volcanic-hosted provinces in which the massive sulfides are underlain by thick (meta-)siliciclastic sediments. The same mineral equilibria may also buffer the sulfur- and metal-carrying capacity of basement fluids, giving rise base metal deposits in overlying carbonate basins. Magmatism can be an essential heat source,

notably for mobilizing adequate concentrations of Cu in the fluids of the Iberian Pyrite Belt, but magmatic fluids are not an essential ingredient and the composition of the magmas is therefore not critical for deposit composition.

Acknowledgments

Appendix A. Supplementary data

Supplementary data associated with this article can be found, in the online version, at doi:10.1016/j.chemgeo.2007.10.011.

References

Almodovar, G.R., Saez, R., Pons, J.M., Maestre, A., Toscano, M., Pascual, E., 1998. Geology and genesis of the Aznalcollar massive sulphide deposits, Iberian Pyrite Belt, Spain. Mineralium Deposita 33, 111–136.

Anderson, G.M., 1975. Precipitation of Mississippi Valley-type ore fluids. Economic Geology 70, 937–942.

Anderson, I.K., Ashton, J.H., Boyce, A.J., Fallick, A.E., Russell, M.J., 1998. Ore depositional processes in the Navan Zn–Pb deposit, Ireland. Economic Geology 93, 535–563.

Barrie, C.T., Hannington, M.D., 1999. Classification of volcanic-associated massive sulfide deposits based on host rock composition. In: Barrie, C.T., Hannington, M.D. (Eds.), Volcanic-associated massive sulfide deposits; processes and examples in modern and ancient settings. . Reviews in Economic Geology, vol. 8. Society Economic Geologists, pp. 2–12.

Barriga, F.J.A.S., 1990. Metallogenesis in the Iberian Pyrite Belt. In: Dallmeyer, R.D., Martinez Garcia, E. (Eds.), Pre-Mesozoic Geology of Iberia. Springer Verlag, Heidelberg, pp. 369–379.

Bischoff, J.L., Dickson, F.W., 1975. Seawater-basalt interaction at 200°C ad 500bars: implications for origin of sea-floor heavy metal deposits and regulation of seawater chemistry. Earth Planetary Science Letters 25, 385–397.

Bolas, H.M.N., Hermanrud, C., Teige, G.M.G., 2004. Origin of overpressures in shales: constraints from basin modeling. AAPG Bulletin 88, 193–211.

Caritat, P., Baker, J.C., 1992. Overpressure release, cross formational porewater flow and diagenesis. In: Kharaka, Y., Maest, A. (Eds.), Proceedings 7th International Symposium on Water Rock Interaction. Balkema, Rotterdam, p. 1161.

Carmichael, R.S., 1989. Practical Handbook of Physical Properties of Rocks & Minerals CRC Publisher. Boca Raton. 741 pp.

Carvalho, D., Barriga, F.J.A.S., Munhá, J., 1997. Bimodal siliciclastic systems — the case of the Iberian Pyrite Belt. In: Barrie, C.T., Hannington, M.D. (Eds.), Volcanic-associated Massive Sulfide Deposits: Processes and Examples in Modern and Ancient Settings. Reviews in Economic Geology, vol. 8, pp. 375–408.

Conde, C., Mathaii, S., Geiger, S., Tornos, F., Herrington, R., 2005. Heat and fluid modeling of the shale-hosted massive sulphides in the Iberian Pyrite Belt, Spain. Abstracts GAC-MAC-CSPG-CSSS meeting, Halifax, 2005, 238.

Cooke, D.R., Bull, S.W., Large, R.R., McGoldrick, P.J., 2000. The importance of oxidized brines for the formation of Australian Proterozoic stratiform sediment-hosted Pb–Zn (Sedex) deposits. Economic Geology 95, 1–18.

Corbett, K.D., 2001. New mapping and interpretations of the Mount Lyell mining district, Tasmania: a large hybrid Cu–Au system with an exhalative Pb–Zn top. Economic Geology 96, 1089–1122.

Costa, I.M.S.R., 1996. Efeitos mineralogicos e geochimicos de alteraçao mineralizante en rochas vulcanicas felsicas de Rio Tinto (Faixa Piritosa Iberica, Espanha). Dissertaçao de Mestrado, Universidad de Lisboa. 200 pp.

Fallick, A.E., Ashton, J.H., Boyce, A.J., Ellam, R.M., Russell, M.J., 2001. Bacteria were responsible for the magnitude of the world class hydrothermal base metal sulfide orebody at Navan, Ireland. Economic Geology 96 (4), 885–890.

Fouillac, A.M., Javoy, M., 1988. Oxygen and hydrogen isotopes in the volcano-sedimentary complex of Huelva (Iberian Pyrite Belt): example of water circulation through a volcano-sedimentary complex. Earth Planetary Science Letters 87, 473–484.

Fowler, A.D., Anderson, M.T., 1991. Geopressure zones as proximal sources of hydrothermal fluids in sedimentary basins and the origin of Mississippi Valley-type deposits in shale-rich sequences. Transactions Institution Mining Metallurgy 100, b14–b18.

Francheteau, J., Needham, H.D., Choukroune, P., Juteau, T., Seguret, M., Ballard, R.D., Fox, P.J., Normark, W., Carranza, A., Cordoba, D., Guerrero, J., Rangin, C., Bougault, P., Cambon, P., Hekinian, R., 1979. Massive deep sea sulfide ore deposits discovered on the East Pacific Rise. Nature 277, 523–528.

Galley, A.G., 2003. Composite synvolcanic intrusions associated with Precambrian VMS-related hydrothermal systems. Mineralium Deposita 38, 443–473.

Garavito, A.M., 2006. Chemical osmosis in clayed sediments. Field experiments and numerocal modelling. Ph.D. Thesis, Vrije, Amsterdam, 150 pp.

Garven, G., Freeze, R.A., 1984. Theoretical analysis of the role of groundwater flow in the genesis of stratabound ore deposits.1. Mathematical and numerical model. American Journal Science 284, 1085–1124.

Gemmell, J.B., Sharpe, R., Jonasson, I.R., Herzig, P.M., 2004. Sulfur isotope evidence for magmatic contributions to submarine and subaerial gold mineralization: conical seamount and the Ladolam Gold Deposit, Papua New Guinea. Economic Geology 99 (8), 1711–1725.

Gleeson, S.A., Yardley, B.W.D., Munz, I.A., Boyce, A.J., 2003. Infiltration of basinal fluids into high grade basement, South Norway: sources and behaviour of waters and brines. Geofluids 3, 33–48.

Graf, D.J., 1982. Chemical osmosis, reverse chemical osmosis and the origin of subsurface brines. Geochimica Cosmochimica Acta 46, 1438–1441.

Goodfellow, W.D., Lydon, J.W., Turner, R.J.W., 1993. Geology and genesis of stratiform sediment-hosted (sedex) zinc–lead–silver sulphide deposits. In: Kirkham, R.V., Sinclair, W.D., Thorpe, R.I., Duke, J.M. (Eds.), Mineral Deposit Modeling. Geological Society Canada Special Paper, 40, pp. 201–251.

Goodfellow, W.D., Peter, J.M., Winchester, J.A., Staal, C.R.V., 2003. Ambient marine environment and sediment provenance during formation of massive sulfide deposits in the Bathurst mining camp: importance of reduced bottom waters to sulfide precipitation and preservation. Economic Geology Monograph 11, 129–156.

Hamilton, J.M., Delaney, G.D., Hauser, R.L., Ransom, P.W., 1983. Geology of the Sullivan Deposit, Kimberley, B.C., Canada. Mineralogical Association of Canada Short Course Handbook 9, 31–83.

Hannington, M.D., 1999. Auriferous polymetallic massive sulfides and the VMS-epithermal transition: a new exploration target. In: Hodgson, C.J., Franklin, J.M. (Eds.), New developments in the geological understanding of some major ore types and environments, with implications for exploration. Short Course, pp. 101–123.

Hanor, J.S., 1994. Physical and chemical controls on the composition of waters in sedimentary basins. Marine and Petroleum Geology 11, 31–45.

Heinrich, C.A., 1990. The chemistry of hydrothermal tin(-tungsten) ore deposition. Economic Geology 85 (3), 457–481.

Hemley, J.J., Cygan, G.L., Fein, J.B., Robinson, G.R., D'Angelo, W.M., 1992. Hydrothermal ore forming processes in the light of studies in rock-buffered systems: I. Iron–Copper–Zinc–Lead Sulfide solubility relations. Economic Geology 87, 1–22.

Hennigh, Q., Hutchinson, R.W., 1999. Cassiterite at Kidd Creek: an example of volcanogenic massive sulfide-hosted tin mineralization In: Hannington, M.D., Barrie, C.T. (Eds.), Economic Geology Monograph 10: The Giant Kidd Creek Volcanogenic Massive Sulfide Deposit. Western Abitibi Subprovince, Canada, pp. 431–440.

Hinman, M., 1996. Constraints, timing and processes of stratiform base metal mineralisation at the HYC Ag–Pb–Zn deposit, Mac Arthur River. Economic Geology Research Unit Contribution 55, 56–59.

Jupp, T., Schultz, A., 2000. A thermodynamic explanation for black smoker temperatures. Nature 403, 880–883.

Kyle, J.R., Saunders, J.A., 1996. Metallic deposits of the Gulf Coast basin: diverse mineralization styles in a young sedimentary basin. In: Sangster, D.F. (Ed.), Carbonate Hosted Lead Zinc Deposits, Society Economic Geologists Special Publication, 4, pp. 218–229.

Large, R.R., Doyle, M., Raymond, O., Cooke, D., Jones, A., Heasman, L., 1996. Evaluation of the role of Cambrian granites in the genesis of world class VHMS deposits in Tasmania. Ore Geology Reviews 10, 215–230.

Large, R.R., Bull, S.W., McGoldrick, P.J., Walters, S., Derrick, G.M., Carr, G.R., 2005. Stratiform and Strata-bound Zn–Pb–Ag Deposits in Proterozoic Sedimentary Basins, Northern Australia. In: Hedenquist, J.W., Thompson, J.F.H., Goldfarb, R.J., Richards, J.P. (Eds.), Economic Geology — One hundredth anniversary Volume. Society of Economic Geologists, Littleton, pp. 931–964.

Leistel, D.L., Bradley, D., Lewchuk, M.T., Symmons, D.T.A., Marsily, G., Brannon, J., 2002. Mississippi Valley-type lead zinc deposits through geological time: implications from recent age-dating research. Mineralium Deposita 36 (8), 711–740.

Leistel, J., Bonijoly, D., Braux, C., Freyssinet, P., Kosakevitch, A., Leca, X., Lescuyer, J.L., Marcoux, E., Milesi, J.P., Piantone, P., Sobol, F., Tegyey, M., Thiéblemont, D., Viallefond, L., 1994. The massive sulphide deposits of the South Iberian Pyrite Province: geological setting and exploration criteria. Documents BRGM 234, 236 pp.

Leistel, J.M., Marcoux, E., Thieblemont, D., Quesada, C., Sanchez, A., Almodovar, G.R., Pascual, E., Saez, R., 1998. The volcanic-hosted massive sulphide deposits of the Iberian Pyrite Belt. Review and preface to the special issue. Mineralium Deposita 33, 2–30.

Liu, W., McPhail, D.C., 2005. Thermodynamic properties of copper chloride complexes and copper transport in magmatic–hydro-thermal solutions. Chemical Geology 221, 21–39.

Lydon, J.W., 1983. Chemical parameters controlling the origin and deposition of sediment-hosted stratiform lead–zinc deposits. In: Sangster, D.F. (Ed.), Mineralogical Association Canada Short Course handbook, 9, pp. 175–250.

Mantero, E., Alonso-Chaves, F.M., Azor, A., 2005. Geometría y Cinemática de un Sistema Imbricado de Cabalgamientos en la Faja Pirítica Ibérica (Zona Sudportuguesa). Geogaceta 39, 47–50.

Marcoux, E., 1998. Lead isotope systematics in the giant massive sulphide deposits in the Iberian Pyrite belt. Mineralium Deposita 33, 45–58.

Marcoux, E., Leistel, J.M., 1996. Mineralogy and geochemistry of massive sulphide deposits. Iberian Pyrite Belt. Boletin Geologico Minero 107 (3–4), 117–126.

Marcoux, E., Moelo, Y., Leistel, J.M., 1996. Bismuth and cobalt minerals: indicators of stringer zones to massive-sulfide deposits, South Iberian Pyrite Belt. Mineralium Deposita 31, 1–26.

Mathur, R., Ruiz, J., Tornos, F., 1999. Age and sources of the ore at Tharsis and Rio Tinto, Iberian Pyrite belt, from Re–Os isotopes. Mineralium Deposita 34, 790–793.

Michalik, M., 1997. Chlorine containing illites, copper chlorides and other chloride bearing minerals in the Fore-sudetic copper deposit (Poland). In: Papunen, H. (Ed.), Mineral deposits: research and exploration. Balkema, Rotterdam, pp. 543–546.

Moreno, C., Sierra, S., Sáez, R., 1996. Evidence for catastrophism at the Famennian–Dinantian boundary in the Iberian Pyrite Belt. In: Strogen, P., Somerville, I.D., Jones, G.L. (Eds.), Recent advances in lower Carboniferous geology. Geological Society Special Publication, 107, pp. 153–162.

Mottl, M.J., McConachy, T.F., 1990. Chemical processes in buoyant hydrothermal plumes on the East Pacific Rise near 21°N. Geochimica Cosmochimica Acta 54, 1911–1927.

Moura, A., 2005. Fluids from the Neves Corvo massive sulphide ores, Iberian Pyrite Belt, Portugal. Chemical Geology 223, 153–169.

Munhá, J., Relvas, J.M.R.S., Barriga, F.J.A.S., Conceiçao, P., Jorge, R.C.G.S., Mathur, R., Ruiz, J., Tassinari, C.C.G., 2005. Os iso-topes systematics in the Iberian Pyrite Belt. In: Mao, J., Bierlein, F. (Eds.), Biennial SGA Meeting. Mineral Deposit Research: Meeting the Global Challenge. Springer, Beijing, pp. 663–666.

Nehlig, P., Cassard, D., Marcoux, E., 1998. Geometry and genesis of feeder zones of massive sulphide deposits: constraints from the Rio Tinto ore deposit (Spain). Mineralium Deposita 33, 137–149.

Nesbitt, B.E., Muehlenbachs, K., 1994. Paleohydrology of the Canadian Rockies and origin of brines, Pb–Zn deposits and dolomitization in the Western Canada sedimentary basin. Geology 22, 243–246.

Plumlee, G.S., Leach, D.L., Hofstra, A.H., Landis, G.P., Rowan, E.L., Viets, J.G., 1994. Chemical reaction path modeling of ore deposition in Mississippi Valley-type Pb–Zn deposits of the Ozark Region, US Midcontinent. Economic Geology 89, 1361–1383.

Quesada, C., 1992. Evolución tectónica del Macizo Ibérico (una historia de crecimiento por acrecencia sucesiva de terrenos durante el Proterozoico Superior y Paleozoico). In: Gutierrez Marco, J.C., Saavedra, J., Rábano, I. (Eds.), Paleozoico Inferior de Ibero-América. Mérida, Junta de Extremadura, pp. 173–192.

Reed, M.H., 1983. Seawater–basalt reaction and the origin of green-stones and related ore deposits. Economic Geology 78, 466–485.

Reed, M.H., 1998. Calculation of simultaneous chemical equilibria in aqueous–mineral–gas systems and its applications to modeling hydrothermal processes. In: Richards, J., Larson, P.B. (Eds.), Techniques in hydrothermal ore deposits geology. Reviews in Economic Geology, vol. 10, pp. 109–124.

Relvas, J.M.R.S., Tassinari, C.C.G., Munha, J., Barriga, F.J.A.S., 2001. Multiple sources for ore forming fluids in the Neves Corvo

VHMS deposit of the Iberian Pyrite Belt (Portugal): Strontium, Neodymium and Lead isotope evidence. Mineralium Deposita 36, 416–427.

Relvas, J.M.R.S., Barriga, F.J.A.S., Longstaffe, F.J., 2006. Hydro-thermal alteration and mineralization in the Neves-Corvo volcanic-hosted massive sulfide deposit, Portugal. II. Oxygen, Hydrogen, and Carbon Isotopes. Economic Geology 101, 791–804.

de Ronde, C.E.J., 1995. Fluid chemistry and isotopic characteristics of seafloor hydrothermal systems and associated VMS deposits: potential for magmatic contribution. In: Thompson, J.F.H. (Ed.), Magmas, Fluids and Ore Deposits, 23. Mineralogical Association Canada Short Course, pp. 479–509.

de Ronde, C.E.J., Hannington, M.D., Stoffers, P., Wright, I.C., Ditchburn, R.G., Reyes, A.G., Baker, E.T., Massoth, G.J., Lupton, J.E., Walker, S.L., Greene, R.R., Soong, C.W.R., Ishibashi, J., Lebon, G.T., Bray, C.J., Resing, J.A., 2005. Evolution of a submarine magmatic-hydrothermal system; Brothers Volcano, southern Kermadec Arc, New Zealand. Economic Geology 100, 1097–1133.

Russell, M.J., 1983. Major sediment-hosted exhalative zinc+lead deposits; formation from hydrothermal convection cells that deepen during crustal extension. In: Sangster, D.F. (Ed.), Short Course in Sediment-hosted Stratiform Lead–Zinc Deposits. Mineralogical Association Canada, pp. 251–282.

Saez, R., Almodovar, G.R., Pascual, E., 1996. Geological constraints on massive sulphide genesis in the Iberian Pyrite Belt. Ore Geology Reviews 11, 429–451.

Sánchez España, J., Velasco, F., Boyce, A.J., Fallick, A.E., 2003. Source and evolution of ore-forming hydrothermal fluids in the northern Iberian Pyrite Belt massive sulphide deposits (SW Spain): evidence from fluid inclusions and stable isotopes. Mineralium Deposita 38, 519–537.

Scott, S.D., 1992. Polymetallic sulfide riches from the deep: fact or fallacy? In: Hsu, K.J., Thiede, J. (Eds.), Use and Misuse of the seafloor. Wiley & Sons, New York, pp. 87–115.

Sheppard, S.M.F., 1986. Characterization and isotopic variations in natural waters. In: Valley, J.W., Taylor, H.P., O Neil, J.R. (Eds.), Stable Isotopes in high temperature geological processes. Reviews Mineralogy, vol. 16, pp. 165–184.

Simancas, J.F., Carbonell, R., Gonzalez Lodeiro, F., Perez Estaun, A., Juhlin, C., Ayarza, P., Kashubin, A., Azor, A., Martínez Poyatos, D., Ruiz Almodovar, G., Pascual, E., Saez, R., Expósito, I., 2003. Crustal structure of the transpressional Variscan orogen of SW Iberia: SW Iberia deep seismic reflection profile (IBERSEIS). Tectonics 22 (6), 1962–1974.

Silva, J.B., Oliveira, J.T., Ribeiro, A., 1990. Structural outline of the South Portuguese Zone. In: Dallmeyer, R.D., Martinez García, E. (Eds.), PreMesozoic Geology of Iberia. Springer Verlag, Heidelberg, pp. 348–362.

Solomon, M., Heinrich, C.A., 1992. Are high heat producing granites essential to the origin of giant lead–zinc deposits at Mount Isa and Mac Arthur River, Australia? Exploration Mining Geology 1, 85–91.

Solomon, M., Quesada, C., 2003. Zn–Pb–Cu massive sulphide deposits: Brine pool types occur in collisional orogens, black smoker types in backarc and/or arc basins. Geology 31, 1029–1032.

Solomon, M., Tornos, F., Gaspar, O.C., 2002. Explanation for many of the unusual features of the massive sulfide deposits of the Iberian Pyrite Belt. Geology 30, 87–90.

Spirakis, C.S., Heyl, A.V., 1995. Evaluation of proposed precipitation mechanisms for Mississippi Valley-type deposits. Ore Geology Reviews 10, 1–17.

Stampfli, G.M., Borel, G.D., 2002. A plate tectonic model for the Paleozoic and Mesozoic constrained by dynamic plate boundaries and restored synthetic oceanic isochrons. Earth Planetary Science Letters, 196, 17–33.

Sverjensky, D.A., 1984. Oil field brines as ore forming solutions. Economic Geology 79, 23–27.

Sverjensky, D.A., 1989. The diverse origins of Mississippi Valley-type Zn–Pb–Ba–F deposits. Chronique Recherche Miniere 495, 5–13.

Tornos, F., 2006. Environment of formation and styles of volcanogenic massive sulfides: the Iberian Pyrite Belt. Ore Geology Reviews 28, 259–307.

Tornos, F., Solomon, M., Conde, C., Spiro, B.F., in press. Formation of the Tharsis massive sulfide deposit, Iberian Pyrite Belt: geological, lithogeochemical and stable isotope evidence for deposition in a brine pool. Economic Geology, in press.

Tornos, F., Gonzalez Clavijo, E., Spiro, B.F., 1998. The Filón Norte orebody (Tharsis, Iberian Pyrite Belt): a proximal low-temperature shale-hosted massive sulphide in a thin-skinned tectonic belt. Mineralium Deposita 33, 150–169.

Turekian, K.K., Wedepohl, K.H., 1961. Distribution of the elements in some major units of the Earth's crust. Geological Society of America Bulletin 72, 175–192.

Urabe, T., 1987. Kuroko deposit modelling based on magmatic hydrothermal theory. Mineral Geology 37, 159–176.

Velasco, F., Sanchez España, J., Boyce, A., Fallick, A.E., Saez, R., Almodovar, G.R., 1998. A new sulphur isotopic study of some Iberian Pyrite Belt deposits: evidence of a textural control on some sulphur isotope compositions. Mineralium Deposita 34, 1–18.

Wilkinson, J.J., Eyre, S.L., Boyce, A.J., 2005. Ore-forming processes in Irish-type carbonate-hosted Zn–Pb deposits: evidence from mineralogy, chemistry, and isotopic composition of sulfides at the Lisheen mine. Economic Geology 100, 63–86.

Yang, K., Scott, S.D., 1996. Possible contribution of a metal-rich magmatic fluid to a sea-floor hydrothermal system. Nature 383, 420–423.

Yang, K., Scott, S.D., 2005. Vigorous exsolution of volatiles in the magma chamber beneath a hydrothermal system on the modern sea floor of the eastern Manus back-arc basin, western Pacific; evidence from melt inclusions. Economic Geology 100 (6), 1085–1096.

Yardley, B.W.D., 2005. Metal concentrations in crustal fluids and their relationship to ore formation. Economic Geology 100, 613–632.